

SEALED-CELL NICKEL-CADIUM BATTERY APPLICATIONS MANUAL

GODDARD SPACE FLIGHT CENTER
GREENBELT, MD

DEC 79

NASA Reference Publication 1052

Sealed-Cell Nickel-Cadmium Battery Applications Manual

Willard R. Scott and Douglas W. Rusta

Written Under Contract NAS5-23514 for NASA/GSFC
by TRW Systems, Redondo Beach, California

Floyd E. Ford, GSFC Technical Representative

DECEMBER 1979

NASA

REPRODUCED BY
**NATIONAL TECHNICAL
INFORMATION SERVICE**
U.S. DEPARTMENT OF COMMERCE
SPRINGFIELD, VA. 22161

5

BIBLIOGRAPHIC DATA SHEET

1. Report No. NASA RP-1052	2. Government Accession No.	3. Recipient's Catalog No. N80 160 95	
4. Title and Subtitle Sealed-Cell Nickel-Cadmium Battery Applications Manual		5. Report Date December 1979	6. Performing Organization Code 711
		8. Performing Organization Report No. G-7824	
7. Author(s) Willard R. Scott and Douglas W. Rusta		10. Work Unit No. 506-23-22	
9. Performing Organization Name and Address Goddard Space Flight Center Greenbelt, Maryland 20771		11. Contract or Grant No.	
		13. Type of Report and Period Covered Reference Publication	
12. Sponsoring Agency Name and Address National Aeronautics and Space Administration Washington, D.C. 20546		14. Sponsoring Agency Code	
15. Supplementary Notes Written under contract for NASA/GSFC by TRW Systems, Redondo Beach, California (Floyd E. Ford, GSFC Technical Representative)			
16. Abstract This manual covers the design, procurement, testing, and application of aerospace-quality hermetically sealed nickel-cadmium cells and batteries. Its focus is on cell technology, cell and battery development, and spacecraft applications. Written for spacecraft battery and electric power-system engineers, it summarizes and interprets applicable NASA, military, and general technical literature, for the period from 1967 to 1977. It discusses long-term performance in terms of the effect of initial design, process, and application variables and presents design guidelines and practices when applicable.			
17. Key Words (Selected by Author(s)) Nickel-cadmium battery, Spacecraft battery, Secondary battery, Energy storage (spacecraft), Electrochemical battery, Hermetically sealed cell		18. Distribution Statement STAR Category 20 Unclassified-Unlimited	
19. Security Classif. (of this report) Unclassified	20. Security Classif. (of this page) Unclassified	21. No. of Pages	22. Price*

NOTICE

THIS DOCUMENT HAS BEEN REPRODUCED FROM THE BEST COPY FURNISHED US BY THE SPONSORING AGENCY. ALTHOUGH IT IS RECOGNIZED THAT CERTAIN PORTIONS ARE ILLEGIBLE, IT IS BEING RELEASED IN THE INTEREST OF MAKING AVAILABLE AS MUCH INFORMATION AS POSSIBLE.



Sealed-Cell Nickel-Cadmium Battery Applications Manual

Willard R. Scott and Douglas W. Rusta
TRW Systems, Redondo Beach, California



National Aeronautics
and Space Administration

**Scientific and Technical
Information Branch**

1979

j. b

All measurement values are expressed in the International System of Units (SI) in accordance with NASA Policy Directive 2220.4, paragraph 4, except for the following: the ampere-hour is used rather than the coulomb because it is traditional within the battery community.

PREFACE

Since 1967, Government agencies have sponsored numerous contracts and technical meetings for improving the design, performance, and service life-time capability of sealed-cell nickel-cadmium batteries. Much of the work has been focused on improving manufacturing controls, documentation, and the overall quality-assurance aspects of cell procurement and battery production. For the most part, data and information generated by these contractual efforts have been dispersed but in a form unsuitable for direct application to other design efforts. In 1975, the National Aeronautics and Space Administration/Goddard Space Flight Center (NASA/GSFC) began to develop a battery applications manual that would: (a) present an integrated view of the state of the art, and (b) present data, information, design guidelines, and design practices of direct use and benefit to battery and electric power-system designers. Accordingly, in May 1976, NASA awarded Contract NASS-23514 for preparing this manual with the objective that its subsequent use would save battery-system designers time and effort that would otherwise be spent in searching the recent voluminous battery literature and in separating fact from conjecture. This manual, which covers the available nickel-cadmium literature through September 1977, is the product of this project. As principal investigator and coauthor, Dr. Willard R. Scott was responsible for all aspects of cell and battery technology and applications; Douglas Rusta, as project manager and coauthor, was concerned with overall manual development and with preparing technical material on battery and battery-system development, defining interfaces between the battery and other spacecraft equipment, and describing aerospace and terrestrial applications.

Several sources of data and information were used in developing this manual, particularly NASA and unclassified military reports and publications. These listings were obtained from the following sources:

- A machine search of the National Technical Information Service (NTIS) data base
- A machine search of the NASA/GSFC Library data base

- D.D. Abbott and I.S. Mehdi, "Batteries: A Literature Review and State of the Art in 1975," five volumes, Contract JPL-953984, Boeing Report D180-18849-2
- "Battery Information Index," Battelle Memorial Institute, June 1972
- "Nickel-Cadmium Batteries – A Bibliography with Abstracts," Report NTIS/PS-76/0466, June 1976
- G. Halpert and W. Webster, Jr., "Secondary Aerospace Batteries and Battery Materials – A Bibliography," NASA SP-7027, August 1969
- P. McDermott, G. Halpert, S. Ekpanyaskun, and P. Nche, "Secondary Aerospace Batteries and Battery Materials – A Bibliography," NASA SP-7044, July 1976
- E. Brooman, "An Annotated Bibliography of the Thermal Properties of Primary and Secondary Cells," Report AFAPL-TR-70-34, June 1970

The NASA/GSFC Battery Workshop Proceedings (1968 through 1977) and the Power Sources Symposium Proceedings (through 1976) were additional sources of bibliographic listings. Other sources included the results of a questionnaire survey of 17 private and Government organizations concerned with aerospace-battery applications and of separate visits to GSFC and to the Naval Weapons Supply Center at Crane, Indiana for the purpose of identifying and collecting unpublished data and information.

CONTENTS

	<i>Page</i>
SECTION 1—INTRODUCTION	1
1.1 History and Background	1
1.2 Organization	5
SECTION 2—CELL DESCRIPTION	9
2.1 Introduction	9
2.2 Electrode Reactions	9
2.3 Cell Design and Construction	12
2.4 Cell Manufacturing	47
2.5 Reference Cell Design Data	58
2.6 Lightweight Cells	62
SECTION 3—CELL PROPERTIES AND PERFORMANCE	65
3.1 Introduction	65
3.2 Static Properties of Cells	66
3.3 Initial Performance Characteristics	78
3.4 Long-Term Performance Characteristics	134
SECTION 4—CELL FAILURE ANALYSIS AND MECHANISMS	179
4.1 Introduction	179
4.2 Systematic Approach to Degradation/Failure Analysis	179
4.3 Degradation and Failure-Analysis Terminology Applicable to Cells and Batteries	180
4.4 Observed Degradation and Failure Modes	186
4.5 Underlying Causes of Degradation and Failure	191
4.6 Effect of Cell Design on Degradation Processes	209
4.7 Effect of Operating Conditions on Degradation Processes	216

CONTENTS (Continued)

	<i>Page</i>
SECTION 5—CELL AND BATTERY PROCUREMENT	221
5.1 Introduction	221
5.2 Cell Procurement Process	222
5.3 Cell Specification Document	225
5.4 Request for Proposal	231
5.5 Manufacturing Control Document	234
5.6 Battery Engineering Support to Quality- Assurance Activities	237
5.7 Cell Acceptance	239
5.8 Battery Procurement	239
SECTION 6—CELL AND BATTERY TESTING	245
6.1 Introduction	245
6.2 Acceptance Testing	245
6.3 Qualification Testing	262
6.4 Life Testing	262
6.5 Special Accelerated Testing	269
6.6 Miscellaneous Tests	272
SECTION 7—BATTERY SYSTEM DEFINITION	275
7.1 Introduction	275
7.2 Electric Power System Design Considerations	275
7.3 Types of Electric Power Systems	289
7.4 Methods of Temperature Control	302
SECTION 8—BATTERY SYSTEM DESIGN	325
8.1 Introduction	325
8.2 Requirements and Constraints	325
8.3 Methods of Charge Control	329
8.4 Methods of Cell and Battery Protection	352
8.5 Methods of Discharge Control	370
8.6 Synthesis of Battery-System Configurations	379
8.7 Analysis of Battery-System Configurations	388

CONTENTS (Continued)

	<i>Page</i>
SECTION 9—BATTERY DESIGN AND DEVELOPMENT	409
9.1 Introduction	409
9.2 Definition of the Battery Configuration	410
9.3 Battery Manufacturing	426
9.4 Battery Acceptance Testing	429
9.5 Battery Qualification Testing	434
9.6 Battery Storage, Maintenance, and Installation	437
SECTION 10—APPLICATIONS	445
10.1 Introduction	445
10.2 Battery-System Hardware Descriptions	445
10.3 Advanced Battery Systems	454
10.4 Terrestrial Applications	457
REFERENCES	459
APPENDIX A—DEFINITIONS	491
APPENDIX B—AUTHOR INDEX	497
APPENDIX C—ORGANIZATION INDEX	503
APPENDIX D—SUBJECT INDEX	505

SECTION 1 INTRODUCTION

1.1 HISTORY AND BACKGROUND

The majority of spacecraft flown in the two decades of the space era have contained energy storage systems composed of nickel-cadmium batteries. This fact is due to the high cycle-life capability, good specific energy, and relatively simple charge-control requirements of the nickel-cadmium system. Because the reliability of the system has been quite good, nickel-cadmium batteries have been used for extended manned missions, as well as for unmanned applications. In unmanned applications mission length has increased up to ten-fold in 20 years.

A large part of this success is attributable to the availability (for the first time in the 1950's) of significant quantities of hermetically sealed cells. Originally developed for commercial purposes, the earliest sealed nickel-cadmium cells were not suitable for aerospace application. They were small in capacity and often exhibited the effects of seal unreliability, poor thermal design, nonoptimum electrochemical design, and lack of control of materials and processes. As time progressed, sponsoring government agencies, cell buyers, and cell suppliers identified and addressed many problems. By the late 1960's, cells were available in capacities up to 50 Ah, seal problems were less frequent, and several domestic suppliers were offering designs that emphasized light weight. Depths of discharge had risen from about 5 percent to 15 to 20 percent in low-altitude orbit applications and up to 40 percent for the batteries of geosynchronous orbit spacecraft.

As more demands were made of the nickel-cadmium system, more development efforts were initiated to obtain better performance and reliability. Government space agencies provided the impetus and direction for this work with leadership provided by skill groups at the Goddard Space Flight Center (GSFC), the Jet Propulsion Laboratory (JPL), and the U.S. Air Force Aero Propulsion Laboratory. The primary goal was to obtain a cell that would meet standards of aerospace quality through what was necessarily an evolutionary process in the environment produced by a young

and dynamic space program. Among many important issues that were addressed during these years were:

- the determination and solution of the causes of common cell failures
- the establishment of the relationship between operating temperature and cycle-life performance
- the development of improved methods of charge monitoring and control
- the investigation of the effect of changes in cell design on long-term performance
- the solution of design problems associated with larger cells and batteries
- the development of failure-analysis techniques
- the establishment of controlled cell manufacturing and test procedures

Aerospace contractors, independent research organizations, and battery cell suppliers contributed to these studies by participating under government-sponsored development projects and by sharing experiences otherwise obtained from work performed for commercial space activities.

The National Aeronautics and Space Administration (NASA) understood the importance of disseminating the information obtained from these activities and of encouraging the sharing of experiences as a means of ensuring the development of good application practices and uniform product characteristics. This understanding was demonstrated in three important ways. First, a long-term cell evaluation project was established at the Naval Weapons Supply Center, Crane, Indiana (NWSC/Crane), which continues today. The NWSC/Crane test programs represent the most important single source of comparative real-time and accelerated life-cycling test data for the aerospace battery community. NWSC/Crane testing efforts have been summarized with regularity with raw data always available to organizations with legitimate need. Second, NASA has sponsored the publication of a series of periodic monographs (of which this document is one) that summarize the state of the art and provide a valuable source of

reference material (References 1 and 2). Finally, NASA has sponsored and hosted annual battery workshops at the Goddard Space Flight Center since 1968.

These workshops provide an opportunity for representatives from all organizations concerned with the design, manufacture, test, and application of sealed aerospace-quality cells and batteries to exchange problems and solutions, development status reports, experiences, and views regarding perceived trends in technology. The maintenance of peer contact has proved to be important in keeping channels of communication open throughout the industry, and the published transcripts of the meetings have become an important source of battery design information.

Throughout the 1970's, interest intensified in several areas. Perhaps the most important of these has involved studies of ways to further improve cell reliability. Work has proceeded along several lines: (1) definition and better understanding of cell-design variables; (2) definition and control of cell manufacturing processes; and (3) definition of correct application procedures. The results of these efforts have been a general upgrading of cell procurement specifications and the agreement of the cell suppliers to work under a predetermined set of manufacturing controls.

Another area of interest, which is closely related to efforts made in improving cell reliability, concerns the question of extending the service life of the nickel-cadmium system. It is generally understood that early cells were usually designed for obtaining high values of specific energy with less attention paid to design aspects that are now known to strongly influence long-term operation. Continued study indicated that proper specification of certain cell-design variables is essential if the full cycle-life capability of the nickel-cadmium system is to be realized. Cooperation between users and suppliers has resulted in cell specifications that are now somewhat more self-consistent in terms of expected performance and actual weight. Many controlled tests and experiments have demonstrated the influence of depth of discharge and temperature on cycling performance. It is now clear that maintenance of controlled low operating temperatures is very important in achieving long life. Data obtained from accelerated tests indicate that proper in-orbit reconditioning of batteries—particularly in geosynchronous orbit applications—may also provide extensions of service life. Future work will undoubtedly focus on the benefit of these approaches. Other, more fundamental work will address the relationship between cell-design and manufacturing variables and cycle-life performance.

Battery system weight continues to be a major area of interest. Much progress has been made in the art of packaging nickel-cadmium cells into batteries. In early configurations, 20 to 30 percent of the total battery mass was devoted to structure, thermal-control auxiliaries, and wire and connectors. Today, advanced designs require only 5 to 15 percent of the total mass for the same functions. Lightweight, long-life cells that weigh about 25 percent less than conventional cells are under development. About half of the reduction is obtained through the use of smaller electrodes of high specific energy; the remaining half results from the scaling of other cell components and the use of thin-wall cell containers.

The economic realities of the 1970's, coupled with the future availability of the Space Transportation System in the 1980's, have provided motivation for searching for ways to standardize spacecraft hardware. For some years, work within NASA has been directed at the system, component, and device levels. Two results of these efforts will be the development of a Standard 20-Ah cell and a Standard 22-cell battery that contains this cell (Reference 3). The effort at the cell level has provided an opportunity for developing specifications and manufacturing controls that reflect the experience gained over many projects and many years.

Most of the developments outlined in the previous four paragraphs have occurred since the last general NASA publication on batteries (Reference 2) was published in 1968. At that time, relatively little performance data were available from the literature, and what there was often represented cell configurations that are now considered to be either obsolete or non-representative of those manufactured today. Significant investigations that were then under way were not reported until several years later.

This document updates the record and provides both an overview and an interpretation of the progress made in the last decade. Although titled as an applications manual, the approach taken is less toward that of a "cookbook" and more toward that of a summary. This is justified because the state of the art in nickel-cadmium cell and battery design is still in considerable flux, with much work to be done before precise rules can be defined for battery-system synthesis and hardware implementation.

A review of the literature has revealed many areas in which data are either missing, incomplete, or so specific to an application that it requires first-hand evaluation by the prospective user. Relatively few controlled experiments have been documented in detail. This is not surprising because much development work has been performed in the context of either

specific projects or organization-funded research and development activities. General publication of results is difficult to accomplish in the former case and often prohibited for proprietary reasons in the latter case. A questionnaire survey of private and government organizations was conducted to identify present concerns and future needs. The results of the survey guided the selection and organization of material in this manual.

Material is presented at three levels—cell, battery, and system. To fulfill the objective of showing how nickel-cadmium cells can best be used in spacecraft application, this manual has been written for both battery and power system engineers because their efforts are closely interrelated during the conceptual and preliminary phases of design. It has therefore been necessary to include collateral material, not found elsewhere in concise form, for providing information necessary to understanding past applications and current trends in design. The importance of a thorough definition of design requirements and constraints to the success of a battery system development effort has been emphasized. The viewpoint expressed is not parochial. Many requirements are determined at the spacecraft system and subsystem levels and may often not be translated in sufficiently clear terms to the battery-component level. The avoidance of such a situation is ultimately the responsibility of the battery designer.

Therefore, the following sections encompass a dual approach to battery system design. The battery is viewed as a system component with definite requirements, constraints, and interfaces. Full understanding of the meaning of each of these enables specification of the correct cell for a particular application. The cell, in turn, is examined as a device whose initial and final performance is dependent on many variables—some directly associated with the intended application and others associated with fundamental design and manufacturing considerations. Any practical cell design or mission application involves a series of compromises regarding these aspects. If the user is helped in developing an understanding of how the significant parameters that affect performance and reliability may be balanced and how mission objectives can be satisfied, this manual will have served its intended purpose.

1.2 ORGANIZATION

The manual is organized into 10 sections. This section provides an overview of the book. Sections 2 through 6 describe the design and performance of the sealed nickel-cadmium cell. Sections 7 through 10 deal with the application of the cell to batteries and battery systems. Although data and

information useful for battery system design appear throughout the manual, cell-level design data are presented mainly in Section 3.

Section 2 contains a general description of the modern aerospace-quality sealed nickel-cadmium cell. The treatment contains only as much theory as required to demonstrate the operation of the cell as a secondary (rechargeable) energy-storage device. Each cell component is discussed and the variables critical to its design and manufacture are identified. Quantitative measures of electrochemical and mechanical properties are provided for typical cells and, in particular, for cells identified throughout this manual as reference designs.

Three reference cell designs are identified. Each represents a particular group of cell configurations and has been applied during the last 5 years. They are used only as a well-defined baseline configuration against which cells within the groups can be compared. Therefore, the description and discussion of the reference cells is not meant as a recommendation for their use in new applications.

Section 2 and subsequent chapters introduce definitions of terminology that may or may not be familiar to the reader. Some workers in the field may disagree with certain proposed definitions. It is believed that clear, precise language is necessary for good technical communications, and an attempt has been made to be consistent in meeting this standard.

Section 3 contains a summary of data on the physical and electrical properties of a variety of cells. The material is arranged in three groups: static properties, initial performance characteristics, and long-term performance characteristics. The first two groups describe so-called "new" cells—those that have experienced only a small number of discharge/charge cycles for stabilizing their characteristics. The last group contains examples and estimates of changes to the characteristics that may be expected with continued service. These results may be used to perform sizing calculations based on end-of-mission requirements.

Section 4 considers the causes of change in cell performance characteristics throughout the service period. The discussion is focused on the relationship of cell design and manufacturing variables on degradation and failure phenomena. The treatment requires careful definition of what is meant by degradation and failure and requires the introduction of terminology from the disciplines of failure physics and analysis.

Section 5 addresses the general subject of cell and battery procurement methodology and practice. The total procurement cycle is discussed, from the preparation of specifications to the disposition of hardware after it has been received and accepted, but before it is integrated into the next hardware level.

Section 6 is concerned with all aspects of cell and battery testing and, in certain areas, serves as an adjunct to Sections 4 and 5. Alternative testing philosophies are described and evaluated with special reference to the impact on project time and cost.

Sections 2 through 6 deal with topics at the cell and battery levels without direct discussion of application beyond the categorization of performance variations and other considerations in terms of general mission specifications (orbit characteristics, design life, etc.). Throughout the discussions, there is a presumption that the cells and batteries will be operated properly in orbit to maintain energy balance and temperature control. The entire question of what constitutes proper application at the battery and power system levels is the subject of Sections 7 through 10.

Section 7 presents a general review of electric power subsystem design methodology. The role of the battery system is emphasized to show how it affects, and is affected by, the operation of the power subsystem. This section also contains a review of thermal design principles and techniques as they are used in providing thermal control of cells, batteries, and battery auxiliaries.

Section 8 examines aspects of battery system design, including the selection and application of electronic controls and protection functions. The treatment is based on a loosely connected series of cases or examples, each considered in detail, that identify problem areas in application and offer alternative methods of solution. Design guidelines are introduced when appropriate.

Section 9 continues the progression from the general (the electric power system) to the specific (in this case, the battery as a component). It discusses battery development and provides an outline of a general development plan from the conceptual design phase, through manufacture and component-level testing, to subsequent prelaunch storage and logistic activities.

Section 10 concludes the manual with illustrations of battery system hardware representative of the recent, present, and expected conditions of the

state of the art. Terrestrial applications of sealed nickel-cadmium cells are briefly discussed.

The following terminology has been used throughout this manual: cell battery, battery system, and electric power system. It is appropriate here to define these and other related terms. A *battery* is defined as an assembly of *cells*, connected electrically in series, together with whatever auxiliaries may be integrally mounted, such as cell protection or charge/discharge control circuitry, telemetry and command interface circuitry, reconditioning networks and controls, heaters and heater controls, other thermal control devices, and radiation shields. The battery assembly is identified by both a configured-item identification number and an assembly drawing with associated parts list.*

A *battery system* is a complete energy-storage system and includes all batteries and other components or functions that are related to the batteries and that are required for their operation and maintenance. By this definition, charge controllers or discharge regulators that may be contained in another component, such as a power-control unit, are part of the battery system. If dedicated to the batteries, active thermal-control equipment, such as heat pipes or thermal louvers, form a *battery thermal-control system* that is part of the battery system.

The spacecraft electric power subsystem is referred to as an *electric power system*. It contains the battery system, other power sources such as the solar-cell array, and regulation, conversion, and distribution equipment. By this terminology, a spacecraft also contains a *thermal-control system*, a *structural system*, a *command and telemetry system*, an *attitude-control system*, a *propulsion system*, and one or more payloads.

*Some batteries are composed of physically separate subassemblies or modules that may or may not be identical in electrical and mechanical configuration. For the purposes of this manual, it is assumed that the battery consists of all subassemblies so defined that are connected electrically in series and are necessary to its function.

SECTION 2 CELL DESCRIPTION

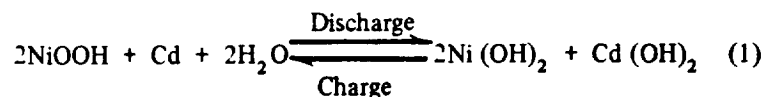
2.1 INTRODUCTION

This section presents an overall description of the sealed nickel-cadmium cell and includes sections on the electrochemistry of the cell system, the design and construction of present-day cells, and the manufacturing process used to produce commercially available cells. Much of the information presented on cell design and manufacturing has not been published and was obtained by reviewing cell-design data supplied during the process of cell procurement and from private communications with vendors and users.

The discussion of electrochemistry is nontheoretical and covers only the material required to understand and deal with cell design and performance. The description of the state of the art of cell design covers the design of cell components and presents typical properties data. Electrical characteristics of components are given, but electrical performance at the cell level is not included here because it is the subject of Section 3. References 4, 5, and 6 contain more general information on cell design. Additional details beyond those in this manual may be found in the references cited in the following sections.

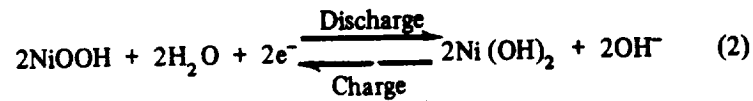
2.2 ELECTRODE REACTIONS

The main overall reaction involved in energy conversion in a nickel-cadmium cell may be written as

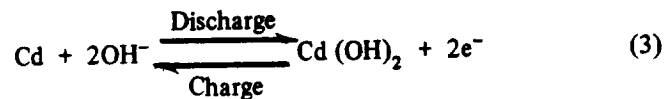


The charged form of nickel-active material is most often written as NiOOH as a matter of convenience if not of convention. Although this formula implies an oxidation state (valence) of 3 for nickel, the exact composition of the charged nickel is uncertain (References 7, 8, and 9).

The corresponding half-cell reaction that occurs at the nickel-hydroxide electrode (connected to the normally positive terminal) is



in which charging results in the oxidation of nickel hydroxide and discharging results in the reduction of NiOOH. The half-reaction at the cadmium electrode (connected to the normally negative terminal) is

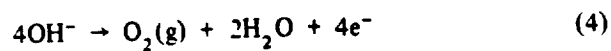


in which charging results in the reduction of Cd(OH)₂ to Cd and discharging results in the oxidation of Cd to Cd(OH)₂. The sum of reactions 2 and 3 is reaction 1. Thermodynamic constants for each electrode reaction and for the cell reaction are summarized by Bauer (Reference 2). Other data on the open-circuit potential have been published (References 7 and 10).

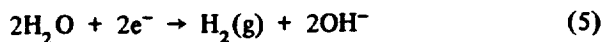
One mole of water per mole of NiOOH is consumed during discharge and is regenerated during charge. No net change in the amount of OH⁻ occurs during reaction 1, although the OH⁻ concentration varies during cycling (Reference 11).

According to equation 1, charge or discharge involves a transfer of exactly 1 faraday (26.8 Ah) per mole of Ni(OH)₂ or NiOOH. Although this relationship is approximately true, there is evidence (References 4 and 9) that certain kinds of nickel-hydroxide electrodes can be charged to a nickel-oxidation state well above +3.0, and that the discharge can produce more than 1 faraday per mole of Ni(OH)₂ which is widely used as a reference for expressing the observed utilization of nickel-active material in a cell. This gives a conversion factor of 0.288 Ah per gram of Ni(OH)₂. The corresponding factor for Cd(OH)₂ is 0.366 Ah per gram.

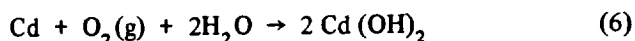
During overcharge, one or both of two additional reactions may occur. Oxygen is normally evolved at the charged positive electrode according to half-reaction



Also, depending on its state of charge and its physical condition, hydrogen may be evolved on the negative electrode according to half-reaction



In a new, properly designed and manufactured sealed cell, considerable uncharged, electrochemically active $\text{Cd}(\text{OH})_2$ remains when oxygen evolution begins at the positive electrode (Section 2.3.3.6), and, hence, reaction 3 proceeds from right to left instead of reaction 5. In addition, the oxygen from reaction 4 reacts with charged cadmium at the negative electrode according to reaction



This process is known as oxygen recombination. When the oxygen pressure is constant, no net change occurs in the state of charge of either the nickel-hydroxide (positive) electrode or the cadmium (negative) electrode.

When a cell that is designed to be positive-limiting on discharge* is discharged beyond the capacity of the positive electrode, the potential of that electrode shifts by more than 1 volt in the negative direction, and reaction 5 takes place on this electrode. Because some capacity usually remains in the cadmium electrode when the nickel electrode is exhausted, reaction 3 continues to occur in the discharge direction.

Because the electrode potential of reaction 5 is more negative than that of reaction 3, the cell voltage at that point is negative. As overdischarge continues, the usable capacity of the cadmium electrode is also eventually exhausted, at which time the cadmium-electrode potential becomes more positive by over 1 volt, and reaction 4 occurs. The cell voltage under these conditions is about -1.5 volts.

Reaction 5 produces hydrogen gas at a rate equivalent to the discharge current involved (418 cm^3 of H_2 per Ah at standard temperature and pressure), and, unless most of this hydrogen is recombined or escapes from the cell, high pressure will result. Since the rate of dissipation of hydrogen gas is normally very low (in the absence of devices that catalyze recombination with oxygen), the discharge rate during reversal must be kept small. The quantitative aspects of rate-versus-hydrogen pressure during overdischarge have been studied by Ritterman (Reference 12).

*A cell is positive-limiting on discharge when the discharge capacity to a given end voltage is determined by the electrode potential of the positive electrode and not by that of the negative electrode.

2.3 CELL DESIGN AND CONSTRUCTION

This section presents and correlates certain details of design and construction of modern hermetically sealed, sintered-plate nickel-cadmium battery cells. The material is presented as background information and is intended to serve as the basis for discussing the effect of design variations in Sections 3 and 4.

2.3.1 General Design Requirements for Space Applications

By far, the largest use of nickel-cadmium batteries in space applications is for orbiting spacecraft, whether for Earth orbiters, lunar orbiters, Mars orbiters, or others. Such applications take advantage of the inherently long cycle life of the nickel-cadmium cell as compared to other types of sealed cells.

The cell and battery design requirements for orbital applications are:

- Capability to withstand launch vibrations and shock environments
- Integrity of the hermetic seal maintained throughout thousands of electrical cycles involving pressure and thermal changes
- Low thermal resistance from plate stack to spacecraft heat sink
- Long cycle life under a wide range of conditions
- Stable long-term voltage regulation
- Maximum coulombic efficiency
- Maximum useable energy per unit weight
- Stable long-term overcharge characteristics

This section describes how the design and construction of the cell contributes to the achievement of these requirements. Section 2.3.2 discusses the design of individual cell components, and Section 2.3.3 discusses the design of the cell as a whole, including the interrelationship of components.

2.3.2 Cell Components

The cell components of greatest potential impact on cell performance and life are the plates,* separators, container and seals, and electrolyte. For a summary of additional information, see Reference 5. Two excellent bibliographies on cell materials have been published (References 13 and 14).

2.3.2.1 Plate Design

A sintered plate consists of a porous metal substrate, called a plaque, whose pores are partially filled with an electrochemically active material. The plaque consists of a matrix of sintered-nickel particles attached to a supporting base, usually referred to as the grid. Many design variables can affect plate behavior and, hence, cell performance and life. Some of these are discussed in the following paragraphs.

Plaque Design—The variables involved in plaque design include grid type, material, and thickness, plaque thickness, porosity (void fraction), and pore size.

Two types of grids are generally used: perforated sheet metal and metal screen. Each is made as either solid nickel or nickel-plated steel. The sheet is usually 0.08 to 0.1 millimeter (0.003 to 0.004 inch) thick and is about 40 percent perforated. Typically, screen grids are made from wire about 0.3 millimeter (0.01 inch) in diameter and have up to eight wires per centimeter (20 per inch). Currently, only a wet slurry coating is used with perforated sheet grids, and only a dry powder coating is used with screen grids. (See the following description of the plaque-making process.) Although the screen can be slurry-coated, perforated sheet is usually unsuitable for dry-coating because it does not retain dry nickel powder properly.

From a reliability standpoint, the perforated sheet-grid/slurry-coated plaque design appears to be superior to the screen-grid/dry-coated type for spacecraft applications. Several deficiencies of the latter may be cited. For example, the individual wires at the edges of the screen grids are difficult to control, even when the plaque is coined, and tend to become

*The term "plate" is used in this manual to designate the physical entity consisting of a flat structure made up of an electrical conductor and the active material. A number of plates welded together become a "plate group." The term "electrode" is reserved for a plate or plate group that operates electrochemically in an electrolyte.

bent toward the adjacent plate, thereby shorting the cell. The tabs must be welded to the remainder of the plaque, and this weld is often a point of relatively high resistance, which causes hot spots that can soften or melt the separator that leads to plate-to-plate shorting in the tab area. High voltage or charge and low voltage or discharge can also result. Finally, dry-sintered plates undergo considerably more swelling and buckling with cycling because the sintered matrix is relatively weak and is largely on one side of the screen grid. Therefore, any swelling of the sinter (normal for chemically impregnated positive plates)* tends to distort the plate.

The thickness of plaque now being produced by different manufacturers ranges from 0.5 to 0.9 millimeter (0.02 to 0.035 inch). Plaque for positive plates often is of a different thickness than that of plaque for negative plates. When the negative-to-positive capacity ratio is low (e.g., less than 1.25), the negatives may be thinner; when this capacity ratio is high (e.g., 1.5 or greater), the negatives are usually thicker than the positives. Table 1 gives thickness data for plates in some typical spacecraft cells.

Table 1
Thicknesses of Plates in Spacecraft Cells¹

Manufacturer	Positive (mm)	Negative (mm)
Eagle Picher	0.63 to 0.70	0.68 to 0.78
General Electric	0.69 to 0.71	0.80 to 0.82
SAFT ²	0.83 to 0.88	0.82 to 0.90

¹ Uncoined area; coined areas are thinner.

² From cells supplied by SAFT-America (formerly Gulton Industries, Alkaline Battery Division); plates manufactured by SAFT-France.

The thicker the plaque of a given void fraction, the greater the amount of active material that can be impregnated and, thus, the greater the initial capacity per unit plate area and the lower the ratio of inert plate weight to initial capacity. On the other hand, the amount of active material that can be impregnated is limited in practice by the amount of sinter corrosion

*See Section 2.4.2.

that is permitted by the blockage of pores and by accumulation of surface buildup. (See Section 2.4.) Thin plates are better for high-rate operation (i.e., charge and discharge rates well above the 1C rate);* however, spacecraft batteries are rarely designed for true high-rate operation, since cycle life may be shortened under these conditions. Plaque (and plate) thickness is thus not easily optimized, and the choice is often dictated by the capabilities of the cell manufacturers' equipment and processes.

The void fraction (or porosity) of the sintered-nickel matrix before impregnation is a key parameter. Table 2 gives representative data. For plaque of a given thickness, the strength of the sinter, the resistivity, and the average pore size are related to sinter void fraction (Reference 15). Therefore, control of this property provides indirect control over a number of other properties that affect plate performance and life.

Table 2
Void Fraction of Aerospace Plaques and Plates¹
(percent of total plate volume)

Manufacturer	Plaque		Plate ²	
	Positive	Negative	Positive	Negative
Eagle Picher	83 to 87	83 to 87	(3)	(3)
General Electric	75 to 80	80 to 85	25	34
SAFT ⁴	(3)	(3)	29	32

¹ Measured by water absorption.

² Remaining after impregnation.

³ Data not available.

⁴ From cells supplied by SAFT-America; plates manufactured by SAFT-France.

The void fraction of plaque for spacecraft cell plates ranges from 75 to 90 percent of sinter volume, depending on the manufacturer and whether the material is used for positive or for negative plates. The void fraction of the negative plaque is usually higher.

*When used to designate a charge or discharge rate, the symbol "C" stands for a current in amperes numerically equal to the cell capacity in ampere-hours.

The void fraction for positive plaque has been optimized with respect to initial capacity and handling during manufacturing. However, heavily loaded plates made from such plaque by the chemical impregnation method undergo considerable thickening with cycling (References 16 and 17). Also, after several hundred cycles, positive-plate capacity and utilization* of active material decrease relative to their initial values when plaque void fraction is above 75 to 80 percent, (Reference 18), whereas the opposite trend is observed below 75 percent. Because, for a given plate thickness, plate weight per unit area increases as void fraction decreases, however, design tradeoffs at the plaque design level are possible.

Relatively few data are available on pore size and pore-size distribution in sintered-nickel plaque. One reason for this is the difficulty and expense of making the measurements. It has been reported that the mercury intrusion method that is often used for measuring pore size in other applications is not valid for sintered nickel (Reference 15). Available data show a range from 1 to over 100 microns calculated pore diameter, with averages in the range of 10 to 20 microns (References 19 and 20). Figure 1 shows the surface of a sintered-nickel plaque as seen under the scanning electron microscope.

Reference 18 shows that the average pore size increases as void fraction increases and that utilization in positive plates decreases as pore size increases. Thus, optimization of a cell design for specific energy should include consideration of plaque pore size as well as void fraction.

The edges of plates used in most aerospace cells are "coined." Coining is the process of stamping the sinter to densify it and thereby to strengthen the edges. Because coining is normally done before impregnation, the amount of active material absorbed by the edges is less than that in the uncoined area; hence, the weakening effect of cycling on the sinter structure is less at the edges. Different manufacturers use different degrees of thickness reduction, ranging from 15 to 50 percent of the uncompressed thickness. Tests have shown (Reference 17) that the beneficial effect on positive plates is insignificant unless the thickness reduction is greater than 30 percent. Figure 2 shows the appearance of properly coined edges.

The average width of the coined border is usually constant for a given manufacturer and independent of the size of the plate. Thus, the percentage of total plate area affected by coining increases as cell size (and plate size) decreases. For an average coined width of 1.5 millimeters,

*In this manual, utilization = (capacity obtained on discharge ÷ theoretical capacity calculated from the amount of active material present).

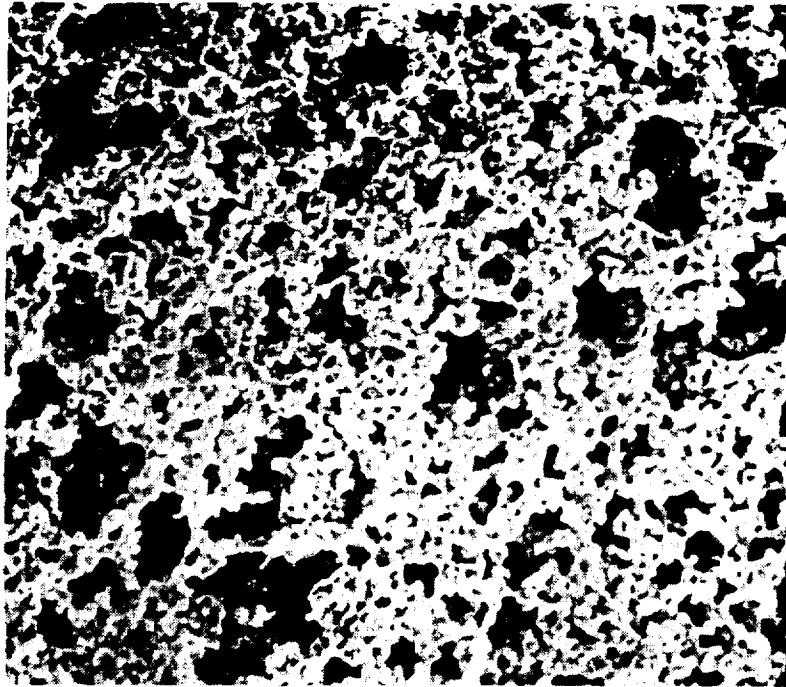


Figure 1. Sintered-nickel plaque surface as seen under the scanning electron microscope (500X).

which is typical, the coined area amounts to 7 percent of total plate area in a 20-Ah cell and 11 percent in a 6-Ah cell, representing a tradeoff between the potential benefits of coining and the specific energy obtained from a cell.

The practical benefit derived from coining negative plates is less than that obtained from coining positive plates because the negatives are inherently less brittle and have less tendency to swell on cycling. Coining of positive plates made by the vacuum impregnation process has provided distinct strengthening and stabilization of edges (Reference 17). The edges of plates made by electrochemical impregnation are more mechanically stable and thus, up to the loading level at which capacity per unit plate area is equal to that of chemically impregnated plates, do not require coining. However, because more highly loaded plates are weaker, they benefit from coining.

ORIGINAL PAGE IS
OF POOR QUALITY

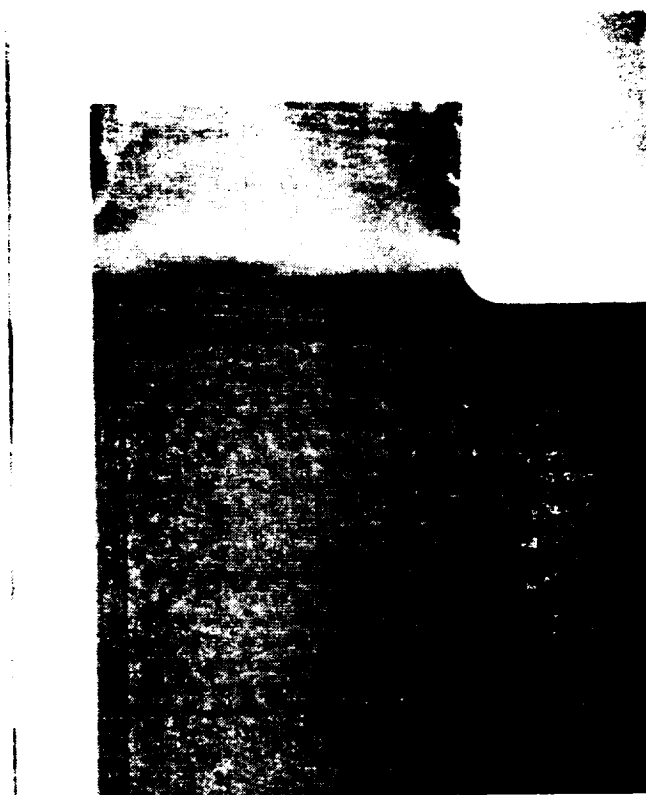


Figure 2. Coined edges of a plate near the plate tab (3X).

Composition of Impregnated Materials—Impregnated materials are those chemicals that are deposited in the pores of the plates by the impregnation process. (See Section 2.4.2.) Not all of these materials are electrochemically active in some plate designs. The active part of impregnated material contained in the positive plates is referred to as positive (or nickel) active material, and that contained in the negative plates is referred to as negative (or cadmium) active material.

Most manufacturers use additives to improve performance in various ways. These additives are usually injected at the time of impregnation by coprecipitation with the active materials. Although many additives to the nickel active material in positive plates have been tested (References 17 and 20 through 24), only cobalt and cadmium are now used commercially to a significant extent. Cobalt compounds are added to positive plates to increase the utilization of positive active material. (See the section on "Sizing and Coining" later in this document.) It has not been clearly

established if cobalt takes an active part in the electrochemical reaction. Although the amount of cobalt used varies among manufacturers, it is usually in the range from 5 to 10 mole-percent based on the nickel-active material deposited.

A small percentage of cadmium is incorporated into the active material of positive plates of some designs to act as antipolar material* (Reference 20). Cadmium material has also been added to reduce the rate of fading of the positive-electrode voltage with cycling.†

Loading Level—Whether electrochemically active or inactive, the total weight of material in final converted form (after drying) that is absorbed by a plate during impregnation is referred to as the "loading." The loading level is expressed in one of several ways: (1) weight per unit area of plate; (2) weight per unit volume of plate; or (3) weight per unit of plaque void volume. These may be interconverted if the plate thickness, density, plaque void fraction, and extent of corrosion during impregnation are known. Cell manufacturers' specifications are usually in terms of weight per unit area. Table 3 gives these data for plates from several spacecraft cell manufacturers and the values for weight per unit of plate volume calculated from area loading data and thickness data from table 1.

Loading values expressed as weight per unit of void volume are ambiguous and can be misleading unless the point in the process at which the said volume is measured is specified. This is because the volume internal to the plate available for occupation by active material (which is properly referred to as the void volume before impregnation) increases during impregnation and formation, and the increase may be considerable (e.g., 25 percent) when high loading levels are used and corrosion of the sinter during impregnation is severe. Thus, the value for weight per unit of plaque void volume (measured before impregnation) will be greater than the weight per unit of available internal volume after impregnation. Methods of determining the latter volume are subject to considerable uncertainty. The authors of this manual estimate that the value of weight per unit of available internal volume in commercial plates now available for spacecraft cells is about 2.0 g/cm^3 for positives and 2.3 g/cm^3 for negatives. These values are approximately the same as those reported by Dunlop (Reference 25).

*Antipolar material is used to provide temporary protection against the effects of reversal. Cadmium hydroxide becomes charged as the positive electrode becomes discharged, thus holding the voltage more positive until all the cadmium material is charged.

†G. G. Rampel, General Electric Battery Division, private communication.

Table 3
Manufacturers' Specifications for Loading
Commercially Available Plates¹

Manufacturer	Positive Plates (g/dm ²)	Negative Plates (g/dm ²)
Eagle Picher	12.2 to 12.8	13.3 to 16.0
General Electric	13.5 to 14.7 ²	16.3 to 17.5 ²
	12.8 to 14.0 ³	15.4 to 16.6 ³
SAFT (Type VO) ⁴	14.0 to 16.0 ⁵	17.0 to 17.7 ⁵
	16.0 to 16.5 ⁵	17.7 to 18.7 ⁵

¹Applicable before formation; composition of impregnated material is unspecified.

²1969 to 1974.

³1975 to present.

⁴Plates manufactured by SAFT-France.

⁵Two loading levels used at cell manufacturer's discretion (1968 to 1975).

Special Plate Treatments—Plates may be given special treatments* so that they perform better in certain applications. Such treatments normally result in the deposition of material at or near the gross surface of the plates (as opposed to being uniformly distributed with the active material in the pores). Examples of treatments now in use are Teflonation of negative plates and silver treatment of the negatives.

Negative (cadmium) plates are Teflonated (Reference 26) by at least one manufacturer as an option. The amount of Teflon used is less than 1 percent of plate weight. By reducing the wettability of negative-plate surfaces, Teflonation reduces the amount of electrolyte redistribution (Reference 27). Teflonation also appears to reduce the amount of cadmium active material deposited in the separators during cycling (Reference 27). Sections 3 and 4 contain more specific data.

One manufacturer also offers a silver treatment of negative plates (Reference 28) as an option. The amount of silver material deposited is approximately 0.1 percent of plate weight. This treatment is claimed to increase the

*As used here, special treatments are applied by operations other than the normal plate-manufacturing process. Thus, they do not include additives incorporated during impregnation or formation.

oxygen-recombination rate capability of the negative-plate surfaces, particularly at low temperatures. No comparative test data demonstrating such an effect has been published.

2.3.2.2 Separator Design

Separator materials for sealed aerospace cells should exhibit the following characteristics:

- Physical strength as a mechanical spacer between positive and negative plates
- Minimum electrolytic resistance (good conductivity in electrolyte)
- Protection against plate-to-plate shorts
- Resistance to chemical degradation by electrolyte or active materials
- Dimensional stability over the operating temperature range
- Effectiveness in preventing migration of particles and colloidal or soluble substances between plates of opposite polarity
- Cushioning of plates against mechanical shock
- Retention of sufficient electrolyte to perform the battery reactions under operational acceleration fields
- Sufficient physical strength to provide easy handling
- Permeability to gasses

In general, only highly porous, so-called "absorber-type" separators (as opposed to the barrier type used in silver-electrode cells) are used in sealed cells. These absorbers are usually nonwoven, felt-like products that permit maximum transfer of oxygen between the positive and negative plates to facilitate oxygen recombination and to control overcharge pressure. Figure 3 shows the open structure of this type of separator.

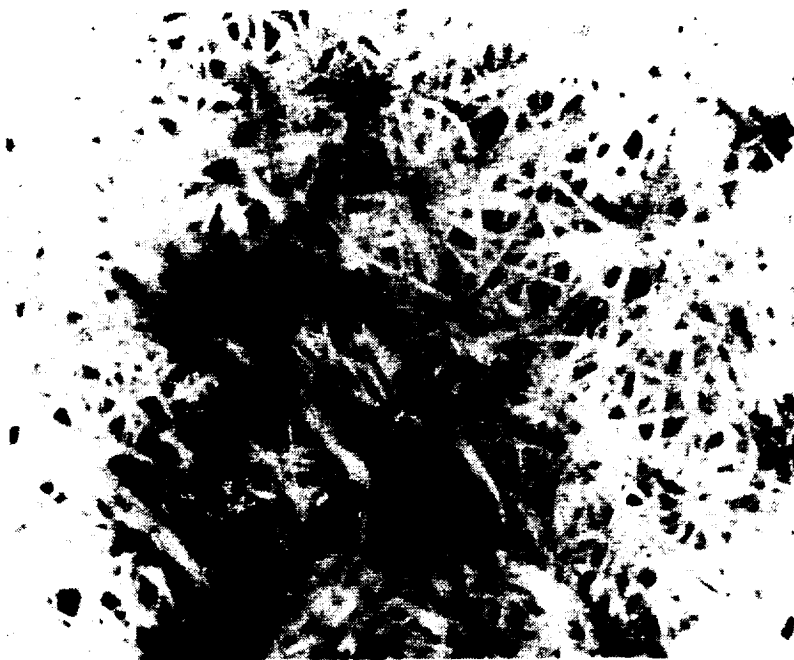
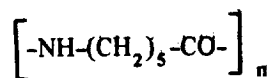


Figure 3. Nylon (Pellon 2505) separator as seen under the optical microscope (50X).

Pellon Type 2505 Separator—Essentially all spacecraft cells made for use in the United States during the past 8 years have been made with a single separator product, Pellon Type 2505* (formerly 2505 ML, for "maximum loft"). Table 4 shows some characteristics of this material, taken from the manufacturer's literature and from Reference 29. Pellon Type 2505 separator fiber is made from nylon-6, which is a polymer of 6-aminocaproic acid, $H_2N-(CH_2)_5-COOH$. Known as a polyamide, this polymer is of the formula,



where n is approximately 200. Table 5 shows typical properties of nylon-6 as used in fibers.

*Product designation of the Pellon Corporation, Lowell, Massachusetts.

ORIGINAL PAGE IS
OF POOR QUALITY

Table 4
Properties of Separator Materials

Designation	Filament Material	Weight Per Unit Area (g/m ²)	Thickness, (Cady gage)		Breaking Strength		Electrolyte Absorption (wt-%)	Air Permeability (CFM ft ² at 0.5 in. H ₂ O)
			(mm)	(mils)	MD ¹ (kg)	AMD ² (kg)		
Pellon 2505	Nylon	60 ± 8	0.38 ± 0.07	15 ± 3	2.3	3.2	800 (min)	200 (min)
Pellon 2505 K4 ³	Nylon	60 ± 8	0.20 ± 0.05	8 ± 2	2.3	3.2	200 (min)	(4)
Pellon 2140	Polypropylene	65 ± 8	0.20 ± 0.05	8 ± 2	2.7	5.4	400 (min)	(4)
GAF WEX 1242	Polypropylene	60 ± 8	0.25 ± 0.05	10 ± 2	(4)	(4)	250 (min)	75 (min)

¹ Parallel to the machine direction ² Across the machine direction ³ Hot calendared ⁴ No data available

Table 5
Properties of Plastic Fibers Used in Separators¹

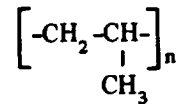
Polymer	Density (g/cm ³)	Melting Point (°C)	Glass Transition Point (°C)	Tensile Strength (psi)
Nylon-6	1.14	228	50 to 70	(75 to 90) × 10 ³
Polypropylene	0.91	180	-10 to +25	(2)

¹ From Reference 30, pp. 400 and 418 ² Data not available

The amide groups (-CO-NH-), which link the hydrocarbon groups of the polymer together, react slowly with the hydroxide ions (OH-) in the electrolyte so that the wettability of the filament surfaces increases for a time after the cell is first filled. This same reaction can eventually lead to decomposition of the polymer and, hence, to degradation of the properties of the separator (Reference 30). (See Chapter 4.)

Other Separator Materials—The only other material for absorber separators used in a significant number of sealed cells is polypropylene. This material has been used by the Canadian Defence Research Establishment in a number of Canada-sponsored satellite programs and by the United States when high temperatures are unavoidable.

Polypropylene is a hydrocarbon of the formula,



Because of its structure and the fact that it contains no nitrogen or oxygen as does nylon-6, polypropylene is chemically quite different from nylon-6; it is less wettable and more resistant to the action of the electrolyte and oxygen in the cell. Consequently, the filament surfaces are less wetted by electrolyte, and the separator offers more chemical resistance to the cell environment than does nylon.

Many types of polypropylene absorber separators from different sources have been tested (References 31 through 35). Two products for which the most data are available are listed with their properties in table 4. The properties of the polypropylene polymer material are shown in table 5.

Manufacturers have offered a few specialized nonwoven products that contain both nylon and polypropylene fibers. Also, fibers made of Teflon and other unusual materials and variations having different fiber diameters (deniers) have been available in limited quantities for testing. Wettability and electrolyte retention of these materials are different from those of the more standardized products. However, no long-term comparative test data appear to be available to indicate their relative merits.

Structure and Pretreatment—Nonwoven separators are made from what is known as “staple fiber,” which is highly contorted as spun, as opposed to the straight-type fiber used for weaving. To produce a coherent product that retains a certain thickness and shape, the fibers are compressed and bonded at contact points. Nylon filaments are usually bonded chemically, whereas polypropylene filaments are bonded with heat. Bonding methods vary widely from one material to another, and the bonding materials and processes are generally proprietary.

Because nonwoven materials are highly porous and compressible, they can be made thinner and denser by using heat and compression either during or after the bonding operation. This process is known as “calendaring.” For example, Pellon Type 2505-K4 is a calendared version of Type 2505 and, hence, has the same fiber content and weight per unit area as that of the thicker product. Although nonwoven nylon products with less and more weight per unit area than that of Pellon 2505 are available (e.g., Pellon 2506 and Pellon FT 2117), they have been little used for spacecraft applications.

Nonwoven polypropylene products have been made inherently more wettable by radiation grafting of hydrophilic side-chains onto the polymer or by incorporating a surfactant in the fiber during manufacture (Reference 35). The long-term effectiveness of these materials has yet to be demonstrated.

Form of Separators—In completed cells, separators are deployed in one of several general forms: (1) the so-called “accordion fold” configuration, (2) “U-folds,” and (3) “bags.” In the accordion-fold style, a continuous length of separator is used to interleave between all plate surfaces, with a sharp fold between each layer. In the U-fold style, a separate piece of separator is folded around each plate with the sides open. In the bag form, separate pieces of separator product are cut for each positive plate, folded over, and heat-sealed along two edges to form a flat bag that is open at the top. Because cell manufacturers tend to make separators for all of their cells in the same form, only one form is normally available from any one manufacturer. No comparative data appear to be available on which to base a choice between these forms.

2.3.2.3 Case and Cover Design

The “lower” part of the cell enclosure surrounding the plates is referred to as the case (or sometimes the “can”), whereas the “top” part, usually bearing the terminals, is referred to as the cover or cover assembly (figure 4).

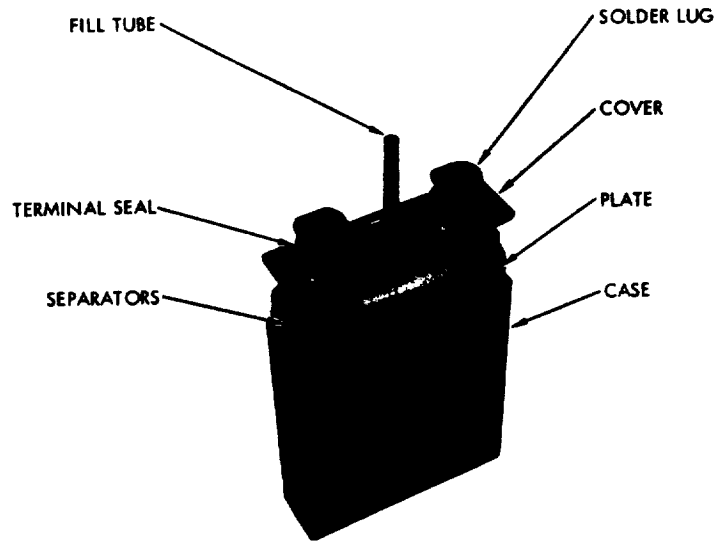


Figure 4. Hermetically sealed nickel-cadmium cell mechanical assembly.

Wall Materials—The walls of essentially all commercially available spacecraft nickel-cadmium cells made to date in the United States have been made of 300-series stainless steels, usually Type 304 or 304L. A new lightweight case made from a carbon fiber and epoxy resin composition is currently under development (Reference 36). Ordinary plastic materials do not conduct heat well enough to be used for spacecraft applications.

Some properties of metallic wall materials used are shown in table 6. Because it has been suggested for special applications, properties of nickel 200 are included for comparison.

Type 304L, whose carbon content is lower than that of 304, is required for the cover to prevent "sensitization" and loss of corrosion-resistance, which can occur in the higher-carbon 304 stainless steel because of the oven-brazing operations used for fabrication. Type 304L is also advisable for the case to ensure that the wall material does not become "sensitized" when the cover is welded to the case.

Wall thickness of the case is typically between 0.4 and 0.8 mm (0.016 to 0.032 in.). The current trend is toward thinner case walls to reduce weight, including thicknesses below 0.4 mm. Relatively few data are available on

Table 6
Properties of Cell Case Materials

Alloy	Carbon Content (Max. Wt-%)	Density (g/cm ³)	Electrical Resistivity (ohm-cm)	Thermal Conductivity (watts cm ⁻¹ C ⁻¹)
Stainless Steel Type 304	0.08	7.8	90×10^{-6}	0.15
Stainless Steel Type 304L	0.03	7.8	90×10^{-6}	0.15
Nickel 200	—	8.7	8×10^{-6}	0.7

the deformation of case walls because of the internal pressure of thinner-wall cases, which must be greater than that of heavier case walls. The lower practical limit of case thickness for 304 stainless-steel material has not yet been determined. The ability to make a reliable case-to-cover weld may establish the lower limit; however, good welds have been made in production with wall thicknesses as low as 0.3 mm (0.012 in.).

For spacecraft applications, welded (so-called "fabricated") cases are generally preferred to drawn cases. Drawn cases have a cross section that tapers down from top to bottom, resulting in uneven compression of the separators. Also, the wall thickness cannot be held to close tolerances during drawing, which results in variable outside or inside dimensions and variable cell weight.

Cover-Assembly Design—As shown in figure 4, the cover assembly consists of a cover plate, terminal seals, and normally a "fill tube" used during cell manufacturing to add electrolyte and to measure internal pressure by means of an external gage. The assembly is usually prefabricated before it is attached to the plates. Some cell manufacturers subcontract this assembly; others manufacture the assembly in-house from purchased piece parts.

In the past, the fill tube has been attached to the cover plate mainly by welding. As total testing and observation time has increased, instances of leakage at the base of the pinch tube have accumulated. Although some of these cases have involved continuous use of gage fittings on the fill tubes and, hence, higher-than-normal stresses in the joint, this experience suggests that the fill-tube-to-cover weld joint may be a potential weak point.

Several users have evaluated brazing this joint, and brazing appears to provide a stronger, more reliable joint than welding.

As the cover dimensions are increased (as is usually the case for cells of 50-Ah capacity and above), more attention must be paid to flexing of the cover plate. Such flexing can place great stress concentrations on the terminal seals and, hence, lead to a higher probability of seal failure. Heavier gage material can be used in larger covers, or reinforcement can be added only where needed when weight is critical.

Terminal Seal Design—The main power terminals (so designated to distinguish them from auxiliary terminals that may be present in cells containing auxiliary electrodes) consist basically of the terminal conductors and, for insulated terminals, the insulator seals. This section discusses these two parts separately.

The main terminal conductor (sometimes called a post or stud) may be made of either nickel or stainless steel. Nickel conductors are appreciably lighter for a given current-carrying capacity because nickel has a higher electrical conductivity than stainless steel. However, unless all the other metal parts (flanges, etc.) that are brazed to the post have compatible brazing characteristics, it may not be practical to use nickel for the post material. Thus, the entire terminal must be designed as a whole for manufacturability, optimum conductivity-to-weight ratio, and reliability.

Because the caps, flanges, and collars used in some insulated terminal designs are relatively thin, they must be protected from corrosion by the atmosphere while on the Earth's surface. This is especially true when these parts are made of Kovar or of nickel-iron alloys with no chromium content. Protective coatings may be required when these materials are exposed to other than a dehumidified environment.

The "combs" (the lower ends of the posts that mate with the plate tabs) are part of the terminal conductors. The choice of materials for the combs is more restricted than for the posts. Mechanical strength and weldability with the plate-tab material are important requirements. Stainless steel is generally used because it has the best combination of desired properties.

Copper or nickel solder lugs on the tops of the terminal posts are now available from all cell manufacturers, with nickel being the preferred material. These lugs are usually brazed onto the terminal posts at the same

time that other brazes in the terminal assembly are made. Such lugs (figure 4) usually have multiple holes for attaching cell interconnecting leads. The lugs may be solder-coated by the cell manufacturer, if desired.

Insulator seals are used to electrically insulate either one or both of the power terminal conductors from the metal cell case and, at the same time, to form part of the overall hermetically sealed cell enclosure. Two basically different types of terminal-seal structures may be distinguished on the basis of the bond type—the ceramic-to-metal braze type and the compressed-polymer type. Although the latter types are promising, they are not now commercially available on nickel-cadmium cells and, to the knowledge of the authors, have not been flown. Reference 37 reviewed the background and state of the art of these seals as of 1967; a more recent survey does not appear to be available.

Figure 5 shows cross-section diagrams of several terminal designs with different ceramic-to-metal insulator seals. Most cells flown before approximately 1972 had insulator seals of one of the four types shown in figure 5. Since 1972, one manufacturer has continued to supply cells with Type A terminals, whereas another manufacturer has changed from Type B to Type D. The Type C terminal containing glass-to-metal seals is used on small cylindrical cells made by only one manufacturer and is not considered to be suitable for long-life applications.

Table 7 lists the significant design characteristics of Types A, C, and D. The butt-type geometry is inherently stronger and permits a greater ceramic-to-metal bond area than the compression geometry (Reference 32). However, when properly made, both types are satisfactory for space applications. The nickel-braze material is more inert to the cell environment than unprotected copper-silver alloy (References 32 and 38), but terminals made with the latter are normally supplied with a nickel plating over the copper-silver surfaces internal to the cell. When this plating is sufficiently adherent and pore-free, no significant reaction with the underlying braze material occurs.

The cavity between the post and the cup of the Type A terminal can be a problem because it may trap impurities during manufacturing or collect moisture, solder flux, etc., during ground testing. These problems can be dealt with by proper attention to quality control and by filling the void with a suitable polymeric sealant before use.

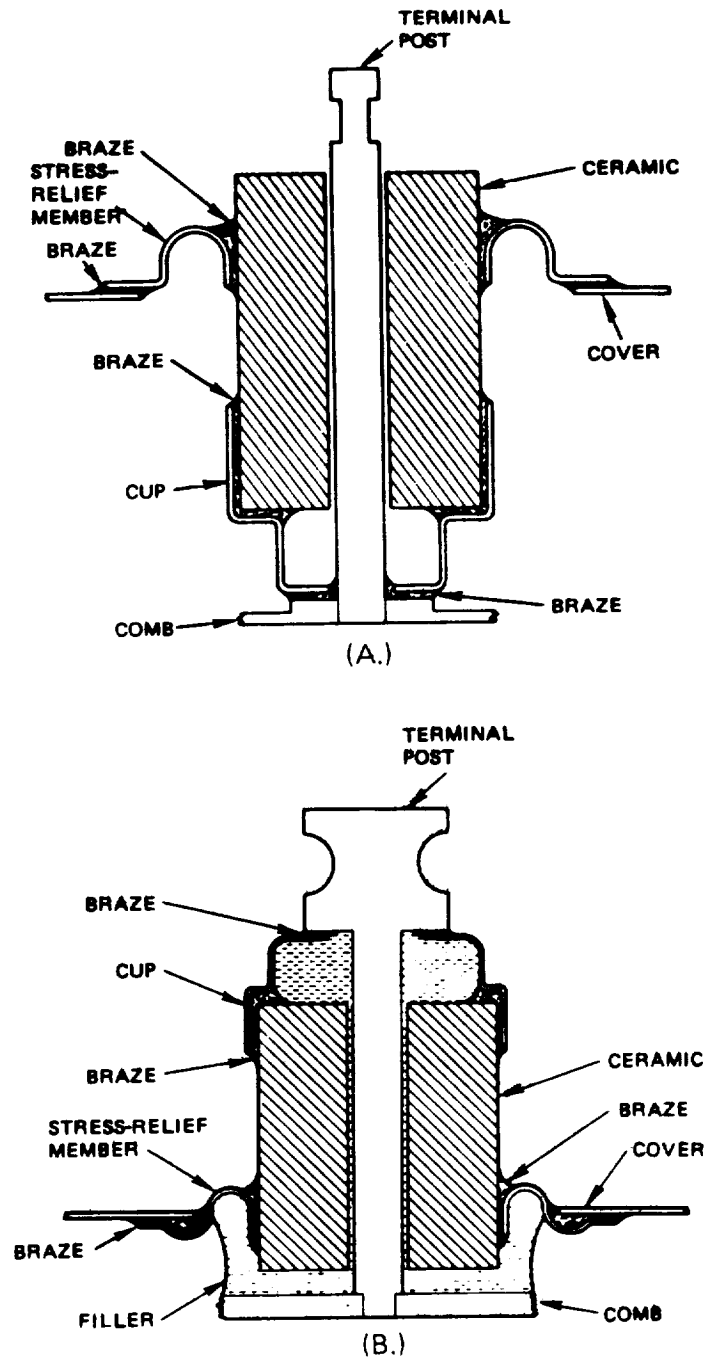


Figure 5. Cross-section diagrams of widely used terminal seals.

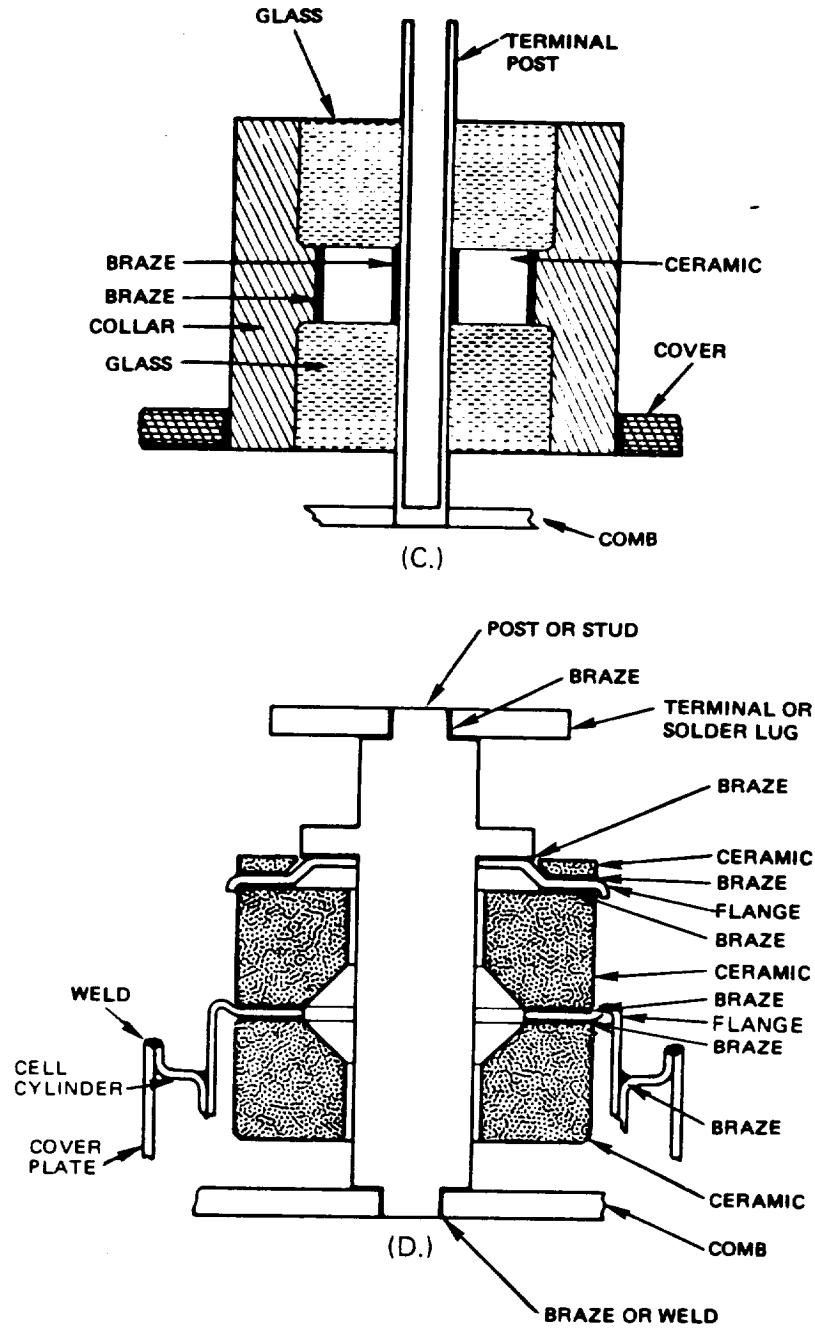


Figure 5. Cross-section diagrams of widely used terminal seals (continued).

Table 7
 Characteristics of Terminal-Seal Designs in Current Use

Characteristic	Type Designation (from figure 5)		
	A	B	D
Interface geometry	Compression	Compression	Butt-type
Metal piece-part material	Nickel-iron alloy and stainless steel	Nickel	Nickel
Ceramic-to-metal braze material	Copper-silver eutectic	Copper-silver-palladium	Nickel
Metallization	Titanium hydride	Titanium hydride	Titanium

2.3.2.4 Electrolyte Composition

Potassium hydroxide (KOH) solution is used exclusively as the electrolyte in spacecraft cells. The concentration of KOH added to different cell designs ranges from 28 to 34 percent by weight. Some suppliers offer a choice of concentrations; others offer only one, with special development testing required for any other concentration. Reference 5 contains a review of KOH electrolyte properties and effects.

For long-life applications, the trend is toward lower electrolyte concentrations (below 32 wt-%) because they appear to result in less swelling of the positive plates during cycling. However, good comparative data for the effects of different concentrations are lacking at this time.

Lithium hydroxide (LiOH) may be added to the electrolyte for special applications, but the value of this additive is not clear-cut. Considerable evidence exists for increased charge efficiency at higher temperatures (over 35°C) relative to that in the absence of lithium (References 20 and 39 through 41). There appears to be no beneficial effect on charge efficiency at temperatures below 20°C. On the other hand, Yamashita (Reference 42) reports that lithium causes the sintered-nickel substrate to become brittle and increase in resistivity. Thus, unless the operating temperature cannot be kept down and charge rate is low, the use of lithium in the electrolyte

cannot be recommended for spacecraft applications, particularly not for long-term missions. (See the section on "Oxygen Evolution and Pressure on Overcharge" later in this document.)

Although carbonate is almost always present to some extent in potassium hydroxide solution, cell manufacturers can limit this impurity to 3 wt-% (as K_2CO_3) in the solution as it is first added to the cell. Concentrations up to 3 wt-% in new electrolyte may be insignificant because when electrolyte enters the cell, the concentration of carbonate usually increases rapidly with cycling to a level over 10 wt-% as carbonate is extracted from the plates into solution. (This occurs even with plates that have been "decarbonated"* because this operation does not normally remove all the carbonate that is initially present.) Section 3 describes the effect of carbonate in the electrolyte on cell performance.

2.3.3 The Cell as an Entity

This section describes the design and structure of the hermetically sealed nickel-cadmium cell as a completed entity ready to operate. The topics covered include geometric considerations, capacity ratios, electrolyte quantity, and precharge. The range of these variables available in commercial spacecraft cells is shown in relation to cell capacity, and practical limits are indicated. The implications of these variables for cell size and mass are discussed qualitatively. A more quantitative assessment of their impact on electrical performance and on specific energy is contained in Section 3.

2.3.3.1 Plate Area and Number of Plates

By the proper choice of plaque thickness, plaque porosity, and quantity of active material impregnated per unit pore volume, the total area of positive plates necessary for delivering a specified initial capacity may be varied over a considerable range. Positive plate area per unit of measured capacity is also a function of the impregnation and formation processes and the electrolyte level, among other variables. Chemically impregnated positive plates produced commercially, which are loaded to approximately 2 g/cm^3 of pore volume, initially exhibit ratios ranging from 3 to 4 Ah/dm^2 [†] and a utilization of 80 to 90 percent. Electrochemically impregnated plates exhibit about 25 percent higher initial utilizations and therefore require correspondingly less plate area per unit capacity delivered.

*Subjected to an operation designed to remove carbonate from the plates before cell construction.

[†] Plate areas by convention are expressed in square decimeters (dm^2) and are areas of plate material (i.e., only one of the two faces is counted). The total gross surface area (counting both faces) of 1 dm^2 of plate would be 2 dm^2 .

As plate area per unit capacity increases, the ratio of "inert" weight (i.e., grid and nickel sinter) to active-material weight increases, and, hence, the initial cell specific energy decreases. In addition, for a given area per plate, the number of plates in parallel must also increase, thereby increasing the thickness of the cell. Alternatively, the cell-case width and/or height may be increased to accommodate more plate area. This alternative approach is limited primarily by the problems of handling large plates during cell assembly, as well as by the implied increase in size and weight of the external battery-support structure.

Greater plate area per unit capacity is required for high-rate operation (e.g., for charge and discharge rates $> 2C$) to minimize polarization losses. However, for geosynchronous orbit applications, such high rates are not necessary, and thicker plates may be used. Lower positive-plate area results in higher polarization during charge and discharge and, hence, higher voltage on charge and lower voltage on discharge.

Table 8 shows the number of positive plates and the total uncoined positive-plate areas in catalog-item sealed aerospace cells from the two largest domestic suppliers of spacecraft cells. As table 8 shows, the SAFT plates are thicker and have a greater weight of active material per area. The fact that plate area is not strictly proportional to rated capacity results from variations in the method of rating and in utilization as a function of cell size.

Table 8
Number and Area of Positive Plates in Spacecraft Cells¹

Rated Capacity (Ah)	General Electric		SAFT-America	
	Number of Plates	Area (dm ²) ²	Number of Plates	Area (dm ²) ²
6	10	2.52	9	2.3
12	11	5.01	10	4.37
15	11	6.75	10	5.50
20/24 ³	11	9.54	9	7.29
50	16	21.33	(4)	(4)
100	(4)	(4)	15 ⁴	39.18 ⁴

¹ Reference design cells; see Section 2.5.

² Uncoined area only.

³ The same cell is rated differently by different organizations.

⁴ Design not standardized.

The usual cell contains one more negative plate than positive plate. Cells have been made with more or less negative plates than is normal for achieving variations in the ratio of negative-to-positive capacity. (See Section 2.3.3.5.)

2.3.3.2 Plate-Separation Distance

The distance between adjacent plate surfaces in the cell affects other design parameters and properties:

- The separator pore volume, the amount of electrolyte the separator can absorb, and the ability of the separator to compete with the plates for electrolyte increases as the separation increases.
- The probability of a plate-to-plate short caused by plate buckling or bent corners or edges decreases as the as-built separation distance increases.
- The percentage reduction in thickness of the separators (caused by thickening of positive plates) is reduced by greater initial separation.
- The ease with which the plate stack may be inserted into the case during cell assembly is greater with less initial compression of the separators (assuming a particular separator material thickness and weight per unit area).
- The internal resistance of the cell is slightly greater at greater separation distance for the same volume of electrolyte added.
- Cell thickness and, to a small degree, cell weight must increase as plate separation increases (assuming that the plate thickness and the number of plates remain constant).

Therefore, many opportunities exist for tradeoffs involving plate-separation distance.

The separation distance in commercially available cells of current design using Pellon Type 2505 separator material averages about 0.018 cm (0.007 in.), which is about 50 percent of the thickness of the separator as

measured by a Cady gage.* At this compressed thickness, the dry porosity of the separator is calculated to be about 75 percent. Therefore, with approximately 0.7 cm^3 of electrolyte per dm^2 of separator (typical of a newly made cell in the discharged state), the remaining porosity (with electrolyte in place) of the separator is about 40 percent. This porosity decreases during overcharge when some electrolyte is forced out of the positive plates. These figures show how separation, separator material, and electrolyte volume interact to affect the oxygen permeability and ultimately the overcharge pressure behavior of the cell.

Some minimum amount of compression of the porous separators is desirable for minimizing the interelectrode resistance, maximizing the rate of passage of oxygen during overcharge, and maximizing the ease of transfer of electrolyte between the plates and separators during cycling.† Therefore, because an increase in separation distance results in decreased compression, greater than normal separation may require a different separator material (thicker in the uncompressed state and possessing more weight per unit area) or the use of two layers of lighter material. Two layers of separator appear to work as well as one (under equal compression).

2.3.3.3 *Electrolyte Quantity*

The quantity of electrolyte that may be used in a sealed nickel-cadmium cell of a given size may vary considerably. The optimum amount depends on the life requirement, operating conditions, and maximum allowable pressure. Quantities as low as 2 cm^3 per Ah of rated cell capacity permit the cell to operate for some period of time before excessive redistribution and drying of the separator occur. On the other hand, amounts up to and beyond 4 cm^3 per Ah are feasible if cell temperature and overcharge are rigidly controlled. Generally, the higher the electrolyte fill level, the longer the useful cycle life. Optimum quantities for different applications have not yet been established.

Different methods are used by different cell manufacturers to arrive at their design point. Some add electrolyte to a given fraction (e.g., 85 percent) of the residual void volume of the dry plate stack, including the separators; others add electrolyte based on the weight of the plates (e.g., 30 percent). The level found in most spacecraft cells is in the range from 4 to 5.2 g ($3 \text{ to } 4 \text{ cm}^3$) per Ah of rated capacity.

*Used for measuring thickness under light compression.

†G. G. Rampel, General Electric Battery Division, private communication.

The maximum amount of electrolyte that can be tolerated without high overcharge pressure is a function of a number of component design variables, such as separator-fiber material (nylon or polypropylene), separation distance, residual porosity of the plates, and whether or not the plates have been Teflon-coated. Quantitative data relating proper electrolyte volumes to these variables are not available, and, hence, the amount for any particular combination of design features is determined by test. Because of this, the quantity that may be used is strongly dependent on the allowable overcharge pressure.

The amount of electrolyte in a cell when it is finally closed ("pinched off") is not necessarily the amount initially added to the dry cell. Some manufacturers remove or add some electrolyte during electrical processing. Thus, to properly identify the electrolyte content, the point in the manufacturing sequence must also be specified.

Clearly, the cell weight is a direct function of electrolyte weight. Thus, the emphasis placed on reducing cell weight has a tendency to cause minimization of electrolyte quantity. Because the length of useful cell service life can depend on the amount of electrolyte present, the cell design process must resolve this conflict.

2.3.3.4 *Internal Void Volume*

The internal void volume is the gas space within the cell enclosure that is not occupied by a solid or a liquid. When the cell is overcharged (or over-discharged) at a given current, any oxygen or hydrogen produced in excess of that which can be recombined builds up a pressure equal to

$$P = \frac{n R T}{V_v} \quad (7)$$

where n is the number of moles of gas present in the cell, R is the universal gas constant, T is the absolute temperature, and V_v is the void volume. Thus, for a given set of overcharge conditions, the end-of-charge pressure will be inversely proportional to V_v .

For a fixed cell-case volume and plate volume, the void volume decreases as electrolyte volume increases. Thus, without independent adjustment of void volume along with electrolyte volume, the end-of-charge pressure can be very sensitive to electrolyte volume.

As the cell size increases, the void volume per unit of rated capacity tends to decrease as shown in table 9. This trend exists because of the desire to minimize cell dimensions and weight as the cell size increases. Therefore, unless higher pressures are allowed, the supplier may be forced to make other changes in the cell design or manufacturing process to lower the pressure. Some of these changes may not be compatible with maximum cell life. Thus, the void volume should be considered in any review of the cell design.

Table 9
Internal Cell Volumes and Void Volumes (cm³)

Rated Capacity (Ah)	General Electric		SAFT-America	
	Case Volume	Void Volume	Case Volume	Void Volume
6	80	20 to 25	90	25 to 30
12	170	35 to 45	195	40 to 45
20/24 ¹	267	60 to 70	291	75 to 85
50	540	110 to 125	(2)	(2)
100	(2)	(2)	1153	150 (est.)

¹This size cell is rated differently by different users.

²Data not available.

2.3.3.5 Negative-to-Positive Capacity Ratio

The literature refers to several kinds of "negative-to-positive ratios." The theoretical negative-to-positive capacity ratio (sometimes referred to as the "material ratio") in a cell is a function only of the negative- and positive-plate active areas and the respective loadings per unit area. Hence, cells made with the same plate materials and with the same number of positive and negative plates will contain the same *theoretical* negative-to-positive capacity ratio. Sealed spacecraft cells are currently made with theoretical negative-to-positive ratios ranging from 1.5 to over 2.

The electrochemically measured negative-to-positive ratio—the one normally referred to in cell specifications—is a function of the theoretical ratio and other variables, including the utilization of negative and positive

active materials, the test temperature, and the charge and discharge rates. In turn, utilization of the negative materials is often sensitive to the number of cycles experienced since reconditioning.

A wide range of negative-to-positive ratios for design have been reported and have been summarized by Gross (Reference 43). It appears that some of these values are theoretical capacity ratios and others are measured ratios. The measurement has not been standardized, and the results can lead to confusion. In a new cell, the measured ratio is always less than the theoretical ratio because the utilization of the negative is less than that of the positive.

In general, optimum negative-to-positive ratios for different applications have not yet been established. This ratio must be coordinated with the selected values of charged and discharged excess negative required. (See following paragraphs.) A conservative minimum value, which has given acceptable performance in many cells in the temperature range from 0° to 25°C, is 1.5 to 1 as measured electrochemically. Gross (Reference 43) discusses guidelines for departure from this ratio.

2.3.3.6 Precharge and Uncharged Excess Negative

It was noted previously that, in positive-limited sealed cells, the negative capacity is designed to be considerably greater than the positive capacity. Thus, by suitable adjustment, the positive electrode can be made to operate at states of charge that are different relative to that of the negative electrode.

The diagrams in figure 6 illustrate three different situations. When the cell has been sealed and remains sealed so that no oxygen or hydrogen can escape and when the internal pressure of oxygen and/or hydrogen remains low, the relative position of the capacity blocks in figure 6 remains fixed (in the vertical direction) by the chemistry of the system. On the other hand, if at any time the enclosure is vented so that oxygen gas escapes during overcharge or hydrogen escapes during overdischarge, the relative state of charge will shift. This change may be shown by a relative vertical movement of the positive capacity block in figure 6. If the cell is again sealed after such venting, the new relative state of charge will then be fixed.

Venting oxygen during overcharge increases the relative state of charge of the negative electrode because no change in the state of charge of the

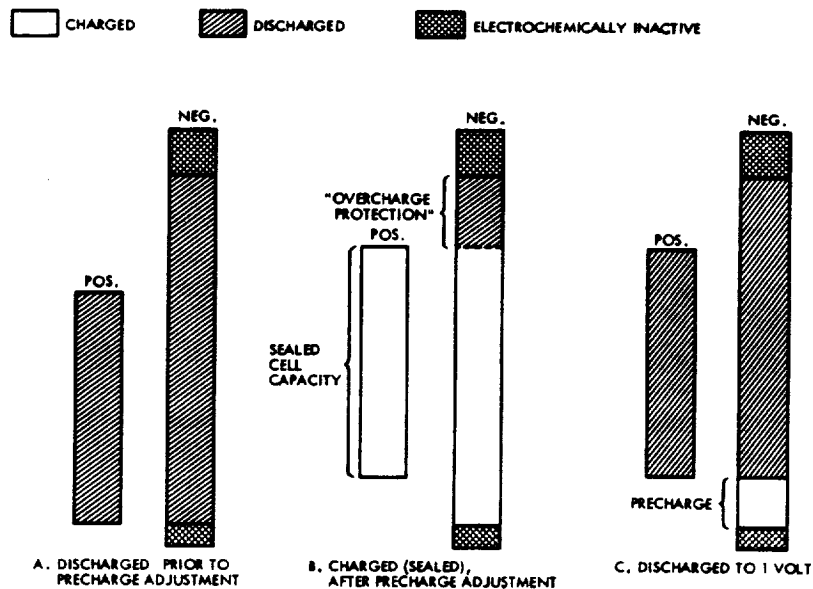
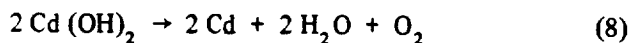


Figure 6. Relative state-of-charge diagrams.

positive electrode takes place (only oxygen evolution according to reaction 4) while the negative electrode is being "charged" according to



Most cell manufacturers install the plates with both positive and negative materials nearly discharged as in figure 6A. Soon after adding electrolyte, the cells are charged, overcharged, and oxygen-vented to increase the relative state of charge of the negative electrode. The ampere-hours of charged-negative capacity change produced by these means is the "precharge." The relative state of charge in a charged cell after venting is then represented qualitatively by figure 6B.

The term "precharge" is sometimes used to refer to the total charged-negative capacity in the sealed cell when the positive electrode is completely discharged (figure 6C). This use of the term can lead to confusion. Because the true state of charge of the negative electrode at the beginning of the adjustment previously described is uncertain, the total charged-negative capacity (measurable by chemical analysis) after the adjustment is usually not the same as the change in charge level produced by the precharge operation. Also, only a part of the charged-negative material may be

electrochemically active (so that it may be discharged at a normal potential). Thus, to avoid confusion, different terms should be used to distinguish between: (a) the total amount of charged-negative material after adjusting precharge, and (b) the amount that is measurable by electrochemical means. The modifying terms "total" and "active" are used in this manual to indicate concepts (a) and (b), respectively.

Some charged excess negative capacity helps to stabilize initial capacity and minimizes capacity-fading during cycling (References 32, 33, and 44). Also, in one report (Reference 45), overcharge pressure decreased as the amount of electrochemically measurable charged excess increased (SAFT cells). However, just how much charged excess is necessary is uncertain, as is the question of how much of the excess must be active. The answers to these questions appear to differ with different applications. A thorough review of this area has recently been published (Reference 43), and some of the results are summarized in Section 3.3.1.2 of this manual.

The amount of negative capacity that remains uncharged when the positive electrode reaches full overcharge (sealed-cell condition) is the uncharged excess negative. That portion of this excess that is electrochemically active is sometimes called the "overcharge protection" because it prevents the evolution of hydrogen gas during overcharge (figure 6B). Because the sum of the charged excess negative capacity, the operating cell capacity, and the uncharged excess negative capacity is roughly a constant equal to the total usable negative capacity under a given set of operating conditions, increased precharge means decreased overcharge protection and vice versa. However, for long-term missions, it is becoming clear that adequate overcharge protection is more important than excess charged negative (References 16, 17, and 46). (See Section 3.3.1.2.) As a minimum, the active uncharged excess should amount to 20 percent of total negative capacity in a new cell.

2.3.3.7 Number of Insulated Terminals

Cells may be designed with either the positive terminal insulated and the negative terminal common with the case or both terminals insulated from the case. Each configuration has relative merits.

The single-insulated design has only one insulator-seal assembly (rather than two) to provide a potential source of leakage and is slightly less expensive. Also, the two outermost (negative) plates need not (and often are not) be insulated from the case walls; therefore, the thermal resistance

between the outer plates and the cell wall is somewhat lower than when an insulating layer is interposed. This difference is not large, however, and usually does not impact the battery thermal design.

On the other hand, the single-insulated cell can be seriously damaged if the positive terminal is accidentally shorted to the case (as with a tool during test setup or battery assembly) because the current can rapidly burn a hole in the case wall. Furthermore, the cases of such cells must always be well-insulated from each other and from grounds to prevent high-current shorting.

The double-insulated design is generally safer to handle because a temporary external short between a terminal and the case will have no appreciable effect. Although the cases must still be insulated from one another in any series-cell arrangement to prevent current from flowing between the bases of the higher and the lower voltage cells in the string, double-insulated terminal cases are more tolerant of variations in insulation resistance (produced by variations in relative humidity while the battery is on the Earth's surface).

Although the statistical probability of cell leakage is twice as great with two insulated seals as with one, the failure rate by leakage of individual terminal seals, involving ceramic-to-metal joints as made by today's technology, is low enough that the factor of two does not significantly affect cell reliability.

2.3.3.8 Cylindrical Versus Prismatic Cell Configuration

Sealed spacecraft-quality nickel-cadmium cells are commercially available in only two proven configurations: cylindrical with a "jelly-roll" plate stack, and prismatic or rectangular with flat, parallel plates. The cylindrical cases have the advantage that, if the ends are heavy enough, no external support is needed to contain cell pressure, thus saving packaging weight. Because a good heat path must be provided, however, the saving is not as great as it might be. Also, only the smaller size cells (10 Ah or less) can be made self-supporting without excessive cell-case weight.

Cylindrical cells normally have a single insulated terminal, with the other terminal being common with the case. Because only a small number of tabs are used to make electrical contact with the plates and because of the difficulty in making strong, low-resistance contacts between the tabs and the

plates, insulated terminal, and case wall, cylindrical cells from some manufacturers are much more subject to high internal ohmic resistance and internal open-circuit failures than prismatic cells.

Nevertheless, when properly made and operated at a low utilization level (i.e., low depth of discharge and discharge rate), cylindrical cells are capable of long useful life. For example, the International Satellite for Ionosphere Studies (ISIS) spacecraft battery and certain others* using cylindrical cells at 10-percent maximum depth of discharge in synchronous orbit have operated successfully for over 10 years in orbit. The use of higher rates and higher depths of discharge produces more rapid degradation of plates in cylindrical cells than in prismatic cells. Most manufacturers do not offer hermetically sealed cylindrical cells in sizes over 6 Ah, and some do not offer this type in designs suitable for space applications.

2.3.3.9 Auxiliary Electrodes

One or more of several types of auxiliary electrodes may be incorporated within the cell. These include: (1) the oxygen-signal, control, or adsorbed-hydrogen (Adhydrode)[†] electrode; (2) the recombination or "full-cell" electrode; and (3) the reference electrode.

Oxygen-Signal Electrode—The oxygen-signal electrode is usually a porous metal surface fabricated on a nickel or noble metal screen or expanded metal substrate. Most signal electrodes have a thin film of Teflon on one side to act as an oxygen-diffusion barrier, and, hence, the response is roughly proportional to oxygen partial pressure in the low pressure range (0 to 25 psia) (References 44, 47, and 48).[‡] Currently, there are no standards for electrode area, and different cell manufacturers make electrodes that range from 10 to 70 cm².

Oxygen-signal electrodes have been physically located: (1) between the outer surface of the outermost negative plate and the adjacent wall of the cell (Reference 49);[‡] (2) in the space between the edges of the plates and the narrow sides (Reference 50) of the case;[‡] or (3) between plates within the plate stack (Reference 51)[‡] Table 10 summarizes the relative merits

*Designed by the Canadian Defence Research Establishment, Ottawa, Canada.

[†]Trademark of SAFT-America, Incorporated.

[‡]H. N. Seiger, "The Active Adhydrode: A Sensor for Monitoring End of Charge in Sealed Nickel-Cadmium Batteries." unnumbered and undated report, Gulston Industries, Inc., Metuchen, New Jersey (now SAFT-America).

Table 10
Analysis of Oxygen-Signal Locations in the Cell

Physical Location ¹	Relief	Advantages	Disadvantages
a	No	Simple to install; electrolyte supply better than for location b.	Remote from O ₂ source; too tightly compressed: wick dries out; electrode shorts to negative plate.
a	Yes	Same as above; compression can be adjusted.	Requires special negative plate; remote from O ₂ source.
b	(2)	Simple to install; not subject to shorting.	Compression too low and variable wick dries out.
c	No	Superior electrolyte supply; near source of O ₂ .	Too tightly compressed; electrolyte supply reduced as plates thicken; may short to either positive or negative plate.
c	Yes	Same as above.	Requires a special negative plate for mounting.

¹See text for definition of locations.

²Not applicable.

of each of these locations. The last line item in this table refers to a configuration in which the electrode is mounted next to a negative plate that has been thinned down to permit the oxygen electrode to fit between two plates without overcompressing the associated separator layers. Although this arrangement has been tested and found to be superior to the others, it has not been flown (Reference 51).

The oxygen-signal electrode is usually connected internally to the cell-case wall and externally to the negative terminal through a resistor. This arrangement puts the inner surface of the case wall parallel to the signal electrode. This raises the question of whether the case wall as an electrode will interfere with the proper operation of the oxygen electrode,

particularly in large cells in which the ratio of cell-wall area to signal-electrode area may be much greater than that of small cells. Recent controlled tests (Reference 51) have shown that no significant difference exists between the signal characteristics whether the signal electrode is connected to, or insulated from, the cell case in 50-Ah cells operating with signal electrodes with areas as small as 10 cm^2 .

The value of the external resistance is not critical within a certain rather wide range, usually extending over more than an order of magnitude between 10 and 200 ohms. Ford (Reference 52) has shown that, within the useful range, there is a resistance value that results in a maximum power dissipation in the load and that overall signal performance is best when using a resistor equal to or close to this maximum power value.

Details of location and method of placement of oxygen-signal electrodes within the cell and the control of the gas and electrolyte environment in the vicinity of the electrode have not received sufficient attention in the past. As a result, the reliability of the oxygen signal has generally been low for long-life applications. It has been shown that careful design can greatly improve oxygen-signal performance (Reference 51). However, the useful life of the signal electrode remains strongly dependent on proper electrolyte distribution in the cell so that separator material surrounding the electrode does not dry out (Reference 51).

Recombination Auxiliary Electrode—The recombination electrode is designed to recombine oxygen and/or hydrogen at high rates and low pressures (References 44, 47, and 48). To do this effectively, such electrodes usually contain a platinum catalyst. The electrodes are connected electrically to the negative terminal through a small resistance. This connection may be made within the cell when access to the resistance for measuring current or voltage is not needed. When the cell is equipped with two insulated power terminals, the connection may be made externally, using the metal container as part of the electrical lead from the enclosed auxiliary electrode.

Recombination electrodes are usually located in the space between the edges of the plates and the narrow sides (and bottom) of the case. To obtain the maximum electrode area, the electrode is often cut as a long, narrow strip and is run around three sides of the plate stack. This strip is surrounded by a wick made of separator material. The Apollo Telescope Mount batteries aboard the Skylab spacecraft were equipped with this type of electrode, as well as with a signal electrode (Reference 49).

Reference Electrodes—Reference electrodes are electrodes (half-cells) having a known and reproducible potential under a given set of conditions. They are often used in the laboratory, for example, to measure the charge and/or discharge voltage of a nickel hydroxide or a cadmium electrode from a nickel-cadmium cell after the opposing electrodes originally together in the cell have been separated. Cahoon has described the general use of reference electrodes (Reference 53).

The mercury-mercuric oxide electrode is most suited for use as a reference electrode in an excess of potassium hydroxide solution in the laboratory. This electrode is not suited to use in a sealed cell, however, because of possibly contaminating the cell with mercury. Instead, a piece of partially charged positive plates can be used to advantage with only a small sacrifice in the consistency of the potential. A cadmium plate should not be used as a reference electrode because originally charged cadmium becomes oxidized (discharged) by reaction with the oxygen in the cell, after which the electrode potential becomes unstable.

The presence of a reference electrode in a sealed cell can be valuable for determining the source of an anomalous cell-voltage behavior without opening the cell. Such an electrode is connected internally to the case wall, and, thus, the voltage behavior of the positive and negative electrodes may be measured separately by measuring the voltage between each power-electrode terminal and the case.* Alternatively, the case may be used as a "reference" electrode in a similar manner if no real reference electrode is present, but the potential of the case is often not sufficiently constant for useful results.

2.3.4 Computation for Optimized Cell Design

From the foregoing, it is apparent that many cell design parameters interact, and, hence, creation of an optimized design involves many tradeoffs. Because the expense of development of cells optimized for a specific application is time-consuming and expensive, the nearest existing design is usually chosen for flight programs. Thus, very few details of the design process have been published.

One exception is the design of a 55-Ah cell with a specific energy of 46 Wh/kg (20 Wh/lb) (Reference 54). This reference lists the parameters considered to influence the design and includes a computer program used to arrive at a final design. Although this program illustrates the approach, the program *per se* is limited in applicability to one cell size.

*This option is open only if both terminals are insulated from the case.

2.4 CELL MANUFACTURING

The information in this section was selected for the general interest of the battery engineer and serves as a basis for the discussion of the effects of manufacturing process variables contained in Sections 3 and 4.

It is recognized that the overall process differs somewhat between each cell manufacturer in that certain materials and/or process steps may be used by one and not by the others. This presentation attempts to identify both the common aspects and the significant differences as practiced by the three major manufacturers of hermetically sealed spacecraft cells in the United States today.

2.4.1 Plate Manufacturing

The manufacture of sealed nickel-cadmium cells may be considered to start with the manufacture of plates. Two of the three major suppliers* of spacecraft cells (i.e., General Electric and SAFT-America) use plates made by similar processes that are closely related to a process originally developed by SAFT in France. The third supplier (Eagle Picher) uses plates made by a considerably different process.

2.4.1.1 *The SAFT-Type Plate-Manufacturing Process*

Figure 7 shows the plate-manufacturing process used by General Electric Battery Products Department and by SAFT-America and referred to here as the SAFT-type process. No published studies of this process as it is implemented in production (i.e., using full-scale production equipment) could be found. However, several studies of similar processes carried out on a pilot scale have been performed (References 8, 15, 55, and 56).

In the SAFT-type process, the grid (or substrate) is made from mild steel. Nickel substrate would be preferable from a chemical standpoint, but nickel is too soft to withstand the action of the machinery involved. The grid is prepared by perforating, cleaning, and nickel-plating the steel strip. The strip is about 0.1 mm thick and is processed in strips about 20 cm wide.

*Marathon Battery Corporation (formerly Sonotone) manufactures small (less than 6 Ah), hermetically sealed cylindrical cells. However, because few of these cells are used for spacecraft applications, Marathon is not classified here as a major supplier. Marathon's plate process is similar to that used by Eagle Picher. (See Section 2.4.1.2.)

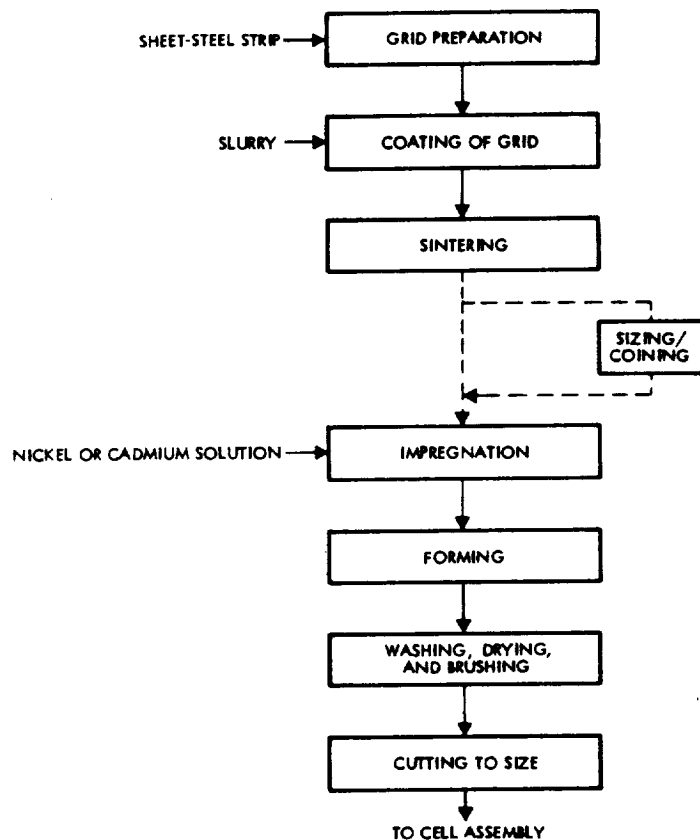


Figure 7. SAFT-type plate-manufacturing process flow.

Preparation of the "slurry" used for coating the grid involves several steps, including preparation of a medium for suspending nickel powder, addition of nickel powder, and removal of air bubbles. Proper and carefully controlled slurry viscosity is necessary for a uniform and reproducible slurry coat.

Coating of the grid, drying of the slurry, and sintering are done in rapid succession, beginning and ending with the material in rolls, as shown in figure 8. The drying removes excess water before sintering. Sintering involves heating to around 1000°C in a reducing gas environment to partially fuse the nickel particles.

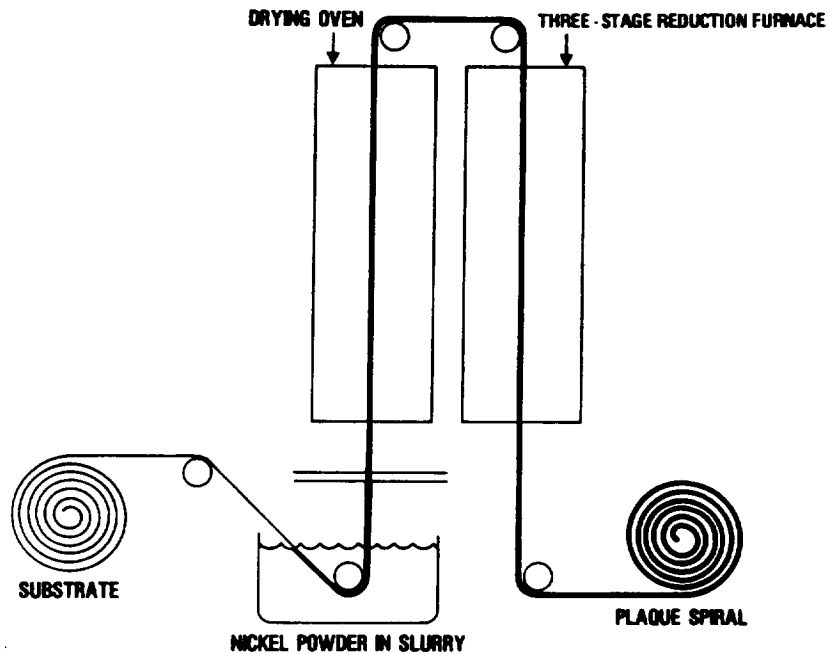


Figure 8. Coating and sintering operations in the SAFT-type plate-manufacturing process.

Sintering temperature and residence time at different temperatures are the process variables that most strongly affect the quality of the plaque (References 8 and 55). Strength increases and resistivity decreases rapidly as the sintering temperature increases in the range from 950 to 1050°C and as the residence time in this temperature range increases from 5 to 15 minutes. On the other hand, void fraction decreases slowly when going through these parameters.

Probably the most critical and the most complex operation in plate manufacturing is impregnation. Plaque is usually, but not always, coined before impregnation to strengthen the plate edges. In addition, some manufacturers lightly compress the plaque before impregnation to control plate thickness.

The type of impregnation now used by most space-cell manufacturers may be referred to as "chemical," as distinguished from the "electrochemical" impregnation process currently under development. Chemical impregnation is performed during a number of "cycles," each typically consisting of the steps of: (a) soaking, (b) drying (optional), (c) precipitation in the pores

using caustic solution, and (d) drying. This sequence is shown diagrammatically in figure 9. Because six to eight such cycles are typically required to achieve presently used loading levels, a total of 24 to 32 steps are required to complete chemical impregnation.* Because of this, the properties of the end result cannot be closely controlled. The extent of corrosion of the nickel sinter is one characteristic that needs more attention, as the degree of swelling of positive plates under cycling is dependent on the residual strength of the sinter of the impregnation. Tests have shown large variations in sinter strength in positive plates from different sources (Reference 20).

After impregnation, the plate material is "formed" by cycling several times in a caustic electrolyte.† In the original SAFT process, this operation is done more or less continuously on long strips of plate material on which conductive rollers act as electrical contacts. In one variation, the strip is cut into short lengths, and these lengths are connected electrically in parallel for cycling. Formation increases the electrochemical activity of impregnated material and reduces the level of impurities carried over from the impregnation baths.

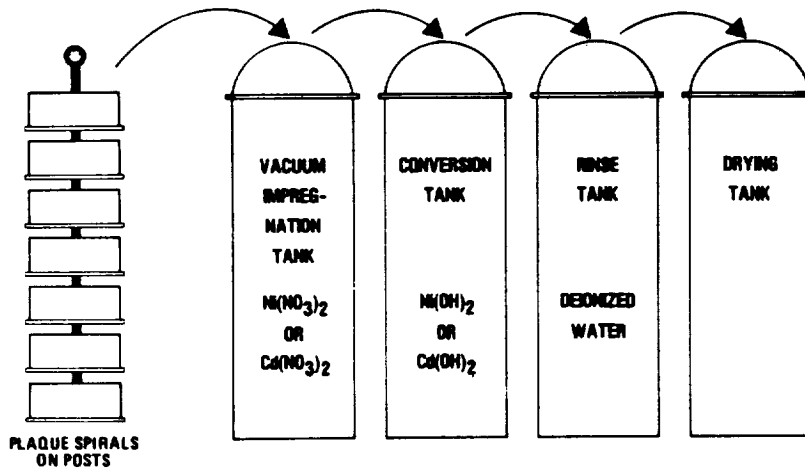


Figure 9. Impregnation of plaque in the SAFT-type manufacturing process.

*By contrast, electrochemical impregnation can be completed in one or two steps.

†This step is also referred to as electrochemical cleaning.

After formation, the plate material is washed free of caustic, dried, and brushed vigorously. This brushing removes active material from the surface and gives the plates a "polished" look. Hard brushing also hardens the plate surface and reduces surface porosity. The relative merits of such brushing for cell performance have apparently not been investigated.

Following drying and brushing, the plate strip is cut into plates of the size required for a particular cell. Cut plate is normally used for cell assembly soon after cutting. However, if the normal flow is interrupted, cut plate may be stored as such. If the dried plate strip is not cut immediately, it is stored as a roll. Such storage is not advisable for plate material to be used in spacecraft cells because the plate takes on a permanent curvature. Storage of cut plate needs special attention because the porous material can absorb carbon dioxide and other volatile contaminants from the environment.

2.4.1.2 Eagle Picher Plate-Manufacturing Processes

Figure 10 shows the plate-manufacturing process used by Eagle Picher for their chemically impregnated plates. This process has been studied under contract to NASA (Reference 57).

Nickel screen is used for the grid, which is cut into rectangles before coating and sintering. Nickel powder is applied dry to each cut piece of screen individually. During the study reported in Reference 57, a mechanical device was developed to improve the reproducibility of the powder-coating step. However, this operation is done by hand in normal production.

The coated screens are then put through the sintering furnace, which runs horizontally so that the loose powder coating remains in place until sintering is completed. The resulting plaques* are then coined and are impregnated in racks in which the plaques are flat with surfaces parallel. In the process normally done by Eagle Picher, plaques are cathodically polarized in caustic at one point during each impregnation cycle. The cycle consists of: (1) immersion in a nickel or cadmium solution, (2) polarization in a caustic solution, and (3) washing, and does not include drying between cycles.

*The term "plaque" is used in this process to refer to the individual rectangles at any point in the process before plates are cut to final dimensions.

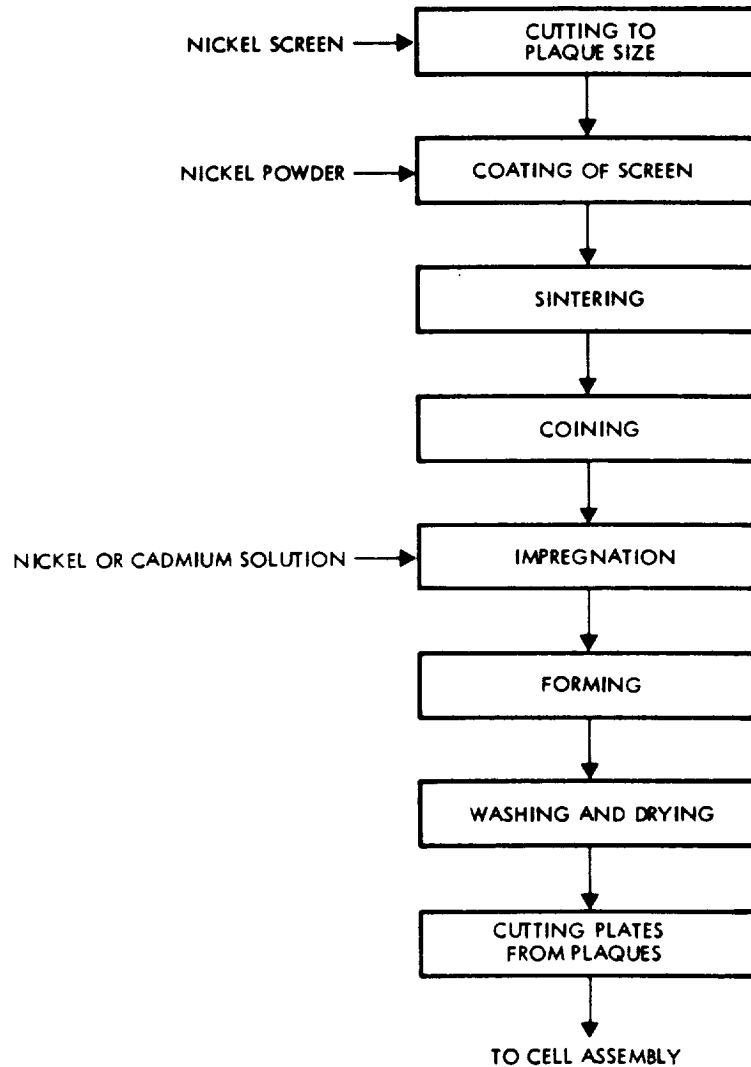


Figure 10. Plate-manufacturing process flow used by Eagle Picher.

Forming is done in batches with many plaques connected in parallel to a current bus. The plaques are then washed and dried to final cutting. During the washing, plaques are brushed by hand to remove surface deposits. Reference 57 contains additional details of this process and the effects of process variations.

2.4.1.3 Electrochemical Impregnation Process

Another plate-manufacturing process being considered for spacecraft cells involves electrochemical impregnation (EI) rather than chemical impregnation (Reference 58). This type of process has been under development for some time, but is not yet in full-scale production (References 32 through 34, 54, and 59 through 61). At least one company is now offering cells with EI plates made on pilot-scale equipment.

The electrochemical method of impregnation involves immersing the plaque in an acidic solution of either nickel (for positive plates) or cadmium (for negative plates) nitrate and passing current cathodic to the plaque (plaque negative in the external circuit). Because material is precipitated in the pores of the sinter as hydroxides practically free of nitrate, separate caustic treatment is not needed as in the SAFT and Eagle Picher processes described previously. The cathodic polarization performed differs from that in the Eagle Picher process in that the former is done in an acid solution and the latter is done in caustic. The remainder of the plate-manufacturing process for EI plates is similar to that described in Section 2.4.1.2.

2.4.2 Spacecraft Cell Assembly and Testing

When the plates have been manufactured, cell assembly can begin. Figure 11 shows the overall manufacturing flow. Figure 12 shows a more detailed sequence of major steps typical of current manufacturing of high-quality spacecraft cells. All manufacturers do not perform all these steps, and the order differs somewhat from one manufacturer to another (References 62 and 63). Some comment on certain steps is in order.

Weight-sorting involves screening the plates to retain those within a specified tolerance around the average weight. Halpert (Reference 64) has shown that such screening reduces the scatter of plate and cell capacities because plate capacity is correlated with plate weight. This correlation is better for plates made by SAFT-France than those made by General Electric Company, however, probably because of a difference in the amount of corrosion in the sinter in plates from these two sources.

Electrochemical testing involves cycling temporary cells in an excess of electrolyte. General Electric Company and SAFT-America subject all chemically impregnated plates for spacecraft cells to this testing. Eagle Picher does not electrochemically test plates after the formation cycling

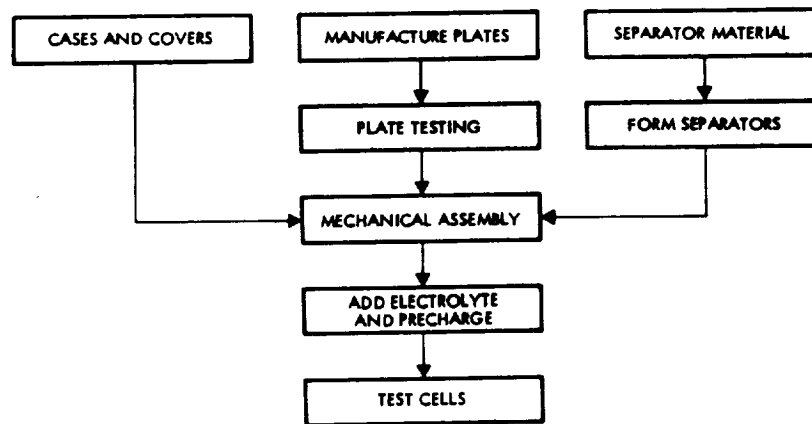


Figure 11. Overall cell-manufacturing flow diagram.

done during plate manufacturing and before cell assembly. The purposes of this test are: (1) to remove residual impurities not removed during first formation and those that may have accumulated during storage; (2) to further increase the activity of impregnated materials, if possible; (3) to serve as a type of acceptance test for the plate material; and (4) to determine if particular combinations of positive and negative plates have the proper flooded-capacity ratio when used together.

Electrochemical plate testing involves several cycles, the number differing with different manufacturers, ending with a discharge to measure flooded capacity. The first part of the discharge is done at the $C/2$ rate and ends at 1 volt (or less in some variations). The cells are then discharged to near zero volts with resistors and driven into reverse, usually at the $C/10$ rate, to complete the discharge of the negative electrode. The first part of the discharge measures the capacity of the positive electrode; the sum of the ampere-hours out on the first part and the last part of the discharge is taken as the capacity of the negative electrode. These two measurements are used to verify that the plate material has the specified negative-to-positive ratio. The significance of this ratio is discussed in Section 2.3.3.5.

A number of criteria have been used to establish the end point of the final discharge of the negative electrodes, including:

- Completion of a fixed discharge time

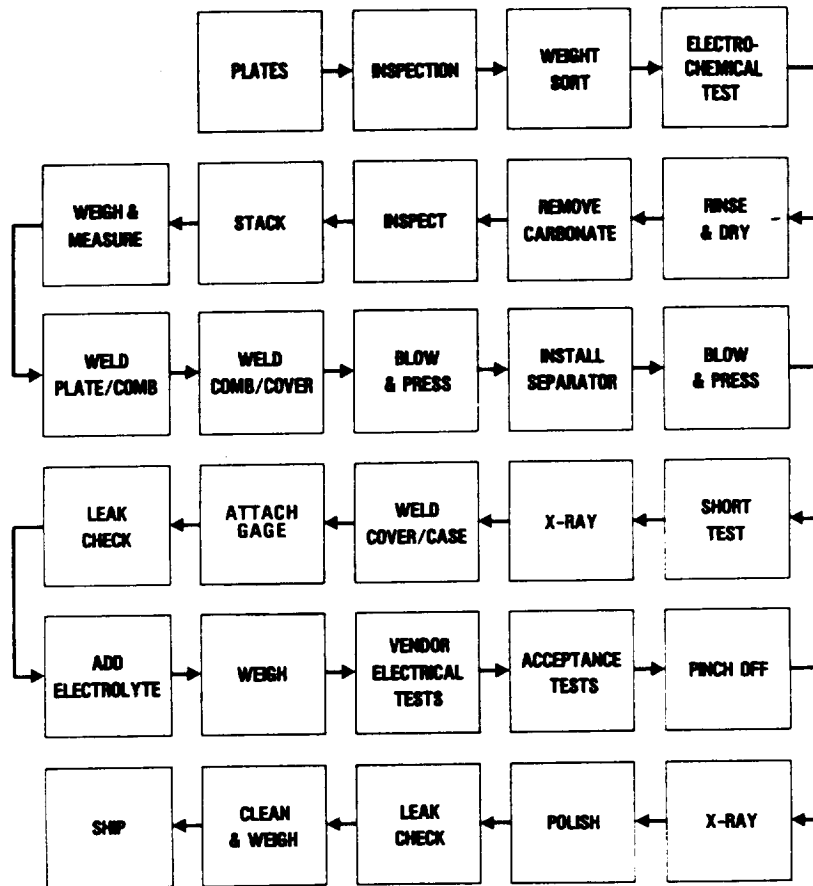


Figure 12. Spacecraft cell assembly and test sequence.

- The point when the first cell in a series string (normally 25 cells in series) reaches a specified voltage, usually either -0.25 or -0.5 volt
- Termination of each cell individually as it reaches a specified voltage, usually either -0.25 or -0.5 volt

Each of these end points results in a different amount of residual undischarged cadmium material left in the negative electrode, with the amount decreasing in the order listed. Lack of control of this process variable was

probably a major contributor to the variability of precharge and charge voltage and pressure behavior observed in these sealed cells before 1968, when an intensive investigation of the effects of such variables began (Reference 47).

The plates from cells that pass capacity requirements for both positive and negative electrodes are washed, dried, and inspected for visible damage. The cells that do not pass either the positive or the negative capacity criteria are rejected. Retesting may be allowed. Users' specifications do not appear to impose plate-lot rejection on the basis of these tests.

Plates that pass inspection are put into packs of the proper number of each polarity, and the plate tabs are welded to the combs. At this point, one manufacturer subjects the plates to a procedure intended to extract soluble carbonate. Because this step involves immersion in caustic solution, the plates must again be washed and dried. Because both the caustic treatment and the subsequent washing may result in loss of cadmium-active material, good control is required to prevent undue reduction in excess negative capacity.

After separators are added, the plate stack is put into a press and is strongly compressed to test for plate-to-plate shorts before inserting the plates into the case. This overcompression facilitates insertion because the separators recover their original thickness slowly, but may damage separator material if compression is not limited.

Radiographic inspection (X-ray) after plate insertion and before welding the cover to the case is advisable for detecting any foreign or loose material and for determining that the plates are properly situated and that the plate tabs are not unduly distorted. The forces involved in inserting the plates often cause the plates to slide or skew, and radiographic viewing is the only available method of detecting these effects. After the cover is welded to the case, radiographic inspection is not as useful but is performed on critical items to determine if the welding operation has introduced any metal particles.

Some manufacturers add only the amount of electrolyte at the start that they wish to remain in the cell at closure. Others may add more initially than they plan to leave in the final cell, and remove some later in the sequence. The latter procedure appears to be necessary in cells with Teflonated negatives when precharge is set by venting at pressures above 1 atmosphere.

Some manufacturers add electrolyte with the cell under atmospheric pressure; others use vacuum in various ways during this step. Each method results in a different degree of filling the pores of the plates with electrolyte and in a different amount of nitrogen gas (from trapped air) left in the cell at closure. No agreement on the best method is apparent from the published literature. Filling under vacuum appears likely to give the least amount of electrolyte distribution during cycling.

Some manufacturers install the plates discharged and must therefore charge the cell and vent oxygen to increase the state of charge of the negative relative to the positive electrode to set the precharge level. One manufacturer installs the negative plates charged and sets the precharge level by discharging the negative electrode, using the case wall as a counter electrode.

Oxygen is vented in two ways: (1) permitting a certain pressure to build up and releasing the pressure to atmospheric, repeating the number of times necessary (by calculation) to vent oxygen equal to the ampere-hours of precharge desired; and (2) venting the cell at slightly above atmospheric pressure and collecting the gas over water. The latter method is easier to control and permits the gas to be easily sampled for analysis to ensure that it is essentially all oxygen as expected.

After setting the precharge level, the cells are subjected to a number of tests that determine if the cells meet the manufacturer's standards of performance. The details of these tests differ with each manufacturer. They usually consist of less than 20 cycles of charge/discharge during which voltage, pressure, and capacity are observed under a set of conditions the manufacturer uses for all cells of that general type. From the manufacturer's viewpoint, conformance to the norm within certain limits indicates a good cell.

During these initial tests, the cells are equipped with removable pressure gages that facilitate examination of an important aspect of initial testing—the determination of overcharge pressure characteristics. Because of the variation in void volume and surface area from cell to cell and from lot to lot, cell manufacturers reserve the right to "rework" cells that have overcharge pressures either above or below a certain range. Such rework may take the form of removing or adding electrolyte, readjusting the amount of excess charged-negative capacity, or performance of additional cycling.

After the manufacturer's standard electrical tests, cells undergo acceptance testing to the buyer's specifications. (See Section 6.) Cells that successfully complete acceptance testing are cleaned and packaged for shipment as the final operation in the production sequence.

2.5 REFERENCE CELL DESIGN DATA

An attempt has been made in this manual to provide performance data keyed as closely as possible to cell design and manufacturing process details. (See Section 3.) When only limited information on these details was available, the approach taken was to identify the manufacturers of the cells for which data are presented and to point out any significant differences in cell behavior that may be correlated with known differences in the design or process.

To implement this approach, the design characteristics occurring most frequently in cells supplied by each of the major cell suppliers in recent years were tabulated and defined as "reference design data" (table 11). Cells whose designs fall within the ranges indicated are referred to as "reference design cells." The authors believe that most of the test and flight data obtained over the past 8 years has come from these reference design cells. Table 11 includes data for the SAFT-France VO23S cell because a considerable volume of test data has been generated in the European space community on this cell, some of which has been included in Section 3. Hence, the VO23S cell represents a useful reference design.

Table 12 lists the outside case dimensions of those spacecraft cells most commonly used in the United States. Figure 13 is a photograph of four of these cells. The exact width and depth depend on the case-wall thickness, which the user may usually specify within limits. The case height is subject to greater variation than any other dimension because it can be adjusted to fit specific space requirements without impacting the plate-stack configuration or the case "footprint." The corresponding dimensions of the SAFT-France VO23S cell are: width 76.2 mm; thickness 29 mm; and case height 160 mm.

Table 13 lists the case volumes and cell masses of those cells listed in table 12. The cells have been selected for comparing those from different manufacturers with similar actual capacities at the various size levels. The masses of specific designs vary as the case-wall thickness, case heights, and electrolyte volume are varied. For comparison, the case volume and mass of the SAFT-France VO23S cell are 354 cm³ (21.5 in³) and 1.015 kg (2.24 lb), respectively.

Table 11
Internal Design Data for Reference Design Cells (from 1969 to the present)

Characteristic	Manufacturer			
	Eagle-Picher	General Electric	SAFT-America ¹	SAFT-France
Rated capacity (Ah)	20 to 45	10 to 30	12 to 20	23 ²
Plaque design	Nickel screen	Perforated, Ni-plated steel	Perforated, Ni-plated steel	Perforated, Ni-plated steel
Substrate type	Dry sinter	Wet slurry	Wet slurry	Wet slurry
Process type	10 to 12	11	9 to 10	12
Positive plate design	70 mm (2.76 in.)	70 mm (2.76 in.)	70 mm (2.76 in.)	70 mm (2.76 in.)
Number used	0.75 mm (0.03 in.)	0.70 mm (0.0275 in.)	0.88 mm (0.035 in.)	0.76 mm (0.03 in.)
Width	0.40 to 0.45	0.40 to 0.45	0.31 to 0.36	0.44
Thickness (uncoated)	1.2 to 1.3	1.1, 4 to 14.6 (before 1975)	16.0 to 16.5	14 to 15
Uncoated area (dm ² /rated Ah)	Chemical	12.8 to 14.0 (1975 and after)	Chemical	Chemical
Loading (hydrate, g/dm ²)	Chemical	Approximately 5	Approximately 5	Data not available
Preparation method	Approximately 5	Cadmium treated	None known	None known
Cobalt content (%) of loading	None known			
Special treatment				

¹Comdex Cotton Industries, Alabine Battery Division.

²For the V0235 cell in particular.

Table 11 (Continued)

Characteristic	Manufacturer			
	Eagle Picher	General Electric	SAFT-America ¹	SAFT-France
Negative plate design Number used	11 to 13	12	10 or 11	13
Thickness	0.75 mm (0.03 in.)	0.82 mm (0.0325 in.)	0.82 mm (0.0325 in.) (low N/P ratio) 0.90 mm (0.035 in.) (high N/P ratio)	0.89 mm (0.034 in.)
Loading (hydrate, g/dm ²)	14 to 16	16.0 to 17.2 (before 1975) 15.4 to 16.6 (1975 and after)	17.0 to 17.7 (low N/P ratio) 17.7 to 18.7 (high N/P ratio)	18 to 19
Impregnation method	Chemical	Chemical	Chemical	Chemical
Special treatment	None	Silver treated; noninflated	None	None known
Precharge (% of total negative)	Data not available	20 to 30	20 to 30	Data not available
Separators				
Thickness, as compressed	0.2 mm (0.008 in.)	0.18 mm (0.007 in.)	0.15 mm (0.006 in.)	0.28 mm (0.011 in.)
Type	Nonwoven absorber	Nonwoven absorber	Nonwoven absorber	Nonwoven absorber
Material	Nylon-6	Nylon-6	Nylon-6	Nylon
Electrolyte				
KOH concentration (% by weight)	31	31 to 34	34	31
Initial specific volume (ml/Ah cap)	1.5 to 4	2.5 to 3	3 to 3.5	3.5 to 4
Negative to positive ratio	1.7 to 1.8	1.6 to 1.8	1.5 to 1.6	1.7 to 1.8
Theoretical	1.3 to 1.5	>1.5	1.3 to 1.5	1.7
Measured (theoretical)				

¹ formerly Gulton Industries, Alkaline Battery Division.

Table 12
Dimensions of Spacecraft Nickel-Cadmium Cells

Rated Capacity (Ah)	Width			Thickness			Height to Shoulder		
	Eagle Picher mm (in.)	General Electric mm (in.)	SAFT- America mm (in.)	Eagle Picher mm (in.)	General Electric mm (in.)	SAFT- America mm (in.)	Eagle Picher mm (in.)	General Electric mm (in.)	SAFT- America mm (in.)
6	53 (2.10)	54 (2.13)	53 (2.10)	22 (0.85)	21 (0.83)	21 (0.83)	89 (3.5)	79 (3.1)	82 (3.2)
9	-	-	53 (2.10)	-	-	22 (0.85)	-	-	94 (3.70)
10	76 (3.0)	76 (3.0)	-	23 (0.9)	23 (0.9)	-	71 (2.8)	84 (3.3)	-
12	76 (3.0)	76 (3.0)	76 (3.0)	23 (0.9)	23 (0.9)	23 (0.9)	103 (4.1)	102 (4.0)	-
15	76 (3.0)	76 (3.0)	76 (3.0)	23 (0.9)	23 (0.9)	23 (0.9)	114 (4.5)	120 (4.7)	-
20	76 (3.0)	76 (3.0)	76 (3.0)	23 (0.9)	23 (0.9)	23 (0.9)	-	160 (6.3)	163 (6.4)
21	76 (3.0)	-	-	23 (0.9)	-	-	167 (6.56)	-	-
24	-	76 (3.0)	-	-	23 (0.9)	-	-	163 (6.5)	-
30	76 (3.0)	76 (3.0)	-	23 (0.9)	23 (0.9)	-	178 (7.0)	174 (6.85)	-
36	81 (3.2)	-	-	37 (1.47)	-	-	146 (5.75)	-	-
50	-	127 (5.01)	-	-	33 (1.31)	-	-	144 (5.65)	-
55	81 (3.2)	-	-	37 (1.47)	-	-	200 (7.87)	-	-
100	189 (7.46)	-	185 (7.30)	37 (1.47)	-	35 (1.40)	185 (7.30)	-	185 (7.30)

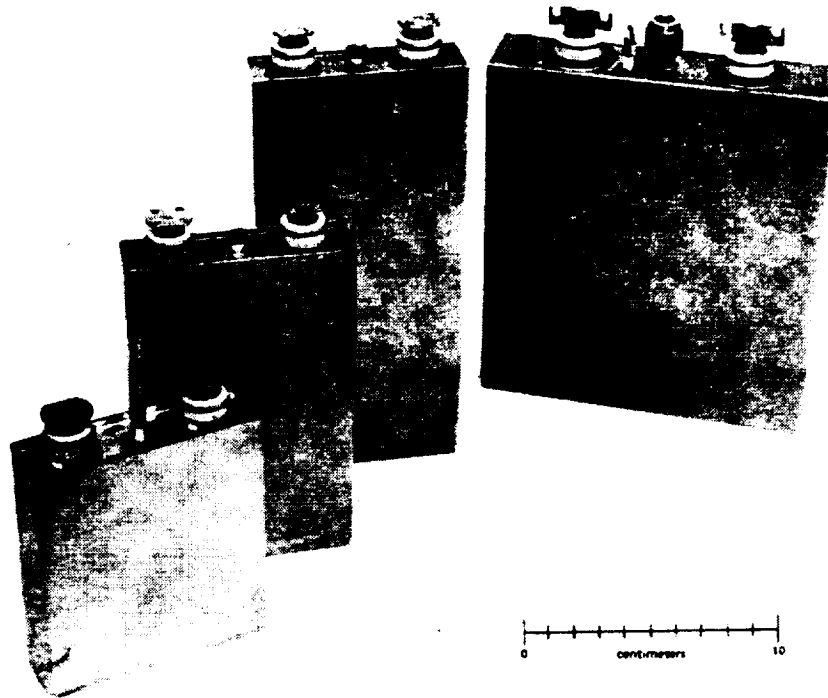


Figure 13. Four typical prismatic spacecraft cells (rated capacities from left to right: 10, 15, 24, and 50 Ah).

2.6 LIGHTWEIGHT CELLS

The term "lightweight" refers to cells with specific energies significantly greater than those of the more standard types of cells. Table 13 shows that the ratio of rated capacity to mass of reference design cells is approximately 24 Ah/kg (10.9 Ah/lb) for the larger sizes. In terms of initial standard capacity,* this ratio is approximately 29 Ah/kg. If the average discharge voltage is assumed to be 1.20, the corresponding maximum specific-energy output (to 1 volt) is calculated to be 34.8 Wh/kg (15.8 Wh/lb).

A number of cells have been built with considerably greater specific energy than this. One of these (Reference 65) is a nominal 20-Ah cell, weighing 0.583 kg, with a specific energy (calculated as above) of 49 Wh/kg.† The

*See Appendix A for definition.

†Eagle Picher Industries, Inc., Type RSN-2A.

ORIGINAL PAGE IS
OF POOR QUALITY

Table 13
Volumes and Masses of Spacecraft Nickel-Cadmium Cells

Rated Capacity (Ah)	Volume*			Mass		
	Eagle Picher cm ³ (in ³)	General Electric cm ³ (in ³)	SAFT-America cm ³ (in ³)	Eagle Picher kg (lb)	General Electric kg (lb)	SAFT-America kg (lb)
6	104 (6.36)	90 (5.51)	91 (5.51)	0.29 (0.64)	0.275 (0.61)	0.30 (0.65)
9	-	-	110 (6.73)	-	-	0.41 (0.90)
10	122 (7.43)	147 (9.0)	-	0.377 (0.83)	0.462 (1.02)	-
12	176 (10.8)	179 (11.0)	-	0.522 (1.15)	0.547 (1.20)	-
15	194 (11.9)	210 (12.9)	-	0.612 (1.35)	-	-
20	-	280 (17.1)	-	-	0.951 (2.10)	-
21	284 (17.4)	-	-	0.910 (2.00)	-	-
24	-	285 (17.4)	-	-	1.0 (2.20)	-
30	304 (18.6)	304 (18.6)	-	1.09 (2.40)	1.10 (2.42)	-
36	440 (26.9)	-	-	1.27 (2.80)	-	-
50	-	604 (36.9)	-	-	2.04 (4.50)	-
55	606 (37.0)	-	-	1.81 (4.00)	-	-
100	1300 (79.5)	-	1220 (74.6)	3.69 (8.12)	-	3.95 (8.7)

*Not including terminal extension.

mass of its plates is 71 percent of the plate mass shown for the standard 20-Ah cell in table 14. Schulman (Reference 46) described another light-weight cell,* which is rated at 34 Ah and made with electrochemically impregnated plates. This cell has a specific energy of 44 Wh/kg at 100 percent depth of discharge. Both of these cells are now undergoing life-testing to establish cycling capability. Further increases in specific energy may be expected from the NASA-sponsored nickel-cadmium battery technology program now underway (Reference 66). Table 14 also shows the mass distribution of a typical cell for reference. The data were obtained from a 20-Ah SAFT-America cell. Because the plates are approximately 50-percent active materials by weight, it may be seen that only 32 percent of the total is active (not including electrolyte). For this reason, most efforts to increase the specific energy of the cell have been directed at reducing the ratio of inactive to active mass.

Table 14
Mass Distribution in a 20-Ah Cell

Component	Mass (g)	Percent of Total Mass
Positive plates	277	29.7
Negative plates	323	34.7
Separator	15	1.6
Electrolyte	93	9.9
Container (case and cover)	219	23.5
Liner	6	0.6
Total	933	100.0

*Manufactured by Yardney Electric Company.

SECTION 3 CELL PROPERTIES AND PERFORMANCE

3.1 INTRODUCTION

This section presents typical properties and performance characteristics of sealed nickel-cadmium cells. Static properties are those that do not involve net-energy conversion; performance characteristics are those that are involved with energy conversion and mass transfer within the cell.

Performance information is presented in two parts: that for initial characteristics, and that for long-term performance. Initial characteristics are considered to be those observed during the first 20 to 50 cycles of operation, and during the first cycles after reconditioning. Long-term characteristics are those observed after several hundred or more cycles and/or several years of service without reconditioning or with ineffective reconditioning. Failure to distinguish between initial and long-term cell behavior in the design of the system can lead to battery-limited power-system operation within the system design life.

Performance data given are primarily for cells designed as described in Section 2.5 (i.e., for so-called "reference design cells"). The effects of departures from these reference designs are indicated in terms of departures from the performance of reference cells taken as the norm. The same treatment is given to variations in processes.

Initial characteristics are similar among cells that are similar in design but made by different types of processes. Thus, initial characteristics are relatively insensitive to process details over a broad range. The user should understand the design aspects that have a direct impact on initial characteristics so that they may be controlled by specification.

Long-term performance or, more specifically, the changes in characteristics resulting from long-term operation are generally more sensitive to both design and process details than initial characteristics. However, because long-term effects cannot be measured during acceptance testing and because the state of the art of performance analysis does not permit reliable predictions from a theoretical standpoint, long-term performance predictions must be based mainly on prior flight and test data and the potential impact of critical design and process aspects. Section 3.4 summarizes available information on these relationships.

Both initial characteristics and long-term performance may be affected by conditions of use. Because use conditions interact adversely with the results of certain designs and processes, some design and use combinations must be avoided. The effect of operating conditions and their limits is discussed under both initial and long-term performance.

The terms used to describe most of the so-called "static" properties of cells, such as mass, length, temperature, impedance, thermal capacity, and thermal conductivity, are relatively straightforward. Other concepts describing dynamic performance, such as those of state of charge, capacity, energy, and heat generation, are functions of many variables and therefore require careful definition if they are to be used with confidence in engineering practice. This section defines these latter concepts in terms of directly measurable variables—cell terminal voltage, cell current, cell-wall temperature, and cell internal pressure—and of various functions derived from them. Cell-wall temperature is considered as directly measurable; internal cell temperature is accessible only with difficulty. Although internal temperature is a more fundamental variable than cell-wall temperature, it can be estimated from external temperature only if the cell heat-generation rate and internal thermal resistances are known.

The electrical power input to, or output from, a cell is an instantaneous performance characteristic that is not normally measurable directly, but it may be determined at any point by multiplying the cell voltage by the current. Note that because it is a photovoltaic cell, a galvanic cell is an energy storage and delivery device and not a power generator, although the sintered-plate nickel-cadmium cell is capable of delivering high power within the bounds of its dischargeable energy content.

3.2 STATIC PROPERTIES OF CELLS

The properties described in this section are mainly inherent in the physical and chemical structure of sealed, sintered-plate nickel-cadmium cells (i.e., properties that do not involve net dc current flow or energy conversion). The following paragraphs describe the static properties of reference designs and the effects of design variations.

3.2.1 Properties of Reference Design Cells

3.2.1.1 Internal Impedance

A knowledge of the effective internal impedance of cells is useful in the design and performance analysis of electric power systems for evaluating the response of the battery to ripple, noise, charging and discharging transients, and other phenomena. In this manual, the term "impedance" is used to refer to the ratio of the observed cell-voltage change to the corresponding change in the alternating current through the cell. Some people refer to this measured value as "internal resistance." This designation is misleading, however, because the impedance of a nickel-cadmium cell at all frequencies outside a narrow band contains a relatively large reactive component (in addition to ohmic resistance), as follows.

Internal Impedance at Low Frequencies—Most impedance measurements for which data are available have been made at frequencies of from 40 to 60 Hz. Figure 14 summarizes the results for prismatic cells made with non-woven nylon separators and shows a plot of impedance versus the fraction $100 \text{ Ah} \div (\text{rated capacity})$. This quotient is used to linearize the plot, recognizing: (1) that impedance should vary linearly with the reciprocal of the plate area, and (2) plate area is roughly proportional to rated capacity.

The solid line corresponds to the smoothed data in References 2 and 67. The dotted lines show the limits of the more reliable data and indicate that the spread is about ± 25 percent over the range of cell sizes and designs included. Although temperature and state of charge are mainly unspecified for these data, it may be assumed that most measurements were made at room ambient. The closeness of the fit of the smoothed data points (circles) to a straight line verifies that the impedance is inversely proportional to plate area.

In a detailed study of impedance of one size of prismatic cell (rated at 23 ampere-hours), impedance was measured as a function of temperature, recharge ratio, and test frequency (Reference 67). Impedance varied within a range of ± 25 percent from the mean with temperature over the range from 0 to $+40^\circ\text{C}$ as measured at 100 to 10^5 Hz. However, at 1 and 10 Hz at 0°C , impedance was a factor of 2 greater than at these frequencies at 20 or 40°C .

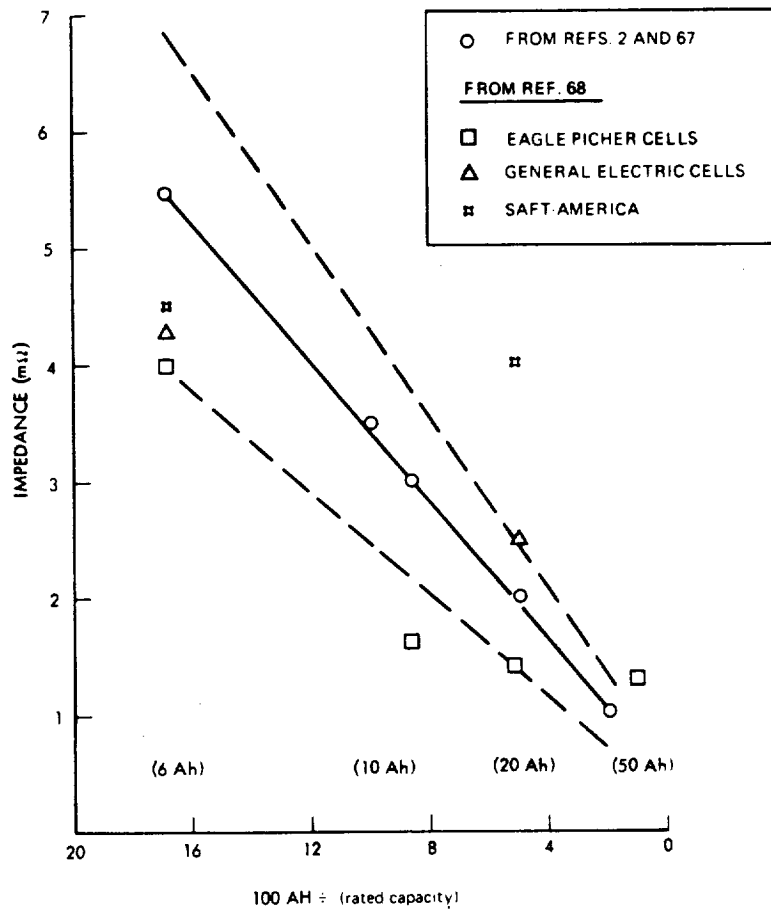


Figure 14. Impedance of new cells at 40 to 60 Hz versus rated capacity.

Variation of impedance with recharge ratio was also within ± 25 percent of the mean and did not show any trends. This result differs from that observed during acceptance tests at NWSC/Crane (Reference 68), in which impedance at end of charge was consistently 20 to 30 percent higher than at lower states of charge. This difference may result from the fact that the measurements on the VO23S cell were made after opening the circuit following a charge.

Measured at low frequency, data for impedance of new cells with adequate electrolyte during discharge (Reference 69) show that impedance decreases by about 20 percent in going from overcharge to discharge and

remains nearly constant at the level shown in figure 15 during discharge (at the 0.5C rate) at least to 100 percent of rated capacity. If inadequate electrolyte is present in the cell as a whole, or if the electrolyte content of the separator is much less than normal, the impedance at depths of discharge approaching 100 percent can be much higher. (See figure 20.)

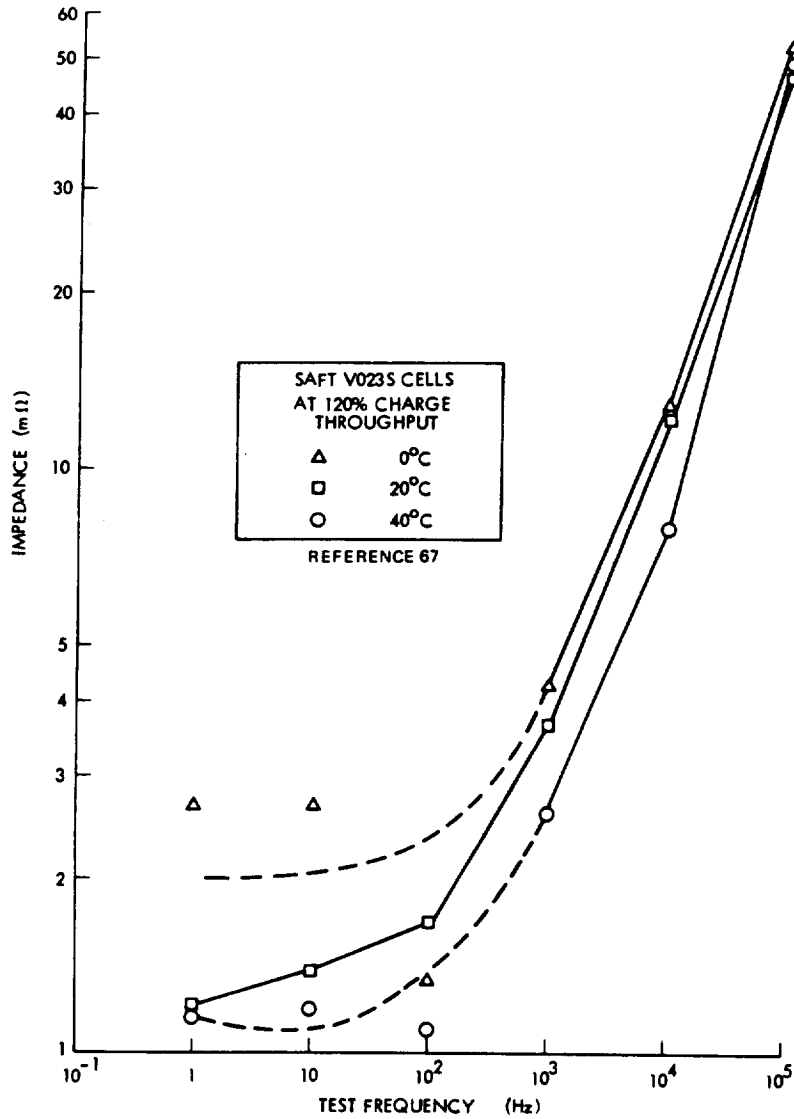


Figure 15. Cell impedance versus frequency.

Impedance Versus Frequency—Figure 15 (from Reference 67) shows impedance data for SAFT VO23S cells, measured at frequencies from 1 to 10^5 Hz after a charge throughput of 120 percent of rated capacity.* (Note that both impedance and frequency scales are logarithmic.) Impedance is relatively constant up to about 100 Hz; it then increases rapidly at higher frequencies.

Reactive Component of Cell Impedance—The foregoing data are for the absolute or scalar value of cell impedance (i.e., without regard to the nature of the impedance). For some applications, the angle between the current and voltage vectors (phase angle) and the relative magnitude of resistive and reactive components is needed.

Figure 16 shows a curve of $\sin \theta$ (θ = measured phase angle) versus test frequency for SAFT VO23S cells, taken from Reference 67 and corresponding to the impedance data in figure 15. Positive and negative values of $\sin \theta$ are associated with net inductive and capacitive reactance, respectively, as shown in figure 17. Similar phase-angle versus frequency data were reported for a 15-Ah cell, measured at 12, 60, and 400 Hz (Reference 69), in which the phase angle at any one frequency changed by only a few degrees in going from the charged to the discharged state.

The behavior shown in figure 16 suggests a simplified equivalent circuit such as the one shown in figure 18. This circuit is similar to that shown by Bauer (Reference 2). Between 30 and 100 Hz, the effects of C_i and L_i on impedance roughly cancel one another, leaving R_i as the measured component. At low- and high-frequency extremes, shunting resistances R_c and R_L , respectively, limit the impedance.

In the region between 30 and 100 Hz, if the effect of R_c and R_L in figure 18 is neglected, the apparent resistance, R_i , and the apparent inductive and capacitive reactances may be calculated using the formula:

$$X = |Z| \sin \theta \quad (9)$$

Therefore, at $\sin \theta = 0$, $X = 0$, and the impedance is purely resistive (ohmic). At 150 Hz, at which $\sin \theta = +0.5$, reactance is inductive and numerically equal to one-half the impedance. At this point, the impedance

*The cells were charged at the 0.1C rate, beginning after a discharge to 1 volt.

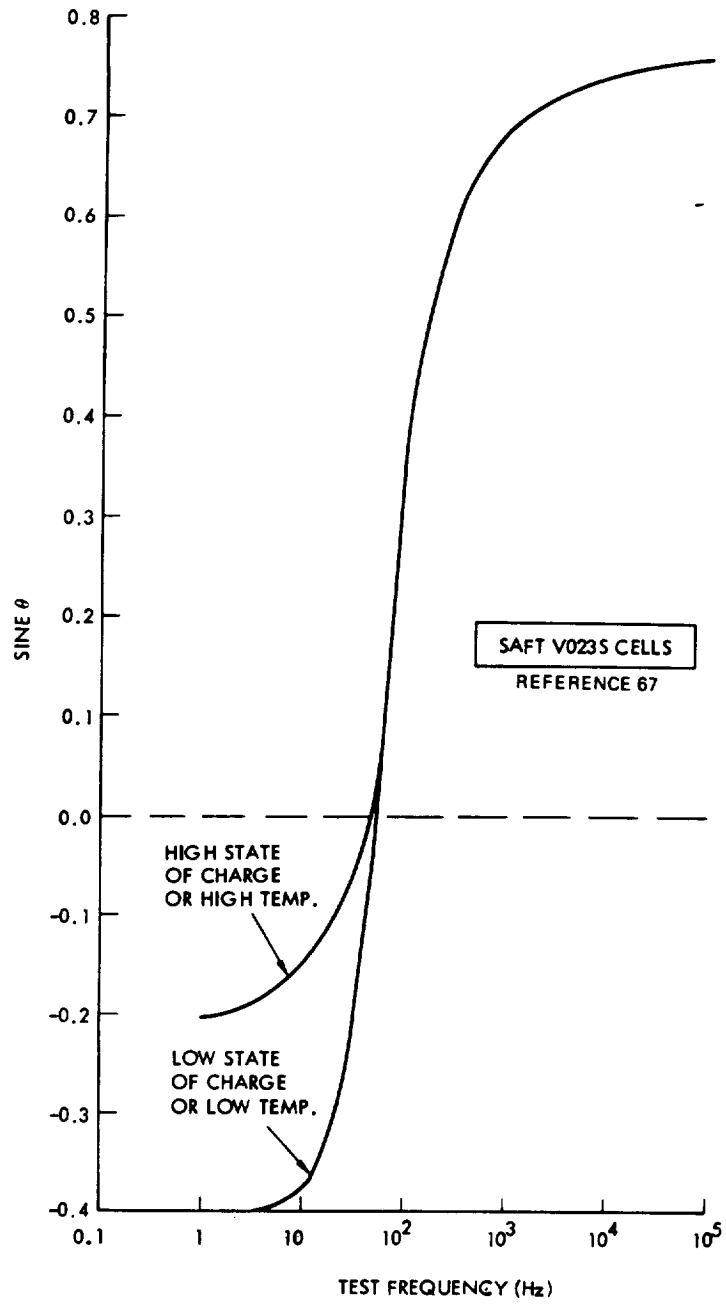


Figure 16. Impedance phase angle versus frequency.

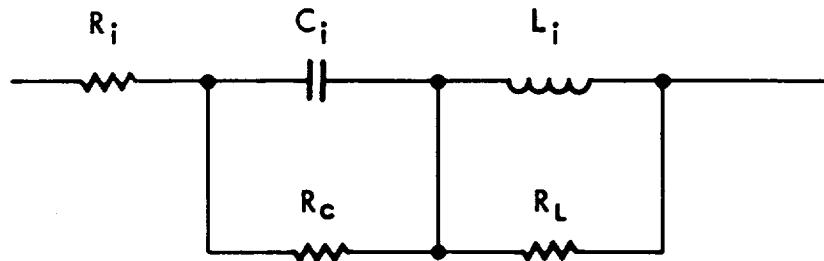


Figure 17. Impedance phase-angle relationships.

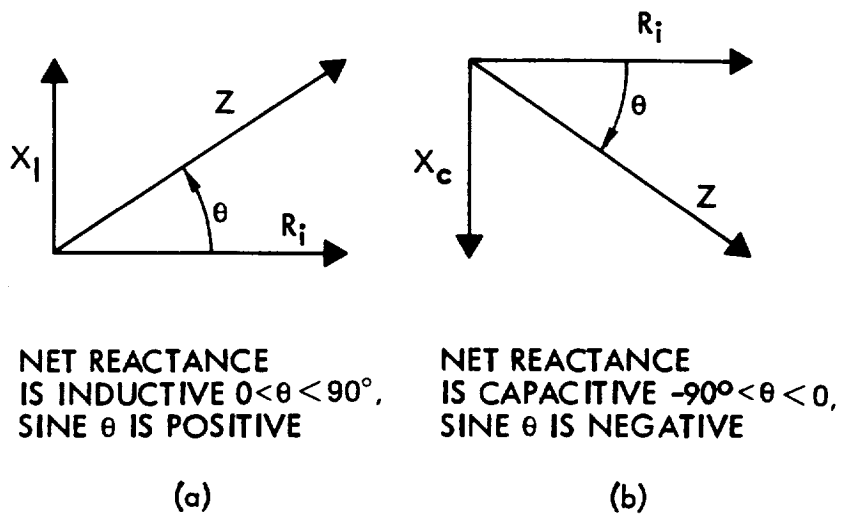


Figure 18. Simplified equivalent circuit for cell impedance.

is about 80 percent resistive, and the effective inductance of these cells (23-Ah rating) is $0.3 \mu\text{H}$. At 30 Hz, at which $\sin \theta = -0.2$, the impedance is 95 percent resistive, the reactance is capacitive, and the effective capacitance is 530 farads.

3.2.1.2 Passive Thermal Properties

The cell thermal properties of interest for battery thermal analysis and design are heat capacity, thermal conductivity, and heat-generation rate. (See the sections on "Heat Generation During Charge" later in this document.)

Values for the heat capacity per unit mass of reference-design prismatic cells (Section 2.5) reported by various sources (References 38, 70, and 71) fall in the range of 0.25 to 0.28 (cal/g)/°C. The variation is probably the result of different percentages of cell weight present as electrolyte. The heat capacity of any specific cell is obtained by multiplying the actual cell mass by this number. Table 15 lists specific heat capacities for individual cell materials. Although data for specific heat capacities of cylindrical cells do not appear to have been published, they should be the same as those of prismatic cells in that the materials and their proportions are about the same.

Table 15
Values for Some Thermophysical Properties of Materials
Used in Nickel-Cadmium Cells (Reference 72, p. 65)

Material	Specific Heat (cal/g/C)	Thermal Conductivity (cgs units)	Specific Gravity or Density (gm/cm ³)
Nickel	0.11-0.13	0.152	8.90
NiO	—	0.00225	7.45
NiO·OH	~0.11	—	—
NiO·H ₂ O	~0.14	≈0.08	—
Ni(OH) ₂	—	—	4.83
Ni ₂ O ₃ ·xH ₂ O	—	—	4.83
Cadmium	0.055	0.23	8.64
CdO	0.081	—	8.15
Cd(OH) ₂	~0.20	—	4.79
KOH (30 percent)	~0.82	0.00135	1.29
Stainless steel (304)	0.12	0.039	8.03
Nylon	~0.40	~0.0006	~1.14

References 70, 72, and 73 have summarized and analyzed data for thermal conductivity of prismatic cells. The conductivity in each of the three mutually perpendicular directions shown in figure 19 are of interest. Most available data are for the X and Y directions (k_x and k_y , respectively),

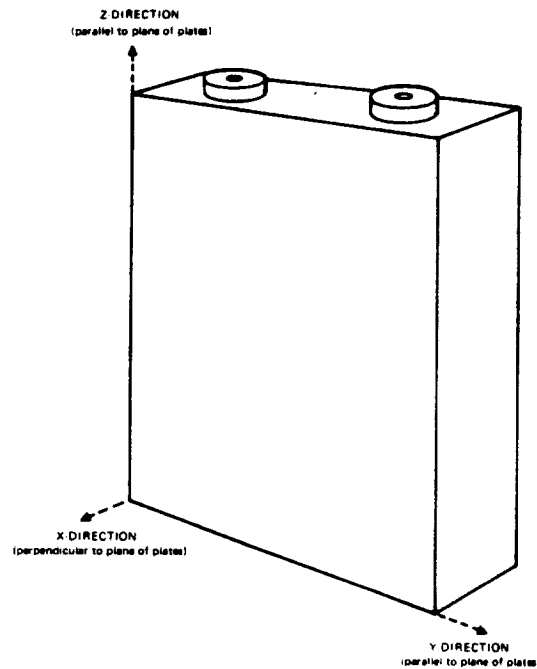


Figure 19. Major directions for heat flow in a prismatic cell.

where k_z is calculated from k_y . The units of thermal conductivity are $[\text{cal}/\text{cm}^2/\text{sec}]/(^{\circ}\text{C}/\text{cm})$ in cgs units and $[\text{Btu}/\text{ft}^2]/\text{hr}]/(^{\circ}\text{F}/\text{ft})$ in English units.

Table 16 is a summary of thermal conductivity values for some reference design nickel-cadmium cells from the literature. These data show considerable scatter and large discrepancies between some calculated and measured values, reflecting difficulties in modeling and/or in making accurate measurements. A slight trend toward lower values of k_x for larger capacity cells is apparent.

A detailed study of thermal conductivity of 20-Ah spacecraft cells (Reference 72) yielded the measured values shown in table 17. These data apply to cells in the fully discharged state. The values for k_x increased linearly with state of charge to a maximum of 12 to 14 percent greater than in the discharged state. Because the cells from which these data were obtained were manufactured before 1969, their designs may differ in some details

Table 16
Cell Thermal Conductivity Data from
the Literature (cgs units)

Manufacturer and Rated Capacity	k_x	k_y
SAFT-America 6 Ah	0.0042 ¹	0.052 ¹
SAFT-America 6 Ah	0.0067 ²	0.019 ²
General Electric 12 Ah	0.002 ¹	0.041 ¹
General Electric 20/24 Ah	0.0016 ²	0.0035 ²
General Electric 50 Ah	0.002 ²	—
100 Ah	0.0016 ¹	—

¹Calculated
²Measured

Table 17
Thermal Conductivities Measured on
20 Ah Cells (cgs units)

Manufacturer	k_x	k_y
Eagle Picher	0.0026	0.0056
General Electric	0.0038	0.0067
SAFT-America	0.0027	0.0070
Average	0.0030	0.0064

from those of the reference cells. However, the differences are believed to be small and, therefore, the values in table 17 should apply to current reference-design cells to within 10 percent. No more up-to-date data were found.

For more detailed modeling and calculation of temperature gradients within the cell, the thermal properties of the individual components must be known. Table 15 lists some of these data. Table 18 lists data for plates and separators as developed in Reference 72. Note that the thermal conductivity of both positive and negative plates decreases when the cell is

Table 18
Thermal Properties of Plates and Separators,
Including Electrolyte (Reference 72)

Component	Thermal Conductivity k_x (cgs units)	Density (g/cm^3)
Positive plate		3.4 to 3.6
Charged	0.00097	
Discharged	0.00144	
Negative plate		3.7 to 3.9
Charged	0.00075	
Discharged	0.0020	
Separator		
(Nylon, Pellon 2505, compressed to 0.25 mm)	0.0006 at 80% saturation	1.2
	0.0003 at 50% saturation	0.9
	0.0002 at 20% saturation	0.3

charged, yet the thermal conductivity of the cell as a whole increases, as mentioned previously. It appears likely that these changes occur in this manner because the amount of electrolyte in the separator increases whereas that in the plates decreases during charge.

3.2.2 Effects of Design and Process Variations on Static Properties

The effects of most design variations on cell dimensions and mass are easily calculated if the change in dimensions and/or weight of the affected components are known. Such changes are most likely to occur as changes in the number or thickness of plates, the average compressed thickness of separators, the thickness of the case wall, or the amount of electrolyte used. The percentage of change in mass may be estimated without a detailed calculation by referring to the mass breakdown given in Section 2.5.

Variations in components such as the case and terminals do not affect capacity or energy output, but variations in the plates or electrolyte usually do. Hence, effects of the latter variations are considered under "specific energy," which takes both electrical output and mass into account. (See Section 3.3.2.2.)

The effects of design variations on properties such as impedance and thermal properties are not easily calculable, and few data are available. The plot of impedance versus capacity in figure 14 indicates that a decrease in plate area is accompanied by a corresponding increase in internal impedance. Decreasing the volume of electrolyte to below the level of about 2 ml/Ah of rated capacity is also likely to result in higher than normal initial impedance. This effect is more severe at higher depths of discharge (Reference 31), as shown in figure 20, and low electrolyte content is therefore of more concern for synchronous orbit applications in which depth of discharge is usually high. Increasing electrolyte beyond that equivalent to about 2.5 ml/Ah does not further reduce the initial impedance of most cells.

Variations in the material of the separator may significantly affect initial impedance. Some cells made with the less wettable separator materials, such as untreated polypropylene, exhibited impedances of up to 50 percent greater than that of their counterparts with nylon separators (Reference 74). This difference was probably caused by a difference in initial

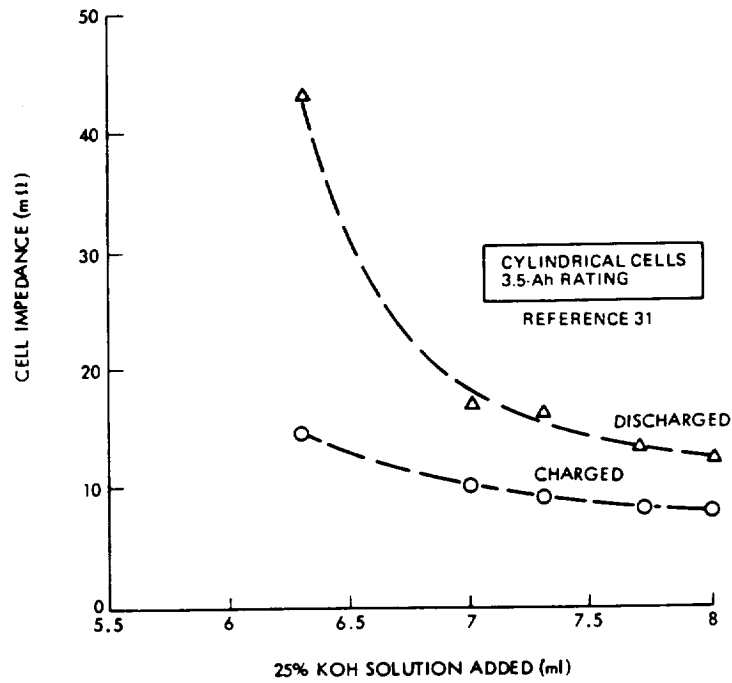


Figure 20. Effect of electrolyte level on cell impedance.

electrolyte distribution between the two types of cells in question. Polypropylene separators may also make impedance more sensitive to electrolyte level because a difference of 50 percent in impedance was seen between pore fills of 70 and 80 percent (Reference 74).

Because the specific heat of a nickel-cadmium cell as a whole appears to be independent of design variations for reference-type cells (Reference 72), heat capacity will be simply proportional to cell mass. On the other hand, thermal conductivity increases as the number of plates per unit cell thickness increases, as separator thickness decreases, and as volume of electrolyte per unit of plate stack volume (percent of pore fill) increases. The amount of electrolyte in the separators has the largest single effect when the level is low. (See table 18.) This relationship suggests that, although cells may have adequate thermal conductivity when new and, hence, when electrolyte distribution is normal, the thermal conductivity can decrease significantly with electrolyte redistribution, causing an increased internal thermal resistance.

3.3 INITIAL PERFORMANCE CHARACTERISTICS

This section describes the dynamic performance characteristics of hermetically sealed, sintered-plate, nickel-cadmium cells that are most useful for design and performance analysis of working spacecraft electric power systems. Initial characteristics have been defined as those to be expected within the first 50 or so repetitive cycles of cell life or soon after effective reconditioning. Thus, no appreciable voltage degradation is included. These data provide a frame of reference for comparing subsequent performance.

Separate data is given for short cycle (90- to 180-minute cycle length, as for low Earth-orbit applications) and for long cycle (12- to 24-hour cycle length, as for Earth-synchronous and other medium- to high-altitude applications). This division recognizes the significant differences in operating conditions between these two major application areas. The long-cycle data also applies to interplanetary probes and orbiters.

Charge data for one-at-a-time cycles* is given separately from that for continuous cycling. Discharge data is given separately.

*A one-at-a-time cycle is one of a set of only a few cycles, usually performed under a given set of standard conditions, before and after which the conditions are different (e.g., the cells may be cycling continuously). Before each charge of a one-shot cycle, cells are either discharged to 1 volt or are discharged on a resistor to zero or near-zero volt (as specified). Charging is usually prolonged and taken to a higher state of charge than for regular cycling.

Composite data typical of the cells of all manufacturers are presented when available, but data for cells with widely differing behavior are not combined. Significant performance differences exist among cells from different sources, resulting from certain design or process differences, that the battery engineer must consider.

A few words about the method used to express variables is in order. Charge and discharge currents are expressed as far as possible in so-called "normalized" form (i.e., the current in amperes divided by cell capacity in ampere-hours). The manufacturer's rating (C_R) is used as the divisor in this manual. Other methods of normalization used include: (1) dividing by the capacity actually measured under a specified set of conditions; (2) dividing by the area of the positive plates in the cell; or (3) dividing by the weight of positive active material in the cell. These divisors for current often provide more accurate or internally consistent relationships between cells of one specific design. However, when specific design details are lacking, the rated capacity is considered to be the most practical common denominator for use as a scaling factor for different cells. With a knowledge of factors such as the foregoing, the designer can convert to other scales if desired.

The scales for charge throughput and discharge output are normalized by dividing ampere-hours by the rated capacity (C_R). When appropriate, "true" state of charge, as defined in the Appendix A, is used as the dependent variable rather than charge throughput. Although true state of charge is more difficult to determine than charge throughput, certain characteristics (such as instantaneous charge efficiency and heat rate) are much more closely related to true state of charge, and, hence, this type of plot is more broadly useful.

Voltage data are presented as voltage per cell. Such data are usually the average of 5 to 30 cells operating in series. Data on the spread between the highest and lowest cell voltages are given when significant and when data are available. Unless otherwise noted, the temperatures given are cell-wall temperatures. When cell-wall temperatures are not available, ambient temperature is indicated.

3.3.1 Initial Charge Characteristics

This section describes initial charge characteristics, including data for active charge (that portion of charge in which the charge efficiency is high), overcharge (when charge efficiency is low or zero), and trickle charge (when charge rates are usually less than 0.03C following a charge at a higher rate).

3.3.1.1 Charge Data for Reference-Design Cells

Charge Voltage and Current—The voltage of a nickel-cadmium cell on charge is a function of a number of operating variables, including temperature, charge rate, initial state of charge, state of charge at the point of interest, and immediate prior history. In addition, charge-voltage characteristics, although generally similar in shape for different designs, vary in shape as a function of design details, such as plate area per ampere-hour, plate loading, pore size, and electrolyte level. Because of the variables involved, no satisfactory general approach to predicting charge voltage has been developed. Also, charge voltage is not controlled directly by the cell-manufacturing process in the present state of the art. Hence, initial voltage characteristics are not single-valued but are distributed over a range, even for cells from the same lot. System design must consider this range.

Transient Charge Characteristics—Figures 21 through 25 show typical voltage curves for charge during one-at-a-time cycles using continuous, constant current in the absence of voltage-limiting for reference-design cells from several sources. The rate of voltage increase per unit of charge increases after a throughput equal to the prior discharge. At higher rates and/or lower temperatures, the voltage subsequently either rises to a new nearly constant level or passes through a maximum and then decreases somewhat. The former voltage behavior occurs when the cell-wall temperature is rigidly held at the test temperature; the latter behavior, which is much more commonly observed, occurs as the cell-wall and internal cell temperatures rise considerably above the test temperature because of overcharge heating. Rigid control of cell-wall temperature requires complete immersion of cells in a well-stirred liquid bath; operation of cells in circulating air results in significant rise of wall temperature.

Figure 26 shows charge-voltage data at charge throughputs of 100 and 120 percent as a function of cell temperature and charge rate, cross-plotted from the voltage data in figure 25. The charge rates are those that are appropriate for long-cycle applications. However, not all types of cells have voltage characteristics that are straight lines over the entire range. Because the overcharge characteristics of specific cells may vary from one design to another, they can be measured under operating conditions if voltage is to be used to terminate charge.

These data are not used as such for designing charge control for short orbit operation, as the battery under these conditions reaches the voltage limit before recharge is complete and is then typically permitted to taper-charge

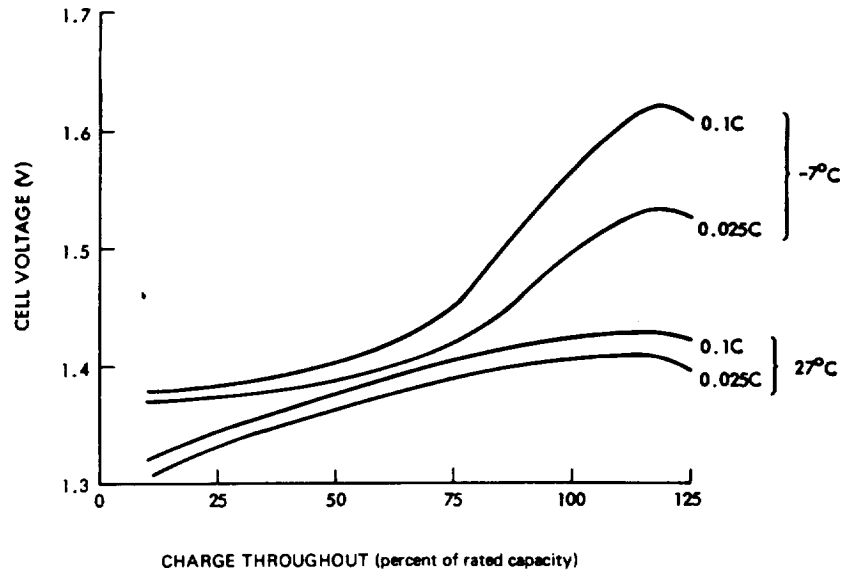


Figure 21. Charge voltage versus throughput for Eagle Picher cells (charge rate and temperature as parameters).

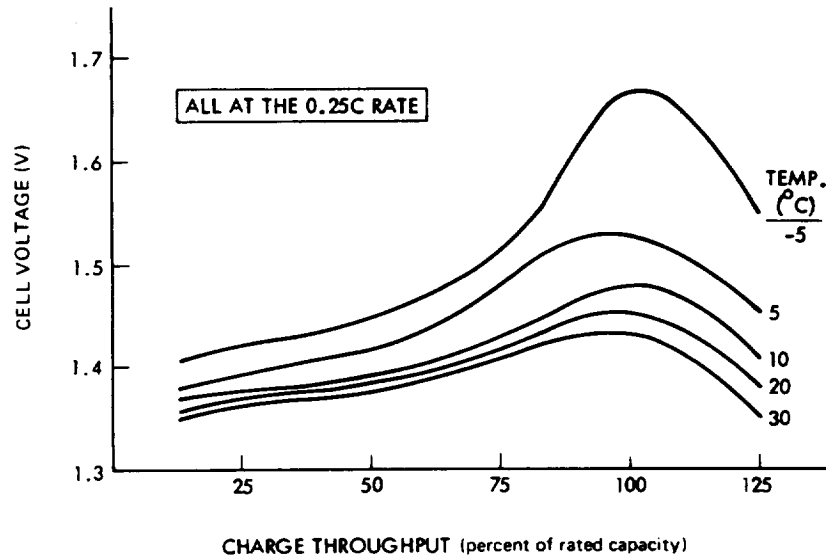


Figure 22. Charge voltage versus throughput for Eagle Picher cells (temperature a parameter).

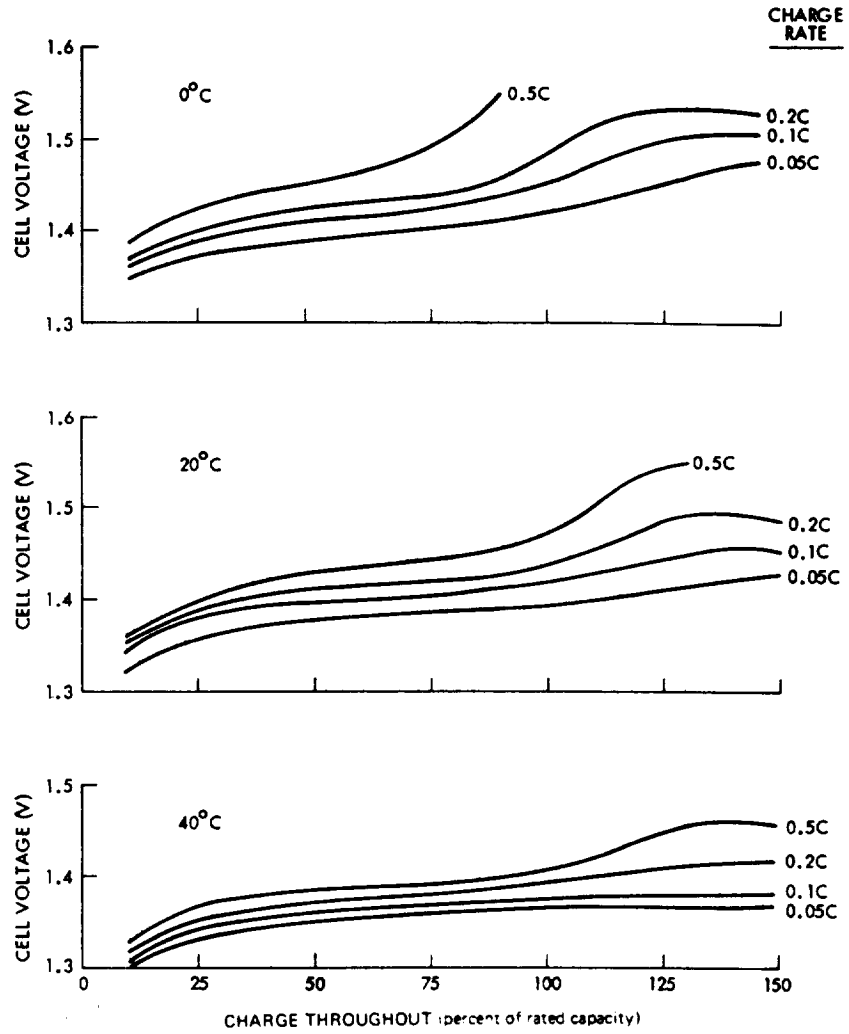


Figure 23. Charge voltage versus throughput for General Electric cells (charge rate a parameter).

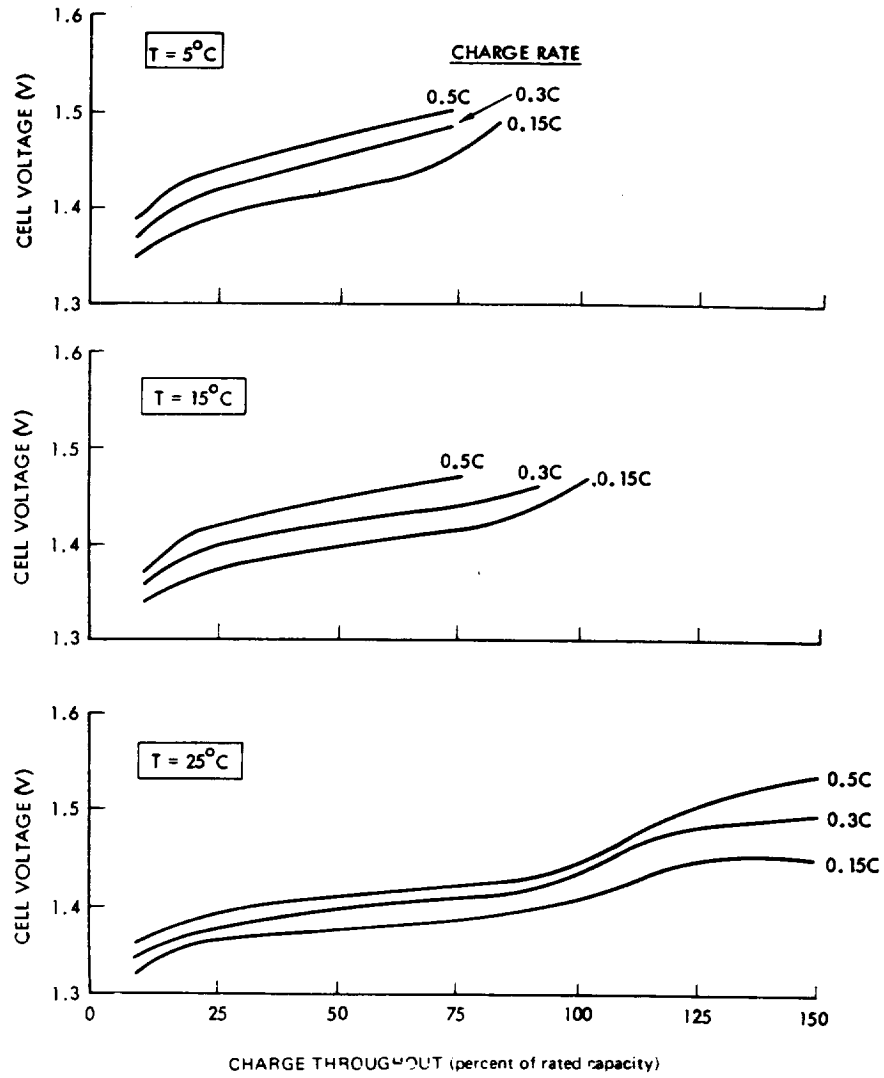


Figure 24. Charge voltage versus throughput for SAFT-America cells (charge current a parameter).

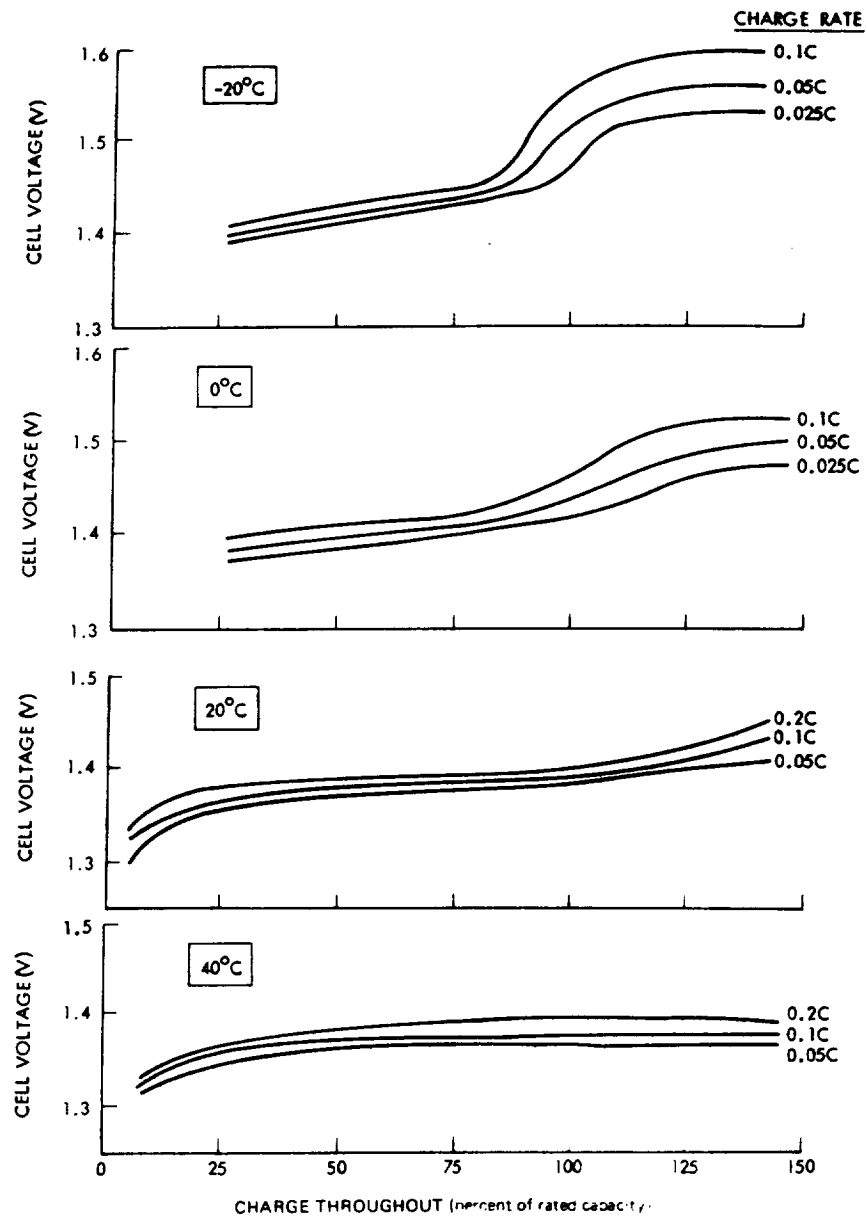


Figure 25. Charge voltage versus throughput for SAFT-France VO23S cells (Reference 75).

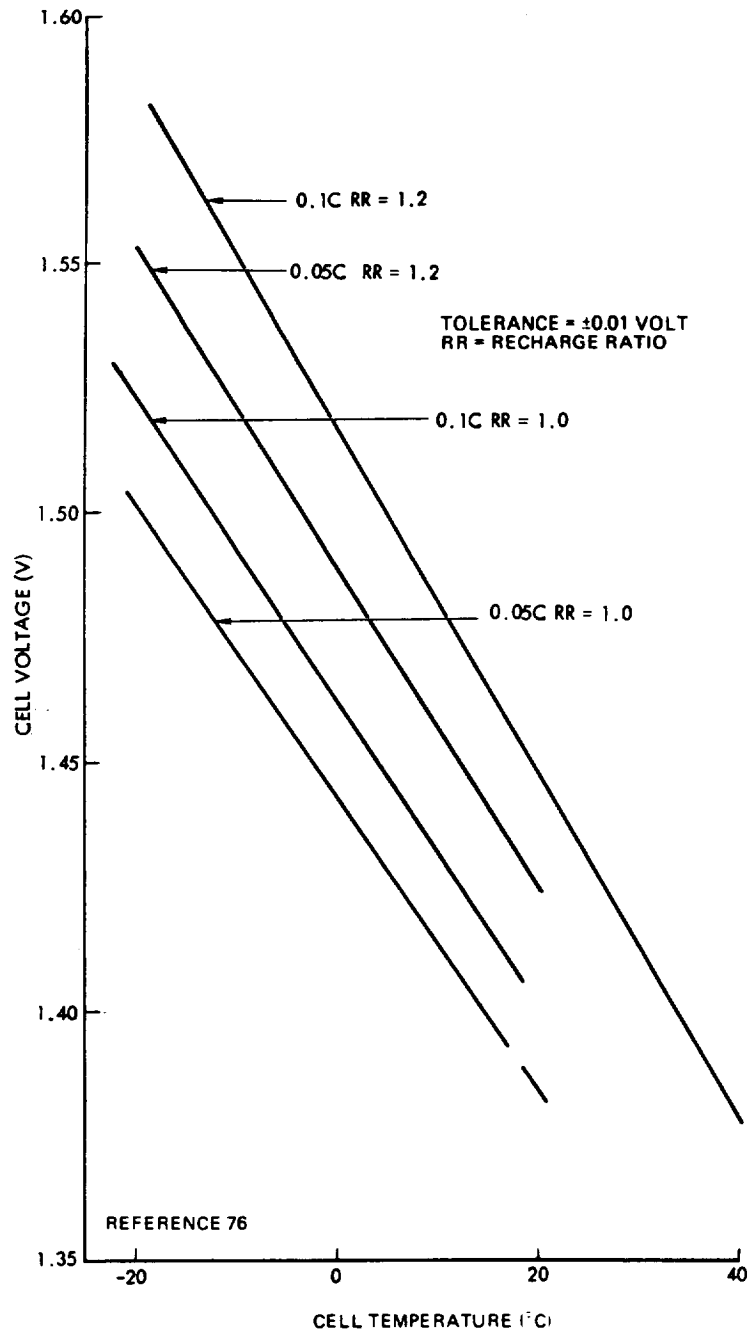


Figure 26. Charge voltage versus temperature and charge rate (recharge ratio a parameter).

at the limit until the end of the charge period. (See "Methods of Charge Control," Section 8). In this mode, recharge ratio is a function of initial charge rate, cell temperature, and voltage limit at a given temperature, as shown in figure 27 for one type of cell operating at a 15-percent depth of discharge (Reference 77). Figure 28 shows similar characteristics for cells from another manufacturer for cells discharged to 1 volt after each recharge.*

Steady-State Overcharge Voltage—In a cell in good condition that is positive-limited on overcharge, cell voltage tends to level off when overcharge is continued at constant current and temperature beyond the region of the voltage rise. The steady-state overcharge voltage is a function of internal cell temperature and charge rate. Figures 29 and 30 show typical average steady-state overcharge voltage data for two types of cells for which consistent data are available. The voltage of individual cells during overcharge may vary from the averages shown, with the variation increasing from ± 0.01 volt at 30°C to ± 0.02 volt at 0°C . The range of normalized current below 0.03C is regarded as the trickle-charge region and, except

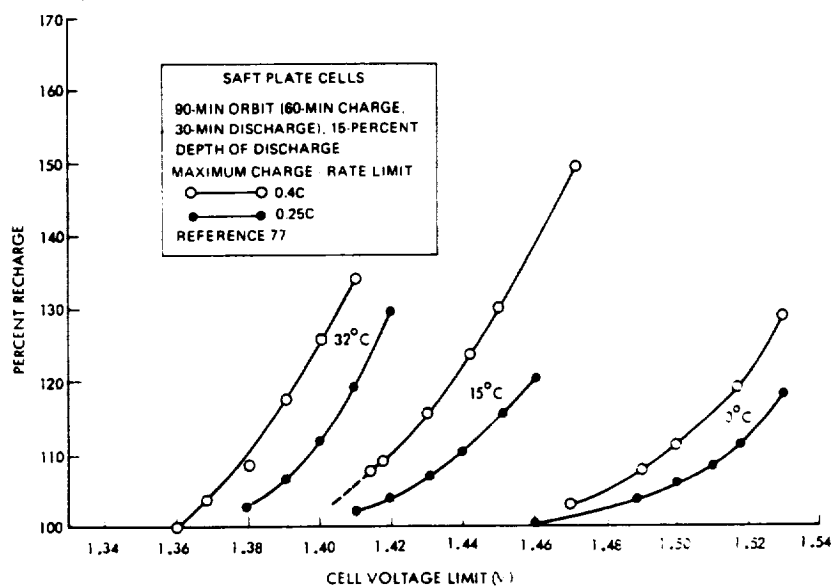
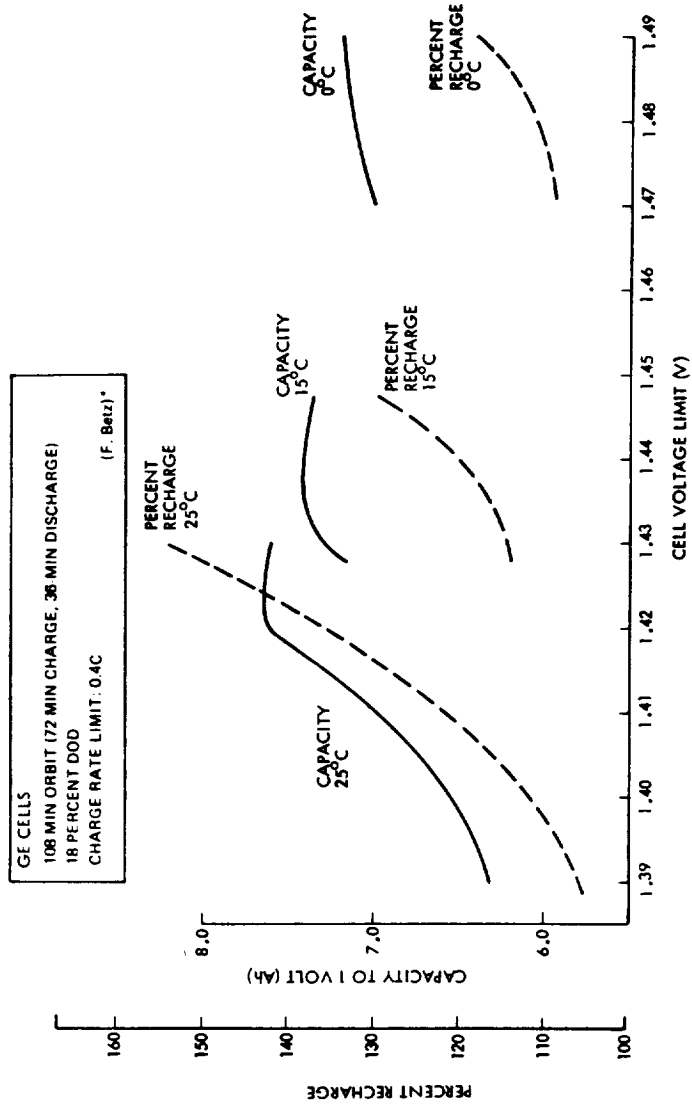


Figure 27. Percent recharge — voltage-limit relationships for 90-minute cycling at 15-percent depth of discharge (SAFT-America cells).

*F. Betz, Naval Research Laboratory, Washington, D.C., private communication.



* F. Betz, Naval Research Laboratory, Washington, D.C., private communication.

Figure 28. Percent recharge — voltage-limit relationship for 108-minute cycling at 18-percent depth of discharge (General Electric cells).

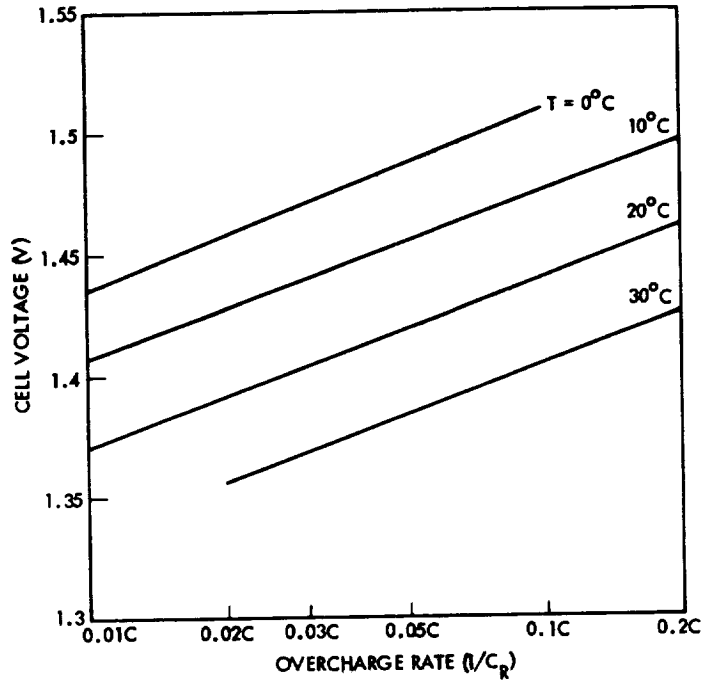


Figure 29. Normalized current versus overcharge voltage for General Electric cells (temperature a parameter).

at very low temperatures, is not normally used for active charging because of low charge acceptance. The voltages shown were measured after 12 to 24 hours of constant-current charging. Voltages may differ somewhat from those shown immediately after switching down from a greater current or if the cells are only partially charged when the current is reduced.

Maximum Allowable Voltage on Charge—If the voltage of a cell rises to a certain value above the normal range during charge, hydrogen gas may be evolved from the cadmium electrode. Whether hydrogen will be evolved cannot be stated with certainty because it is usually not known to what extent the high cell voltage is due to the negative electrode and to what extent it is due to the positive electrode. In the absence of information on individual electrode potentials, the worst may be assumed, and all abnormal cell-voltage rise may be attributed to the negative only. Under these conditions, the voltage at which a significant fraction of the charge current will be converted to hydrogen is shown in figure 31 (Reference 76).

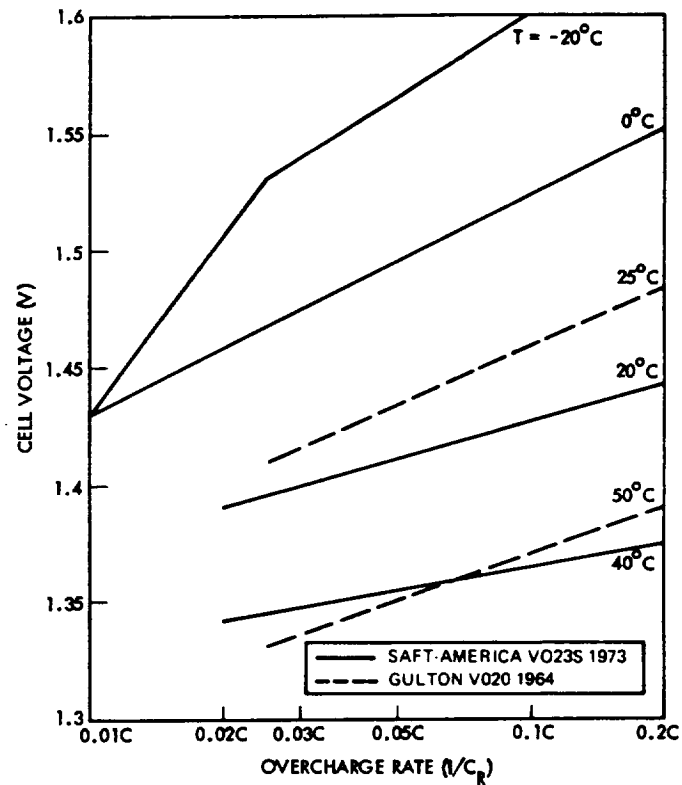


Figure 30. Overcharge voltage versus overcharge rate for SAFT-America cells (temperature a parameter).

As shown, maximum safe voltage is a function of cell temperature and charge rate. The rate effect shown is only for cells with an internal impedance of $50/C_R$ milliohms, which is typical of new cells with adequate electrolyte (figure 14). If the impedance is much greater than this, the maximum voltage levels are higher accordingly, and the difference between high and low rates becomes larger. Also, if the potential of the positive electrode is abnormally high, the cell voltage for hydrogen evolution will be correspondingly higher. It is because the hydrogen-evolution voltage of the cell is a function of all these variables that the condition of the cell must be completely defined to specify a voltage; in older cells, the negative electrode potential must be known to predict the probability of hydrogen evolution.

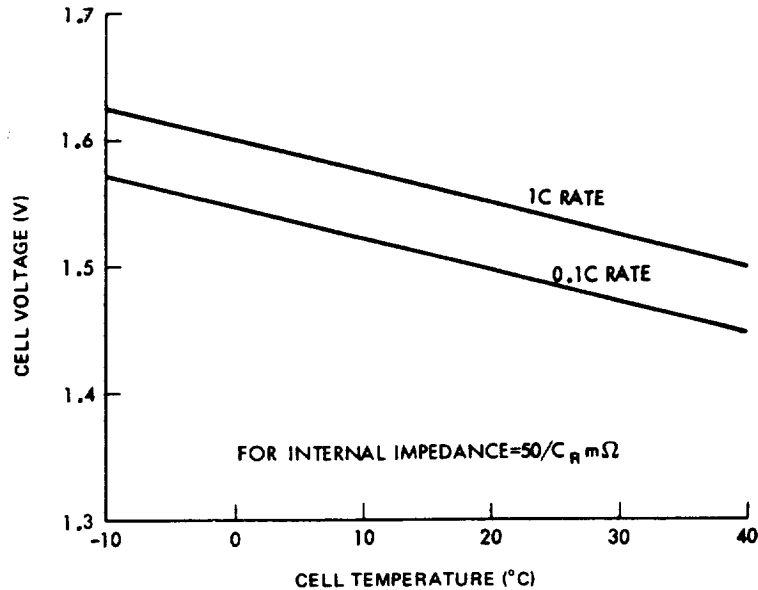


Figure 31. Charge voltage for significant hydrogen evolution.

End-of-Charge Current—When overcharge current is controlled by applying a voltage limit rather than vice versa, overcharge current becomes the dependent variable. Because true steady-state current is rarely reached in short-cycle operation, end-of-charge currents will be higher than those in figures 29 and 30 after charging under a voltage limit for only 60 to 80 minutes. End-of-charge currents under voltage-limit control are quite sensitive to the value of the voltage.

Oxygen Evolution and Pressure on Overcharge—Oxygen is usually the main gas responsible for pressure buildup during overcharge in cells with adequate overcharge protection. Although the rate of oxygen evolution from the positive electrode during overcharge may be calculated from the charge current and the incremental charge efficiency, oxygen pressure during overcharge is the most highly variable and unpredictable performance parameter the designer must deal with. This is because oxygen pressure is cumulative and depends not only on the rate of generation but on the rate of recombination at the negative electrode. The latter rate is, in turn, a function of the temperature at the plate surfaces, the amount and distribution of electrolyte in the cell, the nature of the negative-plate surfaces, and the residual void volume within the sealed container. Because pressure characteristics are a function of so many variables and because the amount

of electrolyte added can be varied to adjust overcharge pressure, pressure behavior can vary significantly from cell to cell and from lot to lot. A maximum overcharge pressure is usually listed in the cell specification, ranging from 50 to 80 pounds per square inch gage (psig). Limits on the low pressure side and on electrolyte quantity are also needed for minimizing problems from electrolyte redistribution. (See Section 4.5.3.3.)

Figure 32 shows the general effects of temperature and charge rate on oxygen pressure after extended overcharge in new SAFT cells containing about 3 ml of electrolyte per ampere-hour (Reference 76). The corresponding overcharge-voltage data appear in the previous section.

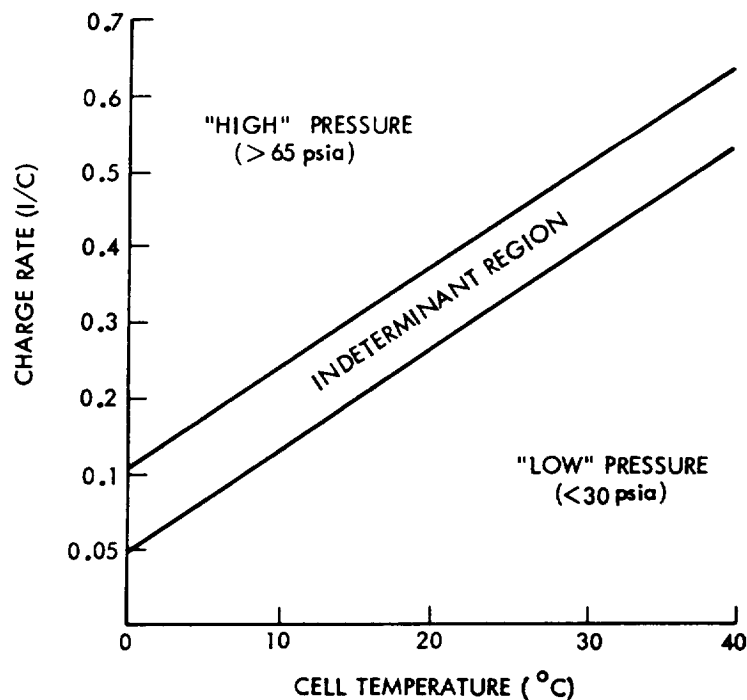


Figure 32. Overcharge pressure diagram for SAFT VO23S cell.

Charge Efficiency and Charge Acceptance—Some charge efficiency information in the literature is misleading because it is not labeled as either coulombic or energy efficiency.* Furthermore, average efficiency data are

*See Appendix A for definitions.

often not distinguished from incremental efficiency* data. This section describes both overall and incremental coulombic (ampere-hour) efficiency data, which may be combined with charge-voltage data to calculate energy efficiencies if desired.

Overall Charge Efficiency—Overall ampere-hour charge efficiency, as measured by the ratio of ampere-hours discharged to total ampere-hours charged, is a function of cell temperature, charge rate, recharge ratio, and discharge conditions. Figure 33 shows data for charging at 23 to 25°C ambient under conditions in which the recharge ratio was limited to unity. Some data have been published for cells made before 1969 that indicate much lower charge efficiencies than those in figure 33, particularly at lower charge rates. These older data may have been obtained on cells that contained impurities and may not represent cells made in recent years.

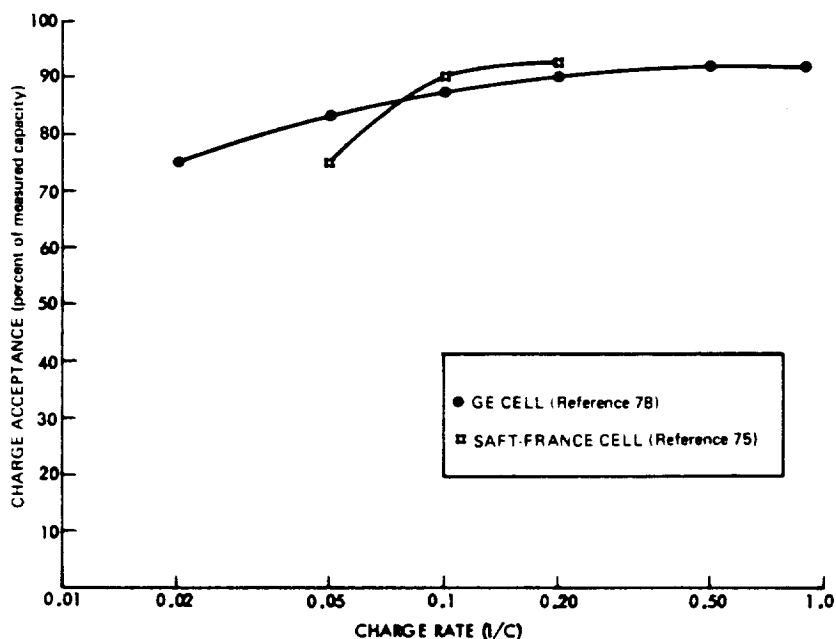


Figure 33. Charge acceptance at 23 to 25°C for 100 percent of rated ampere-hour throughput.

*See Appendix A for definitions.

Figures 34 through 36 show data that illustrate how overall efficiency depends on charge rate and throughput for one type of cell. These curves are for recharge after discharging to 1 volt and are taken from a report of a detailed experimental study of charge efficiency (Reference 75). Similar but less complete data for General Electric 50-Ah cells have been published (Reference 38). The position of the curves in the region from 0- to 25-percent charged is uncertain because the data there are erratic. This apparently results from an inherently nonreproducible charge acceptance at low states of charge. Charge efficiencies ranging from 22 to 85 percent after only a few-percent charge, beginning with a completely discharged cell, have been reported in connection with tests for internal shorts (Reference 79).

Maximum Achievable State of Charge—As charging is continued into overcharge and beyond, the dischargeable capacity of a cell at constant temperature and charge rate increases to a value that is dependent on temperature and rate and then levels off. This value is the maximum state of charge achievable under the given conditions. At lower temperatures, this level is reached at lower charge rates and/or with less overcharge than at higher temperatures.

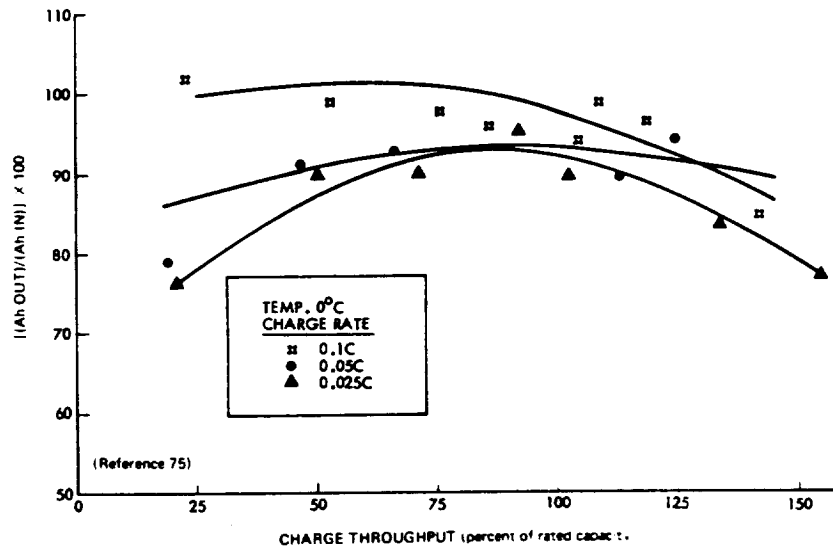


Figure 34. Overall charge efficiency versus throughput at 0°C (charge rate a parameter (SAFT)).

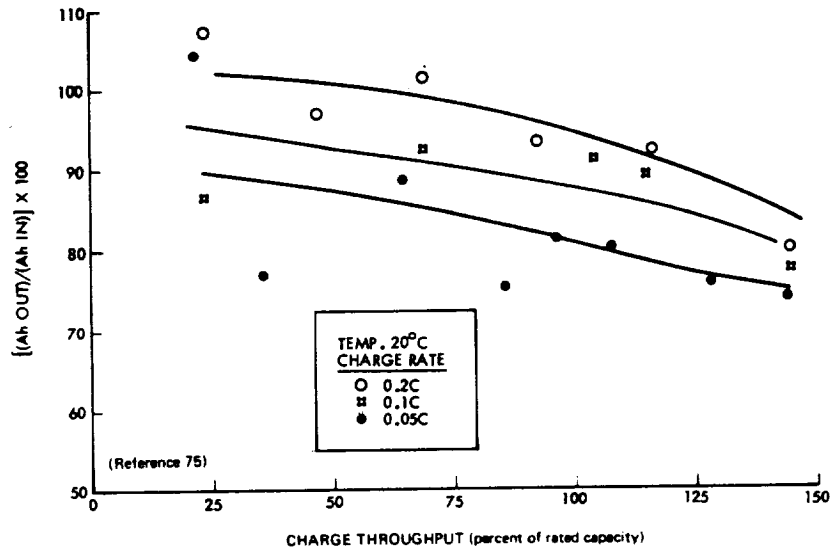


Figure 35. Overall charge efficiency versus throughput at 20°C (charge rate a parameter (SAFT)).

Figure 37 shows initial capacities as a percentage of rated capacity after returning 1.20 to 1.25 times the measured ampere-hour capacity as a function of temperature and charge rate for a SAFT VO23S cell (Reference 75). Charging was begun immediately after discharging at 0.5C to 1 volt. Measured capacities were greater than rated in the temperature range from -20 to +20°C.

Figure 38 shows capacities as a percentage of measured capacity after returning 1.0, 1.2, and 1.5 times the measured ampere-hour capacity (Reference 75). In the tests represented by figures 37 and 38, the 0.2C rate was not used below 20°C. The higher capacities at 0°C resulted from the fact that the capacity used for reference was measured with a throughput of 1.2 times measured capacity, beginning with the cells discharged to zero volts with 1-ohm resistors. Note that capacity was lowest with the lowest recharge ratio (1.0) at all temperatures and was the highest with the highest recharge ratio (1.5) at the higher temperatures (except at 40°C at the 0.2C rate). At -20 and 0°C, however, no difference occurred at the 0.05C rate between a 1.2 and a 1.5 recharge ratio. Cases have been reported in which capacity was greater after a lower recharge ratio than after

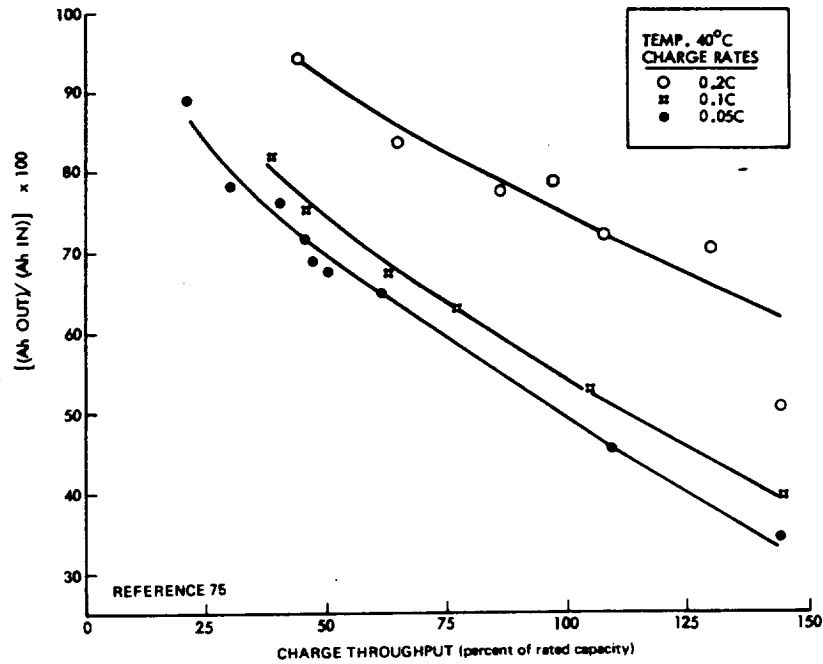


Figure 36. Overall charge efficiency versus throughput at 40°C (charge rate a parameter (SAFT)).

a higher recharge ratio. This effect is probably caused by a self-discharge resulting from a rising internal cell temperature produced by overcharge heat generation. More positive thermal control sufficient for limiting internal temperature rise to less than a few degrees above the control temperature should prevent capacity drop on overcharge.

In some cells, maximum achievable capacity at a given temperature is proportional to the logarithm of the relative charge rate (References 23 and 80). This relationship may be expressed as

$$\frac{C}{C_R} = k \log \frac{I}{I_R} \quad (10)$$

where C_R is a reference capacity (e.g., rated or standard capacity), and I_R is the charge rate corresponding to C_R .

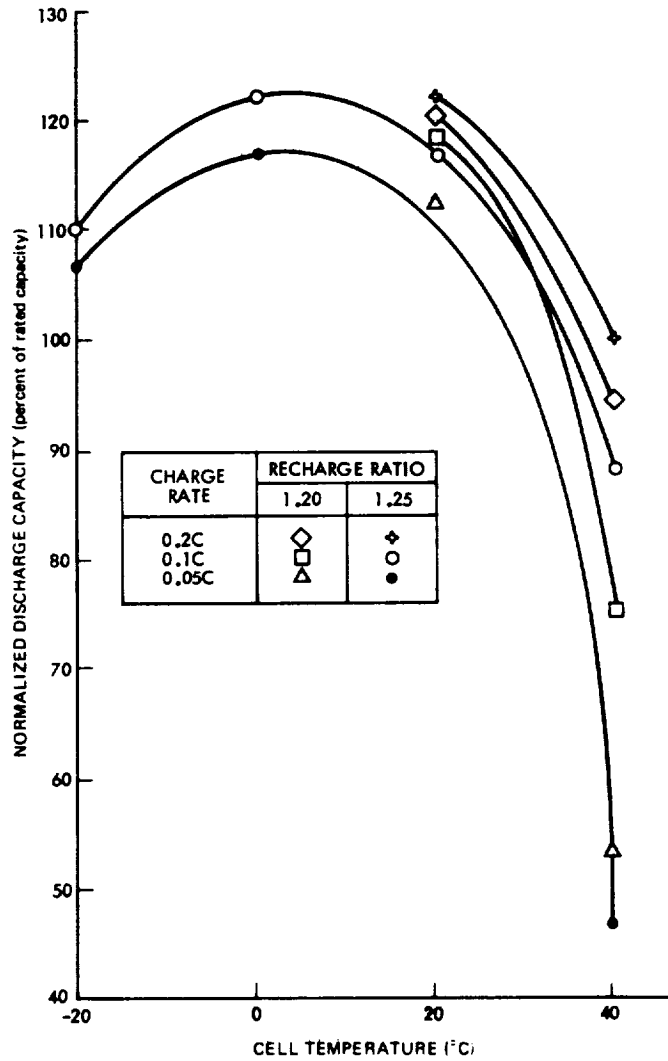


Figure 37. Discharge capacity as percent of rated versus temperature (charge rate and recharge ratio as parameters (SAFT)).

Incremental Efficiency—Incremental (instantaneous) coulombic efficiency data are useful for battery-system design and analysis because they permit a calculation of battery state of charge and heat-generation rate as a function of time on charge. Incremental efficiency data are displayed here: in plotted versus charge throughput and in plotted versus true state of charge.

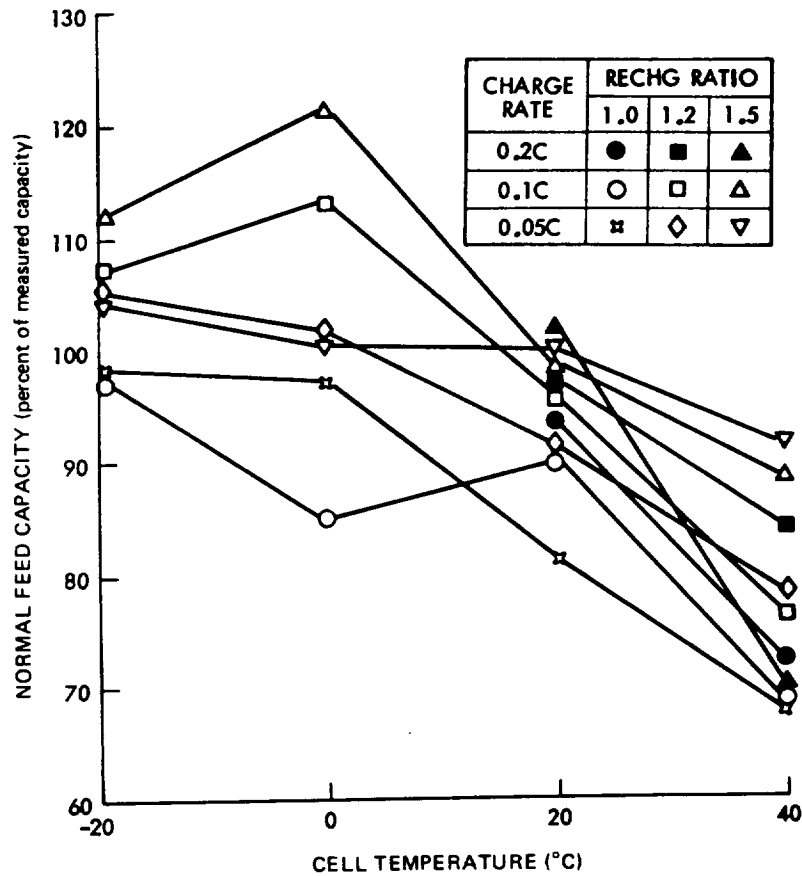


Figure 38. Discharge capacity as a percent of measured versus temperature (charge rate and discharge ratio as parameters (SAFT)).

Figure 39 shows plots of incremental efficiency versus charge throughput for SAFT cells (Reference 75), where the charge began after a discharge to 1 volt and capacity was measured at the 0.5C discharge rate.

Data for charge efficiency based on actual (true) state of charge is more fundamental and more useful for battery-performance analysis computations than data based on charge throughput. Bauer showed sets of curves for incremental charge efficiency plotted versus true (calculated) state of charge as a function of charge rate for several temperatures (Reference 2). These curves represent a synthesis of data from a number of sources. No new curves of this kind appear to have been published since that time.

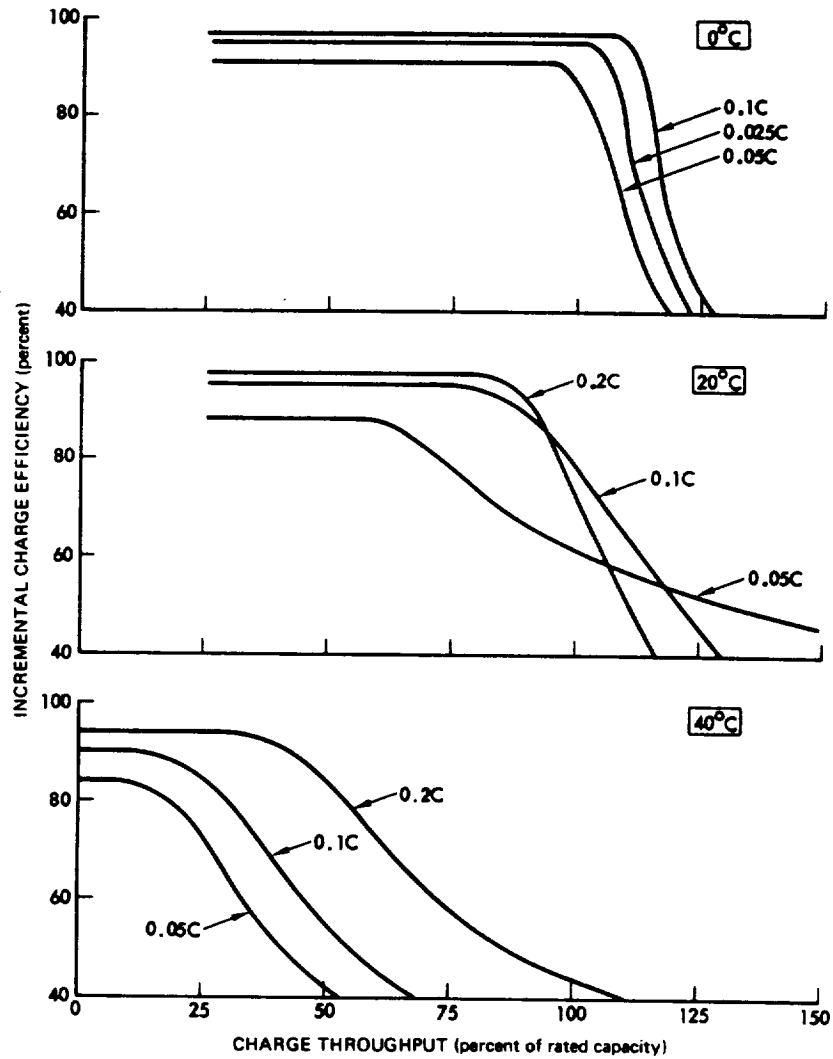


Figure 39. Incremental charge efficiency versus throughput for SAFT VO23S cells (charge rate a parameter) (Reference 75).

Figures 40 and 41 show families of incremental charge efficiency curves for 0 and 30°C, respectively, updated by the present authors using available new data. The characteristics of the SAFT cell change relatively little between 0 and 20°C. The most significant change from previously published

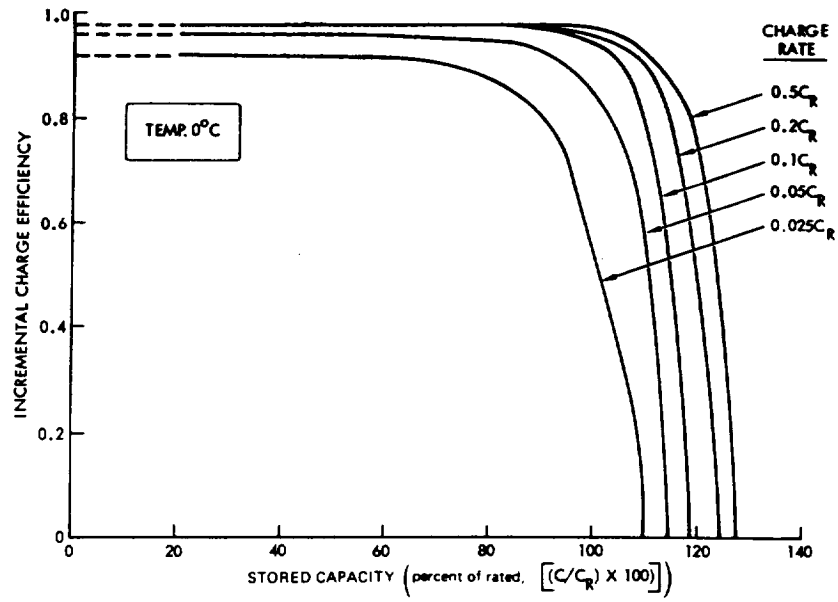


Figure 40. Incremental charge efficiency at 0°C versus stored capacity (charge rate a parameter).

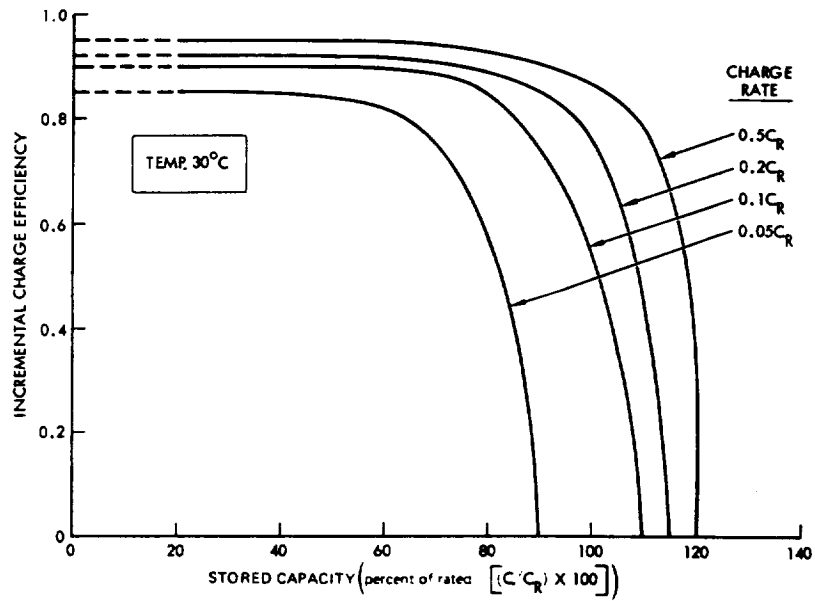


Figure 41. Incremental charge efficiency at 30°C versus stored capacity (charge rate a parameter).

data (Reference 2) is an increase in the achievable state of charge for many of the curves, as indicated by the data in figure 37, cell manufacturer's test data, and acceptance test data from the NASA evaluation program at NWSC/Crane.

As shown, these curves are believed to apply most accurately under the following conditions:

- a. Charging begins after a discharge to 1 volt/cell.
- b. Charging is at a constant current, except as noted in c.
- c. Cell voltage does not exceed limits shown in figure 27. If the appropriate limit is reached, charging continues at the voltage limit.
- d. Cell design and thermal control are such as to keep the internal cell temperature within 5°C of the given temperature.
- e. The following discharge, which is the measure of the state of charge reached, is begun within 1 hour after the main charge ends (i.e., open circuit or trickle charging after the main charge does not last more than 1 hour). Also, the discharge is performed at the given temperature, at the 0.5-C_R rate, and to 1 volt per cell.

Note that, because true state of charge cannot be measured directly when discharge is incomplete, the validity of these efficiency data for cycling to normal depths of discharge (e.g., 25 to 75 percent) cannot be determined directly. However, oxygen-evolution data (Reference 81), and the fact that the shapes of the charge voltage curves are similar for different initial states of charge, indicate that the data in figures 40 and 41 can be used to estimate efficiencies for charging from a nonzero state of charge by compressing the curves toward the right to fit the curve into the range of state of charge being used.

Charge Retention on Open Circuit—Nickel-cadmium cells gradually lose charge when standing on open circuit because of thermal decomposition of the charge material in the positive electrode. The rate of such loss is a function of temperature and state of charge and is usually determined by fully charging a group of cells and then discharging samples after different times on open-circuit stand.

Figure 42 shows a composite plot of open-circuit charge-retention data from several sources for stand periods of up to 90 days. The solid lines are curves through points for a single-cell design obtained in one study (Reference 82). Note that the self-discharge rates of cells of different designs, and made by different manufacturers, differ significantly, particularly at temperatures above 20°C. Also, considerable scattering of values around the trend lines shown is usually observed.

More data exists for charged open-circuit stand at room temperature over a 7-day period than for other stand temperatures and times because these conditions are often used for internal-short testing. Data from two sources

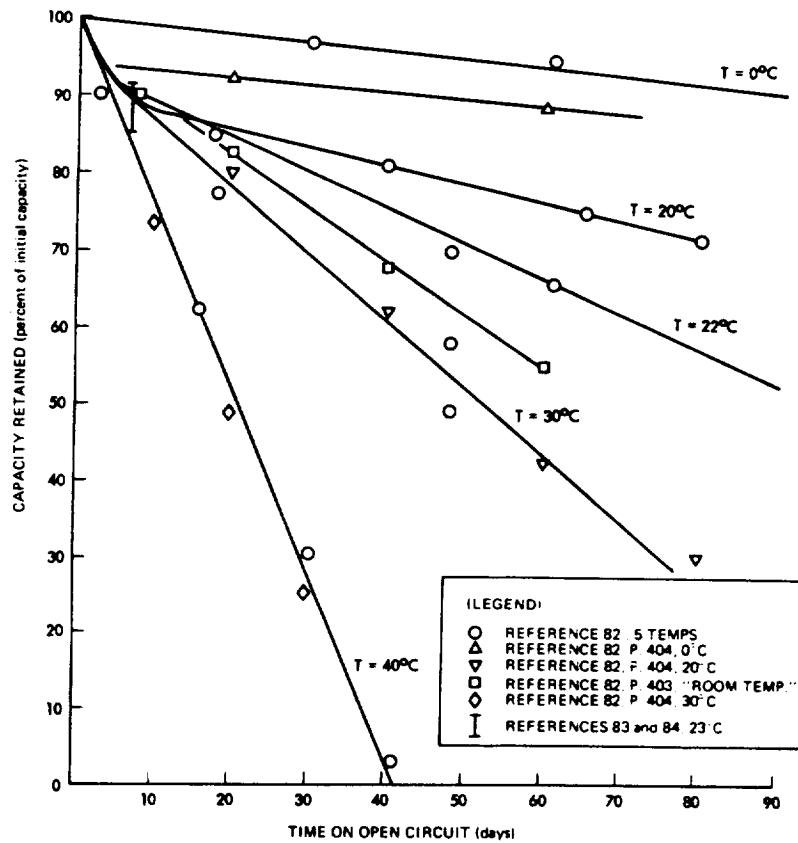


Figure 42. Average charge retention on open circuit versus stand time (temperature a parameter).

(References 83 and 84) show that capacity retention after 7 days ranges from 85 to 90 percent for cells from several U.S. manufacturers. During such a stand, the cell voltage normally decreases from 1.39 to 1.40 volts after the first hour to 1.29 to 1.30 volts after 168 hours. In the interim, the rate of change of voltage is linear with the logarithm of elapsed time (Reference 83).

Heat Generation During Charge—The total amount of heat generated by a sealed nickel-cadmium cell during charge, Q_c , is the sum of the heat generated by the charging of active materials, $(Q_c)_1$, and the heat generated by the overcharge reaction, $(Q_c)_2$:

$$Q_c = (Q_c)_1 + (Q_c)_2 \quad (11)$$

Because of the variation that usually occurs in the quantities that affect heat generation during charge, these heats are best calculated by integrating heat-rate functions over the charge time or by some equivalent summation of heat increments.

One or more of several expressions for heat-generation rate during active charge may be used, depending on the type of data available. The following equation is a modification of one given by Bauer (Reference 2):

$$(q_c)_1 \Big|_{T,p} = \frac{d(Q_c)_1}{dt} \Big|_{T,p} = -I_c \eta_c \left[(E_{rev} - E_c) + \frac{T|\Delta\hat{S}|}{F} \right]^* \quad (12)$$

where

$$(q_c)_1 = \frac{d(Q_c)_1}{dt} = \text{rate of heat generation from the main cell reaction in watts}$$

$$I_c = \text{cell current during charge in amperes, using the convention that charge current is positive (i.e., } I_c = |I_c|)$$

*For practical use in battery-system design, heat rates and heats are given here as heat generated (i.e., liberated) by the cell; hence, the signs of these quantities are opposite to those called for by thermodynamics convention.

η_c	=	incremental (instantaneous) coulombic charge efficiency
E_{rev}	=	reversible EMF of the cell (volts)
E_c	=	measured cell terminal voltage on charge
T	=	absolute temperature, deg K
$\Delta\hat{S}$	=	the entropy change per equivalent (joules K^{-1})
F	=	Faraday constant = 9.65×10^4 coulombs per equivalent
p	=	internal cell pressure

Equation 12 is strictly accurate only if temperature and pressure are constant. However, negligible error is introduced if the temperature varies as much as 20°C during charge or if pressure changes as much as 10 atmospheres. Therefore, in subsequent equations of this kind, the subscripts indicating constants p and T are dropped.

In equation 12, efficiency, η_c , and cell voltage, E_c , are functions of temperature, charge rate, and state of charge. As noted earlier, state of charge is a function of initial state of charge, charge temperature, and charge rate. Thus, evaluation of $(q_c)_1$ under actual operating conditions can be quite complex and is best done by computer. On the other hand, if I_c , η_c , E_{rev} , and E_c are assumed to be constant or if average values are estimated, corresponding constant average values of $(q_c)_1$ can be calculated for limited periods of time during charge.

The value of $\Delta\hat{S}$ for use in equation 12 is somewhat in doubt: reported values (Reference 2), range from -40 to -50 joules K^{-1} (-10 to -12 cal K^{-1}). This degree of uncertainty can effect the relative accuracy of the calculated heat rate that varies from small to large depending on the value of $(E_{rev} - E_c)$. Note that on charge $E_c > E_{rev}$; therefore, $(E_{rev} - E_c)$ is negative. Thus, $(\dot{Q}_c)_1$ will be zero when $|(E_{rev} - E_c)| = T |\Delta\hat{S}|/F$. At normal battery operating temperatures, the latter term $\cong 0.15$ volt.

The main source of uncertainty in using equation 12 is the term, E_{rev} . According to the derivation of equation 12 (see, e.g., Reference 2, p. 12), E_{rev} is the thermodynamic reversible potential of reaction 1. It is known that E_{rev} is a function of cell temperature. Values ranging from 1.25 to

1.30 are quoted in reviews of data for this quantity (References 2 and 85). It is uncertain if, at a given temperature, E_{rev} is a fixed value or a function of the state of charge of the cell.

A somewhat different expression for $(q_c)_1$ that does not contain the term, E_{rev} , and that is adapted from an equation for discharge derived by Brooman (Reference 73) is shown in the following equation:

$$(q_c)_1 = I_c \eta_c \left[(E_o - E_c) - T \left(\frac{\partial E_o}{\partial T} \right)_p \right] \quad (13)$$

where E_o = measured open-circuit cell voltage, and the other quantities are as defined for equation 12. Subscript p indicates constant pressure. Brooman does not give values for E_o or indicate how E_o might be measured. The only self-consistent set of data found for E_o is that published by SAFT (Reference 75) and plotted in figure 43. As may be seen, values for E_o were functions of temperature and recharge ratio (i.e., state of charge). Comparison of figure 43 with figure 27, which contain data from the same charges, gives values for $(E_o - E_c)$ ranging from -0.03 to -0.05 volt in the temperature range of 0 to 20°C. The slopes of the curves in figure 43 at 10°C, which give an estimate of $(\partial E_o / \partial T)_p$, range from -8 to -11×10^{-4} volt K⁻¹. Bauer gives a value of -2.3×10^{-4} volt K⁻¹ for dE/dT , where E refers to the reversible potential (Reference 2). It is apparent that the E_o values shown are not truly reversible potentials, but quasi-stable open-circuit values associated with the charging process.

A third expression for heat rate during active charge, also derived from one presented by Brooman (Reference 73), which contains no equilibrium or open-circuit voltage terms, is shown in the following equation:

$$(q_c)_1 = -I_c \eta_c \left(\frac{|\Delta \hat{H}|}{F} - E_c \right) \quad (14)$$

where, as before, $(q_c)_1$ is the rate of heat generation in watts, \hat{H} is the enthalpy or heat-content change in joules per equivalent, and I_c , η_c , F, and E_c are as defined for equation 12. The value of $\Delta \hat{H}$ at 25°C is well established at -140×10^3 joules (equivalent)⁻¹, thus making the first term in the parentheses in equation 14 equal to 1.45 volts at 25°C. The value of $|\Delta \hat{H}|$ should increase as temperature decreases, but no low-temperature values were found. Even so, equation 13 appears to be simpler and may be more reliable than either equation 12 or 13.

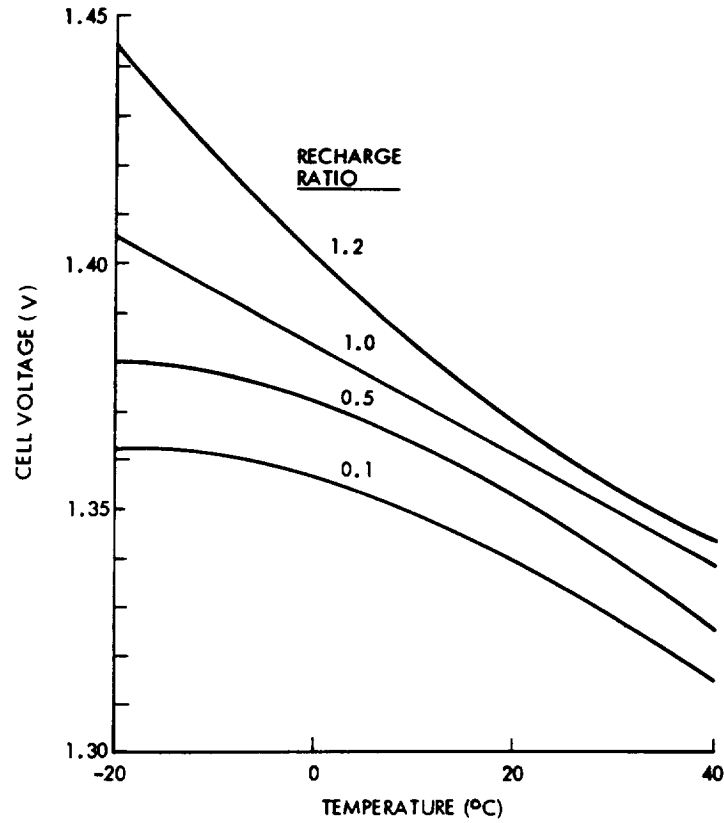


Figure 43. Open-circuit voltage versus temperature (recharge ratio a parameter (SAFT)).

The corresponding expression for calculating the rate of heat generation from the oxygen-transfer (recombination) reaction is as follows:

$$(q_c)_2 = I_c (1 - \eta_c) E_c \quad (15)$$

where $(q_c)_2$ is the rate of heat generated (liberated) in watts, and I_c , η_c , and E_c are as defined for equation 12. The rate of total heat generation during charge is therefore given by:

$$\begin{aligned} q_c &= (q_c)_1 + (q_c)_2 \\ &= -I_c \eta_c \left(\frac{|\Delta \hat{H}|}{F} - E_c \right) + I_c (1 - \eta_c) E_c \end{aligned} \quad (16a)$$

$$= -I_c \left(\frac{\eta_c |\Delta \hat{H}|}{F} - E_c \right) \quad (16b)$$

To calculate the total heat generated during charge or during any part of charge, equation 16 may be integrated with respect to time, and the result may be evaluated between the desired time limits. Thus,

$$\begin{aligned} Q_c \Big|_{t_1}^{t_2} &= \int_{t_1}^{t_2} q_c dt \\ &= - \int_{t_1}^{t_2} I_c \left(\frac{\eta_c |\Delta \hat{H}|}{F} - E_c \right) dt^* \end{aligned} \quad (17)$$

equation 17 shows that, if I_c , η_c , and E_c may be assumed constant for any part of the charge, the integral is evaluated as

$$Q_c \Big|_{L,\eta,E} = - I_c \cdot \left(\frac{\eta_c |\Delta \hat{H}|}{F} - E_c \right) \cdot (t_2 - t_1) \quad (18)$$

3.3.1.2 Effects of Cell Design Variations on Initial Charge Characteristics

Table 19 lists the qualitative effects of a number of cell design variations on key charge characteristics. These variables have the largest expected effects and are those over which the user has some degree of control by specification or approval of the manufacturing control document.

The higher the loading in positive plates, in terms of active material per unit gross area, the higher the overcharge voltage will be at a given charge rate, I/C, because the higher current density results in a more positive nickel-hydroxide electrode potential. Thicker plates with the same volumetric loading as thinner plates will have higher area loading than the thinner plates. This also implies that, at end of charge, the electrode reaches the oxygen-evolution potential at a lower state of charge and overall charge acceptance is therefore lower.

*Like q_c , Q_c is defined here as heat generated by the cell (not heat absorbed), and, hence, its sign is opposite to that of the thermodynamic heat change.

Table 19
Effects of Cell Design and Process Variables on
Charge Characteristics Relative to those of Reference-Design Cells¹

Variable Parameter	Active-Charge Voltage	Overcharge Voltage	Overcharge Press Rise	Initial Maximum Achievable Capacity
Plate loading	0	Increase ¹	Increase ¹	Increase ¹
Plate area	Decrease	Decrease	Decrease	0
Negative plate teflonation	0	Decrease	Decrease	?
Negative/positive ratio	0	See text	See text	+/-
Plate separation distance	0	Increase	Increase	?
Substitution of polypropylene for nylon	0	0	?	-
Final electrolyte volume	0	Increase	Increase	Increase
Void volume	0	0	Decrease	0
Precharge level	?	See text	See text	+
Decarbonation of plates	Decrease	Decrease	Decrease	0

¹All effects indicated are for an increase in the variable level or for the addition of a process, relative to that for reference-design cells (Section 2.5). ? = effect not clear cut; 0 = negligible or only slight effect.

Elder and Jost (Reference 80) found that positive plates made from a denser carbonyl-nickel powder (INCO 287) gave lower utilization under a wide range of conditions than plates made from a less dense powder (INCO 255), even though the unimpregnated plaque-void fractions differed by only 3 percent. End-of-charge voltage and pressure were higher with the former material. Denser plaque and the addition of cobalt to the active

material made charge voltage more sensitive to charge rate. Elder and Jost expressed their results in the form of the equation:

$$\text{Parameter} = k_0 + k_1 (\text{charge level}^*) + k_2 (\text{charge rate}) \quad (19)$$

where the parameter may be end-of-charge voltage, discharge capacity, etc. The calculated values for the constants are given in Reference 80 for various combinations of design factors.

High-loading of the negative plates also increases charge voltage (References 86 and 87), but to a lesser extent than with positive plates because the large excess of cadmium-active material present results in a lower initial negative electrode-current density. Lower loading facilitates charging at high rates and/or at low temperatures by keeping the negative overvoltage low and, hence, minimizing hydrogen evolution. Data for hydrogen-evolution electrode potentials are summarized by Gross and Glockling (Reference 88).

Within certain limits, negative-plate loading strongly affects overcharge pressure (due to oxygen evolution from the positive electrode), because the recombination rate decreases as loading increases and, hence, residual porosity and exposed nickel-sinter surface area decreases. Maurer (Reference 32) showed that a difference of 10 percent (from 30 to 40) in pore volume filled can result in a 10-fold difference in pressure. Because this effect is sensitive to the amount of electrolyte in the cell, these two design aspects must be coordinated.

Cell manufacturers claim that teflonated negative plates (Section 2.3.2.1.4) result in lower overcharge pressure at a given temperature, charge rate, and electrolyte level than nonteflonated plates with the same loading level. However, the independent effect of the teflonation treatment is obscured because more electrolyte is usually added to these cells to bring their pressure level up to that observed for nonteflonated negatives.

The ratio of negative-to-positive capacity in a cell (Section 2.3.3.5) does not *in itself* affect initial charge characteristics. It does affect the total excess negative capacity available and, hence, affects the total amount of charged excess negative and uncharged excess negative capacity that can be provided. A certain fraction of the total charged excess negative is referred to as "precharge" (Section 2.3.3.6). The exact effects of precharge and uncharged excess cadmium on initial charge behavior has been debated at

*The term "charge level" as used here is equal to (charge throughput)/(theoretical capacity).

length (References 32, 33, and 45), but still remains uncertain. An excellent review of this and related factors has recently been published (Reference 43), from which tables 20 and 21 are taken. Ford (Reference 45) and Turner (Reference 89) have reported that overcharge oxygen pressure decreases sharply as the precharge level is increased over a range of a factor of 5 in new cells. Font (Reference 90) found only a small decrease in pressure over a similar range of precharge. However, such an effect appears to diminish as cells are cycled. There is general agreement (References 32 and 45) that precharge should not be increased solely to reduce oxygen pressure in an attempt to compensate for other design defects.

Table 20
Qualitative Effects of Precharge¹ Level
(Reference 43)

	Little Precharge	Much Precharge
Oxygen pressure	High	Low
Capacity	Low	High
Cell beginning-of-charge voltage	High	Low
End-of-charge voltage ²	Low	High
Voltage recovery following short	High	Low

¹Precharge obtained at the expense of uncharged excess cadmium.

²High end-of-charge voltage is caused by the reduced amount of uncharged excess cadmium that can occur at high precharge levels.

Maurer (Reference 45) has attributed the effect of increasing precharge on initial oxygen pressure to an increase in porosity and surface area for recombination. Thus, any such effect would be expected to also be a function of negative loading level and electrolyte distribution, neither of which are directly controllable. Maurer has recommended that 10 percent of the negative be precharged (with a negative-to-positive ratio of 1.7) to avoid generating bursts of hydrogen when cells are charged from the completely discharged state.

Table 21
Qualitative Effects of Uncharged
Excess-Cadmium Level*

	Low	High
Cell end-of-charge voltage	High	Low
Cell end-of-discharge voltage	Low	High
Tolerance to high charge rate	Low	High
Tolerance to low temperature overcharge	Low	High
Tolerance to effects of separator degradation	Low	High
Tolerance to increase of positive capacity	Low	High

*Uncharged excess cadmium obtained at expense of charged excess.

Most cells made by existing commercial processes contain approximately 10 percent of the negative capacity as elemental cadmium (charged) material before any precharge adjustment is made. Although this material is initially electrochemically inactive, it may be measured by chemical analysis. This material may become partially activated after relatively few cycles, causing charge behavior to change accordingly. For this reason, charge behavior should not be finally judged until at least 20 to 30 cycles have been performed. This general approach may present the need for a smaller amount of added precharge, permitting a larger amount of uncharged excess negative material to remain.

A minimum of precharge is required for low-pressure operation in the temperature range from 0 to 20°C; greater precharge is required at both lower and higher temperatures, however, with the difference increasing as temperature extremes increase. Also, less precharge is needed at lower charge rates ($\leq 0.1C$) than at higher rates.

Finally, because various reactions within the cell tend to increase the amount of charged excess negative (Section 4), it is wise to err on the low side for initial precharge. However, precise data on quantitative relationships are lacking.

The amount of uncharged excess-negative material initially in the cell is at least as important for controlling charge behavior as the amount of precharge, particularly for applications such as synchronous orbit in which cells spend relatively long periods on charge. Dunlop (Reference 91) has shown that, in synchronous orbit tests, high end-of-charge voltage and hydrogen pressure correlated with a low level of electrochemically active uncharged excess-negative capacity. Ford (Reference 45) described how high voltage and pressure on overcharge may develop during prelaunch testing if insufficient uncharged excess negative is present. Maurer (Reference 32) points out that the utilization of the negative and, hence, the activity of the uncharged excess-negative capacity decreases as operating temperature decreases and charge rate increases. These relationships are largely responsible for the high end-of-charge voltage and the increase in hydrogen in the cell when operating at very low temperature (Reference 92). At spacecraft battery operating temperatures from 0 to 25°C, the extreme temperature effect can be ignored.

The minimum amount of electrochemically active uncharged excess negative should be 30 percent of the positive capacity for spacecraft operations (20 percent of the total active negative for a negative-to-positive ratio of 1.5), as measured on a new cell. However, the maximum possible amount of uncharged excess negative should be installed for any application that involves many cycles (>10,000) or long mission life (>3 years). This can be achieved by using the largest possible negative-to-positive ratio, achieving the highest possible utilization of negative material and minimizing added precharge. Increasing the negative-to-positive ratio should be done without increasing the negative plate loading over commercially available levels and may therefore reduce the initial specific energy levels. This is one of the more important tradeoffs, involved in optimizing cell design for a given application.

There appears to be little direct effect on charge characteristics of varying the separation (distance) between plates over the practical range of 0.1 mm to 0.3 mm (0.004 to 0.012 inch). Greater separation with no change of electrolyte volume will result in greater porosity of compressed separator material and, hence, lower overcharge pressures. Greater separation requires a larger and therefore heavier container. Other advantages of greater separation are discussed under long-term effects and failure determinants. Variations in charge behavior sometimes attributed to different

separator fiber material (e.g., polypropylene versus nylon) are more likely attributable to differences in the amount of electrolyte present and the distribution of electrolyte.

With a given design of the plates, plate separation, separator material, and dry void volume, the maximum amount of electrolyte that may be added before observing high and variable overcharge pressure is limited, as illustrated in figure 44. The weight of electrolyte per unit capacity that may be added without pressure problems is a function of many cell-design parameters. For example, teflonation of negative-plate material resulted in lower peak voltage and lower pressure (Reference 93) and permitted higher steady-state charging rates over a wide range of temperature with more electrolyte than possible with standard-type negative plates.

The residual void (gas) volume in a cell will affect the overcharge pressure considerably. The smaller the void volume, the higher the pressure will be under a given set of temperature, charge rate, and overcharge conditions. Any change in case dimensions or electrolyte volume without a change of plate-pack dimensions can change the void volume. A trend toward lower void volumes per unit cell capacity as capacity increases was noted in Section 2.3.3.4.

A final aspect of charge characteristics is oxygen-signal (or adhydrode) electrode voltage in cells equipped with these auxiliary electrodes. In general, two methods and locations of installation are used. One method places the auxiliary electrode with its plane perpendicular to the plane of the cell plates and locates it along one edge of the plate stack in the space between the edges of the plates and a narrow side of the case. The other method places the auxiliary electrode with its plane parallel to that of the plates and locates it either between an outside plate and a broad face of the case or in the plate stack between a positive and a negative plate. If adequate electrolyte is added and the electrolyte is well-distributed, initial signal-voltage behavior is usually normal and essentially the same for both configurations when nylon separator material is used (Reference 51). When the auxiliary electrode is located at the edge of the plate stack, signal voltage can be marginal and erratic with polypropylene separator material, presumably because of the lesser wicking capability of this material. Initial oxygen signal electrode performance was good with polypropylene separators when the auxiliary electrode was placed flat between two plates in the plate stack (Reference 51).

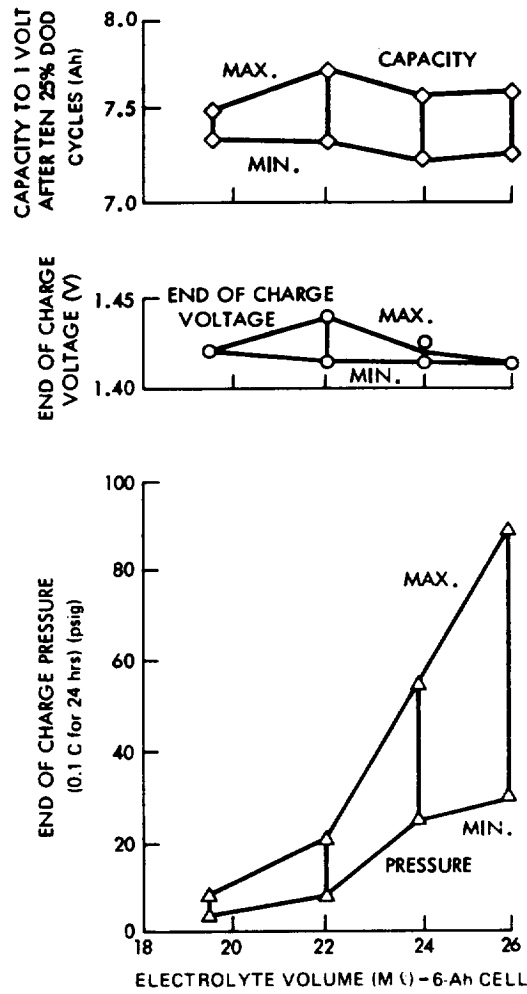


Figure 44. Discharge performance versus electrolyte level.

3.3.1.3 Effects of Cell-Manufacturing-Process Variations on Initial Charge Characteristics

In addition to design variations, certain manufacturing-process variations can affect initial charge characteristics. Some of these variations represent differences between the entire process as performed by different manufacturers; others represent changes that one manufacturer may elect to make in his process sequence from time to time.

Only a few organized studies of the effects of process variables have been published, and these dealt with only a few particular plate materials, some of which have not been produced commercially (References 8, 15, and 57). Very little such information is available for the processes used by the two largest suppliers of spacecraft nickel-cadmium cells in the United States.

One study (Reference 15) included both dry-sinter (loose powder) and slurry-coated sinter substrates, together with three types of impregnation, among other variables. Although some charge data are shown, the data were not analyzed to show the effect of those variables on initial charge characteristics.

Another study of process variables that involve only a dry-sintered plate process (Reference 57) found that the use of ten-flooded-formation cycles during platemaking gave significantly lower overcharge voltages and pressures in test cells than either one- or three-formation cycles. Note, however, that the cell assembly and test process used to make the test cells did not include any open-cell-formation cycling other than that done during platemaking.

Flooded-formation cycling (electrochemical testing) can remove a significant quantity of cadmium-active material from negative plates, and indeed this procedure is intended to remove loosely adherent material before the plates are installed in sealed containers.* The last discharge of the procedure is designed to determine if the resulting group of plates has retained the minimum required capacity of both positive and negative plates. Because the part of this discharge below zero volts is usually run at a low rate (e.g., 0.1C), it indicates the presence, but not necessarily the high-rate activity, of the excess cadmium material in the negative plates.

Another variable of the open-cell-formation procedure that apparently affects subsequent cell-charge behavior is the voltage to which the flooded cells are taken on the last discharge before the plates are washed and dried. Among other things, this discharge is used to establish that the minimum required electrochemical negative-to-positive ratio is present.* This involves discharging the cells into reverse, usually at the 0.1C rate. Different manufacturers have used cutoff voltages ranging from -0.25 to -1.0 volt. Some workers associate abnormally high end-of-charge voltage with cutoff voltages that are more than -0.5 volt negative, although no cause-and-effect relationship has been established. The difference is attributed to a difference in the amount of undischarged cadmium left in the negative

*G. G. Rampel, General Electric Battery Division, private communication.

plates with different end voltages. There appears to be sufficient weight of empirical evidence to support recommending a cutoff voltage no lower than -0.5 volt at the 0.1C rate. At the 0.5C rate often used for testing for excess negative capacity during acceptance testing, an end voltage of -1.0 volt is more appropriate.

A process step that affects initial cell-charge performance through its effect on negative plates is decarbonation. Certain manufacturers use this procedure to reduce the amount of carbonates in the plates before the cell is sealed.* Different procedures have been used, including "flushing" the cell with electrolyte either with or without cycling, overcharging, and then replacing the electrolyte and soaking the plates in electrolyte before assembling the final cell. All such procedures increase the porosity of the negative plates by removing solid material from the pores, thus increasing the effective void volume of the cell. Without compensation with added electrolyte, end-of-charge voltage and pressure are often lower with decarbonation than without. Decarbonation also removes active material from the plates along with the carbonate and may discharge part of the charged-cadmium content of the negative plates.

3.3.2 Initial Discharge Characteristics

The initial discharge characteristics (those observed before significant degradation has occurred) are less sensitive to cell design than charge characteristics. However, as in previous sections, discharge data for cells of known design are presented before an attempt is made to generalize.

3.3.2.1 Discharge Characteristics of Reference-Design Cells

Discharge Voltage—Discharge voltage is most often shown as a function of normalized output. Falk and Salkind present a comprehensive summary of such discharge curves for both vented (flooded) and sealed (starved) cells (Reference 5, pp. 325-334 and 384-389, respectively). However, these data are mainly for discharge rates in the range from 1C to 10C, which is used for terrestrial applications but not for spacecraft for which long cycle life is required.

Figure 45 shows average discharge-voltage curves that are typical of recently made reference-design spacecraft cells in the size range from 10- to 50-Ah capacity operating at an average temperature of 10°C. These cells

*G. G. Rampel, General Electric Battery Division. private communication.

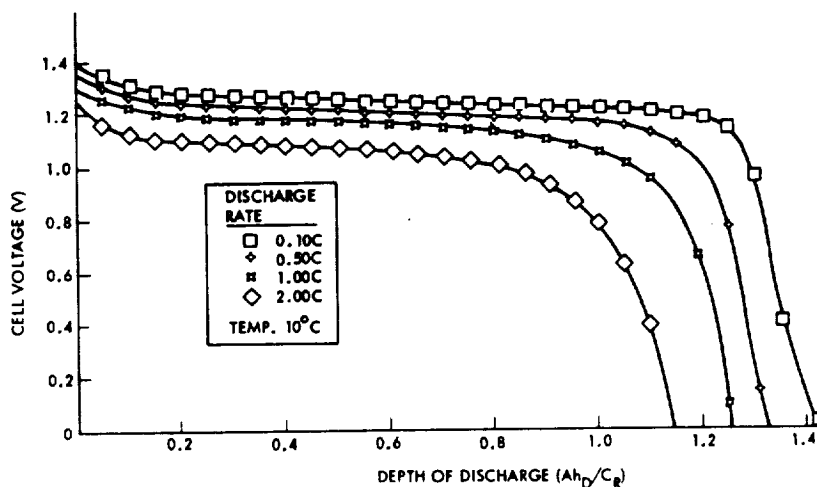


Figure 45. Discharge voltage versus depth of discharge for new cells at 10°C (discharge rate a parameter) (General Electric).

have an actual initial standard capacity that averages 120 percent of the manufacturer's rating (C_R). For cells with other ratios of actual-to-rated capacity, the scale of figure 45 can be adjusted accordingly.

Figure 45 shows, within 0.005 volt, the same discharge voltage at mid-discharge for operation at temperatures other than 10°C in the range from 0 to 20°C that is recommended for high-reliability designs at any given discharge rate. Lower temperatures increase the slope (negative) of the plateau, increasing the beginning of discharge voltage and decreasing the end of discharge voltage. Higher temperatures have the opposite effect on the plateau slope. These statements assume that charge control is properly adjusted to compensate for effects of temperature on charging characteristics.

The most important part of these curves is the "plateau" at which the voltage changes only slowly with ampere-hours out. At a given state of charge, this plateau voltage is approximately a linear function of discharge current over a wide range of current. This behavior lends itself to another kind of data display—current-voltage (I-V) curves—in which I-V relationships are shown as straight lines. This format may facilitate computer processing of the data. Bauer showed diagrams of this type for discharge at several temperatures (Reference 2). Section 3.3.3 contains I-V diagrams for currently manufactured cells.

Overdischarge voltage characteristics below zero volts (in the region of voltage reversal) may be used for predicting cell and battery voltage at end of discharge under abnormally prolonged loads. Figure 46 shows typical curves for new reference-design General Electric or SAFT-America type cells. These curves are extensions of those in figure 45 for the corresponding discharge rates. The plateaus shown by the curves in the region from -0.2 to -0.6 volt lend themselves to straight-line I-V formatting as previously described.

Gas Evolution and Pressure During Discharge—No gas evolution reactions occur during discharge in the normal discharge-voltage range (above zero volts). However, if discharge begins immediately after a charge at a moderate rate and low temperature, pressure may increase briefly at the beginning of discharge because of a delay in the normal gas evolution during charge. Other than this, the pressure normally decreases during discharge due to recombination of accumulated oxygen in the absence of oxygen evolution. If the gas in the cell at end of charge is largely hydrogen (usually occurring only after some degradation), the pressure decrease during discharge may be quite small because the rate of hydrogen recombination is low.

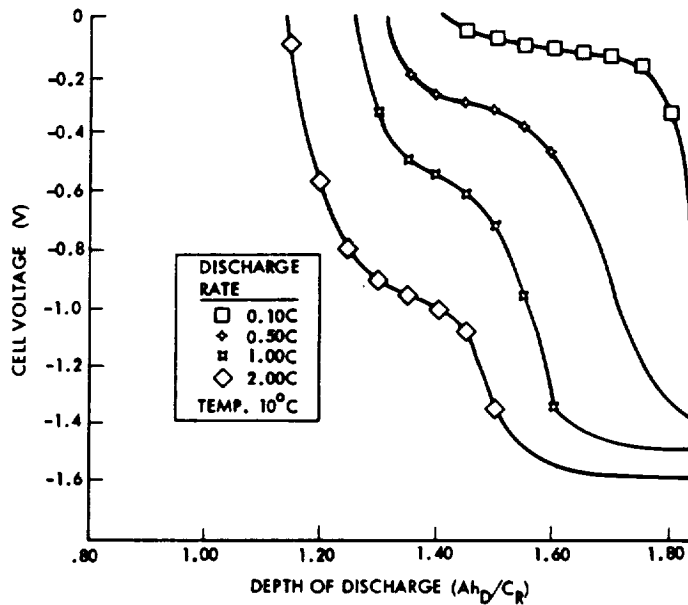


Figure 46. Overdischarge (reversed) voltage versus depth of discharge for new cells at 10°C (discharge rate a parameter).

During overdischarge and reversal of a new cell, hydrogen will be generated if the cell is positive-limited on discharge. The voltage plateaus below zero volts in figure 46 indicate that hydrogen is being evolved from the nickel-oxide electrode after the normal electrode reaction has been exhausted. If the cell is negative-limited on discharge (a condition that occurs in some new cells even though the cell is designed to be positive-limiting), the negative plateau, which occurs at about the same voltage as that of positive-limiting, indicates oxygen evolution from the cadmium electrode. In either case, because most of the discharge current goes to generating gas, pressure rise may be rapid at high discharge rates and, if not checked, can distort or rupture the case.

Reference 94 showed that, if the voltage of a cell is kept from going more negative than -0.2 volt during discharge (as by shunting the necessary discharge current), the rate of pressure rise may be kept to less than 30 psi per hour in reversal. If this pressure is caused by hydrogen alone, the pressure rise per cycle can accumulate to much larger values on repetitive cycling, especially if cycle time is short.

After extensive cycling, some cells can be reversed on discharge with little or no pressure rise (Reference 95). The mechanism of this effect is not known. A theory of hydrogen recombination during reversal has been proposed (Reference 12), but the rate of this process as reported is far too low to explain lack of hydrogen evolution at discharge rates up to 0.5C and greater. Although bridging between positive and negative electrodes by conductive cadmium filaments has been postulated, most tests for shorts in such cells have been negative.

Heat Generation During Discharge—The rate of heat generation during discharge may be calculated in a manner analogous to that previously described for the charge process in the section on "Charge Retention on Open Circuit," using equations analogous to equations 12, 13, or 14. There are:

$$(q_D)_{\text{gen}}]_{T,p} = -I_D \left[(E_{\text{rev}} - E_D) + \frac{T|\Delta S|}{F} \right] \quad (20)$$

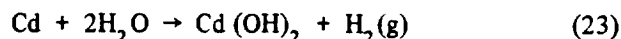
$$(q_D)_{\text{gen}}]_{T,p} = I_D \left[(E_o - E_D) - T \left(\frac{\partial E_o}{\partial T} \right)_p \right] \quad (21)$$

$$(q_D)_{\text{gen}} \Big]_{T,p} = - I_D \left(\frac{|\Delta H|}{F} - E_D \right) \quad (22)$$

where $(q_D)_{\text{gen}}$ is the rate of heat generation (i.e., heat evolved) during discharge,* and I_D is the discharge current, with the sign of I_D being negative (i.e., $I_D = -|I|$, where $|I|$ is the absolute value of cell current).

Equation 20 is the simplest to use because it contains the least uncertain quantities. (See Section 3.3.1.1 for discussion.) As the quantity $\Delta H/F$ equals 1.45 volts at 25°C, the heat rate is theoretically zero at a cell voltage of 1.45 volts and increases as the cell voltage decreases on discharge. By substituting values for discharge voltage from figure 45 into equation 20 it can be shown that the heat rate increases gradually during the voltage plateau and then increases rapidly as the cell voltage drops toward zero. This characteristic has been verified by measurements made with heat meters that have essentially zero heat capacity relative to the cell (Reference 71).

Data could not be found for heat rate during overdischarge involving hydrogen and/or oxygen evolution. It is assumed that the rate can be calculated by using the foregoing equations, but that values of E_{rev} , E_o , and ΔH , corresponding to the reaction that is actually occurring during reversal (which is not the primary cell reaction), must be used. For positive-limited cells, the overall reaction in reversal is as shown in the following equation:



Discharge Capacity and Energy Output—Discharge capacity (in ampere-hours or coulombs) to 1 volt, measured under controlled conditions, is useful primarily for evaluating the quality of new cells and for matching cells in new condition for inclusion in a battery. The use of 1 volt for cutoff is based on the facts that, for a new cell in good condition, very little energy can be withdrawn below 1 volt and that the voltage is decreasing very rapidly at that point at useful discharge rates. Figure 47 shows the average capacity obtained from a new cell discharged at the 0.5C rate as a function of the cutoff voltage. This curve was derived from the data in figure 45,

*As with heat generation during charge, the sign of the discharge heat rate is made positive in this manual when heat is evolved by the cell, and, thus, the sign is opposite from the thermodynamic heat loss.

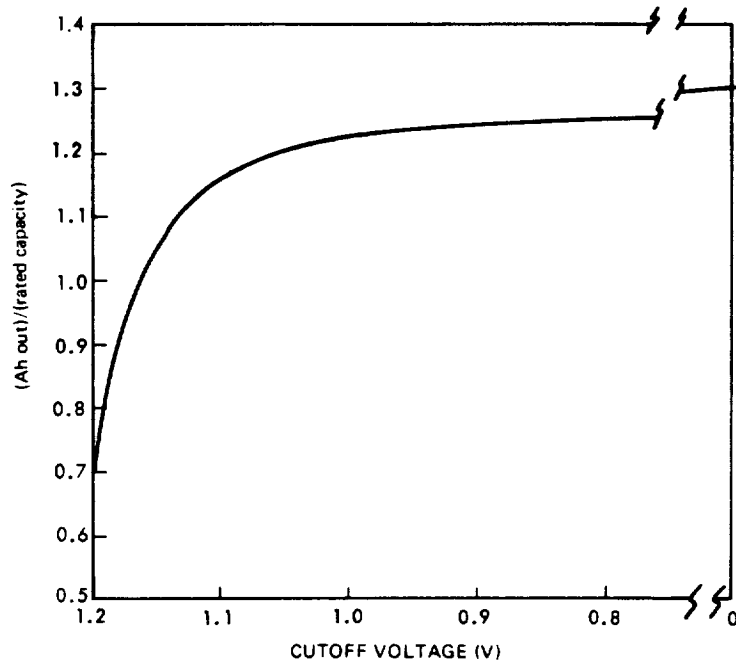


Figure 47. Capacity versus end-of-discharge voltage for new cells at 10°C (0.5C discharge rate).

which implies charging and discharging under standard conditions.* However, the shape of this curve changes significantly during cycling so that more and more capacity is obtained at lower voltage. Therefore, a cutoff of 1 volt is not necessarily appropriate for measuring the useful capacity of cycled cells, as discussed later under long-term effects.

Knowledge of relative capacity (i.e., actual capacity as a fraction of rated or standard capacity) achievable under a prescribed set of conditions is useful in sizing a battery for a given application. Achievable relative capacity is a function of cell temperature, charge rate, state of charge at the beginning of recharge, and extent of recharge. A previous section, "Charge Efficiency and Charge Acceptance," contained data for various types of cells.

When cells are charged at constant current without a time limit, the instantaneous charge efficiency eventually approaches zero as the capacity approaches its limiting value. Under such conditions, the achievable

*See Appendix A for definitions.

capacity may be estimated from efficiency versus state-of-charge diagrams (e.g., figures 40 and 41) by noting the capacity at which the incremental efficiency becomes zero.

For cells of a given design and mass, standard capacity is a measure of quality. For comparing cells of different designs and weights, specific capacity, or capacity per unit mass, gives a useful figure of merit. Although specific energy is often used for this purpose, it implies that the discharge voltage curve, or at least the average voltage on the plateau, either is known or can be assumed. Specific capacity is a design-related parameter that is relatively independent of the voltage of the plateau and therefore independent of specific use conditions.

Discharge energy is the time-integral of the product of voltage and current (power output). Thus, energy discharged above some cutoff voltage indicates how long the cell will support a constant power load above that voltage. The ampere-hour capacity indicates how long the cell will support a constant current load above a given lower voltage limit. Inasmuch as most spacecraft loads require constant power rather than constant current, discharge energy is a better measure of the ability of a cell to perform in a spacecraft power system than ampere-hour capacity.

Relatively little energy data are available because of the added cost of the equipment and time required for acquiring the needed intermediate voltage data and for making the computations. Modern automatic data-acquisition systems can easily obtain the input data, and a low-cost computer can make the necessary calculations either on-line or off-line. Because cell manufacturers have not yet availed themselves of this type of equipment, however, cells cannot now be cost-effectively tested for energy content at the manufacturer's plant. However, requirements for minimum discharge energy can and should be applied when selecting cells for batteries.

Most energy output values are obtained from constant-current discharge data. If the cell voltage remains relatively constant (on the plateau) throughout the discharge, constant-current discharge is adequate. If the voltage at the end of discharge begins to drop, a constant-current load will result in higher capacity and energy output than that of a constant-power load. Hence, the latter produces the more realistic data for cells intended for spacecraft usage.

When battery mass is of prime concern, specific energy* (i.e., energy per unit of cell mass) is a useful figure of merit if it is used in a definitive

*Specific energy is also referred to as "energy density."

manner. A rough approximation to output energy can be obtained by multiplying the ampere-hour capacity by the average discharge voltage (\bar{V}_D), if known, or by the mid-point voltage on the plateau. For new cells discharged to 1 volt at the 0.5C rate, this voltage is close to 1.2 volts; hence, much published specific-energy data have been calculated simply by multiplying specific capacity by 1.2. At higher discharge rates and after multiple cycles, average discharge voltage and capacity are less than they were initially; therefore, in-service specific energy is quite sensitive to the method and extent of use. Data in table 13 show the initial standard specific energy* (for $\bar{V}_D = 1.2$ volts) of commercially available reference-design cells to be 35 to 37 watt-hours per kg (16 to 17 Wh/lb) to 1 volt.

Utilization—Utilization describes the fraction of active material in an electrode or cell that is converted to electrical output on discharge. It may be expressed as the number of coulombs or ampere-hours per unit mass of active material present or as ampere-hours divided by the ampere-hours calculated as theoretically equal to the mass of active material. Expressed as a percentage, the latter fraction is often referred to as the “electrochemical efficiency.” This concept should not be confused with charge efficiency.

The theoretical coulombic equivalent of nickel-hydroxide [$\text{Ni}(\text{OH})_2$] for a 1-electron per mol change according to equation 1 is 0.288 ampere-hour per gram; for cadmium-hydroxide [$\text{Cd}(\text{OH})_2$] for a 2-electron per mol change is 0.366 ampere-hour per gram. Because the actual electron change per mol of $\text{Ni}(\text{OH})_2$ taking place on a nickel-hydroxide electrode is uncertain (Reference 9), the expression of utilization as a function of mass is preferred. Inasmuch as the active materials constitute approximately 25 percent of the cell mass in current designs, maximum utilization is a key to maximum specific energy.

3.3.2.2 *Effects of Cell Design Variations on Initial Discharge Characteristics*

This section considers the effects of cell-design (including component design) variations on the initial discharge characteristics of sealed nickel-cadmium cells. The characteristics discussed are voltage, utilization, specific capacity, and specific energy as observed during the first few cycles of operation under new-cell conditions. Section 3.4 covers the effects of such variations on long-term cell performance.

*Corresponds to the standard capacity; see Appendix A for definitions.

Most published data on effects of cell-design variables are for initial capacity because it is the most quickly and easily measured. In some cases, data are also given on utilization, energy, or specific energy. Because much of the data were obtained on electrodes operating under flooded conditions, they must be interpreted before they can be applied to complete, starved electrolyte cells.

Many variables affect utilization and specific energy, and many of them interact. A summary of the effects of some of the more important variables follows. References 5 and 96 contain additional information.

Plate (Plaque) Thickness—Within the range of discharge rates (up to 1C) used for most spacecraft applications, corresponding to current densities up to about 2 ampere/dm², little effect on voltage and capacity per unit area is observed because the thickness of the positive plates is varied by ±50 percent about the 0.8- to 0.9-mm (0.028- to 0.032-inch) range now offered by manufacturers if other variables such as plaque void fraction and area loading* are constant (Reference 5). At much higher discharge rates, utilization in thinner plates is distinctly greater than in thicker plates. Thickness of plates should not be confused with thickness of active material.

With a given impregnation procedure, loading and therefore capacity (to a first approximation) increases linearly with plaque thickness in the range from 0.7 to 1 mm (0.025 to 0.04 inch) (Reference 54). Thus, plaque thickness must be controlled if capacity per unit of plate area is to be uniform.

If the area loading is to be increased over levels now used (table 11), plate thickness may be increased to keep the volumetric loading (grams per unit volume of void) nearly constant. However, such thicker plates are subject to lower cycle life, as described in Section 3.4. With the area loading levels shown in table 11, plate thickness cannot be decreased significantly without causing the volumetric loading to become too high, thus reducing utilization.

Void Fraction and Pore Size—Void fraction (also referred to as porosity) and average pore size are discussed together because, with a given type of nickel powder and sintering procedure, average pore size increases as void

*Loading of active material per unit of apparent plate area.

fraction increases. This relationship can be modified, but not basically altered, by use of a pore former during plaque manufacture (References 8, 54, and 87).

Utilization of active material decreases as the void fraction (and pore size) increases (References 56, 59, and 97). Seiger et al. (Reference 56) show a linear relationship over the range from 72- to 90-percent void. Hence, if loading per unit area is held constant, capacity per unit plate volume will decrease with increasing void fraction. However, if the impregnation process is fixed as it is in commercial-cell manufacturing operations, higher void fraction will result in higher loading, compensating for the lower utilization during early cycling of the cell. Thus, Seiger et al. calculate that measured, flooded, positive-electrode capacity per unit volume of plate should vary by 1.2 percent (from 0.476 to 0.470 Ah/cm³) over the range of sinter void fraction from 77 to 85 percent. Seiger et al. further determined that the void fraction for maximum initial capacity per unit positive-plate volume is 77 percent and showed how the capacity per unit mass of positive plates depends on sinter void fraction.

Utilization has been shown to be constant and at a maximum when average pore size is below approximately 20 microns, decreasing sharply as pore size increases (References 59 and 97). Because utilization decreases as material thickness increases (Reference 17), the effect of pore size in the 10- to 50-micron effective diameter range appears to be the result of a variation in the average thickness of active material. Most published data apply to loading levels well below those now available; therefore, it is not certain how well the foregoing relationship holds at higher loadings. Also, pore size indicated was measured by the mercury-intrusion method in all cases, and this method has been shown (Reference 15) to indicate surface pore size but not necessarily pore size in the bulk of the sinter.

Table 22 shows average pore-size data for plaque used in positive plates for commercially available spacecraft cells. Therefore, pore size of available

Table 22
Available Plaque Pore Size Data (Positive Plates)

Manufacturer	Effective Average Pore Diameter (microns)	Reference and Date
Gould	10 to 15	56 (1966)
General Electric	10 to 20	98 (1969)

plate material appears to be optimum for maximum initial capacity per unit area. However, pore size is not directly controlled by cell manufacturers during platemaking; it is the net result of the type of nickel powder used, the density and viscosity of slurry used, and the sintering conditions. Being a function of so many variables, pore size is a potential source of trouble if it increases significantly from the normal range. Note that reports of a study of cell-manufacturing variables (Reference 57) did not mention plaque pore size.

Sizing and Coining—Sizing, or compaction of the plaque to control or reduce thickness before impregnation, reduces utilization at a fixed pore-fill fraction* (Reference 59). This effect may cause a manufacturer to load the plates excessively to compensate for the resulting reduction in capacity per unit plate area. Sizing is therefore usually undesirable. However, if thickness variations are excessive, they can lead to cell-behavior variations, making sizing a practical necessity. Closer control over unsized plaque thickness is preferable.

Coining reduces capacity per unit overall plate area (and, hence, per unit plate weight) in proportion to the fraction of area coined and to the thickness reduction used. Plate material that is compressed to less than 70 percent of its uncoined thickness is essentially inert. If present in a border approximately 2 mm wide, such coining corresponds to about 5 percent of the total plate area and associated capacity in a 20-Ah cell. Coined areas of positive plates having a thickness greater than 80 percent of the uncoined thickness provide little protection against physical damage during handling and against decomposition because of cycling in the cell (Reference 20).

Loading—Few data published during the last decade were found that relate capacity to loading level with other variables held constant. In one study involving plate material not currently available (Reference 54), flooded capacity of positive plates was proportional to loading over a range from 3.2 to 7 Ah/dm² (0.48 to 0.61 Ah/cm³ of total plate volume) for plates 0.7 to 1.2 mm (0.0264 to 0.048 inch) thick, respectively. The initial porosity of all plaque was about 80 percent (by mercury intrusion). The volumetric loading increased with plaque thickness because corrosion of the sinter increased with thickness. Utilization averaged 95 percent at the 0.5C discharge rate for these tests. Utilization of positive electrodes in

*The fraction of the original pore volume (after compaction) filled with solid active material.

starved cells made from the thicker plates and using an 80-percent electrolyte pore fill was 75 percent. This is the utilization level seen initially in General Electric and SAFT cells made with chemically impregnated plates. This large difference between flooded and starved utilization of positive-active material makes the use of flooded-capacity data to predict the starved capacity versus loading relationship rather uncertain.

A study of process variables (Reference 57) found that, at 23°C, capacity in electrolyte-starved cells was relatively constant with positive-electrode loading in the range from 11 to 15 g/dm² and was more than proportionately lower at a loading level of 8 to 10 g/dm². The lower utilization at the lower loading levels was probably due to insufficient electrolyte rather than lower loading *per se* because 5 percent less electrolyte was used in these cells.

The sensitivity of utilization to electrolyte level noted here is discussed in more detail later. In starved cells, more electrolyte can be added to compensate for the effect on capacity of reduced loading over a range of 10 percent (Reference 93). This fact will tend to obscure any clear elucidation of the effect of loading alone on capacity.

The positive-active material in reference-design cells amounts to approximately 15 percent of the cell mass. Therefore, a 10-percent increase in positive loading would result in a 1.5-percent increase in cell mass. Thus, the capacity and energy output must increase by more than 1.6 percent to produce an increase in specific energy. In addition, an increase in loading of positive plates can affect the long-term performance of the cell in ways that may be more serious than the impact on cell mass for a given application. (See Section 4.)

Effect of Cobalt in Positive-Active Material—The effect of cobalt (as an additive to positive-active material) on initial charge acceptance and capacity has been a subject of a number of studies. One of these (Reference 23) showed that 20-percent* Co (OH)₂ was optimum within the range of 5 to 40 percent tested. This study emphasized higher-temperature (e.g., 65°C) performance, in which charge acceptance (at the 0.1C charge rate used) without additives proved to be poor. At 25°C, utilization with 10- to 15-percent cobalt was nearly the same as that for 20-percent cobalt—10 to 20 percent greater at the 1C discharge rate than without cobalt.

*Because the molecular weight of Co (OH)₂ is almost identical to that of Ni (OH)₂, a given weight percent is numerically the same mole percent. Hence, it is not necessary to designate which type of percentage is meant.

The increase in discharge capacity (to 1 volt) produced by introducing cobalt is accompanied by a decrease in the plateau voltage (Reference 20). Thus, although added cobalt increases initial specific capacity, it may not increase specific energy deliverable to a constant power load.

Another study involving electrochemical impregnation (Reference 20) found that 10 percent cobalt was optimum for capacity at the 1C discharge rate when high-temperature performance was not required. This study showed that, based on $\text{Ni}(\text{OH})_2$ content, utilization of active material increased faster than the increase in total weight of $\text{Ni}(\text{OH})_2$ plus $\text{Co}(\text{OH})_2$ as the percent of cobalt in the mixture was increased in the range from 0 to 10 percent, then decreased at higher cobalt percentages. These results were obtained at loading levels well below those of currently available spacecraft cells, however, and information on the effect of cobalt use at higher plate-loading levels is not available.

A third study (Reference 80) included a wider range of conditions than that of the preceding work. This study showed that the results from cobalt addition at 4.4 percent (the only level tested) is dependent on many variables. At high charge rates and recharge ratios of less than 1, the cobalt increased charge acceptance, whereas, at low charge rates and considerable overcharge, little benefit occurred (at 4.4 percent) at 23°C. The foregoing results indicate that the level of cobalt tested here was too low for optimum effect. Many interactions with other design variables and operating conditions were observed, and the results are presented in the form of coefficients of general equations for capacity as a function of charge rate, charge coefficient,* and discharge rate.

No data were found for comparative testing of cobalt additive at temperatures below 23°C. Because of the inherently better charge acceptance of $\text{Ni}(\text{OH})_2$ at lower temperatures, considerably less benefit would be from cobalt at 0°C than at 25°C. However, there appears to be no disadvantage to carrying cobalt in the range of 5 to 10 percent of the positive-active material in cells used at low temperature.

In general, cobalt levels above 10 percent (as $\text{Co}(\text{OH})_2$) should be necessary only if the cell must operate at high temperatures and maximum capacity is required. Cycle life will still be short under these conditions, however, and testing of the particular plate material to be used for high temperature performance is advisable.

*Charge coefficient = (ampere hours charged)/(ampere hours of measured capacity).

Effects of Negative-Electrode Design on Initial Discharge Characteristics—

As with positive electrodes, two aspects of electrode design are distinguished: (1) intrinsic aspects, such as plaque structure and loading level; and (2) overall aspects, such as total negative-plate area, negative-to-positive ratio, and precharge level.

The degree of impact of negative-electrode design variations on initial cell discharge voltage and capacity is small for cells designed to be positive-limited (as are all sealed cells in commercial use today), but it is large for cells designed to be negative-limited, such as those studied under recent contract efforts (References 99 through 101). However, any design aspect that affects negative-material utilization will affect the amount (mass) of material required for achieving a given negative-to-positive ratio and will therefore affect the mass and initial specific capacity of a positive limited cell.

Gross (Reference 88) summarized published information on sintered nickel-cadmium-plate design, including the points that maximum initial utilization at normal discharge rates occurs at low active-material loading levels and with sinter pore size in the range from 10 to 20 microns. Because low loading and small pore size both imply low cadmium-plate capacity per unit plate mass, tradeoffs are involved in reaching an optimum. Such tradeoffs must also consider the expected changes in cadmium-electrode activity with cycling, which are much greater than those for the nickel-hydroxide electrode. Section 3.4.1 describes cycling effects.

In one study, including indium compounds as part of the active material in sintered cadmium plates improved utilization, particularly at high rates and/or low temperatures (Reference 90). Indium has not been used commercially because, for most applications, the degree of effect does not justify the high cost of this material.

Evidence for a beneficial effect of added nickel hydroxide on initial capacity is contradictory. Because all tests show that nickel additions result in a second, lower cell-voltage plateau on discharge after cycling, this additive does not appear to be beneficial in the long run (Reference 88).

"Teflonated" cadmium plates have a somewhat lower initial utilization than nonteflonated plates (Reference 54); therefore, a given electrode mass provides a smaller initial excess over the positive capacity. However, because life-test data to date indicate that teflonated negatives exhibit less fading with cycling (Section 3.4.1.6), no additional mass may be needed for an adequate negative excess at end of life.

Nonsintered cadmium-plate designs, such as the so-called "sponge" type and various pressed composition types have been proposed for spacecraft nickel-cadmium cells. These materials have significantly lower mass for a given negative capacity than sintered plates but suffer from much more rapid fading with cycling. Nonsintered cadmium plates have been flown in silver-cadmium cells but not in sealed nickel-cadmium cells.

When adequate excess negative capacity is installed, the only overall aspect of negative-electrode design known to affect initial capacity is the precharge level. Seiger reports that an amount of precharge (by venting oxygen) equal to 20 percent of the positive capacity is required to obtain the maximum cell capacity from a new cell (Reference 8). However, one study showed that this effect of initially added precharge disappeared after 10 cycles, after which capacity with no added precharge equaled that in cells with large amounts of precharge (Reference 102). This result, obtained by using a 130-percent recharge ratio, is consistent with the effect of cycling and overcharge described by Maurer (References 32 and 45), whereby inactive excess charged negative is converted to active charged excess and therefore has the same effect as that of precharge added by adjustment.

The effect of separator design on initial capacity is not well-defined. Occasional comments appear in the literature to the effect that lower capacity was observed with a polypropylene separator than with a nylon separator (i.e., Pellon 2505). No such difference has been observed under controlled test conditions in programs in which special attention was given to obtaining adequate electrolyte in the cells (References 51 and 103). The authors believe that the lower initial capacities that some observed with polypropylene were due, not to the separator material *per se*, but to the fact that the electrolyte present in the cell or in the separator was insufficient to provide full capacity.

When the cell is finally sealed, the amount of electrolyte, if too small, can result in low discharge voltage and/or capacity. The optimum amount for a particular cell design is a function of plate and separator design and, more specifically, of the residual dry void volume of the plate stack. For cells made with chemically impregnated plates such as those now commercially available, initial capacity is affected when the level of electrolyte is less than about 2.5 ml/Ah of capacity. With electrochemically impregnated plates, this effect occurs at about 3 ml/Ah per ampere-hour, presumably because of the higher plate void volume per ampere-hour.

3.3.2.3 *Effects of Manufacturing-Process Variations on Capacity*

Initial specific capacity and specific energy of cells are probably affected by many process variables. Discussion of all such variables is beyond the scope of this manual. Those having the greatest effect per unit of cell mass are considered here. Although they were produced by different processes, products (plates and cells) with the same physical properties are compared.

Whether the plaque used for impregnation is made by the dry (loose) or by the slurry-coated sinter process does not appear to affect initial flooded capacity of positive plates having a given thickness, plaque void fraction, and loading level. On the other hand, whether the plaque is impregnated by the chemical or by the electrochemical precipitation process has a sizeable effect. Generally, utilization of active material in chemically impregnated (CI) plates during flooded formation cycling is about 0.26 ampere-hour per gram (from manufacturing test data) or 90 percent of theoretical. Utilization of electrochemically impregnated (EI) plate is reported (Reference 17) to be 0.31 to 0.33 ampere-hour per gram (110 to 115 percent of theoretical) under similar conditions. Because the ratio of starved-cell capacity to flooded capacity is about 0.85 for both types of plates, less active material and less plate material (and mass) are needed for a given capacity for EI plates, and initial specific capacity and specific energy will be correspondingly greater.

In one study, increasing the number of electrical cycles first used on newly impregnated positive-plate material (referred to variously as first formation or electrochemical cleaning) increased the initial capacity of positive plates (Reference 57). Thus, variations in details of initial formation appear to be responsible for some observed low and/or variable capacity in completed cells. Most manufacturers perform additional formation cycling of plates in the form of open cells before assembling the spacecraft cell. This tends to minimize the effect of variations attributable to earlier formation processing. The cell user is normally not in a position to influence the procedure for either of these formation steps, but should attempt to determine if they are properly controlled.

3.3.3 **Initial Cyclic Charge and Discharge**

Previous sections described charge and discharge behavior immediately following the reconstituting effect of complete discharge as obtained on a resistive short-down (i.e., before significant change in the cell physics and

chemistry has occurred). This section reviews differences from the initial behavior observed to the result from limited continuous cycling* (such as that used for acceptance testing). This information applies to about the first 50 cycles at the beginning of cell life, during which it is assumed that the cells are shorted down several times.

During continuous cycling, the cell is charged and discharged differently than for a one-shot cycle. The cell is charged for a shorter period of time and often with an imposed voltage limit, and discharge is not carried to completion, but usually is limited to a value considerably less than the rated capacity. Under such conditions, the cell usually does not have time to become as fully charged or as fully discharged on any one cycle as on the longer one-shot type cycle, and cell behavior is modified accordingly.

The cell voltage and internal-pressure profiles during continuous cycling are functions of cycle length, operating temperature, depth of discharge, charge rate, and charge-control method used. During acceptance testing and capacity measurement of cells, as well as during eclipse seasons in a synchronous equatorial orbit, cycle length is on the order of 24 hours, temperature is usually 5 to 25°C, and charge rates are 0.05C to 0.1C. Under such conditions, the behavior shown in figure 48 is typical of a system operating at 0 to 15°C, in which charge control involves switching from a constant 0.1C rate to a constant 0.01C rate for overcharge. Auxiliary (oxygen signal) electrode voltage and cell temperature are also shown for reference. As may be seen, cell voltage, pressure, temperature, and auxiliary electrode voltage rise together as the cell approaches full charge. The dashed-line extensions indicate the behavior to be expected if charging were continued beyond the point at which switching to the lower level occurred. The degree of increase in cell voltage (and pressure) is less at higher temperatures, as shown by figures 21 through 25. The extent of temperature rise is a function of the thermal design of the cell, the battery structure, and the heat sink. (See Section 8.)

Figure 49 shows a typical initial performance profile of a cell operating in a 100-minute cycle without voltage-limiting on charge. Higher charge rates are involved than those normally used for longer cycles, and, consequently,

*Continuous cycling as used here means that more than one cycle is performed consecutively and that each discharge or charge follows the previous opposite half-cycle either immediately or with an intervening period of trickle charge or open circuit that lasts for only a fraction of the normal cycle period.

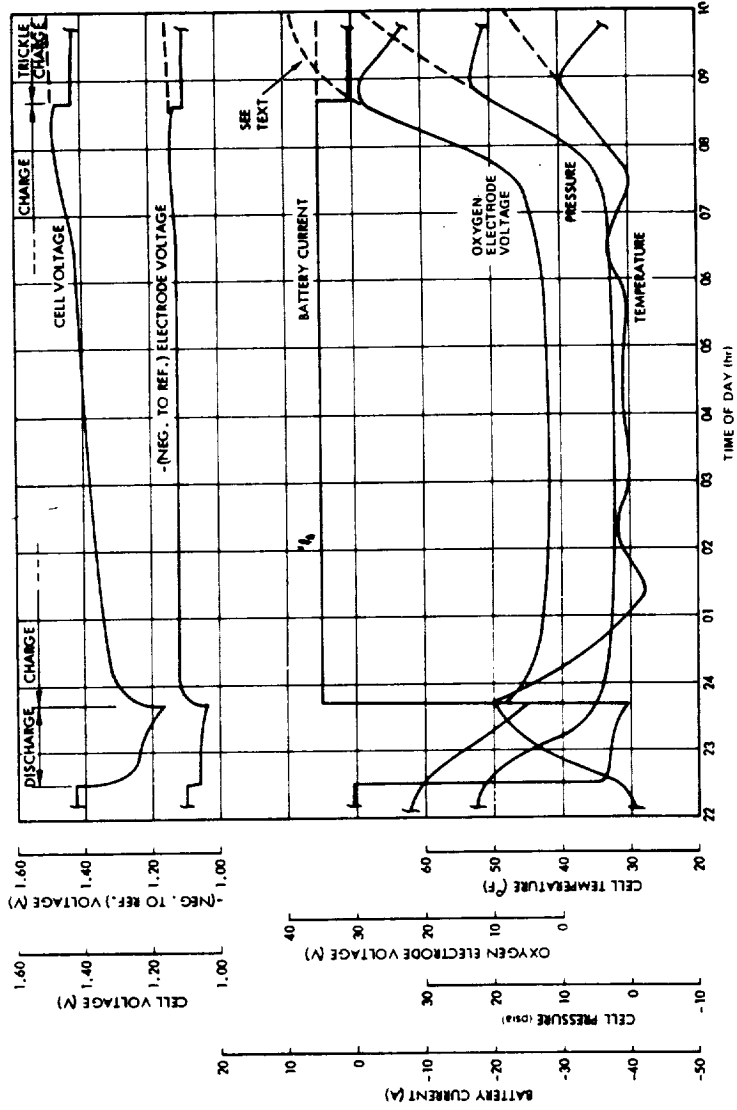


Figure 48. Typical cell performance characteristics in a 24-hour cycle.

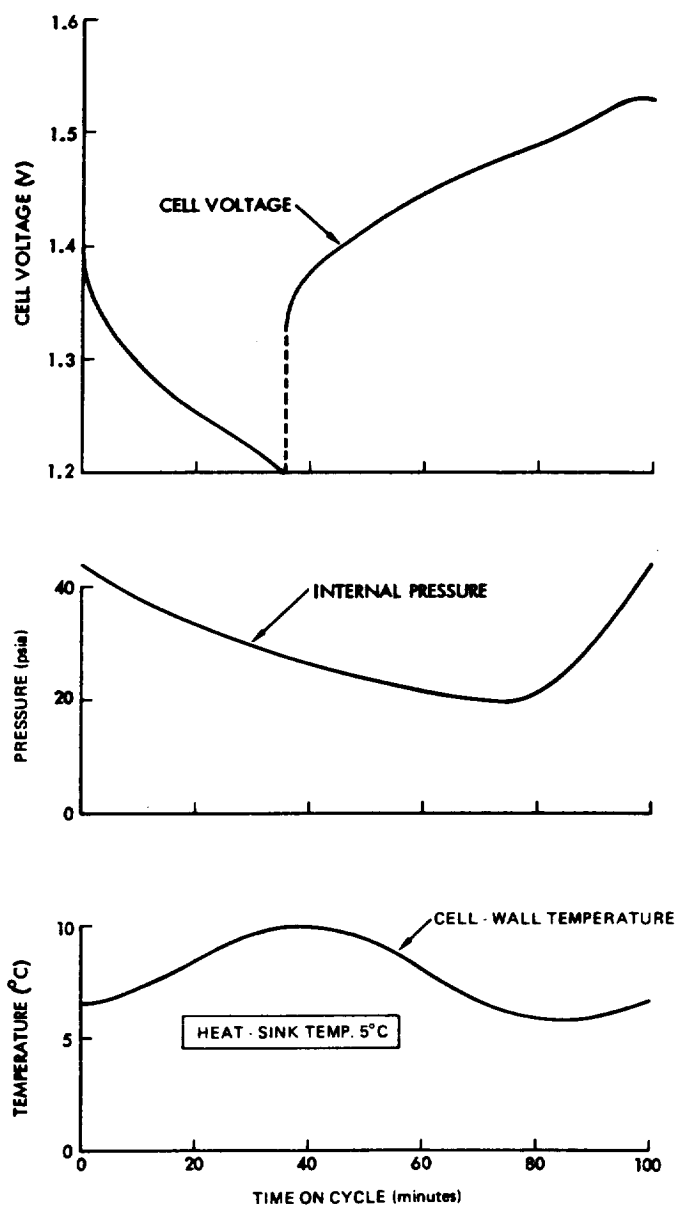


Figure 49. Typical cell performance characteristics during 100-minute repetitive cycling without voltage-limiting.

end-of-charge voltage is higher. For depths of discharge over 10 percent, charge voltage must be limited at moderate to cool temperatures to limit overcharge and, hence, to prevent pressure buildup.

Data for a cyclic operation may be displayed for analytical purposes in the form of families of current-voltage (I-V) curves as a function of state of charge and cell temperature. Figure 50 shows one such family of curves that is appropriate for initial cycling of reference-design General Electric cells. The I-V characteristics of recent vintage SAFT-America cells are similar except that charge voltages are higher at states of charge above 0.8. Consistent voltage data for Eagle Picher cells were insufficient for constructing a curve set. The position of these curves changes significantly with additional cycling without reconditioning; therefore, different sets are needed to represent different stages of voltage degradation.

3.4 LONG-TERM PERFORMANCE CHARACTERISTICS

As defined here, "long-term" covers more or less continuous use for periods ranging from a few weeks to 10 years or longer for which data may be available. Data on observed ranges and trends of key performance parameters are summarized and correlated. The information is intended for use in battery design in that it may be used to "size" the battery (i.e., to select the the initial cell capacity and number of cells required for meeting system requirements and to select the operating conditions and controls that best fit the system constraints). The information is separated into that applicable to low-Earth (short-orbit) use, and that applicable to high-altitude and other long-cycle use. This is done to facilitate use of the data for specific applications and because many aspects of performance differ significantly between short and long cycles.

3.4.1 Performance Under Continuous Short-Cycle Conditions

This section presents information relating to essentially continuous-type cycling with cycle times ranging from 90 minutes to 3 hours. Most data are available for cycle periods in the range of 90 to 110 minutes. Table 23 lists references from which most of the data summarized here were taken. In terms of both total cells tested and length of time on test, the largest single test program is that at NWSC/Crane. Each NWSC annual report (Reference 68) describes this program. A majority of the analysis reports listed in table 23 deal entirely with data from the NWSC/Crane test program.

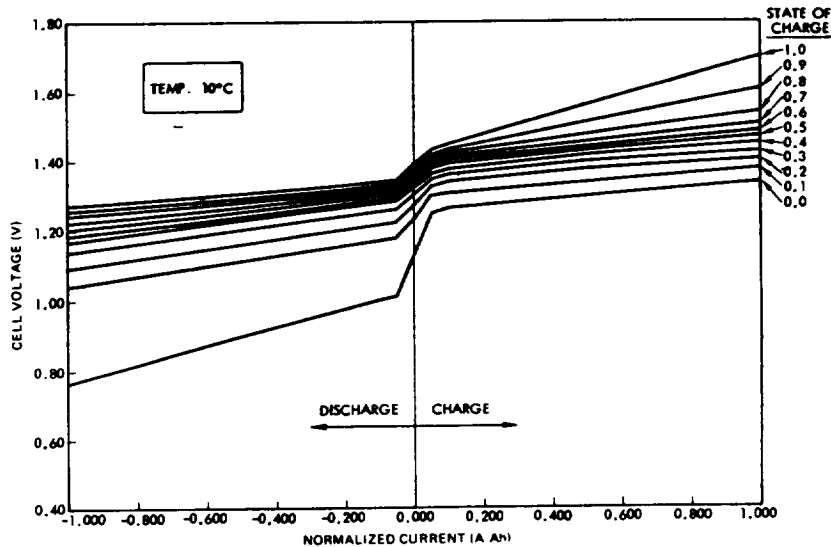


Figure 50. Current-voltage curves for cycling at 10°C (state of charge a parameter).

The types of information sought for inclusion here include: (1) cell voltage during cycling, (2) cell pressure during cycling, (3) cell capacity after cycling, and (4) life expectancy. Each of these was to be related to cell operating temperature, charge parameters, depth of discharge, and number of cycles and/or total operating time. Discussions on both qualitative and quantitative relationships that available data indicate follow:

3.4.1.1 Charge-Voltage Characteristics During Short Cycling

Constant-Current Charging—Although straight constant-current charging (i.e., with no voltage limit) is rarely used in short orbit, a knowledge of the voltages that would result is useful in understanding the basis for design of more practical means of charge control. One published account shows voltage during true constant-current charging in a 90-minute cycle (Reference 104) and includes results at 0, 20, and 40°C and depths of discharge 5, 10, 30, and 50 percent. In these tests, after 1 year of cycling, the charge voltage

Table 23
Data Sources for Short-Cycle Testing and Analysis

Reference No.	Type of Information Contained						Test Parameters				Cell Brands Included	Cell Types and Rated Capacities
	Raw Data	Results Summaries	Analysis	Reliability Analysis	Flight or Ground	Temperatures (°C)	Depth of Discharge (% of Rating)	Charge Rates				
68	X	X			Ground	-20, 0, 10, 15, 25, 40	10, 15, 20, 25, 40, 60		Eagle Picher, America GE, SAFT, Sonotone	Cylindrical: 3.5, 4.5 Ah Prismatic: 6, 8, 10, 12, 20, 50 Ah		
104	X	X	X		Ground	0, 20, 40	5, 10, 30, 50		SAFT-America SAFT-America	Prismatic		
19	X	X	X		Ground	0, 25			GE	Prismatic: 20 Ah		
105		X	X		Ground							
106		X	X		Ground							
49, 107	X	X			Ground			10 to 20				
(1)		X	X		Both							
(2)	X	X			Ground							
108	X	X			Ground	5 to 20	15 to 20	0.3 to 0.5C	SAFT-America	Prismatic: 20 Ah		
109, 110			X		Ground							
111			X		Ground							
112			X		Ground							
113			X	X	Ground							
114		X			Ground							

1. Gibson, "Long-Life Ni-Cd Battery Evaluation," Aerospace Corporation, Los Angeles, California, approximately 1972.
 2. Thierfelder, "Test Report for NSF Cells and Batteries," General Electric Company, Valley Forge, Pennsylvania, June 1976.

exhibited a short plateau at 1.35 to 1.45 volts. This plateau voltage increased with decreasing temperature but was independent of depth of discharge. The end-of-charge voltage, on the other hand, increased sharply as temperature decreased and as depth of discharge increased, as shown in table 24.

Table 24
End-of-Charge Voltages on Constant-Current Charge
in 90-minute Cycles After 5000 Cycles (Reference 104)

Temperature (°C)	Depth-of-Discharge (percent)			
	5	10	30	50
0	1.57	1.61	1.63	1.67
20	1.43	1.47	1.55	1.55
40	1.45	1.45	1.45	—

Although the reference does not state the recharge ratio for these tests, it is estimated from the shapes of the voltage curves to be 1.25 or greater. The increasing voltages at higher depths of discharge result from the fact that charge current must increase as depth of discharge increases in order to adequately recharge the cells in the 60-minute charge period.

Because most of the voltages in table 24 may result in rapid gas evolution (figure 31), they tend to cause a net pressure increase from cycle to cycle, leading to excessive pressure and internal temperatures after many cycles. To prevent this occurrence, a voltage limit is usually applied. Most low-Earth-orbit related testing and applications over the last 10 years have involved such a voltage limit.

Charge Current-Voltage Performance Using Voltage-Limited Charging—

Figure 51 shows voltage and current characteristics typical of 100-minute cycling with a charge-voltage limit. If curves 1A and 1B represent the behavior of a cell that has not been previously subjected to extended continuous cycling, then curves 2A and 2B and 3A and 3B represent two

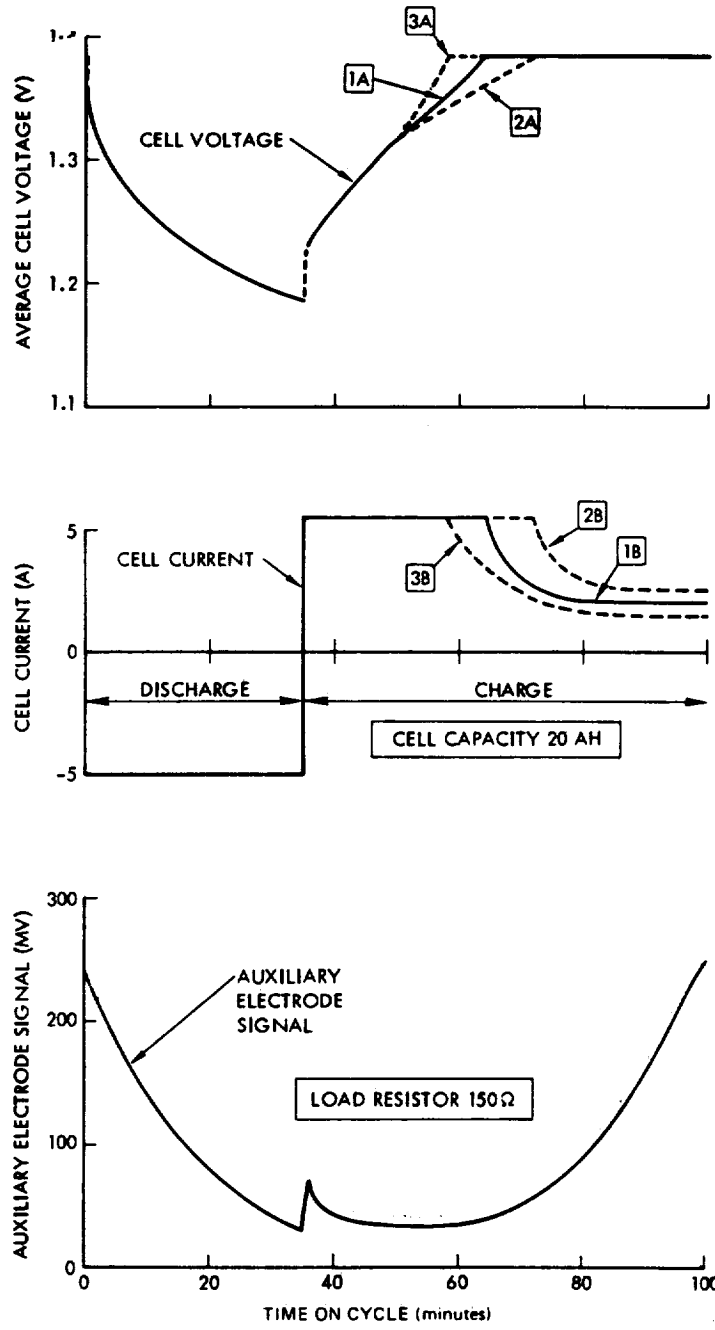


Figure 51. Cell voltage and current during 100-minute cycling with voltage limiting.

ways that the voltage-current characteristics have been observed to change with cycling. On curve 2A, charge voltage versus time is below that for curve 1A, the voltage limit is reached later, and, as for curve 2B, the current remains higher than that for curve 1B. The opposite is true for curves 3A and 3B.

Most cells progress from curve 1 in the direction of curve 2 during the first several hundred cycles on life test (References 68, 115, and 116). After that, the characteristics of better performing cells tend to remain in the region between curves 1 and 2, whereas those of cells that experience unusually rapid fading or that have inadequate active uncharged excess negative capacity tend to move toward curve 3. Furthermore, life-cycle test data (Reference 68) indicate that lower charge-voltage limits (at a given temperature) tend to keep charge-voltage characteristics low and suppress the development of high charge-voltage behavior. The lower voltage limit causes the current to cut back at a lower state of charge, making charge voltage less sensitive to variations in the condition of the negative electrode.

When using voltage limits that have been found best for long cycle life, the end-of-charge current at the beginning of cycle is about 25 percent of the maximum available charge current (before voltage limiting), the exact fraction depending on cell temperature. As cycling continues under a fixed-voltage limit (which is usually adjusted to give a recharge ratio of less than 1.10 at moderate temperatures at the beginning of cycling), the end-of-charge current and recharge ratio gradually increase. Without adjustment of the voltage limit, end-of-charge current can increase by as much as 50 percent before it stabilizes. When end-of-charge current increases in this way, the voltage limit must be decreased if the recharge ratio is to be kept close to its initial value. This adjustment was made during many of the low-Earth-orbit life tests performed at NWSC/Crane (Reference 68). The degree of this change appears to be greater for General Electric cells of more recent vintage than it is for older cells and SAFT-America cells.

The foregoing analysis applies strictly only when each cell is controlled with an individual voltage limit. When many cells are operated in series in a battery with a voltage limit applied at the battery terminals, as is usually the case, all the cells are charged at the maximum current for the same period of time, all cells experience the same current taper, and cell-voltage divergence around the average per-cell limit voltage occurs. This divergence increases with recharge ratios greater than 1.0 and with the number of cycles (Reference 49). Selection of cells that were more closely matched for capacity decreased the observed cell divergence.

The recharge ratio at a given voltage limit also undergoes similar changes early in cycle life (References 49, 77, and 116), correlating with the changes in the time the charge current begins to taper. An increase of 25 percent during the first 400 cycles is not uncommon, and this increase is usually followed by a period of relatively constant recharge. Figure 28 showed the relationship between recharge ratio, temperature, and voltage limit for 20-Ah SAFT-America cells operating at 18-percent depth of discharge after the recharge ratio had stabilized. It has also been shown (Reference 49) that, at a given temperature and voltage limit, the recharge ratio obtained in a 90-minute cycle increases as the depth of discharge decreases, as shown in figure 52. This figure also shows the range of recharge ratios obtained under various other operating conditions with the temperature-compensated voltage limit curve shown in figure 53.

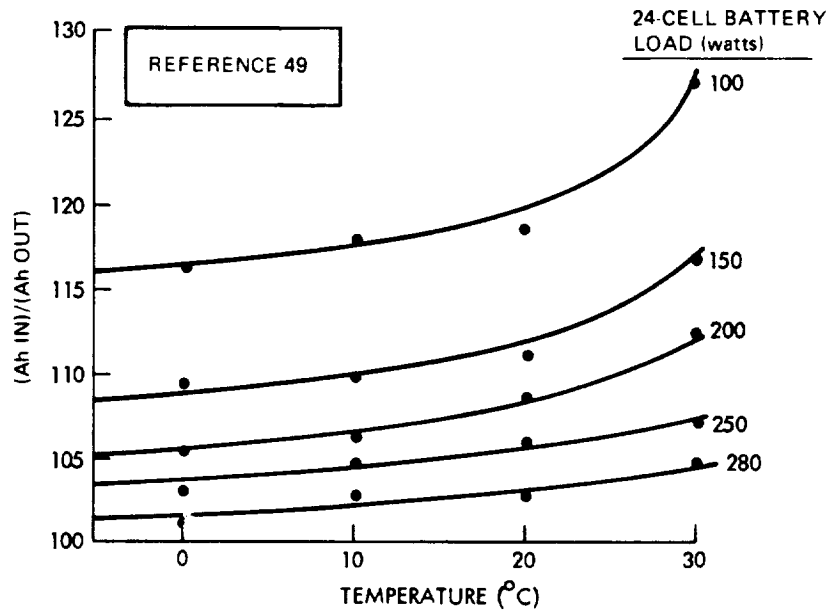


Figure 52. Recharge ratio versus temperature (battery load a parameter).

Toward the end of cycle life, the trend of recharge ratio at a fixed voltage limit becomes unpredictable, depending on whether the cells degrade by shorting or by high impedance behavior. If the voltage limit is the only means for adjusting recharge ratio, multiple voltage-limit levels may be required to compensate for changes in cell end-of-charge characteristics.

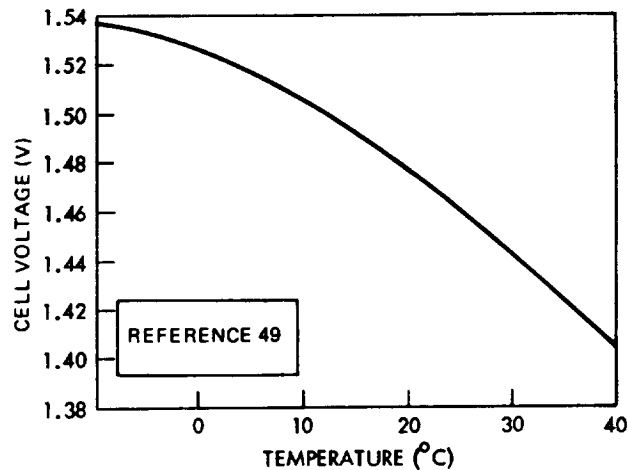


Figure 53. Typical charge-voltage limit (temperature compensated).

The rate of change of these charge I-V characteristics with cycling is less at lower operating temperatures and is almost negligible for the first 2 years at 0°C when the recharge ratio is adjusted to the range from 1.03 to 1.10 (Reference 68). By contrast, at a temperature of 25°C and above, the rate of change of charging characteristics varied widely and apparently at random during tests that involved commercially produced reference-design cells manufactured over the past 8 years.

3.4.1.2 Discharge Voltage Characteristics During Short Cycling

Both capacity trends and the trend of discharge voltage with number of cycles as a function of operating conditions must be considered in selecting the initial cell capacity and proper conditions of use. Although almost all available short-cycle (i.e., 3-hour cycle or less) tests have been run with constant current discharge, many spacecraft loads are mainly constant power, and discharge current increases as battery voltage decreases on such loads. Therefore, to deliver a given power level for a given eclipse period, a lower voltage battery must discharge at a higher rate and to a greater depth of discharge than a higher voltage battery and, hence, will be subjected to a greater stress.

Two aspects of discharge voltage are of concern: the average voltage and the end-of-discharge voltage. The first determines the ampere-hours of discharge required on a constant power load; the second determines the

maximum discharge rate and whether the battery voltage will remain within the range required for proper operation of the system. Average discharge voltage may be defined as equal to (watt-hours discharged)/(ampere-hours discharged). The denominator of this fraction is easily calculated but the numerator must be evaluated by integrating volt-amperes over the discharge time interval. For constant-power discharge, the ease of calculating numerator and denominator is reversed. No average voltage data were found for either kind of testing.

When the discharge voltage versus ampere-hours curve is nearly a straight line, the mid-discharge voltage is a good approximation to the average discharge voltage. This is the case early in cycle life for low depths of discharge and for low-temperature operation (References 68 and 104). Under less favorable operating conditions, the mid-discharge voltage may decline only slightly, whereas the end-of-discharge voltage drops sharply, indicating a rapid decline in voltage during the last half of discharge. Therefore, knowledge of both mid-discharge and end-of-discharge voltages permits a visualization of the shape of the discharge voltage curve and, hence, some estimate of the degree of voltage regulation that is obtainable. The annual reports of the NWSC/Crane test program (Reference 68) contain considerable data on mid-discharge voltage.

Table 25 shows data from 35 representative packs of cells on low Earth-orbit life tests at NWSC/Crane. The table includes only cells made by General Electric and SAFT-America because insufficient long-term test data were available for cells from other manufacturers. No cell failures had occurred in any of the packs shown within the number of cycles shown for each.

In table 25, cell packs are listed in order of increasing operating temperature and increasing depth of discharge. Test items 1 through 10 involved cells made prior to 1968 before more stringent controls were applied to all manufacturing. Furthermore, spacecraft cells made by General Electric contained plates of significantly different thickness and loading before 1968 than they did after 1968. As shown in a recent report by NWSC/Crane (Reference 117), before 1968 positive plate thickness was 0.86 mm (0.034 inch) and negative plate thickness was 0.74 mm (0.029 inch) in uncycled General Electric cells (i.e., the positive plates were thicker than the negative plates, as were SAFT-America cells at that time). After 1968, plate thicknesses provided by General Electric were as shown for reference-design cells in table 11 (i.e., the positive plates were thinner than the

Table 25
Short Orbit Life Test

Test Item No.	Ambient Temp. (°C)	Depth of Discharge (%)	NWSC/ Crane Pack Number	Cell Mfg.	Vintage (yr.)	Cycle Length (hr)	Total Cycles Included	Charge Voltage Limit (V)	Recharge Ratio Observed	Mid-Discharge Characteristics: Initial Voltage (V) and Trend	End-of-Discharge Voltage Characteristics: Initial Voltage (V) and Trend
1	0	15	16B	SAFT. America	Pre-1968	1.5	27,000	1.48, incr. to 1.55		1.29, constant	1.23 ±0.01
2	0	15	110A	GE	Pre-1968	1.5	32,000			1.28 to 1.29, constant	1.23 ±0.02
3	0	15	111A	GE	Pre-1968	3.0	16,000			1.28 ±0.02	1.23 ±0.02
4	0	15	53B	GE	Pre-1968	1.5	4,000	1.47	1.0	1.29 ±0.01	1.26, decr. lin. to 1.22 at 4,000 cycles
5	0	25	100B	SAFT. America	Pre-1968	1.5	22,000	1.55		1.23 ±0.02	1.17, decr. exp. to 1.12
6	0	25	90C	SAFT. America	Pre-1968	1.5	22,000	1.55		1.25, decr. exp. to 1.20	1.18 decr. exp. to 1.10
7	0	25	13B	SAFT. America	Pre-1968	1.5	27,000	1.55	1.15	1.27 ±0.02	1.24, decr. to 1.20 in 800 cycles, then constant
8	0	25	101B	SAFT. America	Pre-1968	1.5	28,000			1.25 ±0.01	1.19 ±0.02
9	0	25	124A	GE	Pre-1968	1.5	32,000			1.26 ±0.02, decr. lin. to 1.24	1.20 avg. (scattered), decr. lin. to 1.15 avg. (scattered)
10	0	25	125A	GE	Pre-1968	3.0	16,000			1.26 ±0.02	1.20 ±0.02
11	0	25	52C	GE	1968	1.5	8,700			1.27 ±0.03	1.24, decr. lin. to 1.20 avg. (scattered)
12	0	25	50B	GE	1968	1.5	8,900	1.49	1.1 to 1.15	1.27 ±0.02	1.23, decr. exp. to 1.20
13	0	25	92B	GE	1968	1.5	28,000	1.49	1.05 to 1.1	1.26 ±0.01	1.20 ±0.01

Table 25 (Continued)

Test Item No.	Ambient Temp. (°C)	Depth of Discharge (%)	NWSA/ Crane Pack Number	Cell Mfg.	Vintage (Yr.)	Cycle Length (hr)	Total Cycles Included	Charge Voltage Limit (V)	Recharge Ratio Observed	Mid-Discharge Characteristics: Initial Voltage (V) and Trend	End-of-Discharge Voltage Characteristics: Initial Voltage (V) and Trend
14	0	40	UMC	GE	1972	1.5	3,600	1.49		No data	1.21, decr. exp. to 1.13
15	0	40	01H	GE	1972	1.5	11,000	1.49	~1.03	1.23, decr. lin. to 1.22	1.19, decr. exp. to 1.14 at 16,000 cycles, then constant
16	0	40	01J	GE	1972	1.5	11,000	1.49	1.03 to 1.04	1.25, decr. lin. to 1.22	1.20, decr. exp. to 1.14
17	10	15	04C	SAFT- America		1.5	23,000	1.46	1.0 to 1.1	1.27, decr. lin.	1.21, decr. to 1.17 at 7,000 cycles, then constant
18	10	15	04E	SAFT- America		1.5	15,000	1.45	±1.08	1.28 ±0.01	1.22, decr. lin. to 1.205
19	10	16	7C	GE		1.6	14,000	1.44	1.03 to 1.07	1.30 ±0.02	Scattered to 3,500 cycles then constant at 1.23 to 1.24
20	20	25	95B	GE		1.5	29,000	1.45	1.05 to 1.15	1.27 ±0.01 to 16,000 cycles then decr. to 1.24	1.21, rolling off to 1.14
21	20	25	14E	GE		1.5	14,000	1.446		1.27, leveling off at 1.26	1.22, decr. exp. to 1.19, then constant
22	20	25	14F	GE		1.5	13,400	1.446	1.1 to 1.18	1.28, leveling off at 1.27	1.22, decr. to 1.16 in 4,000 cycles, then incr. to 1.20
23	20	25	14G	SAFT- America		1.5	8,000	1.45	1.15	1.26 ±0.02	1.23, decr. exp. to 1.17
24	20	25	04F	GE	1974	1.5	3,400	1.49		No data	1.25, decr. lin. to 1.15
25	20	25	01G	GE	1974	1.5	11,000	1.43	1.05	1.26 ±0.01	1.24, decr. exp. to 1.20, at 1,500 cycles, then constant
26	20	25	01I	GE	1974	1.5	11,000	1.43	1.07	1.28, decr. lin. to 1.26	1.24, decr. exp. to 1.20 at 2,000 cycles, then constant

Table 25 (Continued)

Test Item No.	Ambient Temp. (°C)	Depth of Discharge (%)	NWSC/ Crane Pack Number	Cell Migr.	Vintage (yr.)	Cycle Length (hr)	Total Cycles Included	Charge Voltage Limit (V)	Recharge Ratio Observed	Mid-Discharge Characteristics: Initial Voltage (V) and Trend	End-of-Discharge Voltage Characteristics: Initial Voltage (V) and Trend
27	20	25	01D	SAFT-America		1.5	15,000	±1.46	1.08	1.26, decr. lin. to 1.24	1.20, decr. lin. to 1.15
28	20	29.5	07D	GE		2.0	6,000	1.425	1.1	1.28, decr. lin. to 1.27	1.24, decr. exp. to 1.22
29	25	25	83A	GE		3.0	14,000	1.39 inc. to 1.42		1.25 ±0.01	1.18, decr. exp. to 1.10
30	25	25	05B	GE		1.5	7,900	±1.28		1.27 ±0.02	1.19, decr. erratically to 1.15
31	25	25	017B	GE		1.5	9,000	±1.28		1.28, decr. exp. to 1.26	1.20, decr. exp. to 1.14
32	25	25	09F	Eagle Picher		1.5	Recond. each 2,000 cycles	1.416	1.1 to 1.2	1.28 ±0.01	1.25, decr. lin. to 1.15 in 2,000 cycles
33	40	15	47C	GE		1.5	5,800	1.39	1.1 to 1.3	1.28, decr. lin. to 1.22	1.24, decr. to 1.1 in 3,000 cycles, then to 0.85
34	40	25	42C	GE		1.5	8,900	1.38, inc. 1.45		1.25 ±0.02	1.10, incr. to 1.14
15	40	25	10C	GE		1.5	7,800	1.38	1.0 to 1.1	1.25, decr. to 1.23	0.9, incr. to 1.13

1. End of Charge Voltage (EoC) (V).
 a. All packs were limited with voltage limited, charge limited, EoC/V is established by a test-equipment setting.
 b. 1.55 V/cell at 0°C, and in the early years of the operation, was later found to be anomalously high and damaged. The 0°C limit was subsequently set at 1.46 V/cell.
 c. The limit is subject to charge-shifting testing, usually to a lower value.
 d. Limit voltage decreases as test temperature increases.
 2. Recharge Ratio.
 a. The recharge ratio is dependent on the temperature and charge-voltage limit.
 b. Target recharge ratio as function of test temperature were (approx.): 1.05 at 0°C, 1.10 at 15°C, and 1.15 at 25°C.
 3. Discharge Voltage Data.
 a. "Initial Voltage" is the voltage after the first few hundred cycles. Up to that point, the discharge voltage decreases more rapidly than after that point.
 b. The "slope" is the average rate of change in voltage with respect to the number of cycles completed. "Lin" indicates a linear change with cycles; "exp" indicates an exponential slope to the voltage versus cycles curve, wherein the rate of decrease of voltage with cycles is decreasing as the test proceeds.

negative plates). The thickness of the plates supplied by SAFT-America in their standard spacecraft cell has remained unchanged; however, some variation on thickness and loading is available on special order from this company.

In table 25, note that different tests have progressed to different numbers of cycles and that the final discharge-voltage data apply at the end of the number of cycles completed. Analysis of the discharge data in table 25 reveals that:

- For mid-discharge voltage behavior:
 - Initial mid-discharge voltages ranged mainly from 1.25 to 1.29 volts with extremes at 1.23 and 1.30 volts. No correlation of this voltage with either test temperature or charge-voltage limit is apparent. Midvoltages were slightly lower at higher depths of discharge.
 - The trend of the mid-discharge voltage was either constant (± 0.02 volt) or decreasing linearly with cycles at a rate of 1 to 2 mV per 1000 cycles in the test temperature range from 0 to 25°C. The rates of charge increased with temperature and depth of discharge.
- For end-of-discharge voltage behavior:
 - Initial end-of-discharge voltages ranged mainly from 1.20 to 1.24 volts with extremes at 1.18 and 1.25 volts. Higher values are associated with lower test temperatures and lower depths of discharge.
 - With some exceptions, final end-of-discharge voltages ranged from 1.20 to 1.23 volts at lower temperatures and depths of discharge, and between 1.15 and 1.20 volts at higher temperatures and depths of discharge. Generally, the higher the voltage at any point in the test, the more rapidly the voltage decreased with cycling. Although rates of charge varied widely between packs, they tended to be greater at higher temperature. The rate of decay between the initial and the final voltage levels ranges from 5 to 20 mV per 1000 cycles when linear and from 20 to 40 mV per cycle-decade when exponential. At a given combination of temperature and depth of

discharge, the final voltage was roughly the same for most cells and represents a first plateau on the overall discharge-voltage characteristic (figure 54).

Table 25 and the foregoing summary show that, at all depths of discharge, operation in the temperature range from 0 to 20°C results in high in-cycle discharge voltages and less in-cycle voltage degradation than operation at higher temperatures. Section 3.4.1.3 describes capacity performance.

In another analysis of NWSC/Crane data (Reference 114), end-of-discharge voltage data for 60 packs (screened as described in Section 3.4.1.5) at 2000, 4000, 6000, 8000, 10,000, and 12,000 cycles were compiled in relation to test temperature and depth of discharge. Table 26 lists the averages of these data over all packs in each temperature and depth of discharge category at 6000 and 12,000 cycles. However, these voltage data should be applied with caution because the cycling involved was not truly continuous as it would be in many low-Earth missions. During most tests, the cycling was interrupted every 88 days for a capacity measurement and occasionally by power outages and test equipment malfunctions that resulted in open-circuit periods. These types of interruptions result in an

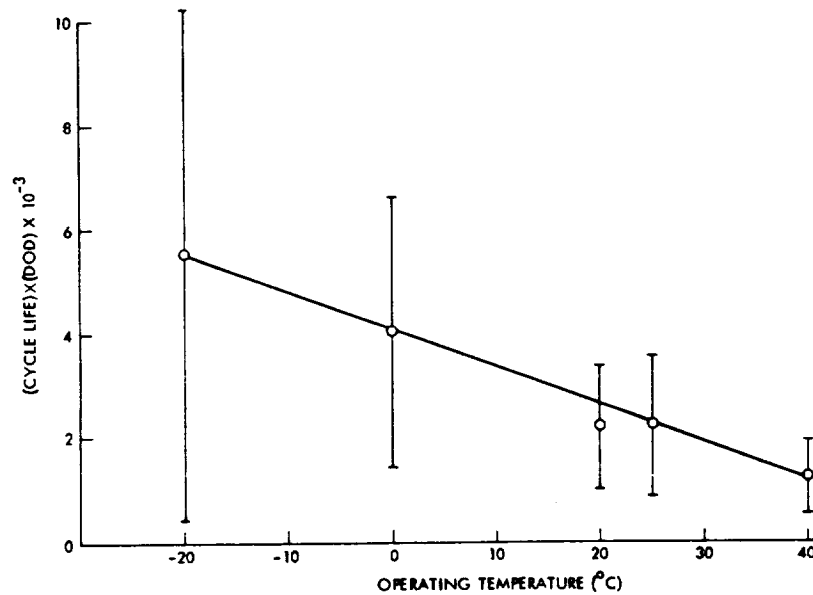


Figure 54. Depth of discharge per cycle life product as a function of operating temperature.

Table 26
End-of-Discharge Voltage Summary, NWSC/Crane
Low-Earth-Orbit Life Tests

Temperature (°C)	Depth of Discharge (%)	End-of-Discharge Voltage Per Cell (average of all appropriate cell packs)	
		At 6000 Cycles	At 12,000 Cycles
0	15	1.220	1.205
	25	1.175	1.163
	40	1.145	1.130
20	15	1.190	1.190
	25	1.176	1.173
	40	1.14(2) ¹	1.12(1)
25	15	1.14(1)	1.12(1)
	25	1.13(2)	1.10(2)
	40	1.10(2)	1.05(1)
40	15	(2)	(2)
	25	1.040	(2)

¹The number in parentheses following a voltage indicates that only that number of packs were present in the data base used to calculate the average.

²Insufficient data.

increase in end-of-discharge voltage above the trend line immediately after cycling is resumed, but this effect disappears within a relatively few cycles.

For comparison, note that the end-of-discharge data from two other ground tests in which cycling was not interrupted (References 115 and 116) show initial values of approximately 1.24 volts and decay rates of 20 mV per cycle-decade at 25 to 30°C over a 5000-cycle test (General Electric cells) and 15 mV per cycle-decade at 5 to 10°C over a 3000-cycle test (SAFT-America cells), both at 15- to 18-percent depth of discharge. SAFT-America cells of the same design on board the OAO-2 (Orbiting Astronomical Observatory) spacecraft in orbit (Reference 62), operating at 10 to 15°C and 15 percent depth of discharge, exhibit an average end-of-discharge voltage that remained in the range of 1.238 ±0.025 volts

throughout the first 15,000 cycles (approximately 3 years), with no detectable downward trend after the first few months of operation. The same type of SAFT-America cells on the HEAO-A (High Energy Astronomical Observatory) spacecraft in orbit at 5 and 10°C and 12 to 15 percent depth of discharge have shown a decay rate of about 15 mV per cycle-decade for the first 4000 cycles. These rates of change of discharge voltage are all significantly less than those indicated in table 25, suggesting that uninterrupted testing and/or actual use may often be less strenuous than on-the-ground testing as performed at the NWSC/Crane facility.

The previous paragraphs deal with the voltage at the end of the regular discharge, which lasts about 0.5 hour, associated with low-Earth orbits. If, after extended cycling (at depths of discharge below 30 percent), cells are permitted to discharge beyond the regular time, the voltage at any given output is below what it is before cycling, and two voltage plateaus are evident (References 62 and 77). The average voltage levels of these plateaus first decrease with the number of cycles and then appear to approach a lower limit after several thousand cycles. At 10 to 15°C and 15-percent depth of discharge, Ford (Reference 77) found the higher plateau to be at 1.18 to 1.19 volts and the lower plateau to be approximately 1.05 volts, as shown in figure 55. At higher temperatures, these voltages can be expected to be lower. As the number of cycles increased, the transition between these two plateaus occurred earlier in the discharge. In one test

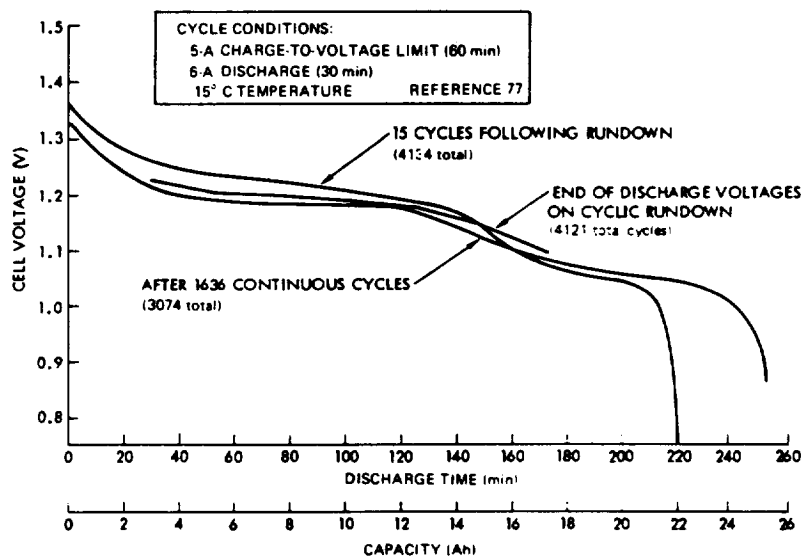


Figure 55. Second plateau voltage behavior after low-Earth cycling.

(Reference 77), the upper plateau had disappeared after 11,697 consecutive cycles without a complete discharge. Similar experience from other, less well-documented sources indicates that this voltage behavior is typical of low-Earth cycling and must be considered during design.

3.4.1.3 Capacity Trends During Short-Cycle Operation

The main impact of the declining voltage characteristic described previously is its effect on cell and battery capacity to a given end voltage. If the lower voltage limit of the power-system bus is too high and, more specifically, if it corresponds to an average cell voltage greater than that of the lower plateau, then loss of some usable capacity will occur earlier in cycle life than if the lower voltage limit is set at 1.0 volt per cell. This effect is illustrated graphically by two capacity versus cycle versus end-voltage plots in the "13th Annual Report of the Cycle Life Test" by NWSC/Crane (Reference 118). For example, the capacity down to 1.1 volt per cell was consistently less than 75 percent of that to 1.0 volt per cell at 0°C and 25 percent depth of discharge.

These data also show that the capacity to a given end voltage decreases more rapidly at higher temperature and at higher in-cycle depth of discharge. At the same time, operation at lower temperature (0°C compared to 25 or 40°C) compensated for the severe rate of loss of capacity that would be expected from operation at both high depth of discharge and high temperature. During testing, similar effects of operating temperature on capacity were found (Reference 49) for a much smaller population of cells from one supplier in the form of 24-cell batteries.

The 6th annual report of the NWSC/Crane test program (Reference 119) contains much data for trends of capacity to 1 volt per cell. More recent NWSC/Crane annual reports show some additional plots. These data show that, although the general trend of capacity is downward in the long run, the capacity of some cells and cell packs increases during the first several thousand cycles of regular testing. These increases occur mainly at low temperatures and probably result from either incomplete formation of the positive plates during cell manufacturing or inadequate active excess charged-negative capacity at the beginning of cycling.

The decline in capacity normally observed at 0°C is roughly linear with cycles and occurs at a rate of about 5 percent per year for most types of cells at depths of discharge up to 25 percent. This slope remains nearly constant for 4 to 5 years on test. At 25°C, the rate of loss is more unpredictable, ranging from 25 to 50 percent per year during the first year and

becoming much lower as the capacity approaches the number of ampere-hours discharged during regular cycling. The only apparent effect of depth of discharge is to vary the lower limit to which the capacity tended.

Note that the capacity figures referred to here were obtained on the second of the two discharges performed during capacity checks at 88-day intervals on the NWSC/Crane program. The second discharge usually gives higher capacity than the first, and the difference averages about 25 percent. Thus, an analysis of the first discharge-capacity data, which is not readily available in many cases, would be expected to show higher rates of loss than those indicated above.

Some of the foregoing capacity data were obtained during the earlier years of the NWSC/Crane tests when higher charge-voltage limits and higher recharge ratios were used than are now believed to be necessary. Ford (Reference 77) has shown that, when operating at 15-percent depth of discharge, the recharge ratios shown in table 27 as a function of temperature are sufficient to maintain an adequate margin of capacity to a 1.0 volt per cell lower limit.

Table 27
Recharge Ratios for Maintaining
Capacity in a 90- to 100-Minute Cycle
at 15 Percent Depth of Discharge

Temperature (°C)	Recharge Ratio (Ah in/Ah out)
0	1.04
15	1.09
32	1.15

These values were derived by using charge-rate limits in the range from 0.25C to 0.6C. This type of information has not been developed for depths of discharge greater than 15 percent. Various tests have shown that higher recharge ratios are needed in 24-hour cycles in which depth of discharge is over 50 percent and charge rates are 0.1C or less. (See Section 3.4.3.)

The cause of the large variability in rate of capacity loss at 25°C and above is not now known, but it may be inherent in the plate materials involved. Thus, if a significant residual capacity must be maintained in low-Earth missions beyond 1 year, the surest approach is to operate the battery at an average temperature below 20°C.

3.4.1.4 Auxiliary Electrode Performance During Short-Orbit Cycling

At a given operating temperature, the output of the oxygen-signal auxiliary electrode with a given load resistance is a function of the partial pressure of oxygen (at a given state of charge) in the cell (References 44, 47, and 48) and the distribution of electrolyte in the vicinity of the oxygen electrode (Reference 48), neither of which are directly measurable. As cells are firmly constrained while being cycled, considerable pressure can accumulate before being detected if no pressure transducer is attached. Even when total pressure is measured and found to be constant, the partial pressure of oxygen at a given point in the cycle may vary from time to time. Thus, variations in auxiliary electrode signal output during life testing are to be expected.

The trend of signal voltage under actual low-Earth-orbit test conditions has been toward lower values with prolonged cycling (References 49, 68, and 120), although some increase in signal may be observed in the meantime. Ford (Reference 120) reports that, in a low-Earth-orbit application, oxygen electrodes performed well in SAFT-America cells over a number of years. Output voltages at end of charge were sensitive to recharge ratio, as expected from the relationship of oxygen pressure to recharge ratio. A loss of signal sensitivity occurred in some cells after cycling, which was attributed to an effect of hydrogen generated because the cells had become negative-limited on charge. No direct experimental proof that hydrogen was the cause was reported. Tests showed that normal signal behavior could be restored by decreasing the recharge ratio at which the initial (relative high) charge rate was reduced. Thus, stable operation of the oxygen-signal auxiliary electrode for multiyear missions appears to be dependent on the degree to which loss of overcharge protection and electrolyte redistribution within the cell can be controlled. In the absence of such controls, it is advisable to provide several selectable levels of trip voltage for charge control, in a manner similar to that often implemented for the battery charge-voltage limit, to accommodate up to a two-to-one range of variation.

3.4.1.5 Cell Failure Rate and Cycle Life in Short-Cycle Operation

To perform battery reliability assessments as usually required during spacecraft system design, cell failure-rate or life-expectancy data are necessary. Failure rate is defined as the average of the hazard function and is developed mathematically in Section 8.7.4.1. The life expectancy of a cell is the mean operating time or the mean number of cycles to failure. In an

application or test in which cycling is regular and continuous, operating time and number of cycles are directly interconvertible and either measure of life can be used without ambiguity. However, when cycling is intermittent, as in eccentric and geosynchronous equatorial orbits, mean time to failure and mean cycles to failure cannot be interconverted without a definition of the mission profile. Therefore, there may be anywhere from a few to several hundred charge-discharge cycles per year in different intermediate and high-altitude Earth orbits. For low-Earth-orbit (short-cycle) testing as performed at NWSC/Crane and for most other low-Earth-oriented ground tests, cycling is done more or less continuously (except as noted earlier), and about 5500 cycles per year are completed for 90- to 100-minute cycling. It has therefore become customary to express life expectancy in this operating mode in terms of mean cycles to failure or, as the term is often abbreviated, mean cycle life.

A number of reports published during the past 8 years present cell failure-rate and/or cycle-life data, mostly from analysis of the NWSC/Crane test results. Reference 112 describes an extensive computerized analysis of data from several ground-test programs as of 1971. A complex cell-reliability model is generated with submodels for failure rate as a function of aging, quality-related failures, and dormancy (when applicable), and the constants calculated for each submodel are given as a function of test temperature, depth of discharge, and a third variable depending on the submodel. The data analysis showed that, in terms of instantaneous failure rate* versus cycles:

- There was no significant difference between the results from 1.5-hour cycles and 3-hour cycles.
- There was no significant difference between the results from cylindrical and prismatic cells.
- After the first 2000 cycles, larger cells had slightly higher failure rates than smaller cells.
- Cells manufactured by General Electric had the highest overall long-term reliability.
- In the range from 5000 to 15,000 cycles, the failure rate at 40°C was an order of magnitude greater (10^{-4} hr^{-1} versus 10^{-5} hr^{-1}) than at 0°C.

*Instantaneous failure rate is the same as the hazard rate, and may be used to calculate cell reliability as described in Section 8.

- After the first 2000 cycles, the failure rate increased with cycles at 25 and 40°C but decreased at 0°C.
- After the first 2000 cycles, the failure rate for 40-percent depth of discharge was about five times that at 25-percent depth of discharge at 25°C. No similar analysis was shown for 15-percent depth of discharge at 0°C.
- A minimum failure rate was found at a recharge ratio of 1.15 at 20 to 25°C over a range of depths of discharge and charge rates.
- Cell failure rates from the aggregate of ground-test data available at the time of the study (1971) were an order of magnitude greater than those estimated from orbital operations, which ranged from 10^{-4} hr⁻¹ to 10^{-6} hr⁻¹. Reference to sources of these figures was given in the report.

Reference 111 contains another thorough analysis of NWSC/Crane test data. This report shows a useful tabulation of most cell packs tested, categorized by cell manufacturer, special cell features, test temperature, and depth of discharge, as well as total cycles completed, number of cells starting each test category, and number of individual cell failures to the date of the study (1972). A particular objective of this study was to determine the relative merits of pooling failure data from cells of different manufacturers versus keeping such data segregated. The conclusion on this point was that cell-failure distributions for cells from different manufacturers were distinctly different. Therefore, such differences should be considered when selecting a source of cells for a specific mission. An extensive set of curves for probability of cell failures as a function of cycles at each combination of temperature and depth of discharge used in the NWSC/ Crane program are shown with separate curves for cells from different manufacturers. Figure 56 is an example of one of these graphs.

A third report (Reference 112) contains information similar to that in Reference 111 updated to 1974. A tabulation shows pack start and completion dates but not individual cell-failure data. Plots of calculated mean cell cycle life versus depth of discharge for five test temperatures are shown. An approximate linear relationship between the product [(mean cycle life) × (depth of discharge)] and test temperature was found, as shown in figure 54. The diagonal line in this figure corresponds to the equation:

$$F(T) = \overline{\bar{n} \cdot \text{DOD}} = -(70.7) T + 4015 \quad (24)$$

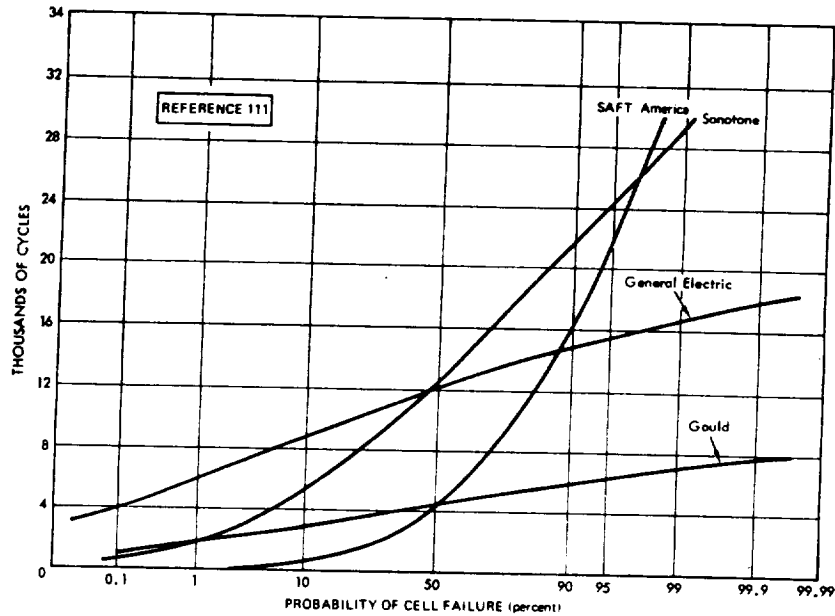


Figure 56. Probability of cell failure versus number of short cycles for cells from four manufacturers.

where \bar{n} is the mean cycle life, and DOD is expressed as a fraction of 1. This reference contains no data on failure rates *per se*.

A more recent study of this type (Reference 114), published in 1975, contains tabulations of results of 90-minute cycle tests at NWSC/Crane where certain factors were out, such as cylindrical cells, cells made with other than nylon separators, failures caused by leakage through defective or broken seals, failures attributable to shorting as a result of silver migration from the terminal braze alloy, and failures caused by malfunction of test equipment. These tabulations show individual cell failures and removals by cycle number—information published in the first few annual reports of the NWSC/Crane program, but not since that time.

The analysis approach used leads directly to cell reliabilities rather than to failure rates. Reliability was calculated for different sets of temperature

and depth of discharge for a design life of 6000 cycles, using three different data bases, as follows:

- A. Tests at NWSC/Crane only, including tests that began when the program began in 1963
- B. Tests at NWSC/Crane only, but excluding tests begun before mid-1966
- C. Tests as in B, plus orbital data from a number of spacecraft in low-Earth orbit with batteries operating in the range from 10 to 25°C and 15- to 25-percent depth of discharge (DOD)

Table 28 shows the results of these calculations. Note the significantly lower cell reliabilities calculated from data base A and the similarity in the results from data bases B and C. These comparisons indicate that cells that began cycling at NWSC/Crane before mid-1966 usually experienced much higher failure rates early in life than cells beginning tests later. This improving trend continued past 1966 and is expected to continue indefinitely. Therefore, inclusion of data from the older packs in reliability calculations will give estimates that are significantly lower than those that are appropriate for modern cells. For this reason, the cell failure rates and failure probability data in References 121 and 122* are not appropriate for modern cells procured under currently enforced controls and quality-assurance requirements.

Table 28
Estimated Cell Reliabilities at 6000 Cycles for
Three Data Bases Versus Operating Conditions
(Reference 123)

Temp. (°C)	Data Base A DOD (%)			Temp. (°C)	Data Base B DOD (%)			Temp. (°C)	Data Base C DOD (%)		
	15	25	40		15	25	40		15	25	40
40	0.7232	0.4500 ¹	0.4208	40	(2)	0.9596	0.960 [~]	40	(2)	0.9755	0.960 [~]
25	0.9798	0.8000 ¹	0.7424	25	1.0000	1.0000	0.9891	25	0.9999	0.9972	0.9891
20	1.0000	0.9950	1.0000	20	1.0000	0.9974	0.8596	20	1.0000	0.9974	0.8596
0	0.9402	0.8694	0.8864	0	1.0000	0.9726	0.9605	0	1.0000	0.9726	0.9805

¹Point estimate used for these values. All other values are Weibull-fitted values.
[~]Insufficient data.

*See also J. D. Dunlop, COMSAT Laboratories, private communication.

The foregoing cell-failure rates from Reference 113 were based on ground-test data only. On the other hand, analysis restricted to orbiting spacecraft data (Reference 121) based on 304 spacecraft operating through 1970 gave a battery-cell mean-failure rate estimate of $22 \times 10^{-9} \text{ hr}^{-1}$. The 90-percent confidence limits were at $0.11 \times 10^{-9} \text{ hr}^{-1}$ and $100 \times 10^{-9} \text{ hr}^{-1}$. Reference 121 does not state how the spacecraft involved were distributed among low-Earth and higher altitude missions. This estimate is two orders of magnitude lower than that calculated from the earlier years of the NWSC/ Crane test program (Reference 113). The foregoing failure-rate estimate value is certainly over-optimistic because it was derived under the assumption that, if a battery had not failed, no cells in the battery had failed. Also, it was derived from flight applications involving depths of discharge that averaged only 10 percent.

It is often necessary to perform a preliminary battery reliability estimate before the operating conditions have been fully defined. To do this, a generalized cell reliability estimate must be synthesized. Reference 114 calculated such generalized values for each of the three data bases described earlier, but omitted data for the highest temperature (40°C) and highest depth of discharge (40 percent) in table 28. Table 29 shows the results. The difference between the cell reliabilities for data base A and those for data bases B and C may appear small, but the difference in unreliability (1-R) (i.e., 0.09 versus 0.01) is large, and this difference is reflected in the 22-cell battery reliability values shown in table 29.

Table 29
Calculated Lumped Cell and 22-Cell Battery Reliabilities
for 6000 Cycles Using Different Data Bases (Reference 114)

Data-Base Designation	Number of Cells in Data Base	Generalized Cell Reliability for 6000 Cycles	Battery Reliability
A	237	0.9116	0.1306
B	170	0.9935	0.8663
C	764	0.9968	0.9319

Data base C was further used in an effort to produce a generalized cell and battery reliability model to fit the available NWSC/Crane test data (Reference 122). The result was a temperature and depth-of-discharge dependent model of broad usefulness. This model was used to generate figure 57, which shows mean cell cycle life as a function of depth of discharge with temperature as a parameter, and figures 58 and 59, which show cell reliability as a function of depth of discharge at 6000 and 12,000 90-minute cycles. This study also showed that newer cells (past 1968) have a considerably higher reliability estimate under all operating conditions over the cycle life indicated than older cells. This improvement is due in part to improvements in test methods and controls, but in particular to the significant improvements in cell quality produced by the NASA-sponsored high-reliability program begun in 1968.

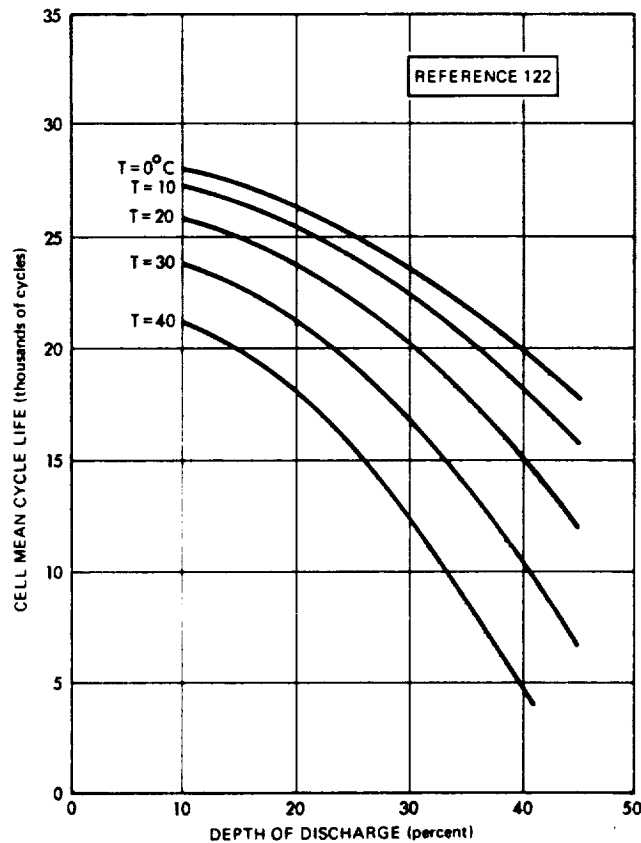


Figure 57. Estimated mean cell cycle life diagram.

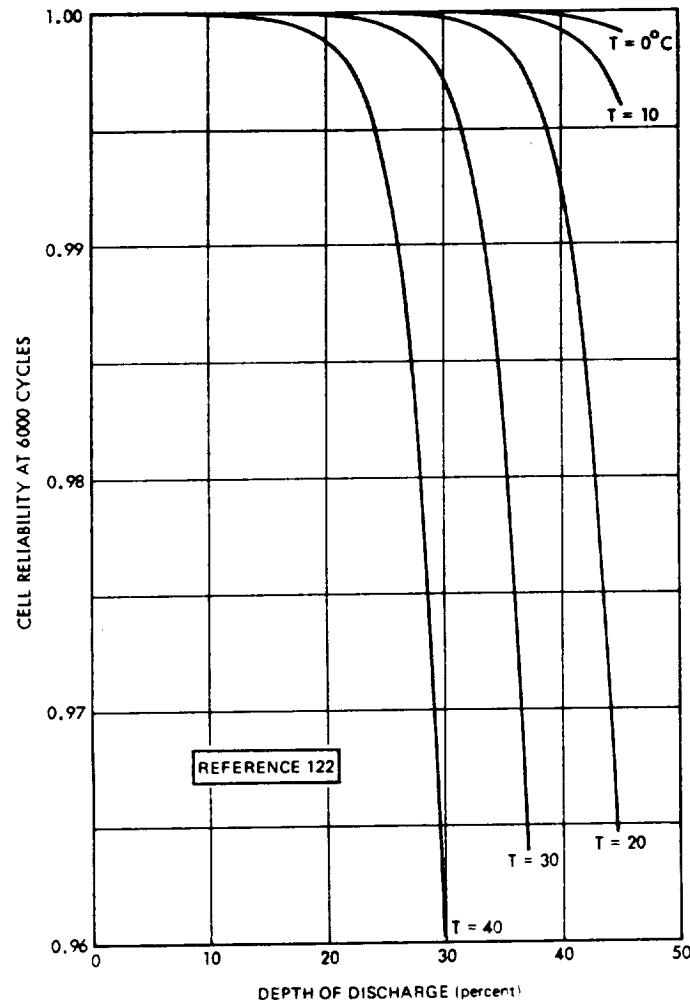


Figure 58. Calculated cell reliability at 6000 90-minute cycles.

3.4.1.6 Effects of Cell-Design Variations on Long-Term Performance in 90-Minute Cycling

Previous sections dealt with performance expected from reference-design cells in low-Earth applications. This section covers differences in low-Earth-orbit cycle performance that are associated with known variations in cell design relative to the reference designs described in table 11. Effects on long-term performance are correlated with design both qualitatively on the

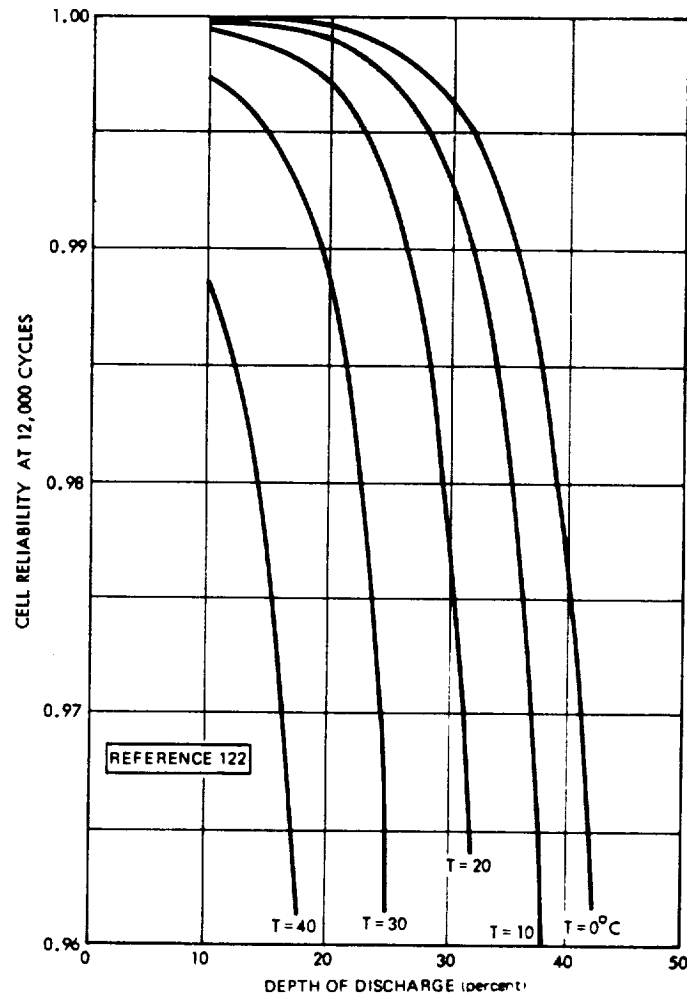


Figure 59. Calculated cell reliability at 12,000 90-minute cycles.

basis of general knowledge and analysis and quantitatively as available data permit. The effects of design are discussed in terms of trends in discharge voltage and capacity and of occurrence of failures as a function of number of cycles and life. Table 30 lists the design variations for which significant data have been or are being generated in the NWSC/Crane test program. Parts of table 30 are redundant because more than one variation is included in many of the packs listed.

Table 30
Cell-Design Variations on Test at NWSC/Crane

Design Variation	NWSC/Crane Pack No.	Other Information
Above-average loading of positive plates (high end of distribution around normal level)	6M	SAFT-America 6-Ah cells (1972-73). Some cells with normal and some with below-normal electrolyte levels.
Decreased loading of positive plates (-10%)	8C, 8D, 8E, 8F, 8G, 8H	GE 12-Ah cells (1973). All cells had teflonated negatives. All cells contained above-normal electrolyte level. 8C, D, E, and H 24-hour cycle testing only.
Decreased loading of both positive and negative plates (-10%)	8F, 8G, 8H	See description above.
Cobalt versus no cobalt in positive plates	9H, 21E, 33D, 45E, 69C	SAFT-America 5-Ah prismatic cells (1969). Some cells had polypropylene separators. Three test temperatures (0, 25, and 40°C) and two DOD (25 and 40 %) used for testing.
Teflonated negative plates	1G, 1H	GE 20-Ah cells (1973). TFE level II. Cells had above-normal electrolyte level. Packs 1I and 1J are reference-design types (nonteflonated negatives; normal electrolyte) tested for comparison.
	8C, 8D, 8E	GE 12-Ah cells (1973). TFE level II. Below-normal positive plate

Table 30 (Continued)

Design Variation	NWSC/Crane Pack No.	Other Information
Teflonated negative plates (continued)	8C, 8D, 8E (continued)	loading. Above-normal electrolyte level. 24-hour testing only.
	18F	GE 8-Ah (1973). Pack 18E is nonteflonated control.
Silver-treated negative plates	7C	GE 12-Ah cells (1973).
Separator material and/or type	9H, 33D, 45E	SAFT-America cells (1969). Electrolyte levels unknown.
Separator material and/or type	2D, 2E, 14E, 22C, 25D, 26D, 31C, 38F, 46C, 49B	Eagle Picher 6-Ah cells (1970). Electrolyte levels unknown.
	9J to 9M, 9O to 9T	Eagle Picher 6-Ah cells (1974). Electrolyte levels unknown.
Electrolyte level above normal	1E, 1F	SAFT-America 20-Ah cells (1973). 20 and 40% above normal.
	1G, 1H, 8C, 8D, 8E, 8F, 8G, 8H, 18F	See above for identification.
Negative precharge level	48C	SAFT-America 20-Ah cells (pre-1968). Three levels of added precharge: 0, 4, and 8 Ah.
	48D	SAFT-America 20-Ah cells (pre-1968). Three levels of added precharge: normal, normal -3 Ah, and normal +3 Ah.
	4C, 4E	

The effect of higher-than-normal loading of positive plates on the trends of electrical output with cycling is not clear from existing data. In one small sample (pack 6M), no significant differences were evident in average end-of-discharge voltage and capacity trends between cells with above-normal loading and those with normal loading over a 5000-cycle test at 20°C and 25 percent depth of discharge. The difference in loading level between the test cells and the norm was 5 to 10 percent. Data for individual cells were perturbed by the presence of different amounts of electrolyte in each cell,* and all cells analyzed had very high percentages of carbonate in the electrolyte at the end of the test. Because cells with lower-than-normal loading of positive plates (packs 8C through 8H) also contain other design variations, the results from these cells (described below under the heading of teflonated negative plates) cannot be simply interpreted to show the effect of variation of positive loading *per se*.

A number of tests (table 30) have been conducted with two levels of cobalt in the positive plates (normal level and none). Because of the number of variables (two kinds of separator material and a range of operating conditions), the smallness of the sample, and the scatter of the data, the results are not clear-cut. On the average, the cells with more cobalt had somewhat longer cycle lives at 25 and 40°C than those with less cobalt, but there was no difference at 0°C. All cells analyzed had a high percentage of carbonate in the electrolyte at the end of the test, and the amount of carbonate was independent of whether the cells contained nylon or polypropylene separators.

Long-term testing of the effects of negative-plate (cadmium) design variables has been limited to life testing of cells that contain negative plates having either a teflonation or a silver treatment, as manufactured by the General Electric Battery Division. In one set of tests involving teflonated versus nonteflonated negative plates (packs 1G, 1H, 1I, and 1J) at 0 and 20°C, no failures occurred in either design over a 2-year period. End-of-discharge voltages of the teflonated design have consistently been slightly below those of the nonteflonated (standard) design throughout the test. Out-of-cycle capacities have declined less than 10 percent to date.

Packs 8C, 8D, and 8E (table 30) with teflonated negative plates are being tested in a 24-hour rather than a 15-hour cycle. In about 600 cycles, end-of-discharge voltage (for a 1-hour discharge at the 0.5C rate) has declined to about 1.17 volts for packs 8C and 8D (0 and 10°C test temperatures)

*Resulting inadvertently from a cell production problem.

and is varying between 1.05 and 1.16 volts for pack 8E (at 20°C). Capacity has declined from an average of 14.5 to 14.2 Ah for pack 8C and 11.4 Ah for pack 8E. Comparison of these data with data from packs 123B (at 0°C) and 109B (at 20°C), which were without teflonated negative plates but tested in a 24-hour cycle, shows that the end-of-discharge voltage and capacity behavior are similar at the 600-cycle point. Thus, more cycle time will be required before the results from packs 8C, 8D, and 8E become significant.

Low-Earth-orbit testing began recently on another group of cells with teflonated negative plates and lower-than-normal loading of both positive and negative plates (packs 8F, 8G, and 8H, table 30). Because these cells also have an above-normal electrolyte level, the effect of teflonation on voltage and capacity may be difficult to detect. Other variables may need to be better controlled because test results to date are not consistent. For example, the average end-of-discharge voltage of the pack 8F cells at 20°C and 25 percent depth of discharge had decreased to 1.15 volts after 3000 cycles, compared to a value of 1.20 volts at the 3000-cycle point for a group of 20-Ah cells of a similar design (pack 1G) under the same test conditions. After 6 months of cycling, the capacity checks were higher than precycling values for both of these packs. This initial capacity increase occurs in many cells with teflonated negatives, particularly when operated at 0°C.

Another comparative test involving teflonated negative plates is under way at NWSC/Crane: that of packs 18E (nonteflonated) and 18F (teflonated). Performance of these packs at 20°C and 25 percent depth of discharge was almost identical for the first 2 years on test. As in the previously described tests that had been in progress for 2 years at the time of this writing, no cell failures had occurred, and no cell teardown analysis data have been obtained on the cells involved.

The second negative plate design variation being tested at NWSC/Crane is the silver treatment. Pack 7C, which has negative plates of this type, has been on test at 10°C and 16 percent depth of discharge for over 4 years with no cell failures. End-of-discharge voltage is stable at approximately 1.24 volts, and capacity decline is normal for these operating conditions. No teardown analysis has been performed on these cells to date. Because the cells are not equipped with pressure gages, the cell manufacturer's claim that the treatment reduced overcharge pressure could not be verified in this pack.

Many cells with the silver treatment have been operating in orbit for up to an equal amount of time with no known problems attributable to the silver. Dunlop* has observed in ground tests that cells with silver-treated negatives appear to be associated with more migration of negative material than those without silver, but no cause-and-effect relationship has been established between these variables. Some users have observed that, although there is a beneficial effect of the silver when the cells are new, the effect diminishes as the cells are cycled.

Many varieties of nonwoven nylon and polypropylene separator materials have been tested in cell cycle life tests since 1968. One series of tests performed early in this period involved Eagle Picher cells (References 32 and 34). Performance of cells with polypropylene separators was comparable to that of nylon separators for the first several thousand cycles in the temperature range from 5 to 25°C. Mid-discharge voltages were the same, and end-of-discharge voltages were 50 to 100 mV lower for polypropylene. In the range from 5000 to 15,000 cycles (1 to 3 years on test), the end-of-discharge voltage decreased further, and end-of-charge voltage increased in the cells with polypropylene separators relative to performance of the cells with nylon separators. These results appear to be consistent with data from the NWSC/Crane tests (table 30), which have been summarized by Hennigan (Reference 34). The electrolyte content of polypropylene separators of the type tested earlier decreased by a factor of three or more during the first 4000 to 6000 cycles of testing. During the same cycling, the electrolyte content of Pellon 2505 type nylon separators decreased only by 10 to 20 percent. In a group of newer polypropylene separator products, two showed rates of loss of electrolyte similar to that of nylon (Reference 124), but last-cycle capacities to 0.75 did not correlate well with electrolyte retention in these cases. One polypropylene product, modified to increase wettability by radiation-grafting of polar side chains, exhibited no better electrolyte retention and last-cycle capacity than most nonmodified polypropylene materials. No useful cell voltage data were obtained during the latter tests because the discharge voltage of the cells fell rapidly with cycling and, hence, was not representative of normal nickel-cadmium cell behavior (Reference 118).

Polypropylene should be superior to nylon as a separator material at temperatures well above 25°C, at which the rate of hydrolysis of nylon increases rapidly (Reference 124). Polypropylene separators have been used successfully in cells that must be subjected to heat sterilization before

*J. D. Dunlop, COMSAT Laboratories, private communication.

launch (References 103 and 124). These cells are required to undergo relatively few cycles (usually less than 500) in the 15 to 25°C temperature range during their service life—a requirement that they meet. One pack of cells tested at NWSC/Crane had polypropylene separators (pack 9H, table 30). When cycled at 40°C and 25 percent depth of discharge, they suffered a rapid loss of capacity (50 percent by the first capacity check), but continued at that level for over 16,000 cycles without failing. This amounts to twice the average number of cycles to failure observed in packs with nylon separators that were tested at 40°C. Teardown analysis showed severe migration of negative material through the separator but no deterioration of the separator material itself. Thus, causes of failure other than separator deterioration are predominant in cells with polypropylene separators operated at high temperatures.

Another design variable of considerable potential impact is electrolyte level. The level in reference-design cells is about 3 ml per ampere-hour of rated capacity. A number of cell packs now on test at NWSC/Crane contain cells with higher-than-normal levels. In one set of three packs (1D, 1E, and 1F), the electrolyte level was the only known variable. After 24 months of cycling at 20°C, the end-of-discharge voltages and capacities of the cells with above-normal electrolyte levels were significantly lower than those for the standard design. A number of other packs contained cells with above-normal electrolyte levels. (See bottom of table 30.) However, these cells also contained one or more other design variations (as described in other sections of table 30) so that the effect of electrolyte level alone is not apparent. Therefore, the value of adding electrolyte above the level in reference-design cells has not been clearly demonstrated in low-Earth-orbit cycle tests to date. Continuation of tests in progress, with the possible addition of more control sample cells, should provide the desired demonstration.

The final design variable to be discussed here is the precharge level. It is difficult to predict the ultimate effect of variations in the precharge level because, with cells having a fixed negative-to-positive ratio (as they do with fixed negative and positive plate material designs), increasing the precharge decreases the excess uncharged excess negative (overcharge protection) and vice versa. Which of these excess negative capacities eventually controls cell behavior probably depends on the use conditions. In NWSC/Crane tests of two packs of cells (48C and 48D) with a wide range of precharge levels (from -3 to +8 Ah in 20-Ah cells), only one cell behaved abnormally (one of two cells with 8 Ah of precharge added); it generated excessive pressure after 500 cycles. Little difference was seen between the electrical behavior of the other cells. Eventual shorting failures appeared to be

distributed randomly among the cells with different precharge levels. In pack 4C at NWSC/Crane after 500 days on test at 10°C and 15 percent depth of discharge, the cell with the highest precharge setting has the highest end-of-charge voltage; otherwise, there is no correlation between precharge level and performance to date. The range of added precharge was quite small, however (4.5 to 6.45 Ah in a 20-Ah cell), and may not have been large enough to make a good test. In pack 4E, tested at 10°C and 14 percent depth-of-discharge, the cells with the largest added amount of precharge had the lowest capacity for the first 18 months on test; after that, the cell with the lowest precharge had the lowest end-of-discharge voltage and capacity. The differences were small (0.02 volt and 1 Ah) for the range of 4 to 1 in the amount of precharging used. These results indicate that, under these operating conditions, variables other than added precharge (over a wide range of precharge level) may limit cell performance more than the precharge level.

3.4.2 Long-Term Performance Under Noncontinuous Short-Cycle Conditions

This section describes the effects on cell performance of interrupting the regular cycling in various ways during 90- to 100-cycle operation. Such interruptions may either occur inadvertently or be performed for various reasons.

3.4.2.1 Effect of Rest, Change of Cycle, or Prolonged Charge

Section 3.4.1 noted that cycling in the NWSC/Crane test program is not continuous, but is interrupted both randomly by equipment problems and, for many tests, regularly for capacity checks. Both of these events result in an increase in discharge voltage in a number of ensuing cycles. This effect usually lasts only for a relatively few cycles, but may show an increase above the overall trend line for several hundred cycles.

Kirsch and Shikoh (Reference 49) report that some capacity lost while cycling at 20°C was recovered by lowering the temperature to 0°C for a number of cycles. This effect was probably gradual and was probably due more to the higher charge efficiency at the lower temperature than to any special effect of the temperature change.

It has been reported that any change of charge rate or discharge rate from that used for regular cycling without a change in cycle timing increases

discharge voltage and/or capacity. Here again, it is likely that this effect results from an increase in the average state of charge of the cell caused by the change in operating parameters.

Prolonged charging at a lower rate than that used for regular cycling should increase voltage and capacity, and some refer to it as one form of reconditioning. Kirsch and Shikoh (Reference 49) show that overcharges of 50 and 100 percent at the 0.1C rate had very little effect after 50 percent of the original capacity had been lost during short cycling at 10 to 20°C. Such charging usually restores capacity only if the capacity loss is temporary and attributable to insufficient charging in regular cycle.

3.4.2.2 Reconditioning During Short-Cycle Operation

As used here, the term "reconditioning" refers to an effect, not to any specific procedure. Many different procedures may be used, and different procedures are needed to be effective, depending on the operating conditions and the underlying cause of performance degradation.

Ford (Reference 77) has shown that, if cells are permitted to discharge down to about 1 volt at the normal in-cycle discharge rate after an extended period of cycling that involves only a 30-minute discharge per cycle, the discharge voltage on subsequent cycles is increased, although the total watt-hour capacity to 1 volt is not increased, and the capacity is not restored to the precycling level. Therefore, this method of "reconditioning" is apparently not optimum under these conditions.

It has been shown that, when observed voltage degradation is not caused by inadequate charging, the greatest actual reconditioning effect, in terms of discharge voltage and watt-hour recovery, is achieved by discharging at a much lower rate than that used for normal cycling (References 123 and 125). During ground testing in which cell terminals are accessible, this can be done by placing a suitable-sized resistor across each cell. Kirsch and Shikoh (Reference 49) showed that this method, applied for 72 hours, restored a battery to essentially full precycling capacity after low-Earth-cycle testing. This procedure is usually not practical in an orbiting spacecraft, however, even if batteries could be taken off the line for the necessary time (usually a minimum of 48 hours) because equipment is not provided for remote connection of cells.

Lanier (Reference 126) recently described a compact, automatic device for implementing full discharge at the battery terminals while preventing any cell from going below zero volts. Repeated use of this device during a

test of over 24,000 cycles resulted in restoring nearly new capacity each time. In addition, charge-voltage divergence was reduced significantly. To use such methods during missions in which there is no natural interruption in cycling, the total battery complement can be divided electrically into two or more series strings of cells, so that one string at a time may be taken off the line for reconditioning.

3.4.3 Long-Term Performance Under Continuous 24-Hour Cycling Conditions

Observed long-term trends in the performance of reference-design cells, used for most high-altitude applications to date, are described first. A discussion of expected effects of certain cell-design and process variations on long-cycle performance follows.

Charge/discharge cycles in a synchronous equatorial orbit occur in groups of about 45 each, often referred to as eclipse seasons, between which no cycling normally occurs. During eclipse season, the cycles last 24 hours; therefore, eclipse seasons last for 45 days. The discharges last for periods that vary from 5 to 20 minutes on the first day and increase to about 72 minutes on the 23rd day. They then decrease again to 5 to 20 minutes on the last day. Because two of these 45-day seasons occur each year, the intervening noncycling periods last for 134 days. Of concern are the behavior patterns: (1) on charge during the eclipse season cycling, (2) on discharge during eclipse seasons, and (3) during the noncyclic periods.

Much less testing has been done for synchronous orbit than for low-Earth orbit, and the amount of published data for the former is correspondingly smaller. The most broadly based known test program in the United States is that at NWSC/Crane (Reference 117). References 29, 38, 125, and 127 through 131 describe more specific synchronous-orbit life tests. References 132 and 133 describe extensive European test programs. These tests cover the temperature range from -10 to +40°C, maximum depths of discharge from 30 to 85 percent of rated capacity, and charge rates from 0.03C to 0.3C.

Orbiting spacecraft provide the other basic source of performance and life data. However, because existing systems provide only battery-level data and the relationship between battery-level data and cell performance is obscure, few useful cell characteristic data have been derived from orbit data.

About half of all synchronous-orbit ground tests have been real-time tests, and the remainder have been various time-accelerated tests. As far as is known, the latter do not involve increased stress levels, but rather involve omitting a large fraction of the noncycling time associated with a real-time orbit. Correlation of voltage performance between real-time tests and time-accelerated tests, in which noncycle time is spent on trickle charge for the few tests that can be directly compared (References 51 and 133), is good for up to the equivalent of 4 years of real time. No comparative data were found for longer missions.

3.4.3.1 Charge-Voltage Current Trends During Eclipse Seasons in Synchronous-Orbit Operation

In each case for which data are available, the voltage trend at the end of charge during eclipse-season cycling has been as if there were a gradual increase in internal impedance on entering overcharge. SAFT-America cells have generally experienced a larger change with time than have General Electric cells. Where charging has been by constant current with no voltage limit or none below 1.55 volts, end-of-charge voltage at a given recharge ratio and temperature has increased gradually but continuously. The rate of increase with time is generally greater at lower temperatures and higher charge rates. At charge rates below 0.05C and at moderate temperatures, the rate of this voltage increase has been typically about 0.005 volt per cell per year (Reference 132). At higher rates and at about 0°C, the charge voltage of pre-1968 General Electric cells increased by 0.05 volt per cell in the first year or two on real-time synchronous-orbit tests, after which it leveled out in the range from 1.54 to 1.58 volts (Reference 117). Although this high a voltage is not desirable, note that a number of these cells have operated for several years at 0°C in this mode without being distorted by high internal pressure while restrained on the large faces. Thus, end-of-charge voltages above 1.5 volts per cell at about 0°C are to be expected on constant-current charging unless an appropriate voltage limit is used.

When a fixed charge-voltage limit has been used, the increasing impedance effect causes the charge voltage to reach the limit sooner as time goes on, causing premature current tapering or current reduction, which can lead to insufficient charge return to support the maximum depths of discharge used in synchronous-orbit applications. Thus, end-of-charge current may decrease by a factor of 2 to 4 over several years. Such a change may cause the operating temperature range of the battery to decrease significantly. Provision of multiple selectable voltage limits almost eliminates this

problem. However, if the increase in this end-of-charge impedance effect becomes too severe, raising the voltage limit will only raise the end-of-charge cell voltages further without appreciably increasing the charge throughput.

The cause of this increasing impedance effect is not fully understood at this time. One possible cause is a reduction in the amount of uncharged excess-negative capacity in the cells. (See Section 4.) However, high voltage on constant current has been seen in cells that appear to have adequate uncharged excess negative. A better understanding of this effect is therefore needed for supporting future long-term communications satellite missions.

3.4.3.2 Discharge Voltage Trends During Cycling in Synchronous Orbit Operation

The voltage characteristic in synchronous cycling that is of most concern for battery design is the minimum voltage that occurs at the end of one or more of the longest discharges in the middle of each eclipse season. The season-minimum end-of-discharge voltage is not a well-defined function of mission time* based on existing data, except at low temperature (-10 to +10°C) and low maximum depths of discharge (30 percent and below). Under the latter conditions, the minimum voltage of good quality cells can be expected to decrease linearly with time, beginning above 1.2 volts per cell and remaining above 1.15 volts for at least 4 years (eight eclipse seasons) (References 132 and 133). As the cell temperature and/or maximum depth of discharge increases, the trend of minimum eclipse-season voltage during continuous operation without reconditioning becomes less predictable from existing data. This appears to be due partly to the wide range of charge rates and charge-control methods used in different tests and partly to inherent differences in cell design and response.

Table 31 is a compilation of minimum end-of-discharge voltage data from many ground tests. These data are plotted in figures 60 and 61, together with data from 24- and 50-Ah battery life tests (References 51 and 125) and from certain orbiting geosynchronous communications satellites. Data for depths of discharge ranging from 60 to 65 percent are grouped in figure 60, and data for the range from 75 to 85 percent are grouped in figure 61. No flight data are included. In all these tests, the batteries were trickle-charged during noncycling periods at rates ranging from 0.01C to 0.03C.

*Because cycling in synchronous and similar orbits is not often continuous, it is generally more useful to relate trends to total mission time than to use the number of cycles completed.

Table 31
Minimum Eclipse-Season End-of-Discharge Voltages
from Simulated Synchronous-Orbit Ground Tests

Temperature (°C)	Depth of Discharge (%) ¹	Data-Source Reference	Average End-of-Discharge Voltage (Year number)					Notes
			2	4	6	10	10	
0	50	134	1.175	1.13	(2)	1.1 to 1.13	Accelerated	
			1.175	1.17	1.16	1.05 to 1.1		Accelerated
	60	135 ¹	1.18	1.16	(2)	(2)	Accelerated, constant DOD	
			1.18	1.17	1.16	(2)	Real time, low charge rate	
	80	135	1.19	1.19	1.17	(2)	Real time, high charge rate	
			1.13	1.1	1.06	(2)	Real time, low charge rate	
	10	30	136	1.17	1.15	1.14	(2)	Real time, high charge rate
				1.20	1.18	(2)	One cycle per day throughput, intermittent, varying DOD	
	20	45	136	1.18	1.17	(2)	One cycle per day throughput, intermittent, varying DOD	
				1.15	1.12	(2)	One cycle per day throughput, intermittent, varying DOD	
30	60	136	1.16	1.12	(2)	One cycle per day throughput, intermittent, varying DOD		
			1.13	1.10	1.17	Real time, high charge rate		
40	45	136	1.19	1.19	1.17	Real time, high charge rate		
			1.15	1.15	1.12	One cycle per day throughput		
60	60	136	1.13	1.05	(2)	Intermittent, varying DOD		
			Erratic	0.9		Intermittent, varying DOD		

¹ All discharges at constant current.

² Test discontinued before this point was reached or data not available.

³ Tests at NWSC X time are done with a long discharge in the middle of each eclipse season to measure capacity. This discharge results in an increase in discharge voltage on the following several cycles.

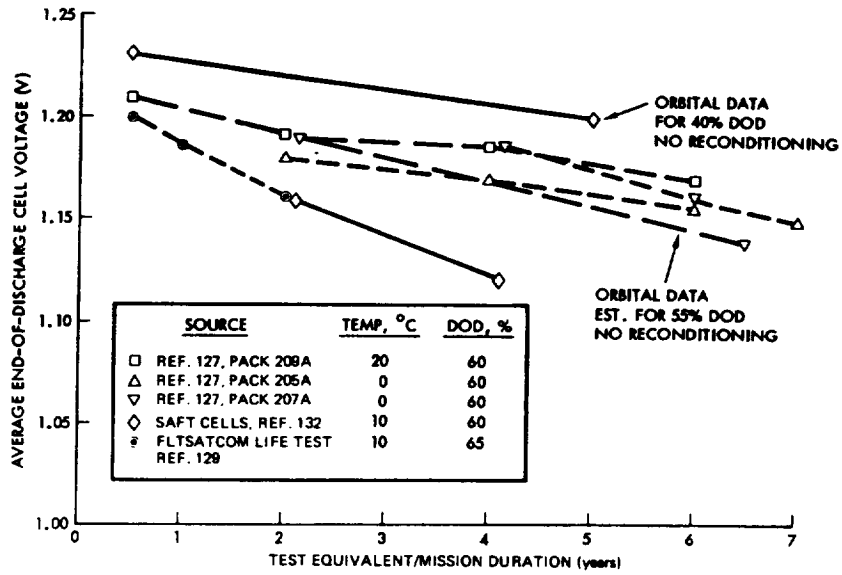


Figure 60. End-of-discharge voltage trends in synchronous orbit (60- to 65-percent depth of discharge).

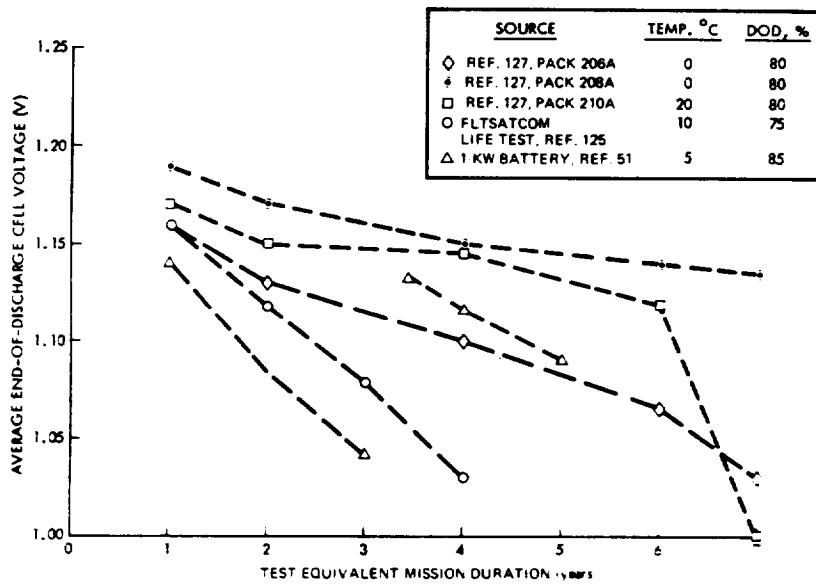


Figure 61. End-of-discharge voltage trends in synchronous orbit (75- to 85-percent depth of discharge; no reconditioning).

Figure 60 shows that the voltage trends from different tests (real-time, accelerated-time, variable discharge, and constant discharge) at any one depth of discharge and temperature fall roughly together over the first 6 "years" of operation,* with some scatter as expected. The voltage levels are appropriate for batteries in good condition at the beginning of the first eclipse season of the mission. Otherwise, the voltage levels may be as much as 0.03 volt lower than that shown.

One aspect the figures do not show is an increasing spread between the highest and lowest voltage cells at end of discharge as the average of a multicell battery falls below 1.1 volts per cell. The voltages of the lowest voltage cells appear to be reaching a second plateau. This plateau is less well-defined than the one that results from cycling at low depth of discharge (Reference 77) and, for some cells, may be located below 1 volt. Much less end-of-discharge voltage spread is observed when a battery is subjected to regular, effective reconditioning during life tests (Reference 125). (See Section 3.4.4.)

3.4.3.3 Capacity Trends During Continuous Long-Cycle Tests

Capacity to any given end voltage decreases gradually with the number of eclipse seasons or total cycles completed in a synchronous-orbit regime. The rate of decline increases as operating temperature increases. The NWSC/Crane tests (Reference 117) provide the only source of in-test capacity data. In these tests, each cell pack was discharged down at the normal test rate in the middle of each simulated eclipse season. Only five cells have been subjected to any one set of conditions, however, and this number of samples is too small to provide clear-cut capacity degradation guidelines at this time.

Capacity trend data are available from another type of long-cycle testing at NWSC/Crane in which the cells undergo an unchanging 24-hour cycle, with a 1-hour discharge each day. Here again, the test packs are periodically discharged down to 1 volt per cell at the test discharge rate. Figure 62 is a plot of the decline of capacity that occurs during one 24-hour cycle test as a function of the lower voltage limit. Note that, in this case, the difference between an end voltage of 1.0 volt per cell and 1.1 volts per cell corresponded to a difference of 18 months of operation at 60 percent depth of discharge.

*In this context, a "year" corresponds to the completion of two simulated eclipse seasons, plus any associated noncyclic operation between seasons.

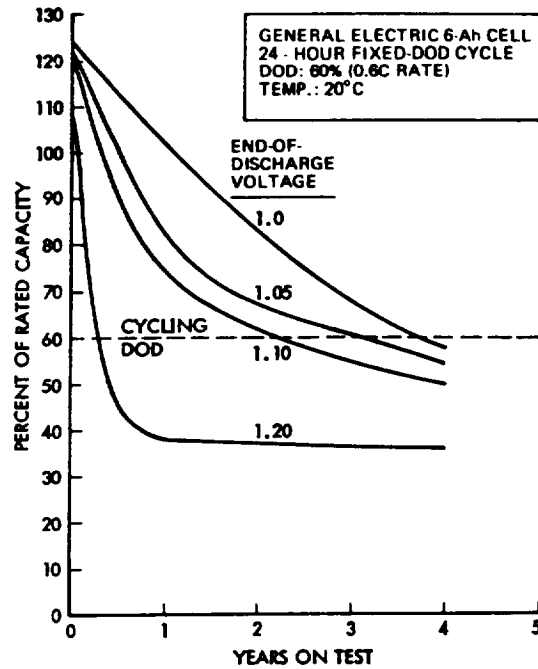


Figure 62. Capacity decline during 24-hour cycling (end-of-discharge voltage a parameter).

3.4.3.4 Cell Failure Rate in Synchronous Orbit

A recent analysis of cell failure data from synchronous satellites and ground simulation tests* resulted in an estimate for the mean failure rate of sealed nickel-cadmium cells in this application of from 100 to 200 per 10^9 hours for a 6- to 8-year mission, depending on the assumptions used. The instantaneous failure rate did not remain constant, but appeared to increase with operating time. This value includes operation under all temperatures prevailing in orbit and the range from 0 to 20°C for ground tests. In contrast to the types of failures seen in low-Earth orbit, less than 25 percent of the total failures involved shorts; most failures resulted from a combination of high voltage on charge and low voltage on discharge.

*Interoffice correspondence No. TDRSS-78-214-030 TRW Data Systems Support Group, Redondo Beach, California.

3.4.3.5 Effects of Cell-Design and Process Variations on Performance in Long-Cycle Applications

No specific cell-design variation tests have been conducted under short-orbit cycle conditions for comparison with those done at NWSC/Crane. (See Section 3.4.1.5.) Krause reports that cells with teflonated negatives are showing results that are superior to those of normal cells in an accelerated synchronous-cycle test at 100-percent maximum depth of discharge (Reference 135). No voltage or capacity data were given.

Nickel-cadmium cells with electrochemically impregnated positive plates have been subjected to various time-accelerated tests for geosynchronous-orbit applications (References 25 and 137). The general result is that discharge voltage is more stable than that of chemically impregnated plates. Little, if any, thickening of the positive plates occurred during these tests. One synchronous-orbit test with cells that incorporate both positive and negative plates made by the electrochemical impregnation process has been reported (Reference 136). The results of testing electrochemically impregnated plates to date must be considered preliminary, however, and much remains to be done to evaluate this development and a number of other potential design and process improvements now being offered by cell manufacturers for synchronous and interplanetary-probe applications.

3.4.4 Effect of Reconditioning on Performance in Synchronous-Orbit Operation

The data and projections discussed in Section 3.4.3 are applicable when no effective reconditioning procedures are used during a test or flight. An "effective" procedure is defined as a procedure that produces a large and long-lasting increase in usable energy per cycle and, ultimately, in useful cycle life. Some procedures referred to as "reconditioning" have little actual beneficial effect and are therefore reconditioning in name only.

To be effective, a reconditioning procedure must consider the degree and nature of degradation in the cells—the greater the degradation and the longer the time since the battery was previously effectively reconditioned, the more difficult it is to achieve true reconditioning. On the other hand, if a well-devised procedure is applied regularly throughout a mission, starting at the beginning, a minimum of difficulty should be encountered in maintaining a battery in condition. Regular reconditioning, by discharge to 1 volt per cell average, has been performed over several years in a number of orbiting satellites with good results (References 78, 125, and 134).

Although a significant increase in discharge voltage is usually obtained by discharging down to 1.0 volt per cell at the 0.3C to 0.6C rate, followed by a full recharge, a much greater and longer lasting increase in discharge energy is usually obtained when the discharge is performed at the 0.05C to 0.01C rate. One life-test has been described (Reference 123) in which, by discharging a battery regularly through a resistor at the 0.01C rate or less down to a low battery terminal voltage (of the order of 1 to 2 volts), near-full capacity was restored in a previously degraded battery and has been maintained throughout more than 30 simulated eclipse seasons (equivalent in cycles to 15 years in orbit). Some cells were reversed near the end of the low-rate discharge, but no ill effects on these cells have been detected. The pressure in one cell that was equipped with a pressure transducer has never exceeded 30 psia during reversal.

SECTION 4 CELL FAILURE ANALYSIS AND MECHANISMS

4.1 INTRODUCTION

This section presents an approach to the analysis of degradation and failure, including a system for classifying these phenomena. The methodology of cell teardown analysis as it pertains to the sealed nickel-cadmium cell is presented briefly, and the significant findings in this area are evaluated. The forms and causes of failure that occur most frequently are then analyzed and classified.

4.2 SYSTEMATIC APPROACH TO DEGRADATION/FAILURE ANALYSIS

Cell degradation or failure analysis has been defined as the process of determining the nature and underlying causes of observed anomalous behavior (References 138 and 139). This information may serve as the basis for corrective action. Defined in this way, failure analysis is considerably broader than teardown analysis *per se*. A complete degradation/failure analysis of a battery cell should involve the following steps:

- Gathering and analyzing available data
- Postulating one or more theories as to the cause of the failure
- Performing electrical testing and teardown analysis of the cell in question to verify the theory
- Correlating electrical behavior with the physical/chemical conditions inside the cell and developing a description of the process of degradation

These steps were first described in detail with respect to nickel-cadmium cells by McCallum et al. (References 138 and 140 through 143). These reports also contain additional references in this field. Progress in the area of failure analysis has been impeded by the lack of a widely accepted frame of reference and method of describing cell-degradation/failure phenomena. McCallum et al. (References 138 through 143) developed one

method that consists of a system of concepts, terms, and definitions designed for organizing information describing failure, its characteristics, and its underlying causes. This conceptual framework is summarized here because it is widely applicable and because many of the details are necessary to the discussion of relationships between degradation and cell-design and process variables that follow. On the basis of the author's experience, certain modifications to the system as originally published have been included.

4.3 DEGRADATION AND FAILURE-ANALYSIS TERMINOLOGY APPLICABLE TO CELLS AND BATTERIES

4.3.1 Degradation and Failure

The term "degradation" may be defined as a significant and persistent change in performance or in some characteristic, relative to that observed when the cell or battery was new, in a direction that reduces usefulness or manageability. The term "failure" is more specific, being defined as the inability of a cell or battery to deliver on discharge or accept on charge a prescribed quantity of electrical energy within a prescribed set of limits (Reference 138). The limits referred to are the "failure criteria."

Because the concept of degradation includes failure as a special case, degradation may be described without any judgment regarding failure, but failure implies degradation beyond prescribed limits. Users establish the criteria of failure to fit their applications.

Although most clearly defined when applied to whole cells or batteries, the term "degradation" may also be applied to cell components and to their particular characteristics. For clarity, additional modifying terms should be used when referring to a specific case. These modifiers should specify the device level (i.e., battery, cell, or cell component, if known) and the deteriorated characteristics. For example, one might have "battery charge-voltage degradation," "cell-capacity degradation," or "separator wettability degradation."

As previously defined, failure can be either reversible or irreversible. For example, the inability of a cell to meet performance requirements is usually irreversible if it results from an irreversible open circuit, a high impedance, or a shorted condition. If the inability exists only under a particular set of operating conditions, a change in these operating conditions or the application of an appropriate reconditioning procedure may

eliminate the "failure." This type of failure is usually exhibited as a gradual decline of end-of-discharge voltage to a point less than a tolerable limit. Often, however, operating conditions cannot be changed or reconditioning cannot be performed in a given application, so that an otherwise reversible failure may become permanent.

4.3.2 Degradation/Failure Modes Defined

The term "failure mode" is widely used to refer to all aspects of cell degradation or failure. McCallum et al. (References 138 and 140) proposed that the term "mode" be used in a more restricted sense—to identify only the directly measurable parameter or combination of such parameters that exhibited deterioration or exceeded prescribed limits. Use of this definition confines a degradation/failure mode to a description in terms of electrical quantities, such as voltage, current, ampere-hours, and watt-hours. Restricting these definitions to electrical quantities was based on the fact that cell-level electrical (i.e., current/voltage) degradation can impact battery electrical performance and on the assumption that characteristics such as internal cell pressure and temperature cannot have a direct impact. It was also recognized that pressure and temperature data often are not available for individual cells; therefore, mode definitions should not require that these parameters be specified. However valid these points may be, it has become evident that information other than electrical can help considerably in understanding the cause of failure, and pressure and temperature data should therefore be included in the description of the failure mode when they are available. This broader definition will therefore be used in this manual.

Table 32 is a matrix of the various categories of data and the choices within each category that are useful to describe a degradation/failure mode. The term "electrical degradation/failure mode" refers to mode descriptions that include only electrical quantities.

An example of a degradation mode would be "abnormally low cell voltage, high pressure, and high temperature at end of discharge." The corresponding electrical degradation mode would be "low cell voltage at end of discharge." A related electrical failure mode would be "cell voltage below 0.5 volt on discharge before rated capacity output (temperature and rate specified)." Failure modes are discussed further in Section 4.4.

Table 32
Expanded Cell Degradation/Failure Mode Description Matrix

Operating Condition	Midcharge and/or Mid-Discharge	Cell Voltage ¹ End of Charge and/or End of Discharge ²	Overcharge	Internal Pressure End of Charge and/or End of Discharge	Temperature End of Charge and/or End of Discharge
Active Charge	High ³ Normal Low ³	High Normal Low	(4)	High Normal Low	High Normal Low
Overcharge	(4)	(4)	High Normal Low	High Normal Low	High Normal Low
Discharge	Normal Low	Normal Low	(4)	High Normal Low	High Normal Low

¹ Preferably at constant current. Rate should be specified. Conversely, if the battery is charging under a voltage limit or discharging at constant power, the current behavior may be described.

² EOC = end of charge involving normal charge return used for regular cycling; EOD = end of discharge to depth used for regular cycling.

³ High and low are relative to expected normal range.

⁴ Not applicable.

4.3.3 Degradation/Failure Determinants Defined

McCallum and Miller distinguished two levels of causes of degradation/failure modes (Reference 138). The most immediate and predominant cause was called the "determinant." The determinant was defined as that single cell component, together with the electrical condition and/or behavior of that component, that directly produced the degradation/failure mode of interest (References 138 and 140). It is advisable to broaden the definition to include more than one component because two or all three of the components that may often be determinants (i.e., positive electrode, negative electrode, and separator) may share the responsibility for abnormal cell behavior, and one should not be rejected over the others. For example, the cell terminal voltage (V_T) may be modeled as

$$V_T = E_p - E_N + I R_i \quad (25)$$

where

- E_p = the electrode potential of the positive electrode at current I
- E_N = the electrode potential of the negative electrode at current I
- I = cell current (positive on charge; negative on discharge)
- R_i = interelectrode ohmic resistance, where R_i is largely a function of the resistance across the separator

Thus, each term on the right-hand side of equation 25 corresponds to one determinant of V_T .

Therefore, in the analysis scheme used in this manual, a failure mode may have several determinants but each determinant is concerned with only one component.

Examples of possible determinants of the degradation mode "low voltage at end of discharge" might be "excessive polarization* of the negative

*Polarization of either electrode is the difference between the observed electrode potential with current flowing and that on open circuit. Thus, if $(E_O)_p$ and $(E_O)_N$ are the open-circuit potentials, the respective polarizations are $E_p - (E_O)_p$ and $E_N - (E_O)_N$, where E_p and E_N are as defined for equation 25. With the sign of I defined as for equation 25, $E_p - (E_O)_p$ is positive on charge and negative on discharge, and $E_N - (E_O)_N$ is the opposite.

electrode at end of discharge” and “excessive IR-drop across the separators.” Note that these descriptions state the existing electrical response of components, but do not state the cause for the response or how the observed condition may be developed. These latter aspects are the subject of the failure mechanisms, as described in the following section. Determinants are discussed further in Section 4.5.2.

4.3.4 Degradation/Failure Mechanisms Defined

The term “failure mechanism” is often used interchangeably with the term “failure mode” to refer to all aspects of the failure process. It is also used loosely to refer to the behavior of a cell component (e.g., the “plate-swelling mechanism” or the “separator dry-out mechanism”). The term “mechanism” may also be used in failure analysis to refer to or describe the sequence of steps or reactions leading from the original condition of a component to the condition described by a determinant. In this manual, the term “mechanism” will be used only in the sense last defined. Furthermore, the term “specific mechanism” will be used to describe the detailed physical or chemical changes involved in any single step in a sequence.

Examples of physical or chemical processes involved in specific mechanisms include:

- Solution of an ionic solid in the electrolyte
- Precipitation of a dissolved substance
- Corrosion of a metal
- Diffusion of protons or charged ions through a solid phase
- Diffusion of dissolved substances through the electrolyte
- Expansion and contraction
- Chemical reactions such as hydrolysis, oxidation, and reduction

Mechanisms of degradation are more difficult and costly to determine than determinants and are therefore often neglected. Yet a knowledge of mechanisms is essential in designing meaningful accelerated tests and, ultimately, in eliminating a failure determinant. Section 4.5.3 contains examples of degradation mechanisms.

4.3.5 Degradation/Failure Description Summary

The terminology for analysis and classification of degradation/failure phenomena described in the preceding sections as as follows:

<u>Category</u>	<u>Quantities</u>
Modes	Voltage, current, time, ampere-hours, watt-hours, pressure, temperature, etc.
Determinants	Electrical, physical, and electrochemical
Mechanisms	Physical and chemical

Figure 63 is a diagram of the structure of this system. The literature (e.g., Reference 106) describes other systems of classification using similar terms, but the one shown is used in this manual.

Figure 63 shows that avenues to be investigated increase rapidly as the depth of the analysis is increased. Depending on the extent of an analysis, certain mechanisms may be presumed but may remain unverified.

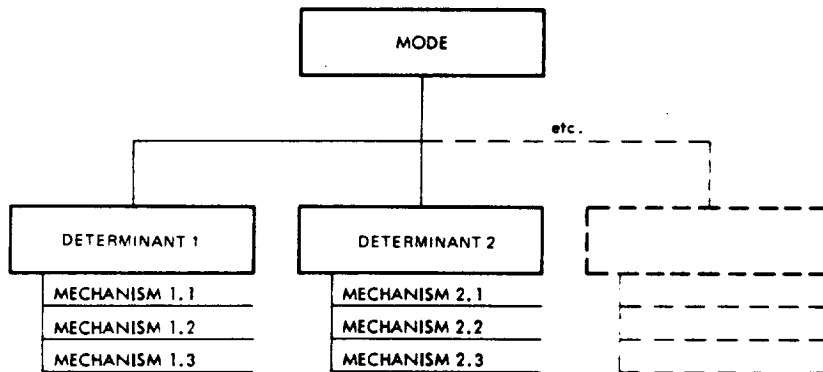


Figure 63. Degradation/failure process description scheme.

Judgment and experience may be used to establish "most probable" mechanisms in the absence of physical evidence. The distinction between presumed and demonstrated mechanisms is often not clear in literature references.

Although this overall method of description is most applicable at the cell level, it is also applicable to batteries with appropriate modifications. The degradation mode of a battery would describe characteristics measurable at the battery (cell string) power terminals, as well as average battery temperature and, possibly, average cell pressure if it can be determined. Battery-degradation determinants would include individual cells as a whole because the cells are the main active "component" of a battery. High-resistance connector contacts and solder joints are other possible battery-degradation determinants.

4.4 OBSERVED DEGRADATION AND FAILURE MODES

This section discusses and classifies observed degradation/failure behavior according to the system described in Section 4.3. These discussions provide a basis for examining the underlying causes presented in subsequent sections. See Section 3 for data on frequency of failure as a function of number of cycles or operating time.

4.4.1 Low Voltage at End of Discharge

The degradation mode "low voltage at end of discharge" is the most frequent observed cell degradation characteristic (References 68 and 106), and it impacts battery voltage performance most directly. Low end-of-discharge voltage is classified as either a degradation mode or a failure mode, depending on the severity of the voltage discrepancy, the shape of the voltage-discharge time curve, and the minimum allowable voltage.

In most common uses, the voltage behavior referred to is that observed during continuous cycling under use conditions (i.e., the "in-cycle" behavior). The end-of-discharge versus output behavior out-of-cycle or under noncyclic conditions is often quite different from in-cycle behavior. (See Section 4.4.2.)

Because the phrase "low voltage at end of discharge" describes only a single point in the charge/discharge cycle, it provides little information on which to base a failure analysis. To improve the description, cell voltage at several points in the operating electrical cycle could be included in the mode

description. Table 33 lists several types of voltage behavior that have accompanied low end-of-discharge voltage. Theoretically, each of these combinations may occur with different pressure behavior, but elevated pressure (greater than 1 atmosphere) is most frequently found in cells with low discharge voltage (References 68 and 106). Each combination of behavior factors shown in table 33 (i.e., each different complete mode description) may imply a different degradation mechanism.

Table 33
Cell-Voltage Behavior Variations of the
Low End-of-Discharge Voltage Mode

Variation Number	Mid-Discharge Voltage*	End-of-Discharge Voltage	Mid-Charge Voltage*	End-of-Charge Voltage
1	Normal	Low	Low to normal	Low to normal
2	Normal	Low	Low to normal	High
3	Low	Low	High	High
4	Low	Low	Low	Low

*Beginning-of-discharge and beginning-of-charge voltages are normal for all variations of this mode.

4.4.2 Loss of Capacity

The capacity of a cell is normally defined as the number of ampere-hours (or coulombs) of electrical output obtained on discharge to a predetermined end voltage when the cell is charged and discharged under a specified set of conditions. Some workers use the term "capacity" to refer to output obtained under continuous-cyclic operating conditions unique to their application (the so-called "in-cycle" capacity). Others use the term to refer only to output under a fixed set of standard conditions (e.g., temperature 25°C, 0.1C-rate charge for 24 hours, 0.5C-rate discharge to 1.0 volt), regardless of the conditions for any particular application (the so-called "out-of-cycle capacity"). Because the measured capacity of a given cell and the rate of change of capacity are usually different under different operating conditions, the various capacity values reported in the literature can be confusing and difficult to compare.

When in-cycle capacity is referred to, the foregoing definition of capacity indicates that "loss of capacity" is another name for "discharge voltage reaching some lower limit after a decreased ampere-hour output" during cycling; therefore, the loss of capacity results automatically from the low end-of-discharge voltage-degradation mode. When out-of-cycle capacity is referred to, loss of such capacity may or may not correlate with decreasing in-cycle end-of-discharge voltage. During short-cycle operation and at lower depths-of-discharge, the in-cycle end-of-discharge voltage may decline considerably over the first several thousand cycles (e.g., from 1.2 volts to between 1.0 and 1.1 volts), yet the out-of-cycle capacity to 1.0 volt may decrease only slightly. This situation is most likely when the charge and/or discharged rates used for capacity measurement are much different from those used for normal cycling. On the other hand, during 24-hour-cycle operation using a high depth-of-discharge, out-of-cycle capacity may decline considerably while in-cycle end-of-discharge voltage changes little.

Figure 64 shows these distinctions graphically. Discharge-voltage curve 1 represents that of a new cell, with C_1 capacity to 1.0 volt. After several thousand cycles involving discharge to the point at which D_1/C_1 is the depth of discharge, the total discharge-voltage curve may resemble curve 2, in which the end of discharge voltage at D_1 is below 1.1 volts, but capacity at the 0.5C rate to 1 volt is still C_1 (Reference 77). On the other hand, cycling to D_2 (e.g., for a geosynchronous-orbit application, in which D_2/C_1 may be 0.6 to 0.8) may result in voltage curve 3 with only a small voltage loss at D_2 but a 20 percent loss of capacity from C_1 to C_2 (Reference 17), as measured at the 0.5C rate. Thus, in the absence of a more universal and precise definition of the term "capacity," decrease of end-of-discharge voltage and loss of capacity may occur independently, and, hence, both are classified as degradation/failure modes.

4.4.3 Low Voltage on Charge

The phrase "low voltage on charge" is used here to refer to behavior in which charge voltage may be as much as, but not more than, about 0.05 volt below the normal expected value and discharge voltage is normal. Behavior in which both end-of-charge and end-of-discharge voltages are somewhat low, but not indicative of a short, is classified as a low end-of-discharge voltage mode. (See variation 4 in table 33.) Very low voltage is discussed in Section 4.4.4.

Table 34 lists the variations of low-charge-voltage behavior. Such behavior is usually clearly evident only during constant-current charging. If charge voltage is limited, the behavior shows instead as an abnormally high current

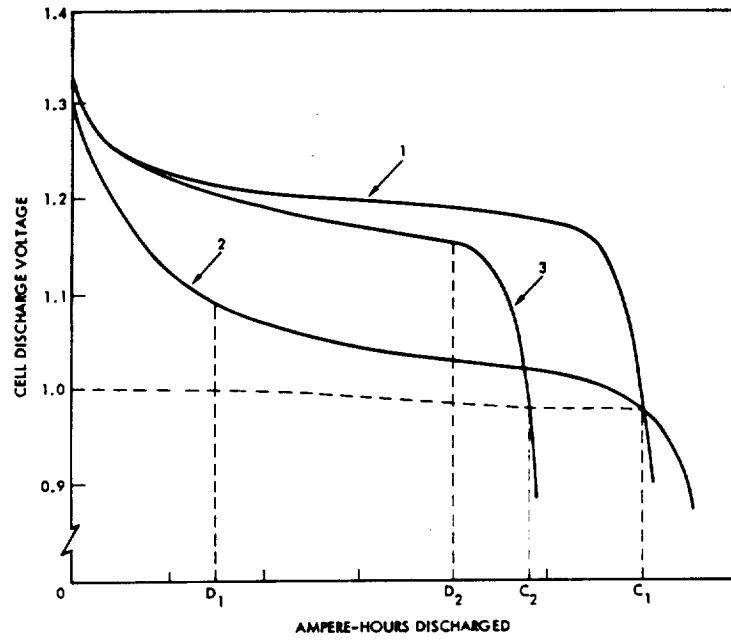


Figure 64. Degradation of discharge voltage with cycling.

Table 34
Variations of Low-Charge-Voltage Mode

Mode Variation Number	End-of-Discharge Voltage	Midcharge Voltage	End-of-Charge Voltage
1	Normal	Normal	Low
2	Normal	Low	Low
3	Normal	Low	Normal

after the voltage limit is reached. When tested in a low-Earth-orbit cycle, General Electric cells exhibit this behavior more than cells of other manufacturers, and the effect is greater the lower the voltage limit value. This type of low-charge-voltage behavior is not classified as a failure mode because it does not signify cell failure if that discharge voltage is normal. It is considered a degradation mode, however, because it represents a persistent and undesirable departure from the original behavior.

4.4.4 Shorted-Failure Mode

The term "shorted" is commonly used to describe an observed behavior in which the cell voltage is significantly less than normal throughout the charge/discharge cycle. Actual voltages may range from only a few millivolts to over 1 volt and may vary considerably during a cycle. Terms such as "hard," "soft," "high resistance," etc., may be added to the term "short," depending on the observed voltage. Ordinarily a cell in the shorted condition cannot be fully or adequately charged under the conditions of use, even though the short may be of the high-resistance type (Reference 68).

4.4.5 High Voltage on Charge

"High voltage on charge" usually means "higher than normal voltage at end of charge," and "end of charge" most often means a recharge ratio of 1.0 or greater. This behavior may be observed when a cell is charged at constant current without a voltage limit or as part of a number of cells in a series battery on which a voltage limit is applied at the battery terminals. When a voltage limit is applied to an individual cell or to the terminals of a small group of cells, or when a large fraction of the cells in a battery with voltage-limiting show similar "high-voltage" behavior, the tendency toward high end-of-charge voltage is seen as low end-of-charge current (Reference 68). The cell therefore behaves as if there were an abnormally large increase in internal impedance at end of charge. No clear dividing line exists between the range of charge voltage referred to as "high charge voltage" and that indicative of a high internal impedance.

Charge voltage alone is not a criteria of failure because failure is judged only on discharge. High charge voltage can contribute to a failure by preventing adequate recharge during cycling when the maximum charge voltage across the battery is fixed. Even in this case, however, a single high-voltage cell in a 20- to 24-cell battery will have a negligible effect on recharge, unless that cell is essentially an open circuit. Batteries have operated satisfactorily as a source of energy on discharge with one (or more) cells

going to abnormally high voltage at end of charge. Therefore, the type of high charge voltage usually observed, in itself, is not classified as a failure mode. Such behavior may be associated with a true failure mode, as shown in table 33 for low-discharge-voltage mode variations 2 and 3. High charge voltage can be considered a degradation mode, however, because the term describes a persistent and undesirable departure from normal behavior.

4.4.6 Open-Circuit Failure Mode

An unusual type of cell-voltage behavior is characterized by a relatively high voltage at all times during charge (equal to the voltage applied at the battery terminals) and a very large negative voltage at all times during discharge with no current flow. This behavior is commonly referred to as an "open circuit." However, whether or not the cell is truly an open circuit internally can be determined only by teardown analysis. The term "open circuit" is classified as a failure mode even though it does not specify voltage or current because it stands for a well-recognized set of current/voltage symptoms.

4.4.7 Other Degradation Characteristics

Many characteristics other than those described in the previous sections are referred to in literature as degradation or failure modes. These include cadmium migration, separator deterioration, separator dryout, plate deterioration, and high pressure (Reference 68). According to the classification system described in Section 4.3, these are degradation/failure determinants, not modes, because they refer to conditions within the cell that are not apparent until the cell is opened and, hence, destroyed as a hermetically sealed device. Degradation/failure determinants are discussed in the following sections.

4.5 UNDERLYING CAUSES OF DEGRADATION AND FAILURE

In general, degradation and failure of cells are produced by the effects of certain incompletely reversible responses of internal cell components to imposed operating conditions. As the operating conditions become more "severe," such as by increasing the temperature and/or charge and discharge rates, the rates of degradation processes usually increase. This section identifies the component or components and conditions of same that are responsible for various externally observed degradation/failure modes (i.e., the determinants of each mode), describes the methods and results of teardown analysis, and reviews available information on degradation/failure determinants.

4.5.1 Teardown Analysis

4.5.1.1 Definition and History*

Teardown analysis is the process of opening and disassembling a cell and inspecting, testing, and analyzing the internal components. When done in connection with a failure analysis, the purpose of these tests and analyses is to establish the determinants of the degradation or failure and, if possible, to obtain information that may lead to a postulation of the mechanism of the degradation process involved. However, teardown analysis *per se* does not include an actual determination of the mechanism.

Observations from teardown analysis appeared in the literature well before the experimental procedures were published. The early annual reports from the evaluation program at NWSC/Crane contained some of the first published observations from relatively large numbers of failed cells (Reference 68). Kent (Reference 106) summarized much of this information. Information on teardown analysis procedures began to be published around 1968; since that time, development effort on procedures and the practice of cell-teardown analysis have grown rapidly. One of the first published accounts of a complete cell failure-analysis system and cell-teardown analysis procedure was that of McCallum and Faust (References 140 and 144). These methods and concepts were developed further by Reed and McCallum (Reference 142), McCallum and Miller (Reference 138), Halpert (Reference 19), Dunlop (Reference 45), Parry (Reference 145), Kröger (Reference 146), and others. References 142 and 147 contain complete procedures for teardown analysis of sealed nickel-cadmium cells. Stofel describes a similar procedure in less detail (Reference 148).

4.5.1.2 Cell-Teardown Procedures

As described in Reference 147, cell-teardown analysis may consist of the following steps:

- Gas sampling and gas analysis
- Extraction of electrolyte
- Electrolyte analysis (for KOH, carbonate, nitrate, etc.)

*The term "failure analysis" is sometimes used in the literature to refer to teardown analysis as defined here. However, as defined in Section 4.2, failure analysis has a much broader scope, and teardown analysis can be performed in the absence of a failure.

- Inspection of components
- Chemical analysis of positive plates for:
 - Charged and discharged nickel-active material
 - Carbonate
 - Nitrate
 - Additives
- Chemical analysis of negative plates for:
 - Charged and discharged cadmium-active material
 - Carbonate
 - Nitrate
 - Additives
- Electrochemical capacity measurements of positive and negative plates
- Physical property measurements on positive and negative plates, including:
 - Weight
 - Thickness
 - Void fraction (porosity)
 - Mechanical strength
 - Surface area
 - Crystal structure

Reference 147 also contains procedural details, calculations, and data sheets. The procedure may be varied to disassemble the plate stack before extracting the electrolyte so that the electrolyte content of individual

plates and separators may be measured to determine electrolyte distribution. Also, testing and analysis of separators can be added, if desired, using tests and data given in References 29 and 149.

The most difficult part of cell-teardown analysis is the chemical analyses of plates, particularly of positive plates. After some cycling by direct extraction with ammonium hydroxide/chloride solution* as described by Reed and McCallum (Reference 142) and Parry (Reference 145), positive-plate analysis has not been satisfactory because of interference by residual charged nickel-active material. The procedure originally described by Kröger (Reference 146) and detailed in Reference 147 is more generally useful.

Although older methods of analyzing negative plates (References 142 and 145) worked better than those for positive plates, the method given in Reference 147 is recommended. Some question remains as to whether the extraction step cleanly separates discharged cadmium material (Cd^+) from charged material (Cd^0). Another method that is free from this uncertainty involves treating the sample with a dilute nonoxidizing acid whereby hydrogen gas is generated by any Cd^0 that is present.† The details of this method have not been published. Some organizations use atomic-absorption (AA) spectroscopy to determine nickel and cadmium in solution rather than the wet-chemical methods described in Reference 45. When an AA instrument is available, it can save time because physical separation of constituents is usually not necessary. Also, AA can be used to advantage to analyze for cobalt, iron, silver, and other metallic elements that may be present in small concentrations in the sinter.

4.5.1.3 Results of Teardown Analyses of Nickel-Cadmium Cells

The results of teardown analyses performed on failed‡ cells from the test program at NWSC/Crane through the year 1967 (Reference 68) were summarized and statistically analyzed in Reference 106. During this period, the analysis was limited to visual inspection and recording of conditions observed in failed cells.

*Sometimes referred to as "Muspratt solution."

†D. Maurer, Bell Telephone Laboratories, private communication.

‡For the definition of failure used in the NWSC/Crane program at that time, see the reports listed in Reference 68.

Table 35 shows the distribution of the five most frequently occurring characteristics. Most of these cells had been tested in either a 1.5-hour or a 3-hour cycle. The "migration" referred to is that of cadmium-active material, subsequently identified as cadmium hydroxide. Evidence of migration was seen as deposits on negative-plate surfaces and in the voids of separators. The practically identical frequency of "separator deterioration" suggests that the first two items in the table should be combined. However, "migration" was seen in the absence of appreciable "separator deterioration" at low operating temperature (0°C). The "deposits" listed were found on the inner surfaces of the terminals, on tabs, on plate edges, and on the inner surfaces of cell containers in different cells. The chemical composition of the deposits was apparently not determined. The "blisters" occurred mainly on the positive plates, with the sinter being loose in some cases and in place in others. These results apply to cells made during the period 1963 to 1966, well before the NASA model high-reliability cell specification was drafted and more stringent quality controls were implemented beginning in 1969 (Reference 150).

Table 35
Frequency of Occurrence of Characteristics Found
by Teardown Analysis (NWSC/Crane, 1964 to 1967)

Designation of Characteristic ¹	Percent of Total Number of Cells Opened ²
Migration	54
Separator deterioration	53
Deposits	40
High pressure	34
Blisters	22

¹The names shown are those used in the references.

²A total of 320 cells were included in this summary.

Unfortunately, no summary or analysis of teardown information from NWSC/Crane for the period from 1969 to the present has been published. A review of the more recent annual reports from the NWSC/Crane test program (Reference 68) shows that the frequency of failure has decreased substantially for cells made after 1968, and occurrences related to impurities (such as deposits) and to poor workmanship (such as short separators or bent plates) have all but disappeared. Migration and separator

degradation continue to be the most frequently observed effects in cells undergoing low-Earth-orbit testing, and the percentage of these effects has increased as the percentage of other effects has decreased.

References 19, 38, 117, and 151 also contain accounts of migration and/or separator deterioration obtained from teardown analysis. These results apply to cells tested under normal operating conditions of temperature, charge rate, and discharge rate. Although some teardown results from accelerated testing (involving elevated temperatures or rates) at NWSC/ Crane have been published, data on migration or separator degradation were not included (References 152 and 153).

Other frequently observed effects associated with degradation and failure include thickening of positive plates (References 17, 25, and 154), and redistribution of porosity and active material in positive plates (References 17, 25, and 154), weakening and crumbling of positive-plate sinter (References 17 and 117), migration of electrolyte out of the separators into the plates (References 155 through 158), flooding of the pores in negative plates (References 91, 155, 156, and 159), and a buildup of carbonate concentration in the electrolyte (References 19, 68, 91, 152, 153, 156, 157, and 158). All of these phenomena often occur together in the same cell, making the overall degradation process quite complex.

4.5.2 Degradation/Failure Determinants

This section describes the determinants of the more important degradation/failure modes that were reviewed in Section 4.4, including both demonstrated and nondemonstrated but probable determinants. Much of the information presented was obtained from teardown analysis. In some cases, experimental proof of a determinant was obtained in the course of failure analysis; in most cases, however, it is known only that certain internal conditions were found in cells that had failed, and the determinants can only be presumed.

4.5.2.1 Determinants of Low End-of-Discharge Voltage Modes

Table 36 lists all possible determinants of the four most frequently occurring low end-of-discharge voltage degradation modes as defined in table 33. These determinants also apply to the loss-of-capacity failure mode. In table 36, any or all of the items shown in one of the four numbered rows for a particular point in the electrical cycle (i.e., mid-discharge, end-of-discharge, midcharge, and end of charge) may contribute at that point.

Table 36
Determinants for Low End-of-Discharge Voltage Degradation Modes

Mode Variation Number from Table 33	State of Charge	Positive Electrode	Negative Electrode	Separator
1	End of discharge	Excessive polarization (-)*	Excessive polarization (-)*	High IR drop
2	End of discharge	Excessive polarization (-)	Excessive polarization (+)	High IR drop
	End of charge	Excessive polarization (+)	Excessive polarization (-)	High IR drop
3	Mid-discharge	Excessive polarization (-)	Excessive polarization (+)	High IR drop
	End of discharge	Excessive polarization (-)	Excessive polarization (+)	High IR drop
	Midcharge	Excessive polarization (+)	Excessive polarization (-)	High IR drop
	End of charge	Excessive polarization (+)	Excessive polarization (-)	High IR drop
4	Mid-discharge	Excessive polarization (-)	Excessive polarization (+)	High IR drop
	End of discharge	Excessive polarization (-)	Excessive polarization (+)	High IR drop
	Midcharge	Abnormally low polarization	Abnormally low polarization	Not applicable
	End of charge	Abnormally low polarization	Abnormally low polarization	Not applicable

*See footnote on page 183 for a definition of polarization. The sign in the parentheses gives the direction of polarization. Negative polarization of the positive electrode and positive polarization of the negative electrode result in a lower cell terminal voltage, and vice versa, as indicated by equation 25.

In all cases in which the results of cell-failure analysis were reported by McCallum and coworkers for low end-of-discharge voltage failures (References 140 through 143), "loss of capacity" from both positive and negative electrodes was observed, but significant increases in internal resistance were measured in some but not all of the failed cells. The term "temporary loss of capacity" was used in the references to indicate that the capacity measured in the flooded state after removal from the original cell was significantly greater than that observed in the original cell. Although electrode discharge-voltage curves were not reported, it is surmised that excessive polarization at end of discharge, as indicated in table 36, was observed. In most cells, the degradation in the voltage of the positive electrode was sufficient to impact the cell voltage under the test conditions, but that of the negative electrode had not progressed to that extent.

Published data from the use of reference electrodes in starved cells undergoing short-cycle testing (References 15, 20, and 59) show that both electrodes usually develop excess polarization (often referred to as "fading") as cycling continues, with the positive electrode exhibiting excess polarization relatively early in cycle life and the negative electrode following by several hundred to several thousand cycles. Because of this difference in rate of response between the positive and negative electrodes, tests of short duration and certain types of accelerated tests can lead to the conclusion that only the positive electrode can be responsible for long-term cell voltage changes (Reference 19).

In contrast to the foregoing behavior, only the negative electrode became strongly polarized in a synchronous-orbit test involving a deep maximum depth-of-discharge (84 percent of rated capacity) and a temperature of 0 to 15°C during discharge (Reference 51). This is one example of how operating conditions can determine the relative importance of the determinants.

Data available for internal impedance before and after cycle testing and for failed cells (References 51, 87, 141, and 160) show a wide range of impedance behavior. With nylon separators and/or at test temperatures of 25°C or below, impedance changes are small and do not correlate with low end-of-discharge voltage (Reference 141). With polypropylene separators and at elevated temperatures, impedance often increases sharply during cycling, and the higher impedances correspond with the lower cell end-of-discharge voltages (References 51 and 160). However, it is believed that, in most cases in which impedance increased considerably in cells with polypropylene separators, insufficient electrolyte had been added when the cell was made.

4.5.2.2 *Determinants of Low-Charge-Voltage Modes*

The possible determinants of the low-charge-voltage modes described in Section 4.4.3 are the same as those shown in the last two lines of table 33. The separator cannot be a determinant here because any increase in separator IR drop from the normal new-cell value (which is of the order of a few milliohms as shown in figure 14) would only increase charge voltage, not decrease it.

4.5.2.3 *Determinants of the Shorted Failure Mode*

The possible determinants of the shorted failure mode described in Section 4.4.4 include two types of shorting paths within the cell—electronic (metal-to-metal) and electrochemical. Electronic shorting is the process whereby electric current flows from one electrode to the other through the cell entirely as electron flow (i.e., without taking part in any electrode reactions). Before 1968, many cases of this type of shorting were caused by the bridging of silver across the insulator of a terminal seal in cells in which high-silver alloys were used as seal braze materials (Reference 68, First through Fourth Annual Reports). Since then, after the use of high-silver alloys was discontinued and/or protective coatings were applied to braze materials, only shorts of the type that occur between plates of opposite polarity or between positive plates and the case have been significant.

Table 37 lists the different forms of plate-to-plate (metal-to-metal) shorting, together with the apparent contributing causes of each. Although items 1, 3a, and 3b result primarily from poor workmanship during cell assembly, they sometimes do not manifest themselves for a great many cycles. Items 2 and 3c result from the response of cell materials to electrical cycling and environmental conditions.

An electrochemical short occurs when an electrochemical reaction, other than the main cell reaction and having a charge and/or discharge voltage much lower than that of the main cell reaction, begins to take place at an appreciable rate in the cell. The one most likely to occur in a nickel-cadmium cell is the cadmium-cadmium cell, which could occur after a certain amount of cadmium had accumulated on the positive plates. Because the voltage necessary for driving this reaction is about 0.2 volt, the occurrence of this reaction may explain why some cells cannot be overdischarged to cell voltage that is more negative than -0.2 volt regardless of how long the discharge is continued (Reference 95).

Table 37
Forms of Plate-to-Plate Shorting

Item	Form	Contributing Cause
1	Metal-to-metal contact at corners or edges	Circumvention or mechanical piercing of separator by sharp edges from bent corners, edges, or substrate burrs
2	Sinter-to-sinter contact	Physical and/or chemical breakdown of separator structure
3	Bridging across the separator	a. Extraneous metal particles in the separators b. Sinter particles in the separators c. Deposition of migrated active materials in separator voids

4.5.2.4 Determinants of High-Charge-Voltage Modes

The two most commonly observed types of high-charge-voltage behavior are characterized in table 32, indicating that they may occur with low end-of-discharge voltage during cycling. However, the possible determinants of the high-charge voltage are the same, regardless of the voltage behavior on discharge and are shown for mode variations 2 and 3 in table 33.

4.5.2.5 Determinants of the Open-Circuit Failure Mode

The possible determinants of an open circuit are: (a) a high resistance or breakage somewhere in the metallic parts of the electrodes or terminals, and (b) a very high resistance across the separators that persists throughout charge, as well as discharge. Condition (a) occurs only rarely in modern spacecraft cells and is irreversible and catastrophic to battery operation. Condition (b) is usually caused by extreme electrolyte redistribution and may or may not be reversible by reconditioning.

4.5.2.6 Summary of Degradation/Failure Determinants

A review of the possible determinants presented in Sections 4.5.2.1 through 4.5.2.5 reveals that a relatively few basic determinants account for all the degradation or failure modes described. Which of these determinants is

operative must be established by failure analysis before a study of the mechanism can begin. Those determinants are:

- Excessive polarization of the positive electrode
- Excessive polarization of the negative electrode
- A relatively high IR drop across the separator
- A shorting path between the positive and negative electrodes
- An open circuit within the cell case

4.5.3 Cell Degradation/Failure Mechanisms

Gross published a comprehensive, qualitative review of degradation/failure determinants and mechanisms in sealed nickel-cadmium cells in which many factors are mentioned as potential sources of trouble (Reference 161). Although this article is a good introduction to cell failure, it does not indicate interrelationships between factors or relative importance of the factors reviewed.

McCallum and coworkers published many reports bearing the term "Failure Mechanisms" in the title, including References 138, 140 through 144, 160, and 162. Although these reports contain considerable information on failure determinants, failure mechanisms are discussed only briefly in the form of theories and are not supported by experimental evidence. The results of this work are discussed further in Section 4.7.

More recently, information relative to failure mechanisms has come from a variety of sources. Certain degradative processes have received special attention, mainly because their effects are easily seen with the unaided eye during teardown analysis or because relevant data are obtained by simple measurements or tests. The following paragraphs discuss these processes, together with others that are considered important but which are not accompanied by visible evidence.

4.5.3.1 Expansion of Positive Plates

Sintered-nickel-hydroxide positive plates tend to expand during cycling, particularly when the cell is overcharged excessively. The expansion occurs within the sintered-nickel structure because of forces within the pores that

result from the considerably different volumes per unit weight of the charged and discharged forms of nickel-active material (Reference 100) and oxygen gas generated on overcharge and trapped within the pore structure (References 163 and 164).

As a consequence of this expansion, the rate and degree of expansion of positive plates increases as the loading level increases and as sinter tensile strength decreases. The controlling sinter strength is in the completed plate after impregnation and formation. In turn, this residual strength is dependent on the strength in the plaque before impregnation and on the extent of corrosion experienced during impregnation. Because the chemical-impregnation process results in less than 5-percent corrosion to get the same capacity per unit area, it results in a stronger sinter and less expansion (Reference 154). Over the long term, expansion of the positive plates must be minimized to ensure high reliability for long cycle life; therefore, cells for long-life applications should be made with positive plates having the greatest possible strength and/or the lowest possible loading level.

4.5.3.2 Electrolyte Redistribution and Separator Drying

Although it has long been recognized (e.g., see Reference 19) that dry separators are a major contributing cause of low-discharge-voltage behavior, only recently has the mechanism by which electrolyte is lost from the separator become clear. Dunlop (Reference 25) has shown that, as the positive plates thicken with cycling, positive active material moves toward the plate surface and, in so doing, greatly reduces the pore size at the surface where contact is made with the separators. The capillary action of the exposed pores is thus increased, causing electrolyte to be drawn out of the separator more strongly than when the cell was new. At the same time, the expansion of the positive-plate sinter provides more void volume inside the plates, where the absorbed electrolyte is trapped so that it cannot be recirculated.

An additional driving force for electrolyte redistribution is described by Seiger (Reference 34), who finds that a certain volume of air is included in the pores of plates when cells are assembled, and, unless special procedures are used (other than those used for normal spacecraft-cell production) during the initial addition of electrolyte, the volume occupied by the nitrogen in this air will eventually become occupied with electrolyte. Some fraction of this electrolyte is likely to come from the separator.

Separator materials that are only weakly wetted by electrolyte further promote electrolyte redistribution because they release their initial electrolyte content more easily and completely than more strongly wetted materials. Thus, the theory predicts and experience confirms (Reference 158) that unmodified polypropylene separators (weakly wetted) should have a greater tendency to dry out in service than nylon separators. On the other hand, life-cycle test results indicate that cells made with teflonated negative plates are less subject to electrolyte redistribution, apparently because the Teflon film makes the plates less wettable and thus inhibits movement of electrolyte into the negative plates.

The effect of temperature on the rate and extent of electrolyte redistribution is not clear-cut. The rate of positive-plate expansion increases and the viscosity of the electrolyte decreases with increasing temperature, and both of these changes are in the direction of increasing the rate of electrolyte distribution. However, because the wettability of separators by electrolyte increases with temperature, the expected net effect is not obvious. The temperature coefficient of wettability for polypropylene fiber is greater than that for nylon, and low-temperature inactive storage of certain cells with polypropylene separators results in some dewetting.*

It is therefore clear that maintenance of proper electrolyte distribution in a sealed cell requires a balance between a number of design factors and process steps. Plates must be strong and must resist expansion; the separator must have some minimum permanent wettability with electrolyte; and special care must be taken to remove all inert gasses from the pores of the plates before completing the addition of electrolyte and to ensure that sufficient electrolyte has been added.

4.5.3.3 Migration of Negative-Active Material

The phrase "migration of negative-active material," or simply "cadmium migration," is used to refer to the condition seen in many cells on teardown after cycling in which dark-colored, solid material is deposited on the outer surfaces of the cadmium plates (outside of the pores in which the cadmium-active material was initially confined) and/or in the separators. This condition is found to a differing extent in all cycled cells, whether or not they have degraded or failed (Reference 68). McDermott (Reference 165) and Gross (Reference 88) summarized the history, effects, and mechanism of migration of negative material in spacecraft nickel-cadmium cells.

*G. G. Rampel, General Electric Battery Division, private communication.

The migrated material was analyzed and found to be almost entirely cadmium hydroxide (i.e., the discharged form of cadmium).^{*} The generally accepted mechanism of migration involves the generation of soluble complex ions containing cadmium, such as $\text{Cd}(\text{OH})_3^-$, in the pores of the negative plates during discharge, the diffusion of these ions toward the positive plates under the influence of the potential field between the positive and negative, and the precipitation of $\text{Cd}(\text{OH})_2$ by decomposition of $\text{Cd}(\text{OH})_3^-$ as the concentration of KOH in the electrolyte decreases or as the temperature decreases. The solid $\text{Cd}(\text{OH})_2$ may precipitate in the mouth of the pores of the negative plates, on the outer surface of the negative plates, or in voids between the separator filaments. Mayer (Reference 166) has shown that carbonate ions in the electrolyte can accelerate the movement of soluble cadmium species from the negative plates in the direction of the positive plates, and this effect has been observed by others (Reference 167).

A relatively high concentration of migrated negative material is often found when the separator is particularly dry. Whether the migration or the dry condition occurs first has not been determined. In such cases, the separators are usually stuck to the negative-plate surfaces to the extent that they cannot be removed for examination without destroying the original structure.

Because the amount of negative-active material that migrates is only a small fraction of the total quantity in the negative plates, the direct negative capacity loss represented is not the main concern. Instead, problems from migrated material arise from other effects; namely, that migrated material can: (a) partially or completely block some of the negative-plate surface pores, reducing access to most of the active material deeper in the pores (References 88 and 167); (b) fill some of the pores in the separator, forcing out the electrolyte and contributing to high resistance across the separators; and (c) lead to internal shorting of the cell. This last point requires more comment.

Pure cadmium hydroxide is a poor conductor of electric current; hence, the question: how does this material lead to a plate-to-plate short? The answer has been speculated upon, and some circumstantial evidence has been published,[†] but no direct proof has been forthcoming. One theory holds that, within the mass of cadmium hydroxide, metallic cadmium is gradually formed and, under the right conditions, can eventually form a

^{*}Occasionally, nickel-active material is also found in the separators.

[†]D. Maurer, Bell Telephone Laboratories, private communication.

continuous, electronically conductive path between adjacent negative- and positive-plate surfaces. Although migration may be severe, not all cells develop shorts due to cadmium migration, apparently because the conditions required for development of a short are not present in all cells. Because these conditions are not understood at this time, the occurrence of shorting from cadmium cannot be predicted with any certainty.

4.5.3.4 Separator Deterioration

Physical deterioration of nylon separator material has been observed in a high percentage of cells that have failed during low-Earth-orbit cycle testing at NWSC/Crane (Reference 68). The literature often states that migration of negative-active material is the cause of the separator deterioration when these occur together, but such cause and effect have not been demonstrated.

Although the literature often mentions "oxidation of (nylon) separator material" as a presumed mechanism leading to separator degradation, recent work (Reference 30) has shown that direct oxidation is not a significant reaction path relative to chemical hydrolysis of the nylon polymer by the alkaline electrolyte solution. The rate of hydrolysis in 31-percent potassium hydroxide solution increased by a factor of 3 for each 10°C increase in temperature. A 10-percent weight loss caused by hydrolysis produces a marked weakening of the structure of the separator, so that it becomes less able to prevent the plates from coming in contact.

4.5.3.5 Loss of Overcharge Protection

The basis of overcharge protection in a sealed nickel-cadmium cell was discussed in Section 2.3.3.6. Such protection may be decreased or lost in several ways: (a) the pores in the negative plates may become blocked with migrated material as mentioned previously (Reference 88); (b) the active-surface area may decrease because of agglomeration and crystal growth (References 88, 168, and 169); and (c) the negative electrode may become more highly charged relative to the positive electrode. The first two items are difficult to detect and have received little attention to date. The last item, which has been studied by Dunlop and Earl (References 91 and 170 through 172), Font (Reference 90), and others, is considered to be one of the primary degradation mechanisms for synchronous-orbit operation.

The cadmium electrode may become charged by loss of oxygen gas from the cell through a leak. Lim (Reference 30) has described a much more probable mechanism involving oxidation of nylon hydrolysis products (from the separator) by reaction with the charged positive electrode, which indirectly increases the relative state of charge of the negative electrode. Lim calculated that, if the material hydrolyzed from the separator is completely oxidized in the cell, all the overcharge protection initially available in a standard General Electric cell would be consumed at the point at which 10 weight-percent of the separator had been hydrolyzed. Reaction-rate data, obtained at elevated temperature and extrapolated to lower temperatures, indicate that a 10-percent weight loss should occur at 25°C in about 7 years. This rate is strongly temperature-dependent, however, as shown by the plot in figure 65. Note that the time to 10-percent separator hydrolysis is extended to 20 years at a temperature of 15°C. Because the hydrolysis reaction proceeds whether or not the positive electrode is charged and any hydrolysis products that accumulate while the cell is discharged would presumably be oxidized as soon as the cell is again charged, the same time-versus-temperature relationship (i.e., figure 65) should apply during discharge and/or shorted storage as applies during cycling and charged storage in flight.

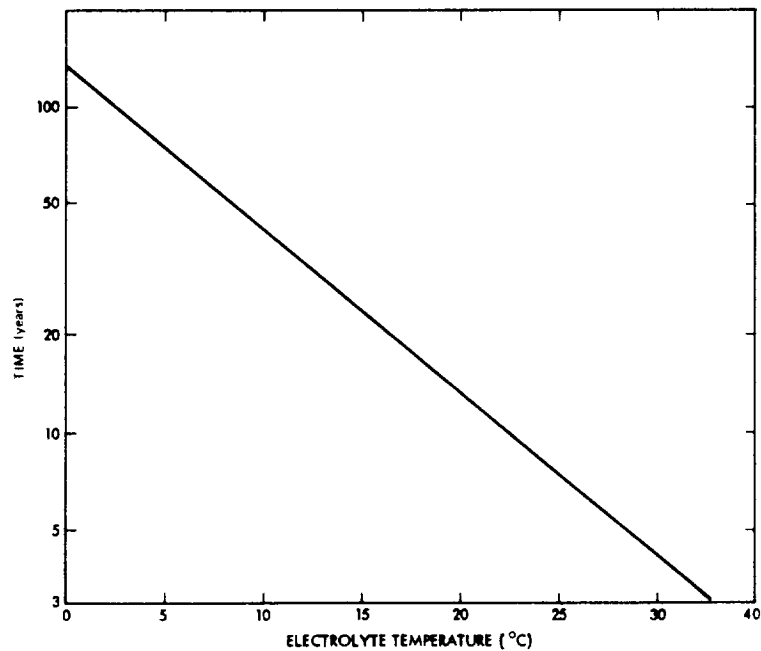


Figure 65. Time to 10-percent hydrolysis of nylon separator versus temperature.

4.5.3.6 Accumulation of UndischARGEABLE Charged Material and Unchargeable Discharged Material

Kröger (References 20 and 59) and Scott (Reference 17) have shown that the percent of active material in the positive electrode that can be effectively discharged at practical discharge rates (usually in the range of 0.3 to 1C) decreases significantly during the first 100 cycles of operation and more gradually after that. Similarly, undischARGEABLE charged cadmium builds up in negative electrodes during cycling (Reference 88) as does unchargeable (discharged) cadmium hydroxide. These accumulations decrease the active areas available for electrochemical reaction and, hence, result in excessive polarization and capacity loss.

One theory proposed for the effect of reconditioning by low-rate discharge is that such operation is able to discharge accumulated charged material that is not discharged during normal cycling. The extra material so discharged is then charged on the following recharge, resulting in the presence of a step increase in the amount of utilizable material for discharge. However, low-rate discharge cannot retrieve accumulated unchargeable material. Such material has been at least partially rejuvenated by prolonged overcharge (Reference 45, p. 99) and by pulse charging (References 173 and 174).

4.5.3.7 Degradation Mechanisms Related to Specific Determinants

The preceding sections described degradation mechanisms in general terms. Interpretation of actual failure-analysis data is facilitated if observations and information on mechanisms can be assigned to specific determinants (as defined in Section 4.3.3 and outlined in Section 4.5.2). To assist in this process, the author has assigned by analysis the most probable immediately underlying causes of each of the most probable determinants (table 38). The mechanisms shown are referred to as "first level" to indicate that additional levels of cause and effect may underlie the phenomena described. Note that different mechanisms may be implied by a single cell component, depending on the nature of the abnormal behavior and where it occurs in the charge/discharge cycle.

4.5.3.8 Interaction Between Degradation Mechanisms

As indicated in Sections 4.5.3.1 through 4.5.3.6 and elsewhere, degradation mechanisms in a sealed nickel-cadmium cell are rarely independent, and many are highly interactive. Figures 66 through 70 show the nature and

Table 38
First-Level Degradation Mechanisms

Determinant		Related First-Level Mechanisms
Component	Electrical Behavior	
Positive electrode	Excessive polarization during active charge	Increased current density due to decreased electroactive surface area Increased plate-surface resistance
	Excessive polarization during overcharge	Decreased electrochemically active area for overcharge Increased oxygen-evolution potential Increased plate-surface resistance
	Excessive polarization during discharge	Insufficient reserve of electrochemically active-charged-positive material at end of discharge Decreased utilization of charged material Increased plate-surface resistance
Negative electrode	Increased polarization during active charge	Increased current density due to decreased electroactive surface area Increased plate-surface resistance
	Excessive polarization during overcharge	Decreased amount of excess negative material (overcharge protection) Decreased electrochemical activity of excess uncharged negative material Decreased electrochemical activity of overall negative electrode (fading) Decreased oxygen-recombination rate capability (increased oxygen-recombination overvoltage) Increased plate-surface resistance

Table 38 (Continued)

Determinant		Related First-Level Mechanisms
Component	Electrical Behavior	
	Excessive polarization during discharge	Insufficient electrochemically active excess charged negative material at end of discharge Increased plate-surface resistance Decreased utilization of charged material
Positive and negative electrodes	Low electrode-potential difference at all times	Positive plate shorted to negative plate by an electronically conducting path
Separators	High IR drop	High electrical resistance due to low electrolyte content

extent of this interaction. These diagrams represent degradation models in which certain, more closely related processes are grouped. The title separations are arbitrary, and, for convenience, a number of phenomena are shown on more than one page.

Note that there are a number of loops where regenerative action may occur (i.e., positive feedback occurs, and high-intensity effects can occur). Note also the prevalence of temperature-sensitive steps and internal heat-generating processes. This explains the generally strong effect of cell temperature that is mentioned throughout the discussion of mechanisms.

4.6 EFFECT OF CELL DESIGN ON DEGRADATION PROCESSES

Sections 3.4.1.6 and 3.4.3.6 described the effects of variations in cell design on electrical performance. This section discusses the effect of design on degradation determinants and mechanisms.

Examination of table 38 and of the degradation models shown in figures 66 through 70 shows that any design of sintered-type positive plates and negative plates will be subject to the same set of degradation processes and that only the relative contribution of the different mechanisms will be affected by variations in plate design. The use of perforated sheet as a

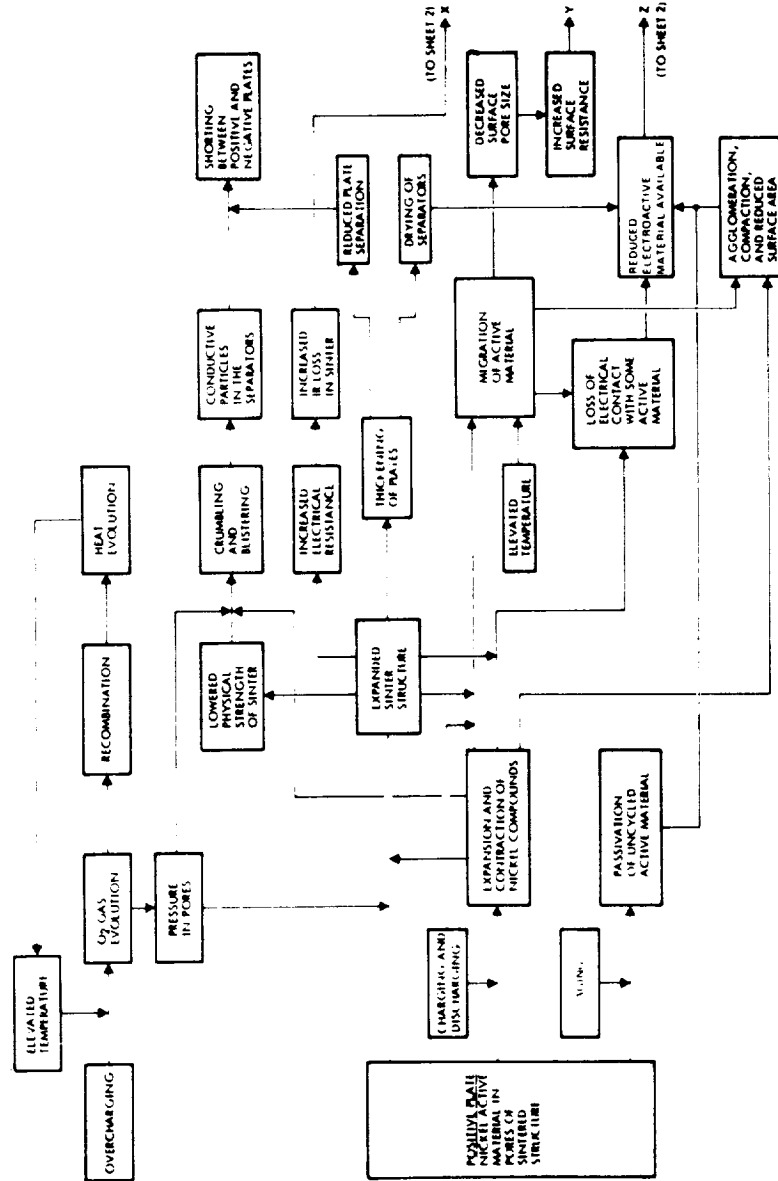


Figure 66. Degradation model for the sintered nickel-hydroxide electrode (sheet 1 of 2).

ORIGINAL PAGE IS
OF POOR QUALITY

ORIGINAL PAGE IS
OF POOR QUALITY

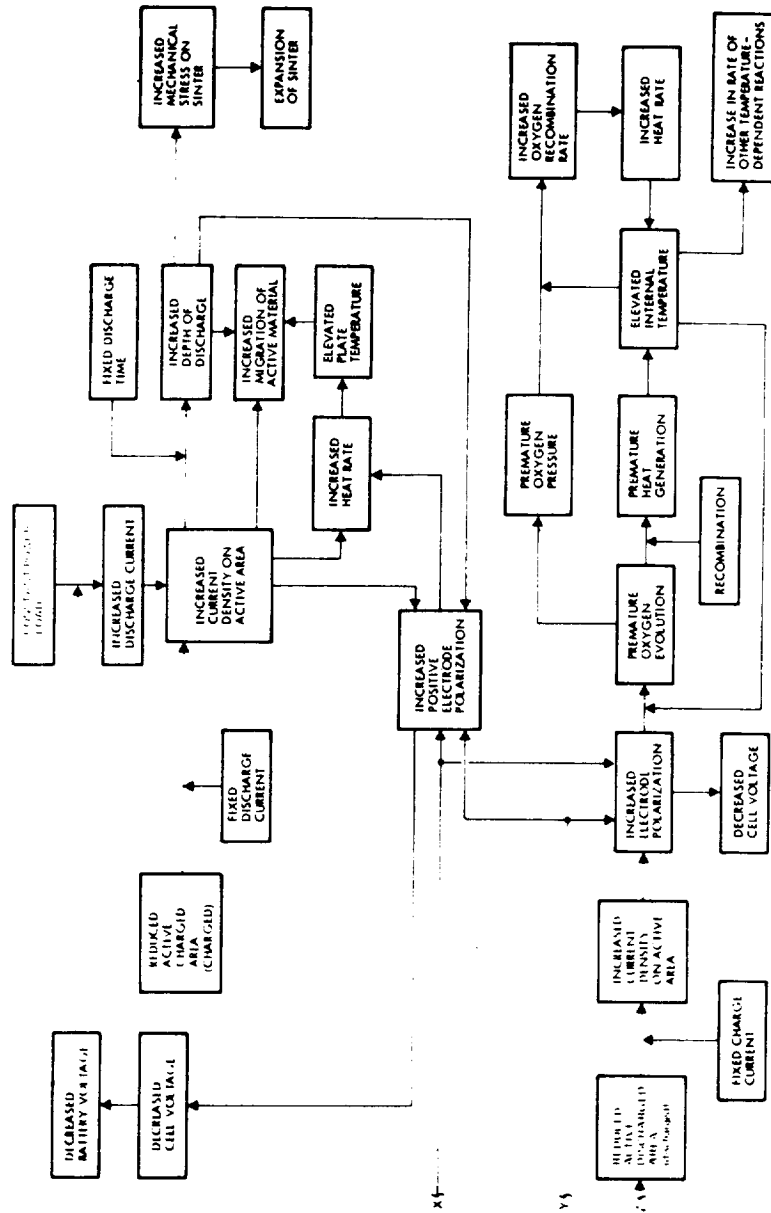
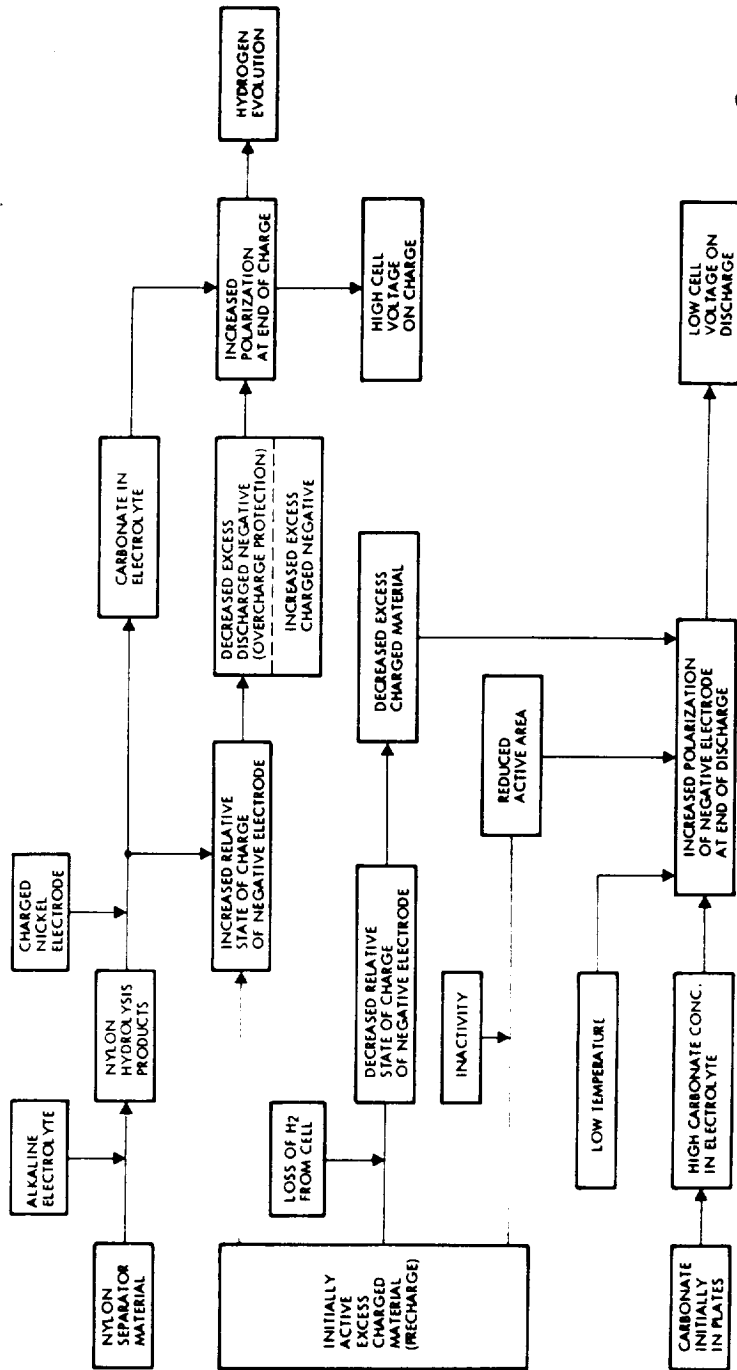
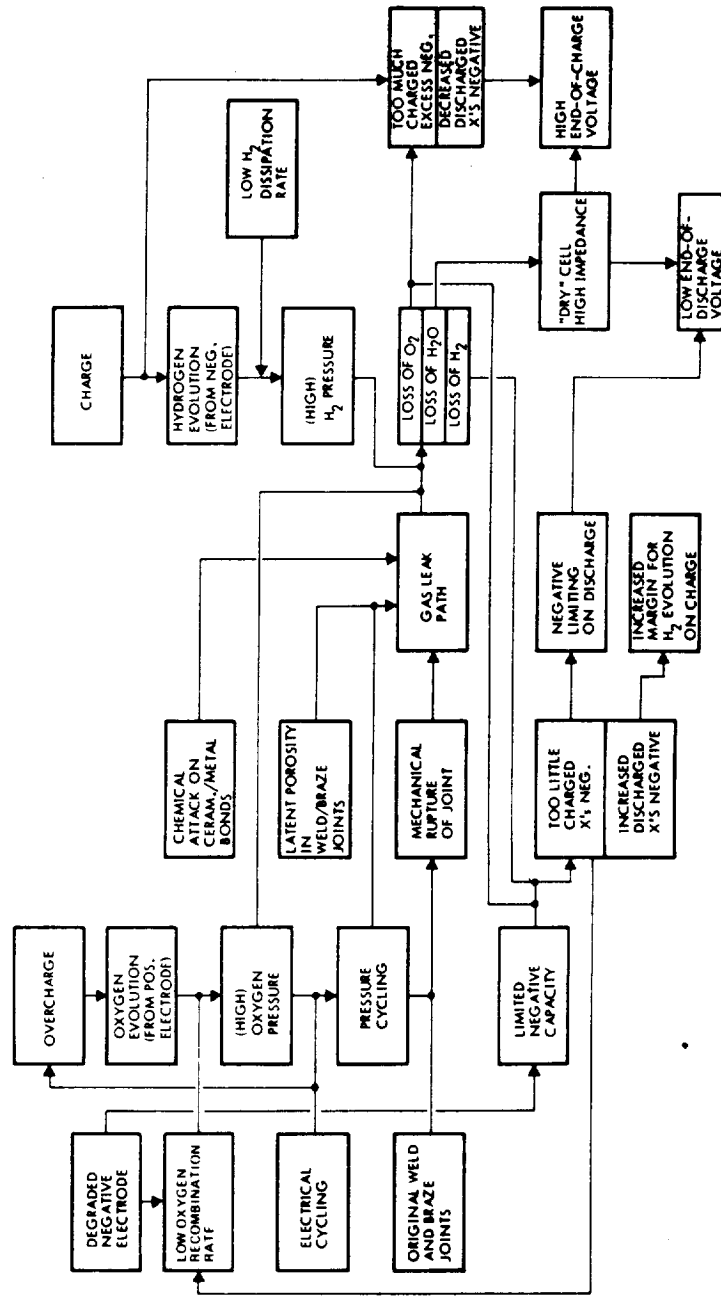


Figure 66. Degradation model for the sintered nickel-hydroxide electrode (sheet 2 of 2).



ORIGINAL PAGE IS
OF POOR QUALITY

Figure 68. Degradation model for the cadmium electrode and separator.



ORIGINAL PAGE IS OF POOR QUALITY

Figure 70. Degradation model for high-charge voltage and high resistance from leakage.

substrate in plates results in less expansion of the grid than the use of wire screen, especially in the direction parallel to the plane of the plates. Heavy loading results in more migration of active material, more pore blockage, and more buildup of material in the separators. Most of these effects are minimized in plates made by the electrochemical impregnation process in which the sintered structure is stronger and the active material is more evenly distributed in the pores than is the case for chemically impregnated plates.

Increasing the ratio of negative-to-positive capacity over a value of about 1.5 to 1 will improve performance only in those cases in which excessive electrode polarization is known to be the controlling determinant. Accomplishment of such an increase by increasing the negative-plate loading or by adding negative-plate area without making other adjustments is likely to result in more migrated negative material and possibly a net loss in mean time to failure. Use of teflonated negative-plate material appears to decrease the amount of negative-material migration substantially, but it demands more attention to proper adjustments of electrolyte during cell manufacturing.

Substitution of polypropylene (or other nonreactive polymer) for nylon in the separators will eliminate the nylon-hydrolysis mechanism and associated decreasing overcharge protection, but it is likely to cause more severe electrolyte redistribution and high internal resistance after cycling. Addition of more electrolyte to the cell tends to offset the effect of redistribution to some degree, but it does not eliminate it, and it may result in high internal pressures early in cycle life.

4.7 EFFECT OF OPERATING CONDITIONS ON DEGRADATION PROCESSES

This section summarizes the effects of operating temperature and depth of discharge on degradation processes.

4.7.1 Effect of Operating Temperature on Degradation Determinants and Mechanisms

The visible evidence of degradation is qualitatively the same in all cells, regardless of the operating temperature, as observed from teardown analysis after tests covering the temperature range from -20 to 40°C (References 19, 68, 106, 152, and 153). These results were reviewed in Section 4.5.1.3.

The relative amount of these effects appears to change with temperature, however, but quantitative data on this point are lacking.

The main effect of temperature on degradation is on the rate of the various processes. The rate of all chemical reactions increases rapidly with increasing temperature (usually by a factor of between 1.5 and 3 per 10°C rise in temperature). Because each reaction (specific mechanism) has its own temperature effect, the distribution of the various processes shown in figures 66 through 70 may be expected to change as temperature changes.

In one of the earliest tests in which temperature was the only applied variable and covered a wide range (-20 to +40°C) (Reference 175), all cell failures occurred by end-of-discharge voltage going below 1.1 volts (pre-selected failure criterion). The main failure determinant—loss of capacity of the positive electrode—was the same at all test temperatures. The authors state that the mechanism of failure was also the same at all temperatures. No investigation of the mechanism was reported, however, although it was speculated that the presence of unusually high concentrations of nitrate and carbonate in the cells was somehow responsible. End-of-discharge voltage data did not fit any of several models tried. Acceleration factors calculated from highly smoothed end-of-discharge voltage data showed no accelerating effect of temperature when there was no temperature gradient across the cells.* It appears that the failure criterion of 1.1 volts at end of discharge was too high for these tests; hence, the results are of little value in predicting the expected long-term effects of temperature.

An accelerated test program involving temperatures ranging from 20 to 60°C is now in progress at NWSC/Crane (References 152, 153, and 176), in which the temperature variable is matrixed with a number of other variables. Most of the electrical testing has been completed, but, because failure analysis and analysis of the data are not complete, the effect of temperature on the mechanism has not yet been determined.

The most obvious visible qualitative effect of increasing operating temperature is an increase in the amount of migrated negative-active material and in the degree of separator degradation, mainly from low-Earth-orbit tests. Although it is not clear in the NWSC/Crane reports (Reference 68), both cadmium migration and separator deterioration are generally minor in cells tested at 0°C.

*Cells with temperature gradients (produced by installing electrical heating elements inside the cells) showed significant effect of the magnitude of this gradient on charge in end-of-discharge voltage with cycling.

4.7.2 Effect of Depth of Discharge and Discharge Rate on Degradation Processes

A great deal of information in the literature suggests that cell cycle life is related to the depth of discharge used for cycling. Most such information comes from low-Earth-orbit cycling, in which failure is most often attributable to internal shorting associated with migrated cadmium material, although the actual failure mode is not clear in many cases.

In one special test at 25°C in which discharge rate was held constant (at 1C) and depth of discharge was varied over the range from 10 to 80 percent (Reference 177), little effect of differing depth of discharge on the capacity of the negative electrodes was seen at any single point in the test. However, a gradual loss of electrode capacity occurred at all depths of discharge over the 1600 cycles performed and at a rate per cycle that increased only slightly with depth of discharge. Reference 172 contains a limited study of the specific mechanism of the observed negative capacity loss but no information on the performance of the positive electrodes in these test cells.

In another special test at 25°C (Reference 85), all the test cells were cycled to 50-percent depth of discharge, and the discharge rate was varied over the range from 0.5 to 8C by varying the discharge time. Poor correlation was seen between the average number of cycles to failure and the different discharge rates, probably because of the high end-of-discharge failure criterion used (1.1 volts corrected for discharge rate by adding the product of internal impedance and discharge current). Both positive and negative electrodes suffered capacity loss, but the severity of the losses did not correlate well with discharge rate. Internal impedance increased by as much as 75 percent in some cells, but remained in the normal range for all cells during the test. No investigation of mechanisms was reported.

From a sophisticated analysis of test data from one of the accelerated tests conducted during the studies described in References 85 and 177, Roeger and McCallum (Reference 162) found that, over the first 3000 4-hour cycles, end-of-discharge voltage decreased linearly with the logarithm of the number of cycles completed. From this, they concluded that, when this was the case, the accessible area of the active material was decreasing by the same ratio during each cycle, where the rate of charge per cycle was a function of discharge rate (depth of discharge constant at 50 percent). On the other hand, loss of capacity from the positive electrodes was found to be more a function of the number of cycles completed than of the charge or discharge rates applied.

Discharge rate is also included as a variable in the current NASA accelerated test at NWSC/Crane, combined with many other variables (References 152, 153, and 176). The data are being analyzed to show the effect of the operating variables, but results are not yet available.

Therefore, at this time, the relationships between degradation determinants and mechanisms on the one hand and depth of discharge and discharge rate on the other are unclear. For a particular application, the user does not have an independent choice of both depth of discharge and discharge rate because, for a given discharge time, these increase and decrease together as the cell capacity is varied (in design). If depth of discharge and discharge rate actually have separate effects on the degradation mechanism, these effects will always be confounded in service. This may explain why much of the available data relating performance to depth of discharge appear to be inconsistent.



SECTION 5 CELL AND BATTERY PROCUREMENT

5.1 INTRODUCTION

The procurement process for sealed nickel-cadmium battery cells, or for complete batteries made with such cells, results in some considerations that are not normally part of similar procurement processes for items such as resistors, capacitors, or solid-state devices. This is because cell manufacturing—at the current state of the art and with the market conditions of the mid-1970's—involves a large number of hand operations and variables, is difficult to maintain under tight control, and is subject to frequent and often unexplained upsets. These factors may combine to produce unexpected quality deviations and delays in deliveries.

A cell is made by first manufacturing many component parts and then assembling the parts into a completed cell, as explained in Section 2.4. Because each of these components is subject to its own variability, for procurement purposes, whole cells should be treated more as “critical assemblies” than as “parts.” Because they are delivered sealed, however, most procurement systems usually treat them simply as parts.

Although parts application specialists are normally available within larger companies to write specifications for, and to assist in the procurement of, most electrical, electronic, and mechanical items, no such battery cell procurement specialists normally exist outside the battery engineering group itself. The battery engineer should therefore be prepared to participate in a wide range of cell and/or battery procurement activities to ensure that the items are delivered to specification and on schedule. This section is designed to assist the battery engineer in performing this important function.

The procurement of batteries (i.e., completed mechanical and electrical assemblies of multiple cells) involves many of the same activities and problems as procurement of cells *per se* and, hence, can be considered as an extension of cell procurement. This section deals first and most extensively with cell procurement; Section 5.8 describes activities that are unique to the procurement of batteries.

5.2 CELL PROCUREMENT PROCESS

In general, cells are procured for new hardware programs under a subcontract arrangement rather than by a simple purchase order. The process of procuring cells by subcontract is similar to that used by government agencies in placing a contract. Figure 71 shows a typical flow of activities and events preceding a procurement, and figure 72 shows the procurement sequence. The sequence applies not only to new procurements, but also to cases in which significant new requirements are introduced that may entail a new or redesigned cell. The sequence may be somewhat abbreviated for procuring a predetermined cell design.

All the activities in figures 71 and 72 are shown in table 39 with primary functional responsibilities and supporting roles identified. Note that battery engineering has primary responsibility for determining the battery and cell design and for creating performance specifications, although other groups are involved with the remaining phases of cell procurement. Throughout the entire process, the battery engineer provides support to all activities. The following paragraphs briefly describe the activities and the role of the battery engineer in each.

Battery specifications precede cell specifications and are derived from electric power-system requirements. When the batteries are to be built in-house and cells therefore procured individually, the battery specification remains an in-house document. When batteries are procured outside, both the battery and cell specifications are used for procurement, as discussed in Section 5.3. The battery engineer is usually responsible for preparing the battery specification, often with assistance from the power-systems engineer and the quality engineer.

The cell procurement specification is normally prepared before issuance of a Request for Proposal (RFP) if it is not already available, and it is the key engineering document on which the procurement is based. The battery engineer has primary responsibility for this specification but draws support from the quality engineer. Cell specifications are treated at length in Section 5.3.

In any action that involves the solicitation of bids, the more complete and definitive the RFP, the more cost-effective the overall procurement. One of

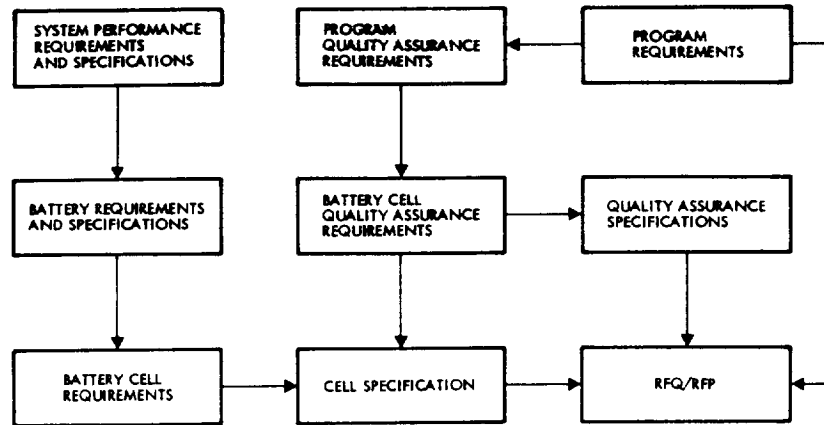


Figure 71. Steps in the development of a battery cell RFQ/RFP.

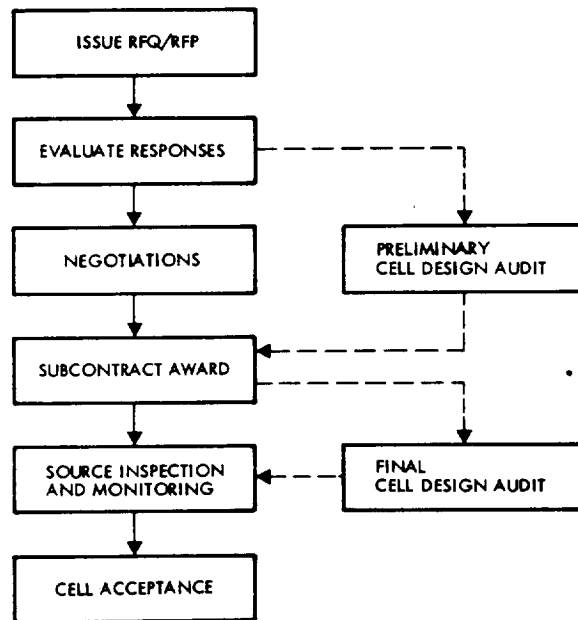


Figure 72. Steps in the cell procurement sequence.

Table 39
Cell Procurement Activities

Activity/Phase	Primary Responsibility ¹	Contribution and/or Support ¹
Prepare battery specification	Battery engineering (BE)	Power system engineering (PSE); Quality assurance (QA)
Prepare cell specification	BE	
a. Design and performance	BE	PSE
b. Quality assurance	QA	BE
Prepare RFP with specimen contract	Procurement	
a. Statement of work		Project engineering (PE); QA
b. Deliverables list		BE; QA
c. Other requirements		QA; BE
Evaluate responses	Procurement	PE; BE; QA
Negotiations	Procurement	PE; BE; QA
Cell design audits	Reliability engineering	BE
Source inspection	QA or government source inspection (GSI)	Government (DCAS); ² BE
Monitoring	Procurement	QA; BE
Acceptance	QA or GSI	Government (DCAS); ² BE

¹ All agencies are those of the buyer unless otherwise stated.

² Defense Contract Administration Service.

the best approaches is to provide bidders with a specimen contract complete with a definitive statement of work, a list of deliverables, and any and all specifications, instructions, and guidelines that constrain the potential supplier. The battery engineer should be familiar with the procurement system of his company/agency and should contribute to the RFP package as early as possible.

Procurement personnel evaluate the responses to an RFP, and any subsequent negotiations, with the assistance of cognizant project, battery-engineering, and quality-assurance representatives. During negotiations, any significant differences in position between the buyer and proposer on the cell specification and, if possible, on the Manufacturing Control Document (MCD) should be resolved. Section 5.4 discusses these activities.

After contract award, a source inspection program is implemented, and monitoring activities are initiated—first at the user's plant and later at the supplier's facility. These activities are outgrowths of a quality-assurance plan prepared by the user and coordinated with an MCD prepared by the supplier. Sections 5.5 through 5.7 present guidelines for the engineering support of this phase of procurement and acceptance activities.

This general review of the cell procurement process has identified a number of key documents and activities that require special attention by the battery engineer. These include the cell specification, the RFP or purchase order package and consequent negotiations, and the monitoring of production and quality-assurance operations.

5.3 CELL SPECIFICATION DOCUMENT

This section is intended as an engineering guide to the preparation of an effective cell specification rather than a general treatise on the preparation of specifications. Individual company procurement manuals and federal publications (Reference 178) contain complete information for preparing specifications.

5.3.1 Types of Specification Documents

Several types of specification documents, identified in terms of the arrangement of certain material and the degree of generality, are used: (a) the detail

specification, (b) the general specification, and (c) the standard specification. They are described in the following paragraphs with reference to their use for cell procurement.

5.3.1.1 Detail Specification

A detail specification contains all the details pertaining to a specific cell in the main body (basic content) of the text. This type of specification usually covers only one cell size.

5.3.1.2 General Specification and Specification Sheets

In a "general specification," only those requirements applicable to a broad class of cells are included in the main body of the text. Particular requirements defining dimensions, capacity, weight, configuration, and test details appear on separate pages that are usually referred to as "specification sheets." Therefore, a general specification, with one or more specification sheets attached, forms a complete specification.

This approach permits changing of cell particulars when necessary without revising and reissuing an entire specification. General specifications can also aid the procurement process because they can be made available for review by the cell manufacturer well in advance of a particular procurement, thereby permitting plenty of time for accommodation. A single general specification can be used for many procurements, eliminating the need to negotiate common requirements each time. This can help to reduce costs and to provide a rational basis for developing a general MCD.

A variation on the standard specification consists of the preparation of only the general quality-assurance requirements as a general specification document. All design and performance requirements are then issued for particular cells as required.

5.3.1.3 Standard Specifications

The use of general specifications as previously defined above, with the accompanying benefits obtained by simplified documentation, still permits each company to impose separate and different requirements. As developed by NASA, the standard cell-specification concept goes a step beyond and provides for both a general specification that would be standardized throughout the industry and standardized detail specifications for selected

cell sizes. By this means, the cost of procurement could be reduced, and the overall uniformity of cells made to these specifications could be increased significantly.

5.3.2 Specification Form and Content

Specifications that conform to the requirements of Reference 178 are constructed around a six-section outline with the headings: (1) Scope, (2) Applicable Documents, (3) Requirements, (4) Quality Assurance Provisions, (5) Preparation for Delivery, and (6) Notes. Only Sections 3 and 4 are discussed here.

5.3.2.1 Requirements

Because the long-term performance of the cell is component- and process-sensitive, it is necessary to specify certain aspects of components and process steps in order to have better control over performance of the finished cell. It is advisable to separate requirements for components and processes from those for the whole cell and to place these under separate headings. Alternatively, this may be done by putting all requirements for components under the heading of "Design Requirements" or under a heading such as "Details of Components." Such separation will ensure that both in-process and end-item requirements will receive the individual attention desired.

Of the many topics that may be included under "Requirements," design (and construction) and performance require the greatest care in preparation. To simplify the design requirements section, it is advisable to put all visually observable and directly measurable aspects, such as external dimensions, cell weight, overall configuration, and external finish, etc., under separate headings. Design requirements would then include only the less obvious aspects, such as materials of construction, details of terminal-seal design, number and thickness of plates, separation distance, quantity of electrolyte, and precharge level.

Requirements for design should not conflict with requirements for performance. The information in Sections 2, 3, and 4 should prove helpful in making these assessments, and the cell manufacturers should be consulted.

In a cell specification, performance requirements normally deal only with the behavior and output of the cell as a whole. They are expressed in terms of the voltage, current, and pressure relationships during the passage of electricity and of quantities such as capacity and energy derived from

voltage/current/time data. These may be subdivided into requirements under "normal environment" conditions (e.g., moderate temperature, ambient pressure, etc.) and requirements under various nonnormal environmental conditions, such as at temperature extremes, during and after vibration or shock, and under constant acceleration.

The different types of performance characteristics presented in Section 3 are candidates for inclusion in a specification. Other characteristics may be needed for specific applications, yet others may sometimes be included for reference and for comparing data with that of cells previously purchased.

5.3.2.2 *Verification of Requirements*

In a properly constructed specification, each specific requirement statement (in the "Requirements" section) is accompanied by a corresponding method for verification (usually located in the "Quality Assurance" section). The method specified may be a test, a physical measurement, a chemical analysis, or a documented calculation. Practical considerations dictate that requirements that must be verified on all individual cells during acceptance testing must be capable of such verification in a relatively short period of time (usually a few weeks) to expedite completion of the procurement cycle. Verifications that require longer periods fall into the category of qualification tests.

Design requirements are verifiable if they are sufficiently specific. Thus, requirements for items such as the material of the case, the concentration of the electrolyte, and the excess charged-negative capacity may be verified in a short time by known methods, although a given contract may require that verification of any of these aspects be performed only infrequently.

On the other hand, requirements such as "the cell shall be designed for a useful life of 5 years" or "the cell shall be designed for a minimum of 10,000 cycles" can be verified only by theoretical analysis within the time constraints for cell acceptance. Furthermore, at the present state of the art, no manufacturer can design a cell specifically for a given cycle life or guarantee that a given design will last for many years. Therefore, such broad statements should not be included in design requirements but should be placed under a separate heading such as "Life and Reliability" or "Intended Use." The overall design may be made subject to analysis by the design-audit process. (See Section 5.4.)

By the same argument, performance requirements placed in the "Requirements" section should specify only initial characteristics (as defined and used in Sections 2 and 3). Because long-term or end-of-life performance and reliability cannot be verified for procurement purposes, statements as to desired limits, if included, should be placed under a heading such as "Life and Reliability." As such, they may be considered as performance goals and may serve as guidelines for cell design. Until the cell becomes qualified by life-testing, the probability that the cell will achieve the goals may be assessed by analysis in lieu of test. The results of this analysis then may be made one subject of a cell-design audit. (See Section 5.4.)

If a given cell design has been qualified and the ability of that design to meet the performance requirements has been officially demonstrated, the procurement problem then becomes one of ensuring that the same design is accurately reproduced. This effort is a matter of quality assurance and is discussed in the following section.

5.3.2.3 Quality-Assurance Provisions

The quality-assurance portion of the specification is the result of a joint effort by the battery engineer and the quality engineer to reflect the unique aspects of the cell-production process. This activity is greatly facilitated if the MCD to be used is in hand so that the manufacturing steps and the supplier's proposed quality plan are known.

The quality requirements should cover both materials that are processed and the final product. Particular attention should be given to the more critical components, such as plates, terminal seals, and separator material. Generally, these items should receive more rigorous inspection, screening, and testing than is normally performed by cell supplier in the manufacture of commercial cells.

Requirements for the qualification of cells are always included in the "Quality Assurance" section. Complete and specific descriptions of all qualification tests and associated pass/fail criteria should be provided, especially for those tests that are not part of the acceptance-test sequence. By this means, the cell supplier can determine what testing the cell must pass to be qualified and may be guided in his design accordingly. He may also be able to point out possible conflicts between the design requirements and these test requirements.

Qualification testing usually consists of a series of tests, some of which are the same as those used for acceptance, plus others performed under more

extreme operating conditions and/or environmental stress levels. Although long-term life testing on the ground may be involved, more often, the final qualification status results from actual spaceflight application. Different approaches to the qualification testing of cells are discussed further in Section 6.

The requirements for the acceptance of cells form another major part of the Quality Assurance provisions. They usually include two main items:

- Delivery by the seller of a certificate of conformance stating that the cells in question: (1) conform with the requirements of the specification, and (2) were made to the same design, using the same materials and processes, as the cells already qualified or otherwise approved
- Satisfactory completion of acceptance testing

Before the order is closed out, the battery engineer, together with his purchasing agent, should verify that all data, samples, and other nonhardware items required by the contract were received in good order. He should also attempt to validate foregoing items (1) and (2) of the certificate of conformance.

In a specification, requirements for cell acceptance normally follow those for qualification. According to standard format, subsections on responsibility for testing, sampling instructions, special test conditions, and a list of the test sequence are given here. Details of the test methods are described later in the cell specification under "Test Methods." The substance of these tests is discussed in Section 6 of this manual.

The buyer may elect to have the manufacturer perform only part of the acceptance testing, and the buyer perform the remainder. It is never advisable to permit the supplier to do no acceptance testing, however. If he performs no tests and if the cells fail to pass some part of the testing at the buyer's facility, the supplier has a right to question the proper conduct of the test, and the cells may have to be returned to the supplier for resolving the problem. For this and for other reasons, some suppliers choose to perform certain acceptance tests even when they are not required by contract to do so.

Performance of some, if not all, acceptance testing by the supplier offers certain other advantages. It expedites the availability of acceptable cells; it is usually less costly than when the tests are done at the buyer's facility; and it permits testing to be done with accompanying pressure measurements

(before pinch-off) if desired. The main disadvantage of acceptance testing by the supplier is that his test equipment and controls are usually not as refined as those available at the buyer's plant, particularly for thermal control. The supplier usually uses only air as the cooling fluid, with the result that cells are operated near the upper limit of the test tolerance. This results in lower charge voltage and higher discharge voltage than if the cells were operated near the lower end of the temperature tolerance, where they tend to be when the heat path is through metal clamps to a liquid-cooled heat sink. If the acceptable performance limits are too narrow, this type of temperature control difference can be sufficient to result in passing a test at the supplier but failing to pass after receipt at the destination.

Another type of acceptance test that should be considered for obtaining greater control of internal design and processing is teardown analyses. Randomly selected cells can be opened, the internal parts visually inspected, and certain measurements and tests made quickly and inexpensively concurrent with the main electrical testing activities. Advance suitable acceptance criteria must be negotiated with the cell manufacturer.

5.4 REQUEST FOR PROPOSAL

The RFP defines the content of the proposal, as well as the scope of the work to be done after contract award. The battery engineer should assist in formulating both sets of requirements and should participate in subsequent proposal evaluations.

The supplier should be required to defend his proposed design when: (a) a qualified cell cannot satisfy battery performance and life requirements; (b) the fine details of cell design are left to the supplier; and (c) when the supplier proposes to use a different design from one already qualified to meet an old set of performance requirements. This is best done by requiring that a description of the cell design, detailed down to the level of all proposed changes, be included in the proposal response, together with a discussion of why the proposed design is expected to meet the performance and life specifications. The discussion of cell-design parameters contained in Section 3 may be used as a guide for the type of design information to be requested. A discussion of the design and the rationale for its selection may be a part of negotiations; if so, the request for proposal should so state.

Generally, all future significant spacecraft cell production is expected to be performed with reference to some version of an MCD. * Because the content of the MCD can affect cost and schedule, it is advisable to attempt to resolve any significant differences between the buyer and supplier regarding the MCD. Therefore, if the MCD to be used has not already been established at the time the procurement action is initiated, one or more copies, updated to reflect specification and contract requirements, should be required as part of the proposal. The document may then become the subject of subsequent negotiations.

Also of interest to the battery engineer are requirements for tasks that follow the award of a contract. Postaward requirements should be identified by a "specimen contract" that later becomes the final contract after modifications that result from negotiations.

The primary contract requirement is for the delivery of cell hardware. Formulation of this requirement is greatly simplified by reference to the cell specification, which defines individual cell characteristics in detail. The only other information that the RFP must define is how many cells are required and when they are to be delivered.

Because most cell procurements call for delivery of items in addition to cells, however, the request for proposal must also define these nonhardware items and their delivery schedules. These items may be conveniently summarized in a list or table that identifies how many of each must be produced, when, and to whom each is to be delivered. Such a table is similar to the Contract Data Requirements List, DD Form 1423, associated with many government contracts. This list should include, as applicable, the following items:

- Cell-design package
- Cell-design audit
- Manufacturing Control Document
- Master production schedule
- Material and production records
- Quality control reports
- Samples
- Acceptance test data sheets
- Certificate of Conformance for cells

*See Section 5.5 for a definition and discussion of the MCD.

A cell-design audit should be conducted if a new design is to be built or if new drawings or revisions to existing drawings or procedures are necessary for updating a design that was previously reviewed and approved. This review should be held after the supplier has completed the drawing/design package to be used for production. The battery engineer should submit a copy of the design package to the buyer for his review well before the review meeting is scheduled.

The master production schedule, a key item needed for properly monitoring the work flow, should include:

- Shipping dates with quantities of deliverable cells
- Production milestones for each production group of cells, including at least:
 - Availability of plate material
 - Completion of aerospace formation
 - Filling with electrolyte
 - Completion of acceptance testing
- Due dates of any production reports, samples, data packages, and other required software

The material and production records required should include as a minimum copies of:

- Evidence of acceptability of the plate material used
- Evidence of acceptability of the separator material used
- Data sheets from the aerospace formation (open cell) test operation
- Selected data sheets on which other data are recorded during production
- All manufacturing travel cards

The evidence of acceptability of plates and separator material, which may be in the form of certificates of conformance, should show both as-determined and required values and the applicable drawing reference with revision number and date of revision. The formation data permit the engineer to review the manufacturer's decision to either use or reject groups or

lots of plate material. The travel cards and other in-process data sheets are of value in tracking the effectivity of events or changes to the process when other sources of schedule information are incomplete.

Specifications for these items have not usually been invoked in the past. Yet, to ensure that what is wanted is obtained, it is advisable to include minimum specifications for content, format, and type and quality of reproduction of software as attachments to the contract. Blank forms and/or completed examples of acceptable material should also be attached, if possible.

A key item on the foregoing list of deliverables is the MCD. As noted, it is recommended that arrangements be made to deliver this document with the proposals to ensure adequate time for review. Because this document is of central importance to the control and documentation of cell design and processing, it is discussed in detail in the following section.

5.5 MANUFACTURING CONTROL DOCUMENT

The MCD, sometimes referred to as a Process Identification Document (PID), is a document package prepared by the manufacturer to define the details of cell design and the process steps to be used. Whereas the specification defines what is to be made and how it (the cell) should work, the MCD defines how it will be made and how the intent of the specification is to be carried out. The use of this type of documentation has increased rapidly during the last 5 years, and many prime contracts now require its use for cell procurement.

5.5.1 MCD Format and Content

In general, an MCD contains the following items and sections:

- Revision record
- Table of contents
- Engineering drawings
- General engineering documents
- General quality-control procedures
- Process flow chart
- Process step to document cross-reference table
- Material control procedures and forms
- Step-by-step manufacturing and test instructions
- Step-by-step quality-control instructions

- Travel card forms
- Data sheet forms
- Customer acceptance test procedure

Except for special items that individual customers may add, the main body of the MCD tends to be the same for all sizes of spacecraft cells made by one supplier. Only certain drawings (e.g., of the plates and of the completed cell assembly) and specific values of charge and discharge current defined for the purpose of test need to be different. The customer-required acceptance test procedure, which is a part of the MCD, usually exhibits the most variations of any section of the document.

The format, and to a lesser degree the content, of the MCD varies considerably from one supplier to another at the present time. These differences make comparative evaluation difficult for the cell user. It is hoped that in the future the standard cell program sponsored by NASA will result in a more standardized format.

A number of pertinent drawings, procedures, and operating instructions may not be distributed with the MCD because they may be considered proprietary by the manufacturer. However, all pertinent documents should be included at least by reference to the document number. All such document callouts should include a current revision number/letter and corresponding date.

5.5.2 Engineering Review of MCD

In the first submittal of the MCD, the buyer is responsible for determining if the design and process are adequately defined for his application. The cell design is defined in an engineering sense by the applicable drawing "tree." Usually only a small part of this tree, consisting of a number of top-level drawings, is included in distributed copies of the MCD. Experience has shown that they do not provide adequate visibility for verifying design control to the level required to obtain long-life spacecraft cells. One approach to improving this situation is to include a complete tree diagram in terms of all the drawing/document numbers. Because plate design is basic to cell design, this tree should identify the positive and negative plates to be used in the cell. The battery engineer should review all parts of these documents that impact cell design before final approval of the MCD. If some drawings cannot be permitted outside the factory, they should be reviewed on the premises. Once a given drawing revision has been reviewed, any subsequent revision should be considered to constitute an official revision to the MCD and should be so handled. The contract provisions that cover the use of the MCD should make this point clear.

The same approach should be followed throughout review of the process steps described in a first-submittal MCD. Documents referenced but not supplied should be reviewed at the supplier's facility. Options exercised for repair or rework of material failing to pass an inspection or test step should be identified, and the applicable rework/retest procedures should be documented. Adequate record keeping and data gathering should be ensured through the use of appropriate manufacturing travel cards and data sheets. Although the manufacturer's travel cards are not normally designed to follow rework, rework can sometimes be the cause of subsequent abnormal cell behavior.

Although users may not be able to directly influence the way certain manufacturing operations are performed, they can often exert strong influence on the manufacturer's quality-control program. Thus, the battery engineer should review the quality plan presented in the MCD from his point of view and should make recommendations to his quality-assurance engineer during the review process. For example, possible improvements might take the form of additional inspection steps, greater depth of coverage for key steps, or additional inspection data to be taken.

5.5.3 Standardized Manufacturing Control Documents

The creation of new MCD's and their review are time-consuming activities. Furthermore, the continual introduction of new and unfamiliar instructions into the production sequence is often counterproductive because of the time needed to accommodate each change.

These problems can be minimized by the use of a standardized MCD or standardized control document modules. Because a high percentage of cell assembly and initial test operations performed by a given manufacturer are essentially the same for all spacecraft cells made regardless of the buyer's specification, a large portion of the complete document could be prepared in advance in standardized form. Only those portions unique to the particular cell ordered would have to be prepared in original form.

This approach is facilitated by the use of general specifications, particularly those for quality assurance. Quality requirements tend to be the major source of differences from program to program and from company to company. Formatting the MCD so that the Quality Control Plan is a separable module, with inspections and tests keyed to the process flow diagram, would expedite the review and approval process. Use of standard specifications when applicable would also simplify this process.

5.6 BATTERY ENGINEERING SUPPORT TO QUALITY-ASSURANCE ACTIVITIES

The role of the user's quality-assurance function in cell procurement is not only verifying that the delivered items meet the specification requirements, but also ensuring that manufacturing is performed in accordance with the approved MCD. The latter task is essential because of the strong dependence of long-term cell performance on certain process details as discussed in Section 3. This task is best performed by verifying that the manufacturer's quality-assurance organization is performing in accordance with the quality plan in the MCD.

Verification of conformance to the MCD is sometimes difficult because the written instructions are often incomplete and/or unclear, and are therefore subject to differing interpretations by different personnel. In such cases, the buyer's quality representative may be required to judge if a deviation is in the spirit of, or only in the letter of, the instruction. It is here that the battery engineer should contribute by analyzing the degree of potential impact of the deviation on ultimate cell performance.

Before cell production begins, the buyer's quality engineer prepares a quality-assurance plan covering source inspection (inspection at the manufacturer's plant by a representative of the buyer) and production monitoring (tracking manufacturing activities at the supplier's facility). The details of this plan are based mainly on the process sequence and on the manufacturer's quality plan as described in the MCD.

In developing the plan, it is important to assign priorities to the operations so that key steps are given proper attention. The battery engineer is in the best position to assign these priorities because of his knowledge of the process. When many cells are to be manufactured in a relatively short time, several production lots may be in process at one time. Under these conditions, proper quality-assurance coverage of only the high-priority steps can be a full-time job for one man. At such times, direct support by the battery engineer at the manufacturer's plant may be advisable.

To be effective, the source inspection plan should address the following activities at the manufacturer's plant:

- Reinspection of materials or hardware (after the manufacturer's inspection), usually on a random sample basis

- Verification that various approvals have been accomplished and associated paperwork has been properly completed
- Review of data sheets and quality-control record forms for conformance with manufacturers' standards and contractual requirements
- Verification that equipment setups are proper, that equipment is in calibration, and that operations are being performed according to the MCD
- Verification that the latest revisions of operating instructions are being used on the floor
- Verification of conformance of cells to preshipment acceptance requirements and of the completeness of the data package
- Communications of events that may impact schedule and of questions of interpretation by either telephone or teletype to the buyer
- Preparation of periodic reports to the buyer's quality engineer or quality management

Monitoring normally consists of following these activities, tracking the status of cells, and responding to communications from the supplier and from the source inspector as production proceeds. These activities permit the user to anticipate receipt of cells and, if necessary, to assist the supplier in a timely manner to avoid delay in deliveries. Such monitoring is made necessary by the limited spacecraft-cell production capacity and staff maintained by the cell manufacturers.

To best support procurement as production proceeds, the battery engineer should know the status of each batch of cells as production continues. If possible, production schedule information should be obtained at weekly intervals down to the level of the number of cells at each operation. In this way, the effectivity of any process change that is made during a production run can be established with minimum risk to the entire production run. This problem is difficult at best, however, because cells are not individually serialized until near the end of the process, and manufacturing sublots are not separately identified. It is evident that only more rigorous accountability than has been customary will improve traceability to process details.

5.7 CELL ACCEPTANCE

Acceptance of cells is the last step in the cell-procurement cycle in which the battery engineer is involved. Acceptance is usually accomplished in two stages: (a) a provisional acceptance at the supplier's location, and (b) a final acceptance at the buyer's plant. The second stage is necessary because of the possibility that adverse shipping conditions may permanently degrade cell performance beyond specification limits.

The source inspector normally receives notice from the buyer's quality-assurance in-house personnel that a group of cells have completed acceptance, that other cells have not passed all requirements and are being held for retest, or that the supplier requests a waiver on one or more cells. As much information on the nature and distribution of the data in question should be transmitted at this time so that the battery engineer can make the required judgments. Similarly, to expedite the decision on final acceptance, data obtained from any final acceptance testing at the user's plant should be made available immediately to the battery engineer.

5.8 BATTERY PROCUREMENT

Any company charged with designing or building a spacecraft electric power system must make a "make-or-buy" decision regarding the batteries (i.e., whether to make the batteries in-house using purchased cells or to buy the batteries from an outside source). If the company has the facilities, equipment, and experienced personnel to assemble and test batteries, economics usually dictate a "make" decision. If these capabilities are not available, battery assemblies must be procured.

Two types of qualified outside sources are available: (a) another spacecraft contractor with power systems and battery assembly capability, and (b) cell manufacturers who also make batteries. Most prime contractors for spacecraft systems can now make and test batteries in-house. Of the major cell manufacturers, Eagle Picher Industries, Incorporated, and SAFT-America make batteries, but General Electric Company (Battery Business Department) does not. The supplier does not have to perform all of the activities required for delivering flight-ready units to a spacecraft. The buyer may retain the design activity as well as qualification testing; the latter may be done in-house after receipt of the hardware. The supplier normally performs acceptance testing. Thus, many practical combinations of tasks and performing organizations are possible.

For a final procurement decision, a number of technical and cost trade-offs must be evaluated. Table 40 summarizes the considerations associated with selecting either type of outside source or of performing the entire job in-house. The table shows that, for new and critical designs for which a high degree of optimization is necessary for meeting weight or performance requirements, the design work is best performed in-house. However, if the design is not critical, especially if a standardized design can be utilized, outside sources for batteries may prove most cost-effective.

5.8.1 Specifications for Battery Procurement

A cell specification and a battery specification are both normally used as separate documents for battery procurement. This practice reflects the fact that the cells used to make the batteries should be manufactured, tested, and accepted in the same manner as if they were to be delivered as individual cells. Therefore, the cell specification need be no different from that described in Section 5.3. Obviously, for mutual compatibility, certain requirements must be coordinated with those in the battery specification.

The battery specification used for outside procurement may be nearly the same as that prepared during a battery design program, but it should also contain certain requirements that may not be included in a specification written for internal use only. For example, a battery procurement specification should contain procedures and criteria for selecting cells to be used for battery assembly out of the many available cells (all of which are individually acceptable) and for assigning cells to individual battery assemblies. Section 6 discusses such criteria.

A related set of requirements concerns the range and limits of individual cell voltages at end of charge and end of discharge during battery acceptance testing. Such requirements recognize the fact that occasionally the process of constraining the cells in a battery case or the performance of battery-level testing at levels beyond those experienced during cell acceptance testing will cause some cells to behave poorly. When cells of this kind are present, a battery should not be considered acceptable even though the battery terminal voltage falls within prescribed limits.

Formulating definitive and adequate battery acceptance and qualification test requirements and associated pass/fail criteria demands more care than that for individual cells, because a completed battery represents much more time and cost. The specification of these requirements should not be

Table 40
Relative Merits of Buying Versus Making Batteries

Procurement Option*	Advantages to User	Disadvantages to User
Spacecraft contractor designs, builds, and acceptance tests batteries under a subcontract arrangement	<ul style="list-style-type: none"> a. Fixed design cost b. Fixed recurring cost c. Does not require in-house facilities for cell receiving, cell testing, and battery assembly 	<ul style="list-style-type: none"> a. Limited design attention b. Limited interaction with subsystem design c. Limited optimization d. Manufacturing methods and technology not under control of user
Prime contractor designs; spacecraft subcontractor builds to print and acceptance tests batteries	<ul style="list-style-type: none"> a. Design may be optimized with minimum effort b. Fixed recurring cost c. Does not require in-house facilities for cell receiving, cell testing, and battery assembly 	<ul style="list-style-type: none"> a. Design costs may escalate b. Manufacturing methods and technology not under control of user
Cell/battery manufacturer designs, builds, and acceptance tests batteries	<ul style="list-style-type: none"> a. Minimum design cost b. Low recurring cost c. Does not require in-house facilities for cell receiving, cell testing, and battery assembly 	<ul style="list-style-type: none"> a. Minimum design sophistication b. Little interaction with subsystem design c. Minimum capability to adapt to changing program requirements

Table 40 (continued)

Procurement Option*	Advantages to User	Disadvantages to User
Prime contractor designs; cell/battery manufacturer builds and acceptance tests batteries	<ul style="list-style-type: none"> a. Design may be optimized with minimum effort b. Low recurring cost c. Fixed design cost 	<ul style="list-style-type: none"> d. Expect nonoptimized design e. Manufacturing methods and technology not under control of user f. A third party may conduct part or all testing; difficult to control
	<ul style="list-style-type: none"> a. Design costs may escalate b. Manufacturing methods and technology not under control of user c. Limited test control and sophistication 	

*User to conduct all special qualification tests.

merely an extension of cell testing, although the data must relate to cell test data. Section 6 describes cell and battery testing and interpretation of the results.

5.8.2 Monitoring of Battery Production

The procedure for monitoring the procurement of a battery assembly is, at the outset, similar to that for cell production as described in Section 5.6. An MCD should be implemented for the battery assembly and acceptance test phases as a separate document from the one for controlling cell assembly.

SECTION 6 CELL AND BATTERY TESTING

6.1 INTRODUCTION

From the time they are manufactured until they are launched aboard a spacecraft, sealed nickel-cadmium cells and batteries undergo many tests designed for verifying their quality and for ensuring their suitability for flight. Tests may be performed: (a) before the cells are sealed; (b) after the cells are sealed but before they are assembled into batteries; or (c) at the battery level. Some tests provide a basis for formal acceptance or qualification of cell or battery hardware, others provide for monitoring of the manufacturing process. This section reviews these tests in terms of the various test methods used, the success criteria applied, and the degree to which they accomplish their intended purpose, and identifies controversial areas and potential problems.

6.2 ACCEPTANCE TESTING

When cells or batteries are procured to a specification or batteries are assembled to a specification, a number of activities are performed to verify that all requirements are met. These activities are part of the process of verification described in Section 5 and include a set of tests and inspections that are universally referred to as acceptance tests. The acceptance testing of cells or batteries may be performed entirely by the manufacturer or may be divided between the manufacturer and the buyer, with some degree of planned duplication. In either case, the buyer seeks the maximum amount of information useful to his particular application from the tests. However, it is desirable to avoid unique, application-oriented tests during the normal acceptance sequence, particularly during the part of the sequence that is performed by the cell or battery manufacturer. The buyer should perform such special tests after the items have been formally accepted. Otherwise, if negative results from the special tests are obtained or if the cell characteristics are temporarily affected by the special tests, the main purpose of acceptance testing may be compromised. If, on the other hand, maximum use is made of test methods and conditions that are normally used by the manufacturer, it will be possible to take full advantage of the data obtained from prior tests of other similar items. Anomalous results may therefore be

referenced to a large established test data base. During negotiations of the procurement specification and the related MCD, the manufacturer should be told of any special tests that must be included in the acceptance test sequence.

The procurement specification should contain specific instructions as to what tests will be done, what criteria will apply, and which of the tests will be done by the cell manufacturer. Some of the tests, such as those involving cell-pressure measurements, can be done only by the manufacturer.

Because some of the cell manufacturer's acceptance tests are similar or identical to tests in his preacceptance manufacturing test sequence, the dividing line between these two types of tests is often indistinct. This can sometimes lead to confusion as to the responsibilities and options of the manufacturer in the event of failure to meet agreed-upon criteria before and during formal acceptance tests. Therefore, the contract should clearly define the boundaries of the buyer-invoked acceptance tests at the manufacturer's plant and the procedures for disposition of material within those boundaries. Acceptance testing of cells at the cell level differs considerably from acceptance testing of batteries as a whole.

6.2.1 Cell Acceptance Testing

The current approach to acceptance testing of sealed nickel-cadmium cells within the aerospace industry is the result of an evolutionary process that began in the late 1950's. At the outset of the space program, this testing reflected the minimal requirements that were then placed on cell performance and the commercial origins of the device. As the need for improved performance and reliability developed, more attention was given to establishing better methods of screening by cell buyers in both industry and the government. These efforts remained only loosely coordinated until the late 1960's when NASA and the Armed Services began a joint effort to develop manufacturing and test standards at the cell level. This work, which was performed in conjunction with cell suppliers and industrial users, culminated in NASA's "Specification for the Manufacturing of Aerospace Nickel-Cadmium Storage Cells," NASA/GSFC Specification 74-15000 (Reference 179).

The payoff of these efforts, particularly those that concerned the development of standardized cell acceptance-test methods, has been a general improvement in the yield of cells that have successfully passed such testing.

Much of this improvement is due to the refinement of all manufacturing processes and the establishment of controls that provide for early detection and rejection of defective materials. The development and use of improved manufacturing control documentation has encouraged this situation. However, cell rejections still occur during acceptance testing. In general, they reflect the detection of process tolerance problems, particularly when a cell of new design is first manufactured or when process changes are first implemented. Although most cell acceptance failures are not lot-related, occasionally an entire lot may be unacceptable for flight use.

Table 41 illustrates the effect of improved manufacturing process controls and documentation on cell rejection rates for several types of defects observed during four major NASA and Air Force projects. If cells containing such defects were assembled into batteries, the result would be high rates of failure of the batteries to pass battery-level acceptance with high attendant rework costs and accompanying risks to project schedules. As greater emphasis is placed on achieving lower spacecraft component costs, it is natural to question the need for extensive testing at the cell level. However, on the basis of the preceding discussion, a reduction in the level of cell acceptance testing does not appear to be justified at this time. Further reductions in cell defect rates will be necessary before such reductions at the battery level become economically feasible.

Table 41
Trend of Cell Acceptance-Test Failures
Observed on Four Projects*

Defect	Pre-1970	Post-1970
Charge retention	Greater than 1%	Less than 0.5%
Electrolyte leakage	Many problems	Less than 0.2%
Low capacity	Greater than 10%	Less than 0.25%

*TRW data

Despite the availability of NASA/GSFC Specification 74-15000, considerable variation still exists among the cell acceptance-test methods and procedures in current use. One reason is that acceptance tests must be compatible with individual specification requirements, and the NASA specification is

not currently in general use. Another reason is that many projects are ongoing, and it is not practical to change existing practices. Also, some individual organizations have invested considerable effort in developing their methods and procedures, and they rely on the data thus obtained to support current cell and battery design and procurement activities. A final reason is that, for certain mission applications, additional tests and procedures tailored to those applications may be required even though it is desirable not to do them.

6.2.1.1 Cell Acceptance-Test Sequence

The cell acceptance-test sequence may vary from one organization to another primarily in two respects: (a) in the definition of the dividing line between the manufacturer's in-process tests and the buyer's tests, and (b) in the division of formal acceptance tests between the manufacturer's and the buyer's facilities.

Figures 73 and 74 show the entire cell test sequence as defined by NASA/GSFC Specification 74-15000.* Figure 73 shows the final tests in the manufacturing sequence and those tests designated as acceptance tests to be performed by the manufacturer. Figure 74 shows a sequence, referred to in Specification 74-15000 as performance tests, to be performed by the buyer. Figure 74 includes two additional tests that, although they are not always considered to be acceptance tests, have proved to be of general value: a 30-cycle burn-in type test and destructive testing. The latter tests are discussed in Section 6.2.2.

The order of the tests shown in figures 73 and 74 is based on considerable experience and results in a minimum amount of interaction between tests. Therefore, the order should not be changed without careful consideration of all implications.

6.2.1.2 Review of Cell Acceptance-Test Methods

This section describes cell acceptance-test methods. The tests reviewed are those that appear in NASA/GSFC Specification 74-15000.

*This specification is used as both a source and a reference because it has been widely coordinated with, and distributed within, the aerospace industry and the government.

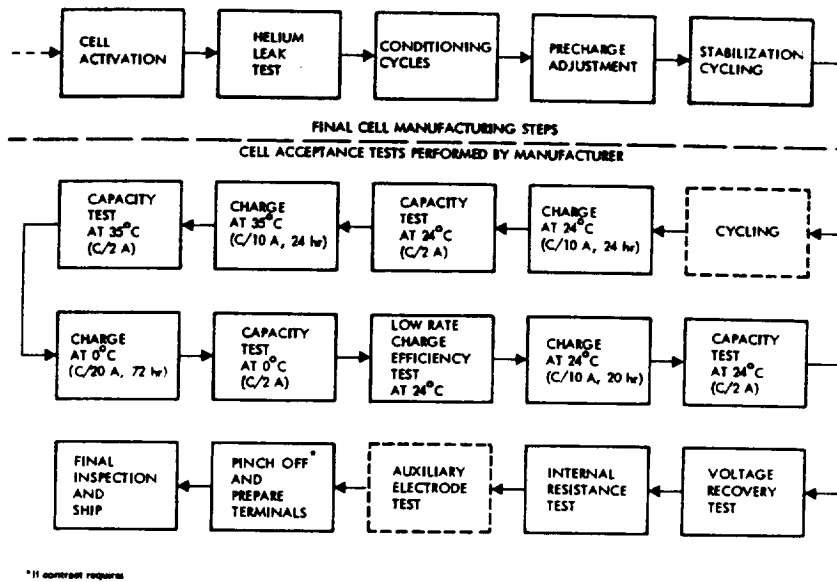


Figure 73. Typical cell acceptance-test sequence performed by the cell manufacturer.

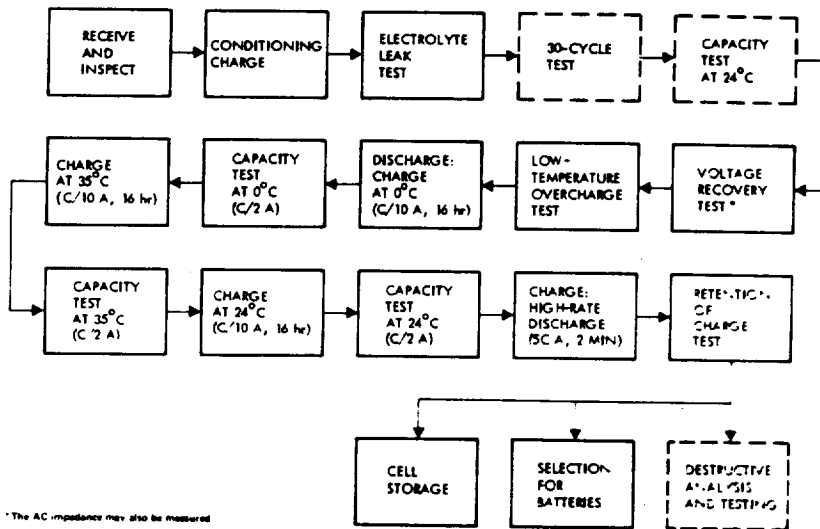


Figure 74. Typical cell acceptance-test sequence performed by the buyer.

Table 42 lists the tests shown in figure 73, together with a brief description of the method specified, suggested alternatives, and authors' comments. Two aspects of the various methods are considered: (1) the test procedure *per se*, and (2) the criteria used for judging the results of the tests. This recognizes the possibility that, although a test procedure may be valid, the pass/fail criteria associated with it may be poorly chosen. Such criteria are often determined by specification performance requirements that may be inappropriate.

Not all of the procedures in table 42 are completely understood, and there is lack of agreement on some of the methods and criteria shown. Several of these points are:

- The actual effect of "stabilization cycling" (item 1 of table 42) on the internal makeup of the cells is not clear. Although the charge and discharge voltages may be stabilized in 10 cycles, indications are that the active capacity of the negative electrode and the activity of the charged excess negative capacity may continue to change for 50 to 100 cycles. Also, there is reason to believe that most positive-plate swelling and electrolyte redistribution takes place after the first 10 to 20 cycles. Furthermore, there appears to be no information available on the effect of the particular depth of discharge used on the subsequent cell performance during acceptance tests. Some users have suggested that the depth of discharge used for stabilization should be the same as that for the intended application. However, no information has yet been made available to demonstrate the advantage of this approach.
- Overcharge tests conducted at 0°C (item 7, table 42) for verifying overcharge protection have occasionally produced results that have not yet been fully explained. Sometimes high cell voltage is observed with low cell pressure; sometimes (but less often) the opposite is seen. Good correlation between low-temperature overcharge voltage and pressure behavior and the amount of overcharge protection provided in the form of excess uncharged negative capacity has not been demonstrated, although it is usually true that little or no overcharge protection results in a high voltage. The presently used upper limit criterion of 1.52 volts may be too harsh and, if interpreted literally, could result in the rejection of good cells. Some cells may peak at slightly above 1.52 volts and then settle down to a much lower voltage. These cells would be rejected by the present criterion. Thus, it is recommended that the basis of judgment in this test be expanded

ORIGINAL PAGE IS
OF POOR QUALITY

Table 42
Cell Acceptance-Test Method Summary

No.	Test	Paragraph and Method Per NASA/GSFC 74.1.5000	Criteria for Acceptance	Alternative Methods and Procedures	Comments
1	Stabilization cycling?	6.4.1 Minimum of 10 cycles at 25-75% depth of discharge (DOD); no temperature is specified	Left to cell manufacturer to recommend	A DOD of 50 to 75% may be used for geosynchronous orbit applications	The manufacturer's preacceptance test sequence may contain sufficient cycling to permit its use as a substitute. The cycling temperature should be as low as possible (down to 0°C) to minimize side effects.
2	Charge and overcharge at 24 ± 2°C cell temperature	6.4.2a Charge at a 0.1C rate for 24 ± 1 hours	Maximum voltage: 1.48 V; maximum pressure: 50 psig		Because voltage and pressure may be quite sensitive to individual cell temperature, temperature data are required. Some cells run warmer than others and may exceed specified limits. A requirement for the maximum rate of change of voltage and pressure at end of charge may be included.
3	Discharge at 24°C	6.4.2b Discharge at a 0.3C rate to 1.0 volt	Minimum capacity: rated ampere-hours at end of discharge (EOD); pressure: 0 psig	The voltage at the half-discharge point may be recorded	A reasonable tolerance on the EOD voltage should be specified (e.g., +0.1 volt, -0.3 volt). An EOD voltage of 1.10 volt should be used to prevent cell reversal if automatic equipment is not used to cut off the discharge at 1.0 volt.
4	Short-down	6.4.2c Place a 1Ω resistor across the cell	Minimum period: 16 hours		Recharge characteristics immediately after a short-down are often different from those obtained for subsequent cycles performed without a prior short-down.

Table 42 (Continued)

No.	Test ¹	Paragraph and Method Per NASA/GSFC 74-15000	Criteria for Acceptance	Alternative Methods and Procedures	Comments
5	Charge and overcharge at 15°C	6.4.2d Change temperature to 15°C and permit it to stabilize for 4 hours minimum; charge at a 0.1C rate for 24 hours	Maximum voltage: 1.45 V; maximum pressure: 50 psig		Maximum pressure should be less than that observed for Test 2.
6	Discharge at 15°C	6.4.2e Discharge at a 0.5C rate to 1.0 volt	Minimum capacity: 55% of that measured in Test 3; pressure < 40 psig		A relatively large spread in capacity is to be expected.
7	Charge and overcharge at 0°C	6.4.2f Change temperature to 0°C and permit it to stabilize for 4 hours minimum; charge at a 0.05C rate for 72 hours	Maximum voltage: 1.52 V; maximum pressure: 50 psig	A prior cycle at 0°C may provide a better test condition.	See text.
8	Discharge at 0°C	6.4.2g Discharge at a 0.5C rate to 1.0 volt	Minimum capacity: 85% of that measured in Test 3; pressure < 40 psig		The 15% capacity decrease is undesirable for applications at low temperature and high depth of discharge and could indicate negative limiting at end of discharge.
9	Short down	6.4.2h Place a 10Ω resistor across the cell for 16 ± 1 hours while stabilizing the temperature at 12°C			Same as for Test 4.

Table 42 (Continued)

No.	Test ¹	Paragraph and Method Per NASA/GSFC 74-15000	Criteria for Acceptance	Alternative Methods and Procedures	Comments
10	Low-rate charge and overcharge at 24 ± 2°C	6.4.2j. Charge at a 0.025C rate for 20 to 11 hours	None specified		The charge acceptance obtained after the preceding short-down will be higher than can be expected during regular cycling. Charge acceptance at this temperature-rate combination and with only 50% of rated capacity throughput can be expected to vary from cell to cell.
11	Discharge at 24°C after a 0.025C charge	6.4.2j. Discharge at a 0.5C rate to 1.0 volt; repeat Test 9	Minimum capacity: 60% of ampere-hours charged		Capacities may be expected to vary widely.
12	Charge and overcharge at 24 ± 2°C and perform an electrolytic leak test	6.4.2k. Charge at a 0.1C rate for 20 hours; perform a leak test	Maximum voltage: 1.48 V; maximum pressure: 50 psig		
13	Final discharge at 24 ± 2°C	6.4.2l. Discharge at a 0.5C rate to 1.0 volt after a 1 hour stand	Minimum capacity: Rated ampere-hours; pressure: >20 psig		A requirement for a maximum difference between capacities measured in Tests 3 and 13 could be used to limit the extent of fading that is acceptable during this test sequence.
14	Short-down at 24 ± 2°C	6.4.2m. Place a 151 resistor across the cell for 16 ± 0 hours	Maximum pressure: 20 ± 1/2 psig		A longer short-down period may be needed if the cell is negative-limited. See Reference 83.

ORIGINAL PAGE IS OF POOR QUALITY

Table 42 (Continued)

No.	Test ¹	Paragraph and Method Per NASA/CSRF: 74-15000	Criteria for Acceptance	Alternative Methods and Procedures	Comments
15	Voltage recovery	6.4.2n. Open circuit for 24 ± 1 hours	Minimum voltage: 1.17 V	Voltage decay test (see text)	More than a one voltage measurement during the 24 hour period is useful. See Reference 83.
16	Internal resistance ^{1/3}	6.4.2n. An instrument is specified	None specified	60-Hz sine wave test (see text)	Impedance should be approximately 50(°C) mΩ. See figure 14 of this manual.

¹ Although many individual tests do not have separate titles in the source document, they are given descriptive names in this table for convenience.

² Tests 1 through 16 are designated by Reference 179 for performance by the cell manufacturer and are therefore designed with this in mind. If they are performed or later repeated at the buyer's plant where more automated test and data acquisition equipment is available, additional refinements and data requirements may be added.

³ Test 16, which includes the acceptance sequence at the cell manufacturer as specified by Reference 179 for cells without auxiliary electrodes. When cells have auxiliary electrodes, some additional tests (not included here) are specified.

to separately specify the maximum voltage during the peak, the duration of the peak, and the voltage and rate of change of voltage at the end of the overcharge period. Any pressure measurements that can be made during this test will greatly facilitate interpretation of the data.

- The voltage recovery test (item 15, table 42) is done to detect internal shorts. It has been shown (Reference 83) that this test method, in which a single voltage measurement is taken at the end of a 24-hour open-circuit stand period, gives results that are relatively sensitive to pretest cell conditioning. Three test methods in general use were evaluated and compared in Reference 83: (1) open-circuit voltage decay after a brief charge; (2) open-circuit voltage recovery after shorting; and (3) open-circuit voltage decay and capacity loss after a full charge. Although all methods were considered to have merit, the first method was recommended for general use. Method 2 showed a sensitivity under ideal conditions that is comparable to that of method 1, but was more affected by the cell's immediate prior history and by conditioning procedures than the other methods. Method 3 was less sensitive than the others but more immune than the others to prior history effects. The results of methods 1 and 2 are adversely affected if the cells are tested in a negative-limited condition. Method 3 is also used to test for charge retention and, as such, may be performed at different temperatures to determine the effect of temperature. Method 1 is sometimes referred to as a charge-retention test. This title is considered to be inappropriate because the method is not suited for that purpose (Reference 83).
- Several methods for measuring internal resistance/impedance (see item 16, table 42) are in use, including: (1) sine-wave ac current and (2) square-wave ac current, both at various frequencies, and (3) high-rate dc discharge current. No data are available to show whether the methods each give the same value for the measured variable. The data in figure 15 show that, without separating the measured voltage into its resistive and reactive components, ac measurements will give erroneously high values for resistance at frequencies above about 300 Hz. Thus, the use of commercially available direct-reading milliohmmeters that apply square-wave current for measuring cell resistance can give significant errors if much high-frequency content exists in the excitation current waveform and the instrument does not discriminate between in-phase and out-of-phase responses.

As greater demands for longer service life and higher reliability are placed on the nickel-cadmium system, tests of greater sensitivity may be required that, in turn, may increase cell rejection rates. Accordingly, as the battery engineer develops new criteria or uses the present criteria, he should not be overzealous in setting tolerances and limits but should allow for the application of engineering judgment to resolve slight variations or inconsistencies in the data.

6.2.1.3 *Cell-Lot and Plate-Lot Acceptance*

Cell specifications normally do not contain provisions for judging the acceptability of cell lots* as a whole; instead, each cell is considered acceptable or not on its individual merits. However, it is possible for a relatively high percentage of cells in a lot to exhibit the same defect or defects, and the buyer should have the prerogative to reject the entire lot until a review can be conducted. The power to take such action must be established contractually in advance, along with the criteria for lot acceptance.

Occasionally, a cell lot will be defective because the plate lot from which it was made was inherently defective. Cell manufacturers rarely reject plate lots as a whole, even though large percentages of the plates may be defective on inspection or test, because no written procedures and criteria for plate-lot acceptance are normally in effect. The authors consider this to be a potentially serious weakness of current quality-assurance practices and something for all spacecraft cell users to consider.

6.2.2 **Other Tests and Analysis**

The sequence of tests shown in figure 74 may or may not be used for contractual acceptance of cells. Table 43 lists the tests enclosed in solid lines in this sequence, together with a brief description of the test method defined in Section 8 of NASA/GSFC Specification 74-15000 (Reference 179) and comments by the authors.

The tests enclosed in dashed lines were added to the buyer's sequence by some organizations, particularly for cells that are to be used in long-life geosynchronous spacecraft. The 30-cycle test, which involves high depths

*The term "cell lot" refers to a manufacturing lot, which is normally defined as all cells made from a single plate lot and manufactured in a group over a relatively short time.

Table 43
Cell Performance Test Method Summary

No.	Test	Paragraph and Method Per NASA/GSFC 74-15000	Criteria for Acceptance	Alternatives	Comments
1	Electrolyte leak test	8.1.1. Immediately after a charge, generating a pressure >0 pug., clean with water and methyl alcohol. Use a swab wet with phenolphthalein solution; red color on swab denotes leakage.	Reject if a positive test occurs after the second cleaning and retest.	Spraying followed by swabbing.	The use of a water-containing indicator solution may cause a false test failure indication on a charged cell.
2	Voltage recovery test	8.2.1. Drain cell with a 10 resistor; open circuit for 24 hours. Measure voltage.	Cell voltage \geq 1.16 volts	Voltage decay test (see text)	More than a single voltage measurement during the 24-hour stand time is useful. See Reference 83.
3	Low temperature overcharge	8.3. Same as Test 7, table 42.	Maximum voltage: 1.52 volts; maximum pressure: 50 pug	Same as Test 7, table 42.	See text.
4	Capacity (at three temperatures)	8.4.1. Two cycles run at each of three temperatures: 0, 24, and 35°C.	Same criteria as in Tests 3, 6, and 8 in table 42.	Eliminate the short-down before the second cycle.	Same as for Tests 3, 6, and 8 in table 42.
5	High rate discharge	8.5. Discharge at a 5C rate for 2 minutes.	Minimum voltage: \geq 1.0 V.		The state of charge and the temperature should be specified. A voltage above 1 volt at the 5C rate implies an internal impedance not much greater than (50/C) m Ω because the IR drop across this resistance will be 0.25 volt.
6	Retention of charge	8.6. Charge at a 0.1C rate for 24 hours, followed by an open circuit stand for 7 days.	Capacity: 80% of initial capacity; cell open-circuit voltage within \pm 5 mV of group average.	Other open-circuit stand times could be used with corresponding residual capacity requirements. (See figure 4.6.)	Additional criteria may be used to make the test more definitive (e.g., voltage should decay on a log time scale and EOD voltage should be greater than 1.28 V). See Reference 83. The test temperature should be not higher than 25°C to achieve 90-percent retention over 7 days.

ORIGINAL PAGE IS
OF POOR QUALITY

of discharge and low temperatures, can be useful for detecting an excessively high rate of fading but, more specifically, an excessively high rate of decrease of negative capacity or precharge. The cycling is usually terminated with a complete discharge at the cycle temperature and may be followed by a capacity measurement at the standard temperature of 24°C, as shown in the flow diagram. This test may be expanded to include a capacity measurement before and after reconditioning before testing for internal shorts.

The other optional item shown in figure 74 is destructive testing and analysis. Since 1970, spacecraft life requirements have been increasing. Recent specifications for geosynchronous-orbit applications require prelaunch storage lifetimes of 4 to 7 years (Reference 180) and service lifetimes of 5 to 10 years; therefore, up to 12 years of total life capability may be required. These lifetime extensions are causing battery users to look for better ways of detecting latent manufacturing cell defects that are not detected by any known nondestructive acceptance tests. These tests may consist of the accelerated cycling of cells to failure and/or of teardown analyses. In the latter case, sample cells are opened, and the components are tested and analyzed for mechanical, electrochemical, and chemical properties. Additional information on teardown analysis appears in Section 4.

Intelsat/Comsat now requires that two cells from each cell (plate) lot be subjected to teardown analysis (Reference 62). Several Air Force projects have incorporated similar requirements into cell and battery specifications. Most companies are now using this form of testing only for engineering evaluation. It is to be hoped that the result of these tests will achieve the status of acceptance requirements in the near future.

6.2.3 Selecting and Matching Cells for Batteries

The process of selecting and matching cells for batteries is not standardized and is hardly discussed in the literature. The process involves the application of engineering judgment on the basis of a detailed review of manufacturing process data, acceptance test data, and data obtained from any other special tests. The objective of cell selection is to ensure uniformity of cell characteristics within the battery and the battery system; cells with performance characteristics that are not similar to the main group of cells are discarded. It is good practice to select the number of cells needed for a battery, plus at least one spare cell for compatible replacement if it becomes necessary.

One or more of four methods are used for selecting and matching cells for batteries: (1) capacity matching, (2) discharge-voltage characteristic matching, (3) charge-voltage characteristic matching, and (4) charge efficiency screening. The method or combination of methods depends on the type of orbit, the maximum depth of discharge, the operating temperature range, and the characteristics of the battery charge controls. The following paragraphs describe these methods and the factors that influence their selection.

Capacity matching is the most common method used to assign cells to individual batteries. In general, the cell of lowest capacity in a series circuit (or string) will establish the capacity of the battery because the discharge must be stopped before that cell is reversed. Capacity matching is therefore more important for geosynchronous applications that require deep depths of discharge than it is for low-Earth-orbit applications. Typical geosynchronous-orbit capacity-matching criteria are ± 1.5 percent for cells within any single battery and ± 2.5 percent for batteries within a spacecraft. By comparison, NASA low-Earth spacecraft projects (Orbiting Astronomical Observatory and High Energy Astronomical Observatory) have required that cell capacities within a battery be matched to within ± 2.5 percent and that battery capacities within a spacecraft be matched to within ± 5 percent.

The capacity data used for matching may be taken from any number of capacity measurements, including those performed during acceptance and performance testing (as outlined in figures 73 and 74) and/or additional tests. The spread in capacities for any group of cells is dependent on the immediate prior history in the test sequence. If the capacity measurement cycle is preceded by a short-down period, the range of values for the test group will usually be quite narrow. If two or three cycles are run without pause after a short-down period, the measured values after the first cycle will be closely grouped, but, after the second or third cycle, the spread of values will become greater. The latter is particularly true at the end of a 30-cycle test if the capacity is measured before reconditioning or short-down.

Capacity is usually measured by using a constant-current discharge. However, for the most part, spacecraft electrical loads are a combination of constant resistance and constant power, predominantly the latter, and the current drawn from the battery is anything but constant as the battery voltage decreases. Thus, if matching were to be performed rigorously, it would be based on energy output rather than on capacity at constant current. This approach has not been used generally because of the added requirements

that it would place on cell test and data-acquisition equipment. However, most modern automatic data-acquisition systems can easily acquire the periodic voltage and current data required and, with the assistance of an on-line computer, calculate the energy data on an essentially continuous basis, if desired.

In the absence of this type of equipment, matching may be improved by including in the criteria, in addition to capacity data, voltages at one or two points on the discharge-voltage curve. These points are best chosen at mid-discharge, where the voltage is between 1.2 and 1.25 volts, and near the end, where the average is about 1.1 volts. The product of these voltages and the corresponding ampere-hour outputs may be used as a substitute for a true discharge-energy calculation.

Matching discharge voltage at the battery level in paralleled multiple-battery systems is usually not required. All the batteries will discharge at approximately the same voltage, and differences among the individual discharge currents will reflect differences in battery current-voltage characteristics. As discussed later in Section 8.5.1, there is a strong tendency toward balanced discharging in the absence of cell failures because of the interaction of conditions of temperature and state of charge. Furthermore, the effect of differences in the resistance of individual battery harnesses usually masks the differences among the discharge-voltage characteristics.

Matching charge-voltage characteristics of cells within a battery can be important if voltage-limited charge controls are used. For example, in low-altitude orbit applications, if the limit is set high so that relatively high recharge ratios are obtained, the range of cell voltages at the end of charge will tend to be wide, suggesting a need for voltage matching. This is one argument for designing such charge-control systems to limit in a manner that provides recharge ratios as low as possible, as was done for the Orbiting Astronomical Satellite (References 62 and 77). With early limiting, the individual cell voltages will tend to be tightly clustered.

From the viewpoint of operating temperature, the need for charge-voltage matching increases as the temperature during charge decreases. Operation at or near 0°C, and particularly with higher charge rates, means that a relatively wide range of cell voltages will be obtained during overcharge in the absence of a voltage limit. More work needs to be done in developing low-temperature tests and associated matching criteria that reflect battery-operating temperature regimes anticipated for longlife missions.

In summary, it is apparent that cell charge-voltage matching is advisable in all situations that depend on charge voltage as a signal or control parameter and in all situations in which charging is performed in the vicinity of 0°C. In lieu of such matching, a reasonable criterion for General Electric and SAFT-America cells is selection within ± 7 millivolts of the group mean voltage following 4 hours of overcharge at 23°C at a C/10 charge rate. Eagle Picher cells may require a wider range. No criterion is needed for matching the charge voltages of multiple batteries if they are charged separately; batteries charged in parallel from a single charge controller may require charge-voltage matching, although the effect of temperature differences between the batteries could mask the effect of differences in the charge characteristics.

Charge-efficiency characteristics of cells become important in applications that involve extremely low or high charge rates. In the former case, it is important to eliminate from consideration the cells that are unable to attain a full state of charge when charged at the low current rates that could occur in certain geosynchronous-orbit applications. For the latter case, it may sometimes be desirable to screen out the cells that contribute excess dissipation and, therefore, exhibit higher operating temperatures than other cells in the battery. Although neither case can be considered a significant problem for most battery applications, of the two, the low-rate charge-acceptance case is encountered most often because of the need for minimizing the area and weight of the solar-cell array.

These different data do not usually result in the selection of a single group of cells. For example, the best match by capacity may not correspond to the best match by overcharge voltage. It is therefore necessary to apply weighting factors to the different types of data. No general rules are obvious. From the foregoing discussion, such weighting must depend on the type of orbit involved, the design of the charge-control method, and the operating temperature range.

6.2.4 Battery-Acceptance Testing

After a battery assembly has been completed mechanically, it is usually given some simple nonoperating bench tests and then subjected to battery-level acceptance testing to specification. Battery-acceptance testing is sometimes done separately and as a prerequisite to qualification testing or as a part of qualification testing. Section 9 describes the sequence and details of such testing.

One aspect of battery-acceptance testing that is usually underemphasized is cell-voltage behavior during battery operation. Individual cell voltages are carefully monitored during cell-acceptance and matching tests for good reason, and they should not be ignored after battery assembly. It should not be assumed that the same voltage distribution observed during cell-level testing will be necessarily observed after the cells are assembled into a battery.

6.3 QUALIFICATION TESTING

The objectives of qualification testing are: (a) to verify that all electrical, mechanical, and thermal aspects of the unit meet specification requirements, and (b) to ensure interface compatibility (insofar as possible) with the spacecraft, the launch vehicle, and ground-handling and electrical support equipment.

Because most cell designs are scaled from previously qualified designs, qualification of battery cells is usually accomplished by analysis. If a cell design is completely new or otherwise unique, qualification testing may be performed. However, such qualification can only be general in nature, because it is essentially impossible to simulate with any degree of accuracy the vibration, shock, acceleration, and thermal environment that cells will experience in an actual battery assembly. For this reason and because most cells used are already qualified as cells and, hence, do not require requalification at the cell level, almost all qualification testing is performed at the battery level.

NASA/GSFC Specification S-711-17 (Reference 181) defines a complete battery-qualification test program for the standard nickel-cadmium battery specified in NASA/GSFC Specification S-711-16 (Reference 182). Table 44 summarizes the battery-level qualification tests identified by the NASA specification and certain other tests that are sometimes performed. Therefore, table 44 is a checklist for both cell- and battery-qualification tests. Section 9.5 describes battery-qualification testing in greater detail.

6.4 LIFE TESTING

As defined previously, acceptance and qualification tests establish compliance with specification design requirements but do not provide verification that a battery will meet the service life and reliability goals for the mission. The term "goal" is used rather than "requirement" because battery service

Table 44
Cell- and Battery-Qualification Test Matrix

Test	Cell Level	Battery Level
Physical inspection	✓	✓
Physical measurements	✓	✓
Magnetic measurements (optional)		✓
Functional tests		
Insulation resistance		✓
Electrical continuity		✓
Capacity	✓	✓
Electrolyte leakage	✓	✓
Voltage recovery (optional)	✓	✓
Charge retention (optional)	✓	✓
Sensor operation		✓
Heater operation		✓
Internal resistance	✓	✓
Humidity	(1)	(1)
Vibration	✓	✓
Shock	✓(2)	✓(2)
Acceleration	✓(2)	✓(2)
Thermal vacuum		✓
Special tests		
High-rate discharge	✓	✓
Thermal cycling		✓

¹Verified by materials analyses rather than by specific test. The shipping container should protect the battery and its cells from humidity exposure.

²Usually most realistically performed at the spacecraft level.

life and reliability are not verifiable quantities in the usual sense. Although cell-procurement and battery-equipment specifications sometimes include specific design requirements for these items, it is neither practical nor possible for a cell manufacturer or a battery supplier to provide direct verification by test that the requirements are met. Missions are measured in years, and it may take years for a properly designed and operated nickel-cadmium battery to exhibit serious degradation or cell failure. Cell and battery reliability can be estimated only on the basis of failure distribution developed for quantities of cells of similar design operated in a similar manner. These circumstances are resolved by reliance on the data collected from the types of life tests discussed in this section.

The usual objectives of cell and battery life testing are:

- To verify that the cell or battery design can meet service life requirements before wearout failure in a simulated space environment
- To obtain degradation and failure data for battery-system reliability assessment
- To obtain beginning-of-life and end-of-life performance data for power-system design analyses, charge-control design analyses, and orbital-operations planning

Two kinds of battery life tests may be distinguished: (a) real-time and (b) accelerated. From a technical viewpoint, real-time tests are preferred because they provide the closest possible simulation of actual flight conditions. Real-time life tests are readily performed for low-altitude orbit missions, which are relatively shorter in duration, but present problems of time and money that increase as the mission length increases. For geosynchronous applications of 5 years or more, real-time tests are usually prohibitive for particular spacecraft projects and are usually performed only in support of long-range development efforts. In lieu of true real-time tests, therefore, certain forms of time-accelerated life tests have been performed.

6.4.1 Real-Time Life Testing

All life tests that have been performed for low-altitude applications have been real-time tests. Certain orbits in this class may exhibit short periods of constant sunlight during which the batteries are not cycled, but such effects

are usually ignored in life testing and cycling continues uninterrupted. With notable exceptions, real-time tests performed for specific low-altitude spacecraft projects are not performed for the full required mission life. No guidelines are known that define the number of cycles that must be accumulated as a minimum for verification of service life.

Real-time life tests that simulated low-altitude orbit discharge/charge profiles have been successfully performed for a number of NASA spacecraft projects (References 62, 77, 116, and 183 through 185). The tests were accomplished by using the charge-control methods planned for the respective projects. Temperatures were selected to bound the predicted operating temperature range (i.e., tests were usually performed in parallel at two or three operating temperatures).^{*} Because of these differences, it is difficult to quantitatively compare the results. Another important source of low-orbit life-cycle data is the series of tests performed under NASA auspices at NWSC/Crane (Reference 68, 12th Annual Report). These tests, which may be referred to as life cycle tests rather than as mission simulation life tests, are a major source of failure data.

As mentioned earlier, real-time life testing for geosynchronous applications is usually impractical for direct support of specific spacecraft projects. Mission-life goals have now reached 10 years, and there are economic pressures for further life extensions. However, certain ongoing tests have been useful in providing design guidelines. For example, the NWSC/Crane real-time geosynchronous life testing of cell packs began in 1967 and continues to the present (Reference 186). COMSAT Laboratories also performed mission-simulation real-time tests (Reference 91), which began 1 to 2 years before the first launch of a particular spacecraft series. Some of these tests have been continued for over 6 years. Finally, a real-time geosynchronous test, which lasted only 18 months but included four simulated eclipse seasons (one at the beginning), has been reported (Reference 51). This test was conducted with a prototype 50-Ah battery whose cells were equipped with active solid-state bypass circuits for controlling overcharge and overdischarge. For detailed descriptions of the test articles, the test equipment, and the test methods, see the referenced reports.

^{*}An alternate method makes use of a variable average battery heat-sink temperature profile throughout the mission.

6.4.2 Accelerated Life Testing

The objective of any accelerated life test is to verify life capability in a shorter period than would otherwise be required if real-time testing were performed. An accelerated test should only hasten normal degradation processes and should not introduce new forms of degradation. Furthermore, if the test is performed in connection with a specific spacecraft project, the test method and conditions should be related as closely as possible to the service conditions to facilitate the interpretation of results.

Two approaches to the life-test acceleration are possible. In one, the overall test time required is shortened without knowingly increasing the stress levels by raising temperature, charge rate, or depth of discharge above their anticipated values. This approach is usually feasible for polar-orbit applications or for higher-altitude applications which experience some extended noncycling periods each year. The other approach involves increasing the operating temperature and/or the stress levels in the cells and, hence, the degradation rates during cycling. Only the latter approach is feasible when the mission involves essentially continuous cycling. This section discusses the former approach; Section 6.5 describes acceleration by increasing stress levels.

Two methods have been used most often to shorten test time without increasing stress. The first, most often used for geosynchronous applications, involves eliminating or reducing intervals of low operational stress such as the continuous noncycling periods corresponding to periods of continuous sunlight in orbit. However, disagreement exists as to whether the results obtained truly account for all of the degradation that would be realized in an actual mission. Because certain degradation processes within the cells are believed to be time-dependent rather than cycle-dependent, their effect would not necessarily become manifest during this type of accelerated life test. Results from this form of accelerated testing were in good agreement with real-time testing under otherwise nearly identical conditions over an 18-month test period (Reference 51), as illustrated in figure 75. Reasonable agreement between the voltage trend from an accelerated test and that from flight data from two spacecraft of the Defense Satellite Communications System (DSCS-II) series is shown in figure 76 over a mission time of almost 5 years.

The second method used for accelerating synchronous tests involves performing a discharge to the same depth of discharge every day of the test, with the depth of discharge made equal to the average of the variable depths

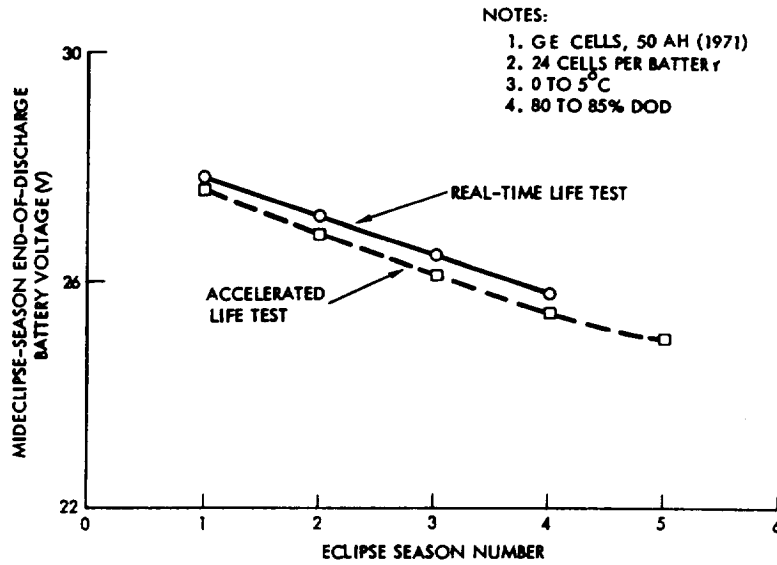


Figure 75. Simulated geosynchronous life-test results for 50-Ah batteries (Reference 51).

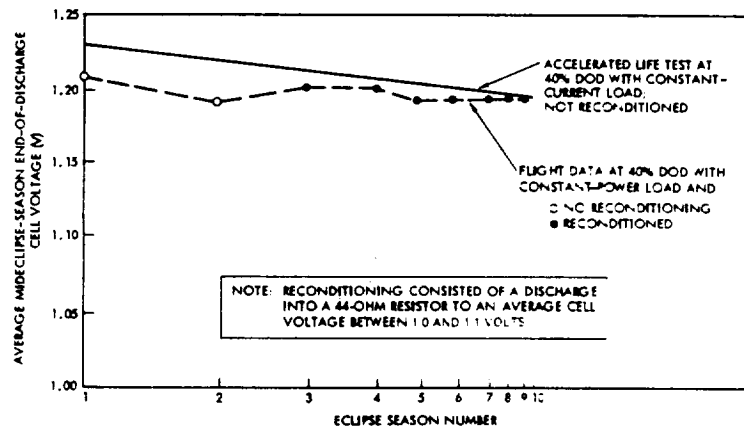


Figure 76. Comparison of DSCS-II battery flight data with simulated geosynchronous accelerated life-test results.

experienced in an actual eclipse season in geosynchronous equatorial orbit. A number of these tests are being conducted at NWSC/Crane (Reference 68, 12th Annual Report) with a 50-percent depth of discharge. Whether these conditions result in the same average stress to the cells that would result from a true eclipse-season simulation is not clear. No attempt to correlate the results with those from other types of accelerated tests has been reported.

Any number of special constraints may be added to life testing to make the results more "realistic" and to meet particular hardware designs and specifications. These may include the use of a specific charge-control method, the use of constant power rather than constant-current loads, the use of cycled-cell temperature profiles to conform with predicted battery temperatures, the simulation of abnormal and partial-failure conditions, and the performance of reconditioning, as appropriate. In particular, the life testing of batteries at more than one temperature level is advisable because the operating temperature is, in all likelihood, the most critical variable and is often the most difficult one to predict.

Life test plans and results should be presented at each battery design review. These tests are costly and usually cannot be repeated within normal spacecraft development schedules. Detailed review and close coordination of all aspects of such tests is therefore mandatory.

Battery reconditioning has been mentioned in connection with accelerated life test procedures. Although the concept of reconditioning batteries in service is not new, recent work performed using deep-discharge reconditioning (Reference 187) has produced test results that are much improved over those obtained with shallow or no reconditioning. Figure 77 shows that over 40 simulated eclipse seasons (equivalent to 20 years of cycling in orbit) have been completed in one life test with no discernable downward trend in minimum end-of-discharge voltage because deep reconditioning was begun between each eclipse season. Accelerated testing performed earlier in this sequence showed that the end-of-discharge voltage decayed relatively rapidly under similar operating conditions when no reconditioning was performed. Similarly, recent data published by NASA/Marshall Space Flight Center (MSFC) and obtained from low-altitude life testing using low-rate reconditioning show a significant change in performance, although improvements in service life have not yet been demonstrated (Reference 175). Reconditioning techniques may therefore play an important role in the design and operation of future long-life battery systems, and their use should therefore be considered when any life-test program is defined.

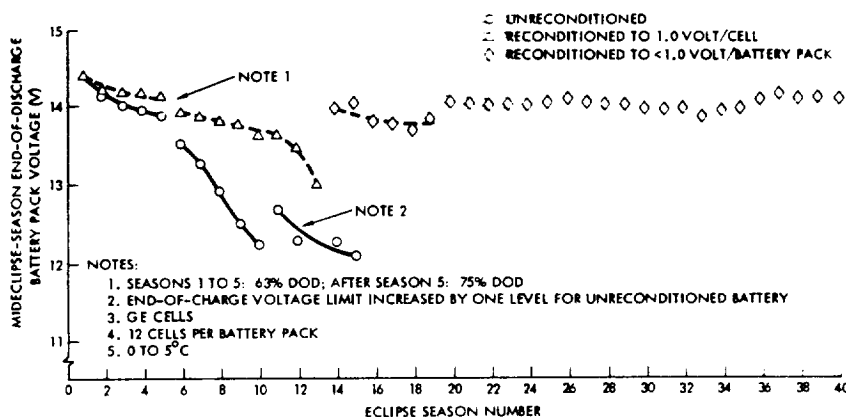


Figure 77. Simulated geosynchronous accelerated life-test results for 24-Ah battery packs.

6.5 SPECIAL ACCELERATED TESTING

The previous section discussed accelerated life testing as it is normally performed for sealed nickel-cadmium cells and batteries in geosynchronous applications. The term "accelerated" was used to denote shortened overall test time relative to a real-time mission. The test-time reductions were obtained by: (a) eliminating those portions of the application profile that contribute relatively little stress to the cells or (b) modifying the usual variable discharge time versus eclipse cycle profile to permit the use of a single depth-of-discharge value that is somewhat greater than the average. It was emphasized that, when these adjustments are made, other test conditions remain close to the expected service conditions.

However, accelerated testing is not usually performed in this manner in other industrial settings. Such tests are designed to hasten expected degradations or failures by stressing the device or component in a particular way or combinations of ways. A basic hypothesis of accelerated testing so defined is that higher stress levels lead to higher rates of degradation. The ratio of the rates of degradation obtained with higher-than-normal and normal stress levels is called the acceleration factor. To distinguish this type of accelerated testing from that discussed in Section 6.4.2, the term "special accelerated

testing" is used throughout the remainder of this section. However, note that "special" has meaning here only in the context of aerospace nickel-cadmium battery technology.

McCallum et al. merged accelerated testing theory with battery technology at Battelle in the late 1960's. In a series of studies that culminated in Reference 139, they attempted to construct a general methodology that could form the basis for the later design of special accelerated test programs. Their approach is described in Section 4. The following discussion of specific methods of achieving test acceleration as they apply to cells and batteries is drawn from the work at Battelle.

McCallum and coworkers investigated the use of elevated temperatures, (Reference 175), elevated depths of discharge (Reference 177), and elevated discharge rates (Reference 85) as means for increasing internal stresses in nickel-cadmium cells. They observed that the number of cycles to failure* generally decreased as temperature, depth of discharge, or discharge rate increased, but this parameter did not appear to correlate with stress levels in their experiments. This result was partially attributable to the fact that the lower voltage limit chosen as a failure criterion was too high and was reached by many cells while the discharge voltage was still on the upper plateau. Better results were obtained by using values on the discharge-voltage curve to calculate a quantity called "quality" (Q_v), defined as a function of discharge rate and the difference between an assumed open-circuit cell voltage and the measured end-of-discharge voltage: i.e.,

$$Q_v = \frac{1}{(I/C)(1.3 - V)}$$

For example, for variable discharge rates (Reference 85), a roughly linear relationship was found between the logarithm of the acceleration factor, (Q_v at rate 2)/(Q_v at rate 1), and the logarithm of the discharge rate over the tested range of 0.5 to 8C. Similar results were obtained for increasing temperature and increasing depth of discharge, although the data were scattered. Different acceleration factors were found from different experiments, however, indicating that other variables were not under control. Thus, the methods for accelerating degradation by increasing stress levels cannot be considered as proven from the results reported. However, these results were indeed promising and bear further investigation using modern cells with greater uniformity than those available earlier.

*"Failure" was defined as an end-of-discharge voltage less than 1.10 volts during regular cycling.

One set of tests using various higher-than-normal discharge rates (Reference 162) showed that, after the data were extensively screened, the end-of-discharge voltage was a straight-line function of the logarithm of the cycle number, at least up to about 3000 cycles at which testing was stopped. The slope of the straight line was a function of discharge rate; therefore, the slope at any normal discharge rate could be calculated from the slope at a higher rate at which the rate of change with the number of cycles was greater. This type of logarithmic relationship was also observed on a cycle-life test performed on recently made SAFT-America 20-Ah cells (Reference 116).

Failure analyses were performed on many of the cells from the accelerated test experiments at Battelle. The results of some of these appear in Section 4. However, the relatively limited scope of these tests and subsequent evaluation studies provided what must now be considered as inconclusive explanations for the results observed. Therein lies one limitation of this type of accelerated testing—the tests and analyses required to determine mechanisms and acceleration factors are often difficult and always expensive. Limited experiments are usually insufficient for determining that the application of various kinds and combinations of stress have not modified the underlying mechanisms.

NASA and the Armed Services are jointly sponsoring a special accelerated test program at NWSC/Crane (Reference 176). The program is directed toward low-altitude cycling and is ambitious in scope; as of October 1977, 594 cells had been placed on test in 103 packs. Although some preliminary results have been published (References 153 and 188), major results will not be forthcoming until detailed analyses are completed.

No similar special accelerated tests have been planned or performed for cells intended for geosynchronous applications. Such methods could be quite useful, however, because: (a) time-accelerated test methods still require considerable test time, and (b) the use of deep-discharge reconditioning with conventional testing causes the cells to exhibit low rates of end-of-discharge voltage decline, thus creating a need for even lengthier tests in order to identify life-limiting mechanisms. If, as it appears, discharge voltage degradation is related primarily to the number of cycles and has little to do with total operating time in a geosynchronous orbit, any method that speeds up cycle-dependent degradation rates should be effective for accelerating geosynchronous-related life tests. (See Section 6.4.2.)

6.6 MISCELLANEOUS TESTS

Two other tests, not as frequently performed, are discussed briefly here. These are parametric tests and heat rate measurements.

6.6.1 Parametric Testing

Parametric testing consists of a group of tests, usually performed on a number of cells at a time, in which charging and discharging are performed over a range of each important operating parameter. Usually temperature, charge rate, and discharge rate are the variables, and others, such as end-of-charge voltage, recharge ratio, and depth of discharge may be added. The purpose of such tests is to obtain performance data over the range of variables used for predicting the envelope of cell and battery behavior to expect in service. The range of conditions may be limited by the range expected or enforced for a particular application. The data may be fed into a computer data file and used for performance simulation.

The task of structuring the test sequence is puzzling because the number of possible combinations is unlimited. In general, it is preferable to begin at the lowest level of temperature, charge rate, and/or discharge rate and to progress toward the highest level. Larger intervals of temperature should be used at the low end than at the high end: 0, 20, and 30 or 35°C provide a good spread for three temperatures. Charge and discharge rates should be varied in geometric series, each differing by a factor of 2 from the next to obtain a good spread of effects.

The proper number of cycles to perform at each combination of variables in order to obtain stable, reproducible data appears to vary with the operating conditions and depth of discharge used. The best compromise is about 5 cycles, with this number increasing as temperature and depth of discharge decreases and vice versa. Some workers short the cells down on resistors between each group of cycles under a fixed set of variables. However, when this is done, one or two extra cycles are needed each time to attain a reasonably steady operating condition.

If time permits, possible bias that may be introduced because of a particular order in which the tests are first run may be compensated for by repeating some sequences in reverse order and combining the data. Some test plans have addressed this potential problem by carrying out sequences in random order. The relative merits of these different approaches are not apparent from data available.

The literature has reported only a few parametric test programs. Two of these were relative to a low-Earth orbit, one involving SAFT-America 6-Ah cells (Reference 189), and the other involving General Electric 50-Ah cells (Reference 38). A third set of tests was more general and involved Eagle-Picher 3-Ah cells (Reference 63).

6.6.2 Heat-Generation Measurement

If the necessary data on cell heat generation under certain conditions are not available and there is reluctance to use general equations for calculating heat effects such as those given in Section 3, actual measurements may be necessary. This step should not be taken lightly, however, because useful and reliable cell heat-rate measurements are very difficult to obtain, particularly those that relate heat rate to varying operating conditions.

Gross (Reference 190) discussed the various methods of heat measurement that apply to battery cells and reviewed the literature through 1968, but he did not include experimental details. Although calorimetric methods have been used most often, they suffer from inherently large thermal mass and, hence, slow response. Reference 71 describes an elegant method involving low-mass heat meters with negligible heat capacity outside the cell that was used to measure essentially instantaneous heat-generation rates in a 50-Ah cell. The results of this study agree well with values calculated from equation 16 in Section 3.

SECTION 7 BATTERY SYSTEM DEFINITION

7.1 INTRODUCTION

This section shifts attention from the device level—the battery cell—to the next higher level of organization. As discussed in Section 3, the term “battery system” represents the battery and certain auxiliary components. The auxiliaries include elements required for charge and discharge control, cell or battery protection, and battery temperature control. They act individually and collectively to establish electrical and thermal interfaces between the battery component and the rest of the spacecraft. However, a battery system that includes these auxiliaries is only part of the electric power system of the spacecraft, although the selection of its configuration may be the most influential decision concerning spacecraft power-system physical and performance characteristics. This section identifies some of the factors that influence the development of a conceptual design of a battery system. Much of the material is presented from the viewpoint of the electric power-system engineer and is meant to serve as background for the detailed discussions of battery-system design principles presented in Section 8.

This section begins with a review of considerations that influence the design of spacecraft electric power systems. The material classifies and describes various types of power systems. The treatment emphasizes the significant role of the battery in system design and illustrates the importance of developing the design of a *total* system—one that reflects not only accommodation of spacecraft load requirements but also those of the battery and its associated elements. The final section describes methods of battery temperature control.

7.2 ELECTRIC POWER SYSTEM DESIGN CONSIDERATIONS

This section identifies and describes major considerations that affect the selection and design of spacecraft electric power systems. It contains general material directed primarily toward establishing definitions of the electrical and thermal interfaces between power-system components and other

spacecraft systems. The material is meant to serve as a background for the descriptions of specific types of electric power systems contained in the following section. Although no single comprehensive guide to the design of spacecraft electric power systems is yet available, the literature of the last decade contains many examples of system studies and applications that contain considerable information regarding synthesis procedures, design methodology, optimization techniques, and special mission-peculiar design problems. Many of these references are cited throughout this and the following section; the reader is encouraged to review these documents first-hand.

7.2.1 Orbital Considerations

The characteristics of the spacecraft orbit or trajectory directly influence the configuration and performance of electric power systems and, in particular, the batteries that they contain. The parameters of a circular orbit define, for example, the number and duration of the eclipse period realized on each calendar day, month, or year of the mission and, conversely, the duration of the sunlit periods—quantities that are essential to sizing a battery and its controls. Figure 78 illustrates the relationship between the maximum number of annual eclipses and the flight altitude of circular Earth orbits. Figures 79 and 80 show the variations in eclipse and sunlit periods for circular equatorial orbits of varying altitude. References 191 and 192 summarize formulas for calculating similar quantities for circular or elliptical orbits of other inclination to the planet's Equator. Reference 193 describes procedures for determining interplanetary trajectories—procedures that enable a designer to calculate the output of the solar array and to estimate the external heat input to battery thermal-control surfaces.

7.2.2 Spacecraft Load Considerations

Electric power requirements of spacecraft equipment vary with the nature of the equipment and the kinds of devices that they contain. Equipment that uses discrete devices, particularly transistors, generally requires voltages in the range of 10 to 30 volts. Equipment that employs integrated circuits requires 4 to 15 volts because of the lower breakdown voltages of micro-circuit components. Vacuum tubes, particularly the output and driver stages of traveling-wave-tube (TWT) transmitters, often require a carefully matched set of up to five or six voltages that may vary from approximately 6 volts for a heater to thousands of volts for an anode. Motors typically operate with a 100- to 400-Vac input, either single or three-phase, derived from an inverter or with a 28-Vdc input (for example, stepping motors).

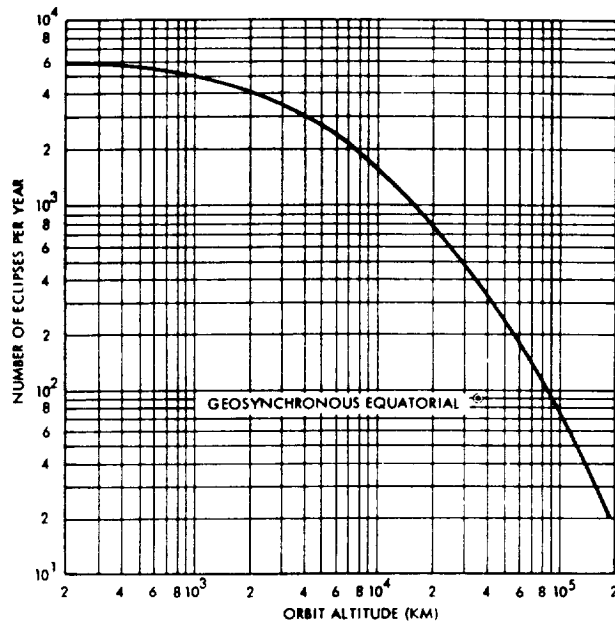


Figure 78. Maximum number of annual satellite eclipses in circular Earth orbits.

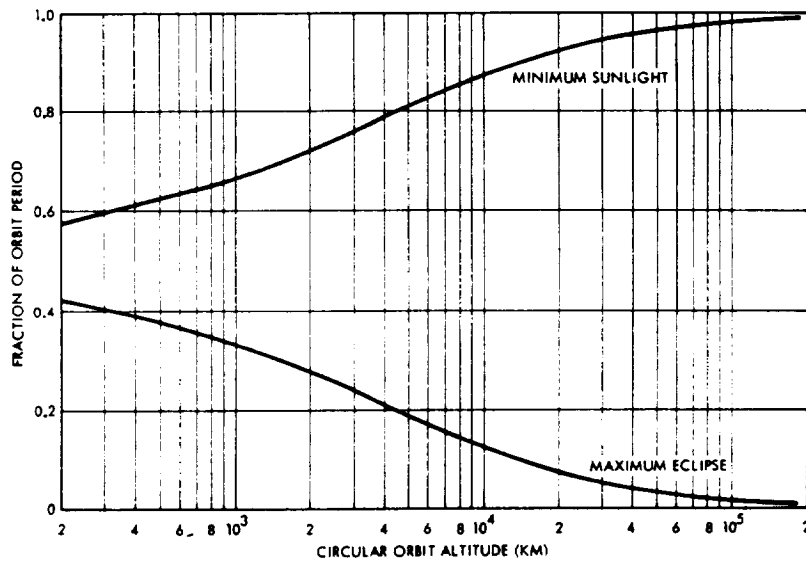


Figure 79. Fractional Sun time of circular equatorial Earth orbits.

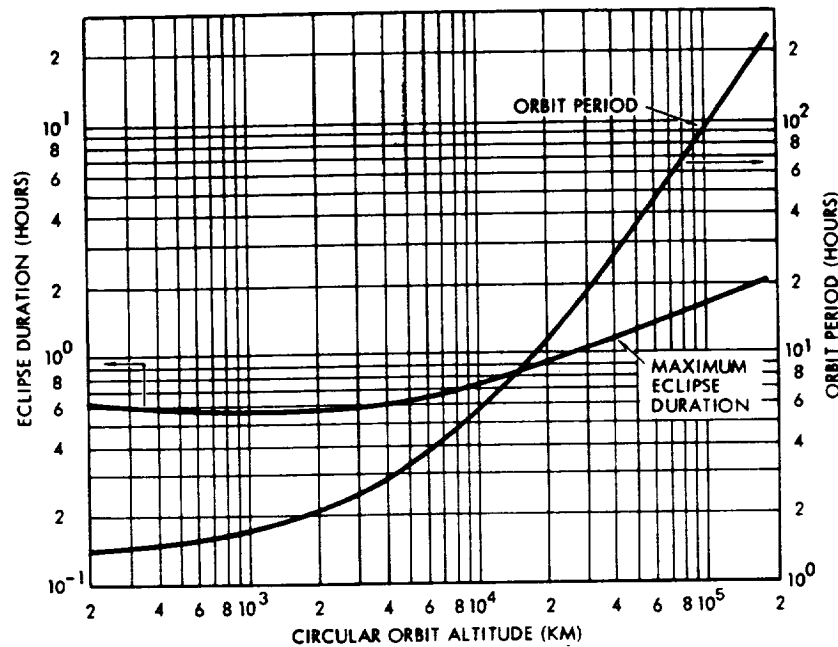


Figure 80. Orbit period and eclipse duration of circular equatorial Earth orbits.

Normally, the quality of power required by most spacecraft equipment is approximately ± 2 to ± 3 percent of nominal input voltage. However, in some cases, notably that of a TWT, voltage regulation requirements can be as severe as ± 0.5 percent, requiring special attention in order to achieve proper equipment operation. Additional problems may be introduced by a requirement for rapid, high-power, pulse trains—a characteristic of radar equipment, some types of guidance equipment, and, at a lower power level, analog-to-digital conversion equipment. If these transients or ripple are permitted to feed directly back to the main power bus, they may interfere with the operation of other equipment that derives power from the same source.

Spacecraft electrical loads are generally of three types: constant current, constant resistance, and constant power. For example, a dissipative series regulator, considered here as a spacecraft load, exhibits a constant-current current-voltage (I-V) characteristic. Heaters used for spacecraft thermal

control are also essentially constant-resistance devices.* Examples of constant-power loads include nondissipative regulators, converters, and inverters.

7.2.3 Electrical Interface Characteristics of the Solar-Cell Array

The I-V characteristics of the solar-cell array can vary considerably because of: (a) the influence of changes in the illumination and temperature of its solar cells, (b) the effect of degradations produced by extended exposure to the radiation and other natural environments of space, and (c) the loss of array output capability resulting from random open-circuit failures within the solar-cell circuitry (Reference 194). The effect of changes in illumination and temperature have the greatest impact. For example, a cold solar-cell-array exiting eclipse in a geosynchronous equatorial orbit will have an open-circuit voltage approximately twice that obtained at steady-state operating temperatures under full illumination. This means that, in the absence of power-source voltage regulation, the input voltage of equipment connected directly to the solar array will be in the vicinity of the open-circuit voltage of the solar-cell array during the early part of the thermal transient interval. Unless the equipment is designed to withstand this voltage stress, its performance will be affected, and its reliability will be reduced.

7.2.4 Electrical and Thermal Interface Considerations for Nickel-Cadmium Batteries

The normal I-V characteristics of nickel-cadmium cells are primarily dependent on cell temperature, state of charge, and prior service history. These dependencies have been illustrated and discussed in Sections 3 and 4. Note that batteries are normally charged at a voltage about 20 to 40 percent above their discharge levels. Thus, if the batteries are connected directly to the power bus during both charge and discharge, they effectively determine the degree of bus voltage regulation. To obtain better regulation, it is necessary to either disconnect the batteries from the bus when they are charged or place a voltage conversion element in series between the batteries and the power bus during either the charge or the discharge periods. Although many battery systems have contained discharge converter/regulators, it is nevertheless desirable to avoid introducing components that contribute power

*The thermal power dissipated by a resistive heater is equivalent to the electrical power, $P = V^2/R$. Thus, the power variation is directly proportional to the square of the voltage variation. This fact should be considered if heaters are connected to an unregulated-voltage power bus.

losses during discharge or that must be capable of passing large currents. Such conversion elements tend to increase the size of the batteries and to cause unwanted thermal dissipations. The electrical interface between a battery and the electric power system is further discussed in Section 7.3 and developed fully in Section 8.

The thermal interface between batteries and other spacecraft systems is of great importance to battery-system design. A battery, unlike most other spacecraft components, is usually a variable source of thermal dissipation throughout an orbit. Section 3 describes the thermal behavior of nickel-cadmium cells, as well as the effect of temperature on long-term cyclical behavior. However, this is only one part of the cause-and-effect relationship that must be considered during the battery-system synthesis process. Battery temperature characteristics are ultimately determined by the selection of the method of temperature control, which, in turn, affects battery-system reliability and may impact the cost and weight of other spacecraft systems and components. It is now generally accepted that, regardless of orbit type, long service life is obtained by maintaining average battery temperature in the region near and above 0°C. In some short-term missions, this requirement may be relaxed without risk to the mission, particularly when conservative discharge/charge duty cycles are used and adequate levels of charge monitoring and control are provided. For longer missions, it is likely that future battery systems will be designed to provide battery operation and in-orbit storage at reduced temperatures. This requirement may cause an increase in battery radiator size or in the size of the solar array because of additional battery-heater power requirements. In certain instances, the requirement may lead to the application of active thermal-control devices, such as heat pipes or thermal louvers. Section 7.4 contains a general review of methods of battery thermal design and control; Section 8 describes the role of charge control in battery-system electrical and thermal design.

7.2.5 Electric Power-System Regulation and Control

The variable I-V characteristics of the power sources make them generally incompatible with spacecraft equipment unless some means of source-load matching is introduced. In the majority of cases, the matching is provided by the converter/regulators or inverter/regulators that are usually required to transform power from the voltage of the primary bus to voltage levels required by the equipment. In the minority of cases, the equipment may utilize power at or near the nominal primary bus-voltage level. In such instances, source-load matching is often achieved by solar-array regulation.

battery-discharge control or regulation, battery-charge control or regulation, or a combination of these methods. The following paragraphs describe significant characteristics of the various regulation and conversion components. (See also References 195 and 196.) Section 7.3 illustrates how they are typically combined into practical electric power-system configurations.

7.2.5.1 Series Dissipative Regulator

The series dissipative regulator shown in figure 81 consists of a voltage reference, a comparator, and a variable resistance device such as a transistor. The output voltage is compared to the reference to produce an amplified error signal that is used to change the equivalent resistance of the linear-control element in the direction and by an amount sufficient to eliminate the error. The series dissipative regulator exhibits constant-current electrical input characteristics for any particular value of output power. It provides a stable, low-impedance output bus that is capable of high-speed response to changes in either input or output. Thus, the regulator is useful in filtering out electrical noise and has sometimes been called an "active filter." However, the requirement that the input voltage always exceed the output voltage plus the saturated voltage drop across the regulating transistor

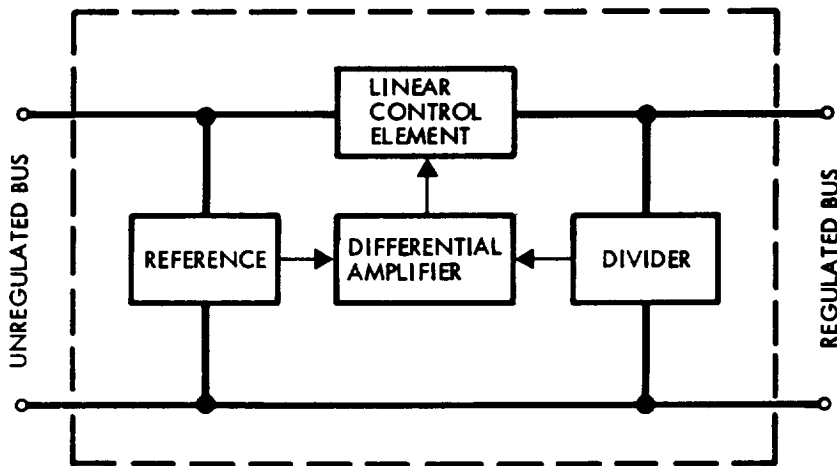


Figure 81. Block diagram of a series dissipative regulator.

means that power is dissipated as heat in the transistor's junction. With unregulated input voltage, this dissipation can be considerable. Nonetheless, when circuit simplicity, low-noise generation, and low cost are desired

characteristics, the series dissipative regulator is often selected, particularly as a means of obtaining voltage regulation at the input to individual loads.

7.2.5.2 Series Switching Regulator

The series switching regulator shown in figure 82 consists of an oscillator-driven semiconductor switch (or switches), a voltage reference, a comparator, a modulator that varies the switch off-time/on-time ratio, and input and output filters. It can be designed in several forms depending on the relationship of input voltage (V_i) to output voltage (V_o):

- Voltage-buck regulator: $|V_i| > |V_o|$
- Voltage-boost regulator: $|V_i| < |V_o|$
- Voltage-buck/boost regulator: $|V_i| \geq |V_o|$ or $|V_i| \leq |V_o|$

The series switching regulator exhibits essentially constant-power electrical input characteristics, subject only to the slight influence of changes in input voltage on its efficiency.

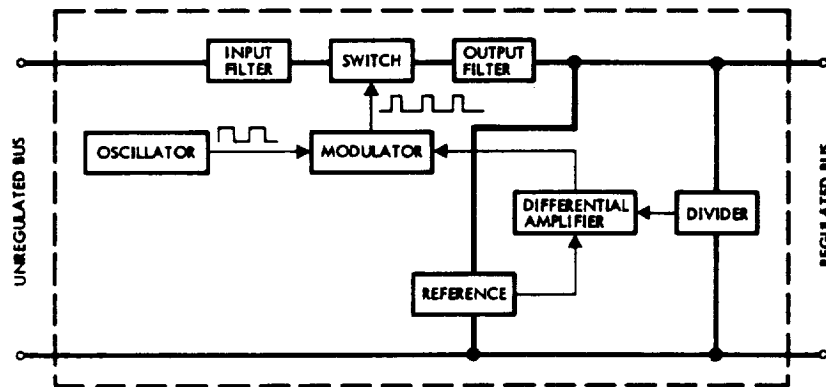


Figure 82. Block diagram of a series switching regulator.

A switching regulator usually operates at higher efficiency than a series dissipative regulator, and, consequently, it has lower and more constant heat dissipation. The efficiency, η , of any switching regulator is

$$\eta = \frac{P_o}{P_o + P_e} \quad (26)$$

in which P_e is the sum of the power losses within the regulator, and P_o is the output power delivered at regulated output voltage, V_o . Reference 196 contains examples of the efficiency characteristics of each type of regulator as a function of input/output voltage ratio for a particular load requirement. Reference 197 displays a general method for calculating the efficiency of a buck-type regulator that can be extended to include the other forms.

Depending on input and output filter design, a switching regulator can provide line and load regulation in the range of 0.1 to 1 percent. A tradeoff is possible between regulation and transient response characteristics. Reference 195 contains a general discussion of the electromagnetic control (EMC) aspects of switching regulator design.

7.2.5.3 Shunt Regulators and Limiters

The shunt regulator is normally used either to limit the voltage of a solar-cell array or to regulate its output voltage. In either case, it is a sink for excess solar-cell array power—power that varies considerably throughout the mission. The shunt regulator/limiter can be designed in several forms:

- Full linear dissipative shunt regulator
- Sequentially controlled full or partial linear dissipative shunt regulator
- Partial linear dissipative shunt regulator
- Switching shunt regulator
- Digital shunt regulator

Dissipative shunt regulators and limiters have been incorporated into most spacecraft electric power systems because of their simplicity and inherent high reliability. However, because they must be capable of handling large amounts of power, they tend to impose a considerable burden on the spacecraft's thermal-control system. Recently developed alternative forms offer reduced dissipation characteristics.

Figure 83 shows a simplified circuit diagram of a conventional full-shunt regulator and how the dissipation is divided between the active control element and the shunt resistor. Maximum transistor dissipation equals $P_{sh}/4$ and occurs when one-half of the rated shunt power is being dissipated. (In this discussion and those that follow, consideration of control-circuit losses has been neglected.)

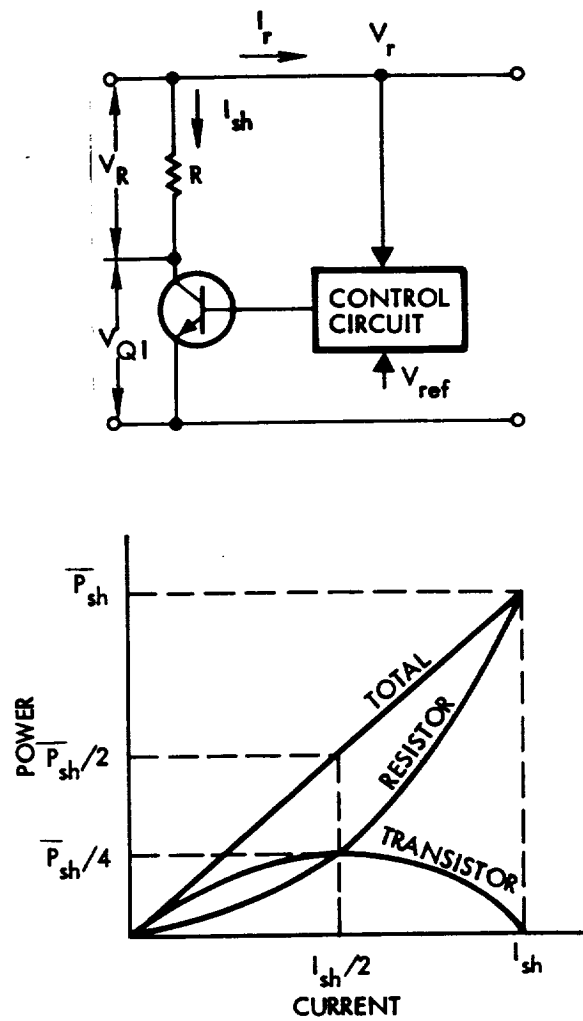


Figure 83. Full dissipative shunt-regulator circuit and performance diagrams.

Figure 84 illustrates how transistor dissipation can be reduced by controlled sequencing of shunt segments in a multiple-segment configuration (Reference 198). For the case shown, each shunt segment is in one of three states: (a) turned completely off; (b) controlled to operate in the linear region; and (c) turned completely on. The maximum current in each segment of a sequenced n -segment regulator is I_{sh}/n . The maximum transistor dissipation occurs with a segment current of $I_{sh}/2n$ and is equal to $P_{sh}/4n$.

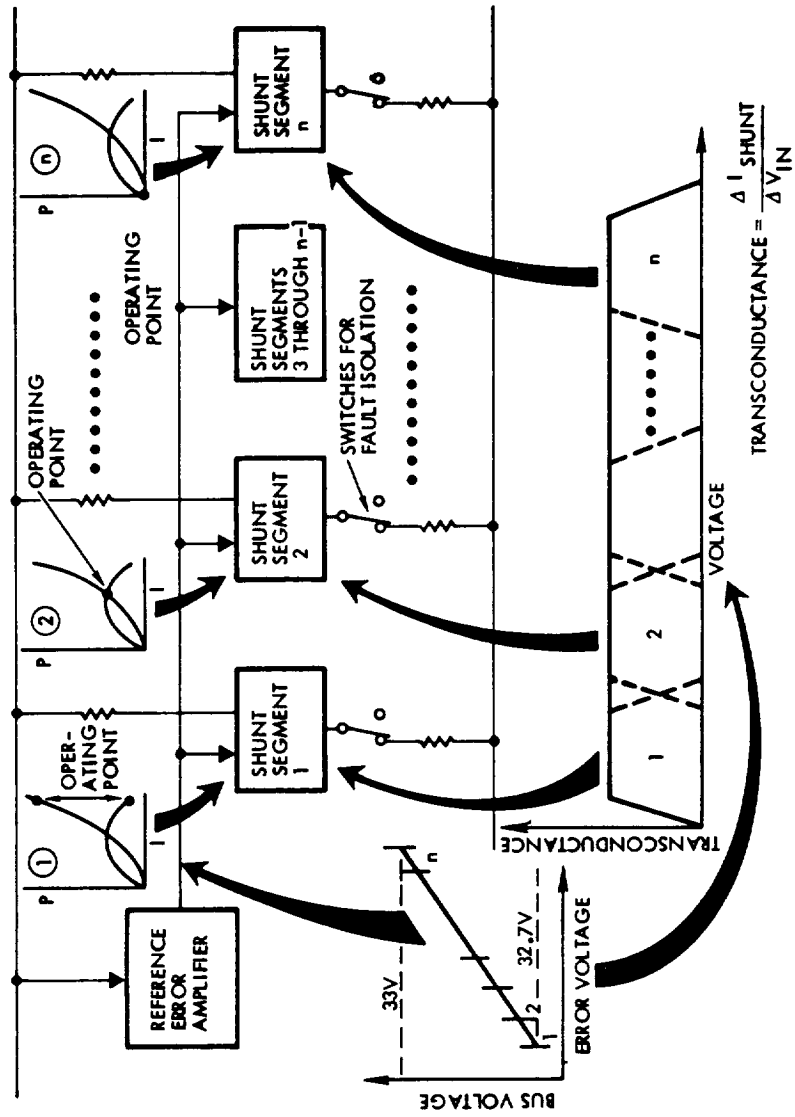


Figure 84. Sequentially controlled full linear dissipative shunt-regulator operation.

The fixed resistor, R , and the variable resistance represented by $Q1$ in figure 83 actually form the lower resistive element of a voltage-divider network. The upper resistive element is the source impedance of the solar-cell array. If a low-impedance source were substituted for the solar-cell array, a fixed series resistor of sufficient size would have to be added to the circuit. The regulator would then become a true shunt regulator of the type often used in other applications for controlling conducted electromagnetic interference on power lines (Reference 195).

Figure 85 is a simplified circuit diagram of a partial dissipative shunt regulator/limiter. The solar-cell array is divided into upper and lower sections with a control transistor placed in parallel with the lower section. The partial shunt regulator thus acts as a linear voltage regulator. With this configuration, the highest voltage at which the upper section can operate is $V_r - V_1$, whereas the specified minimum value of V_{CE} for the control transistor as it approaches saturation is V_1 . Accordingly, the solar-cell array tap point is determined primarily by the I-V characteristics of the array when it is illuminated as the characteristics vary from minimum temperature conditions at beginning of life to steady-state temperature conditions at end of life. Maximum dissipation occurs in the control transistor

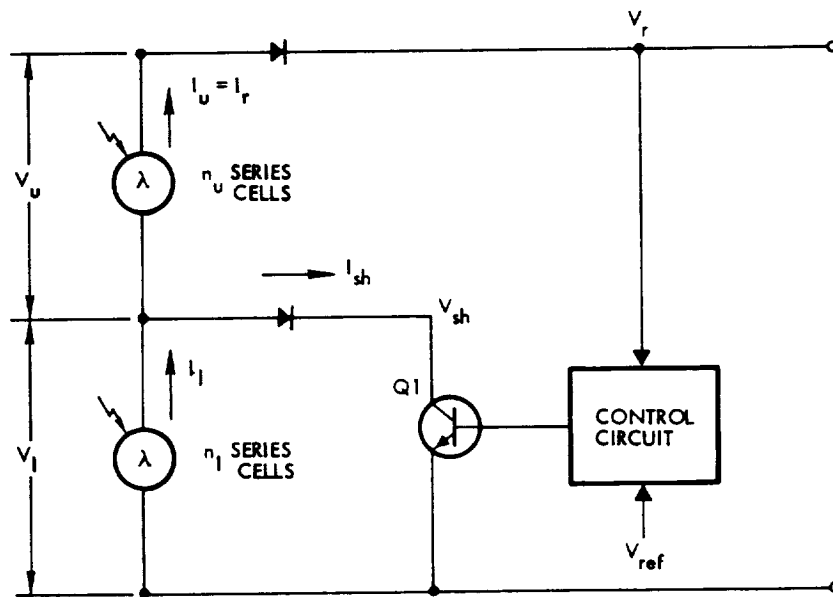


Figure 85. Partial dissipative shunt-regulator/limiter circuit diagram.

when the solar-cell array is unloaded at beginning of life. Nekrasov has outlined a procedure for designing linear partial shunt regulators (Reference 199).

It is sometimes desirable to plot P_{sh} as a function of I_{sh} for the partial shunt regulator in a manner similar to the graph shown in figure 83. This is difficult to accomplish by analytical procedures because of the exponential nature of the solar-cell I-V characteristic curve. Instead, graphical techniques are usually used to measure I_{sh} , as shown in figure 86a for a configuration with a midpoint tap. The shaded area in figure 86a represents P_{sh} . By comparison, the shaded area in figure 86b, a similar graph for a full linear shunt regulator drawn to the same scale, is greater.

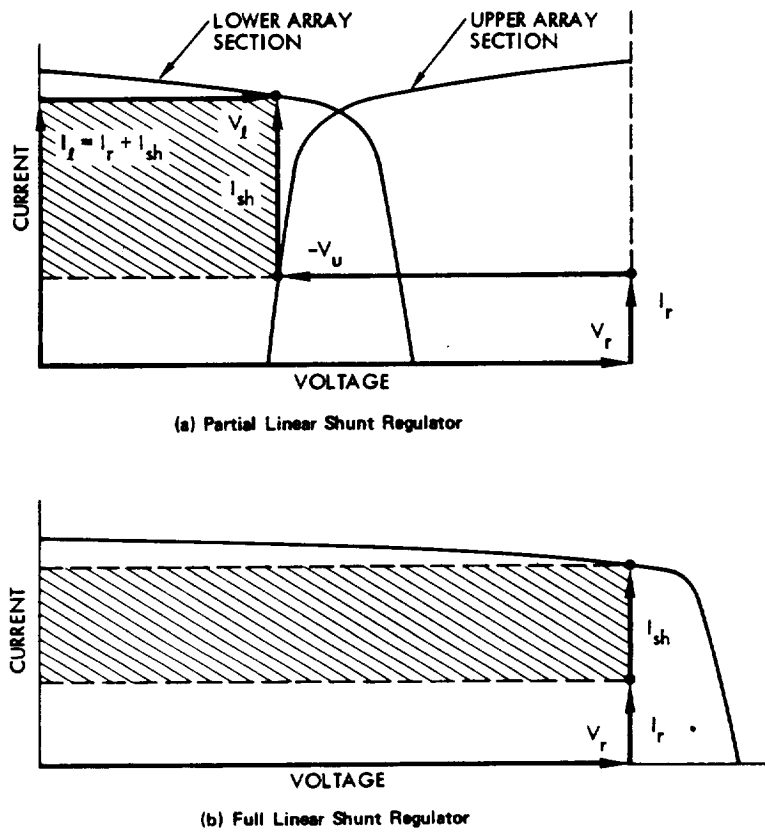


Figure 86. Comparative performances of partial and full linear shunt regulators.

Unlike the full shunt regulator, the partial shunt regulator does not have a collector resistor in series with the control transistor. In the absence of this current-limiting device, it is common practice to make Q1 in figure 85 quadredundant to protect against a collector-to-emitter short circuit. This will reduce the dissipation in each transistor during normal operation but increase the weight of the regulator because the size of each transistor and its heat sinking in the quadredundant circuit is identical to the single control transistor considered previously.

In general, the advantages of dissipative shunt-regulator limiters (both full and partial) are that: (a) essentially no loss of power occurs that otherwise can be utilized by the spacecraft loads or for battery charging, and (b) they provide rapid response to line and load transients. Other shunt-regulator concepts have been investigated in an effort to obtain improved thermal-dissipation characteristics without sacrificing these advantages. A switching shunt regulator can be designed to operate at efficiencies comparable to those of series switching regulators. However, it is relatively more complex than a comparable dissipative regulator, its transient response is poorer, and it tends to be heavier. For these reasons, the switching shunt regulator has not been used. Digital shunt regulators have been examined for high power applications. In concept, they are similar to the sequenced full linear shunt dissipator discussed previously, except that each segment contains only a transistor switch. The switch is connected in parallel across an array segment and is either on or off, depending on the error-sensing and digital-control circuitry. When the switch is on, it is saturated (low dissipation) and effectively shorts out the array segment. An alternative version of this regulator places the switch in series with the array segment; when the switch is open, the array segment is open-circuited. In practice, the digital shunt regulator is augmented with a small dissipative shunt regulator to eliminate bus ripple introduced by the full-on/full-off mode of operation.

7.2.5.4 Power Converters and Inverters

When there are requirements for ac voltages or for dc voltages that differ from that of the primary power bus, it becomes necessary to add some form of power-conversion equipment to the electric power system. An inverter is a dc-to-ac component, and a converter is a dc-to-dc component. It is sometimes convenient to also define a converter as an inverter to which output rectification and filtering has been added.

It is beyond the scope of this discussion to consider in detail the many types of converter and inverter circuits. References 200 and 201 contain

C-4

useful background material for further study. References 202 through 205 describe particular converter and inverter circuits. In particular, Reference 196 describes four commonly used converters and presents calculated values of mass and efficiency for each as a function of output power and modulation frequency. Reference 196 also outlines a method for refining the estimate of efficiency for a typical preregulated converter in terms of output voltage level changes and the incorporation of multiple outputs of differing voltage and power level.

7.3 TYPES OF ELECTRIC POWER SYSTEMS

In generalized form, a spacecraft electric power system is composed of a power source, a power-source controller, a battery system that includes both charge and discharge controls, and combinations of line regulators, converters, and inverters. This discussion assumes that the power source is a solar-cell array, although the configurations described may also accommodate other types of power sources, such as a radioisotope thermoelectric generator (RTG). It is convenient to classify electric power systems by a common characteristic or property. One widely used method is based on the selection of the elements, either series or shunt, used for power-source control. This classification scheme sometimes includes an identification of whether or not the power-source control element is capable of tracking the maximum power-operating point of the source (Reference 206). Another method is based on whether centralized or decentralized power conditioning equipment is used. A third method, which is more informative, categorizes electric power systems by their primary power-bus regulation characteristics. Thus, all spacecraft electric power systems fall within one of the following classes:

- Unregulated-voltage (UV) dc-bus systems
- Limited-voltage (LV) dc-bus systems
- Regulated-voltage (RV) dc-bus systems
- Maximum-power point-tracking (MPT) systems

Another class, regulated ac distribution systems, is not considered here because its systems are not directly compatible with the static energy sources usually found on board spacecraft and are, in fact, usually employed for secondary power distribution and generation. Also, the MPT systems may offer unregulated-, limited-, or regulated-voltage dc buses, depending

on the specific configuration selected. Table 45 lists spacecraft, categorized by primary power-bus regulation characteristics, that represent a wide range of Earth-orbiting missions.

7.3.1 Unregulated-Voltage dc-Bus Systems

Systems included in the unregulated-voltage dc-bus classification exhibit the following general characteristics:

- The primary power bus is usually connected directly to the solar-array bus.
- No active control elements (series or shunt) are incorporated specifically to regulate or limit the voltage of the solar-array bus.
- The batteries are isolated from the primary power bus during a portion of their discharge/charge cycle (usually during charge).
- Spacecraft payloads and most other electrical loads draw power from the primary power bus through power-conversion or power-inversion equipment.

It is worthwhile to consider the implications of the first two items on primary power-bus voltage characteristics. If a battery is connected directly to the bus through a passive bilateral* element (e.g., a resistor), it will provide gross regulation (between ± 10 and ± 20 percent, depending on mission and load conditions) throughout the orbit because of its own discharge/charge characteristics. However, if the battery is disconnected or otherwise isolated from the bus during its period of charge and if no separate means exists for regulating the solar array, the voltage operating point of the system will be determined by the stable intersection points of the solar array and composite load-line $I-V$ characteristics. Under such circumstances, the illumination and temperature characteristics of the array will strongly influence the bus voltage, and bus regulation, in its usual meaning, will all but cease to exist.

The foregoing situation can be tolerated if the equipment connected to the primary power bus is designed to withstand the expected maximum voltage stress, as is the case for at least one major spacecraft project (Reference

*A battery connected to the bus through a diode will regulate the bus if the diode is always forward-biased.

Table 45
Characteristics of Selected Spacecraft

Spacecraft	Design Lifetime (years)	Orbit	Power System Configuration	Primary Voltage (Vdc)	Spacecraft Stabilization	Reference
OAO	1+	LEO	UV	25 to 31.5	Three axis	50
EOGO	1+	EEO	UV	23 to 33	Three axis	207
NTS-1	3 to 5	IEO	UV	24 to 33	GG/Y	208
FLTSATCOM	5	GSEO	UV	24 to 70	Three axis	209
Intelsat-IV	7	GSEO	UV	23.8 to 48	Spin	210
Atmospheric Explorer	1	LHO	LV	-26 to -38	Spin	211
HEAO-B	1	LHO	LV	23 to 33	Three-axis/spin	198
Intelsat-III	5	GSEO	LV	22 to 31	Spin	212
Nimbus-B	1+	LHO	RV	-24.5 ± 0.5	Three-axis	213
NTS-2	3 to 5	HEO	RV	27 ± 1	GG/Y	214
SMS	5	GSEO	RV	29.4 ± 0.2	Spin	215
NATO-III	7	GSEO	RV	29.4 ± 0.2	Spin	216
Telesat	7	GSEO	RV	30.25 ± 0.25	Spin	217
ATS-6	2 to 5	GSEO	RV	30.5 ± 0.6	Three-axis	218
Skylab OWS/AM	0.7+	LEO	MPT	26 to 30	Three-axis	219

Legend: LEO - Low-Earth orbit
 EEO - Elliptical Earth orbit
 IEO - Intermediate Earth orbit
 GSEO - Geosynchronous Earth orbit
 GG/Y - Gravity-gradient stabilized with yaw axis control

209). More often, however, systems in this class will be configured or controlled so as to mitigate the bus-voltage excursion. The following paragraphs describe this type of system.

Figure 87 defines the discharge and charge controls for one of two 22-cell nickel-cadmium batteries contained in the electric power system of a body-stabilized geosynchronous-equatorial-orbit communications satellite. One-half of its flat-panel Sun-tracking solar array provides power to load bus A, and the other half supplies power to load bus B. The following discussion assumes that the bus-tie relay is closed. The system does not contain equipment for solar-array regulation or load-bus regulation.

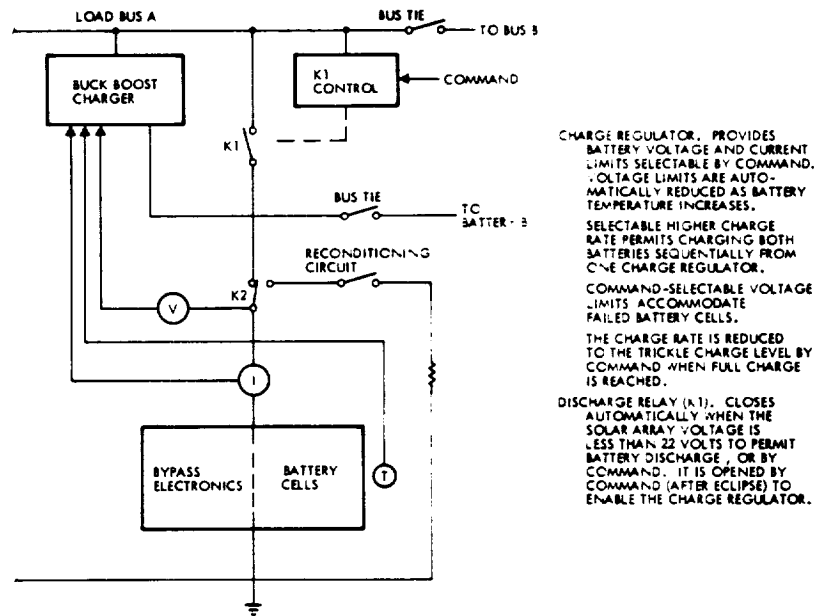


Figure 87. Battery discharge/charge controls.

Relay K1 closes either automatically or by command when the load-bus voltage falls below 22 volts as a result of inadequate array power to support the load, such as upon entry into eclipse. The combined I-V characteristics of the battery and the load establish the load-bus voltage during the discharge period. When the spacecraft exits from an eclipse, the K1 relay is commanded open and the buck/boost battery charger is turned on in controlled sequence. The buck/boost charger accommodates solar-array voltages above and below the battery charge voltage that may occur as a result of

ORIGINAL PAGE IS
OF POOR QUALITY

various combinations of illumination, temperature, degradation, and load. The charger transforms solar-array power not otherwise required by the load to the correct voltage required by the battery for normal current-limited full charge. When the battery voltage reaches one of a family of command-selectable temperature-compensated voltage limits, the charger acts as a voltage regulator to maintain the battery voltage at the limit as the charge current tapers to a lower value. Trickle charge can be initiated by ground command, on which the charger becomes a current regulator.

The operation of the power system is best understood by considering the graphical analyses of each of several important mission conditions. It is convenient to perform the analyses using power-voltage (P-V) characteristic curves because the majority of the load (24 transponders) exhibits constant-power characteristics.

Figure 88 shows the solar-array and spacecraft load P-V curves for end-of-life (EOL) solstice conditions. It is assumed that two transponder failures have occurred to illustrate the compensating effect of thermal-control heaters that are turned on to maintain spacecraft thermal balance. The

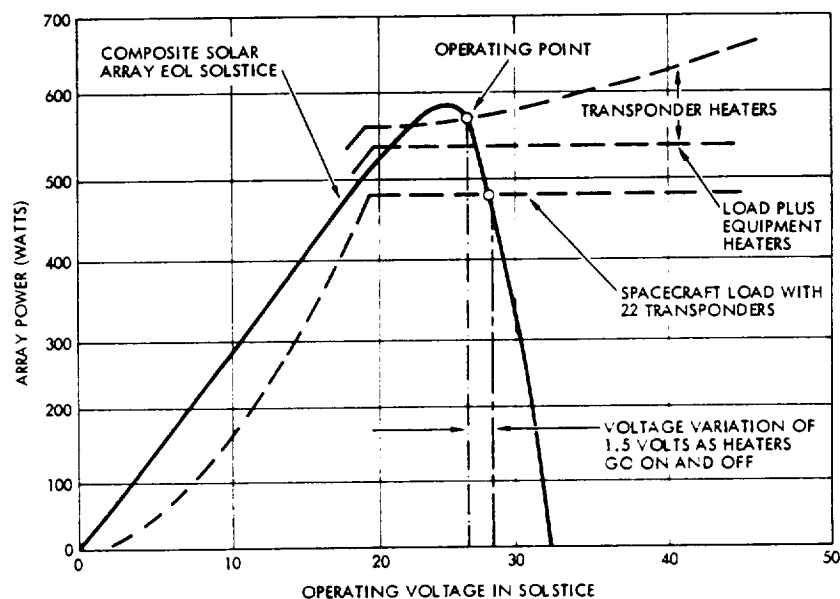


Figure 88. Operating characteristics at end-of-life solstice.

transponder heaters are supplied directly from the unregulated load bus; heaters for other equipment are supplied from a separate regulator and, consequently, appear on the graph as a constant-power increment. With the batteries disconnected from the load bus during sunlight, the stable system-operating point traverses the solar-array P-V curve as shown in figure 88.

As the spacecraft enters an eclipse period during the equinox season, the array power and voltage begin to fall. When the load-bus voltage reaches the 22-volt level, the batteries are automatically connected to the load bus by relay closure and the bus voltage rises to approximately 29 volts. If no cell failures occur, the batteries will discharge to a 24-volt level at the conclusion of the eclipse. As the spacecraft emerges from an eclipse and array power and voltage begin to increase, the batteries are unloaded. Within seconds, the array P-V characteristic will reach point 1 in figure 89. Point 1 lies on

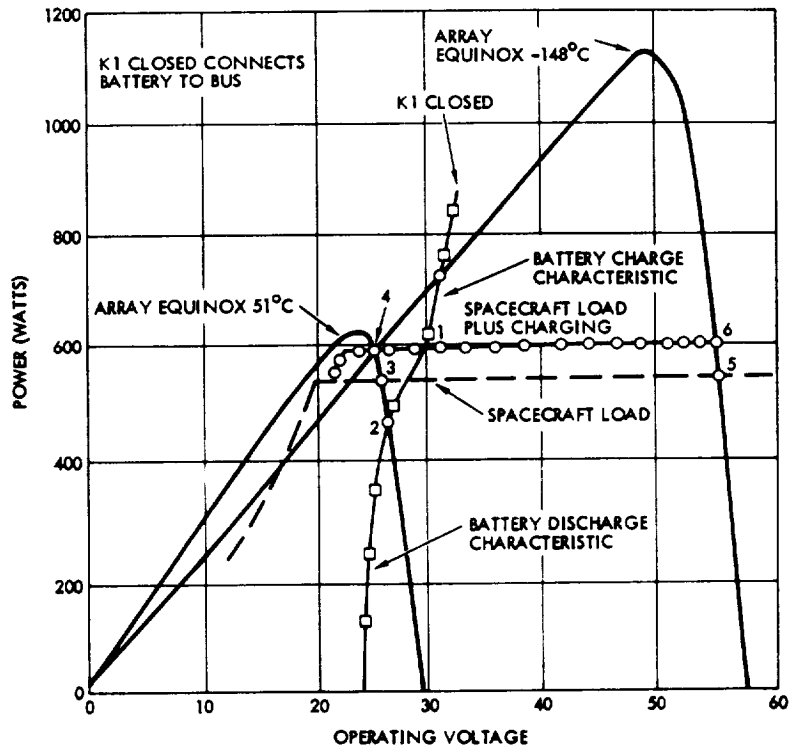


Figure 89. Operating characteristics at equinox under eclipse conditions.

the battery-charge characteristic at approximately 31 volts with the K1 relays closed. When each K1 is opened to remove the batteries from the bus, the load line changes from the battery-characteristic curve to the spacecraft-load characteristic. Thus, early opening of the relays may result in voltage operation between points 3 and 5 before the battery chargers are turned on, and between points 4 and 6 afterwards, as a direct function of solar-array temperature. Figure 90 contains the normal load-bus voltage profile for the equinox-season orbit; the dashed line illustrates the effect of early opening of the K1 relays.

In this system, the buck/boost charger does not significantly affect the operating voltage of the system and could be easily replaced with other types of charge-control circuitry. Maximum values of load-bus voltage are constrained solely by means of system operational control.

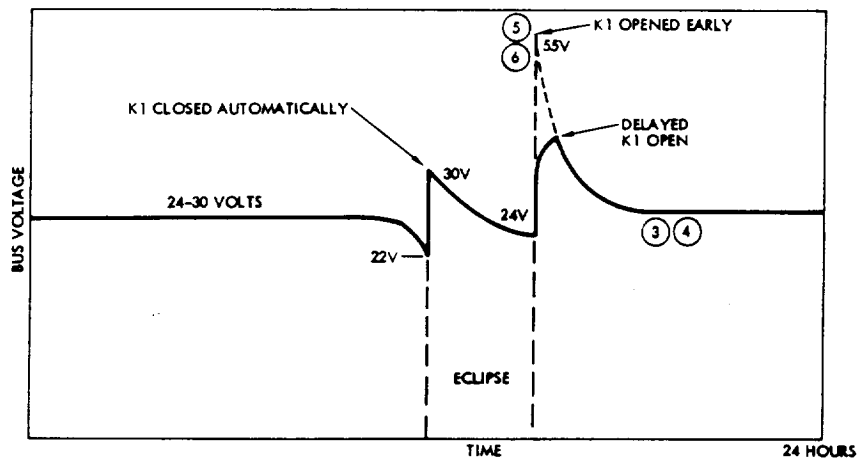


Figure 90. Power-bus voltage characteristics under eclipse conditions.

7.3.2 Limited-Voltage dc-Bus Systems

The majority of spacecraft electric power systems contain some form of equipment for solar-array voltage-limiting because:

- Most missions require autonomous electric power-system operation, which precludes ground control of primary power-bus voltage excursions.

- Much spacecraft equipment **now in use** was designed under policies originally developed for **aircraft equipment** and is therefore meant to obtain its power from a **nominal 28-Vdc** power source.
- Variations in input voltage may affect equipment efficiency with added burdens on the spacecraft thermal-control system.
- It is sometimes possible to utilize the bus-voltage limiter as part of the battery-charge control scheme, thereby obtaining an economical use of circuit parts and a net weight savings over other methods.

An example of the last item is the power-regulator unit system described in Reference 220 and shown in figure 91. It utilizes a series switching regulator to transform power obtained from a solar-array section to the correct voltage required for battery charging. The battery charge bus, which is connected to the load bus through diodes, is thus effectively isolated from solar-array voltage variations. The load bus may also be connected to a separate solar array; however, its voltage is effectively controlled by the characteristics of the batteries as they are charged.

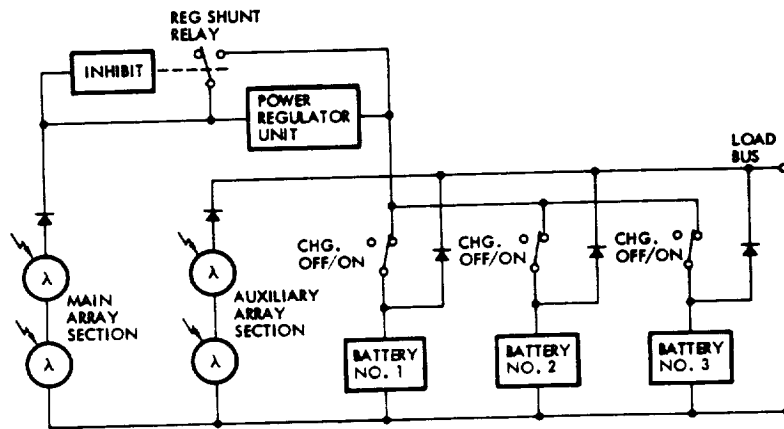


Figure 91. Power-regulator unit system.

Figure 92 shows a simple example of shunt control which provides both bus voltage and battery-charge current control. The single battery is connected directly to the bus through a resistor network. The resistance is used to develop analog signals proportional to both charge and discharge. The signal developed on charge is used to control a full linear shunt dissipator. In this particular flight system (Reference 208), the shunt dissipator was controlled

to limit battery-charge current to one of four commandable charge current limits. The voltage of the load bus is thus established by the battery-charge characteristics; the shunt dissipator does not limit the bus voltage to a particular value.

Graphical analysis techniques can be used to show that the system in figure 92 has a single operating point that is unconditionally stable.

The system shown in figure 92 can be modified to include the ability to charge the battery to a temperature-compensated voltage limit, as well as to selected current limits. It can also be adapted to multiple-battery configurations, but only at the expense of the power lost in the required battery-isolation diodes and with some reduction in overall system reliability. In typical single-battery flight systems, the insertion loss attributable to the current-sensing resistor is about 3 to 5 percent of the battery discharge and charge power.

Other systems have been designed and flown with full, partial, or sequenced full dissipative shunt limiters. Many of these systems have been configured so that the shunt limiters function independently of the battery-charge controls. Regardless of the system configuration selected, the principal reasons for applying solar-array voltage control remain the same.

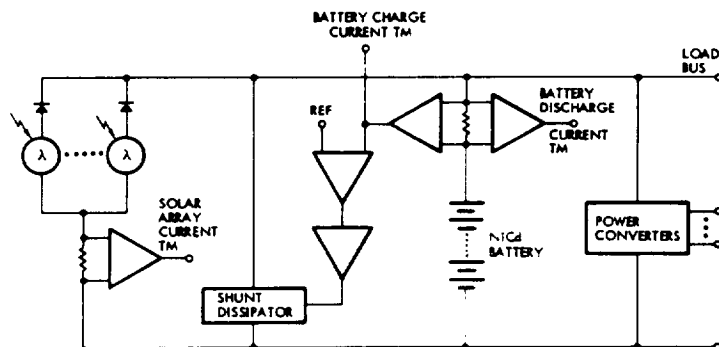


Figure 92. Shunt dissipator control of battery-charge current.

7.3.3 Regulated Voltage dc-Bus Systems

Spacecraft payloads often contain several separate experiment packages—often quite different in function and design. Therefore, to minimize electrical interface problems with, and interactions between, the various equipments, it is sometimes desirable to distribute primary power of known static

and dynamic characteristics. Also, it is sometimes possible to reduce or eliminate preregulation requirements of equipment supplied by the primary power bus if the bus is closely regulated with low-ripple content and if the power is derived from a low-impedance source capable of fast response to load transients.

Bus regulation can be achieved through the use of either series or shunt regulators. Both dissipative and switching series regulators have been applied successfully, although use of the dissipative type has been generally restricted to low-power applications because of semiconductor device limitations* and general difficulties in managing thermal dissipation. Application of either type of series regulator results in a power loss that the solar-array and batteries must accommodate. However, the switching series regulator is capable of tracking the maximum power point of the solar array, which, if accomplished, may result in an increase in energy transfer from the solar array to the loads and batteries during sunlight periods.

Power transfer in regulated-bus systems is improved if a shunt regulator is used for bus control during sunlight periods. However, if this is done, it is necessary to incorporate a separate regulation function for bus control during eclipse periods. This function is always provided by either a buck or boost battery-discharge regulator. If a buck-discharge regulator is used, it is usually configured either as a dissipative regulator or as a switching regulator. If a boost-discharge regulator is selected, it may be either a switching regulator or a converter regulator. Regardless of type of regulator used, the discharge regulator represents a power loss during discharge periods that the battery must accommodate.

The selection of the battery-discharge scheme establishes the allowable range of series cells in the battery. Factors that must be considered in determining the number of series cells are:

- a. Regulated-bus voltage
- b. Minimum allowable voltage drop across the regulator

*The current and power ratings of a power transistor are based on measurements of its thermal characteristics when it is operated as a linear device under steady-state conditions. The application of aerospace part-derating policies always tends to reduce the range of application of any particular device. The application range can be extended by operating the transistor in a switching mode, thereby enabling it to process more average power for the same junction temperature defined as a maximum for linear operation.

- c. Number of allowable battery cell failures if cell bypass circuitry is included in the battery design
- d. Voltage drop across a bypassed cell during discharge under open-circuited, short-circuited, or over-discharged conditions
- e. Lowest value of cell voltage expected during the mission during normal discharge
- f. Highest value of cell open-circuit voltage expected during the mission

Items a through e are used in the analysis to determine the minimum acceptable number of series cells in a battery discharged through a buck-type regulator. The objective of the analysis is to select enough cells to ensure that the minimum required input voltage to the regulator is always maintained or exceeded. Therefore, in the case of item d, it is the maximum value of voltage drop that reduces the terminal voltage of the battery that is of interest.

Items a, b, and f are used in a similar analysis to determine the maximum acceptable number of series cells in a battery discharged through a boost-type regulator. Here again, the objective of the analysis is to ensure regulator operation under specified worst-case conditions.

Certain points should be considered during the process of selecting a battery-discharge-regulator configuration. First is the examination of differences in regulator efficiencies. A buck-type switching regulator is usually 2 to 4 percent more efficient than a boost-type switching regulator; it is 6 to 8 percent more efficient than a boost converter/regulator. The second consideration is the nonlinear relationship between the number of series cells in a battery and their ampere-hour capacity. Specifically, with battery depth of discharge held constant and with the battery discharging into a constant power load,

$$m = - \left(\frac{n}{1+n} \right) \quad (27)$$

where

m = fractional decrease (increase) in the cell ampere-hour capacity

n = fractional increase (decrease) in the number of series cells

Thus, a 25-percent increase in the number of series cells within a battery results in only a 20-percent reduction in cell capacity. If, however, the cell capacity, as well as the depth of discharge, is held constant as the number of series cells increase (or decrease), the power that the battery delivers will increase (or decrease) by the same fractional percentage. This fact means that batteries with buck-type discharge regulators can be adapted to supply late increases in load by adding series cells rather than by respecifying depth of discharge or cell capacity. Because batteries with boost-type discharge regulators are usually sized with the maximum number of series cells permitted by the regulator design, they are somewhat less flexible in accommodating load growth.

In general, the selection of a boost-type discharge regulator implies a buck-type battery-charge controller and vice versa. If a buck-type charge controller is required, it can be either dissipative or switching, and it can be powered either from a separate solar-array section or from the main array. When the charge controller is powered from the main array, it can be used to regulate the primary power bus. This means that near end-of-life, when the solar array has degraded to a point at which it can only support the daytime spacecraft loads and provide charge to the batteries, the shunt regulator is turned off. By comparison, systems that utilize separate battery-charge arrays depend on having some small amount of excess power available at end-of-mission to ensure operation of the shunt regulator and, therefore, maintenance of bus voltage regulation.

If battery-charge power is derived from the main solar array, the compatibility between the number of series cells in the battery and the selected charge controller configuration must be verified. The analysis procedure is similar to that discussed earlier for the discharge regulator. It is not unusual for the analyses of the charge and discharge paths to be repeated one or more times until the proper combination of number of series cells, cell capacity, depth of discharge, and number of separate batteries is reached for the system under consideration.

Thus far, rationale has been given for designing shunt-regulated electric power systems* without discussing specific examples. An interesting aspect of their design, which is beyond the scope of this book, is the method used to sequence and control the operation of the regulators so that the primary

*These systems are sometimes referred to as Direct Energy Transfer (DET) Systems because the solar array is directly connected to the loads.

power bus is regulated continuously. Detailed descriptions of several bread-board and flight systems appear in References 216, 218, 221, and 222.

7.3.4 Maximum-Power Point-Tracking Systems

Maximum-power point-tracking systems contain series or shunt switching regulators that are capable of forcing system operation at the voltage of the solar-array maximum-power point under conditions of high spacecraft and battery-load demand. This type of operation is desirable when:

- a. Additional energy is available from the solar array during periods of thermal transience (References 223 and 224)
- b. Solar-array illumination and temperature characteristics change markedly throughout the mission
- c. The electric power system is required to support high-power loads (Reference 219)

The conditions required for item a usually occur only in low-altitude orbits with Sun-oriented flat-panel solar arrays of rather heavy construction. The duration of temperature rise of such arrays, from eclipse-exit to steady-state conditions, is a significant fraction of the sunlit period. While the array is illuminated and cold, it can generate excess power that, if averaged over the sunlit period, is approximately equal to a 5- to 10-percent increase in average solar-array power. However, this improvement is less pronounced when lightweight solar arrays are used, and it is not realized in geosynchronous orbits because of the extended duration of the sunlight period. In general, any array-power improvement is offset to some degree by the losses associated with the tracking equipment.

The conditions of item b are characteristic of solar-powered interplanetary missions. Reference 225 defines five typical missions and shows how conventional regulators can be combined into system configurations that can adapt to large changes in solar-array I-V characteristics. Reference 226 summarizes an evaluation of several candidate approaches to maximum-power point-tracking for spacecraft with solar-electric propulsion systems.

As item c suggests, electric power systems designed to deliver large amounts of power gain several advantages from the capability of tracking the maximum-power point of the solar array. One example concerns the fact that

high power implies large solar-array area. Application of the tracking concept helps to minimize array area with resulting savings in cost and helps to reduce the effects of solar pressure torques on spacecraft attitude control. Another advantage is that, when peak solar-array power is not required, the tracking regulators act as source-load matching elements, thereby eliminating the need for shunt dissipators. Detailed descriptions of several types of maximum-power point-tracking systems appear in References 227 through 230.

7.4 METHODS OF TEMPERATURE CONTROL

The sensitivity of battery electrical parameters and long-term performance characteristics to temperature is discussed in other sections. It is emphasized that the full operational capability of a sealed-cell nickel-cadmium battery cannot be realized unless its temperature is maintained near and above 0°C during periods of both cycling and long-term storage. This section discusses the problems and solutions associated with achieving this degree of thermal control. In the early years of the space program, a battery system often did not include dedicated thermal-control hardware. Battery temperature control was obtained by standard, usually passive, thermal-control techniques applied as if the battery were but another component with variable dissipation characteristics. Battery temperatures generally ranged from 15 to 35°C, which was adequate for missions of that short duration requiring only shallow battery discharges. Later, as design requirements became more demanding, it became necessary to reduce both the level and the total range of temperature variation. This was accomplished by using charge-control techniques that limited dissipation during overcharge, by incorporating special provisions for battery temperature control, and by reducing thermal gradients within the battery as a design requirement. In recent years, these efforts have resulted in the operation of most batteries in space at temperatures of about 10 to 25°C. Certain other batteries have been operated at between 0 and 15°C to obtain extended service life and/or performance at greater depths of discharge.

The main purpose of a battery thermal-control system is to maintain the temperature of the cell electrodes to within specified limits. However, it is usually impractical to define temperature requirements at the electrode stack level. Instead, separate analyses and tests are performed to establish the thermophysical characteristics of particular cells (e.g., specific heat and

thermal conductivity),* to identify major heat-transfer paths within the cells, and to estimate temperature gradients along the paths. With a cell's thermal behavior thus characterized, the cell-case temperature can be calculated for specific conditions of internal heat generation and external heat sinking. The following section describes the general procedure for mapping thermal gradients within the cell and shows how these procedures may be extended to include evaluation of the heat-transfer path from the cell case to the battery heat sink. Subsequent sections consider the battery as a component whose temperature must be controlled within relatively narrow limits and at lower levels than other spacecraft equipment. Passive and active methods of thermal control are described with emphasis placed on the development of specific configurations of battery heat sinks. Fluid-loop cold-plate design is not discussed because this method of component cooling is usually suggested by other spacecraft requirements, and, because of its complexity, is usually not a candidate as a self-contained battery temperature-control auxiliary. However, further information on fluid-loop control appears in References 94 and 231.

7.4.1 Cell and Battery Thermal Modeling

The predominant heat-transfer mode within a cell or battery is conduction. The general heat-conduction equation that governs the temperature distribution and heat flow in a solid with uniform physical properties and an internal heat source is

$$\frac{\partial^2 T}{\partial x^2} + \frac{\partial^2 T}{\partial y^2} + \frac{\partial^2 T}{\partial z^2} + \frac{q}{k} = \frac{1}{a} \frac{\partial T}{\partial t} \quad (28)$$

where

T = absolute temperature

x, y, z = Cartesian coordinates

q = rate of heat generation per unit volume

k = thermal conductivity

a = thermal diffusivity ($k/C_p\rho$)

*See Section 3.2 for a summary of cell thermophysical properties.

C_p = specific heat

ρ = density

t = time

If the system contains no heat sources, equation 28 reduces to the *Fourier equation*,

$$\frac{\partial^2 T}{\partial x^2} + \frac{\partial^2 T}{\partial y^2} + \frac{\partial^2 T}{\partial z^2} = \frac{1}{a} \frac{\partial T}{\partial t} \quad (29)$$

If the system is at steady state but heat sources are present, equation 29 becomes the *Poisson equation*,

$$\frac{\partial^2 T}{\partial x^2} + \frac{\partial^2 T}{\partial y^2} + \frac{\partial^2 T}{\partial z^2} + \frac{q}{k} = 0 \quad (30)$$

In the steady state, the temperature distribution in a body containing no heat sources must satisfy the *Laplace equation*,

$$\frac{\partial^2 T}{\partial x^2} + \frac{\partial^2 T}{\partial y^2} + \frac{\partial^2 T}{\partial z^2} = 0 \quad (31)$$

For the one-dimensional case, equation 31 becomes $d^2T/dx^2 = 0$, which yields, after integration, $dT/dx = \text{constant}$. This result is consistent with the basic relation for heat transfer by conduction proposed by Fourier

$$q = -kS \frac{dT}{dx} \quad (32)$$

where

q = rate of heat flow by conduction or \dot{Q}_T

S = area of the section through which the heat flows, taken perpendicular to the direction of heat flow

The sign convention indicates a positive heat flow with a negative temperature gradient.

The second-order partial differential equations 28 through 31 are all linear in that each is of the first degree in independent variable T and its derivatives. Exact solutions are therefore possible if, in general, the boundary conditions are also linear. Solutions have been obtained for simple shapes such as cylinders, spheres, and ellipsoids after transformation of the equations to the corresponding coordinate system. However, with shapes of greater complexity and with dependency on time (transient analysis conditions), the equations are usually too complex for direct closed-form solution, and approximation techniques must be used. Practical methods have been developed on the basis of graphic, numerical, and analog approaches. A concise overview, a comparison of these methods, and a pertinent bibliography appear in Reference 232.

One particularly useful approximation method is based on the analogy between thermal and electrical conduction. A network of thermal-conduction paths may thus be represented by an electrical network containing resistors and capacitors. The network is driven by ideal voltage and current sources that correspond to temperature gradients and heat flows, respectively.

Table 46 defines the thermal/electrical analogies. It follows that, to solve any heat-conduction problem by this method, the following steps apply:

- a. Draw a mechanical schematic diagram of the heat-transfer problem.
- b. Assign and number nodes for the heat source, the heat sink, and each conductive element between the source and the sink. Parallel heat-conduction paths may exist between the source and sink. A single conductive body may be partitioned into small volumes with a node representing the temperature at the geometric center of the volume. Adjacent volumes must then transfer heat by conduction through a common cross-sectional area. The thermal conductance of a contact joint between two bodies is modeled by assigning a node to each opposing surface of the joint.
- c. Draw a thermal schematic diagram for the problem by connecting thermal resistances and capacitances between each node as appropriate. If the thermal capacitance of a path is small, it may sometimes be neglected in favor of simplicity or combined with other capacitances within the network.

Table 46
Analogous Terms for Electric and Thermal Networks

Parameter	Electrical		Thermal	
	Parameter Symbol	SI Unit	Parameter Symbol	SI Unit
Potential (voltage or temperature)	V	J/A·s	T	K
Charge (quantity of energy)	Q	A·s	Q_T	J
Conductivity	γ	$A^2 \cdot s / J \cdot m$	k	$J/K \cdot m \cdot s$
Resistance	R	$J/A^2 \cdot s$	$R_T (= \Delta T / \dot{Q}_T = x/kS)$	$K \cdot s / J$
Capacitance	C	$A^2 \cdot s^2 / J$	$C_T (= \Delta Q_T / \Delta T)$	J/K
Flux (charge or heat-flow rate)	I	A	$\dot{Q}_T (= q)$	J/s
Length or distance	L	m	x, y, or z	m
Area	s	m^2	S	m^2
Time	t	s	t	s
Time constant	$\tau (=RC)$	s	$\tau_T (= R_T C_T)$	s

- d. Draw an equivalent electrical schematic diagram for the thermal network. Include voltage sources necessary for establishing initial conditions analogous to initial temperature, current sources to model the flow of heat, and a common electrical ground point representing the heat sink.
- e. Simplify the electrical network by combining the resistances and capacitances in accordance with standard formulas for adding circuit elements in series or parallel.
- f. Write and solve network equations using Kirchhoff's current and voltage laws. If the network contains capacitors, the equations will be differential equations with solutions given in terms of the voltages across lumped capacitances.
- g. Determine the voltages (temperatures) at other nodes in the network by using the solutions of step f. This is accomplished by retracing the steps taken earlier to simplify the network.

Figure 93 shows a two-node thermal network and its electrical analog. In the latter network, all switches are shown in their position at $t < 0$. At $t = 0$, all switches are switched simultaneously to their opposite state. It is seen that the voltage source is used simply to establish the initial condition for the capacitor. The constant-current source and its shunt switch represent the application of heat to the network as a step function at $t = 0$. The differential equation of the network,

$$C \frac{dv}{dt} + \frac{1}{R} v = i \quad (33)$$

is obtained using Kirchhoff's current law. This equation is of the general first-order form.

$$\tau \dot{v} + v = v_f \quad (34)$$

where v_f is the forcing function. Reference 233 contains its solutions for various forcing functions, which can be quickly determined by Laplace transform methods. However, solution for the case at hand is quite straightforward.

The steady-state voltage across nodes 1 and 2, after the capacitor has become fully charged, is $v_f = IR$. The natural component of voltage is

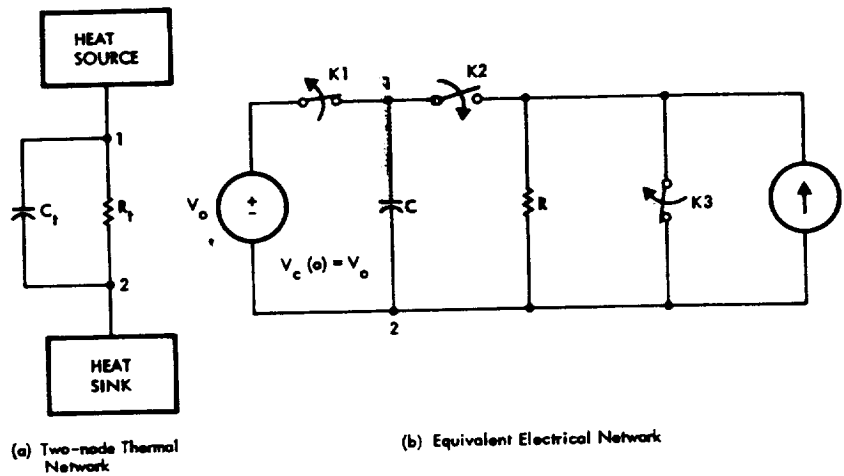


Figure 93. Thermal and electrical network analogies.

determined by setting $i = 0$ in equation 33 and integrating the result to obtain

$$v_n = K e^{-t/\tau} \quad (35)$$

where $\tau = RC$. The total voltage is the sum of the v_f and v_n components, or

$$v = IR + K e^{-t/\tau} \quad (36)$$

The initial value, $v(0) = V_o$, is used to determine K at $t = 0$. Thus,

$$v = IR + (V_o - IR)e^{-t/\tau} \quad (37)$$

which defines the voltage at node 1 as a function of time. It now remains only to transform the solution into an expression that represents the behavior of the thermal system.

Because the voltage, $v(t)$, is measured between nodes 1 and 2, it follows that its thermal analog is a temperature difference. Preserving the convention adopted in the definition of heat conduction (equation 32), $v(t)$ corresponds to $\Delta T = T_2 - T_1$ with $T_1 \geq T_2$. Thus, equation 37 may be rewritten as

$$\Delta T = \Delta T_E + (\Delta T_0 - \Delta T_E)e^{-t/\tau_T} \quad (38)$$

wherein the temperature differences are always taken between nodes 1 and 2 in the same sense, and the subscripts, 0 and E, refer to the initial ($t = 0$) and equilibrium ($t \rightarrow \infty$) conditions, respectively. This is the general temperature-response equation for a body when constant thermal power, Q , is applied at a point (node 1) as a step function at $t = 0$. During the transient period, the amount of heat flowing through the thermal resistance is given by

$$q_r = Q(1 - e^{-t/\tau_T}) + \frac{\Delta T_0}{R_T} e^{-t/\tau_T} \quad (39)$$

By similar analysis, the equation that describes the cooling of a body when its constant thermal input power is removed at $t = 0$ is

$$\Delta T = \Delta T_0 + (\Delta T_E - \Delta T_0)e^{-t/\tau_T} \quad (40)$$

with

$$q_R = Qe^{-t/\tau_T} + \frac{\Delta T_0}{R_T} (1 - e^{-t/\tau_T}) \quad (41)$$

If the heat-sink temperature, T_2 , is known, the temperature of node 1 is completely specified by the appropriate pair of expressions for ΔT^* and q_R . Otherwise, the equations may be used to specify the thermal input to node 2 as part of a separate analysis of its thermal energy balance.

When τ_T is small, the thermal system will reach its steady-state condition rapidly; conversely, a massive body (large C_T), or one connected to a heat sink through a low-conductance (large R_T) path, will reach equilibrium

*Equations 38 and 40 differ in form from those reported on page 32 of Reference 73. The equations in the reference are incorrect because they are based on the transient characteristics of a series RC electric circuit rather than on the parallel circuit of figure 93.

slowly. The literature occasionally observes that networks with large thermal time constants exhibit unstable behavior. (What constitutes unstable behavior is usually not well-defined.) This is not true if the conventional definitions of stability as they apply to analogous electric networks are used. For example, for a first-order system—a system similar to the one being discussed here—to be stable, it is necessary only that τ be positive, or, in terms of the original coefficients of equation 34, that the coefficients of v and \dot{v} have the same sign. A more complex thermal system may be represented by a second-order or higher differential equation. A necessary and sufficient condition for stability of a second-order system is that all coefficients of its differential equation have the same sign. For higher-order systems this is a necessary, but not a sufficient, condition.

An analyst must exercise judgement in constructing thermal-electrical models to prevent insuperable computational difficulties.* For example, in many spacecraft components, it is possible to neglect the thermal capacitance of shims used to conduct heat to a sink. Reducing the heat-transfer problem to a simple network of series-parallel thermal resistances greatly facilitates solution. In other cases in which the conduction path is long or thermal capacitance effects are appreciable, it is necessary to use a ladder network as shown in figure 94. With two RC-pairs in the ladder, a second-order differential equation characterizes the network (Reference 233). With more than two RC-pairs, solution of a second-order difference equation by recursive methods becomes necessary.

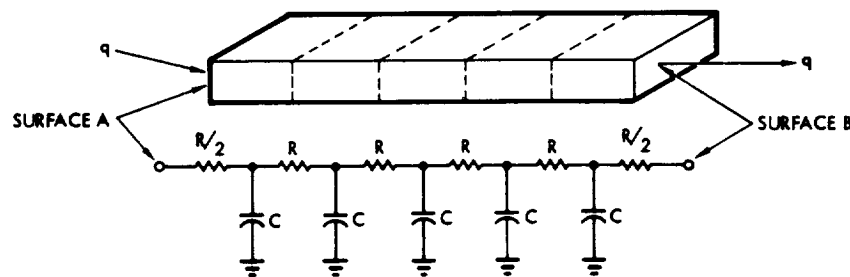


Figure 94. Thermal network for temperature distribution in a slab.

*Many digital computer programs are available for analyzing thermal problems. Even with these, however, it is necessary to tailor node complexity to a level that is consistent with the labor and machine costs associated with their operation.

Figure 95 shows a simple one-dimensional cell model. Under steady-state conditions with constant heat generation at the center of the cell, the temperature difference between either of its surfaces and the center is given by $\Delta T = Q R_{eq}$, where R_{eq} , the parallel combination of resistances, is equal to $R/2$. Extension of the cell model to three dimensions results in the circuit model shown in figure 96. If the temperatures of the six cell surfaces are assumed to be identical and equal to T_2 , the equivalent thermal resistance of the network can be calculated from

$$R_{eq} = \frac{1}{2} \left[\frac{1}{R_x} + \frac{1}{R_y} + \frac{1}{R_z} \right]^{-1} \quad (42)$$

with values of ΔT and T_1 obtained immediately thereafter. In practice, however, the surface of a cell is never isothermal when a significant amount of heat is generated within. This condition exists because the construction of the cell causes it to display anisotropic thermal characteristics. Brooman and McCallum have considered the differences between anisotropic and homogeneous (thermally isotropic) body models of sealed secondary

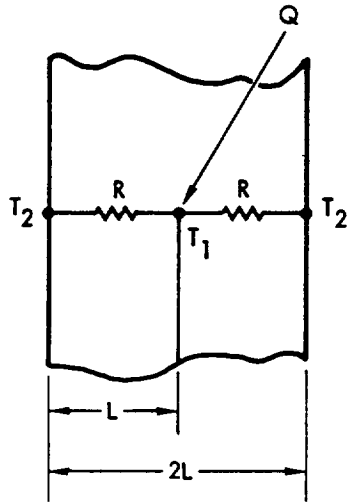


Figure 95. One-dimensional cell model.

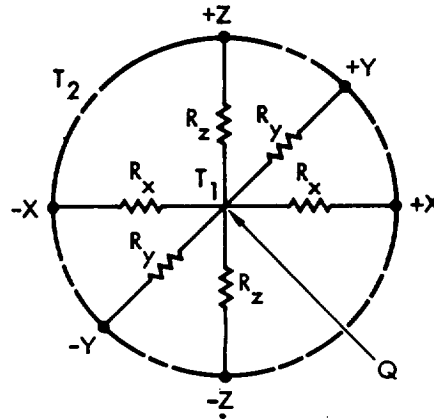


Figure 96. Three-dimensional cell model.

cells (Reference 73). They note that the thermal resistances in the direction (X-axis of figure 96) perpendicular to the electrode stack are relatively small with correspondingly small temperature gradients. By comparison, the

thermal resistances along the remaining pair of orthogonal paths are always greater because of the internal construction of the cell. They conclude that homogeneous-body models of a cell, on the basis of unidirectional conductive heat transfer, are useful in approximating the maximum value of temperature change.

Reference 38 contains another example of battery-cell thermal analysis by the network analogy method. Its approach is noteworthy in that it utilizes a detailed network model for each electrode and separator of the electrode stack.

7.4.2 Space Radiator Thermal Modeling

This section describes procedures for developing a preliminary design of a simple passive radiator that views space—the ultimate heat sink.

Figure 97 is a schematic of a battery (nodes 1 and 2) and its radiator (node 3). The average temperature of the radiator must first be determined subject to the internal and external heat loads impressed upon it. The thermal balance in space of a thin plate (negligible thermal mass) with an insulated heat source on one side is given by

$$\sigma T_3^4 = \frac{\alpha}{\epsilon} (q_s \cos \theta_s + q_e \cos \theta_e) + q_a \cos \theta_e + \frac{q_d}{\epsilon A} \quad (43)$$

where

q = Stephan-Boltzmann constant ($5.6696 \times 10^{-8} \text{ W/m}^2 \text{ K}^4$)

T_3 = plate temperature (K)

α = exterior plate-surface solar absorptance

ϵ = exterior plate-surface hemispherical emittance

q_s = orbit-average solar input (W/m^2)

= fS

f = fraction of the orbit period in which the satellite is illuminated

$$= \frac{1}{2} + \frac{1}{\pi} \arcsin \left\{ \frac{(1-B^2)^{1/2}}{\sin\beta} \right\}^*$$

B = $R/(R+h)$

R = radius of the Earth (6378 km)

h = circular orbit altitude (km)

β = angle between the orbit normal and the Sun's rays

S = solar constant ($1353 \pm 21 \text{ W/m}^2$)

θ_s = angle between the plate-surface normal and the Sun's rays

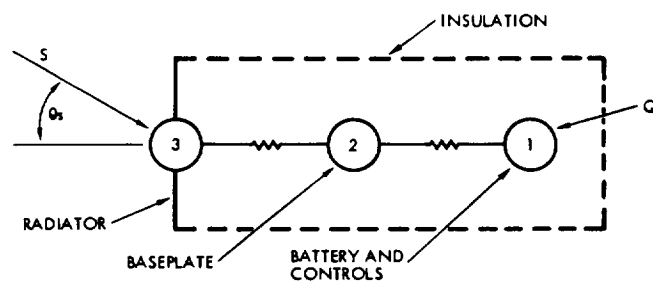


Figure 97. Battery thermal model.

q_e = average[†] Earth-emitted radiation on a plane (W/m^2)

$$= \frac{1}{2} \sigma T_e^4 \left[1 - (1-B^2)^{1/2} \right]$$

T_e = effective temperature of the Earth (280 K)

θ_e = angle between the plate-surface normal and the Earth-satellite line

*If the argument of the arcsin is greater than unity, $f = 1$.

†The maximum value incident on a plane facing the Earth is $\sigma T_e^4 B^2$.

q_a = average* reflected radiation from the Earth to a plane normal to the Earth-satellite line (W/m^2)

$$= \frac{aS}{8} \left[1 - (1-B^2)^{1/2} \right]$$

a = albedo of the Earth defined as the fraction of sunlight striking the Earth that is immediately reflected to space (0.35, average)

q_d = thermal input to the plate because of internal dissipations (W)

A = area of exterior plate surface (m^2)

Table 47 summarizes the representative values of α and ϵ for common thermal-control materials. A wide range of surface-radiation properties can be obtained with these and other materials used either individually or combined in a mosaic configuration.

Equation 43 permits calculation of the steady-state temperature of a radiator in space. The transient temperature response of the battery system (radiator plus battery cells, controls, and baseplate) is estimated by solving

$$Mc_p \frac{dT}{dt} = \epsilon A (\sigma T_E^4 - \sigma T^4) \quad (44)$$

where

m = mass of the battery system (kg)

C_p = specific heat of the battery system ($W \cdot s/kg \cdot K$)

T_E = average equilibrium temperature of the battery system (K)

$$= \Delta T_E / 2 \text{ in equations 38 and 40 with } \Delta T_E = T_{3E} - T_{1E}$$

T = average instantaneous temperature of the battery system (K)

$$\cong \Delta T / 2 \text{ in equations 38 and 40 with } \Delta T = T_3 - T_1$$

*The maximum value reflected to a plane with the Sun directly behind is approximately 16 times the expression given for the average value. With $h = 0.1 R$, the error is about 1 percent.

Table 47
Thermal-Control Material Radiation Properties

Material	α		ϵ	α/ϵ	
	New	Degraded*		New	Degraded*
Second surface mirrors, 0.15-mm silvered fused silica	0.07	0.14	0.78	0.09	0.18
White paint	0.22	0.50	0.88	0.25	0.57
Aluminized Kapton (0.07 mm)	0.44	0.50	0.78	0.56	0.64
Aluminum silicone paint	0.25	0.25	0.28	0.89	0.89
Black paint	0.97	0.97	0.86	1.13	1.13
Vacuum-deposited aluminum	0.11	0.11	0.04	2.75	2.75
Stainless steel, polished	0.40	0.40	0.05	8.0	8.0
Aluminum, unpolished	0.30	0.30	0.03	10.0	10.0

*Seven-year space exposure (estimated).

The steady-state temperature, T_E , is obtained from the solution of equation 43. The effect of internal and external heat inputs to the battery system is thus established. The exact solution of equation 44 for the case of radiative heating is

$$\frac{t}{\tau_{Tr}} + t_{oh} = 2 \left(\operatorname{arctanh} \frac{T}{T_E} + \operatorname{arctan} \frac{T}{T_E} \right) \quad (45)$$

and, for the case of radiative cooling, is

$$\frac{t}{\tau_{Tr}} + t_{oc} = 2 \left(\operatorname{arccoth} \frac{T}{T_E} - \operatorname{arccot} \frac{T}{T_E} \right) \quad (46)$$

where

τ_{Tr} = thermal-radiation time constant

$$= \frac{mC_p}{4\epsilon A\sigma T_E^3}$$

t_{oh}, t_{oc} = constants of integration for heating and cooling, respectively

In practice, the initial temperature is usually known or can be estimated. The constant of integration is determined by solving the equation for $t = 0$. Solution of either equation is facilitated by plotting each with the left-hand side a function of T/T_E .

7.4.3 Heat Pipes

The heat pipe is a device that exhibits a thermal conductivity greatly in excess of that of any known material. It is a fraction of the weight and has several hundred times the heat-transfer capability of metals such as copper, silver, and aluminum. It is ordinarily designed to transport thermal energy at efficiencies greater than 90 percent. Since announcement of its development in 1964 (Reference 234), the heat pipe has been successfully utilized on several major spacecraft (References 235 through 237) for controlling electronic component, solar-array, and battery temperatures.

Figure 98 shows a heat pipe in its simplest form. A pipe is lined with a material suitable for operating as a wick, frequently some kind of woven metal. The pipe is then closed off and evacuated, and a charge of working fluid, sufficient for saturating the wick plus a slight excess, is inserted. If

one end is heated, the liquid is evaporated, and the resulting vapor moves away from the heat source. The heat is removed from the other end of the pipe by radiation, conduction, or convection, causing the vapor to condense back to a liquid. This liquid then travels back to the evaporator end through the wick, where it is again evaporated, and the cycle continues. The device is virtually independent of gravity, and the heat can be applied at any point.

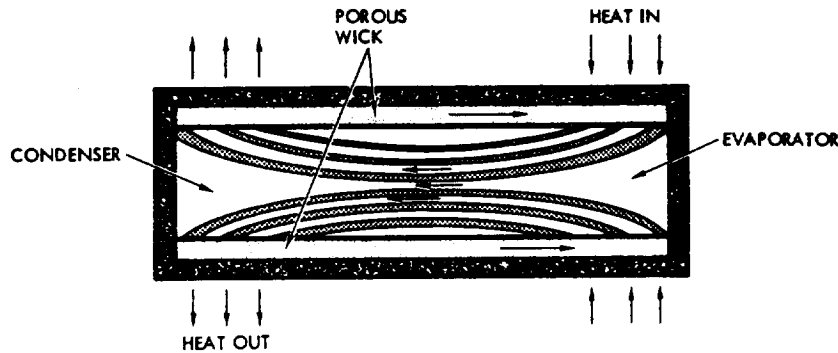


Figure 98. Simple heat pipe.

Either end can serve as a condenser or an evaporator; if the middle is heated, that area becomes the evaporator, and both ends become condensers.

The temperature range over which a particular heat pipe will operate depends on the choice of working fluid. The minimum operating temperature is determined by the boiling point of the fluid, and the maximum is determined by its critical point—the highest temperature at which the fluid can exist simultaneously in both liquid and gaseous phases. Although water possesses many characteristics desirable for a working fluid, it has a relatively high freezing point compared to other candidates. Furthermore, hydrogen-gas generation has been observed with water in the presence of aluminum and stainless steel. Accumulation of this noncondensable gas in the condenser section of the heat pipe degrades its performance. Methanol is usually rejected as a fluid for lightweight heat pipes because it is quite corrosive to aluminum and aluminum alloys. Other candidate fluids, including those of the Freon family, do not perform as well in this temperature range as ammonia. Because ammonia is quite compatible with both stainless steel and aluminum alloys, it is widely used in spacecraft heat pipes.

The detailed design of a heat pipe also involves the selection of materials and configurations for both the pipe and the wick. The pipe material should exhibit a high strength-to-mass ratio, high thermal conductivity, and

fast thermal response. Pipe material strength is an important consideration because high pressures may occur within the heat pipe in addition to the static and dynamic external forces it may otherwise experience. For example, the highest fluid pressures are usually encountered during manufacture when heat pipes are bonded within honeycomb sandwich structures.

The wicking structure must be capable of carrying the specified axial heat flux over the length of the heat pipe without engendering certain limiting mechanisms, such as burnout or boiling. These and other mechanisms combine to establish the capability of each heat-pipe configuration. Eninger has provided a concise general description of the performance limits that must be considered (Reference 238). Design data for wicks appear in the works of several investigators (Reference 239 through 241).

The thermal resistances of the evaporator and condenser of a heat pipe are, respectively,

$$R_e = \frac{T_e - T}{Q} = \frac{1}{U_e A_e} \quad (47)$$

$$R_c = \frac{T - T_c}{Q} = \frac{1}{U_c A_c} \quad (48)$$

where

T_e, T_c = average temperature of the evaporator and condenser, respectively

T = temperature at exit of evaporator

Q = thermal power

A_e, A_c = heat-transfer area of the evaporator and condenser, respectively

U_e, U_c = heat-transfer coefficients of the evaporator and condenser, respectively

The reference temperature, T , may be taken to be the mean vapor temperature or, alternatively, the mean temperature on the outside of the isothermal section of the heat pipe.

Figure 99 shows a thermal network that is applicable for steady-state analysis of the case in which the heat pipe is used as a *thermal transformer* (i.e., as a coupling device between a source and a sink of differing heat-flux densities). To simplify most analysis procedures, the heat-pipe network is usually replaced by a constant-temperature *node* within the general thermal-system model.

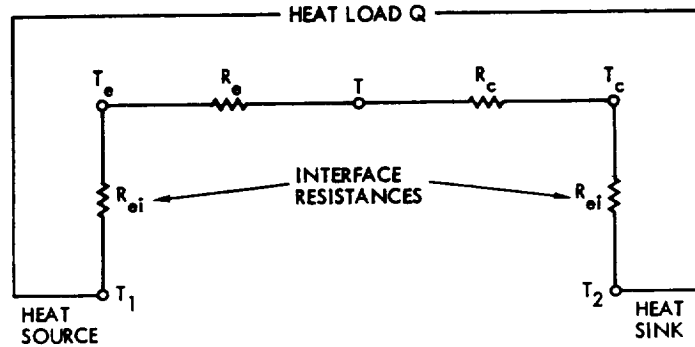


Figure 99. Electrical analog of a simple thermal network for a heat pipe.

From the foregoing discussion and from figure 99, it is apparent that, when a heat pipe is used as a thermal transformer, there will be a difference in temperature between the heat sink (T_2) and the heat source (T_1) that may not be negligible despite the essentially isothermal behavior of the heat pipe. This difference is usually acceptable when the design objective is simply to transport heat from a high-flux region to a spacecraft radiator of low flux density. However, in certain important applications, it is necessary to provide precise control of the source temperature under changing conditions of source power or effective sink temperature, or both. Isothermal operation normally occurs only under constant thermal-power conditions when the source and sink thermal resistances are equal. Therefore, the basic heat pipe must be modified to provide a control function if isothermal operation is to be realized. Such a modification is embodied in the variable-conductance heat pipe (VCHP).

The operation of a VCHP is based on a fact noted earlier (namely, that the presence of a noncondensable gas in the condenser region of a heat pipe will reduce the amount of heat transferred from the condenser). Any noncondensable gas inside the heat pipe will be swept to the condenser end by the flow of the fluid vapor where it will become trapped and will block the

transfer of heat from the vapor to the heat-pipe wall. The result is an effective reduction of condenser area. By deliberately introducing a specific amount of noncondensable gas into the heat pipe and by providing a reservoir at the condenser end, as shown in figure 100, the condenser area can be adjusted to provide a range of heat-pipe temperatures. Precise control is obtained by varying the temperature of the reservoir in response to changes in temperature at the evaporator end of the pipe, causing the noncondensable gas to expand or contract in the condenser region. With this type of control, the temperature of the source can be regulated to within about $\pm 0.5^{\circ}\text{C}$ (Reference 242). The first VCHP placed into orbit was flown on board the Orbiting Astronomical Observatory (OAO-C), which was launched in 1972. Since then, other space applications have been successful (References 243 and 244), and, during the same period, investigators have studied (Reference 245) and developed (References 246 and 247) nickel-cadmium batteries with integral VCHP thermal-control systems.

7.4.4 Thermal Louvers

A thermal-louver system provides controlled heat transfer to space by means of temperature-dependent variations of the effective surface emittance of its radiator. Its function is analogous to that of the heat pipe, except that the heat-transfer mode is radiation rather than conduction, and emittance rather

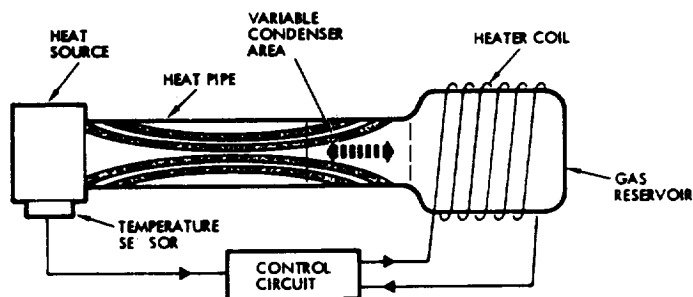


Figure 100. Variable-conductance heat pipe modified for close temperature regulation.

than conductance is the controlled property. However, thermal louvers are less versatile than heat pipes in that they cannot act as thermal transformers and their temperature-control range is usually only about 15°C . Also, thermal louvers are not as mass-effective as heat pipes. For example, a thermal louver, typical of those used on the ATS-6 spacecraft (Reference 248) can control a thermal power variation of 53 watts up to a maximum

dissipation of 61 watts with a corresponding radiator temperature variation of 16.7°C. Based on maximum power dissipation, the power-to-mass ratio of the louver system is 0.078 kW/kg with an areal density of 4.74 kg/m². In contrast, on the basis of a maximum thermal transport of 96 watts, a single constant-conductance ammonia-aluminum heat pipe on board ATS-6 exhibits a power-to-mass ratio of approximately 0.186kW/kg with a lineal density of 0.298 kg/m. Its operating temperature range is 5 to 40°C with a maximum temperature difference of 5.6°C between the evaporator and condenser (Reference 249). The substitution of a variable-conductance heat pipe would result in a reduction of radiator (condenser) temperature variation to about 2°C with only a small reduction in the net power-to-mass ratio of the heat-pipe system.

Despite their performance limitations relative to heat-pipe systems, thermal louvers have enjoyed widespread application on spacecraft of diverse purpose and configuration. One reason is that they are relatively inexpensive to manufacture, install, and test. Another is that they reduce dependence on optical coatings that are subject to degradation from the space environment during long missions. Finally, their technology is both well-developed and proven (Reference 250 through 252). Thermal louvers on board Pegasus, OAO, and Nimbus-D spacecraft have accumulated more than 3.7 million operative blade-hours without failure.

Figure 101 shows a simple thermal-louver system. The steady-state energy balance equation for the system is

$$Q = \epsilon_{\text{eff}} \sigma A T^4 - \alpha_{\text{eff}} AS \quad (49)$$

where

Q = net thermal power transferred from the radiator

ϵ_{eff} = effective emittance of the louver system

σ = Stefan-Boltzman constant

A = exterior radiator-surface active area

T = absolute radiator temperature

α_{eff} = effective absorptance of the louver system

S = solar constant

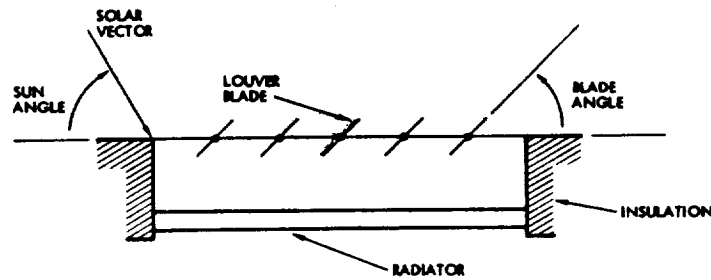


Figure 101. Thermal-louver system.

The effective emittance is a function of the emittance of the baseplate and the angular position of the louver blades as well as the following parameters:

- The conduction path from the radiator to the louver frame
- The external surface area and shape of the louver frame
- The surface emittance of the louver frame
- The radiation leakage paths that exist when the louver is closed
- The louver blade surface emittance

The effective emittance of a radiator with louvers is always less than the surface emittance of the radiator itself. One reason is that the louver occupies 15 to 20 percent of the radiator area. Also, because of their thickness, some blockage occurs when the louver blades are fully open. It is therefore necessary to use the least number of blades compatible with clearance requirements to minimize blade blockage. The effective emittance of a fully open louver is further improved by using blades with highly polished (specular) surfaces. Conversely, the effective emittance of a fully closed louver is minimized by enclosing the ends of the blades to reduce radiative heat losses.

Reference 248 contains calculated values of effective emittance as a function of blade angle. Other analyses and data are reported in References 253 through 255.

The effective absorptance is a function of both the blade and solar-aspect angles and includes the direct and reflected solar energy absorbed by the radiator, as well as the radiation interchange between the blades and the

radiator. Reference 248 contains calculated values of effective absorptance. It is sometimes advantageous to reduce the effect of solar heating by placing the louver system behind a reflecting skin; however, although this improves heat rejection in sunlight, it reduces the heat-rejection capability of the louvers in the shade (Reference 256).

SECTION 8 BATTERY SYSTEM DESIGN

8.1 INTRODUCTION

Section 7 described the relationship of the battery system to the electric power and thermal-control systems.* This section builds on the understanding thus acquired regarding the role of the battery system and concentrates on the definition, analysis, and interpretation of various important aspects of the battery system itself. It emphasizes the thorough definition and understanding of all requirements and constraints and how these matters impact the design. Examples from the authors' experience illustrate the importance of early and complete interface definition. The topics proceed from the general to the specific in a manner that sustains a continuing and parallel discussion of both low- and high-altitude orbit battery-system applications. This approach is helpful for comparing important design details when they differ because of orbit-related mission factors. Cell and battery technology considerations are introduced when they can best serve the narrative. Design guidelines are presented when they are available.

8.2 REQUIREMENTS AND CONSTRAINTS

This section describes mission requirements and constraints in terms of their effect on the design of the battery system and, by implication, of the electric power system. The discussion encompasses a wide variety of design situations. Some of the remarks that follow apply to all battery systems, whereas others apply to specific mission applications. Their presentation is meant to convey that battery-system design should not be performed in an information vacuum, but that all relevant information and data regarding mission objectives, spacecraft system design, and proposed spacecraft operational policies and procedures should be considered early in and throughout the design phase.

It would be convenient to have an available methodology for analyzing requirements and constraints as they apply to the battery, the battery system, the electric power system, and higher levels. It is beyond the scope

*Section 1 contains definitions of terms used in this section and throughout the manual.

of this manual to consider all of the nuances of spacecraft design that are necessary for the full development of such a methodology. However, Reference 232 outlines a general approach, and Section 7.2 discusses other aspects of battery and electric power-system requirements analysis.

8.2.1 Mission Requirements

The mission requirements that have primary effect on the battery system are: (a) the orbit or trajectory parameters, (b) the service and ground-storage times, (c) the spacecraft reliability goal, and (d) special environmental considerations.

The orbit definition is necessary for establishing the discharge/charge cycle profile, including the number of cycles, for the mission. Section 7.2.1 contains the characteristics of circular equatorial orbits and reference lists for the characteristics of other orbits and trajectories. Although it is usually sufficient to design on the basis of the maximum eclipse duration and the maximum number of eclipse periods expected in a year, the designer should recognize that many orbits result in variable eclipse profiles, particularly those at low altitudes with nonzero orbit inclination. Also, the support of peak loads during sunlight periods may add to the number of cycles in an equivalent sense.

The required service time directly affects the depth of discharge and the operating temperature regime selected. These design parameters, plus the allocated reliability goal for the battery system, help in determining the size and number of the batteries. Storage time affects battery-supply and logistic considerations and, therefore, cost to the project, as well as directly influencing performance.

The reliability goal for the spacecraft is the basis for reliability goal allocations at the power and battery-system levels. In general, a reliability goal defined at either the cell or battery level is of limited use; reliability estimates must be made at the battery-system level to incorporate: (a) the unreliabilities introduced by discharge/charge controls and other auxiliaries, and (b) the reliability enhancement provided by redundancy.

Special environments must be defined so that their effect can be determined early in the battery-definition phase. For example, a requirement for magnetic cleanliness aboard a scientific spacecraft may necessitate special wiring practices or may prohibit the use of nickel-cadmium batteries altogether

(References 2, 257, and 258). Similarly, a requirement for sterilization may require a unique cell or battery development effort (References 103 and 259).

8.2.2 Operational Requirements

Spacecraft power systems may be categorized in terms of their operational characteristics. Many may be considered to be automatic in that they operate without direct control from the ground, particularly spacecraft in low-Earth orbits that may not be in contact with ground stations for long periods of time. An incident of failure is handled by automatically switching to redundant channels or by placing the system into a "safe" mode until diagnostic and corrective procedures can be done. Battery discharge or charge control is also automatic. Some military spacecraft are also considered to be autonomous because they must be able to function unattended for long periods with full operational capability even if a failure occurs. Interplanetary spacecraft (flybys, orbiters, and landers) with complex mission profiles and flight trajectories have high levels of autonomy.

Spacecraft in geosynchronous equatorial orbits are candidates for either semiautomatic or manual control from the ground. Commercial communications satellites have been operated in this manner with dedicated ground stations for some years. On-board circuitry is simplified, with many of the decision functions performed by software in ground-based computers.

The operational control philosophy, as it pertains to battery control and protection, must be established early in the definition phase. A decision to operate batteries by ground control, for example, must be considered carefully because it implies the definition of many new requirements for precision telemetry measurements and data processing. Assumptions on the available time for battery reconditioning must be checked against attitude-control-system requirements for stationkeeping if electric thrusters are used (Reference 260) or verified against payload programming schedules.

8.2.3 System Requirements

System requirements are derived from mission requirements, the particular characteristics of payload and housekeeping equipment required to satisfy the mission requirements, and proven design principles, practices, standards,

and procedures. For the battery and power systems, such requirements are primarily those associated with the electrical loads, the environments developed throughout the mission to which the hardware is exposed, and the need to ensure that reliability goals are met.

8.2.4 System Design Constraints

Mission, operational, and system requirements tend to limit the options for design and to impose various constraints on the spacecraft and its equipment. Constraints on the spacecraft configuration affect the batteries in several ways. They must be positioned carefully with respect to the center of mass of the spacecraft and other heavy components. Limitations on solar-array area imply limitations on power for battery charging and for thermal-control heaters. Relatively few locations may be available for adequate thermal radiators, and special provisions may be required for maintaining and controlling the temperature of the batteries to within the range required for long service life. (Batteries should be operated near and just above 0°C; they should not be permitted to operate above 20°C for long service life.)

Prelaunch and launch environments may directly affect the configuration and performance of the battery system. When they are installed on the spacecraft, it may be difficult to cool batteries during ground test and checkout. Charge controls may limit the charge if battery temperatures are above the normal performance range. During ascent, the battery radiators may be blocked by solar panels, or they may be exposed to abnormal insolation for extended periods. Launch-window constraints and ground-station telemetry coverage limitations associated with spacecraft antenna configurations often combine to place the solar array or the batteries in an unfavorable position with respect to the Sun during ascent. Therefore, the batteries may be required to discharge or charge while warm—the latter often at low values and with a periodic current profile because of stowed solar-array characteristics.

Mass limitations usually represent a constraint to the battery system, particularly for missions at high orbital altitudes. The batteries are usually one of the heaviest items on board a spacecraft. For economy, spacecraft mass is usually matched to the capability of the launch vehicle. When the Space Transportation System (STS) becomes operational, apportionments undoubtedly will be made of its payload-to-orbit weight capability, and appropriate corresponding assignments made to each spacecraft payload. There may thus be continued emphasis on battery-mass reductions, as well as battery-cost reductions in the era of the STS.

8.3 METHODS OF CHARGE CONTROL

A wide range of battery charge controls have been developed and successfully applied. Some perform equally well in both low- and high-altitude orbits, whereas others are restricted in use. Some methods are best used as backup to others rather than as primary controls themselves. It would be unnecessarily restrictive to the future development of spacecraft battery and power systems to suggest that one or two approaches have clear advantage over others and should therefore be used exclusively. However, in recent years, certain trends in battery-charge control have become evident.

Typically, on low-altitude spacecraft, approximately one-half of the solar-array power is allocated to battery charging because 35 to 40 percent of the orbit period can be spent in eclipse. The batteries can experience up to 6000 discharge/charge cycles per year exclusive of peak load demands. High-charge currents and fast recharge require moderately complex electronics for controlling overcharge and for preventing undesirable battery heating. Battery overheating was a common problem in early spacecraft. It was difficult to correctly specify simple temperature-sensitive controls that would ensure energy balance, provide overcharge protection, and control thermal dissipation throughout a mission with changing environments and battery I-V characteristics. This was attributable in part to a lack of full understanding of battery-operating parameters and their mutual interaction. For example, early battery systems typically exhibited recharge ratios greater than 1.2 and sometimes as high as 1.6. Their temperatures were often in the vicinity of 30 to 35°C or higher. With continued cycling and corresponding battery degradation, the recharge ratios tended to increase, thereby driving the temperatures yet higher. Single voltage-temperature limits were set too high and were therefore inadequate for their intended purpose. These problems were circumvented on the Orbiting Astronomical Observatory (OAO) by specifying a ground-commandable family of voltage limits that permitted stepwise adjustment of recharge ratios. This, in turn, permitted battery thermal dissipation and temperature to be controlled and reduced and permitted adjustment to accommodate battery-voltage degradation with life. The OAO batteries also benefited from an active thermal-control system.

Table 48 summarizes other low-Earth-orbit batteries and charge controls, with early projects on the left and more recent designs on the right. It is evident that NASA spacecraft now have a strong tendency to utilize the

voltage-limited control method with multiple voltage limits. Higher capacity batteries are favored, and the trend in operating temperature range is generally downward.

Geosynchronous spacecraft encounter approximately 90 eclipses per year, the longest of which takes up 5 percent of the 24-hour orbit period. Available minimum battery-recharge time is 22.8 hours, which can be reduced by peak-load events that may require solar-array/battery load sharing. Because of the extended sunlight period, the solar-array power devoted to battery-charging is only approximately 15 to 20 percent of the total array capability at equinox. Therefore, charge currents are determined primarily by the charge-acceptance characteristics of the battery at low rates.

Table 49 summarizes charge controls used on recent geosynchronous spacecraft. Because most NASA and military spacecraft must operate automatically or autonomously for extended periods, they use the voltage-limited or temperature-limited methods of charge control as reasonably accurate means of determining switchover from high- to low-rate (trickle) charging. Spacecraft with dedicated ground stations utilize telemetered battery data for recharge ratio-estimation and control. All primary battery-charge functions are managed from the ground by the command link, thereby minimizing battery-system complexity.

8.3.1 Current-Limited Charging

In the current-limited or constant-current method of charge control, a regulator limits charge current to one or more selected values. The limits are defined so that charge rates are: (a) high enough to ensure full recharge after a discharge, (b) low enough to limit thermal dissipation during overcharge, and (c) low enough to maintain cell oxygen pressures at safe levels.

The simplest version of this method applies a single current limit throughout the charge and overcharge periods. The limit thus represents a compromise between the requirement for energy balance and the necessities of temperature control and safe charging. For example, a C/20 rate is considered to be safe in terms of cell-pressure stability during overcharge at 0°C; higher rates are permissible at higher temperatures when pressure stability is the only consideration. The C/20 rate provides adequate recharge at 0°C, but requires longer charge periods (higher recharge ratios) at higher temperatures. However, the C/20 rate is too high for extended periods of overcharge because the thermal dissipation produced within the battery tends to drive

its temperature to excessive levels with passive cooling techniques. It is therefore necessary to constrain the application to orbits with short sunlight periods or to use a second, lower limit during overcharge periods. Some early low-altitude spacecraft used the single-limit approach, but it was soon discarded because it could only accommodate depths of discharge of about 5 to 10 percent.

The single-limit constant-current charge-control scheme is no longer used in pure form in any spacecraft application because of the thermal-control problem it engenders. Some dual-limit applications exist in which the higher limit is determined by the capability of the source to deliver current at a rate acceptable for charge but not necessarily for overcharge, and the lower limit is controlled somewhat more carefully during overcharge periods. The following paragraphs present a rationale for selecting high and low current limits.

As mentioned earlier, it is important to select charge-current limits that provide safe charging, especially during periods of continuous overcharge. The current passing through a battery cell during overcharge causes oxygen to evolve from its positive electrodes. The gas is recombined at the negative electrodes. The evolution rate will balance the recombination rate at particular combinations of charge rate, cell pressure, and cell temperature. No increase in pressure will occur at this equilibrium condition unless the rate, the temperature, or both increase. The relationship between these variables, shown in figure 32 for one manufacturer's cells, provides the basis for the selection of the high current limit. Figure 32 shows that, as the charge rate is increased at a particular temperature, there is a transition from a region of low equilibrium pressure to a region of high pressure. Thus, the higher the initial charge rate, the greater the oxygen pressure if any significant period of overcharge occurs and, therefore, the greater the need for prompt action to reduce the charge current to safe levels before pressure builds.

If the initial charge rate is set too high, hydrogen evolution may also occur, particularly with lower cell temperatures. Oxygen evolution on overcharge and hydrogen evolution on charge are discussed in the sections on "Gas Evolution and Pressure During Discharge" and "Maximum Allowable Voltage on Charge," respectively, for new reference-design cells.

Figure 32 is not useful for defining the lower or trickle-charge limit. The use of a current rate at the lower boundary of the indeterminant region (in the "low" pressure region) of figure 32 will result in high heat-generation rates during continuous overcharge and corresponding temperature instabilities. It is necessary, therefore, to reduce the trickle-charge limit to a value

that will maintain charge and provide the desired temperature performance. A C/60 trickle-charge limit will maintain cell capacity at temperature up to 20°C; C/100 has proved to be adequate at temperatures in the vicinity of 10°C. Some data exist to support the use of a C/150 trickle-charge rate with cell temperatures near 0°C, although flight experience has yet to confirm this.

An example of a dual-limit charge-control system in a geosynchronous application is the Fleet Satellite Communications (FLTSATCOM) system recently developed for the Navy. Each of its batteries are separately charged from dedicated-charge solar arrays at rates between C/10 and C/15. When the voltage of a battery reaches a value that corresponds approximately to a recharge ratio (ampere-hours throughput/ampere-hours discharged) between 1.1 and 1.2, it is automatically switched from the charge array to a C/100 trickle-charge array. Trickle-charging is performed at about 10°C.

8.3.2 Voltage-Limited Charging

In the voltage-limited method of charge control, the current rate is controlled indirectly during overcharge. A regulator limits battery-charge voltage so as to reduce charge current from an initial value to a low value that corresponds to a trickle-charge rate. The voltage limit is always defined as a function of battery temperature with a negative slope because, as temperature rises, the current that a cell accepts at particular combinations of voltage and state of charge also increases. Thus, applying a constant-voltage limit will result in a runaway condition during overcharge in which an increase in temperature leads to an increase in current, which results in a further increase of temperature (Reference 261). The definition and application of temperature-compensated battery-voltage limit (BVL) curves has received considerable attention during the last 10 years.

The voltage-limited method was first used in low-altitude orbit applications in conjunction with efforts to increase battery depth of discharge from the very low levels achievable with constant-current charge-control techniques. Controls that permitted depths of discharge up to 20 to 30 percent were designed with a single BVL. Full charge-current rates of up to C/2 were used, sometimes with a current limit and sometimes without, depending on battery temperatures and solar-array characteristics. The design of these systems involved considerable effort in cell current-voltage characterization, BVL circuit design, and computer modeling of battery performance. Particular attention was devoted to the sensitivity of battery-system performance to slight changes in BVL level and slope and, specifically, to changes

in cell and battery characteristics with time and service. It soon became evident, that, for most applications, it was desirable to have available at the end of the mission a different BVL from that used at the start of the mission.

More experience in voltage-limited charge-control methods also indicated that interactions between the battery and its thermal-control system were too complex to predict accurately. Some direct means of controlling battery dissipation was required to compensate for changes that occur in battery heat-generation rates and the surface properties and other characteristics of thermal radiators and associated devices during flight. The use of a single BVL did not permit control of the battery's recharge ratio and, consequently, of its rate of heat generation during overcharge. Also, a single BVL did not compensate for a partial or complete cell short circuit during battery charge. These considerations led to the present general practice of using multiple temperature-compensated BVL's, each selectable by ground command.

The limiting function is used in one of two ways: (a) overcharging is performed with battery voltage held to a value determined by the BVL, or (b) the charge current is switched from the normal full-charge rate to a controlled lower rate when the battery voltage reaches the BVL level. In approach (a), the battery's characteristics determine the value of current that it will accept. Continued charging at a limit results in a tapering of the current in the overcharge region. For this reason, the voltage-limited charging method is sometimes referred to as *tapered-charge control*. In approach (b), the switch-down may be either to a trickle-charge rate or to zero current. Some battery systems have been designed that incorporate both approaches, with the switch-down option used during long periods of continuous sunlight.

Several controllable or measurable battery parameters interact during cycling with voltage-limited charge control. Table 50 shows the effect of increasing one parameter while holding others constant. This is an idealized situation, and no statement is made on the relative magnitudes of the changes. In practice, a moderate change of one parameter (e.g., depth of discharge) will affect another parameter (particularly in a short-period orbit with passive battery temperature control), thereby shifting the overall equilibrium

of the discharge/charge cycle. The net effect of such a change on recharge ratio may therefore be quite small.

However, the I-V characteristics of a cell are nonlinear with temperature and state of charge (SOC) so that it is only possible to evaluate accurately the total effect of parameter changes: (a) by performing a test under simulated spacecraft environmental conditions, or (b) by performing a computer simulation using a reasonably representative set of cell I-V characteristics for the discharge/charge cycle being considered.

Table 50
Charge-Control Parameter Sensitivities

Increase	Time to Reach Limit	True SOC at Limit	Taper Current		Recharge Ratio
			Final Value ¹	Asymptotic Value ²	
Voltage limit	+	+	+	0	+
Full charge current	-	-	-	0	-
Temperature	+	?	+	+	+
Average cell voltage ³	-	-	-	?	-
Depth of discharge	+	0	+	0	-

¹Applicable to short cycles only.

²See text.

³Change resulting from a change in cell characteristics.

A distinction is made between the final and asymptotic values of taper current. The asymptotic value of taper current is that value of current that is approached if overcharging is continued for a much greater period of time than the interval ordinarily referred to as the charge period. (Constant cell

temperature during overcharge is assumed for the purpose of this discussion.) In a long-period cycle, these values may be the same. In a short-period cycle, the final, or end-of-discharge, value may be greater because of the onset of discharge.

The battery's characteristics and its temperature determine the asymptotic value. Figures 29 and 30 show asymptotic values of overcharge current taken at constant current without voltage-limiting for reference-design cells. It is not known if the same results would be obtained if similar tests were conducted under voltage-limited conditions.

Figure 102 shows some of the BVL's that have been used in low-altitude orbit applications. The diversity is attributable to several factors. Those with shallow slopes represent early battery-system designs that were operated at temperatures between 15 and 30°C. The general opinion then was that higher values of recharge ratio (>1.1) were required for maintaining energy balance and that higher values of overcharge current were therefore required.

Some attempts were made to tailor BVL's to the thermal-control capability of the battery, thereby achieving stable operation at somewhat lower temperatures (Reference 262). Because such designs were quite sensitive to the level of the BVL in the cooler regions, relatively low values of recharge ratio were obtained, which caused some concern about whether or not the batteries would be fully recharged.

These concerns were dispelled by Ford (Reference 77), who conducted extensive cell-characterization and cycling tests for the Orbiting Astronomical Observatory project and correlated the test results by using BVL's with significantly steeper slopes than those in prior use. His approach was to use a limit that was reached before the threshold of the overcharge region, typically at 60 to 70 percent of recharge, while maintaining the battery temperature at 5 to 15°C. Overcharge thermal dissipation was therefore controlled and reduced, which, in turn, helped to achieve the reduced operating temperatures desired for long service life. Ford's work demonstrated that the low recharge ratios that resulted from this approach were adequate for long-term short-cycle operation with a 15-percent depth of discharge.

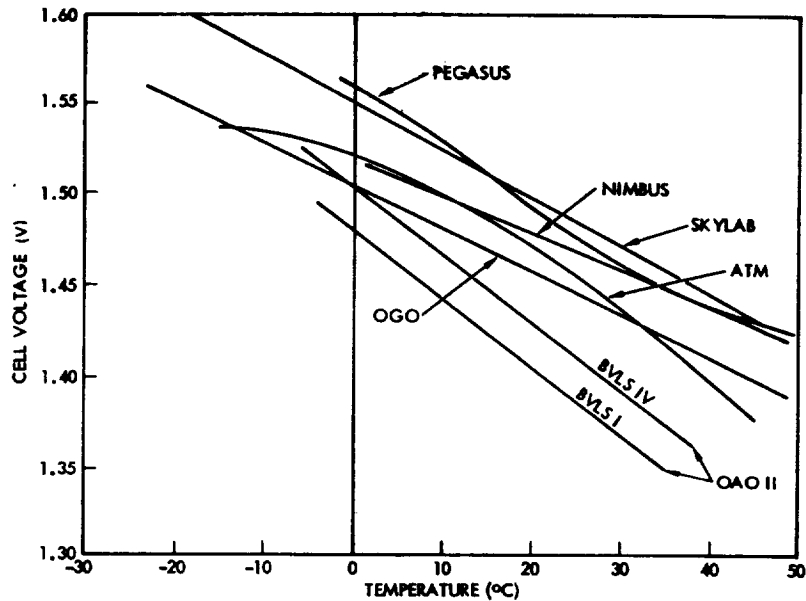


Figure 102. Comparison of voltage limits used in low-altitude orbit applications.

Figure 103 defines the family of BVL's used for OAO-3. OAO-3 batteries have completed over 5.5 years of successful operation in orbit with a 16- to 18-percent depth of discharge and a temperature of about 7°C. Their BLV levels are varied between levels 1, 2, or 3, depending on spacecraft off-pointing requirements, and have never been set above level 4. Other recent applications of this approach include the Orbiting Solar Observatory I (OSO-I) and the High Energy Astronomy Observatory (HEAO), both in low-altitude orbits. Figure 103 compares the BVL's of OAO-3, OSO-I, and HEAO. Each family contains eight linear curves spaced at essentially equal distances at the temperature end points. Normal operation is usually at the third or fourth level counted from the bottom. (Table 54, which appears in a later section, defines the BVL's used for engineering characterization tests for the Multimission Modular Spacecraft (MMS) now being developed by NASA.)

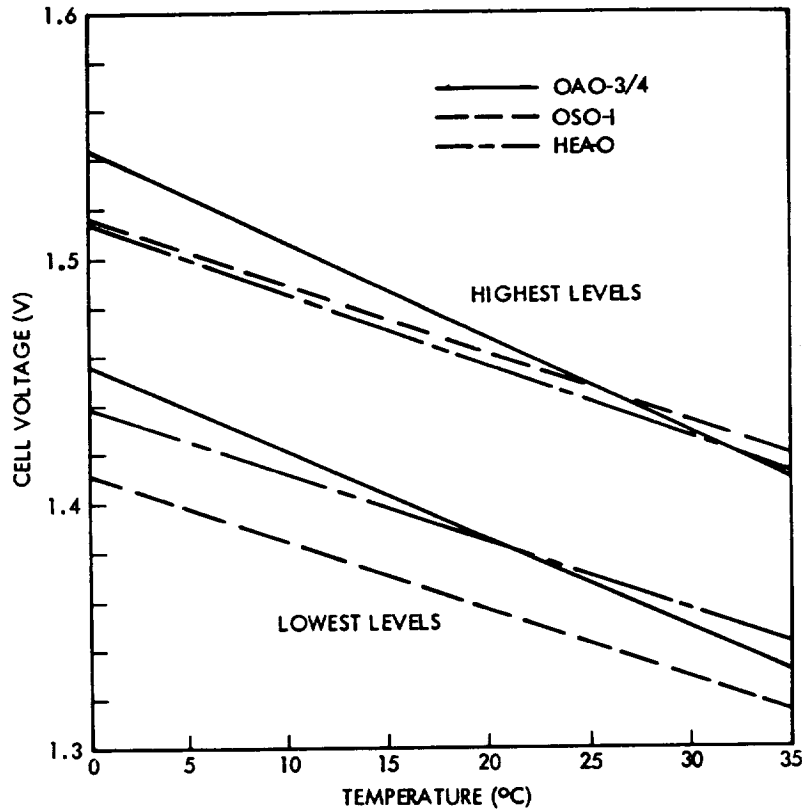


Figure 103. BVL families used in recent low-altitude orbit applications.

Figure 104, reproduced from Reference 77, shows the relationship between voltage limit, full charge current, temperature, and recharge ratio obtained from OAO characterization tests of SAFT-America 20-Ah cells. The test cycle was 100 minutes (35 minutes discharge and 65 minutes charge) with a 15-percent depth-of-discharge. Figure 104 also shows values of recharge ratio that are said to be the minimum values required for maintaining battery capacity at each of the test temperatures. Because the minimum values were not obtained directly, they must be interpreted as representative minimum values for the particular discharge/charge cycle and for cells of a particular vintage. They were deduced after analysis of NWSC/Crane life-cycling test data, which showed good capacity retention over many thousands of cycles when such values of recharge ratio were used:

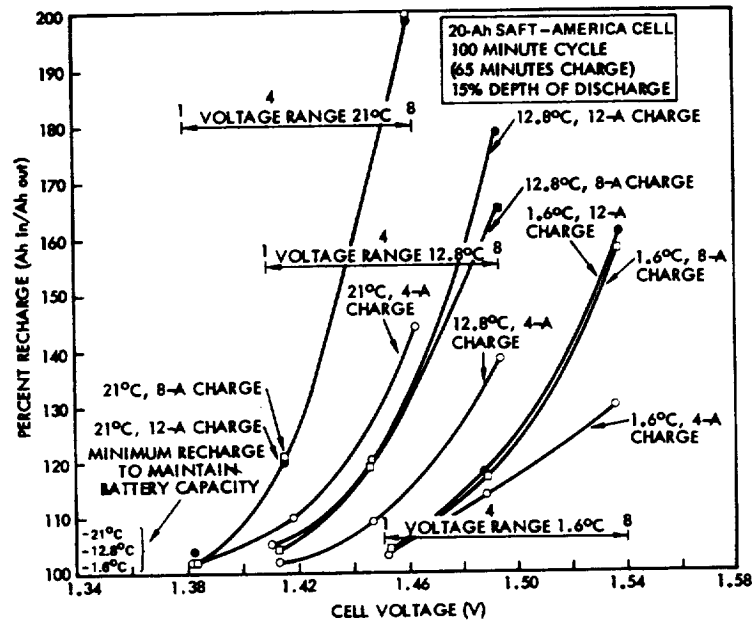


Figure 104. Recharge ratios for voltage-limited charging of OAO-3 cells.

Figure 105 shows OSO-I characterization test results for 12-Ah cells in a similar application.* The data were taken after a minimum of 16 cycles or after the recharge ratio remained stable within a 1-percent variation for three consecutive cycles. Table 51 lists other data taken in the same test. The long-term performance of the OSO-I cell is represented by the data taken for NWSC/Crane test pack 7C. The pack was operated in the OSO-I regime (10°C average temperature, 1.429-volt limit, approximately) for over 30 months (over 22,000 discharge/charge cycles) with a recharge ratio of about 1.05. The voltage limit corresponds to the fourth BVL counted from the bottom of the family.

*W. Webster. NASA/Goddard Space Flight Center, private communication, January 1975.

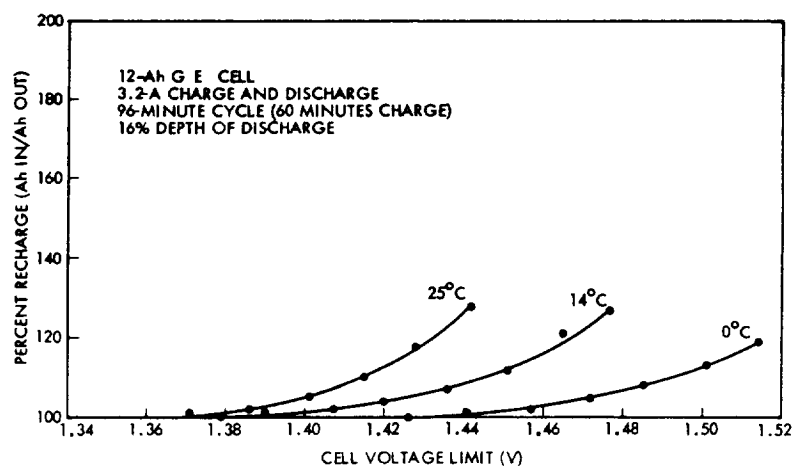


Figure 105. Recharge ratios for voltage-limited charging of OSO-I cells.

Voltage-limited charging has been used in geosynchronous orbits, as well as in low-altitude orbits. (See table 49.) Little detailed documentation of test and flight experience exists for these missions. Instead of attempting comparisons of the data that are available, two cases will be examined to illustrate the performance of this charge-control approach with a long-period orbit: the Applications Technology Satellite 6 (ATS-6) and the FLTSATCOM system.

Reference 218 gives the status and performance of ATS-6 after 2 years in orbit. Each of its batteries is normally charged at a controlled C/10 rate to a single temperature-compensated BVL (Reference 263). The batteries experienced 1123 discharge periods with 71 percent of the discharges in the depth-of-discharge region between 20 and 60 percent. The BVL was selected to cause the onset of voltage-limiting to occur at a recharge ratio of about 0.95. During the course of the mission, the battery-voltage characteristics on charge tended to increase, thereby causing the limit to be reached earlier at a recharge ratio of 0.8. The end-of-discharge voltages decreased significantly, particularly during the phase when the batteries were not being fully recharged. The immediate problem was resolved by reverting to standby C/20 constant-current charge control, which has proved adequate for continued operation. A similar problem was encountered during the Intelsat-III mission. The lesson to be learned from these experiences is that single

Table 51
OSO-I Characterization Test Results

Voltage Limit Per Cell (V)	Time to Limit (min)	0°C		Time to Limit (min)	14°C		Time to Limit (min)	25°C	
		En. of Discharge Current (A)	Pressure (psia)		End of Discharge Current (A)	Pressure (psia)		End of Discharge Current (A)	Pressure (psia)
1.371				21	0.50	8.1	22	0.43	8.6
1.379				22	0.50	8.1	24	0.45	9.5
1.386				24	0.40	8.6	25	0.55	11.1
1.390				25	0.43	9.4	28	0.68	15.4
1.401				27	0.54	11.8	29	0.95	22.0
1.407				29	0.71	17.8	29	1.30	30.8
1.415				30	1.04	23.7	31		
1.415				31	1.28	31.3			
1.420			6.7						
1.426	22	0.50							
1.428									
1.436									
1.441	23	0.44	7.3						
1.442									
1.451									
1.457	25	0.47	8.9						
1.455									
1.472	25	0.58	12.8						
1.477									
1.485	26	0.63	16.8						
1.501	27	0.79	24.8						
1.514	28	1.04	36.5						

BVL control may not be adequate for missions beyond 2 years because it lacks flexibility to accommodate changes in battery characteristics, even when it otherwise contributes to a stable thermal balance.

The design of the battery-charge controls for the recently launched FLTSATCOM spacecraft is based on extensive accelerated life-cycle testing (Reference 187). Figure 106 shows the BVL family selected for this mission. Operation throughout the test has been at the fifth level counted from the bottom with recharge ratios of about 1.15. The mechanization used for flight hardware is somewhat different from the approaches described earlier. Full charge is performed at rates between C/12 and C/15 until the temperature-compensated voltage limit is reached, at which time the rate is switched over to a C/100 trickle-charge rate. Therefore, current tapering in the usual sense does not occur in this mode (Mode 1). A second selectable mode (Mode 2) provides tapered current operation, but with a switch-down to the trickle-charge rate at 27°C and switch-up at 21°C. The FLTSATCOM life test was conducted with only Mode 1 control, which will be the primary method of operation of flight battery systems. Mode 2 is considered to be a backup approach that permits higher recharge ratios at the expense of somewhat higher battery temperatures during overcharge. Mode 2 is similar to the approach used successfully for the 5- to 7-year operation of DSCS-II and DSP spacecraft.

8.3.3 Temperature-Limited Charging

The fact that the heat rate of a battery increases as it nears the fully charged state at constant current makes battery temperature a useful alternative to battery voltage for use as a signal that overcharge is commencing. Although some primary charge-control methods have been developed on this basis and applied, the constraints associated with the method have generally relegated its use to that of a backup-control option. One major problem is that it is difficult to predict and to verify the performance of charge controls designed for a particular application.

Battery charging is performed at maximum current rates during the first part of the charge period and is usually performed efficiently, particularly at low temperatures. As the full state of charge is approached, the process becomes less efficient and more of the applied energy is dissipated within the cells as thermal energy. As the electrodes warm, the electrochemical charge reaction becomes even less efficient so that, over a short time (approximately 0.5 hour), a temperature transient develops within the cell.

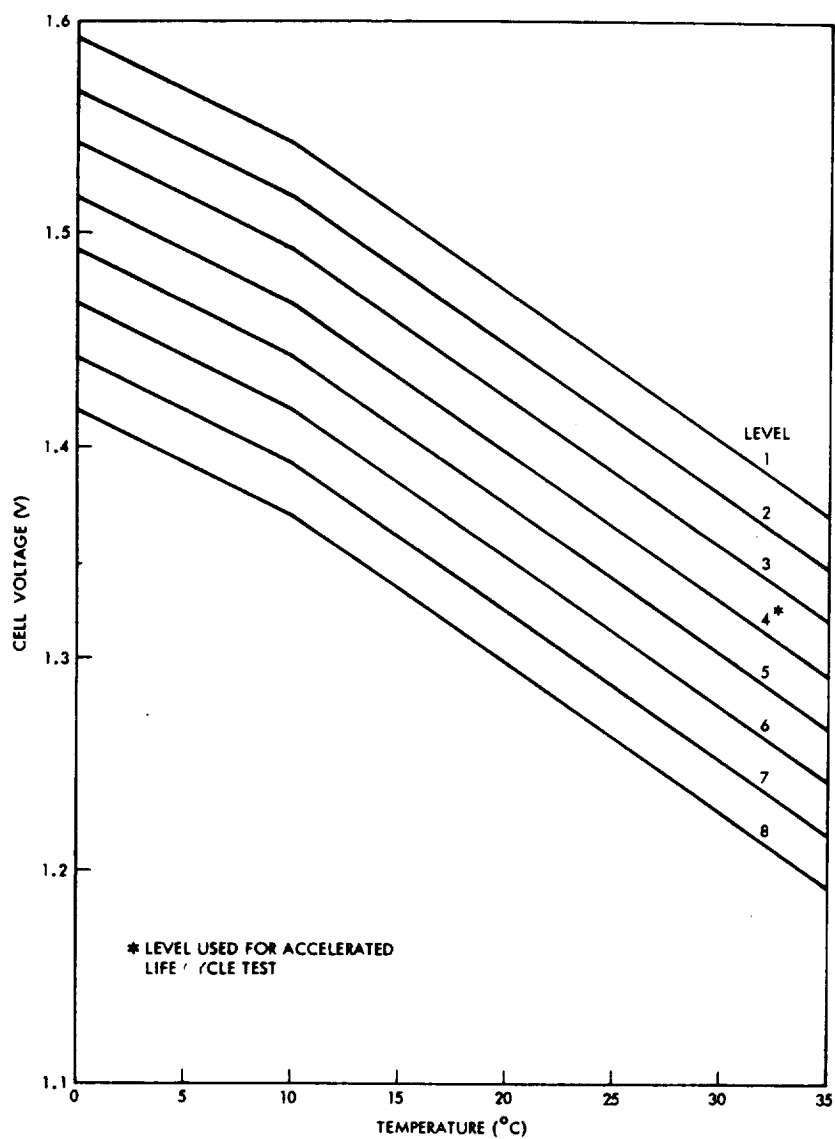


Figure 106. FLTSATCOM battery-voltage limits (cell-level presentation).

The magnitude of the transient is the difference between the mean electrode-stack temperature and the external surface of the cell container. The magnitude depends on the thermal time constant of the cell (primarily the electrode stack) and the forcing function (current). (See Section 7.4.1.) A temperature difference between stack and cell surface will always exist while heat is being generated within the cell. However, during the transient, the difference may exceed the steady-state differential temperature otherwise obtained during extended periods of overcharge. (If overcharge is performed at maximum rates, the average cell temperature will be significantly higher than the temperatures associated with the charge period.)

The effectiveness of using a temperature signal for primary charge control is therefore dependent on the thermophysical properties of the cell and the particular battery-system design application. It is assumed that the temperature sensor is either attached to the cell-container cover near the terminals or embedded in a thermal shim. Therefore, the effectiveness of the method is not necessarily dependent on the overall thermal design of the battery when that design is made to accommodate steady-state conditions of thermal dissipation. With short cycles and high-rate charging, which are usual for low-altitude orbits, there is not sufficient time for the electrode stack to absorb the heat produced and to exhibit a temperature rise before the end of the charge period. A considerable amount of oxygen may be evolved before the temperature signal is sufficient to cause a reduction of overcharge current. This time delay is essentially independent of cell size and is rather an intrinsic characteristic of the cell type. The time scales are much more favorable for long-period orbits, and, accordingly, these are the missions in which the temperature-limited charge-control method is used.

One version of the method that has been used on several military spacecraft permits a battery to charge at full rate until its temperature reaches 27°C. The current is then reduced to a trickle rate and maintained at that level until the battery cools to 24°C, when the full charge rate is restored. If the temperature of the battery reaches the switch point beyond the end of discharge, the discharged battery is automatically placed on trickle charge until it cools. In this application, the battery thermal-control system is designed so that battery temperature after maximum discharge does not reach the switch point.

The foregoing temperature limits reflect a compromise between a desire to maintain average battery temperatures at low levels and the realities of the particular missions and spacecraft configurations. Operation has proved

satisfactory for geosynchronous missions of 3 to 7 years with 40- to 55-percent depths of discharge. The charge controls are quite simple (figure 107). Discharge occurs through the closed relay contacts when the battery is below the thermal switch setting; otherwise, discharge is through the diode/resistor pair. Full charge occurs through the closed relay until the battery temperature limit is reached. When the relay is open, the resistor limits trickle-charge current. The battery is always connected to the bus through the diode to support peak discharges. A shunt regulator limits bus voltage.

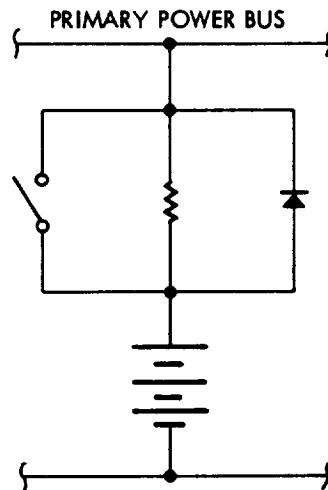


Figure 107. Controls for temperature-limited charging.

The temperature limits can be lowered if the battery's thermal-control system is adjusted to provide a lower average battery-operating temperature. Few data are available on the performance of temperature-limited systems operated at lower temperatures, although there is some evidence that a significant lag exists between the pressure buildup within a cell at cold temperatures and the measured increase in its temperature (Reference 51). This effect could cause the cells to exhibit higher average pressures as cycling proceeds.

Other mechanizations involving temperature have been suggested as a means for charge control. One approach is based on the measurement of the temperature difference between the battery and a reference point on the

spacecraft structure (Reference 264). With a known thermal resistance between the measurement points, the controller acts as a form of heat meter that is independent of reference temperature level. An increase in battery temperature because of overcharge may therefore be detected directly and may be distinguished from the effect of external heat inputs to the battery. Another approach involves the determination of rate and sense of temperature change. This implies the use of controls with a memory function that may now be practical with the advent of low-cost microprocessor technology.

Despite limited application as a primary method of direct charge control, the use of temperature as a control parameter is widely used as backup to other methods. Most charge-control systems, whether automatic or ground commanded, include overtemperature and undertemperature protection functions. Overtemperature protection usually involves placing the battery into a trickle charge or low-rate (reconditioning) discharge mode until its temperature has cooled to a second, lower limit. Overtemperature limits in the range of 30 to 45°C have been used with the upper limit to some extent—a reflection of past applications with high average battery temperatures. The selection of a value for an overtemperature limit is somewhat arbitrary because it is not usually a primary control parameter. However, sustained operation above 25 to 30°C has a strong negative effect on service life, and, beyond 40°C, the possibility of failure because of overpressure effects becomes significant. For these reasons, it is recommended that the overtemperature limit be maintained at or below 35°C.

Undertemperature protection ensures that the battery will not be operated at temperatures: (a) that are detrimental to its long-term performance characteristics, (b) that are beyond the range of the primary charge controller, or (c) that could produce immediate damage. The latter could result if a failure placed the battery in an open-circuited condition with no external source of heat. It would therefore cool at a rate dependent on the characteristics of its thermal-control system and could, in the extreme, reach temperatures at which electrolyte in its cells would freeze (< -60°C).

Undertemperature limits in the range of -5 to +10°C have been specified. When the limit is reached, heaters, which are usually located between the battery and its mounting surface, are activated. Normally, the heaters are powered only during certain trickle-charge periods when external sources of heat are reduced (e.g., when the battery's radiator receives no solar input). Battery heaters represent an additional power requirement that must be met by the solar array.

8.3.4 Pressure Limited Charging

This method is motivated by the fact that oxygen is evolved at an increasing rate as the point of full charge is approached and, depending on the rate of simultaneous recombination of the gas, a net pressure increase will occur within the cell. The rise in pressure can be used to generate a signal for charge control in one of two ways. When the pressure reaches a limiting value, the charge current can be switched from a high to a low, or trickle-charge, rate. Alternatively, the signal can be used to modify the shape of a temperature-compensated battery or cell voltage limit used for primary charge control. In either case, the effect is to provide a reduction in charge rate in response to pressure. However, the pressure within an otherwise normal cell may fluctuate to an extent that it may become difficult to use it as a signal source. Also, unknown accumulations of hydrogen tend to make total pressure-sensing unreliable as an end-of-charge indicator.

Cell pressure can be measured with a pressure transducer or gage or with an externally mounted strain gage (Reference 38). Neither method has been widely used in flight spacecraft. Pressure transducers have limited accuracy and repeatability at pressures near atmospheric ambient and are not sensitive to small changes in pressure. The installation of a pressure transducer means that a feedthrough must be installed in the cover, thereby possibly affecting the cell's reliability.

A strain gage bonded to the surface of a true pressure vessel will detect pressure changes within the vessel that are sufficient to cause surface deflections. Prismatic cells, which are usually packaged in a compressed stack, offer few surfaces appropriate for mounting a strain gage. Those that are available are usually the cover or the narrow sides and are quite stiff. Deflections at low values of pressure are small, making calibration of the gage difficult. Hysteresis effects interfere with the repeatability of the measurements.

An alternative to these methods involves the use of cells equipped with a third or auxiliary electrode that produces a current in proportion to oxygen pressure when it is connected through a resistance to the negative electrode. The voltage signal developed across the resistive load can be used to control charge parameters. The theory and design of auxiliary electrodes are discussed in Section 2.3.3.9. References 52 and 265 contain an example of detailed application. These references describe the development of auxiliary electrode controls that were used as a backup to the primary charge-control system of the Orbiting Astronomical Observatory battery. Reference 49

describes the characterization and development of primary charge controls using auxiliary electrode signals for the Skylab Apollo Telescope Mount (ATM) power system. References 266 and 267 describe other uses of third-electrode cells in primary charge-control applications. In all cases, the work applied to low-altitude Earth-orbit applications.

Cells equipped with auxiliary electrodes will provide service in the geosynchronous orbit on board the International Ultraviolet Explorer (IUE) Spacecraft (Reference 93). Considerable data and experience have already been obtained with similarly equipped cells as part of the development of an advanced geosynchronous orbit battery for the U.S. Air Force (Reference 51). Implementation was unusual in that every cell was equipped with an auxiliary electrode that was used to control the level of a temperature-compensated voltage limit dedicated to the cell. This forward bypass circuit thus provided effective closed-loop control of two parameters at the cell level: overcharge current and pressure—both as function of temperature.

Despite the efforts cited, pressure sensing and control with an auxiliary electrode are at a less advanced stage of development than some of the methods of charge control described in earlier sections. Although cell manufacturers have provided cells with functional third electrodes, the nature of their designs have not been investigated rigorously, and uniform specifications have not been developed or applied. Differences between third-electrode cells made by various suppliers are not well understood. Available characterization data have been taken for only a relatively small population of cells. Life-cycling test data and flight experience generally show that auxiliary electrode performance is unstable over long periods and, in particular, following changes in battery-system operating conditions.

Certain application problems must be considered before selecting this method of charge control. First is the question of the variation of pressure characteristics between cells in a battery. Under normal conditions, a wide range of pressures will be obtained; yet a single cell, equipped with an auxiliary electrode, will provide total charge control based only on its own performance. There is also the question of cell-to-cell variations in the sensitivity of the auxiliary electrode to pressure. The charge controls must provide for initial adjustment to compensate for these variations. Throughout a mission, the sensitivity to pressure may change because of certain phenomena (e.g., electrolyte redistribution within the cell). (It is assumed that the behavior of the negative electrode of the cell, to which the auxiliary electrode is referenced, is normal throughout the mission. Little is known about the interaction between the negative and auxiliary electrodes over

long periods of cycling.) Finally, there is the question of the behavior of the auxiliary electrode as a function of temperature when it delivers current to a fixed value of load resistance. There appears to be little doubt that uniform behavior can be obtained within a narrow temperature range with repetitive cycling by proper selection of a resistance value. But, if the temperature increases, the sensitivity to pressure with a fixed-load resistance may decrease even though the auxiliary electrode itself tends to exhibit increasing sensitivity with increasing temperature when properly monitored. The net effect is one of self-compensation because the oxygen-recombination rate is higher at higher temperatures. Nevertheless, adjustment of the load resistance should be considered if the range of control is to be extended beyond a narrow temperature regime. (See also Section 3.4.1.4.)

For these reasons, the auxiliary-electrode charge-control technique cannot be considered so much more advantageous than other charge-control methods as to warrant its use as a primary method of control without other types of backup controls. As more is learned about specifying and producing third-electrode cells and as improved circuits are developed for compensating for changes in auxiliary-electrode characteristics caused by long-term cycling effects and temperature variations, this situation may change. Until then, the method should be generally restricted to the following circumstances:

- a. Batteries operated with repetitive cycling between 0 and 15°C—The nickel-cadmium system is most sensitive to overcharge current in this regime.
- b. As a method of augmenting the primary charge-control system—The auxiliary-electrode controls should be set so that they do not interfere with the normal range of recharge-ratio adjustment provided by the primary controls.
- c. With other means provided for limiting the generation of hydrogen—The oxygen-signal characteristics are believed to be affected by the presence of significant amounts of hydrogen.
- d. Minimal effect on battery-system reliability—If the battery contains only one cell equipped with an auxiliary electrode and its proper charge control depends on that cell's performance, there will be a significant effect on battery-system reliability if the cell or the auxiliary electrode fails.

- e. As a technique for monitoring the characteristics of a battery in orbit—Useful information regarding the typical performance of cells may be obtained through the telemetry system.

The decision to incorporate auxiliary-electrode controls into a battery system should be made with clear objectives in mind. Item e may be reasonable enough because the data obtained are useful in determining the effect of charge management procedures instituted in response to changes in battery performance throughout the mission (Reference 50).

8.3.5 Recharge-Ratio Control

Of the four methods described, two (temperature-limited and pressure-limited control) do not generally permit direct adjustment of the recharge ratio. Automatic versions of single-limit constant-current controls do not provide for such adjustments. The voltage-limited or ground-controlled dual-limit constant-current methods do, however, and that explains their wide use.

In all automatic systems in which recharge-ratio control is obtained, it is accomplished by indirect means, such as the switching to a different voltage or current limit. Therefore, values of recharge ratio are provided in steps that cannot be accurately predicted beforehand. Each step corresponds to a new equilibrium condition for the cycle in response to changes in state of charge and temperature. This granularity is usually not a problem with voltage-limited control based on the use of a family of BVL's. However, the effect of changing a constant-current limit can be significant.

A more direct method of recharge-ratio control is to perform an ampere-hour integration with respect to time to determine the specific point of charge cutoff. (Charge cutoff is defined as a reduction of charge current to zero or to a trickle-charge level that, under subsequent charging, has little additional effect on the recharge ratio.) The integration is required for discharge, as well as charge, with the values retained for computation of the recharge ratio. The calculations may be performed by either ground-based computer using telemetered battery current, voltage, and temperature data or an on-board ampere-hour meter. The former approach is practical for geosynchronous applications with dedicated ground stations, whereas the latter is necessary for low-altitude missions or for interplanetary spacecraft. On the OAO-2 and -3 spacecraft, an ampere-hour meter was connected to each battery. A self-contained ampere-hour meter was also used aboard the

Skylab Airlock Module for both charge-control and monitoring functions. This meter is discussed at the system level in Reference 219 and described in detail in Reference 229.

Both the development of advanced on-board computers and the current expansion of microprocessor technology open new avenues for developing compact, low-cost, "smart" charge controls. Reference 268 surveys the prospects for Earth-orbiting spacecraft and Reference 269 considers specific approaches applicable to interplanetary missions.

One limitation to using direct methods of recharge-ratio control is the requirement for battery performance data in a format that correlates recharge-ratio values with discharge/charge cycle parameters, operating mode (cycling or storage), temperature, control parameters (current voltage and pressure), and service history and time. To use the method in a primary charge-control mode, these data must be obtained by extensive cell characterization and life-cycling tests. Even when the method is used as an adjunct to the primary controls, some testing is necessary for verifying the recharge-ratio criteria planned for mission operation. This was indeed the case for the Skylab applications (Reference 49).

Another issue involves the question of measurement and computational accuracies. In the future, the former may be of more concern than the latter, particularly with the availability of dedicated on-board ampere-hour meters that are independent of spacecraft processors and data-bus configurations. Low-loss accurate current sensors are required with the capability of measuring a wide range of currents on both charge and discharge. The capability to accurately measure other battery parameters will be key to the full realization of the potential of this method.

8.4 METHODS OF CELL AND BATTERY PROTECTION

The degree of protection a battery cell may require is directly proportional to increasing depth of discharge, temperature, and mission length. As these parameters increase, the possibility of overdischarge or overvoltage on charge also increases. Protection from the effect of these stresses takes the form of either circuitry designed to limit currents through the affected cell when either degraded condition develops or battery-level charge management decisions based on voltage-current measurements made at the

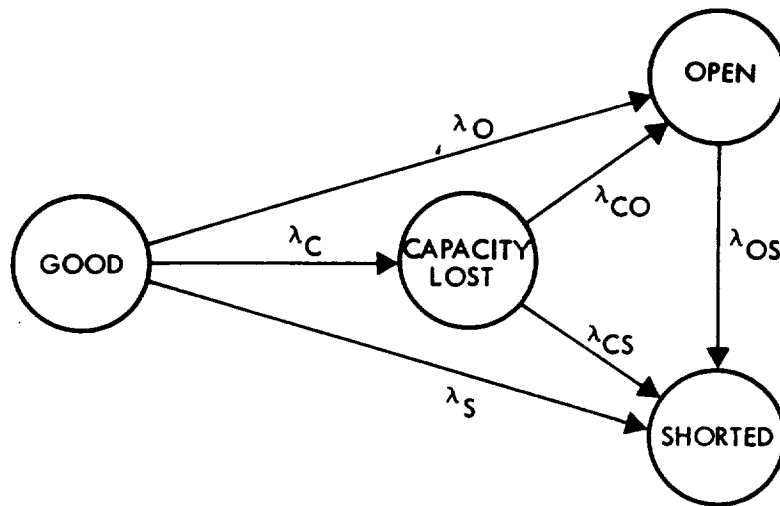
cell level. When properly implemented, either approach ensures that excessive pressures do not develop in a failing cell that might otherwise lead to rupture of the hermetic seal and consequent leakage of cell gasses and/or electrolyte.

At the battery level the term "protection" is used in a somewhat different sense. Avoiding overpressure within the cells is still a major concern. However, in the absence of specific cell-level protection against such effects, it is common practice to size the battery system conservatively and to provide sufficient charge-control capability so that cell overpressure becomes improbable. Battery-level protection, instead, refers to provisions in the battery or battery-system design that accommodate the effects of an open-circuited cell or one or more short-circuited cells. Both types of failures represent a far greater potential loss of available battery-system capacity than the partial failure of one or two cells when the cells are individually protected. The accommodation of open-circuit failures may be in the form of either additional (redundant) batteries or a simple bilateral network that bypasses current around the defective cell. The accommodation of complete short-circuit failures requires no special provisions other than ensuring that the battery system is initially designed to maintain the voltage of the primary power bus above its specified minimum value if such failures occur. The accommodation of partially shorted cells—an issue of greater complexity—is discussed in subsequent sections.

8.4.1 Failure Modes and Protection Requirements

Battery cells are prone to any of three general modes or states of failure: (a) short-circuit (zero impedance), (b) excessive capacity degradation manifested as reduced cell terminal voltage (finite variable impedance), and (c) open circuit (infinite impedance). Figure 108 illustrates the transition from a state of "good health" to one or more of these states of partial or full failure (Reference 270). Six transition paths are realistically possible.

The strong left-to-right progression from state to state is not meant to imply that states "to the right" exclude the types of failure associated with states "to the left." For example, in a capacity-lost-to-opened transition, it is not assumed that the cell regains capacity. Rather, all failures are assumed to be permanent. It is assumed in each case, however, that the effect of the succeeding state on the terminal characteristics of the cell will dominate those of all preceding states. Thus, if a cell has lost capacity and then suddenly experiences an open circuit, the open condition is assumed to govern the cell's behavior.



λ IS A MARKOV TRANSITION RATE

Figure 108. Cell-state transitions.

This assumption appears to be reasonable on physical grounds for each of the transitions shown in figure 108. For example, consider the open-to-short transition. Opens will normally be caused by excessive impedance in the ionic conduction path between plates (e.g., drying-out of the separator), whereas a cell short is most likely to be caused by some inadvertent conducting path between plates (e.g., fragmented sinter material) that bypasses the ionic path. Therefore, if a cell has experienced an open and then becomes shorted, the short condition should dominate. Similarly, the left-to-right character of the permissible state transitions of figure 108 is not meant to imply that right-to-left transitions are physically impossible. However, under the foregoing assumption about dominance of terminal characteristics, such transitions would not affect the performance of the cell.

If a cell suffers a complete short circuit, conduction through the cell is ohmic, and no electrochemical reactions occur. In particular, a completely shorted cell will not exhibit voltage or pressure effects associated with overcharge or overdischarge. Therefore, the cell does not require or benefit from self-protection circuitry. However, this failure mode is rarely seen in pure form.

Most cell failures fall into the capacity degradation class, and nearly all cell failures exhibit some behavior associated with this class as the transition is made from a state of good health to a state of failure. (Note, however, that improper charge control and/or cell design may also produce symptoms similar to those observed for cells with states within the capacity degradation class.) These cells continue to behave as electrochemical devices and are capable of overcharge and overdischarge reactions in varying degrees. Some form of cell protection may therefore be required to accommodate such partial or complete failures if the battery-system design requires operation with failures present.

If a cell develops a complete open circuit,* the battery containing the cell is lost unless there are provisions for bypassing discharge and charge currents around the affected cell. This failure mode is rarely seen in pure form but is probable enough to warrant consideration in developing the design of long-life battery systems.† The presence of cell-level or battery-level redundancy is usually sufficient to accommodate the open-circuit failure mode.

8.4.2 Battery-Level Redundancy

Two or more parallel-connected batteries are used for most low-Earth-orbit (LEO) missions. Redundancy is provided in the form of extra batteries. If cell failures occur, the affected batteries are removed from service, and those that remain share operation at deeper depths of discharge. The battery system is always sized to accommodate the event—however unlikely—that enough failures occur at the beginning of the mission to effectively eliminate redundancy for the remainder of the mission. The value of maximum depth of discharge selected for the sizing calculation is determined by cycle life characteristics and battery-system reliability considerations.

Battery systems used in LEO missions may experience from 500 to 30,000 discharge/charge cycles in typical applications, with most missions falling within the range of 3,000 to 10,000 cycles. Thus, in general, the maximum depth of discharge for LEO missions is constrained to shallow levels. (See Section 8.7.4.) At or above these levels (for systems with all batteries in

*This includes the condition of high internal impedance caused by loss of electrolyte from the separators.

†A survey of failure-mode distribution data conducted by TRW in 1977 revealed the following breakdown: capacity degradation: 72.5 percent; short circuits: 22.0 percent; and open-circuits: 5.5 percent.

service), a failing cell is unlikely to reverse in voltage during discharge so abruptly that the event remains unnoticed during routine examination of battery telemetry data. In the past, this has been an important consideration because, with notable exceptions, batteries in LEO spacecraft have been operated at warm temperatures, which would contribute to overpressure effects during reversal. Also, the LEO spacecraft can be out of sight of a ground station for several successive orbits.

The situation is similar for higher orbits with longer eclipse and orbit periods but with fewer discharge/charge cycles. In these orbits, batteries are operated at greater depths of discharge and for longer mission times. Consideration must therefore be given to the margin between the specified value of maximum depth of discharge (with no redundant batteries remaining in service) and the expected capability of the nickel-cadmium system as demonstrated by life-cycle tests and orbital performance measurements. If too little margin is provided, cell reversals will probably occur during normal discharges near the end of the mission. At the present time, there is no general agreement regarding an appropriate value for this margin. The single published guideline was developed in 1973 for general application to U.S. Air Force geosynchronous spacecraft (Reference 271). It suggests reducing the expected (mean) cell cycle-life characteristic curve—determined by analyzing observed data—by approximately 20 percentage points over a 40- to 70-percent range of depth-of-discharge values to derive an acceptably safe value of maximum depth of discharge. However, the work leading to this recommendation was necessarily qualitative because applicable data were sparse, and the study did not consider the effect of reconditioning or, in a parametric sense, the effect of operating temperature. Although more data are now available, comprehensive analyses have not yet been reported that define geosynchronous service life capability as a function of maximum depth of discharge, temperature, cell configuration, reconditioning policy, and charge-control method or the confidence limits associated with the definitions. Furthermore, the capability definitions based on accelerated life-cycling tests and limited orbital data must eventually be reconciled with real-time performance data if a high level of confidence in the capability definitions is to be achieved. Until these tasks are performed, estimates of life capability and margin will be based on engineering judgment supported by the analysis of the trend of available test and flight data.

The preceding discussion provides a brief overview of the state of affairs concerning the evaluation and prediction of geosynchronous battery mission life and reliability. Various approaches are reflected in the recent literature, and it is evident that they are being formulated in response to: (a) particular customer concerns and requirements, (b) the availability and quality of test

and flight data, (c) the variability of cell-design features from project to project, and (d) a general awareness that certain cell materials and manufacturing processes may have inherent limitations in terms of meeting long-service lifetime requirements.

Certain issues have been thoroughly discussed throughout the industry. In the applications area, the beneficial effect of low-temperature operation of batteries in both low- and high-altitude orbit applications has received widespread acceptance on the basis of an overwhelming amount of flight and ground test data. Other issues are being investigated and discussed. For example, the effect of reconditioning and the definition of correct reconditioning procedures and schedules are under debate. In the area of cell design, some investigators contend that improvements in performance and reliability might be obtained if a cell were specifically developed for geosynchronous applications and, in particular, for long-life service. This general situation is reflected in table 52, which summarizes views expressed by representatives of several battery-system developers at the 1976 Goddard Space Flight Center Battery Workshop. This table shows the diversity of opinion in the industry regarding expected capabilities and design guidelines based on the expectations.

8.4.3 Cell-Level Redundancy

Individual battery cells may be equipped with circuitry designed: (a) to accommodate an open-circuit failure, or (b) to protect the cell or its battery from the effects of overdischarge and/or overvoltage on charge if it should develop. If item b is completely satisfied, item a is also satisfied, but the reverse situation is not necessarily true. On Intelsat-IV spacecraft, open-circuit failures are accommodated by bypassing each cell with diodes in both directions (Reference 210). Intelsat-V spacecraft batteries will also be protected against open-circuit cell failures and will include provisions for measuring individual cell voltages. Intelsat-III battery cells had reversal protection circuits (Reference 212). The FLTSATCOM batteries have circuits that protect against both overdischarge and overvoltage on charge. A brief survey of other applications of cell and battery protection circuits appears in Reference 272.

Table 52
Geosynchronous Battery-Capability Limits Circa 1976 (Reference 46)

Mission Length (years)	Percent Depth of Discharge Based on Rated Capacity			Operating Temperature Range (°C)	Battery-System Developer	Battery Reconditioning Policy ¹
	Guideline Maximum	Flight Application	Expected Capability			
7	50 to 60			10 to 25	Philco-Ford	High-rate SDR
6 to 7			55 ²	4 to 17	Hughes	SDR
8		58		2 to 15	RCA	High-rate DDR
10	75		75 to 85 ³	5 to 15	TRW	Low-rate DDR

¹ Shallow discharge reconditioning (SDR) or deep discharge reconditioning (DDR); see Section 3.4.4.

² Percent of actual capacity.

³ See also Reference 49.

8.4.3.1 Open-Circuit Failure Protection

The simplest form of open-circuit protection involves the use of diodes connected in parallel with the cell to permit the passage of charge and discharge currents. A single diode is sufficient in the discharge direction. Under conditions of normal discharge, it does not conduct. If the cell develops an open circuit at any time during discharge, the diode will conduct all of the battery current with a forward voltage drop determined by the device itself. Battery terminal voltage is reduced by an amount that is equal to the sum of all normal cell-voltage contributions lost to open-circuit failure and of all forward voltage drops of the discharge bypass diodes that are forced to conduct.

A somewhat similar situation exists during charge. Here, however, it is necessary to use multiple diode junctions in series to obtain a forward characteristic that does not limit normal charge currents by limiting the cell's voltage. Thus, when silicon diodes are used, it is necessary to have three in series because the forward voltage of each device is typically in the range of 0.6 to 0.8 volt, and the cell must be permitted to charge in the vicinity of 1.5 volts. With normal cell operation, a negligible amount of charge current is bypassed.

If a cell develops an open circuit, the charge bypass diodes will conduct all of the charge current. The battery terminal voltage will increase an amount (for each bypassed cell) equal to the difference between the total forward voltage drop of the diodes and the normal cell voltage contribution that is lost because of the failure. This significantly affects the selection of battery-level temperature-compensated voltage limits if such a scheme is used for charge control. For example, if a single voltage limit is used, a cell failure will cause the limit to be reached earlier, thereby reducing battery recharge.

Accommodating thermal dissipation in the diodes when they are conducting is an important design consideration. The instantaneous dissipation within a discharge diode is about 3.5 times as great as within an unfailed cell that carries the same current. This establishes the design requirement for a thermal shim if it is used to control both cell and diode temperatures. Discharge diode dissipation is always greater than the dissipation in a single-charge diode. Cell discharge dissipation is always greater than the cell dissipation obtained during trickle charge and is nearly always greater than the heat generated during overcharge at safe current rates. In general, paralleling diodes to reduce thermal dissipation is not feasible because of inevitable differences in forward I-V characteristics and junction temperatures.

Although other passive devices have been suggested as replacements for the silicon diode to achieve a reduction in thermal dissipation, they suffer in comparison. For example, germanium devices exhibit a lower application temperature range, higher reverse leakage currents, and less radiation resistance. Schottky-barrier power rectifiers have been considered because their forward voltage is in the range of 0.3 to 0.6 volt. However, they are less reliable than silicon diodes and may be more reliable than the battery cells they are meant to protect.* Also, Schottky devices have reverse leakage currents in the mA range rather than in the nA range, as is the case with most good silicon P/N junction diodes.

8.4.3.2 Active-Element Failure-Protection Circuits

Active-element failure-protection circuits, usually referred to as active-bypass circuits, provide cell-level redundancy in an equivalent sense. The circuits act to either place a low-impedance path around a failing or failed cell or limit the cell's voltage in the overdischarge or overcharge regions. An example of the former is the use of a single-pole double-throw (SPDT) relay to disconnect and bypass a cell from its battery, leaving the cell's terminals open-circuited (Reference 273). Another example is the installation of a single-pole single-throw normally open relay across each cell to provide a current path on relay closure. Design considerations in such applications include selection of adequate relay contact ratings and circuit application procedures (Reference 274), circuit power consumption (i.e., if magnetic self-latching devices are not used), electrical state indication provisions, relay performance in vibration, and shock environments, weight, and volume.

Relay protection implies significant added battery weight because large relays are usually required to handle the maximum expected discharge current. A designer is usually faced with two specific considerations: (a) contact life at nominal current ratings, and (b) limitations on the maximum current-carrying capability of the contacts. Derating policies normally applied to power relays, particularly in battery-control applications, tend to limit the choice to relays of the largest space-qualified size.

*The usual failure mode of all diode types is a short circuit through the junction, possibly followed by an open circuit if sufficient power is available to burn the short open. The metal semiconductor barrier at the junction of the Schottky tends to diffuse into the silicon. This effect is undesirable and leads to a higher incidence of short circuits.

Active bypass circuits usually limit cell voltages in the overdischarge or overvoltage on charge regions by linear control of current passed through a shunt transistor placed in parallel with the cell. On overdischarge, the limit is set within the range of -50 to -200 millivolts. That is, the protected cell is not permitted to reverse in voltage on discharge to a value more negative than the preset limit. The extreme limit of -200 mV is usually associated with values of cell current at the threshold of the range of currents that contribute to rapid pressure buildup when the cell reverses. The relationships between reversal voltage, overdischarge current, temperature, cell design and construction, age and service history, and failure pathology are not amenable to exact description. Much of a cell's behavior during reversal depends on: (a) the amount of residual available capacity in the negative electrode when the positive electrode is exhausted,* and (b) the physical causes of the capacity degradation process. A reversed cell will pass a specific value of discharge current when its voltage is limited to a particular value, but the exact value of current cannot be predicted with a high level of confidence in the statistical sense. When the discharge bypass circuit is properly designed, it will pass the majority of the discharge current; however, characteristics of the cell always determine the ratio of the shunted current to the cell current.

Hydrogen is generated during early reversal with the maximum theoretical rate given by

$$\frac{\Delta P}{\Delta C_{od}} = \frac{3600 RT}{2 VF} \quad (50)$$

where

ΔP = pressure increment ($\text{kN}\cdot\text{m}^{-2}$)

ΔC_{od} = overdischarge capacity increment (Ah)

3600 = seconds per hour

R = gas constant ($8.314 \text{ J}\cdot\text{K}^{-1} \text{ mole}^{-1}$)

T = absolute temperature (K)

2 = number of electrons per molecule of generated hydrogen

*A positive-limited cell configuration is assumed.

V = cell void volume (m^3)

F = Faraday's constant ($9.65 \text{ E}+04 \text{ A}\cdot\text{s}\cdot\text{mole}^{-1}$)

Observed rates are generally below the theoretical, leading to the hypothesis that hydrogen recombination takes place at low but measurable rates during overdischarge (Reference 12). Some experimental work indicates that deliberate reversal of unfailed cells—as might occur toward the end of a low-rate deep-reconditioning discharge—can be accomplished with stable cell pressures below 30 psig if the current through the reversed cell is maintained at sufficiently low rates:

- New 24-Ah General Electric cells: C/120 to C/60
- New 12-Ah SAFT-America cells: C/260 to C/130
- Extensively cycled 12-Ah SAFT-America cells: C/130 to C/65

If the cell reversal voltage is limited to -50 mV or is held more positive, cell currents in these ranges are realizable (Reference 275).

If a cell is permitted to overdischarge at normal rates, the negative, as well as the positive, electrode will usually be eventually discharged and the reverse potential will reach -1.3 to -1.5 volts. Both oxygen and hydrogen will be generated, and internal pressures of several hundred psi will be observed if terminal seals have not otherwise leaked or the cell case has not ruptured. The intermediate region between -0.2 and -1.3 volts is associated with rapid pressure buildup at normal discharge rates and should also be avoided.

It has been suggested that no two cells will exhibit identical behavior in the reversal region because of individual differences and, usually, because of diverse reasons for degrading to the failed condition. Cells seldom reach a state of failure in swift, dramatic fashion; the degradation is gradual over many cycles. In any particular discharge, the failing cell may contribute some energy before it reverses. Even if relatively high currents are present within the cell, whether or not it is protected, the period of gas evolution may be only a fraction of the total discharge period. The literature does not report simulations of the cumulative effect of gradual cell degradation.

Analysis of the effect is difficult and can be accomplished only under rather restrictive assumptions and constraints. It is reasonable to believe, however, that the rate of pressure buildup within a failing cell will double in proportion to the rate of degradation. If discharge bypass protection is provided, the model will have a sigmoid (s-curve) shape.

The active-discharge bypass circuit should be capable of shunting the maximum expected value of battery-discharge current without reaching saturation, with accompanying loss of control of the voltage limit. The effect of cell failures should be considered in calculating maximum discharge current. In a multiple-battery system, a maximum number of tolerated cell failures are usually specified for each battery. The mechanical packaging of the power-handling elements of the bypass circuitry must include adequate provisions for thermal control if failures occur in adjacent cells within the same battery. Power for transistor drive circuits and reference circuits should be derived from a stable external source. The use of adjacent cells to provide auxiliary power is not recommended because the simultaneous reversal of two electrically adjacent cells will result in a loss of protection for one of the cells.

A similar approach has occasionally been used for overcharge protection. A separate shunt transistor with its own reference and control circuitry is used for current bypass. For adequate protection, it is necessary to provide a temperature-compensated voltage limit. The voltage limit is usually designed to prohibit excessive generation of hydrogen during overcharge, particularly at temperatures in the vicinity of 0°C. (See figure 31.) When the charge-control system utilizes a family of temperature-compensated battery-voltage limits, the higher levels may permit high battery-level charge voltages at cold temperatures. With such a condition, hydrogen evolution at or near full charge rates may occur in one or more high-voltage cells. The situation is aggravated by the tendency for the range of individual cell voltages to increase at cold temperatures. The cell-level overcharge protection feature acts to limit this condition. This approach is not required in low-altitude orbit applications (depth of discharge < 20 percent) that utilize BVL families set low to control overcharge.

8.4.4 Cell Parameter Sensing

Longer missions and the use of greater depths of discharge have combined to create a desire on the part of battery, system, and operations engineers for more battery-performance information in greater detail. At the time of

this writing, it is understood that at least three future geosynchronous spacecraft (Intelsat-V, Tracking Data Relay Satellite, and the Satellite Business Systems Satellite) will include provisions for monitoring and continuously telemetering cell-level voltage measurements. In all cases, the data will be used not only as an alternative to active cell-level protection, but also as an integral element of the battery charge-control system. Short- and long-term operating procedures will be based on periodic analyses of the I-V data received at the spacecraft ground-control station. If a cell exhibits undervoltage on discharge or overvoltage on charge, a scenario involving load and charge management of the affected battery will be developed to maximize its energy contribution while ensuring that the cell and battery are operated safely.

Certain questions naturally arise regarding this approach to cell protection and battery charge control. Foremost among these is whether sufficient information can be obtained from normal battery telemetry data to permit correct charge-management decisions. Figure 109 shows a TRW estimate of the variation in end-of-charge cell voltage that may be experienced by one or more cells in a battery operated from -5 to $+5^{\circ}\text{C}$ for 10

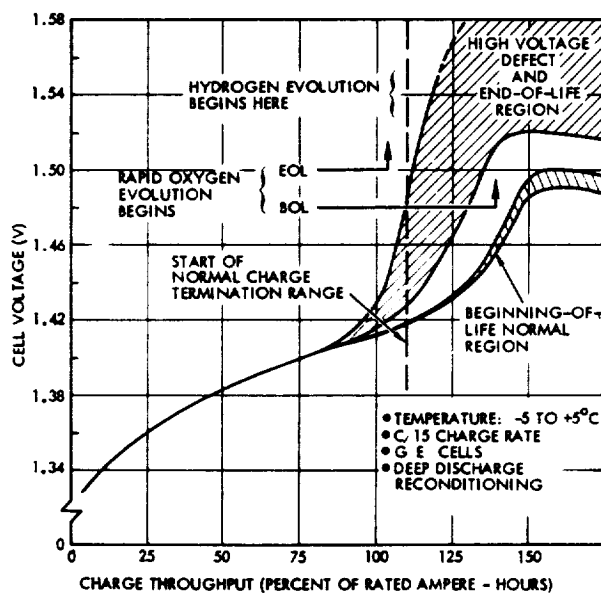


Figure 109. Cell-level charge-voltage characteristics predicted for a 10-year life.

years. The estimates are based on real-time geosynchronous tests at 0°C conducted at NWSC/Crane (packs 203A, 205A, and 206A) and on data from the U.S. Air Force Aero Propulsion Laboratory (USAF/AFAPL) Long-Life Battery Advanced Development Project.

The beginning-of-life (BOL) curve represents a recharge from a shorted condition. The charge throughput required to reach the point of rapid voltage rise is therefore greater than that required during continuous cycling above 1 volt. However, the relative position of the curves on the voltage scale is believed to be valid for normal eclipse-season cycling.

It is seen that a minimum increase in end-of-charge voltage of 0.02 volt per cell is predicted, with the maximum increase being of the order of 0.1 volt. Voltages at which rapid oxygen evolution may begin at BOL and end of life (EOL) are indicated to show the onset of pressure rise. At EOL the oxygen-evolution voltage is closer to the hydrogen-evolution voltage than at BOL. This assertion is based on the assumption that the oxygen overvoltage on the positive electrode remains approximately the same throughout life and, hence, that the change in cell voltage is due mainly to a shift of the potential of the negative electrode at end of charge.

Figure 110 shows the corresponding battery terminal-voltage characteristics during charge of a 24-cell battery. The two upper solid curves bound the region of uncertainty in predicting the average and distribution of cell voltages at the end of 10 years in orbit. It is assumed that only a fraction of the cells will show high voltage in the worst case. The range of uncertainty of battery voltage at EOL in the region of recharge ratio of interest (100 to 130 percent) is seen to be about 0.5 volt. The dashed curve shows one example of a characteristic that could result from a number of combinations of cell voltages and voltage distributions, two of which are indicated on the figure 110. More than one cell at higher voltage would produce other curves within the uncertainty band. Therefore, even if the battery-voltage sensor and telemetry channel were capable of essentially "infinite" resolution, one or more high-voltage cells could not be distinguished from a smaller increase in average cell voltage by observation of the battery terminal voltage on charge.

We now consider whether voltage degradation on discharge can be detected by monitoring battery-terminal voltage. Figure 111 shows various typical cell discharge-voltage curves, each with a single discharge. These curves were synthesized from the aggregate of real-time available synchronous-orbit data. Curve A represents cells early in life, whereas curves B, C, and D

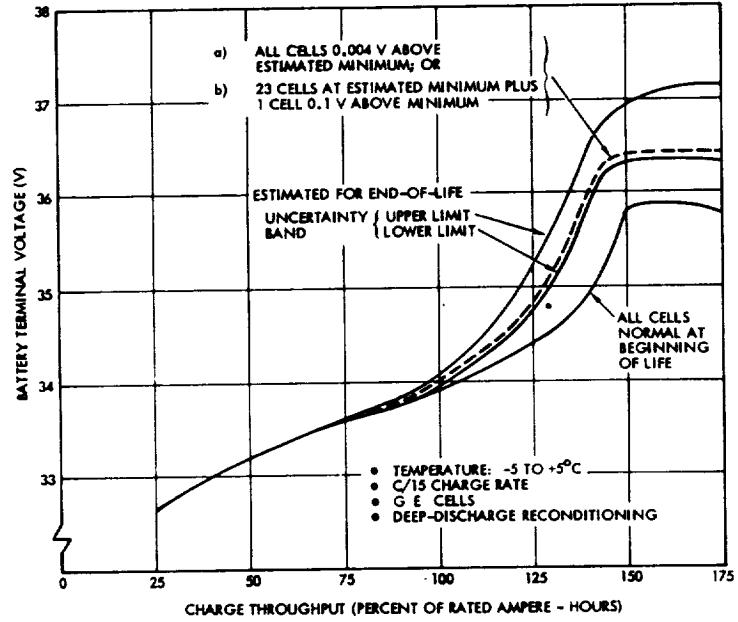


Figure 110. Battery charge-voltage characteristics predicted for a 10-year life.

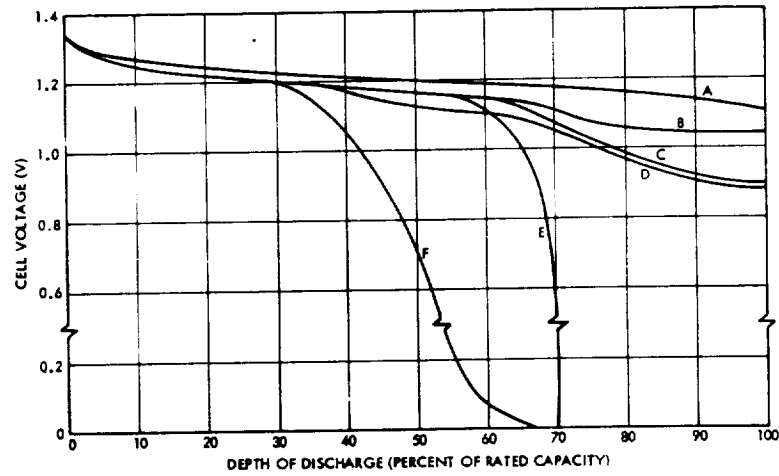


Figure 111. Cell discharge-voltage characteristics.

represent three cases of typical cell-voltage behavior projected for a 7- to 10-year service life. Curve B is believed to be much more probable than curves C or D when cell processes are normal and when low-rate deep-discharge reconditioning is used regularly. The point in the discharge at which the curves begin to fall below the plateau is uncertain; early incidents (curve D) have been observed. This type of voltage degradation is often seen under the expected operating conditions and has even been observed after reconditioning, but to a lesser extent.

Curves E and F show two ways that a few cells have reached zero volts during an eclipse-season discharge (other than when the cell is internally shorted). For this analysis, it is assumed that the cell voltage levels off within the normally observed range of 0 to -0.3 volt.

Figure 112 shows several examples of 24-cell battery voltage resulting from the more probable distributions of cell voltages. It is seen that, when no cells are shorted, the discharge voltage at the beginning of discharge does not change much throughout life, but the decrease in voltage at the end of discharge increases as cycling increases. On the other hand, if a cell is shorted, the discharge voltage begins immediately at about 1.3 volts lower

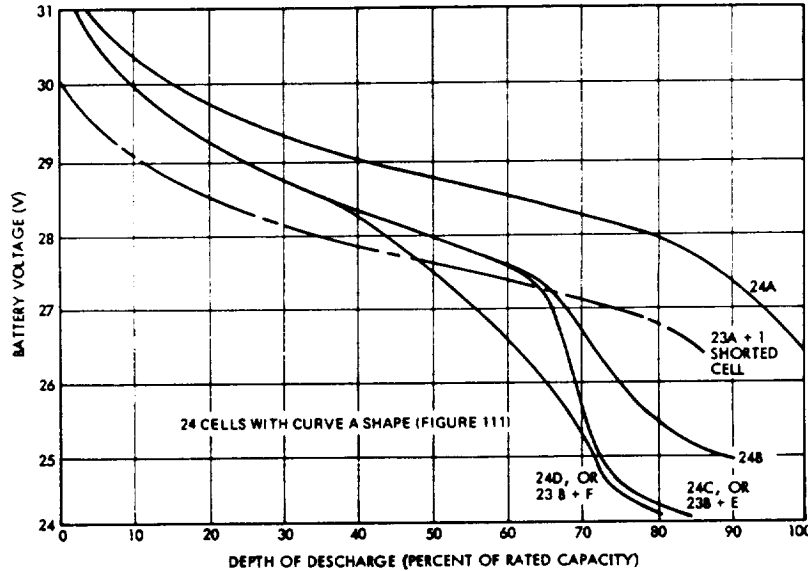


Figure 112. Battery discharge-voltage characteristics.

than normal and continues at about 1 volt below normal throughout the discharge. Therefore, if the battery voltage were to be followed closely by telemetry throughout a complete discharge before and after the occurrence of a shorted cell, it should be possible to detect such a short by comparing the two curves. If only a spot check of voltage near the end of discharge is made, the effects of a short could not be distinguished from those of other forms of cell-voltage degradation, as indicated by the intersection of the broken curve with all three of the lower solid curves in figure 112.

It would appear that, if a cell in the battery behaves as shown by curve E or F (figure 111), it could be easily detected by watching the battery terminal voltage. Abrupt as the cell-voltage change may be at the end of discharge, the effect on the battery terminal voltage characteristic will not be distinguishable from that resulting from a number of other, more probable cell-voltage distributions. As shown by the lower two solid curves, the battery-voltage curve resulting from all 24 cells discharging on curve C is practically identical to that for 23 cells discharging on curve B and one cell on curve E. Similarly, the battery terminal-voltage curve for all cells discharging on curve D is practically identical to that for 23 cells on curve B and one cell on curve F detected by monitoring these currents. With multiple batteries whose output terminals are connected at a common point, the current-sharing characteristics under these conditions will be no more useful than battery terminal voltage for distinguishing between one cell reversing on overdischarge and a large number of cells in a battery going to some slightly lower than usual voltage at end of discharge. It is therefore concluded that, regardless of the fineness of resolution of the battery voltage and current telemetry from spacecraft to ground, overdischarge of an individual cell with degraded capacity cannot be reliably detected in a battery that has operated for a few years simply by observation of battery terminal voltages and currents. Cell reversals and possible further damage to degraded cells cannot be reliably prevented by management from the ground on the basis of such data alone.

A related issue concerns the question of whether a small number of battery-voltage sensing points, or taps, can be used to provide data for battery-control decisions. It can be shown analytically that taps at the first cell, or at the quarter- and half-battery points (referenced to the grounded terminal), may provide voltage measurements of sufficient accuracy to permit detection of an anomalous cell within the group. However, above the half-battery point, the probability that a defective cell will remain undetected increases dramatically. Therefore, the use of a limited number of sensing taps does not provide information that is uniformly complete or accurate regarding the condition of all cells within a battery.

Cell-voltage scanning for cell protection is a developing art from both the hardware and operational viewpoints. Little published information is yet available that describes circuit techniques, and none is available that describes flight experience with the circuits. Reference 276 considers cell-parameter sensing as part of the development of a microprocessor-controlled battery-protection system and identifies some of the problems that must be overcome in developing the measurement system. Table 53 summarizes typical measurement system requirements. Other cell-voltage scanning systems under development may require even closer measurement accuracies.

Table 53
Typical Battery Measurement Requirements
for Geosynchronous Spacecraft

Measurement Level	Parameter	Requirement ¹	Specified Level or Range
Cell	Voltage	Range Accuracy ² Repeatability ² Frequency of measurement	+0.6 to +1.6 Vdc <±0.030 Vdc <±0.015 Vdc <60 seconds
24-cell battery	Voltage	Range Charge Discharge Accuracy ²	33.6 to 37.4 Vdc 0 to 33.6 Vdc
		Charge Discharge	±0.5% of 37 Vdc ±1.0% of 33 Vdc in range of 24 to 33 Vdc
		Frequency of measurement Charge Discharge	300 seconds 60 seconds
	Current	Range (0- to 5-Vdc output) Low (charge) High (discharge) Accuracy ² Low range High range Frequency of measurement	0 to 5 Adc 0 to 50 Adc ±3% of 50 Adc ±3% of 5 Adc <60 seconds
	Temperature	Range Accuracy ² Frequency of measurement	-10°C to +40°C ±0.75°C Concurrent with battery-voltage measurement

¹ Redundant measurements required for battery-level parameters.

² Includes telemetry channel errors and 10-year component drift/aging effects.

8.5 METHODS OF DISCHARGE CONTROL

Batteries are discharged to the primary power bus either directly, through isolation diodes, or through discharge regulator/converters. The insertion of any power-handling element between a battery and the power bus introduces voltage and power losses that must be accommodated by an increase in battery size, in the form of either additional cells or cells of larger capacity. In synthesizing an electric power system, the first, or baseline, approach examined should always be one that utilizes the direct-discharge method because it will usually result in batteries of minimum size. The baseline system must satisfy all performance requirements, including bus-voltage regulation, safe charge control of individual batteries, and system reliability allocations.

When batteries are connected in parallel directly to a bus or to a bus through isolation diodes, their ability to share the load current in equal parts becomes important. An imbalance between discharge currents means that the batteries will each have different depths of discharge and, possibly, different temperatures. It is necessary to consider separately what this may mean in either low-altitude or geosynchronous-altitude orbit applications. In the former case, with depths of discharge up to 30 percent, such imbalances are normal and may result from: (a) temperature differences between batteries during charge, (b) mismatches in the impedance of the power cables, and (c) imbalanced battery capacities. In the absence of cell failures such as short-circuits, these conditions have different and sometimes self-compensating effects on the cells during cycling with the net result that, within certain limits, the overall energy balance of the cells is affected little or not at all. Special tests recently performed at NASA/GSFC have determined these limits for state-of-the-art low-altitude orbit applications.* Later paragraphs of this section summarize some of the test results.

The effect of failed or severely degraded cells in one, two, or more paralleled batteries is not usually a problem from the viewpoint of current-sharing in low-altitude orbit applications because the battery containing these cells will be effectively decoupled from the rest of the battery system during all or most of the discharge period. The normal batteries will run at deeper depths of discharge, but this will be no worse than the case in which failed batteries have been disconnected with no redundancy remaining for the rest of the mission. The worst-case values of depth of discharge so obtained for the "good" batteries, and the corresponding profiles of "good"

*Floyd E. Ford, NASA/GSFC, private communication, February 1978.

battery temperature, should be examined to ensure that: (a) the battery system can support the mission in the absence of redundancy, and (b) the power system undervoltage requirements will be met. The situation involving battery-level redundancy in geosynchronous applications is similar. A failure in a battery may be tolerated (if secondary effects of localized heating are not severe), or the weak battery may be disconnected.

Unbalanced discharge currents are more of a problem with paralleled batteries that have cell-level protection. Such batteries are designed for continued service with one or more failed cells and may be operated with depths of discharge in the 60- to 75-percent range. A serious imbalance between battery currents can result in the early exhaustion of one or more of the batteries, leading to a significant reduction in power-bus voltage at end of discharge. Also, as the end of discharge is approached, the batteries containing bypassed cells will deliver most of the discharge current. For a particular system, this value of current may represent the maximum condition for the design of the discharge bypass circuit and relays or other devices connected in series in the discharge path.

This section discusses the load-sharing characteristics of batteries discharged in parallel directly to a load bus. Later paragraphs describe approaches for achieving discharge current balance among batteries in geosynchronous applications.

8.5.1 Parallel Battery Operation

Batteries installed aboard a spacecraft and operated in parallel during discharge behave with slight differences from one to another because of inevitable differences between: (a) their local thermal-control system characteristics, (b) their power distribution cabling, and (c) their initial capacity, I-V, and charge efficiency characteristics. These differences are reflected in the instantaneous performance of each battery, but, if more than one are present, the interactions are so complex that they defy analysis by any method other than detailed computer simulation. Testing is another matter, however, and the following paragraphs present certain results developed by NASA/GSFC that should prove useful in developing low-altitude spacecraft batteries.

A starting point for this discussion is the consideration of the relationship between battery temperature, state of charge, recharge ratio, and I-V characteristics. Temperature differences between batteries during discharge do not cause significant differences in their discharge I-V characteristics.

(This presumes that the comparisons are made at the same values of true state of charge with batteries of identical capacity.) However, temperature differences during charge can result in each battery being at a slightly different state of charge at the beginning of the discharge period. When batteries are charged in parallel from a common voltage-limited source, the initial charge currents will be imbalanced because of differences in temperature and state of charge, but their initial voltages will be similar. With low BVL levels, the coldest battery will tend to limit the others. With high BVL levels, the reverse situation will tend to occur. In a two-battery system, the battery at the higher temperature will exhibit the higher final value of taper current, although no definite statement can be made regarding the relative values of the true states of charge of the batteries at the same point in the cycle.

Figure 113 shows data taken during a load-sharing test recently performed at NASA/GSFC during the development of the electric power module of the Multimission Modular Spacecraft (MMS). Two batteries were charged in parallel from a single charger that had battery voltage-limiting capability. Table 54 defines the levels of the family of temperature-compensated battery-voltage limits (BVL's) that were used for the test. A 100-minute cycle was used with 64 minutes of charge time. The batteries were discharged in parallel. Battery A was maintained at an average temperature of 10°C. Battery B was permitted to range 10°C above and below the temperature of battery A.

Figure 113 shows the variations in recharge ratio with temperature difference for each battery when four voltage limits are successively used. The maximum percent depth of discharge obtained with each battery when battery B is at 20°C is shown at the right-hand side of the figure.

Two points are evident from this figure. First, under ideal conditions, both batteries might be expected to exhibit the same recharge ratio when their temperatures were identical, and this is nearly the case. The fact that the trend lines for each battery with a particular BVL are not perfect mirror images of one another is due to inevitable differences between the characteristics of the batteries (true capacity and current-voltage, for example) and to experimental technique. Second, it is seen that, with a 10°C temperature difference between the batteries, only a small difference exists between the maximum depths of discharge even though large differences exist between the corresponding values of recharge ratio. With the higher BVL levels (5, 6, and 7), the recharge ratio of the warmer battery is generally and noticeably higher than that of the cooler battery. The lowest BVL

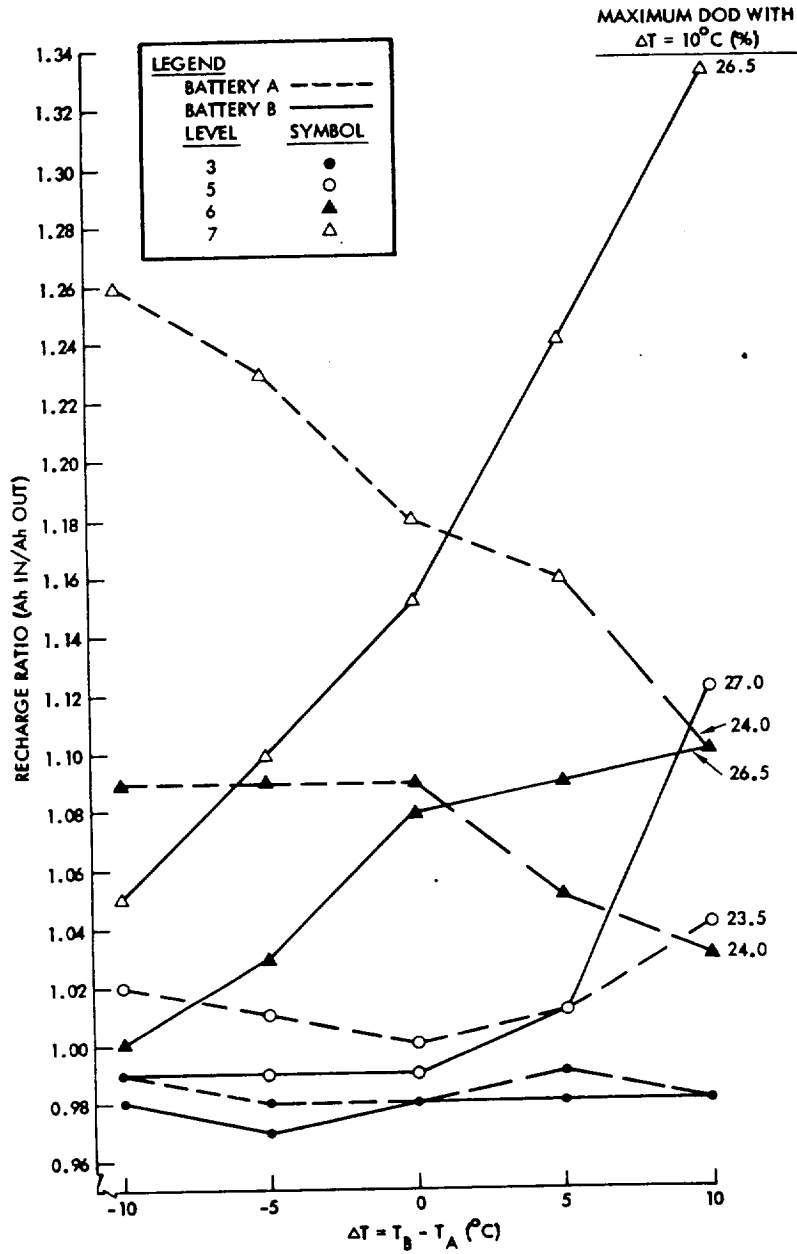


Figure 113. Recharge ratio for paralleled batteries as a function of battery-temperature difference.

Table 54
Battery-Voltage Limits for the Multimission Modular Spacecraft

BVL Level	BVL* as a Function of Cell Temperature (volts/cell)		
	0°C	10°C	20°C
8	1.520	1.497	1.473
7	1.500	1.477	1.453
6	1.480	1.457	1.433
5	1.460	1.437	1.413
4	1.440	1.417	1.393
3	1.420	1.397	1.373
2	1.400	1.377	1.353
1	1.380	1.357	1.333

*Level 8: 1.520 ± 0.015 V at 0°C
 Slope: -0.00233 ± 0.00020 V/°C
 Separation: 0.020 ± 0.002 V between levels
 Range: -10 to +35°C with level 8 specified at 0°C

(level 3 in this experiment) shows the same trend, but it is much less pronounced and the recharge ratios obtained are all less than unity. Data taken in a separate test confirm this latter fact. The load-sharing test demonstrated that temperature differences between batteries, obtained when the batteries are cycled under short-orbit conditions, do not contribute to significant differences between their depths of discharge and that the differences in depth of discharge that are obtained are relatively insensitive to limiting voltages if the limits otherwise permit adequate battery recharge. It has also been demonstrated that, if a BVL level that limits the amount of overcharge in each battery is not used, the resulting differences in generated heat may cause even larger temperature differences between the batteries and general thermal instabilities.

If each battery has independent charge controls, the effects of temperature differences between batteries are further reduced if the controls permit each battery to reach a full state of charge. Because temperature has little effect on discharge I-V characteristics, the battery currents will be essentially equal. The independent charge controls provide flexibility in controlling the recharge ratios for each battery and, therefore, battery overcharge. The need for this flexibility must be weighed against the additional complexity and cost as compared to that obtained with the parallel-charge approach.

In every spacecraft, the resistance across the battery harness from the terminals to the bus will vary from battery to battery. Most of the variation results from differences in cable lengths. Other variations may result from slight differences in the insertion losses of elements (current telemetry resistors, diodes, relays, etc.) placed in series with the batteries in their discharge paths. In a separate test, NASA/GSFC determined the effect of differences in discharge-path resistance on the current-sharing capability of two batteries in the test configuration previously described. Figure 114 shows the general variation of recharge ratio and depth of discharge with

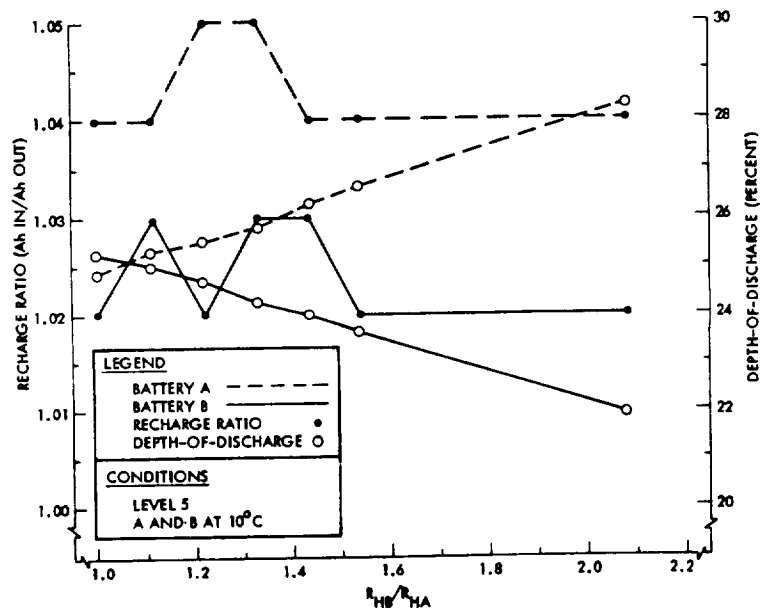


Figure 114. Recharge ratio and depth of discharge for paralleled batteries as a function of harness-resistance ratio.

ratios of equivalent harness resistances. As the ratio of (or the difference between) harness resistances increases, the difference between the depths of discharge of the batteries also increases. The battery with the lowest discharge-path resistance attains the highest depth of discharge and the highest recharge ratio and vice versa. This result suggests that differences between the internal impedances of paralleled batteries tend to be masked by the discharge path resistances, if the latter are large by comparison. Thus, in most applications, the presence of an isolation diode in each discharge path will tend to equalize current-sharing between normal batteries.

Other factors that influence cell and battery I-V and charge efficiency characteristics are sometimes considered in terms of their effect on parallel battery-system performance. For systems with batteries charged and discharged in parallel, it is common practice to require that the batteries be closely matched in capacity to minimize differences in I-V characteristics in terms of the state-of-charge parameter. A typical example is the battery system of the Orbiting Astronomical Observatory. Its three 20-Ah batteries are matched to within ± 1.5 Ah, and the cells for each battery are matched to within ± 0.5 Ah (Reference 50). For similar reasons, it is sometimes required that all of the cells be manufactured with plates from the same lot.

8.5.2 Parallel Battery Operation with Cell Protection

Long-life geosynchronous spacecraft batteries often use some form of cell-level protection or, in an equivalent sense, redundancy. To minimize the size of the battery system, the batteries are often discharged directly to the power bus. If one or more cells within one of the parallel batteries are discharged or if cell-protection circuitry becomes operative, the discharge current from the battery will be affected. The discharge voltage of the parallel battery system will be lower than normal, and the other batteries will provide most of the load current until the system voltage reaches the operating range of the low-voltage battery. At that point, the batteries will begin to share current more equally. As the discharge continues, the good batteries will tend toward depletion and their currents will be reduced. The low-voltage battery will therefore deliver most of the load current toward the end of the discharge period. Figure 115 shows a computer simulation of the one example of this situation as it occurs during a maximum geosynchronous eclipse discharge. The three batteries are charged independently so that the effect of battery temperature variations on the discharge currents is small. It is seen that the maximum value of cell bypass current occurs at the end of discharge for the case considered.

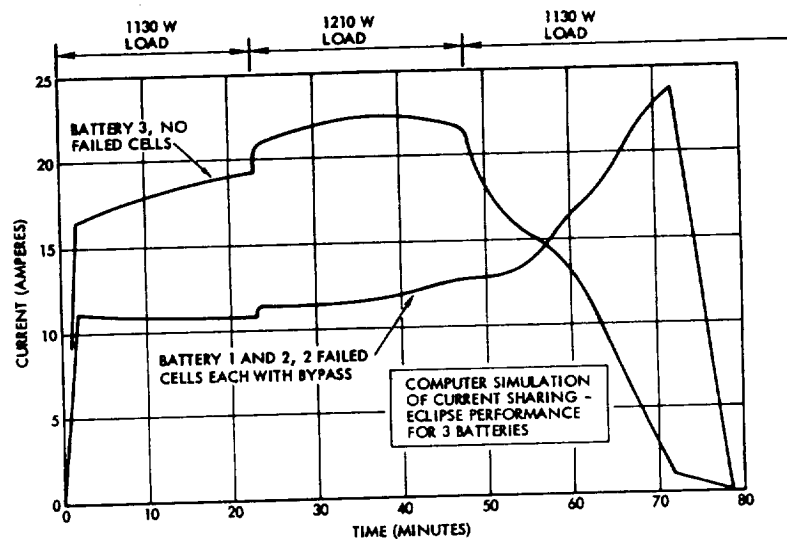


Figure 115. Computer-predicted battery-discharge current-sharing.

If isolation diodes are installed between each battery and the power bus, the current-sharing characteristics will be similar to those described previously. When isolation diodes are used, it is usually to ensure that each battery is charged independently (Reference 277). However, this objective can be achieved by disconnecting each battery from the bus during charge periods with relay controls, leaving only a connection to the bus through a lower-voltage, diode-isolated tap for supporting load peaks and transients (Reference 278). The battery-isolation diodes are usually redundant (parallel or series-parallel) with each diode of a pair capable, after appropriate derating, of conducting the maximum battery current.

The loss of one cell in a battery equipped with equivalent cell-level redundancy can significantly affect the relative states of charge of all other batteries of the parallel battery system. To accommodate this effect, it is necessary to incorporate provisions for balancing the currents or for separate battery-discharge controls.

If one battery of several in parallel develops a low discharge voltage because a cell has failed, the voltage of each of the other batteries can be approximately adjusted to the lower value by either: (a) shorting an unfailed cell and its bypass network with a shunt path through relay contacts, or (b) inserting a resistive or diode network in series between the battery and the

bus. Approach (a) is preferred because it has least impact on battery or spacecraft thermal design. The magnitude of the matching problem depends on the voltage drop actually developed across the bypass network of the failed cell. For example, if a bypass diode is activated because of an open-circuited cell, the battery voltage will be reduced by approximately 2 volts (the contribution of the lost cell plus the diode's forward voltage drop). Removal of one or two cells in a parallel battery lowers the voltage of that battery by about 1.2 or 2.4 volts, respectively. If two cells are removed from each unfailed battery in the system, the battery with the bypassed cell will actually have a higher current at the beginning of discharge and will eventually reach a greater depth of discharge than either of the good batteries—the reverse of the situation encountered when unbalanced current-sharing is tolerated. Of course, because cells are removed from the good batteries, the entire system can store less energy, and all batteries will experience greater than normal depths of discharge. Nevertheless, this approach avoids large disparities between the states of charge of batteries in the energy-storage system.

Another approach, applicable to batteries that are discharged directly to the load bus, involves the use of separate load buses, each dedicated to a single battery. If a cell failure occurs, the battery simply discharges to a greater depth of discharge at a higher current. (A constant power load is assumed.) This split-bus approach has been applied successfully on several of the Intelsat spacecraft, on which multiple transponder loads facilitate the apportionment of the total spacecraft load between the batteries. The definition of balanced load groups between separate buses is more difficult for spacecraft with other types of payloads or mission profiles. Split-bus electric power systems are usually designed as two or more separate power systems with cross-strapping as required for critical functions (e.g., source power for command receiver power supplies) and reliability enhancement.

8.5.3 Discharge Through Regulator/Converters

Many systems contain batteries that discharge through converter/regulators. Most of this type of flight systems have the batteries paralleled at the input to a single but redundant discharge unit. This approach is usually taken because it minimizes the number of parts, weight, and cost associated with the power-conversion equipment. But, as power levels increase, it becomes impractical to perform all of the power conversion in a single unit. Therefore, the concept of modular energy-storage units, each containing a single battery with both discharge- and charge-control functions, becomes attractive.

When each battery in a power system contains its own discharge unit, the batteries are effectively isolated, one from another, during discharge. Such systems are functionally equivalent to the split-bus direct-discharge configurations described previously: As cells degrade or fail (assuming cell-level protection), both discharge current and maximum value of depth of discharge increase. The output power levels of the converter/regulators will be similar—subject primarily to variations introduced by shifts in efficiency caused by differences in converter/regulator input voltages and slight differences between electronic component performance characteristics.

The assignment of a discharge converter/regulator to each battery permits consideration of methods of obtaining forced discharge current sharing. Here, the objective is to maintain equal discharge currents among all batteries regardless of the effects of degradation or of cell failures. Discharge currents are individually sensed, and the corresponding voltage signals are used to develop error signals proportional to the current imbalances. The error signals are used to control the duty cycles of the corresponding converter/regulators. With identical input currents and a common output voltage, the discharge units do not contribute power identically to the load power bus. The circuitry required for this approach becomes complex as the number of energy storage modules increases. The mechanization is, however, relatively simple for a two-battery system. The approach offers the advantage of maintaining the batteries at the same depth of discharge, even though they no longer exhibit similar I-V characteristics. Degradation and cell failures tend to be borne uniformly by all batteries in the system.

8.6 SYNTHESIS OF BATTERY-SYSTEM CONFIGURATIONS

In many respects, the synthesis problem is more complex than the analysis problem. It involves the combination of basic components into particular configurations that each meet the requirements and constraints imposed at the system level. Yet, each component must satisfy certain requirements and must have compatible interfaces with other components and subsystems. In the real world, other factors affect the process. For example, there is usually considerable interest in finding ways to use existing hardware because it has been developed, designed, and tested and therefore represents reduced risk and a potential cost advantage to the project. The designers of power and battery systems must therefore apply considerable ingenuity and creativity to their task, particularly if the mission requirements represent a significant departure from those studied in the past. By comparison, the analysis problem is usually straightforward and, if properly defined, can be solved with standard engineering techniques and methods.

8.6.1 Interactive Roles of Battery-, Power-, and Thermal-System Designers

The importance of a team approach to the development of battery and power systems cannot be overemphasized. The battery is one of the elements that has the most influence on the configuration of the power system, particularly if the spacecraft is designed to orbit the Earth or a planet. Its charge and discharge must be controlled, and, under certain circumstances, its cells must be protected. Its performance characteristics have a direct effect on the size of the solar array and, often, on the voltage level of the primary power bus. It exhibits a variable heat-generation profile with high dissipation peaks relative to many other spacecraft components, yet its temperature must be maintained within close limits at a level below that of other parts of the spacecraft. The performance characteristics of its cells are influenced by a wide range of design, manufacturing, and application variables. These considerations combine to form system and battery-level design problems that usually yield only to an interdisciplinary approach.

8.6.2 Development of Preliminary Power-System Configurations

Before a power system can be synthesized, it is necessary to analyze and define the requirements it must meet. Several types of definition studies can aid this development process.

8.6.2.1 Load Power-Profile Analysis

There may be several load power-time profiles for a particular mission: single-orbit, single-day, single-week, by service mode, by season, or by mission phase. The single-orbit profile is most common and is usually the basis for battery energy-balance calculations. Because the payload duty cycles of some low-altitude Earth surveillance missions vary from orbit to orbit, energy balance is required only over a 14- to 16-orbit "day." Similarly, the loads of some geosynchronous communications satellites may be programmed on a weekly basis to account for periods of heavy or light traffic. Other spacecraft may be designed to serve dual functions, each occurring during different periods of its service lifetime. Separate load profiles are usually defined for geosynchronous spacecraft during the equinox and solstice seasons. Finally, it is always necessary to develop a load power timeline from prelaunch, through launch and ascent, to a point in the final orbit when the spacecraft is fully operational.

Whatever the basis for the load-profile definition, it is not uncommon for the power-system designer to experience great difficulty in assembling accurate load information early in the spacecraft definition phase. Without it, however, there can be no rational basis for power- and battery-system sizing calculations.

The payload power profile is developed by accumulating unit-load power data. The unit or load group power requirements are defined in terms of input voltage, duty cycle, operating mode, transient specifications, and notations of special conditions. Converters that supply power at secondary voltages must be identified in terms of the loads they serve and their efficiencies or losses. A similar profile is constructed for housekeeping power requirements, including those of the power system, and the two combined. Battery-charge power is sometimes not included in the total spacecraft load-power profile but is handled separately in the power-system/battery-system sizing calculations.

A launch/ascent timeline is prepared for: (a) calculating the battery state of charge at liftoff and the drains incurred during ascent when array power is minimal or the spacecraft is eclipsed, (b) identifying solar-array deployment events, (c) ensuring that sufficient loads are maintained to protect the solar-array shunt limiter/dissipator, and (d) evaluating the effect on battery and power-bus voltage regulation of firing pyrotechnic devices.

8.6.2.2 Load-Bus Voltage Level and Regulation Studies

Most spacecraft are designed with nominal +28-Vdc primary power buses because most payload equipment requires power at this voltage level. If a significant amount of load power is required at another level, it is desirable to consider methods of energy generation and storage at that level in order to eliminate losses in conversion/inversion equipment. In some cases, bus voltages in the 56- to 112-Vdc (high voltage) range are used, and, in certain special instances, those in the kilovolt (very high voltage) region may be considered.

If a high voltage load is on during the eclipse period, it can be supported only in one of two ways: (a) low-voltage batteries that discharge to the load through a voltage-boost converter/regulator, or (b) high-voltage batteries that discharge directly to the load. The low-voltage batteries will always be larger in capacity because they deliver the same watt-hours of energy for the load at a lower voltage and they must be sized to accommodate the

inefficiency of the discharge regulator. The high-voltage batteries will be less reliable because they contain about three to four times as many cells in series. With battery-level redundancy applied to both approaches, the system with high-voltage batteries will generally weigh more than one with low-voltage batteries and discharge converter/regulators.

As spacecraft power levels increase, the power losses within cables and harnesses also increase because: (a) the spacecraft dimensions tend to be larger and longer cables are therefore required, and (b) the low-voltage power buses must carry higher currents. Wire weight is directly proportional to current or power and inversely proportional to the voltage drop across a unit length. It is often desired to specify a total voltage drop from the power source to a load so that the increment of power-source weight required for compensating for the voltage drop across the cable is minimized. This condition exists when

$$\Delta V = \ell \sqrt{\frac{\rho\sigma}{m_G}} \quad (51)$$

where

ΔV = voltage drop across a wire of length ℓ (return wire not included)

ρ = density of conductor (wire insulation omitted)

σ = conductor resistivity

m_G = incremental specific weight of the power generator (source)

Reference 279 contains the derivation; however, equation 3.9 of the reference is incorrect. It should be

$$\frac{M}{\ell} = \frac{\Delta M_G}{\ell} = \frac{P}{V} \sqrt{m_G \rho \sigma}$$

The ordinate of figure 3.28 in Reference 279 should therefore be labeled as "Minimum Cable (Power and Return) Weight (lb/ft)."

The foregoing corrected equation shows that the wire or cable mass (M), or the increment of power-source mass (ΔM_G), per unit length varies in direct proportion to transmitted power and in inverse proportion to transmission voltage level. The latter fact is often used as an argument for the use of

high-voltage distribution systems, particularly at higher power levels. There is merit in this approach in many circumstances. However, note that the optimization involves only the power source and the distribution cable. A more complete optimization, as outlined in Reference 280, incorporates the characteristics of postsource and preload conversion equipment.

In addition to influencing the size of the power sources, the cable voltage drops can also affect the voltage regulation of the power buses. When bus voltage is determined by the characteristics of the battery, it may be necessary to design the distribution cable for minimum voltage drop rather than for optimum weight.

Determining voltage regulation requirements is an important preliminary step before system synthesis can begin. Most payload equipment is compatible with a coarsely regulated 28-Vdc power bus. For many components, however, there are specific voltage limits. The lower limits usually have the greatest impact on battery design because they often determine the number of cells in series. The system and battery designers must also consider the specification of the undervoltage limit used for fault detection and isolation because it establishes the battery tap point. When cell-level protection is provided, the effect of cell failures below the tap may influence selection of the limit. If the batteries are connected to the power bus during their charge period, their maximum achievable charge voltage will determine the maximum bus voltage unless the bus is limited by other means.

8.6.2.3 Power-Source Regulation Definition

It is not immediately obvious that the decision to regulate the power source would greatly affect the battery system. However, if no source regulation is provided and the batteries are connected to the bus, the batteries may act as a shunt regulator for the source. When this is the case, care must be exercised to ensure that the batteries are not overstressed during the charge period. Specifically, we refer to a condition in which the charge rate (high), temperature (low), and state of charge (high) may combine so that hydrogen is generated in one or more of the battery's cells.

Conditions that lead to the presence of high-charge currents are maximum solar-array output (e.g., at beginning of life or on eclipse exit when the solar array is below steady-state temperature conditions) and/or reduced spacecraft electrical loads. The combination of low battery temperatures and high charge rates results in a tendency for individual cells within a battery to

diverge in voltage on charge. The cells with higher voltages may therefore enter the voltage region associated with the evolution of hydrogen. (See the section on "Maximum Allowable Voltage on Charge.") Because the recombination rate of hydrogen is low, a possibility exists for the generation of high cell pressures. Given this possibility, the final result is dependent on the duration of gas generation, as well as on the rate.

The critical period occurs during orbits with eclipse durations that produce low-to-intermediate values of battery depth of discharge but are long enough to cool the solar-array significantly. These conditions are most severe when the orbit is at geosynchronous altitude (negligible Earth radiation and albedo to mitigate array temperature excursions) and when the solar array is of lightweight construction. On exit from eclipse into sunlight, the array output power will be at a maximum value that depends on the voltage operating point determined by the battery. Current available from the array at that voltage that is not otherwise required by the spacecraft loads enters the battery. During part of this transient period, the battery current may be at a higher-than-normal charge rate. High rates applied to high state-of-charge cells may therefore result in a period of gas generation terminated eventually when the battery voltage reaches its limit or the transient period ends.

8.6.2.4 Preliminary Definition of Battery-System Thermal and Mechanical Interfaces

It is important to establish the options that are available regarding battery thermal control and physical location early in the system definition phase when spacecraft concepts are still fluid and major shifts in direction have least impact. There is a strong tendency to use familiar, reliable, and simple techniques. Often, these approaches are directed toward use of designs, techniques, tools, and processes that are immediately available or that have proved to be cost-effective in past applications. Thus, there is impetus to apply passive thermal-control techniques to batteries, as well as to other spacecraft components. There is nothing wrong with this, as many successful applications have demonstrated. Note, however, that the development of passive thermal controls for batteries is not a cookbook exercise, particularly when their operating and standby temperature range must be lower than that of other spacecraft components. The requirements of many missions, particularly those in low-altitude Earth orbit can be completely satisfied only by active thermal-control systems. Such needs should be identified early in case they conflict with pre-established ground rules for the project.

The responsibility of the battery designer to the thermal-systems engineer is twofold. First, he must define the temperature-control requirements in unambiguous terms. Second, he must provide complete and accurate heat-generation data for all expected operating modes of the cells and batteries. Although the first is somewhat easier to accomplish during the synthesis phase than is the second, it is no less important.

The responsibility of the thermal-systems engineer to the battery designer is fundamental. He must conceive alternative viable approaches for controlling battery temperature and provide information to support performance, weight, cost, and reliability tradeoffs. In addition, he must justify and document his analytical models and translate key assumptions into appropriate design requirements for the thermal analyst who supports the design of the mechanical packaging of the batteries and their auxiliaries.

The power-systems engineer is responsible for ensuring that these technical interactions take place and that the developing designs are consistent with the overall requirements of the electric power system. He is responsible for overall power-system performance and energy balance. He is also in the best position to identify unusual operating modes or potential failure conditions that may affect the battery and thermal systems.

8.6.3 Development of Preliminary Battery-System Configurations

The starting point in developing a preliminary battery-system design is to completely define the requirements and constraints that it must satisfy. Some of the requirements will have been identified in part during studies directed toward synthesizing the design concept. With the tradeoffs completed and a system configuration selected, it is essential that all of the requirements be reconsidered for completeness and accuracy. If the review uncovers any gaps or inconsistencies, it has served its purpose.

When general requirements are established, it is possible to perform certain well-defined investigations:*

- a. Cell and battery size study and definition—Sizing is performed as part of a reanalysis of the power system defined during the conceptual phase and is done using best available load information. Cell-definition studies are directed toward the preliminary definition of a cell-

*See also Section 9.

procurement specification. Other outputs of this task include definition of preliminary cell current-voltage and heat-generation data for use in subsequent analyses.

- b. Charge-control method and logic definitions—Here, the purpose is to analyze in detail the selected charge-control method to identify all normal and abnormal operating modes, to identify all signal and control parameters and their expected range of values, to establish preliminary tolerance requirements on measurements, and to identify data requirements for the detailed design phase and subsequent test and flight operations.
- c. Definition of thermal-control requirements—This study is conducted jointly with the thermal-system designer to assess the effect of adjusting certain requirements on the battery temperature profile during all operating modes. Issues that were not dealt with in detail during conceptual design studies are examined; for example, requirements for heater power, tradeoffs of radiation area and weight variations in heat-generation profiles, effects produced by repositioning the batteries, effects and advantages produced by relaxing the temperature range during discharge, requirements for battery component thermal design, effect of failures on temperature characteristics, and requirements for auxiliary cooling during ground testing and prelaunch checkout.
- d. Definition of cell-protection methods—If cell-level protection or monitoring is required, a study is warranted to establish the electrical, thermal, and mechanical characteristics of the networks in sufficient detail to support the procurement of long-lead items and the development of preliminary packaging concepts.
- e. Definition of battery reconditioning policies—This area consists of a review of available data to determine if and how reconditioning is to be implemented in terms of controls and sequences of operations. The policy is reflected in the plan for accelerated or real-time cycle-life tests.
- f. Definition of preliminary battery mechanical configuration—The packaging concept must be assessed to ensure compatibility with the spacecraft structure, the equipment and harness layouts, and the thermal-control system. Requirements for control of thermal gradients within the battery assembly must be evaluated with respect to weight, producibility, and cost.

- g. Definition of preliminary battery-system electronic-circuit configurations—The requirements for charge and discharge control, cell protection and monitoring functions, command and telemetry capability, heater controls, power distribution, fault detection and isolation, and power quality and electromagnetic compatibility (EMC) must be translated into circuit concepts to support parts selection and procurement activities and preliminary packaging and thermal design.
- h. Definition of preliminary battery electronic-circuit mechanical configurations—Early decisions must be made on incorporating electronic functions into the battery package. Configurable items must be identified, and steps must be taken toward establishment of their interfaces.
- i. Definition of preliminary battery-system component-mass properties—These characteristics, especially weight and mounting surface area, tend to deviate from early estimates during this phase of design and, accordingly, must be monitored to ensure that individual design decisions will not adversely affect mechanical performance.
- j. Definition of battery-system reliability—Early estimates of battery-system reliability can be improved as the design of system components proceeds. Models are developed for cell and battery reliability, and alternative methods of implementing redundancy are evaluated.

Many other tasks of limited scope must be performed during the preliminary design phase. The foregoing list applies generally to all battery and battery-system designs. The manner in which they are planned and executed may vary from organization to organization or from project to project, but the objectives remain clear: (a) to establish specifications at the battery-system and component level, (b) to perform analyses to support and document the specifications, (c) to define a preliminary cell-procurement document, (d) to establish preliminary circuit and packaging designs on the basis of component specifications, (e) to identify and release long-lead parts, and (f) to identify electrical, mechanical, and thermal interfaces for later definition during the final design phase. Section 9 describes the development process in further detail.

8.6.4 Tradeoff Studies

Tradeoff studies usually involve performance, weight, reliability, and cost, although other factors also play an important part. For example, known customer preferences regarding design approach or the experience and

capability of the spacecraft supplier may limit the range of candidates for comparison. This usually has favorable effect because too many design options may result in a superficial treatment of each.

Most tradeoff studies are performed during the project definition phase or are treated by the organization as proprietary and, therefore, are generally undocumented for the public. Some examples, however, can be found in the literature. They contain a great deal of useful procedural information on the synthesis of power and battery systems (References 196, 197, 206, 225, 281, and 282).

8.7 ANALYSIS OF BATTERY-SYSTEM CONFIGURATIONS

Many analyses are required for defining and designing a battery system. The following sections discuss some that are basic to its development process. The reader is encouraged to familiarize himself with their details even though some of the procedures are somewhat specialized and outside the realm of battery-component engineering. The benefit will be increased awareness of overall performance and interface requirements.

8.7.1 Electric Power-System Modeling

This section discusses methods of modeling and simulating the performance of electric power systems. Procedures for developing approximate graphical analyses of power systems are identified, as well as various types of computer programs that have been used to improve analysis accuracy and to reduce required labor and time. Battery computer programs *per se* are excluded because none are described in the literature, although such models are always incorporated into electric power-system simulation computer programs.

The development of a battery simulation model is usually best accomplished along empirical lines. Battery-cell I-V characteristics are measured under controlled conditions of state-of-charge, temperature, and discharge/charge

cycle specifications (discharge time, cycle period, and maximum depth of discharge) and are arranged in tabular form. The program software merely handles the battery cell as one additional circuit element—albeit, a nonlinear element—that has been characterized parametrically and uses interpolation and other numerical techniques to obtain a solution to a simple system of network equations. Battery-cell dissipation is calculated by the methods described in the sections on “Heat Generation During Charge” and “Heat Generation During Discharge.”

8.7.1.1 Graphical Analysis Techniques

Solar-cell arrays and batteries have nonlinear I-V characteristics that are strongly dependent on other variables (e.g., illumination, temperature, or state of charge). Power control and conditioning equipment also exhibit nonlinear I-V characteristics or, at best, characteristics that are only piecewise linear. The presence of nonlinearities means that analytic solution of system network equations is not usually possible and that computer simulation techniques must be used when accurate, repetitive, system performance calculations are required. Nonetheless, it is often desirable to have at hand the capability of performing a rough but fast check on system operation, particularly when candidate systems are being synthesized. Reference 283 describes a detailed graphical-analysis procedure that may be readily applied to most electric power systems. Reference 225 contains other examples of graphical analysis and shows how the techniques may be used to advantage in performing tradeoffs of candidate electric power systems over a wide range of operating conditions.

One important use of graphical-analysis techniques is the verification of system stability. For a system operating point to be stable, it must satisfy the criterion (Reference 226),

$$\frac{dP_{\text{load}}}{dV} > \frac{dP_{\text{source}}}{dV} \quad (52)$$

Figure 116 shows the I-V characteristic of a converter/regulator superimposed on the I-V characteristic of a solar-cell array. From the origin of the graph to point 1, the input voltage to the converter/regulator is below that required for maintaining regulation, and the load line therefore approximates a constant resistance load. The converter/regulator begins to regulate at point 1, and, as the source voltage increases, the load line follows curve

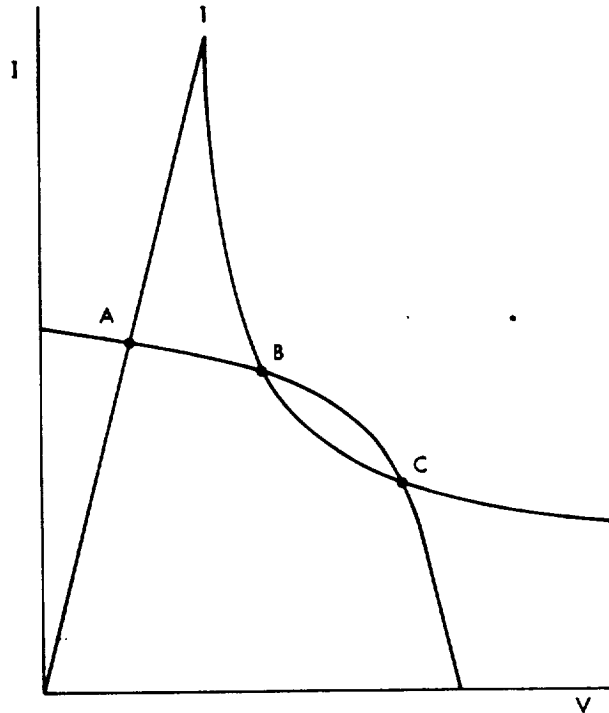


Figure 116. Solar-array characteristics with a constant-power regulator.

1-B-C. The solar-cell I-V characteristic intersects the load line at points A, B, and C. According to the criterion for stability, points A and C are stable, but point B is not.

Although stable operation is necessary, it is not sufficient for proper system performance. In sunlight, under certain combinations of source and load, the system may stabilize at an operating point that satisfies the load demand, but that results in insufficient power for battery recharge. Other conditions may actually result in battery discharge in sunlight, even though there is sufficient solar-array power to support full battery charge (References 283 and 284). Such conditions may result as part of normal system operation or may be associated with partial system failures. In either case, the system designer is responsible for evaluating the performance of each candidate configuration early in the synthesis phase of system development to verify system stability, energy balance, and voltage regulation.

8.7.1.2 *Electric Power-System Simulation Programs*

Design calculations for all but the simplest electric power systems are complex and tedious and must often be repeated many times. Each major supplier of aerospace hardware has developed digital computer simulation programs to reduce labor time and cost and to improve accuracy. Although no two programs are alike in detail, they share common features within certain categories.

Many computer programs perform complete simulations of electric power-system performance throughout single or multiple orbits or specified trajectories. One group of such programs evolved under NASA auspices for the Television Infrared Observational Satellite (TIROS) and Lunar Orbiter spacecraft series (Reference 285) and for the Nimbus series (Reference 286). A similar program was developed for the OAO missions (Reference 62).

The programs contain subroutines that each model one of the major system components. In a typical example, the subroutines are called by a main program that contains the system network equations and the integration routines necessary for determining system energy balance. Iterative procedures are used to converge on the system operating point—the same operating point that could otherwise be obtained by graphical methods. The solar-array and battery models are semiempirical. Their I-V characteristics are inputted as measured data selected for the particular mission and translated for their predetermined temperature profiles. (In the case of the solar array, other translations are required; for example, for illumination intensity, for radiation and other space environmental effects, etc.) In the particular case of the battery model, tables of measured battery cell voltage data are stored in the computer's memory. The voltage data are a function of state of charge (independent variable), charge and discharge current rates, and temperature.

Intermediate values are obtained by interpolation, using a special subroutine. The program requires battery temperature profiles as input data, but calculates the heat-generation profiles for the batteries as part of the simulation. The temperature predictions can therefore be improved by successive iterations of the separate electrical and thermal-system computer programs. Versions of this basic program have been used in the design of low (References 62 and 285 through 287), intermediate (Reference 208), and geosynchronous (Reference 263) orbiting spacecraft.

A second group of programs has been developed in response to analysis requirements imposed by large, complex, geosynchronous satellites. In such spacecraft, the thermal-design problem is more difficult and demands more accurate estimates of unit-level dissipations, especially those that vary with time. Accordingly, simulation programs have been developed that incorporate multinode thermal models of key components, such as the batteries. Temperatures, as well as dissipations, are calculated at each orbit time-step and are immediately used in calculating system electrical parameters. The electrical/thermal calculations are performed successively until total energy balance is achieved. The time counter is then advanced one interval, and the process is repeated. The general approach taken in the development of these programs has been analytical, with battery and solar-cell data processed at other times with other software. References 288 and 289 describe one of the system simulation programs of this group. Reference 290 describes another program, which was developed for the simulation of interplanetary missions.

All of the system simulation programs just identified contain a model of the battery's electrical characteristics and, in some cases, of its thermal characteristics. These models are usually in subroutine form and are often used to obtain general performance predictions. Their effectiveness usually depends on an associated data base of measured battery parameters. Other investigators have taken a different approach and have attempted to develop cell performance models based on the use of equivalent electrical circuits. One model is based on a diode/resistor/capacitor network (Reference 291); another uses only resistors (Reference 292). Such approaches are clever and usually reproduce battery characteristics with fidelity if the particular underlying assumptions and constraints are not violated. Usually, however, the circuit approach is not quite as flexible in application as techniques that make direct use of empirical data.

8.7.2 Cell- and Battery-Sizing Calculations

If all decisions that must be made in performing battery-system sizing calculations were organized into a logical pattern, the resulting flow chart would take several large pages and be a confusing network of boxes and crisscrossing lines. The process is interactive with other power- and thermal-system analyses and is iterative in nature. This section describes a few fundamental steps that apply to all battery systems in any phase of the design process.

The size of a battery (in the electrical sense) depends on the energy it must deliver during discharge. Stated somewhat differently, the battery must deliver current at a voltage above a minimum value for a period of time. Although the current may be constant, it usually varies as a result of either the load type (constant power, resistive) or load programming during the discharge. An estimate of the average value of current during discharge is usually sufficient for preliminary sizing.

As more cells are added to a battery, the average discharge current required to support a constant power load is reduced. The opposite is true for a constant resistance load. By definition, changes in battery voltage do not affect the current required of a constant current load. Constant power loads are dominant in most spacecraft, and it is usually adequate to use a constant-power I-V relationship for analysis. (The exception is when there are significant heater loads.)

It is therefore clear that the starting point in sizing is the determination of the number of series cells in the battery. Sections 8.3 and 8.4 describe certain aspects of the analysis with regard to accounting for voltage drops produced by elements in series with the battery and the effect of cell-protection circuitry. Let it suffice to simply restate that the battery must make up all voltage losses on discharge between the battery terminal and the primary power bus. These may include diode, relay contact, current-sensing resistor, or discharge regulator insertion losses, as well as battery harness losses.

The effect of these voltage drops must be measured against the undervoltage limits specified for the power system. Three types of undervoltage limits are possible, and all may be present in a particular design. The first type is a limit imposed on the primary bus for fault detection and is of concern only in terms of the selection of a battery tap point for a fault-isolation current path to the bus. The second is a limit defined for the primary bus to protect loads that are sensitive to sustained undervoltage conditions. The third type of limit is imposed at the battery output terminal as a means of battery protection. It is applicable only when the battery's voltage is independent of the voltage of other batteries within the power system.* The battery must have sufficient voltage under normal and tolerated (by design) abnormal operating conditions, with all series losses accommodated, to exceed these limits with some margin.

*This requirement can be circumvented when batteries are connected in parallel during discharge by applying a limit to groups of cell groups in each battery. A battery is disconnected when one of its cell groups develops an undervoltage condition.

With the number of series cells established, it is a simple matter to calculate the average battery-discharge current under normal and exceptional conditions. The battery-discharge voltage determines the load-bus voltage, which may then be used to calculate the load current from knowledge of the I-V characteristic of the spacecraft load, either directly (assuming a constant power load) or graphically. If the battery is connected directly to the load bus through passive elements, the battery current is equal to the load current. If a regulator is in the discharge path, it will modify the current in accordance with its characteristics as power converter.

The number of batteries must be established on the basis of a reliability analysis of the mission. Section 8.7.5 contains an outline of the applicable techniques. However, because the results of this separate task are not available at the time of preliminary sizing, it is necessary to assume a number that is consistent with the type of redundancy envisioned. With battery-level redundancy, the minimum allowable number of operative batteries will establish the preliminary value of maximum depth of discharge for each operative battery. With cell-level redundancy, there will be at least two batteries and perhaps more.* The preliminary value of maximum depth of discharge is computed on the basis of all operative batteries but with a predetermined combination of cells bypassed. (The combination may provide for unequal numbers of bypassed cells in each of the batteries. For preliminary sizing, however, the computation is simplified by considering that all batteries are equal in terms of the number of operative and bypassed cells.)

Because the average battery current is divided between the operative batteries, the capacity discharged from each battery is thus approximately the product of its average discharge current and the discharge time.

For the initial calculation, a preliminary value of maximum depth of discharge may be assumed. It will be based on an analysis of the mission requirements and an assessment of the battery thermal environment for the proposed spacecraft. In particular, the number and kind of discharge/charge cycles and the expected operating temperature range will determine the initial estimate. See the data summarized in Sections 3.4, 8.3, and 8.4.

*Although it is conceivable that a single battery with cell-level redundancy could be used in certain applications, a case can usually be made for having a second battery. Some of the arguments for the second battery are: (a) that series elements could fail, leading to a complete loss of a single battery; and (b) that the power system is vulnerable to the effect of faults that could occur during the time that a single battery is being reconditioned.

A preliminary value of battery and, therefore, cell capacity is obtained by dividing the capacity discharged by the preliminary maximum depth of discharge. As the design process continues, these calculations may be repeated several times until final values are obtained.

The procedure outlined here is traditional. It is based on the tacit assumption that the maximum depth of discharge, when selected as a result of documented industry-wide experience with similar applications, will have associated discharge characteristics of a particular kind (i.e., the cell voltage will be above a particular level at end of discharge, and, after the required number of discharge/charge cycles have been achieved, the cell capacity will be above a particular minimum value (percent of initial rated capacity)). Neither the voltage level nor the value of minimum capacity are identified explicitly in the underlying analyses. Therefore, no data or procedures are available, based on life-cycle test results, for sizing the battery on the basis of end-of-mission requirements.

8.7.3 Battery Electronics Design Analysis

As in battery thermal design, the battery engineer is not usually responsible for the detailed design of electronic auxiliaries mounted to the battery or of the major discharge/charge control elements. He interprets the mission requirements as they affect battery performance, service time, and reliability and analyzes the impact of constraints imposed on the battery system by the spacecraft and electric power-system configurations. He must usually define battery electrical performance characteristics for the power-system and power-equipment design engineers, often on the basis of incomplete data. Nevertheless, his models of cell and battery behavior are essential to the development of energy-storage and power systems.

The battery engineer is responsible for more than simply providing a characterization of battery performance. He must play an active part in defining limits, set-points, tolerances, and mode transitions for each of the electronic circuits that interfaces with the battery. In this regard, he must develop a general understanding of circuits in common use and their particular limitations. There are no clear procedures for obtaining this knowledge and experience, and it is beyond the intent of this book to attempt to define a methodology. Instead, a few short topical discussions are presented to illustrate some of the concerns that may require attention by the battery engineer or by the power systems engineer.

Three aspects of power component design and analysis are of specific importance to the battery engineer: circuit technique, device selection, and specifications. The following topics fall into one or more of these areas:

- It is generally not possible to regulate more than one parameter at a time. For example, a charge controller may limit current in an early mode with one circuit and limit voltage in a later mode with a second circuit. Although the controlling element may be a single device, two independent regulating networks are required for controlling it, one overriding the other.
- Current sensing may be accomplished by measuring the voltage drop across a resistive network (which produces a power loss) in series with the battery and noting the polarity of the analog signal. Alternatively, a magnetic amplifier may be used with a wire-loop flux detector to generate an analog signal proportional to current. Although the latter method introduces essentially no insertion power loss, it requires a separate regulated power supply with its accompanying inefficiency.
- A temperature-compensated battery-voltage limit (BVL) has a tolerance band that is a function of the circuit, the desired slope, shape, and accuracy of the limit curve, and the devices used within the circuit. Part of the tolerance may result from predictable time-related drifts, and part may be random. When a family of BVL's is defined for a long-term mission, the intercurve spacing should account for probable drift effects and for predicted end-of-mission battery-voltage performance. The overall spacing should accommodate a specified number of shorted or degraded cells and must provide adequate resolution for controlling overcharge and heat generation. Decreasing end-of-charge voltages are to be expected at end of mission in low-altitude orbit applications. The opposite case is typical for higher orbit applications.
- Solid-state thermal switches (SSTS) used for controlling battery heaters or for generating signals used for charge control generally have hysteresis characteristics at both the open and close switch points. These SSTS characteristics should be considered as part of a detailed electrical thermal performance simulation.

A long list of similar items culled from experiences obtained on many hardware projects could be added to the foregoing. Such a list is not required for support of the point we now make, namely, that interaction leading to mutual understanding is required between all contributors to a battery system design in order that requirements and constraints be satisfied with low cost and risk to the project.

8.7.4 Battery-System Reliability Analysis

Reliability is defined as the probability that a system, subsystem, component, or part will perform its intended functions under defined conditions for a specified operating period (Reference 293). Explicit in the definition is the concept that equipment performance can be represented by probabilistic models, as well as by deterministic models. As the art of reliability engineering has developed, it has shown that probabilistic effects strongly influence both short- and long-term equipment characteristics. In the broadest sense, short-term effects are attributable to: (a) design misjudgments or misapplication of parts or processes, and (b) variations in the manufacturing quality control of items ranging from the smallest device to those at the system level. Long-term effects are the failures or degradations that are not easily predicted by deterministic methods but that are expected, even though the design and application of the equipment is conservative, it has been manufactured to high standards, and it has been operated in the manner for which it was designed. Earlier sections of this manual considered various aspects of cell and battery reliability in terms of proper identification and control of their design and manufacturing variables. This section discusses the methodology ordinarily used for estimating the probability of mission success for the battery system, as well as one of the two major contributions that reliability engineering has made to the development of a battery system. The other major contribution is a formal Failure Modes and Effects Analysis (FMEA).*

*The FMEA process is not described in detail because each manufacturer of aerospace equipment has usually defined procedures that fit within his Product Assurance Organization's policy guidelines. It is assumed that a battery designer in such an organization is familiar with the applicable policies. It is sufficient to note that an FMEA usually includes detailed analyses of electrical, mechanical, and thermal functions down to the piece-part level. Their objectives are to identify critical items, single-point failures, and actions to eliminate or control single-point failures.

8.7.4.1 Quantitative Measures of Reliability

Let T be a random variable representing the service life of a device, component, or system. Then the reliability of the device or system as a function of the length of operating time, t , is defined by

$$R(t) = P(T > t) \quad (53)$$

in which the probability, $P(T > t)$, is referred to as the probability of survival or the probability of failure-free operation. The *reliability function*, $R(t)$, has the following characteristics:

- $R(t)$ is a decreasing function of t
- $0 < R(t) \leq 1$
- $R(0) = 1$ and $R(\infty) = 0$

Alternatively, the unreliability of a device, component, or system at time t is given by

$$Q(t) = 1 - R(t) = P(T \leq t) \quad (54)$$

where $P(T \leq t)$ is referred to as the probability of failure, and $Q(t)$ is the *cumulative distribution function* (cdf) of service time, T . The derivative of $Q(t)$ with respect to t is $q(t)$, the *probability density function* (pdf).

Another important reliability function is the instantaneous failure rate or *hazard function* defined as

$$H(t) = \frac{q(t)}{1 - Q(t)} = - \frac{d}{dt} \left[\ln R(t) \right] \quad (55)$$

The reliability function and the pdf can be expressed explicitly in terms of the hazard function,

$$R(t) = \exp \left[- \int_0^t H(t) dt \right] \text{ for } t > 0 \quad (56)$$

$$q(t) = H(t) R(t) \text{ for } t > 0 \quad (57)$$

The *mean failure rate* for a time period, t , is defined as the average of the hazard function, or

$$h(t) = \frac{1}{t} \int_0^t H(t) dt \text{ for } t > 0 \quad (58)$$

When an exponential reliability function is used, $h(t) = H(t) = \lambda$ and the term *failure rate* (λ) is then synonymous with the terms, hazard function and mean failure rate.

The *mean time to failure* (MTTF) is the expectation of T or, simply, the expected time to first failure,

$$\text{MTTF} = E(T) = \int_0^{\infty} t q(t) dt \quad (59)$$

These equations are the basis for all reliability calculations. They are used in conjunction with models of failure characteristics of the device or system (or service function) that are fitted either to experimentally obtained life test results or to data obtained from service histories, or both.

8.7.4.2 Cell Reliability Models

If a representative sample of battery cells from a population is subjected to continuous, repetitive, discharge/charge cycling under controlled conditions (e.g., depth of discharge, charge and discharge rates, temperature, voltage limit, and cycle period), the reliability function can be estimated as

$$R(c) = 1 - \frac{n_f}{n_t} \quad (60)$$

where n_f and n_t are the number of cells failed and tested (sample total), respectively, and the number of cycles, c , represents operating time. However, most testing is actually performed with test packs containing small groups of series-connected cells. When a pack is judged to have failed, possibly because of only one problem cell, it is usually removed from the test.* Under such conditions of cell discontinuation, at any point in the test,

*A definition of failure is not required for the purpose of this discussion.

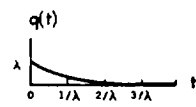
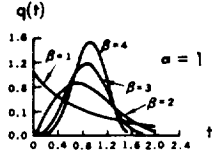
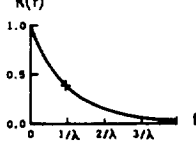
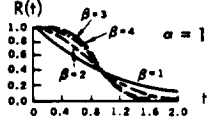

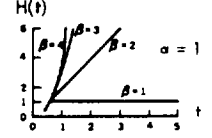
$$R(c) = 1 - \frac{n_r}{n_o - n_r} \quad (61)$$

where n_o and n_r are the number of cells originally on test and removed before cycle c , respectively. A plot of equation 58 appears as a series of steps rather than a smooth curve because $R(c)$ changes value only at the cycle times when a failure or a pack removal occurs. The basic cell reliability modeling problem is one of fitting an analytic expression for $R(c)$ or $R(t)$ to the empirically derived reliability function so that discontinuation data are handled in a manner that is mathematically consistent with the way that failure data are treated. The method of maximum likelihood is a classical statistical approach that is suited to this problem. It has been applied in connection with the development of a general reliability model for low-altitude orbit battery systems (Reference 122).

It is beyond the scope of this manual to describe in detail the specific models used in reliability work. Instead, this section describes two distributions—exponential and Weibull—that are of prime importance in battery cell reliability estimation work. Figure 117 summarizes the mathematical form of these distributions and their associated reliability and hazard functions. References 294 through 296 contain further information. The remaining discussion refers primarily to the reliability function because it can be calculated directly from failure data.

The exponential is the most frequently used reliability function because it is simple and because its associated constant-hazard function is representative of a wide variety of devices when they are properly used and maintained within a controlled environment. But, this distribution is not satisfactory for modeling a population of devices such as nickel-cadmium cells that may exhibit pronounced wearout with extended service in addition to the effect of random failures. The Weibull model provides a better fit. By adjusting the Weibull parameters, α (scale) and β (shape), it is possible to match the $R(c)$ obtained from equation 59 or 60 for a particular cell-test category with small error (References 114, 122, and 297). The Weibull distribution contains the exponential distribution when $\beta = 1.0$. The mean failure rate obtained with the Weibull model is $t^{\beta-1}/\alpha$.

Figures 57 through 59 of Section 3 display part of the results obtained from an analysis of 90-minute discharge/charge cycle data obtained from two sources: (a) the continuing NASA-sponsored cell-test project at the Naval Weapons Support Center (NWSC), Crane, Indiana (NWSC/Crane), and (b) a government and industry-wide survey of available low-Earth orbit-flight

PARAMETER	EXPONENTIAL	WEIBULL (TWO PARAMETER)*
MEAN	$E(t) = 1/\lambda$	$E(t) = \alpha^{1/\beta} \Gamma(\frac{1}{\beta} + 1)$
VARIANCE	$V(t) = 1/\lambda^2$	$V(t) = \alpha^{2/\beta} [\Gamma(\frac{2}{\beta} + 1) - \Gamma^2(\frac{1}{\beta} + 1)]$
DENSITY FUNCTION, $q(t)$	$q(t) = \lambda e^{-\lambda t}$ 	$q(t) = \frac{\beta}{\alpha} t^{\beta-1} \exp(-t^\beta/\alpha)$ 
RELIABILITY FUNCTION, $R(t)$	$R(t) = \lambda e^{-\lambda t}$ 	$R(t) = \exp(-t^\beta/\alpha)$ 
HAZARD FUNCTION, $H(t)$	$H(t) = \lambda$ 	$H(t) = \frac{\beta}{\alpha} t^{\beta-1}$ 

*SOMETIMES EXPRESSED IN TERMS OF β AND δ , WHERE δ IS AS DEFINED AND $\delta = \alpha^{1/\beta}$

Figure 117. Characteristics of selected reliability models.

and ground-test data (References 114 and 122). The analysis utilized a Weibull distribution, and the calculated Weibull parameters are reported in Reference 122. Figure 57 plots the estimated mean cell cycle life (MTTF)

as a function of depth of discharge and operating temperature. Figures 58 and 59 show the calculated cell reliabilities at 6,000 and 12,000 cycles, respectively, as functions of these same parameters.

Note that battery-cell reliability modeling is a developing art and is subjective in terms of both model selection and the selection and interpretation of the cell-failure data base. For example, Reference 297 reports the results of a Weibull treatment of a data base similar to that used in developing Figures 57 through 59; however, the calculated Weibull parameters and cell reliability predictions are different, probably because of differences in the approaches to handle the effect of temperature and depth of discharge on the calculated parameters. Earlier attempts to apply Weibull techniques (References 111 and 298) also involved complex formulations of the Weibull parameters in terms of temperature and depth of discharge. Finally, note that European investigators (Reference 113) found that, for certain categories of failure exhibited in the unscreened NWSC data, a Gompertz model* produced a better fit to the empirical reliability function than the Weibull model. It is clear that the Weibull model presented in this section should be considered for use primarily for preliminary analysis and design. Greater reliance on the model should be withheld pending the development of a thorough understanding of the cell-test data base that it reflects and of refinements that may result from considering other data subsequently collected. The model of Reference 122 is valid only for 90-minute orbit applications. At the present time, comparable cell reliability analysis data are not available for the 24-hour orbit or for intermediate-altitude orbits.

8.7.4.3 Battery Reliability Models

In addition to the complement of series-connected cells, a battery reliability model may include other related elements such as regulators (charge and discharge), cell-protection circuits and their power supplies, power switches (relays or solid-state devices), battery-reconditioning circuits, heaters and associated controls, isolation diodes, and transducers for monitoring electrical and thermal parameters. When an element is present, it must be represented in a reliability block diagram. A complete reliability block diagram shows all redundant and nonredundant elements and provides a visual representation of the total battery reliability calculation. Each block must define, as a minimum, a hazard function and a duty cycle. The hazard function is specified because, when the elements of a system are nonre-

*The Gompertz model is of the form $R(t) = \exp \left[-a/b (e^{bt} - 1) \right]$ and has a corresponding mean failure rate of $(a/bt) \exp(bt)$.

dundant and can fail independently, it is simply the sum of the hazard functions of the elements, whether or not the hazard functions are each derived from the same reliability function. This fact is apparent from consideration of the form of equation 56 and the general reliability calculations shown in figure 118. The calculation procedure is simplified considerably

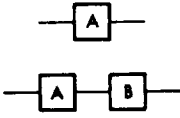
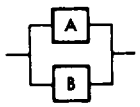
<p>GENERAL DEFINITION</p>	$R = e^{-\int_0^t H(t)dt}$ <p>WITH HAZARD FUNCTION $H(t)$</p>
<p>EXPONENTIAL MODEL</p>	$R = e^{-\lambda t}$ <p>WITH MEAN FAILURE RATE λ</p> $= e^{-[\lambda_1 d + \lambda_2(1-d)]t}$ <p>WITH INDEPENDENT FAILURE MECHANISMS, DUTY CYCLE D, AND $0 \leq d \leq 1$.</p>
	$R = R_A$ $R = R_A R_B$ $= R_A^n \text{ FOR } n \text{ IDENTICAL ELEMENTS}$ $= \prod_{i=1}^n R_i \text{ IN GENERAL}$
<p>FULL-TIME REDUNDANCY</p> 	$R = R_A + R_B - R_A R_B$ $= 1 - (1 - R_A)^n \text{ FOR } n \text{ IDENTICAL ELEMENTS}$ $= 1 - \prod_{i=1}^n (1 - R_i) \text{ IN GENERAL}$
<p>STANDBY REDUNDANCY</p>	<p>SEE REFERENCE 295, PAGE 256, FOR THE GENERAL CASE, OR REFERENCE 299, PAGE B-9, FOR THE APPROXIMATE CASE WITH MONITORING AND SWITCHING FUNCTION NEGLECTED.</p>

Figure 118. Evaluation of simple reliability block diagrams.

when failure rates associated with the exponential distribution are used or if the reliability of the element is precomputed, as can be the case when a Weibull cell reliability model is used.

Battery systems may be either nonredundant or redundant. The choice depends on: (a) the numerical reliability allocation for the battery system, and (b) judgments made regarding risk to the mission resulting from failure of a nonredundant battery system. In the early days of the space program when payload weight was constrained and missions were short, nonredundant batteries were often chosen; in recent times, however, this approach has been rarely taken for new spacecraft designs. The amount of redundancy and its method of implementation are now affected, more often than not, by considerations beyond those of mathematical reliability prediction because nickel-cadmium cells are prone to varying degrees of wearout. Nevertheless, interest appears to be increasing regarding the possibilities of developing improved predictive tools for both reliability and end-of-mission battery performance estimates. Motivation for this interest comes primarily from the desire to extend mission times, coupled with the availability of a growing data base of ground-test and flight-battery performance data. The remaining paragraphs of this section outline several approaches to battery and battery-system reliability modeling.

The reliability of a single battery without cell-level redundancy is easily calculated by using the formulas shown in figure 118. Several batteries, each with its own auxiliary elements (regulators, diodes, etc.), may be connected in parallel for supporting the eclipse and peak-load demands. Extra batteries are required for meeting the desired battery-system reliability requirement. If $R_B = R_B(t)$ is the reliability of one battery, the reliability $R_S = R_S(t)$ of an entire battery system in which k batteries out of m must successfully operate is given by

$$R_S = \sum_{x=k}^m \frac{m!}{x!(m-x)!} R_B^x (1 - R_B)^{m-x} \quad (62)$$

Battery-level redundancy is therefore based on the assumption that an anomalous condition—one open cell, one or more short-circuited cells, or several severely degraded cells within a battery—is sufficient for removing the battery from the system. The individual batteries within the system must therefore be sized for reliable operation with k operative batteries.

Equation 62 does not directly account for the effect of cell failures on the depth of discharge and temperature of affected and unaffected batteries within the system. This limitation may be dealt with by calculating the cell reliability by the Weibull method for values of depth of discharge and temperature that are representative of the ranges of these parameters traversed as batteries are removed from service. A precise analytical solution to this general problem is complex and requires computer solution (Reference 299).

Cell-level redundancy introduces significant additional complexity to the estimate of battery-system reliability. The redundancy is achieved by some form of bypass circuitry that compensates, as a minimum, for open-circuited cells and that may also provide protection from the effects of overcharge or overdischarge. The action of the bypass circuits, combined with the behavior of the cell under a particular failure mode, results in a lower voltage from the protected cell than that generally obtained from each of the other unfailed cells in the battery. The resulting voltage degradation at the output of the single-battery system may be tolerated if the output voltage is above the minimum level required by the subsystem. Otherwise, the battery will have failed. A single-battery system, redundant at the cell level, is sized to accommodate one or more cell failures before battery failure occurs.

Several approaches to estimating the reliability of a battery with cell-level redundancy have been taken. The simplest involves conventional analysis techniques. The reliability of an element—a cell and its bypass circuits—is calculated by using the formulas for full-time or standby redundancy, whichever is appropriate. The reliability of a series string of these elements is then computed by using equation 62 with m equal to the total number of series elements and k equal to the minimum number of series elements required for sustaining battery operation. The reliabilities of the complete battery and the battery system (if multiple parallel batteries are used) are then calculated by using standard expressions from figure 118.

This conventional approach requires simple definitions of cell failure (e.g., open-circuited, short-circuited, or severely degraded). The latter corresponds to a situation encountered in life-cycling tests in which a minimum discharge voltage limit criterion is not met. In practice, the degraded mode occurs far more often than the others. Usually, however, it is difficult to separate the effect of random failures of cells that exhibit degraded voltage behavior from the behavior of other cells in the battery that are merely

experiencing normal degradations associated with battery use. Two approaches have been developed that deal with this problem in the context of estimating the reliability of batteries with cell-level redundancy.

The first approach, which applies to a single-battery system only, utilizes a Markov reliability model (References 94 and 270). In the Markov approach, states are defined that correspond to various numbers and kinds of failures, and state-transition probabilities are determined from the mean failure rates of the various parts of the system. (See Section 8.4.1 and, in particular, figure 108.) One of the main advantages of this approach is that the failure rates of some parts of the system can be permitted to be dependent on the good/failed status of other parts of the system. As an example of why this is desirable in a battery reliability model, suppose that a cell suffers a loss of capacity. It will then tend to go into voltage reversal on deep discharge, which will cause hydrogen gas to be evolved at the positive electrode. In turn, this effect will increase the hazard of seal failure because of hydrogen pressure, after which loss of electrolyte may occur with consequent open-circuiting of the cell. The reverse voltage limiting action of a discharge bypass circuit will strongly inhibit this sequence of events if the circuit itself has not failed. Thus, the capacity-loss to open-transition rate of a cell is substantially influenced by whether the associated discharge bypass circuit is working. This transition rate will also be influenced by the reverse voltage limiting capability of the bypass circuit, with more negative limits on reverse voltage resulting in higher transition rates. Likewise, bypass circuit failure rates may be assumed to be influenced by the states of the respective cells (e.g., if the cell is good, the bypass circuit will remain in a "standby" condition and can therefore be represented by a lower failure rate). Another advantage of a Markov model is that it permits failure rates to be time varying. Thus, time-increasing failure rates may be used to represent a "wearout" type of cell degradation.

The Markov reliability modeling technique has not yet been applied to multiple-battery systems. Extension of the method is not trivial because a significant amount of computation is required for a single battery. An alternative approach has been developed and applied that accounts for the interaction (load sharing) of multiple batteries with cell-level redundancy under various conditions and combinations of cell failure and degradation (References 300 and 301). The modeling process is based on the performance of a Monte Carlo simulation of the battery system. Network equations are written that represent the battery system and preserve the identity of each cell. The conditions at a mission point (e.g., an eclipse season) are simulated to determine the voltage-profile contribution of each cell and the

current sharing between batteries. Before the simulation, a state or condition is assigned at random to each cell. Associated with each state is a discharge I-V profile that lies somewhere in the continuum between a "good" and a "poor" cell and that is defined as a function of the cumulative amount of stress to which the cell has been exposed before the point in the mission that is being simulated. If bus voltage exceeds the minimum requirement, the simulation is declared a success, and the next mission point is simulated; if not, the total mission is declared a failure. This process is repeated until many total missions have been simulated. The ratio of the number of successful missions to the number of missions simulated is an estimate of battery-system reliability.

SECTION 9 BATTERY DESIGN AND DEVELOPMENT

9.1 INTRODUCTION

The design and development of sealed nickel-cadmium batteries for spacecraft use require the careful attention of the battery engineer. The complete definition of the battery-system and battery configurations is the first key step that leads to the proper selection of the cell and to the correct specification of the battery.

The electrical design requirements are derived from the power system requirements. The mechanical design requirements are determined by general requirements imposed on all spacecraft components and by a series of trade-offs and analyses performed to meet weight, volume, and cost criteria at the spacecraft level. Thermal-design requirements are developed similarly and are also strongly influenced by the special need to impose temperature constraints and controls on the battery for achieving the required lifetime. The contribution of each engineering discipline to satisfying these requirements must be planned, coordinated, and reviewed continuously throughout the design phase.

The selected method of thermal control is by far the most critical factor in attempts to achieve long service life and to improve performance. This aspect of battery system design is emphasized in earlier sections and is continued at the battery-component level. However, correct specification and procurement of cells and careful attention to packaging cells into a battery are of no less importance. A packaging approach must be selected that minimizes weight and yet provides good structural support for the cells—during both dynamic launch operations and over operational periods in which the structure is subjected to fatigue from pressure and thermal cycling. Formal design reviews should be held throughout the design activities to ensure that these requirements are met and that all interfaces are correctly defined. The reviews should also verify that manufacturing can build the battery as designed in an economical manner.

The following sections deal with the design, manufacture, test, and storage of sealed-cell nickel-cadmium batteries.

9.2 DEFINITION OF THE BATTERY CONFIGURATION

The definition of a spacecraft battery configuration is an iterative and, at times, complex process. Considered simply as a component without auxiliaries, the battery requires the support and coordination of electrical/electrochemical, mechanical, and thermal-design specialties. The addition of auxiliaries, such as integrally mounted charge or cell-protection circuitry, introduces the element of electronic design and may add to the complexity of packaging and heat-transfer problems. All of these disparate skills must interact effectively if the requirements and constraints imposed on the battery and battery system are to be satisfied.

A new battery design usually evolves through three distinct phases – conceptual design, preliminary design, and final design. Each phase involves certain key activities that relate to one another as shown in the design process flow chart (figure 119). This flow chart shows the major activities that typically occur during the design, manufacture and test, integration, and flight of a battery as planned and executed by a prime spacecraft contractor. Though somewhat elaborate, this flow chart is representative of the work that must eventually be done during the course of a spacecraft project. Many activities involve functional groups outside the group primarily responsible for the battery. This is simply a reflection of the numerous interfaces between the battery and other spacecraft systems and components that must be analyzed and defined. When a single organization produces both the spacecraft and the battery system hardware, the project may be structured in different ways to obtain the necessary levels of coordination. The resulting work flow plan might be different in detail from figure 119, but it should produce the same desired results. When a spacecraft contractor purchases battery hardware, the activities differ somewhat from those shown in figure 119. The spacecraft contractor must perform many activities of the conceptual and preliminary design phases so that requirements for, and constraints on, the battery are properly defined in sufficient time for procurement. The battery equipment specification and electrical schematic level on the battery supplier should include these definitions. Section 5 describes the special considerations that apply to such a procurement.

The conceptual design phase is devoted to reconciling the battery or battery-system design originally proposed with the provisions of the negotiated contract and any other agreements made between buyer and seller. Requirements for the battery system are reassessed in light of revised requirements defined for the electric power system. Electrical, mechanical, and thermal design constraints are identified, and their impact on the battery system is

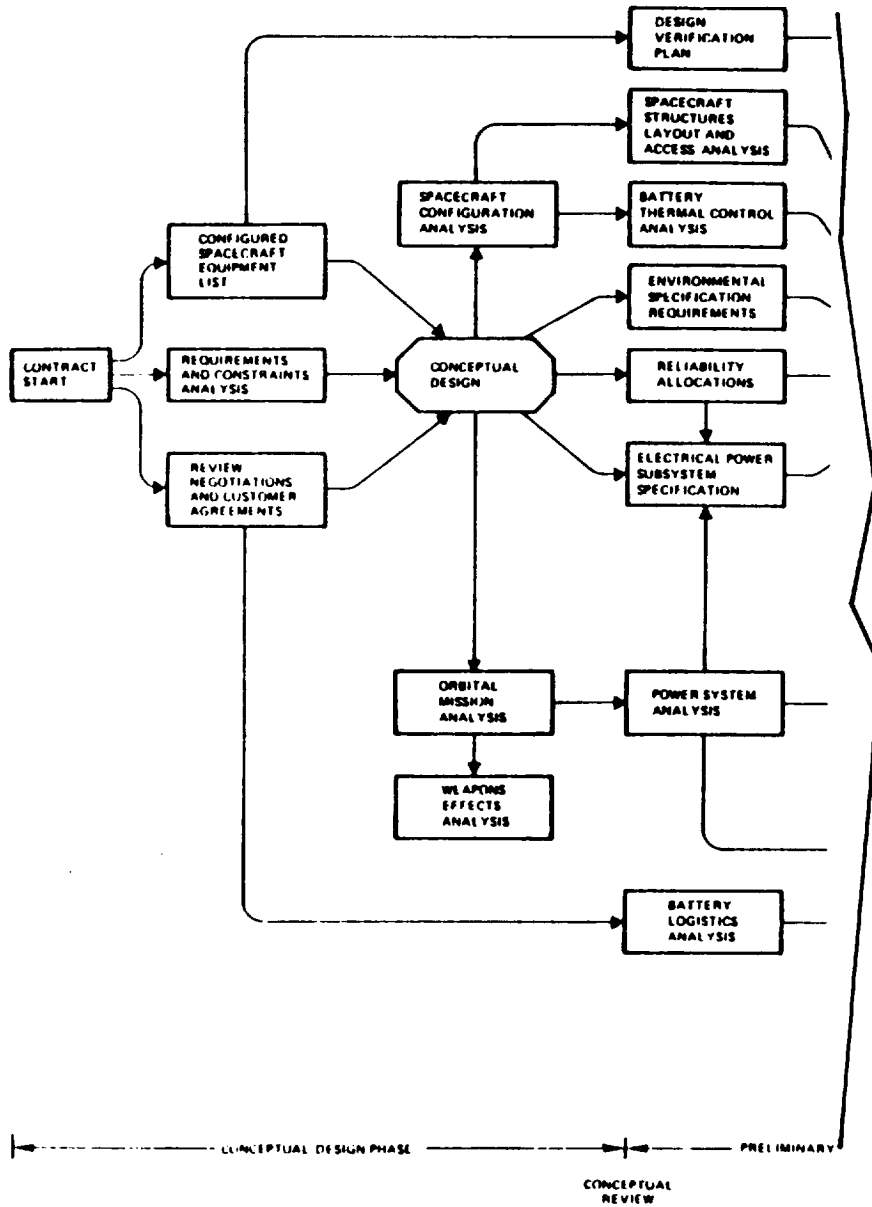


Figure 119. Typical battery design and development process flow chart (sheet 1 of 3).

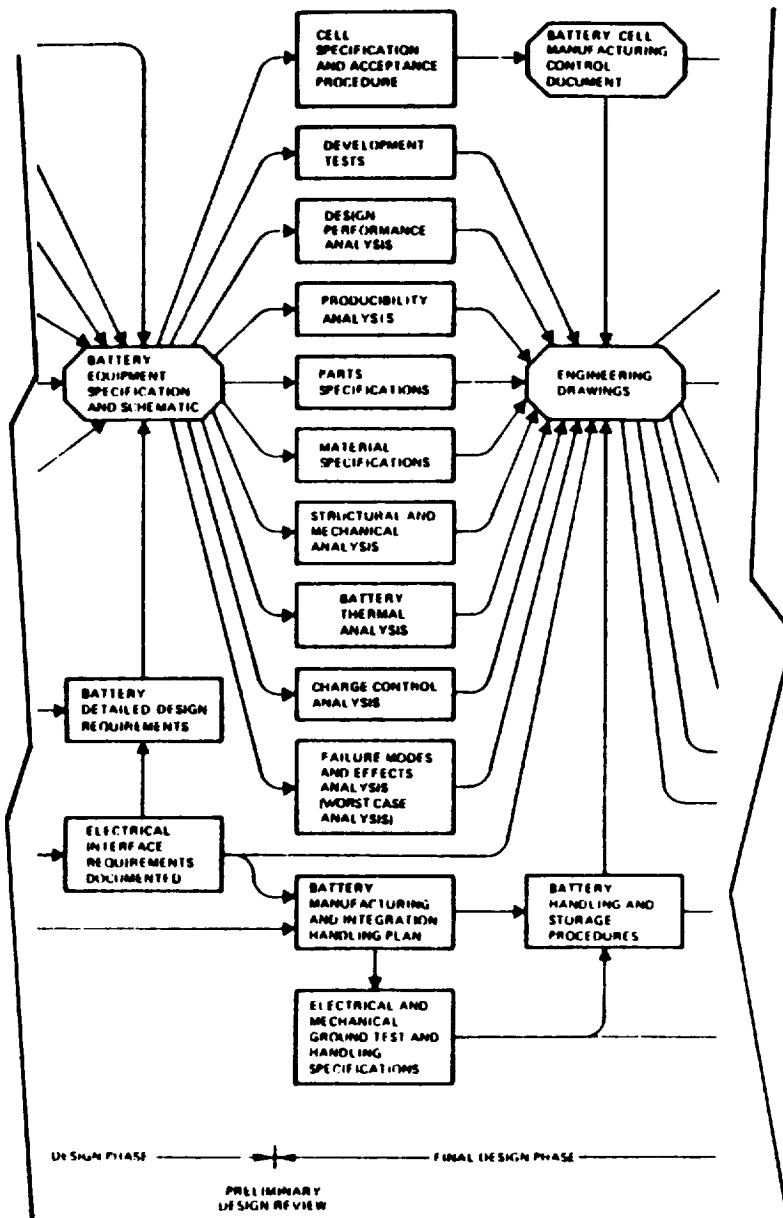


Figure 119. Typical battery design and development process flow chart (sheet 2 of 3).

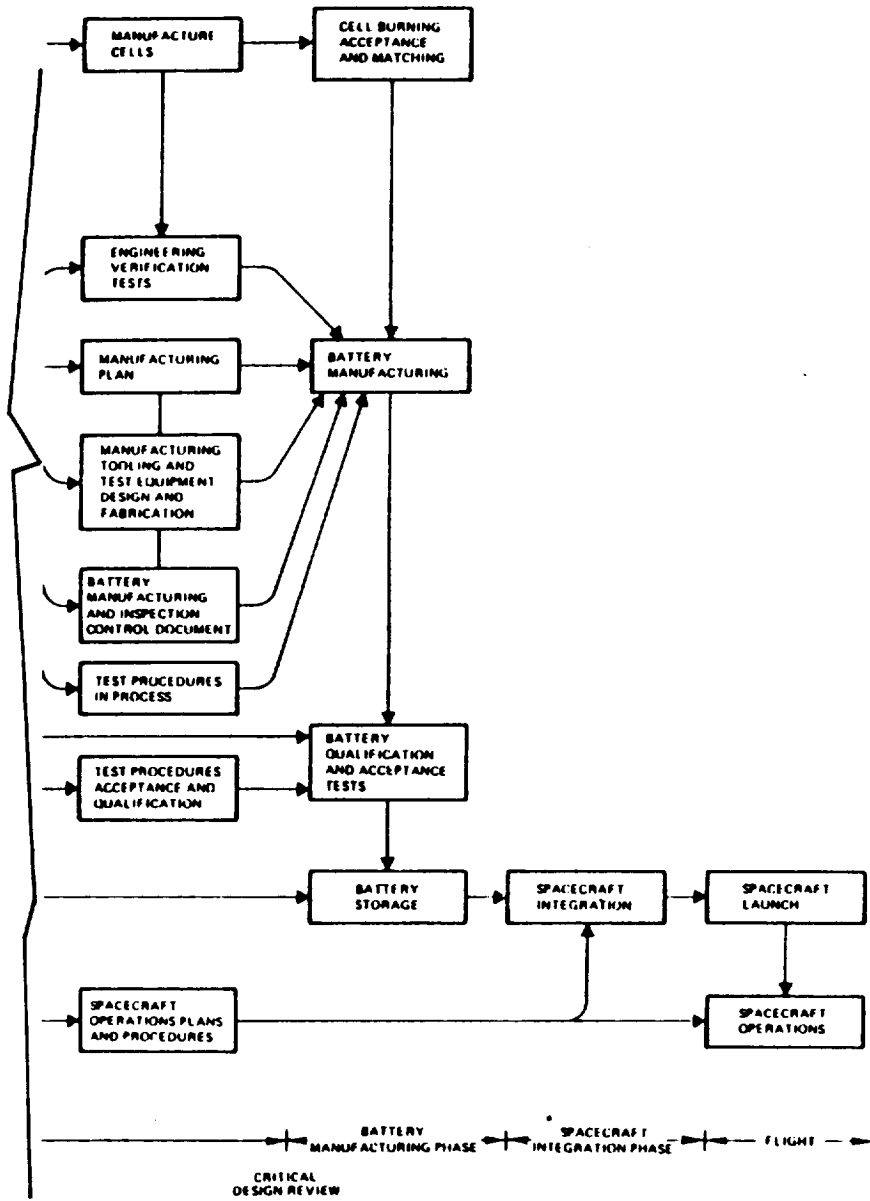


Figure 119. Typical battery design and development process flow chart (sheet 3 of 3).

determined. Critical interfaces are analyzed, and tradeoffs are performed to achieve an appropriate balance between performance, weight, cost, and reliability. The output of these efforts is a conceptual battery-system design that represents a point of departure for preliminary design activities. The number of batteries, the number of cells in each battery, the size of the cell, the selected redundancy approach, the method of charge control, the operating and in-orbit storage temperature ranges, and the packaging concept are determined. Preliminary estimates of battery weight, volume, mounting-surface area, and heat-generation profiles are developed.

The preliminary design phase is concerned with the engineering analyses required for preparing a battery equipment specification and an electrical schematic diagram. Two analyses are performed: (1) those that are necessary for a firm definition of all interfaces between the battery, its auxiliaries, and other spacecraft systems and components; and (2) those performed in conjunction with general electric power-system analyses and sizing calculations. The cell procurement process is usually under way during this phase with a preliminary version of the cell procurement specification available for review and negotiation with the selected supplier.

The final design phase encompasses all of the detailed analyses and liaison required for preparing specifications, drawings, and test plans and procedures that the battery and its auxiliaries require. Manufacturing plans and procedures are developed, and tooling and special test equipment are designed and released for manufacture or procurement. The battery cell Manufacturing Control Document (MCD) is finalized. Cell manufacturing begins, and engineering verification and characterization tests are conducted.

A design review usually concludes each design phase. When the third, or critical, design review is successfully completed, the component is released for manufacture and test.

9.2.1 Analysis of Requirements and Constraints

The analysis of requirements and constraints is the most critical step in the battery-design process. The requirements for the battery system and the batteries *per se* are derived from an evaluation of constraints and interfaces that is determined by:

- Launch trajectory and orbit or mission trajectory characteristics
- Spacecraft electrical power requirements

- Spacecraft thermal-control system capability and performance characteristics
- Spacecraft structural configuration and dynamic-response characteristics
- Natural or manmade radiation environments
- Special considerations such as generated magnetic moment characteristics or sterilizability
- Battery-system and component reliability allocations
- Component producibility guidelines and goals
- Spacecraft integration plans that identify battery logistic schedules, support equipment requirements, and power-system and battery-system checkout and test objectives.

The importance of complete and early definition of interface requirements cannot be overemphasized. These requirements should be defined before the preliminary design review (PDR) and documented in a power-system specification and/or in an interface requirements document issued to include the battery system and its configured (separately identified) components.

9.2.2 Electrical Design

The development of the electrical design of a battery system involves several major activities. This section discusses the activities that are directly concerned with the battery component. Specific discussion of design activities that are necessary for developing battery auxiliaries (e.g., charge or discharge control and power conversion circuitry) is beyond the scope of this manual. This should not be an inconvenience because the general design process for electronic equipment development is quite well-known. The main problem that confronts the responsible battery-system designer is that of coordinating parallel design activities to ensure that requirements are met, that interfaces are compatible, and that engineering verification tests are properly defined and conducted.

9.2.2.1 Electrical Performance Analyses

Electrical performance analyses are usually performed in conjunction with power-system analyses and may be coordinated with spacecraft thermal-system design analyses. Before and during the conceptual design phase, it is

usually sufficient to use approximate calculation techniques. For the preliminary and final design, the analyses are simplified, particularly for low-altitude orbit applications, through the use of computerized cell- and battery-simulation models. Section 8 describes simulation models that apply to both performance and reliability calculations.

The performance analyses are conducted to determine the following parameters as they vary throughout selected discharge/charge cycles:

- Battery state of charge
- Battery charge and discharge currents
- Battery charge and discharge voltages
- Battery heat-generation and temperature profiles

The selected cycles represent key in-orbit situations that involve extremes of eclipse or full sunlight duration, extremes of insolation on battery heat rejection surfaces, cell or battery failures within specified acceptable limits, or cases of anticipated degraded cell performance. The results of these analyses are used in the final determination of battery electrical dimensions (i.e., number of cells and cell capacity), in the assessment of electric power-system voltage-regulation characteristics, and in the prediction of battery-system reliability.

The electrical performance analyses are updated several times during the engineering phase as the power-system load requirements change. Past experience has shown that a positive battery-load growth margin is necessary at the time of the conceptual design review to avoid major changes to the battery design after the preliminary design review. The battery engineer must negotiate design margins vigorously to ensure that they are adequate and that the opportunity for minimizing cost and schedule risk to the project is not lost.

9.2.2.2 Battery-Cell Selection

The primary output of the electrical performance analyses is the required size of the cell in terms of its rated capacity. However, this calculated size is not necessarily the size finally selected. Each supplier of sealed nickel-cadmium cells has a catalog of sizes that have been flight-qualified and

otherwise subjected to developmental testing and documentation. As may be expected in a competitive market, two or more suppliers may offer a cell at or near the same value of rated capacity. Therefore, it is almost always desirable to coordinate the electrical performance analyses with the available qualified cells to minimize project risk and the costs associated with developing a significantly different cell design. This does not mean that efforts for minimizing battery-system weight must be completely compromised. An existing qualified cell design/size may be scaled up or down in the direction of larger or smaller cells that are also qualified with little risk, if the same plate and separators are used, the same plate area per unit capacity and plate separation distance are used, the same ratio of electrolyte-to-plate area or void volume is used, and the same processing is used.

The cells from each manufacturer will exhibit certain characteristics unique to that supplier's design and manufacturing process. The performance characteristics of most concern that tend to be different are:

- Voltage and pressure increase on overcharge, especially at low temperatures ($< 10^{\circ}\text{C}$), is much greater in some manufacturers' cells.
- End-of-charge voltage increases with cycling more rapidly in some cells; therefore, for missions exceeding 2 or 3 years, voltage-limited charging from a fixed bus is not compatible with such cells.

9.2.2.3 Cell Development Testing

Tests should be performed to confirm that the selected cell design will perform as expected in the particular environments and operational regime to which the batteries will be exposed. Stable cyclical operation should be demonstrated with charge control performed by using nominal values of control parameters with expected operating temperature profiles and limits. Typical methods for demonstrating these capabilities are:

- Parametric electrical characterization tests
- Extended cycle tests
- Charge control verification tests (may be conducted as part of parametric characterization tests or electrical subsystem tests)
- Overcharge-rate safety-verification tests (applicable to any system operating at low temperatures in overcharge)
- Reconditioning verification tests

9.2.2.4 Definition of Battery Heat-Generation Profiles

The design of battery thermal controls must be based on a definition of the heat-generation profiles over the orbit for the range of expected operation conditions. Preliminary estimates of heat rate versus time may be made manually by using equations such as those in the section on "Heat Generation During Charge," with charge efficiency data as shown in the section on "Charge Efficiency and Charge Acceptance." As the design progresses, a large number of repetitive calculations of heat-rate profiles may be needed, and a computer program that includes the heat-generation equation will greatly facilitate this work. To minimize the impact of uncertainties in the values of charge efficiencies, results of the computations may be validated at certain points by results from direct measurements of heat rates on the cells to be used.

For low-altitude orbit applications, sufficiently accurate estimates of average battery temperature may be obtained from orbit-average values of heat dissipation because instantaneous maximum and minimum temperatures do not depart far from the average. For geosynchronous orbits, variations in heat rate are widely separated in the orbit, and, consequently, battery temperature varies over a wider range (e.g., 20°C or more) unless an extremely efficient active thermal-control device (such as a heat pipe) is used. Because of this variation, point-to-point temperature calculations are usually necessary for the longer orbits. This is particularly necessary if battery temperature is used as an input to the charge-control logic, either directly to terminate charge at a selected battery temperature or to compensate a voltage-limit level for battery temperature.

9.2.2.5 Preparation of Cell-Procurement Specifications

Cell-procurement specifications must be prepared to procure the cell designs needed for each specific design application. General guidelines for preparing this specification appear in Section 5.

NASA has developed a specification (NASA/GSFC 74-15000) for manufacturing spacecraft-quality cells (Reference 302). This specification reflects the analysis of more than a decade of observations of cell-procurement activity on NASA-sponsored spacecraft projects and the experience gathered on related activities involving cell and battery standardization. In its present form, it does not conform to format requirements for procurement for military programs, but the technical content may be used as the basis in any format. (See Section 5.)

The degree of applicability of the NASA specification to a particular project is usually decided after: (a) evaluation of the mission requirements,

(b) evaluation of the technical data available to the buyer for the cell he has selected, (c) reassessment of the buyer's procurement experience with the selected supplier, and (d) consideration of customer requirements and concerns.

9.2.2.6 Negotiation of a Manufacturing Control Document

Cells should not be procured for a spacecraft project without a full set of manufacturing control documentation. The battery engineer should carefully review the Manufacturing Control Document (MCD) to ensure that it is complete and that it will satisfy the objective of process control and repeatability. Detailed guidelines for this review appear in Section 5.

NASA has supported the development of MCD's at the following cell manufacturers:

- Eagle-Picher Industries, Inc., Electronics Division
Joplin, Missouri 64801
- General Electric, Battery Business Department
Gainesville, Florida 32601
- SAFT-America, Inc.
Valdosta, Georgia 31601
- Yardney Electric
Pawcatuck, Connecticut 02891

The development of a new and significantly different MCD for a spacecraft cell can be a lengthy process and, hence, should be considered with caution.

9.2.2.7 Preparation of Cell Acceptance and Qualification Test Procedures

Cell acceptance and qualification test procedures vary widely throughout the industry. For example, government and commercial sponsors sometimes disagree on what procedures are best. NASA/GSFC 74-15000 (Reference 302) establishes one set of requirements and procedures that can be used totally or selectively to accept and qualify cells. (See Section 6.)

Cell qualification test procedures are usually not required except for completely new cell designs. When they are invoked, the qualification test

procedures should include the acceptance tests described previously and other tests that verify that the new design will withstand the specified environments and intended application:

- **Vibration** – Three-axis vibration based on a mission overstress safety factor 1.5 times greater than the expected force transmissibility at resonance experienced when the cell is installed in the battery assembly.
- **Shock** – Demonstration of a shipping/handling and a mission shock survival capability
- **Storage** – Determination of effects of shorted, open-circuit, and trickle charge
- **Duty-cycle capability** – Performance of an accelerated life test or partial real-time test to demonstrate that the new cell design meets the specification and will provide stable performance in the intended application

9.2.2.8 Specifications for Battery Auxiliaries

Batteries often include temperature sensors, heaters and heater controls, cell-protection circuitry, and other accessories. The battery equipment specification must specify these auxiliaries. If the auxiliaries require unique devices, new device procurement specifications may be necessary. These specifications should be identified early in the design phase to ensure that approvals are obtained for space application in sufficient time for device procurement. Such devices and parts are often long-lead procurement items.

9.2.2.9 Battery Schematics and Outline Drawings

The electrical design activity includes the preparation of the battery electrical schematic, interface data sheets, the parts list, and wiring diagrams. The electrical schematic defines the battery electrical circuitry up to the connector interface. Complete electrical interface definition is usually documented separately on data sheets that define for specific functions both source (input) and load (output) characteristics on both sides of the interface. The parts list identifies the electrical and electronic parts for use by procurement, reliability, and manufacturing planning. The wiring diagram defines the battery harness configuration and is made in conjunction with mechanical-packaging concept development. Both the schematic and wiring diagrams should contain definitions of electrical test points and cabling.

9.2.3 Mechanical Design

The objective of the mechanical design activity is to integrate the battery cells, sensors and controls, and structure into a single package. The mechanical design requirements, identified by the battery equipment specification, include:

- Weight
- Size and envelope constraints, including mounting orientation
- A mounting interface that is compatible with the spacecraft structure in terms of the dynamic launch environment defined at the interface
- Provisions for containing cells without deformation with maximum predicted cell pressures (usually 100 to 300 psig)
- Provisions for containing cells without damage or deformation during dynamic launch environments (with a safety factor of 1.5 times the expected force transmissibility at resonance)
- Ability to withstand low-cycle fatigue stresses induced by thermal and pressure cycling within the cells throughout the battery service life
- Provisions for adequate heat-transfer paths to meet thermal-gradient design requirements
- Provisions for external cooling during ground test operations
- Compatibility with spacecraft-level requirements for accessibility and replaceability
- Compatibility with manufacturing tooling and spacecraft-integration handling fixtures
- Compatibility with radiation hardening requirements

The mechanical design activity performs the following analyses and tasks in developing and demonstrating the mechanical design:

- Materials are reviewed and selections are made to meet weight, strength, and thermal-design requirements. Materials selection trade-offs should be made before the PDR to ensure that these requirements

are met and that availability, workability, and cost considerations are satisfied.

- Thermal analyses are performed on power-handling and temperature-sensing devices and parts to ensure that they are maintained within safe operating temperature limits under worst-case failure/degradation operating modes.
- Structural analyses are made to define the shape and dimensions of load-bearing members. These analyses should not be overly conservative at the predicted qualification levels to avoid unneeded weight in the battery and in the spacecraft structure at the mounting interface. Structural analyses are typically required for:
 - Dynamic loads at liftoff
 - Preloading applied to cells in the battery assembly
 - Loading that results from pressures generated within cells during worst-case or abnormal operations
 - Battery mounting fastener and mounting panel insert integrity under dynamic loading at liftoff and separation
- Detailed battery mass properties analyses are prepared by PDR and maintained current as the design progresses. This is an estimate of battery weight and center of gravity based on piece-part data (estimated or measured).
- Manufacturing methods reviews are scheduled regularly as the mechanical design progresses to ensure that the battery is manufacturable and that proper assembly tooling is designed and provided. The equipment must be repairable.
- Detailed parts and assembly drawings are prepared to define the mechanical design and assembly. Preliminary drawings of the assembly and schematics should be available by PDR. Final drawings made to the standards of the manufacturing drawing system should be presented at the critical design review (CDR) with final release to manufacturing after CDR approval.
- Assembly procedures are developed by manufacturing with support and review by both electrical and mechanical design engineers. The

assembly procedures should include precise definition of all sub-assembly tasks, final assembly tasks, and in-process inspections. Safety precautions should be defined in the assembly procedures.

9.2.4 Thermal Design

The battery-system thermal design often directly and significantly affects the spacecraft thermal-system design. Therefore, the thermal characteristics of the battery itself must be accurately defined. The main source of heat dissipation in a battery is the battery cells. However, if the battery also comprises power resistors, diodes, or other semiconductor devices that may carry heavy currents during certain operating modes, the overall heat-dissipation profile must be determined. Section 9.2.2.4 gives the calculation of the profile for the cells. The calculation for other parts is more straightforward after currents and voltages are established. If semiconductor devices are used to bypass cells during overcharge or overdischarge, calculating the division of battery current between the cell and the bypass device can be difficult.

As implied previously and discussed in Section 8, considerable interaction occurs between several design specialists. The battery engineer gives and receives information to a thermal-system component designer and a component thermal-design specialist. The thermal engineers also interact with the electric power-system engineer. Other key contributors to the overall design process are the spacecraft electrical- and mechanical-system engineers and the structural-system engineer.

When a thermal-control concept has been established and requirements have been defined for the battery-system components, the thermal-system component designer is responsible for translating the concept into hardware that satisfies other allocations of weight, cost, and reliability. At the battery level, the main objectives of the thermal analysis and design activities are to:

- Define and minimize thermal gradients between the cells within the battery package
- Define and minimize thermal gradients between the cells and the heat-rejection surface aboard the spacecraft
- Maintain the temperature of electrical and electronic auxiliaries mounted to the battery within specified limits
- Define the position and mounting of temperature sensors and heaters

- Select thermal-control materials and coatings and analyze their effect
- Analyze and design integrally mounted thermal-control auxiliaries
- Analyze battery thermal performance during ground operations with external cooling
- Develop thermal simulation models of the cells and the primary heat-transfer paths
- Prepare battery thermal-design verification test plans and provide technical support to the verification tests

The battery engineer is responsible for coordinating these activities and for ensuring that the resulting definitions are compatible with electrical and mechanical requirements for the battery. Incomplete or inadequate thermal-design analyses have resulted in both prelaunch and postlaunch problems for several spacecraft. Less obvious are the effects on long-term operational performance that may occur because of neglect in developing the battery thermal design during the spacecraft definition studies and conceptual design phases. Therefore, the importance of the role of the battery engineer in identifying, guiding, and monitoring thermal-system and thermal-component design activities during this early period cannot be over-emphasized.

Section 3 summarizes cell thermal properties, and section 7 describes battery thermal-design techniques. Although this information can be used for preliminary design, detailed cell data used for design should be validated by the test for the actual components used. Battery-cell cyclical and incremental charge efficiencies vary with design. Beginning-of-life to end-of-life charge and trickle-charge rates significantly affect resultant battery heat-dissipation characteristics. Thus, it is necessary to perform thermal analyses at the beginning- and end-of-life design points for all battery systems. The resulting thermal performance predictions should be incorporated into electric power- and thermal-control system models to verify total spacecraft energy balance.

9.2.5 Battery Equipment Specification

A battery equipment (or component) specification is mandatory for each spacecraft battery. It defines battery-design and interface requirements and establishes the basis for acceptance, qualification, and handling of the component. The battery equipment specification is derived from, and referenced

to, the electric power-system specification. A preliminary version of the specification should be approved at the time of PDR before the detailed design phase is begun.

NASA has developed specifications for a standard nickel-cadmium battery that can be used as models for other battery equipment specifications. Reference 182 describes the design and acceptance requirements for the standard battery, and Reference 181 describes the requirements for qualifying the standard battery. These specifications provide guidelines for aerospace nickel-cadmium battery design and design verification that reflect a general consensus among Air Force, Navy, and NASA battery technology centers.

9.2.6. Design Reviews

Scheduled design reviews are important milestones in the design and development process because they provide an opportunity to detect problems that might otherwise remain undetected until budgets and schedules or spacecraft performance are finally impacted. They also facilitate dissemination of design details to all concerned personnel. An effective review should be preplanned to ensure that all aspects of the design are covered and, if problems are discovered, that proper resources are brought to bear on their solution. Technical specialists, both independent and those involved with the design, should be given an opportunity to review a design summary data package before the review so that questions and comments can be properly formulated. The responsible battery engineer and key contributors to its design should present the design and provide answers to the questions at the review. Customer representatives, as well as functional and project management representatives of the project contract, should be present. Product Assurance and Reliability Engineering representatives should attend all major design reviews. Minutes of the meeting should be taken, and action items, agreements, and expressed concerns should be recorded. The tone of the meeting and all related activities should be constructive rather than adversary.

At least six reviews are usually performed during a typical battery development project:

- Conceptual design review – Before beginning battery component specification, review of battery interfaces and performance requirements; definition of a baseline design
- Preliminary design review – Identification of updated battery performance and interface requirements; presentation of the cell specification

and design/development plans; review of analyses and tradeoffs made in support of configuration detail definition

- Critical design review – Review of the final design, additional analyses, and engineering development test results; determine if the design is ready for release to manufacturing
- Manufacturing readiness review by engineering – Review of the design with manufacturing to interpret drawings and design data
- Manufacturing readiness review by manufacturing – Review of manufacturing and inspection plans, procedures, and tooling to verify the battery producibility
- First article open-box review – Review of first battery assembly before closing and beginning the acceptance tests to confirm that the as-built configuration meets design requirements and workmanship standards

A design review checklist for each of these events appears in table 56.

9.3 BATTERY MANUFACTURING

The manufacture of sealed-cell nickel-cadmium batteries requires skilled personnel and facilities comparable to those required for producing aerospace electronic equipment. Mechanical assembly and electrical wiring operations are performed in a contamination-controlled environment. Special tools and fixtures are required for assembly and handling. This is usually necessary for assembly because the cells are often packaged under a compressive preload and, therefore, part tolerances must be verified, matched, and adjusted with shimming techniques; for handling, this requirement is simply because the complete battery assembly is relatively heavy and awkward to move and position.

Each battery represents the application of a considerable amount of materials technology. Certain surfaces must be electrically insulated from one another. Certain joint thermal conductances must be maximized. Materials and coating must be compatible to avoid corrosion problems during prelaunch storage and handling—problems that may occur either in the battery component or at the interfaces between it and temporary fixtures. In some designs, cell cases are modified before battery assembly by applying coatings or electroplating, by attaching thermally conductive shims by bonding, or simply by applying a dielectric layer.

Table 56
Design Review Checklist*

Task	Conceptual Design Review	Preliminary Design Review	Critical Design Review	Engineering Manufacturing Readiness Review	Manufacturing Engineering Readiness Review	First Article Open-Box Review
Interface Analyses						
Thermal	P	P	F			
Electrical loads	P	P	F			
Charge/discharge controls	P	P	F			
Sensors	P	P	F			
Command/telemetry requirements	P	P	F			
Spacecraft equipment layout	P	F				
Battery envelope drawing		P	F	F	F	
Battery mounting drawing		P	F	F		
Cable/harness description	P	P	F	F	F	
Electrical ground equipment		P	F	F		
Thermal-test support equipment		P	F	F		
Handling fixtures		P	F	F		
EMC requirements		P	F			
Radiation requirements		P	F			
Magnetic requirements		P	F			
Space charging requirements		P	F			
Electrical Design Analyses						
Electrical compliance						
Requirements analysis	P	U	F			
Capabilities analysis						
Capacity sizing	P	U	F			
Voltage regulation	P	U	F			
Life verification	P	U	F			
Reliability						
Success analysis	P	U	F			
FMEA		P	F			
Electrical design description						
Cell description definition	P	F	F	F		
Battery description	P	U	F	F		
Cell specification	P	U	F			
Battery specification		P	F			
Development plan	P	F				
Manufacturing logistics plan		P	U	U	F	
Spacecraft logistics plan		P	F			
Charge-control requirements	P	U	F			
Sensor specifications	P	U	F			
Test equipment design	P	U	F			
EAGE equipment design	P	U	F			
Electrical procedures						
Development test		P	F			
Cell acceptance test			P	U	F	
Battery manufacturing test			P	U	F	
Battery acceptance test			P	U	F	
Battery qualification test		P	U	U	F	
Storage and reconditioning		P	U	U	F	
Spacecraft preparation			P	U	F	
Spacecraft integration			P	U	F	
Spacecraft operations			P	U	F	

*P = Preliminary, F = Final; U = Update. EMC = Electromagnetic compatibility, FMEA = Failure modes and effective analysis, EAGE = electrical auxiliary ground equipment.

ORIGINAL PAGE IS
OF POOR QUALITY

Table 56 (Continued)

Task	Conceptual Design Review	Preliminary Design Review	Critical Design Review	Engineering Manufacturing Readiness Review	Manufacturing Engineering Readiness Review	First Article Open-Box Review
Mechanical Design Analyses						
Requirements analyses	P	U	F			
Reliability analysis	P	U	F			
Spacecraft interface requirements definition	P	U	F			
Assembly outline	P	U	F			
Battery assembly		P	U	F		
Weight/strength tradeoffs	P	U	F			
Mass properties	P	U	F			
Long-lead parts list	P	F				
Assembly parts list		P	F			
Cell-to-cell interconnector design			P	U	U	F
Accessibility analysis		P	U	F		
Producibility analysis		P	U	U	F	
Detailed drawings			P	U	U	F
Assembly procedures			P	U	U	F
Handling requirements			P	U	U	F
Handling fixture design			P	U	U	F
Safety analysis			P	F		
Thermal Analyses						
Cell thermal data	P	U	F			
Verification of compatibility with spacecraft thermal system	P	U	F			
Battery thermal analysis						
Heat generation profiles	P	U	F			
Heater sizing		P	F			
Heater controls definition	P	U	F			
Temperature sensing definition	P	U	F			
Thermal verification						
Test plan		P	F			
Test procedure		P	F			

*P = Preliminary, F = Final, U = Update.

A key aspect of battery manufacturing involves the understanding and support of the product assurance function within the battery manufacturer's organization. Many manufacturing operations are unique to the battery product line, and their definition and implementation should be coordinated with quality engineers and inspectors in the earliest stages of development to ensure that product assurance objectives are met. Therefore, an appropriate theme for the manufacturing phase is that of teamwork among contributors with various skills and functions.

Detailed planning is essential to the economical production of high-quality components. This is particularly true for nickel-cadmium batteries because their cells are normally considered to have a limited shelf life when stored under ambient environmental conditions. (Storage at reduced temperatures provides sufficient shelf lifetime extensions for most projects.) Plans are therefore needed that reflect best use of battery manufacturing personnel and facilities and that are coordinated with logistic constraints and top-level production schedules for the spacecraft project. Among these are the following documents:

- Facilities allocation plan
- Capital equipment allocation plan
- Tool, fixture, and special test-equipment development plan
- Battery manufacturing control document
- Manufacturing flow chart
- Personnel training plan
- Manufacturing schedule

The battery engineer should monitor the development of these plans, documents, and schedules to ensure that they are compatible with the battery design and other project schedules. All manufacturing plans should receive final approval as part of the critical design review for the component.

9.4 BATTERY ACCEPTANCE TESTING

Acceptance tests are performed to verify that each manufactured battery is properly assembled and that it complies with the requirements for acceptance.

9.4.1 Test Requirements

Acceptance test requirements are defined by the battery equipment specification and by the spacecraft component environmental specification, if there is one. A typical test sequence is as follows:

- Physical measurements
- Physical inspection
- Functional tests
 - Electrical insulation resistance
 - Electrical continuity
 - Connector bonding resistance
 - Temperature sensor operation
 - Thermostatic switch operation
 - Heater-circuit operation
 - Seal-leakage test
 - Capacity verification test
 - Charge-retention test
 - Peak-load test
- Vibration
- Peak load
- Thermal vacuum
- Capacity tests
- Functional tests
 - Conditioning
 - Seal-leakage test
 - Charge-retention test
 - Electrical insulation resistance
 - Electrical continuity
 - Connector bonding resistance
- Physical inspection

9.4.1.1 Physical Measurements

Battery dimensions and weight are verified by physical measurement. Only those dimensions that are critical to interfaces should be used for acceptance purposes.

9.4.1.2 Visual Inspection

A visual inspection is made to ensure that the battery complies with its drawings and imposed workmanship standards and that no physical damage (cosmetic or structural) has occurred during assembly and in-process testing. The inspection should include solder joints, inserts and fasteners, electrical insulations, degree of cure of potting and encapsulating compounds, and general cleanliness.

9.4.1.3 Functional Tests

Certain tests are necessary for verifying that the battery has been assembled properly and performs as designed. Some of these tests are performed only once, but others are performed both before and after planned environmental acceptance tests:

- Electrical insulation resistance – the resistance between the positive terminal of the battery to the battery case and between the positive terminal of the battery and each externally mounted transducer (thermistor, strain gage, etc.) is measured with a megohmmeter at 100 Vdc for 1 minute. (It is assumed that the battery is used in a negative-ground electric power system.) The measured resistance values shall be greater than 100 megohms.
- Electrical continuity – Each wire in the battery harness is checked to verify the electrical path and terminations.
- Connector bonding resistance – The resistance between the connector shells and the battery case is measured to verify that electrical grounding requirements are met. The resistance should be typically less than 5 milliohms. (This test is a relatively new requirement and is one of the design criteria developed in response to studies of spacecraft space-charging phenomena.)

- Temperature sensor operation – A calibration curve is generated from test data taken over the expected battery temperature range. The data are reviewed to verify proper sensor operation.
- Thermostatic switch operation – The battery is temperature-cycled while in a discharged and shorted state to verify thermal-switch set points and operation.
- Heater-circuit operation – Heater circuits are operated to verify that the proper current is conducted at a selected voltage. Both primary and redundant circuits are verified.
- Seal-leakage test – Seal-leakage tests may be performed after assembly and at selected intervals during testing. The test most often used involves the application of a 0.5- to 1.0-percent phenolphthalein solution around the terminals and exposed cell-weld areas. A red indication is evidence of potassium hydroxide leakage. A second positive indication should be obtained before rejection. A nonaqueous solution is sometimes used to prevent corrosion caused by residual water and to prevent spurious indications caused by the electrolysis of water in the test solution. The seal-leakage test is usually performed during or immediately following an overcharge test.
- Capacity verification test – Capacity verification is accomplished by charging and discharging the battery in a particular manner. The test is performed differently by several companies. A typical method is:
 - The battery is first conditioned with a C/10 charge for 24 hours at $24 \pm 2^{\circ}\text{C}$, followed by a C/2 discharge to 1.0 volt per cell average. (No cell is permitted to discharge below 0.5 volt.) Each cell is then discharged to zero volts through individual resistors.
 - The battery is next charged as it would be during normal spacecraft operations and discharged to 1.0 volt per cell average at the normal spacecraft rate. (No cell is permitted to discharge below 0.5 volt.) Individual cell voltages are monitored to verify uniform voltage behavior. The cycle is repeated several times (three is typical) to determine that measured capacity meets the specification requirement.

An alternate method appears in Reference 182.

- Charge-retention test – This test can be performed in different ways.

NASA uses the voltage recovery method (Reference 182). The charge-retention method is used widely throughout the industry. (See Reference 83.) Proper conditioning of the battery before either test is performed is essential (See Reference 83.)

- **Peak-load test** – A peak load applied at a 3C discharge current rate is used to verify battery performance following vibration. This test usually follows a C/2 discharge for 1 hour, and the 3C rate is applied for 5 minutes. The minimum allowable voltage is usually specified at 1.10 volts for any cell. Care should be exercised to verify that the battery can tolerate the 3C rate.
- **Environmental acceptance tests** – These tests vary from project to project, but they are usually designed to meet certain well-defined objectives. Vibration testing verifies structural, fastener, and harness integrity and demonstrates electrical continuity throughout exposure to an environment similar to that which will be encountered at launch. Thermal-vacuum testing verifies temperature sensor operation and the integrity of adhesive bonds and encapsulants. It is usually performed with temperature limits set 10°C beyond the expected extreme operating temperature limits. The duration of thermal-vacuum testing at the component level should be determined by evaluating the amount of subsequent exposure planned during spacecraft-level tests. (There may be little or no exposure if installation on the spacecraft is delayed until just before launch.) Sufficient testing should be performed to ensure that the battery is adequately out-gassed before launch.

9.4.2 Data Analysis and Acceptance Criteria

Properly written specifications, test procedures, and test data sheets permit unambiguous pass/fail interpretations of the inspection and functional test results. However, additional information is necessary. Individual cell voltages should be monitored to within ± 1.0 mV throughout acceptance testing and recorded. These data are used to determine the degree of voltage balance among the cells. If an imbalance develops, the battery should be examined closely to determine the cause because this condition may signal later failure. Data collected at this time also serve as a basis for comparison with data collected during spacecraft integration and prelaunch checkout tests.

9.5 BATTERY QUALIFICATION TESTING

A battery can be qualified by means of either analysis or testing or both, depending on the amount of new design work required for its development. Minor changes can normally be qualified by similarity to proven designs. Major changes and new designs should be tested to verify that the design is adequate.

9.5.1 Basis for Design Qualification Tests

The purpose of design qualification tests is to demonstrate the ability of the battery to meet all performance requirements without degradation when exposed to environments more severe than those expected during acceptance testing, prelaunch, launch, orbit injection, spaceflight, or reentry. Certain safety margins are included within the qualification test limits:

- Ground mode – Test levels are selected to bound the conditions that are normally expected during fabrication, integration, and test. Ground handling, transportation, and other prelaunch activities that could impose environmental stress (e.g., shock) are usually accommodated by applying special precautions and by using specially designed handling fixtures and packaging.
- Launch mode – Dynamic levels and exposure durations are extended by multiplying predicted levels by a factor of 1.5.
- Orbital mode – One guideline (Reference 303) for setting qualification temperature limits requires that the predicted high- and low-temperature values be extended by 10°C.

9.5.2 Qualification Methods

It is current practice to perform very limited qualification tests on new cell designs—generally only vibration and life tests—and, instead, to concentrate on qualifying complete battery assemblies. Most new cell designs are derived and scaled from proven designs and do not require environmental qualification testing; qualification by analysis is acceptable. Therefore, most qualification testing occurs within three categories:

- Cell-level design verification – Cell-level qualification requirements are contained in cell procurement specifications. Qualification by similarity is usually adequate because most cell-design changes are simply

scaled from previously proven designs. If a completely new design is developed, full dynamic environmental qualification may be performed along with performance characterization tests and life-cycle tests.

- Battery assembly qualification – Battery assembly qualification test requirements are specified in the battery equipment specification and the spacecraft environmental qualification requirements specification. Battery qualification includes all acceptance tests as described in Section 9.4.1. More severe vibration and thermal-vacuum tests are usually used to validate the mechanical and thermal-design features of the battery than those required for acceptance testing. Vibration requirements are determined by spacecraft dynamics analyses on the basis of the method of launch and type of spacecraft structure used.
- Spacecraft interface qualification – Spacecraft interface qualification is as important as the battery assembly qualification tests. It is unrealistic to test large, heavy batteries as separate assemblies for shock survival because the shock characteristics experienced by the battery in a spacecraft are a function of the spacecraft's response to booster separation and other dynamic loads. Therefore, battery qualification for shock should be verified by analysis at the battery level and deferred to spacecraft-level testing. Similarly, the battery electrical and thermal interface test results at the spacecraft level should be carefully reviewed as part of the battery qualification and launch readiness reviews.

Useful guidelines for battery qualification testing appear in Reference 181.

9.5.3 Cell and Battery Test Equipment and Facilities

Cell and battery test equipment are not available as standard equipment. Each battery requires special test features and instrumentation. Standard laboratory facilities are suitable for cell and battery testing.

9.5.3.1 Standard Conditions for Test Areas

Environmental conditions must be controlled so that they do not interfere with handling of the battery. Suitable conditions for performing functional tests before or after environmental exposure are:

- Temperature: 20 to 25°C

- Relative humidity: 30 to 70 percent
- Barometric pressure: room ambient
- Cleanliness: planned and controlled to prevent contamination or degradation in accordance with FED-STD-209B
- Safety and handling requirements: Practices and procedures covering all aspects of cell and battery safety shall be available. Personnel should be trained in their use and periodically reviewed to verify compliance.

9.5.3.2 Measurements

All battery measurements should be made with precision instrumentation. Instrument calibration should be made in accordance with MIL-C-45662A. Tolerances appropriate to the collection of battery test data are:

- Temperature: $\pm 1^{\circ}\text{C}$
- Relative humidity: +0, -5 percent
- Vibration amplitude: sinusoidal, ± 10 percent; random (overall rms level), ± 10 percent; power spectral density, ± 3 dB
- Vibration frequency: ± 2 percent or 1 Hz, whichever is greater
- Shock spectral response: +50, -10 percent
- Acoustics: tolerances on all octave bands, +3 dB and -6 dB; overall spectrum levels, ± 1 dB
- Linear acceleration: +0, -5 percent
- Weight: ± 5 grams or ± 0.1 percent of the total weight, whichever is greater
- Center of gravity: ± 2.5 mm
- Moment of inertia: ± 1.5 percent
- Voltage: ± 0.1 percent of battery voltage; ± 1 millivolt, cell voltage

- Current: ± 0.1 percent of full scale
- Time: ± 1 second
- Impedence: ± 5 percent

9.5.3.3 *Special Equipment*

Batteries are tested with test apparatus and fixtures specially designed to accommodate the battery:

- Battery vibration fixture
- Battery thermal-vacuum baseplate fixture
- Battery electrical performance and functions tester
- Battery cables (for both inside the thermal-vacuum chamber and to the tester)
- Battery-discharge conditioning assemblies
- Battery connector savers (all battery connectors and connector savers to be mechanically keyed to prevent accidents)

9.6 BATTERY STORAGE, MAINTENANCE, AND INSTALLATION

This section presents approaches to battery handling, including the storage, maintenance, and installation of batteries in spacecraft. Much of the available industry data shows that battery handling and logistics methods significantly influence battery performance and life in orbit. A good battery logistics plan can help to reduce project cost and can help prevent in-orbit performance problems. However, some spacecraft-integration concepts in current use may actually shorten the service life of the batteries.

The spacecraft-integration process is most economical if flight batteries are installed and used to support integration testing of the flight spacecraft. The data and criteria discussed in this section are in direct conflict with this cost-effective integration approach. The battery engineer must therefore be prepared to negotiate an approach for battery handling that is usually, of necessity, a compromise between spacecraft-integration economics and potential limitations on ultimate battery life.

9.6.1 Prelaunch Environments

The prelaunch environments for batteries should be carefully defined in the battery component specifications and in a battery handling practice that is used by manufacturing and by spacecraft integration and test to control the battery environment and operation. Several environmental requirements should be considered:

- Exposure of cells to shipping temperatures above 35°C should be limited and monitored. Temperature-sensitive indicators can be included in the cell packages during shipment to verify that selected maximum temperatures have not been exceeded.
- Exposure of cells to room-ambient temperatures should be minimized regardless of whether they are charged or discharged. Suggested limits for batteries that are fully charged are 90 days in trickle-charge storage and 24 hours open-circuit storage per event (5 days of open-circuit storage has proved to be acceptable for a single storage interval).
- During periods of storage, or during standby periods of over 90 days, batteries should be maintained at low temperatures on the order of 0°C. Batteries can be stored as low as -20°C without danger of ice-crystal formation in the cells. Caution should be exercised to ensure proper desiccation within the package during low-temperature storage to prevent corrosion of the cells and battery packaging. Caution should also be exercised to ensure that batteries are not stored at thermal switch-operating points to prevent long-term switch stress and failure.

The following section describes practices for prelaunch handling and environmental controls that have proved to be successful.

9.6.2 Battery Storage and Reconditioning

Since 1960, the aerospace industry has used many methods of battery storage and reconditioning. During the 1960's, batteries were usually stored on trickle charge and were commonly installed aboard spacecraft immediately after acceptance testing in support of spacecraft-integration test and acceptance. Early in 1970, NASA/GSFC (Reference 304) reported a definite trend of early battery failures that indicated that exposure to spacecraft-integration handling and testing caused severe cell degradation. Figure 120 shows the effect to be loss of overcharge capability and very high voltages

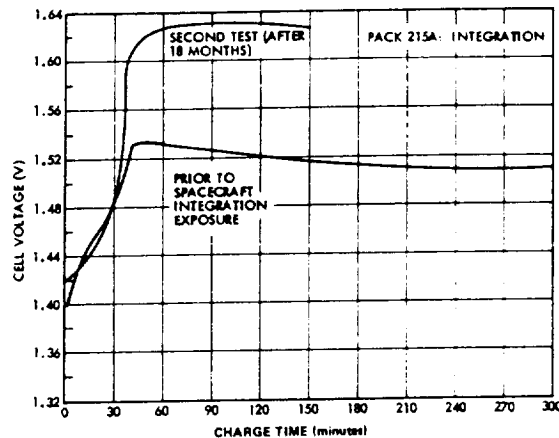


Figure 120. OAO storage test/integration exposure:
Overcharge voltage at 0°C with a C/20 charge.

on charge. Battery test results on several spacecraft projects further corroborated these results.

Beginning in 1970, some users began to reconsider their prelaunch and in-orbit handling procedures (Reference 128). Air Force and NASA programs switched to shorted storage before launch and, in one case, utilized shorted storage in orbit. The Intelsat-IV spacecraft batteries were stored charged and open-circuited during the solstice seasons; most other spacecraft use trickle charge in solstice seasons. The results obtained using shorted storage before launch and in orbit have been excellent. Shorted storage has proved to be effective for up to 5 years before launch without significant subsequent degradation caused by storage (Reference 305).

Long-term open-circuit storage on the ground and in orbit has not been effective, although some success has been reported when storing fully discharged (shorted before storage) batteries on open circuit for short-term periods of up to 60 days (Reference 306). In general, however, open-circuit storage is not recommended.

Trickle-charging of batteries has been used in the past as a storage procedure. However, long-term trickle-charging results in some degradation of the cell separator (Reference 304) and reduces the active surface area of the negative plate (Reference 307). Figure 121 shows typical voltage characteristics after 18 months of trickle charge. These data suggest that, for long

service life, trickle-charging should be limited before launch. Recent data (Reference 30) also show that storage at temperatures at or above room ambient reduces the life of the cells by causing the negative-plate overcharge protection to be reduced. Section 4 describes the mechanism of this process.

Trickle-charging at room-ambient temperatures tends to increase cell temperatures above ambient, further accelerating the degradation processes. When trickle-charging is used, the procedure should limit the upper temperature limits as much as practical, and trickle-charge rates should be minimized to levels required to maintain the cells charged as shown in figure 122.

9.6.3 Battery Standby Operations

The following practices are general guidelines for battery storage and reconditioning:

- Standby trickle charge – The battery should be trickle-charged between $C/75$ and $C/50$ at room-ambient temperatures. Battery temperatures should be maintained below 30°C and, preferably, below 10°C . The trickle-charge rate should be adjusted as a function of temperature in accordance with figure 121. The battery should be discharged and boost-charged before operation. Trickle-charge periods should be limited to a 90-day cumulative maximum for long-life applications.
- Standby open circuit – Fully charged open-circuit storage should be limited to 5 consecutive days as a planned single event. (Twenty-four hours is a preferred limit when several events must be accommodated.)

Fully discharged open circuit storage should be limited to 14 consecutive days. All cells of the battery must be individually short-circuited for at least 16 hours after battery discharge prior to putting the battery on open-circuit stand.

Open-circuit stand intervals over 2 to 4 hours should be followed by special conditioning, such as a short discharge before the reinitiating of charging to avoid possible hydrogen-burst phenomena or other side effects. Batteries subjected to short discharges should always be fully recharged to prevent cumulative capacity degradation effects.

Cumulative open-circuit stand time should be minimized, but exact specification limits have not yet been identified.

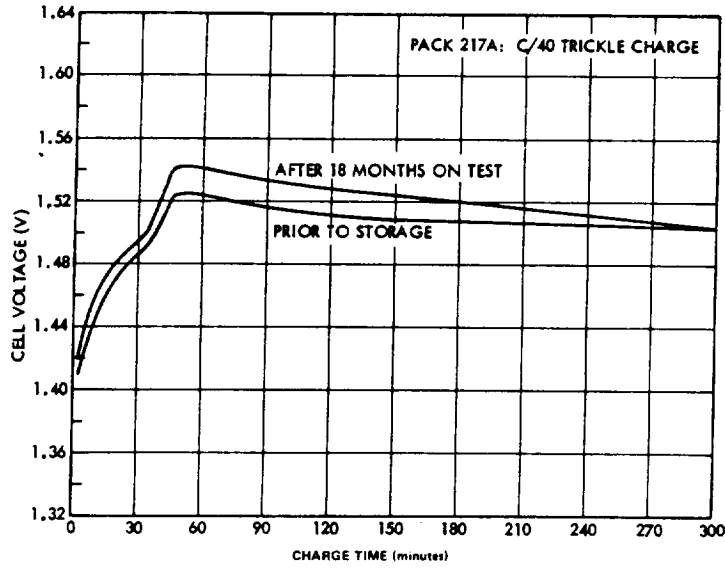


Figure 121. OAO storage test/trickle-charge storage: overcharge voltage at 0°C with a C/20 charge.

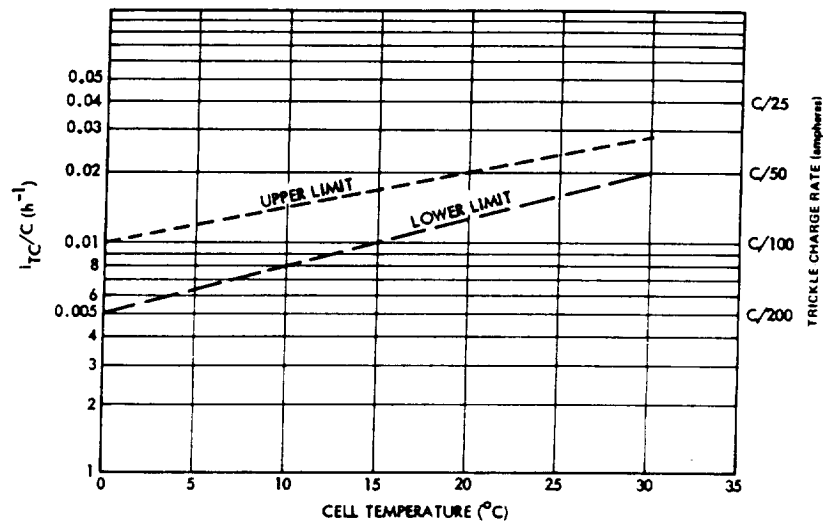


Figure 122. Suggested range of trickle-charge rates for battery storage or standby during ground testing.

- **Battery storage** – Batteries stored over 90 days should be discharged and shorted at the cell level. Practical temperature limits for storage are $-5 \pm 10^{\circ}\text{C}$, but thermal switch operating points should be avoided. Batteries that are stored shorted should be recharged and tested periodically to verify that components are operational and that cell performance remains normal.

Batteries to be stored less than 90 days should be discharged and shorted at the cell level. Although storage at low temperature is preferred, storage at room ambient is acceptable. Again, the thermal switch operating points should be avoided during storage.

Battery storage after activation should be minimized by spacecraft logistics planning. Several spacecraft contractors limit the battery activated life before launch to less than 1 to 2 years. An experimental work (Reference 180) is now in process attempting to define the limits for storage before launch, but this effort has not been completed. Preliminary data show acceptable performance after storage of at least 5 years.

9.6.4 Shipment and Installation

Procedures for shipping and installing batteries into spacecraft vary widely throughout the aerospace industry. Three general approaches have been successfully applied:

- Shipping batteries to the launch site discharged and shorted; charging and testing the batteries at the launch site; and installing the batteries in the spacecraft before placing the spacecraft on the launch stand. Although this concept represents minimum risk to battery life, it provides the least verification of the battery-to-spacecraft interfaces.
- Charging the batteries and installing them in the spacecraft just before shipping the spacecraft to the launch site; shipping the batteries installed in the spacecraft on trickle charge or open circuit with a 24-hour maximum shipping period; and placing the spacecraft directly on the launch stand on arrival at the launch site. Although this practice provides limited verification of the spacecraft interfaces before shipping, it provides no launch site verification of the battery.
- Charging the batteries and installing them in the spacecraft just before the spacecraft acceptance thermal-vacuum and spin-balance tests; testing the batteries during spacecraft thermal-vacuum tests; discharging

and shorting the batteries on the spacecraft following thermal-vacuum testing; shipping the spacecraft to the launch site and then recharging and retesting the batteries at the launch site before placing the spacecraft on the launch stand. This practice requires special cooling provisions at the launch site and a capability of the spacecraft/support equipment for charging the batteries. This concept provides an excellent validation of the battery-to-spacecraft interfaces and battery performance after shipping.

Other approaches or variations of the foregoing can be adopted. However, the battery engineer should not accept any approach unless it is supported by a thorough, well-documented battery and spacecraft logistics plan. As discussed in Section 9.6.2, spacecraft integration checkout and testing with installed flight batteries should be avoided or minimized to reduce risk of battery damage and degradation. The selected approach should reflect this ground rule to the greatest practical extent.

At a lower level of detail, several points are worthy of consideration when shipping and installation procedures are developed:

- Battery connectors and cell terminals must always be protected to prevent personnel injury and equipment damage from shorts. The use of connector savers is recommended for in-transit or standby charging.
- Batteries should not be shipped in a charged state without utilizing special handling practices.
- Batteries should be shipped in packing containers that protect against shock and transport vibration. Containers designed in accordance with Federal Standard PPP-B-566 or PPP-B-636 can be used for shipping batteries. Containers in which the batteries are securely mounted to a support structure are preferred over free-floating package configurations.

Personnel concerned with transporting and installing flight batteries should be completely familiar with the logistics plans, project-specific procedures, and all applicable design practices.

SECTION 10 APPLICATIONS

10.1 INTRODUCTION

This section describes examples of both past and present battery-development activities and briefly considers the role of the sealed nickel-cadmium cell in terrestrial applications. Numerous examples of electric power systems, battery systems, and battery component applications have been identified and discussed in earlier chapters. The purpose here is to catalog some of the most representative items of hardware and, thereby, to simultaneously show features both common and unique to the selected designs. The configurations described have been successful, and some reflect imaginative departures in design. They are offered not as an endorsement of a "correct" design approach, but as a point of departure in the development of future lightweight, low-cost, energy-storage systems of high reliability.

10.2 BATTERY-SYSTEM HARDWARE DESCRIPTIONS

Sections 10.2.1 through 10.2.8 summarize the electrical and physical characteristics of batteries used on certain low-altitude and geosynchronous spacecraft, as well as their environmental capabilities. These data were obtained from Reference 308 and were reformatted for this manual. The spacecraft are listed by increasing battery-cell size. Certain characteristics are included only when applicable.

Reference 308 is part of a final report prepared by the Aerospace Corporation for NASA Headquarters as a consequence of a Standardization and Program Effect Analysis conducted during 1975. Part C of Volume IV, Equipment Compendium, summarizes the characteristics of not only batteries but also battery chargers, discharge regulators, power-control equipment, power converters, series-load regulators, shunt regulators, and solar arrays. This reference also describes the spacecraft from which the hardware examples are drawn.

The final reports for the battery system of the Mariner Mars 1971 mission (Reference 309) and for the battery of the Viking Lander Spacecraft (Reference 103) contain examples of interplanetary mission applications. The former is a complete description of a battery-development project, including aspects of design, manufacture, test, and flight performance. The latter describes the development of a sterilizable battery for a Viking lander.

10.2.1 Synchronous Meteorological Satellite (SMS)

- Design characteristics

Capacity: 3 Ah

Series cells: 20

Cell supplier: Eagle-Picher

Orbit: Geosynchronous

Design life: 5 years (2-year shelf life)

Peak-power output: 729 W for 100 ms

Description: Two batteries per spacecraft

- Design features

Depth of discharge: 60 percent, maximum

Control: Three commandable charge rates

Protection: Undervoltage, 1.0 V per cell; four-cell groups

Other: HM21A-T8 magnesium alloy intercostals and end plates; glass-¹ use epoxy-resin support blocks; cells coated with flat black paint and wrapped in 5-mil Mylar

- Physical characteristics

Dimensions (m): 0.14 long by 0.29 wide by 0.07 high

Weight: 3.4 kg; battery weight/cell weight = 1.10

- Environmental capability

Sinusoidal vibration (peak): 25.0-g thrust axis, 10.0-g other axes

Random vibration: 9.1 g,rms; 2 minutes duration per axis

Acceleration: 25.8 g per axis (qualification level)

Shock (peak): 120 g for 0.7 ms

Maximum temperature: 35°C

Minimum temperature: 0°C

Thermal-vacuum profile: 6-hour soak (nonoperating) at -30°C; 24-hour operation at 0°C; 6-hour soak (nonoperating) at 40°C; 24-hour operation at 35°C

10.2.2 Improved TIROS Operation System (ITOS-D)

- Design characteristics

Capacity: 6 Ah

Series cells: 23

Cell supplier: General Electric

Orbit: Low-altitude

Design life: 1 year

Peak-power output: 93 W (each of two batteries)

- Design features

Capacity: 6-Ah nominal; 17-percent nominal depth of discharge; 28-percent maximum depth of discharge

Control: One temperature-compensated BVL; charge current varies between 0 and 1.5 A; discharge current for both batteries varies between 0 and 3A

Protection: Undervoltage, 1.15 V per cell

Other: Aluminum frame and baseplate; 8-mil H film and thermal grease at interface to baseplate

- Physical characteristics

Dimensions (m): 0.15 long by 0.13 wide by 0.13 wide by 0.3 high

Weight: 9.1 kg; battery weight/cell weight = 1.50

- Environmental capability

Sinusoidal vibration (peak): 5.0 g, all axes (acceptance level)

Random vibration: 10 g, rms; 2 minutes duration per axis

Acceleration (g): Yes (specification not available)

Shock (g, peak): Yes (specification not available)

Maximum temperature: 30°C (operating)

Minimum temperature: 5°C (operating)

Thermal-vacuum profile: Cycle while operating between 45 and -10°C

10.2.3 Atmospheric Explorer C (AE-C)

- Design characteristics

Capacity: 6 Ah

Series cells: 24

Cell supplier: General Electric

Orbit: Low-altitude

Design life: 2.67 years (including 1.33 storage)

Peak-power output: 261 W (three batteries)

- Design features

Depth of discharge: 18-percent nominal; 40-percent maximum; nominal discharge current varies between 0 and 2.7 A

Control: Temperature-compensated BVL used for primary control; charge reduced to 150-mA trickle level when either of two cells equipped with an auxiliary electrode signals that full charge has been reached; 0 to 1.6-A full charge current

Protection: High temperature cutoff

- Physical characteristics

Dimensions (m): 0.15 long by 0.13 wide by 0.30 high

Weight: 22.8 kg

- Environmental capability

Sinusoidal vibration (peak): 4.0-g thrust axis; 1.5-g lateral axes (spacecraft acceptance level)

Random vibration: 8.5 g, rms; 2 minutes duration per axis

Acceleration (g): Yes (specification not available)

Maximum temperature: 40°C

Minimum temperature: 0°C

Thermal-vacuum profile: 24-hour discharge /charge cycling at 0°C followed by 24-hour cycling at 35°C

10.2.4 Small Astronomy Satellite C (SAS-C)

- Design characteristics

Capacity: 9 Ah

Series cells: 12

Cell supplier: SAFT-America

Orbit: Low-altitude

Design life: 18,000 cycles; and 4-year wet-short-circuit shelf life at 0 to 25°C

- Design features

Discharge capability: Maximum discharge rate capability of 30 A for 2 minutes; 1.0 V per cell undervoltage limit

Cell design: 0.015- to 0.030-cm nonwoven nylon separator material (Pellon No. 2505); 304 stainless-steel container and cover

- Physical characteristics

Cell dimensions (m): 0.03 long by 0.06 wide by 0.07 high

Weight: 6.2 kg

- Environmental capability

Sinusoidal vibration (peak): 37-g thrust, 8-g lateral

Random vibration: 16.5 g, rms; 4 minutes duration per axis

Acceleration: 40 g for 3 minutes thrust; 20 g for 1 minute, transverse

Maximum temperature: 25°C operating; 50 nonoperating

Minimum temperature: 0°C operating; -20 nonoperating

10.2.5 Orbiting Solar Observatory I (OSO-I)

- Design characteristics

Capacity: 12 Ah

Series cells: 21

Cell supplier: General Electric

Orbit: Low-altitude

Design life: 1 year

Description: Two packs per battery with 10 and 11 cells, respectively

- Design features

Capacity: 12-Ah minimum at $23^{\circ} \pm 2^{\circ}\text{C}$ after 1 year (5500 discharge/charge cycles) of operation to an average depth of discharge of 15 percent at average charge and discharge current levels of 3.2 A

Control: Eight commandable temperature-compensated BVL's

Protection: Undervoltage, 1.18 V per cell measured at the spacecraft bus; over-temperature, open circuited at 35°C

Other: 40-mil extruded 6063-T6A thermal shims, with 2-mil hard anodize coating; end plates, 7075-T6AL; two titanium tension bars;

fiberglass cell retainers; cells coated with 2-mil black epoxy paint and wrapped with 5-mil Mylar

- Physical characteristics

Dimensions (m): 10-cell pack, 0.31 long by 0.12 wide by 0.12 high;
11-cell pack, 0.33 long by 0.12 wide by 0.12 high

Weight: 10-cell pack: 6.0 kg; 11-cell pack: 6.6 kg; battery weight/cell weight = 1.14

- Environmental capability

Sinusoidal vibration (peak): 12 g at 100 to 200 Hz in thrust axis;
14 g at 30 to 60 Hz in lateral axes

Random vibration: 18.6 g, rms; 4 minutes duration per axis

Maximum temperature: 35°C

Minimum temperature: -10°C

Thermal-vacuum profile: 1×10^{-5} torr; 6-hour soak at 35°C followed by 6-hour soak at -10°C; 10°C/hour maximum rate of change

10.2.6 Applications Technology Satellite 6 (ATS-6)

- Design characteristics

Capacity: 15 Ah

Series cells: 19

Cell supplier: SAFT-America

Orbit: Geosynchronous

Design life: 2 years

Peak-power output: 500 W (two batteries)

- Design features

Control: One temperature-compensated BVL; C/20 and C/60 commandable trickle-charge rates

Protection: Undervoltage, 1.00 V per cell; multiple-cell groups: over temperature, 35°C

Other: 125-mil extruded 6063-T5 thermal shunts with 2-mil type 5 hard anodize; 2024-T351 aluminum frame; end plates secured under 1.03×10^6 N/m² (150 psi) load; cells wrapped in 2.5-mil mylar

- Physical characteristics

Dimensions (m): 0.30 long by 0.23 wide by 0.19 high

Weight: 17.0 kg total; 19 active cells, 12.96; two dummy cells, 0.136; battery weight/cell weight = 1.31

- Environmental capability

Sinusoidal vibration (peak): 12-g all axes

Random vibration: 17 g, rms; 4 minutes duration per axis, operating

Acceleration: 9-g thrust axis; 3.9-g other axis, operating

Maximum temperature: 25°C (operating)

Minimum temperature: 0°C (operating)

Thermal-vacuum profile: -10 to 35°C, operating, at 10⁻⁵ torr

10.2.7 FLTSATCOM

- Design characteristics

Capacity: 24 Ah

Series cells: 24

Cell supplier: General Electric

Orbit: Geosynchronous

Design life: 5 years

Peak-power output: 410 W for 1.2 hours (each of three batteries)

- Design features

- Capacity: 600 Wh per battery above 24 Vdc; >70-percent normal depth of discharge and >85-percent with two failed cells in each of two batteries

- Control: Eight commandable temperature-compensated BVL's control two modes: (1) switch to C/100 trickle charge; (2) current taper

- Protection: Forward and reverse cell-bypass circuits; forward is temperature-compensated voltage limit; reverse limits to -200-mV maximum on discharge; over and under temperature

- Other: Magnesium thermal shims and battery baseplate

- Physical characteristics

- Dimensions (m): 0.39 long by 0.30 wide by 0.22 high

- Weight: 29.9 kg; cells, 22.5 kg

- Environmental capability

- Random vibration (g, rms): Overall level not specified at component level; 3 minutes duration per axis

- Acceleration: 12 g per axis

- Maximum temperature: 32°C

- Minimum temperature: 4°C

- Thermal-vacuum profile: 12-hour soak at -2°C followed by 12-hour soak at 38°C

10.2.8 Defense Meteorological Satellite Program (DMSP)

- Design characteristics

- Capacity: 30 Ah

- Series cells: 17

- Cell supplier: General Electric

- Orbit: Geosynchronous

Design life: 5 years (including 2-year storage)

Peak-power output: 336 W

Description: Two packs per battery with eight and nine cells, respectively; thermal louvers at spacecraft level

- Design features

Depth of discharge: 30 percent, average

Control: One cell in each pack contains an oxygen-signal electrode; selectable charge rates, C/2 maximum; temperature-compensated BVL

Protection: No undervoltage; under temperature (heater)

- Physical characteristics

Dimensions (m): eight-cell pack: 0.34 long by 0.23 wide by 0.13 high

Weight: eight-cell pack, 11.9 kg; nine-cell pack, 12.8 kg

- Environmental capability

Sinusoidal vibration (peak): 15 g each axis, operating

Random vibration: 22.5 g, rms; 2 minutes duration per axis, operating; 155.9-dB acoustic, 2 minutes

Acceleration: 20.7-g axial, 5-g lateral operating

Shock (peak): 15 g, 8 ms each axis, operating

Maximum temperature: 40°C operating, 66°C nonoperating

Minimum temperature: 0°C operating; -43°C nonoperating

Thermal-vacuum profile: cycle while operating between -5 and 45°C at 5×10^{-5} torr

10.3 ADVANCED BATTERY SYSTEMS

This section reviews the latest technical developments identified in the literature and government reports through mid-1977. The major emphases for the advanced development efforts are: (1) to reduce weight for geosynchronous and medium-altitude spacecraft batteries; (2) to increase battery

life capability to over 10 years at up to 85-percent depth of discharge in the longest eclipses of geosynchronous and medium-altitude applications; and (3) to increase battery life to over 5 years at higher depths of discharge than those that can now be used for low-Earth-orbit systems. There are no lightweight developments directed toward low-Earth-orbit applications.

10.3.1 Lightweight Nickel-Cadmium Cells and Batteries

The weight of nickel-cadmium batteries has become an important design variable for geosynchronous and medium-altitude spacecraft. Approaches recently investigated and developed to reduce weight include:

- Reducing battery-assembly structural weight toward design goals of less than 5 percent of total cell weight
- Reducing cell-case weight by reducing thickness of the case walls or by changing to new case materials, such as titanium or graphite fibrous material, that exhibit improved strength-to-weight ratios
- Changing plate-manufacturing processes to improve use of active materials and sinter porosity
- Reducing negative-to-positive plate capacity ratios for selected applications when minimal overcharge protection is required and/or when reconditioning techniques can be used to maintain stable cadmium-electrode activity

Two cell development projects and two battery-assembly development projects have been reported:

- The NATO-III battery (Reference 310) used a cell with a negative-to-positive plate-capacity ratio of less than 1.3:1.0 that yielded a specific energy of 48.5 Wh/kg (22 Wh/lb) based on measured capacity. The battery is a 20-cell, 20-Ah assembly with a measured specific energy of 39.7 Wh/kg (18 Wh/lb). The design utilizes an intercostal structure as shown in figure 123.
- An advanced lightweight nickel-cadmium battery has been developed and qualified (Reference 311) with a cell that provides a 1.5:1.0 negative-to-positive plate-capacity ratio. The cell contains electrochemically impregnated positive plates and exhibits a specific energy of 50.7 Wh/kg (23 Wh/lb) based on measured capacity. The battery assembly utilizes an intercostal structural design, contains fourteen 34-Ah (rated) cells in a monoblock configuration, and provides a

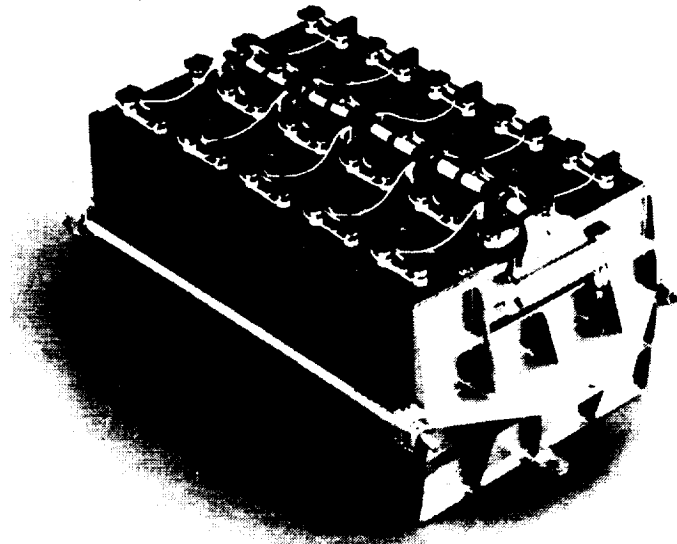


Figure 123. NATO-III battery.

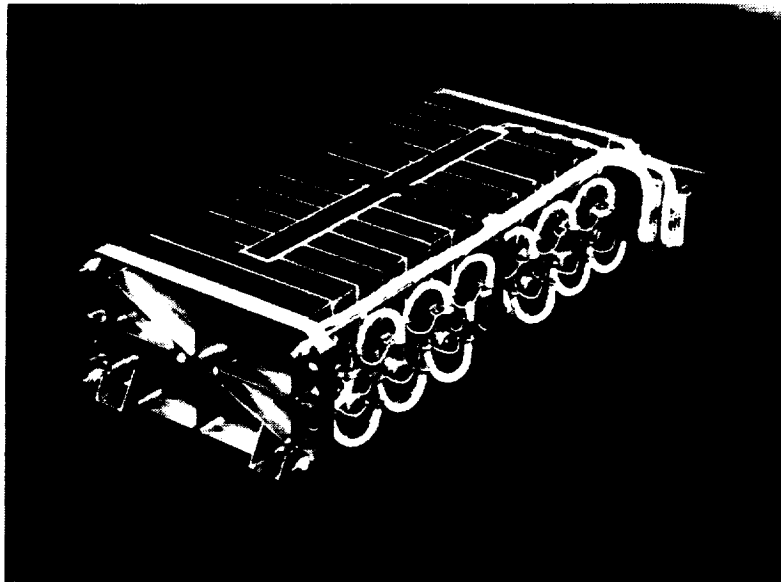


Figure 124. Lightweight nickel-cadmium battery.

**ORIGINAL PAGE IS
OF POOR QUALITY.**

measured specific energy of 46.3 Wh/kg (21 Wh/lb). The unit is shown in figure 124.

Accelerated cycle-life tests have verified the performance of these light-weight battery designs. The technology is new and represents more design risk for spacecraft than the heavier conventional flight-proven designs described earlier. However, the technology is maturing rapidly, and it is expected that these advanced designs will be considered for new spacecraft with severe weight and life requirements (Reference 312).

10.3.2 Trends in Battery-Charge Control

Advanced charge-control development work is being performed primarily with the objectives of achieving compatibility with future on-board spacecraft computer systems and of achieving improved cell monitoring and control capability for long-life battery management. Three studies either have been or are being conducted:

- The Jet Propulsion Laboratory is studying automated power-system management (Reference 269). This study is investigating methods of control and identifying sensors needed for battery control with an on-board computer system.
- The Intelsat-V and NASA/GSFC TDRSS spacecraft projects are developing scanners capable of transmitting a data stream of precisely measured individual cell voltages by telemetry to the ground. Data on all battery cells in the spacecraft can be obtained within 30 seconds if necessary.
- Ampere-hour integrators and associated charge-control logic networks are being studied utilizing newly available microprocessor technology. These studies are new and not well-documented at this time.

Because of the preliminary nature of these activities, most current spacecraft battery-system designs rely on the proven technical approaches reported in Section 8.

10.4 TERRESTRIAL APPLICATIONS

Recently, many consumers have become aware of nickel-cadmium cells because of their use in calculators, electric shavers, and hand power tools. The cells are usually one of the small standard sizes (table 57). They are

higher in initial cost than conventional primary cells such as carbon-zinc or zinc-chloride but have a much lower cost per operating hour because they are rechargeable with good cycle-life capability.

Cell manufacturers sometimes describe their nickel-cadmium products as sealed cells. However, they are not hermetically sealed to the standards of aerospace design by intent; if pressure builds up in a cell, it will vent to protect the user. The imposition of aerospace standards and associated levels of quality control to the cell container, terminals, and fill-tube seals adds to the cost of the cell. Also, the implementation of high-quality seals is more difficult in small cells. The use of the type of cells discussed in this manual in terrestrial applications is therefore relatively infrequent, although a large market exists for various types of vented nickel-cadmium cells.

Vented nickel-cadmium cells are used extensively in aircraft ground-support applications, and a separate literature exists on their design, applications, and special problems. Special nickel-cadmium cells—designed with great tolerance to long-term float-charging and a wide range of terrestrial environments but with low specific energy—are used in telephone communications. Possible terrestrial applications of cells that are similar in construction to aerospace cells include uninterruptible local power systems (military, hospitals, office buildings, and computer installations), power supplies for remote sensors (weather, oceanographic, and geological), or submersible vehicles. In all such applications, the technical requirements must justify the use of more expensive cells.

Table 57
Standard Commercial Cells

Size	Capacity (Ah)	Diameter (cm)	Length (cm)	Weight (g)
AA	0.5	1.42	4.99	22.7
RR	1.0/1.2	2.26	4.24	45.4
C	1.5/1.8	2.59	4.93	68.0
1/2D	2.0/2.3	3.25	3.68	85.0
D	3.5/4.0	3.28	5.89	155.9

References 313 and 314 describe earlier examples of commercial nickel-cadmium cell applications. Reference 315 contains a recent survey of commercial secondary and primary cells.

REFERENCES*

1. Francis, H. T., *Space Battery Handbook*, NASA CR-56514 (N64-25802), 1963.
2. Bauer, P., *Batteries For Space Power Systems*, NASA SP-172 (N69-18042), 1968.
3. Halpert, G., "The 1976 Goddard Space Flight Center Battery Workshop," Proc., Greenbelt, Maryland, NASA TM X-71284 (N77-21550), November 1976.
4. *Encyclopedia of Chemical Technology*, 2nd Edition, Vol. 3, John Wiley and Sons, Inc., New York, 1963.
5. Falk, S. Uno, and Alvin J. Salkind, *Alkaline Storage Batteries*, John Wiley and Sons, Inc., New York, 1969.
6. General Electric Co., "Nickel-Cadmium Battery Application Engineering Handbook," Publication GET-3148, Gainesville, Florida, 1971.
7. Conway, B. E., and E. Gileadi, "Electrochemistry of the Nickel-Nickel Oxide Electrode, Part IV," *Canadian J. Chem.*, **40**, 1962, pp. 1933-1942.
8. Seiger, H. N., *Sinter of Uniform, Predictable, Blemish-Free Nickel-Plaque for Large Aerospace Nickel-Cadmium Cells, Final Report*, NASA CR-132481 (N75-18717), February 1975.
9. Seiger, H. N., "Role of Tetravalent Nickel in Nickel Oxide Electrodes," American Chemical Society Meeting, San Francisco, California, 1976.
10. MacArthur, D. M., "Electrochemical Properties of Nickel Hydroxide Electrodes," *Power Sources 3*, D. H. Collins, ed., Oriel Press Ltd., England, 1970, pp. 91-118.

*Numbers in parentheses are NASA Scientific and Technical Information Service accession numbers.

11. Halpert, G., "Electrolyte Concentration Changes during Operation of the Nickel-Cadmium Cell," NASA TM X-70977 (N75-33497), May 1975.
12. Ritterman, P. F., "Hydrogen Recombination in Sealed Nickel-Cadmium Cells," *Proc. 27th Power Sources Symposium*, Atlantic City, New Jersey, (A77-28153), 1976, pp. 111-114.
13. Halpert, G., and W. H. Webster, Jr., *Secondary Aerospace Batteries and Battery Materials, A Bibliography, 1923-1968*, NASA SP-7027 (N70-22825), August 1969.
14. McDermott, P., G. Halpert, S. Ekpanyaskun, and P. Nche, *Secondary Aerospace Batteries and Battery Materials, A Bibliography, 1969-1974*, NASA SP-7044 (N7716437), July 1976.
15. Holleck, G., *Development of Uniform and Predictable Battery Materials for Nickel-Cadmium Aerospace Cells, Final Report*, NASA CR-130094 (N73-10050), January 1972.
16. "The 1975 GSFC Battery Workshop," *Proc., Greenbelt, Maryland*, NASA TM X-71104 (N76-24704), November 1975.
17. Scott, W. R., *A Study of Degradation of Plates for Nickel-Cadmium Spacecraft Cells, Final Report*, NASA CR-141357 (N75-15164), June 1974.
18. Menard, C., "Recent Development in Porous Structures for Nickel Hydroxide Electrodes," *Proc. Advanced Battery Technology Symposium, Volume 2*, December 1966, pp. 76-98.
19. Halpert, G., "Nickel-Cadmium Battery Test Project—Relationship Between Operation, Life and Failure Mechanism. Vol. III. Analysis of the Cells and Their Components," NASA TM X-63550 (N69-28089), March 1969.
20. Kröger, H., "Nickel Hydroxide Battery Electrode Development," 1st Interim Report, Contract F33-615-69-C-1312, Report GE S-70-1025, General Electric Co., Gainesville, Florida, December 1969.

21. Doran, R., "Further Studies of Aging and Impurity Effects in the Nickel Hydroxide Electrode," *Proc. Second International Symposium on Batteries*, October 1960, pp. 26/1-26/13.
22. Rubin, E. J., and M. J. Turchan, *Nickel-Cadmium Cells, Final Report*, NASA CR-143175 (N75-21792), August 1974.
23. Lerner, S., and H. N. Seiger, *An Investigation of the Nickel-Oxide Electrode, Final Report*, NASA CR-72465 (N69-10584), September 1968.
24. Lerner, S., P. F. Ritterman, and H. N. Seiger, *Investigation of Battery Active Nickel Oxides, Final Report*, NASA CR-72128 (N67-15153), September 1966.
25. Dunlop, J., "The 1976 Goddard Space Flight Center Battery Workshop," *Proc. Greenbelt, Maryland*, NASA TM X-71284 (N77-21550), 1976, pp. 233-242.
26. Rampel, G. G., "Process of Forming Rechargeable Electrodes Utilizing Unsintered Fluorocarbon Binder," U.S. Patent 3,630,781, December 28, 1971; and "Rechargeable Electrodes Utilizing Unsintered Fluorocarbon Binder, U.S. Patent, 3,954,501, May 4, 1976.
27. "The 1973 GSFC Battery Workshop, First Day," *Proc., Greenbelt, Maryland*, NASA TM X-72536 (N75-15152), November 1973.
28. Rampel, G. G., "Cell Having Anode Containing Silver Additive for Enhanced Oxygen Recombination," U.S. Patent No. 3,877,985, April 15, 1975.
29. Baker, H., S. D. Toner, and W. F. Cuthrell, "Evaluation of Separator Materials Used in NiCd Satellite Batteries," Report NBS 10-956. National Bureau of Standards, November 1972.
30. Lim, H. S., et al., "Studies on the Stability of Nylon Separator Material," *Proc. 27th Power Sources Symposium*, Atlantic City, New Jersey, (A77-28126), 1976, pp. 83-85.
31. Jakobi, W., *Research and Development Program on Sealed Nickel-Cadmium Cells for Space Use, Final Report*, NASA CR-55845 (N64-16699), April 1963.

32. "The 1971 NASA/Goddard-Aerospace Industry Battery Workshop, Volume 1," *Proc. Greenbelt, Maryland*, NASA TM X-68828 (N72-27061), November 1971.
33. "The 1971 NASA/Goddard-Aerospace Industry Battery Workshop, Volume 2," *Proc. Greenbelt, Maryland*, NASA TM X-68829 (N72-27062), November 1971.
34. "The 1972 NASA/GSFC Battery Workshop, First Day," *Proc. Greenbelt, Maryland*, NASA TM X-69240 (N73-21956), November 1972.
35. "The GSFC Battery Workshop, 1974," *Proc., Greenbelt, Maryland*, NASA TM X-70822 (N75-16976), November 1974, p. 185.
36. Bauer, J. L., and A. Garcia, "Graphite/Epoxy Nickel-Cadmium Cell Case Development, Final Report," Report 730-3, Jet Propulsion Laboratory, Pasadena, California, December 1977.
37. Scott, W. R., *A Study of the State-of-the-Art of Hermetic Seals for Secondary Alkaline Spacecraft Cells, Final Report*, NASA CR-97888 (N69-12833), March 1968.
38. Levy, E., Jr., E. C. Duncan, C. E. Maiden, W. Michel, and G. I. Cardwell, "Low Earth Orbit Battery Development Project. Final Report," Contract F33-615-73-C-1710, Report AFAPL-TR-72-60. AD-902570L (X73-72130), July 1972.
39. Turner, D. R., W. E. Howden, Y. Okinara, and E. J. McHenry. "Developments Toward an Improved Sealed Ni-Cd Battery. *Power Sources*, D. H. Collins, ed., Pergamon Press, New York, 1966. pp. 349-370.
40. Tuomi, Donald. "The Forming Process in Nickel Positive Electrodes." *J. Electrochemical Soc.*, 112 (1), January 1965. pp. 1-12.
41. Casey, E. J., A. R. Dubois, P. E. Lake, and W. J. Moroz. "Effects of Foreign Ions on Nickel Hydroxide and Cadmium Electrodes." *J. Electrochemical Soc.*, 112 (4), April 1965, pp. 371-383.
42. Yamashita, D., "The Effect of Lithium and the Formation of Active Material from the Nickel Plaque on the Positive Plates of Sintered-Type Alkaline Storage Batteries." *Power Sources*, D. H. Collins, ed., Pergamon Press, New York, 1966. pp. 297-308.

43. Gross, S., *Nickel-Cadmium Cell Designs, Negative to Positive Material Ratio and Precharge Levels*, NASA CR-153904 (N77-27501), June 1977.
44. Voyentzie, P. R., G. Rampel, and W. N. Carson, Jr., "Characterization of Recombination and Control for Spacecraft Nickel-Cadmium Cells Containing Electrodes, Final Report," NASA Contract NAS 5-11547, General Electric Company, March 1970.
45. (a) "NASA/GSFC 1970 Battery Workshop, First Day," *Proc., Greenbelt, Maryland*, NASA TM X-67200 (N71-28659), November 1970.
(b) "NASA/GSFC 1970 Battery Workshop, Sessions 3 and 4," *Proc., Greenbelt, Maryland*, NASA TM X-67186, (N71-28672), November 1970.
46. "The 1976 Goddard Space Flight Center Battery Workshop," *Proc., Greenbelt, Maryland*, NASA TM X-71284 (N77-21550), November 1976.
47. Carson, W. N., Jr., G. Rampel, and I. B. Weinstock, *Characterization of Recombination and Control Electrodes for Spacecraft Nickel-Cadmium Cells*, Final Report, NASA CR-93427 (N68-18826), January 1968.
48. Lerner, S., *Characterization of Recombination and Control Electrodes for Spacecraft Nickel-Cadmium Cells, Final Report*. NASA CR-93244 (N68-17741), June 1967.
49. Kirsch, W. W., and A. E. Shikoh, "Summary Report on Nickel-Cadmium Batteries for Apollo Telescope Mount," Contract NAS8-20055, Sperry Rand Space Support Division, Huntsville, Alabama. June 22, 1970.
50. Ford, F., "Performance of 3rd Electrode Cells in OAO." *Proc. 25th Power Sources Symposium, Atlantic City, New Jersey*, (A73-29581). May 1972, pp. 43-46.
51. Scott, W. R., "Two Kilowatt Long Life Battery." Final Technical Report. Contract F33-615-70-C-1627, Report AFAPL-TR-76-47. AD-B022247L (X78-70547), August 1976.

52. Ford, F.E., "Overcharge Control of Nickel-Cadmium Spacecraft Batteries using the Auxiliary Electrode Signal," NASA TM X-63177 (N68-22377), March 1968.
53. Cahoon, N.C. "The Operation and Use of Reference Cells," *Electrochemical Technology*, 3 (1-2), January/February 1965, pp. 3-9.
54. Puglisi, V.J., and E.L. Ralph, "Development of Nickel Alkaline Batteries for Aerospace Lightweight Secondary Power, Final Report," Contract F33-615-73-C-2012, Report AFAPL-TR-75-64, AD-A022350 (N76-29720), June 1975.
55. Kantner, E., *Production of Uniform Nickel-Cadmium Battery Plate Materials, Final Report*, NASA CR-131914 (X73-75451), 1972.
56. Seiger, H.N., D.F. Pickett, V.J. Puglisi, P.F. Ritterman, and R.L. Oliver, "High Energy Density Sintered Plate Type Nickel-Cadmium Battery Cells, Part 1: The Positive Electrode/Plaque Relationship," Contract F33-615-75-C-2012, Report AFAPL-TR-74-56-I, AD-A000103 (N75-19849), August 1974.
57. Miller, L., *Study of Process Variables Associated with Manufacturing Hermetically-Sealed Nickel-Cadmium Cells, Final Report*, NASA CR-139025 (N74-26501), April 1974.
58. Häusler, E., "Electrochemical Impregnation of Porous Sintered Nickel Grids according to the 'Kandler-process,'" *Power Sources*, D.H. Collins, ed., Pergamon Press, New York, 1966, pp. 287-296.
59. Kröger, H., "Nickel Hydroxide Battery Electrode Development, Second Interim Report," Contract F33-615-69-C-1312, Report AFAPL-TR-71-12, AD-883905 (X71-78940), January 1971.
60. Pickett, D.F., V.J. Puglisi, H.N. Seiger, and R. Oliver, "High Energy Density Sintered Plate Type Nickel-Cadmium Battery Cells, Part 2: Electrochemical Impregnation Methods to Produce Nickel-Oxide Electrodes," Contract F33-615-73-C-2012, Report AFAPL-TR-74-56-II, AD-A002142 (N75-19850), August 1974.

61. Pickett, D.F., "Fabrication and Investigation of Nickel-Alkaline Cells, Part I: Fabrication of Nickel-Hydroxide Electrodes Using Electrochemical Impregnation Techniques," Report AFAPL-TR-75-34-I, AD-A018517, (N76-24737), October 1975.
62. Gaston, S., M. Wertheim, and J.A. O'Rourke, *OAO Battery Data Analysis, Final Report*, NASA CR-130233 (N73-20045), February 1973.
63. Armantrout, J.D., *SMS/GOES Cell and Battery Data Analysis*, NASA CR-156739 (N78-21606), December 1977.
64. Halpert, Gerald, "A Screening and Selection Method for Nickel-Cadmium Cell Plates," NASA TM X-63962 (N70-33091), April 1970.
65. Haas, R.J., and D.C. Briggs, "20 Watt-hour per Pound Nickel-Cadmium Energy Storage for the NATO III Communication Satellite," AIAA Paper 76-287, April 1976.
66. Bogner, R.S., and A.A. Uchiyama, "Coordinated NASA Nickel-Cadmium Battery Technology Program," AIAA Paper 77-516, March 1977.
67. Font, S., "Study of Nickel-Cadmium Batteries for Use in Applications Satellites, Phase 2: Evaluation of Electrical Impedance as a Function of the Frequency at Various Temperatures and Charge States of NiCd V023S Batteries," Contract ESTEC-1358/71-sl, Report ESRO-CR(P)-326 (N74-16813), February 1973 (in French).
68. "Evaluation Program for Secondary Spacecraft Cells." Annual Reports of Cycle Life Test, Contracts W11,252B, W12,397, S23404G, and S53742AG, Weapons Quality Engineering Center, Naval Weapons Support Center, Crane, Indiana, 1965-1976.
69. "The GSFC Battery Workshop, 1974." *Proc., Greenbelt, Maryland*, NASA TM X-70822 (N75-16976), November 1974. pp. 32-38.
70. Brooman, E.W., and J. McCallum, "Heat Transfer in Sealed Nickel-Cadmium Spacecraft Cells and Batteries." Contract AF33(615)-3701, Report AFAPL-TR-69-21, AD-851880 (X69-16296), April 1969.

71. Haugen, H., W.R. Scott, D.N. Stager, and D.W. Zerbel, "Two Kilowatt Long Life Battery," First Interim Report, Contract F33-615-70-C-1627, Report AFAPL-TR-71-43, AD-885779 (X71-81816), June 1971.
72. Brooman, E.W., and J. McCallum, "The Thermal Conductivity of Sealed Nickel-Cadmium Cells," Contract F33-615-69-C-1537, Report AFAPL-TR-71-75, AD-737519 (N72-24055), February 1972.
73. Brooman, E.W., and J. McCallum, "The Thermal Properties and Behavior of Nickel-Cadmium and Silver-Zinc Cells and their Components," Contract AF-33(615)-3701, Report AFAPL-TR-68-41, AD-834300 (X68-18821), June 1968.
74. Crawford, R.L., J.M. Gondusky, P.V. Popat, and E.J. Rubin, "Heat Sterilizable and Impact Resistant Ni-Cd Battery Development, Eighth Quarterly Report," NASA CR-106364 (N69-40742), June 1969.
75. Font, S., "Study of Nickel-Cadmium Batteries for Use in Applications Satellites, Phase 2: Evaluation of Charging Efficiency of V023S NiCd Batteries," Contract ESTEC-1358/71-sl, Report ESRO-CR(P)-325 (N75-16998), February 1973 (in French).
76. Font, S., "Study of Nickel-Cadmium Batteries for Use in Applications Satellites, Phase 2: Evaluation of NiCd Batteries V023S Overcharge," Contract ESTEC-1358/71-sl, Report ESRO-CR(P)-329 (N75-17817), May 1973 (in French).
77. Ford, F.E., "Characterization of the 20-Ah Nickel-Cadmium Cell Used for Energy Storage on the Orbiting Astronomical Observatory," NASA TM X-66093(N73-11040), September 1972.
78. Lackner, J., "The 1976 Goddard Space Flight Center Battery Workshop," *Proc., Greenbelt, Maryland*, NASA TM X-71284 (N77-21550), November 1976, pp. 191-198.
79. "The GSFC Battery Workshop. 1974," *Proc., Greenbelt, Maryland*, NASA TM X-70822 (N75-16976), November 1974, pp. 43-62.
80. Elder, J.P., and E.M. Jost, "Statistical Studies of Rechargeable Battery Systems," *Electrochemical Technology*, 116(5), May 1969, pp. 687-693.

81. Carson, W.N., Jr., J.A. Consiglio, and J.F. Wilbore, "Study of Nickel-Cadmium Cells," NASA Contract NAS 5-9586, Report S67-1116, General Electric Company, Schenectady, New York, July 1967.
82. Font, S., "Study of Nickel-Cadmium Batteries for Use in Applications Satellites, Phase 2: Evaluation of Charge Storage of Charged Ni-Cd V023S Batteries," Contract ESTEC-1357/71-sl, Report ESRO-CR (P)-324 (N74-16812), December 1972 (in French).
83. Scott, W.R., "A Study of Short Test and Charge Retention Test Methods for Nickel-Cadmium Spacecraft Cells, Final Report," NASA CR-143189 (N75-27566), April 1975.
84. Otzinger, B., "VO-75 Nickel-Cadmium Cell, Special Charge Retention Test Program," Report 21329, Electro-Optical Systems, Pasadena, California, April 1974.
85. McCallum, J., E.A. Roeger, Jr., and G.H. Miller, "Rate of Discharge for Accelerated Life Tests of Nickel-Cadmium Cells," Contract F33-615-69-C-1537, Report AFAPL-TR-72-67, AD-748253 (N73-13065), August 1972.
86. Harivell, J.P., B. Morignat, and J. Migeon, "Investigations on the Negative Electrode of Nickel-Cadmium Cells with Sintered Plates," *Batteries* 2, D.H. Collins, ed., Pergamon Press, New York, 1964, pp. 107-127.
87. Rubin, E.J., *Heat Sterilizable and Impact Resistant Ni-Cd Battery Development, Final Report, Volume 2*, NASA CR-109855 (N70-34013), January 1970.
88. Gross, S., and R.J. Glockling, *The Cadmium Electrode, A Review of the Status of Research, Final Report*, NASA CR-149860 (N77-19572), September 1976.
89. Turner, Dennis R., "The Effect of State-of-Charge of the Cadmium Electrode on Oxygen Recombination in Sealed Nickel-Cadmium Cells," *Electrochemical Tech.*, 2(11-12), November/December 1964, pp. 313-319.
90. Font, S., "Improved Nickel-Cadmium Cells for a Communications Satellite at Synchronous Orbit, Final Report," Report DT/SAS-184/72, SAFT-America, Inc., Valdosta, Georgia, April 1972.

91. Dunlop, J.D., and M. Earl, "Evaluation of Intelsat IV Nickel-Cadmium Cells," *Proc. 25th Power Sources Symposium, Atlantic City, New Jersey*, (A73-29581), May 1972, pp. 40-42.
92. Gottlieb, Melvin H., and T.H. Willis, "Operating Characteristics of Sealed Nickel-Cadmium Batteries at Low Temperatures," *Electrochemical Tech.*, 4(11-12), November/December 1966, pp. 515-519.
93. Baer, David A., "Summary of the Manufacturing and Testing of 12-Ah Nickel-Cadmium Cells for the IUE Spacecraft," NASA TM X-71094 (X76-10697), January 1976.
94. Scott, W.R., "Two Kilowatt Long Life Battery," Final Technical Documentary Report, Contract F33615-69-C-1291, Report AFAPL-TR-70-61, AD-876484 (X71-71744), September 1970.
95. Baumstark, G., A. Fitchman, and S. Thornell, *Cell-Core Compression Studies on Nickel-Cadmium Cells, Final Report*, NASA CR-72317 (N68-13010), November 1967.
96. Jakobi, W.W., *Encyclopedia of Chemical Technology*, 2nd ed., Vol. 3. John Wiley and Sons, Inc., New York, 1963, pp. 161-208.
97. Menard, C., "Recent Development in Porous Structures for Nickel Hydroxide Electrodes," *Proc. Advanced Battery Technology Symposium, Volume 2*, December 1968, pp. 76-98.
98. Milner, P.C., and U.B. Thomas, *Advanced in Electrochemistry and Electrochemical Engineering*, Vol. 5, Charles W. Tobias, ed., Interscience Publishers, New York, 1967.
99. Luksha, E., and D.J. Gordy, *Non-Gassing Nickel-Cadmium Battery Electrodes and Cells, Final Report*, NASA CR-128355 (N72-33056). July 1972.
100. Luksha, E., and D.J. Gordy, *Non-Gassing Nickel-Cadmium Battery Electrodes and Cells, Supplementary Report*, NASA CR-130932 (N73-19060), February 1973.
101. Gordy, D.J., *Fabrication and Testing of Negative-Limited Sealed Nickel-Cadmium Cells, Final Report*, NASA CR-143628 (N75-33493). March 1975.

102. Papat, P.V., *Heat Sterilizable and Impact Resistant Ni-Cd Battery Development, Ninth Quarterly Report*, NASA CR-108170 (N70-18977), September 1969.
103. Newell, D.R., *Viking Lander Spacecraft Battery, Final Report*, NASA CR-152618 (N77-20557), September 1976.
104. Garratt, P., and S. Pomroy, "A Study of the Effect of Temperature and Depth of Discharge on the Performance and Cycle Life of Hermetically Sealed NiCd Cells," Report RAE-TR-67026, Royal Air Force Establishment, Great Britain, February 1967.
105. Kent, J.R., "Analysis and Evaluation of Spacecraft Battery Accelerated Life Test Data," NASA Contract W12,397, Report QE/C 70-687, U.S. Naval Ammunition Depot, September 1970.
106. Kent, J., *Analysis and Evaluation of Spacecraft Battery Life Test Data, Phase 2, Summary Report*, NASA CR-107119, (N70-12539), October 1969.
107. Kirsch, W.W., et al., "Experimental Investigation and Model Development of the Skylab ATM Secondary Nickel-Cadmium Batteries, Interim Test Report," Contract NAS8-21812, Report 40M22412, Marshall Space Flight Center, Huntsville, Alabama, May 1974.
108. Johnson, C.R., "HEAO Battery Cell Long-Term Cycle Test (Mod. 100)," Engineering Report 77-8725.6-101, TRW Systems Group, Redondo Beach, California, January 17, 1977.
109. Mauchly, J.W., and J.H. Waite, "Computer Methods for the Reduction, Correlation and Analysis of Space Battery Test Data, Phase I, Final Report." NASA Contract NAS 5-10203, December 1966.
110. Epstein, S.D., J.W. Mauchly, and J.H. Waite, *Computer Methods for the Reduction, Correlation and Analysis of Space Battery Test Data, Phase 2, Part 1, Final Report*, NASA CR-98659 (N69-21107), December 1967.
111. Leary, J., "Statistical Analysis of NiCd Battery Cell Cycle Life Data, Parts I and II." Contract F04-701-72-C-0073, Report TOR-0073 (3420-02)-2. Aerospace Corporation, Los Angeles, California, July 1972.

112. Eliason, J.T., "Preliminary Evaluation of Nickel-Cadmium Battery Reliability," Report SP-250-0834, Sperry Rand Corporation, Huntsville, Alabama, June 1974.
113. Broberg, H., A. Henningson, and A. Loewner, "Space Battery Reliability Assessment," ESTEC Contract 1827/72, Report FTL-C-A16-37, NASA-DCAF-F010430 (X77-70256), October 1973.
114. Robertson, L.G., and E.H. Barnett, "HEAO Battery Reliability Study," Report 26000-200-008, TRW Systems Group, Redondo Beach, California, May 1975.
115. Thierfelder, H., "ITOS Battery Life Cycling Test, Final Report," Report TM-SP-PO-100, RCA, Hightstown, New Jersey, March 1968.
116. Johnson, C.R., "HEAO Battery Cell Life Test (Mod. 100), Final Report," Engineering Report 77-8725.6-108, TRW Systems Group, Redondo Beach, California, February 22, 1977.
117. Harkness, J.D., "Evaluation Program for Secondary Spacecraft Cells: Synchronous Orbit Testing of Sealed Nickel-Cadmium Cells," Report WQEC/C 77-134, Naval Weapons Support Center, Crane, Indiana, June 1977.
118. Harkness, J., "Evaluation Program for Secondary Spacecraft Cells, 13th Annual Report of Cycle Life Test," Contract S53742AG, Report WQEC/C 77-87, Naval Weapons Support Center, Crane, Indiana, March 1977.
119. Harkness, J., "Evaluation Program for Secondary Spacecraft Cells, Sixth Annual Report of Cycle Life Test," Contract W12,397, Report QE/C 77-173, Naval Weapons Support Center, Crane, Indiana, March 1970.
120. Ford, F.E., "Summary of Test Results on Spare Nickel-Cadmium Cells from OAO-A-2 Flight Batteries," NASA TM X-65588 (N76-71921), April 1971.
121. Bean, E.E., C.E. Bloomquist, and J. Finkelstein "More Reliability Data from In-Flight Spacecraft," *Proc., Annual Reliability and Maintenance Symposium, Philadelphia, Pennsylvania, (A73-33625)*, January 1973, pp. 224-237.

122. Robertson, L.G., and L. Gordon, "A Temperature- and Depth-of-Discharge Dependent Weibull Reliability Model for Satellite Battery Systems," Report 76-2286.56, TRW Systems Group, Redondo Beach, California, July 23, 1976.
123. Scott, W.R., "The 1976 Goddard Space Flight Center Battery Workshop," *Proc., Greenbelt, Maryland*, NASA TM X-71284 (N77-21550), November 1976, pp. 199-202.
124. Lim, H., "The 1975 GSFC Battery Workshop," *Proc., Greenbelt, Maryland*, NASA TM X-71104 (N76-24704), November 1975, pp. 915.
125. Scott, W.R., "The 1975 GSFC Battery Workshop," *Proc., Greenbelt, Maryland*, NASA TM X-71104 (N76-24704), November 1975, pp. 154-161.
126. Lanier, R., "A Nickel-Cadmium Battery Reconditioning Circuit," NASA TN D-8508, Marshall Space Flight Center, April 1977.
127. Dunlop, J., "The 1973 Battery Workshop, First Day," *Proc., Greenbelt, Maryland*, NASA TM X-72536 (N75-15152), November 13, 1973, pp. 81-90.
128. Dunlop, J., "The 1972 GSFC Battery Workshop, Second Day," *Proc., Greenbelt, Maryland*, NASA TM X-69239 (N73-21957), November 15, 1972, pp. 24-37.
129. Krause, S., "The 1973 GSFC Battery Workshop, First Day," *Proc., Greenbelt, Maryland*, NASA TM X-72536 (N75-15152), November 1973, pp. 71-79.
130. Armantrout, J., "The 1975 GSFC Battery Workshop," *Proc., Greenbelt, Maryland*, NASA TM X-71104 (N76-24704), November 1975, pp. 137-140.
131. Briggs, D., "The 1975 GSFC Battery Workshop," *Proc., Greenbelt, Maryland*, NASA TM X-71104 (N76-24704), November 1975, pp. 144-148.
132. "Testing of NiCd Cells over Geostationary Orbit Type Cycling Period," Contract ESTEC-1185/70-HP. Report ESRO-CR(P)-504 (N75-10596), January 14, 1974.

133. Fougere, P., "Cycle Life Tests of SAFT Aerospace Sealed Nickel-Cadmium Cells for Space Applications," Report DT/SAS 589/74, SAFT-America, Inc., Valdosta, Georgia, December 1974.
134. Napoli, J., "The 1976 Goddard Space Flight Center Battery Workshop," *Proc., Greenbelt, Maryland*, NASA TM X-71284 (N77-21550), November 1976, pp. 185-190.
135. Krause, S., "The 1975 GSFC Battery Workshop," *Proc., Greenbelt, Maryland*, NASA TM X-71104 (N76-24704), November 1975, pp. 45-48.
136. Pickett, D., "The 1976 Goddard Space Flight Center Battery Workshop," *Proc., Greenbelt, Maryland*, NASA TM X-71284 (N77-21550), November 1976, pp. 55-67.
137. Schulman, I., "The 1976 Goddard Space Flight Center Battery Workshop," *Proc., Greenbelt, Maryland*, NASA TM X-71284 (N77-21550), November 1976, pp. 41-54.
138. McCallum, J., and G.H. Miller, "Failure Mechanisms and Accelerated Life Tests of Nickel-Cadmium Batteries, Part I," Contract F33-615-69-C-1537, Report AFAPL-TR-70-44-I (X70-18112), July 1970.
139. McCallum, J., R.E. Thomas, and J.H. Waite, "Accelerated Testing of Space Batteries," NASA SP-323 (N73-21958), 1973.
140. McCallum, J., and C. L. Faust, "Failure Mechanisms in Sealed Batteries, Part 4, Semiannual Technical Report," Contract AF-33(615)-3701, Report AFAPL-TR-67-48-4, AD-848981 (X69-17161), October 1968.
141. Faust, C.L., and J. McCallum, "Failure Mechanisms in Sealed Batteries, Part 6. Final Technical Report," Contract AF-33(615)-3701, Report AFAPL-TR-67-48-6, AD-854592 (X69-18120), June 1969.
142. Cover, P.W., J. McCallum, and A.H. Reed, "Failure Mechanisms and Analyses of Sealed Batteries, Technical Report," Contract AF-33(615)-3701, Report AFAPL-TR-69-74, AD-859690 (X70-10185), September 1969.

143. McCallum, J., and G.H. Miller, "Failure Mechanisms and Accelerated Life Tests of Nickel-Cadmium Batteries, Annual Technical Report, No. 2," Contract F33-615-69-C-1537, Report AFAPL-TR-70-44-II, AD-730345 (N72-14042), September 1971.
144. Faust, C., and J. McCallum. "Failure Mechanisms in Sealed Batteries, Part 2, Semiannual Technical Report," Contract AF33(615)-3701, Report AFAPL-TR-67-48-II, AD-821895 (X68-12295), October 1967.
145. Parry, John M., "Development of Uniform and Predictable Battery Materials for Nickel-Cadmium Aerospace Cells," Sixth Quarterly Report, NASA Contract NAS 5-11561, Tyco Laboratories, Inc., March 1970.
146. Catotti, A.J., and H.H. Kröger, "Chemical Analysis of Nickel-Cadmium Electrodes," *Proc. 24th Power Sources Symposium, Atlantic City, New Jersey*, (A71-13026), 1970, pp. 4-6.
147. Halpert, G., W.H. Webster, Jr., C.C. Jones, and O. Ogunyankin, "Procedure for Chemical Analysis of Nickel-Cadmium Cell Materials," NASA TM X-70767 (X75-10157), October 1974.
148. Stofel, E., "The GSFC Battery Workshop, 1974," *Proc., Greenbelt, Maryland*, NASA TM X-70822 (N75-16976), November 1974, pp. 246-260.
149. Kelley, J., S. Orenstein, and W. Bulla, *Alkaline Battery Separator Characterization Studies, Final Report*, NASA CR-130154 (N73-16030), June 1972.
150. "Interim Model Specification for High Reliability Nickel-Cadmium Spacecraft Cells," NASA/GSFC Specification S-716-P-23, April 30, 1969.
151. Harkness, J.D., *Evaluation Program for Secondary Spacecraft Cells, Annual Report, Cycle Life Test*, NASA CR-148208 (N76-26687), February 1976.
152. Goodman, L.A., *Accelerated Test Program for Sealed Nickel-Cadmium Spacecraft Batteries/Cells*, NASA CR-148209 (N76-26688), February 1976.

153. Sommerfeldt, E.E., and P.P. McDermott, "Analysis of Data from the Accelerated Test Program on Aerospace Nickel-Cadmium Cells," NASA TM X-71390 (X77-10242), July 1977.
154. van Ommering, G., and A.J. Appleby, *Electrochemical Society, Atlanta Meeting, Extended Abstracts, 77-2*, October 1977, pp. 117-119.
155. Scott, W.R., "The GSFC Battery Workshop, 1974," *Proc., Greenbelt, Maryland*, NASA TM X-70822 (N75-16976), November 1974, pp. 125-130.
156. Scott, W.R., "The 1975 GSFC Battery Workshop," *Proc., Greenbelt, Maryland*, NASA TM X-71104 (N76-24704), November 1975, pp. 201-206.
157. "The 1972 GSFC Battery Workshop, First Day," *Proc., Greenbelt, Maryland*, NASA TM X-69240(N73-21956), November 1972, p. 5.
158. "The 1973 Battery Workshop, First Day," *Proc., Greenbelt, Maryland*, NASA TM X-72536 (N75-15152), November 1973, p. 35.
159. "Proc. Conference on OAO Battery Trouble Shooting, Third Day," Goddard Space Flight Center, Greenbelt, Maryland, October 1968, p. 59.
160. McCallum, J., and G.H. Miller, "Failure Mechanisms and Accelerated Life Tests on Nickel-Cadmium Batteries, Part III," Contract F33615-69-C-1539, Report AFAPL-TR-70-44-III. AD-749129 (N73-14061). August 1972.
161. Gross, S. "Causes of Failure in Sealed Nickel-Cadmium Batteries," *Energy Conversion*, 11 (A71-29701), June 1971, pp. 39-45.
162. Roeger, E.A., Jr., J. McCallum, and G.H. Miller, "Analysis of Accelerated Life Test Data for Aerospace Nickel-Cadmium Cells, Final Report," Contract F33-615-73-C-2024. Report AFAPL-TR-74-75. AD-A002848 (N75-21809), October 1974.

163. Gross, Sidney, "Transient Pressure Considerations in Charge Control of Sealed Batteries," *J. Electrochemical Soc.*, 119(3), March 1972, pp. 347-349.
164. McDermott, P.P., "Study of the Mechanism Associated with the Failure of Positive Plates in Aerospace Nickel-Cadmium Cells when Subjected to High Depth of Discharge at Cold Temperature (0°C)," NASA TM X-70820 (X75-10159), October 1974.
165. McDermott, P.P., *Cadmium Migration in Aerospace Nickel-Cadmium Cells*, NASA CR-144753 (N77-23606), March 1976.
166. Mayer, S.W., "Electrophoretic Mobilities of Cadmium Hydroxide, Nickel-Hydroxide, and Silver Oxide in Nickel-Cadmium and Silver-Zinc Battery Electrolytes, Interim Report," Contract F04-701-74-C-0075, Report No. SAMSO TR-74-163, AD-783853 (N75-11472), July 1974.
167. Barney, D.L., A.J. Catotti, and S.F. Pensabene, "Effect of Carbonate on the Performance of Sealed Nickel-Cadmium Cells," *Power Sources 3*, D.H. Collins, ed., Oriel Press Ltd., England, 1971, p. 119.
168. Hess, H.J., and F.G. Will, *Cadmium Electrode Mechanism Electrode Morphology and Capacity, Final Report*, NASA CR-72777 (N71-21329), March 1971.
169. Chua, D., "Relationship of Electrode Structures and Cell Performance in Sealed, Sintered-Type Nickel-Cadmium Button Cells During Cycling," Thesis (N74-27520), 1974.
170. "The 1971 NASA/Goddard-Aerospace Industry Battery Workshop, Volume 2," *Proc., Greenbelt, Maryland*, November 1971, pp. 378-400.
171. "The 1972 GSFC Battery Workshop, Second Day," *Proc., Greenbelt, Maryland*, TM X-69239 (N73-21957), November 15, 1972, pp. 24-37.
172. "The 1973 GSFC Battery Workshop, First Day," *Proc., Greenbelt, Maryland*, NASA, TM X-72536 (N75-15152), November 13, 1973, pp. 81-90.

173. Wagner, O.C., and D.D. Williams, "Investigation of Charging Methods for Nickel-Cadmium Batteries," *Proc. 26th Power Sources Symposium*, AD-A037699 (N77-80148), 1974, pp. 96-99.
174. "The 1971 NASA/Goddard-Aerospace Industry Battery Workshop, Volume 2," November 17, 1971, pp. 123-143.
175. Brooman, E.W., J. McCallum, E.A. Roeger, Jr., and G.H. Miller, "Temperature and Temperature Gradients for Accelerated Life Tests of Nickel-Cadmium Cells," Contract F33-615-69-C-1537, Report AFAPL-TR-72-66, AD-748252 (N73-13066), August 1972.
176. Hennigan, T.J., "Accelerated Test Plan for Nickel-Cadmium Spacecraft Batteries," NASA TM X-70524 (N74-12741), October 1973.
177. Reed, A.H., and J. McCallum, "Depths of Discharge for Accelerated Life Tests of Cadmium Electrodes," Contract F33-615-69-C-1537, Report AFAPL-TR-72-20, AD-743017 (N72-31088), May 1972.
178. "Standardization Policies, Procedures, and Instructions, Chapter V: Outline of Form and Instructions for the Preparation of Specifications and Associated Documents," Defense Standardization Manual 4120.3-M, Office of the Assistant Secretary of Defense, Washington, D.C., January 1972.
179. "Specification for the Manufacturing of Aero-Space Nickel-Cadmium Storage Cells," NASA/GSFC Specification 74-15000, January 1974.
180. Stanley, C., "Spacecraft Battery Testing. 4-Year Storage Life," USAF/SAMSO Contract F04701-71-C-0131, Report 16439-93-002-601, TRW Systems Group, Redondo Beach, California, April 1976.
181. "Specification for the Qualification of a Standard Nickel-Cadmium Battery," NASA/GSFC Specification S-711-17, March 1976.
182. "Specification for Standard Nickel-Cadmium Spacecraft Battery," NASA/GSFC Specification S-71116. Revision A, February 1976.
183. Bauer, P., and R.H. Sparks, "Nickel-Cadmium Batteries for the Orbiting Geophysical Observatory. Volume II," NASA CR-156678 (N78-72729), February 1964.

184. Sanders, J.A., "ATM Cell Testing and Battery Analysis, Final Report, Volume I," Report 40M21617, Marshall Space Flight Center, Huntsville, Alabama, March 1971.
185. Paschal, L.E., "Experimental Investigation and Model Development of the Skylab ATM Secondary Nickel-Cadmium Batteries," Report 40M22412, Marshall Space Flight Center, Huntsville, Alabama, May 1974.
186. Naval Weapons Support Center, "Results of Continuous Synchronous Orbit Testing on Sealed Nickel-Cadmium Cells," Report WQEC/C 77-134, Crane, Indiana, June 1977.
187. Sparks, R.H., and W.R. Scott, "Application of Nickel-Cadmium Batteries in Deep Discharge Synchronous Orbit Applications," *Proc. 11th IECEC, State Line, Nevada*, (A77-12662), 1976.
188. Naval Weapons Support Center, "Accelerated Test Program for Sealed Nickel-Cadmium Spacecraft Batteries/Cells," Report WQEC/C 76-8, Crane, Indiana, February 1976.
189. Betz, F.E., K.E. Preusse, R.C. Shair, and J. Sylvia, "Parametric Charge Studies for Aerospace Nickel-Cadmium Batteries," *Proc. Fourth Inter-society Energy Conversion Engineering Conference, Washington, D.C.*, (A69-42236), September 1969, pp. 705-709.
190. Gross, S., "Heat Generation in Sealed Batteries," *Energy Conversion*, 9, (A69-34780), June 1969, pp. 55-62.
191. Wolverton, R.W., ed., *Flight Performance Handbook for Orbital Operations*, John Wiley and Sons, Inc., New York, 1961.
192. Cunningham, Fred G., "Calculation of the Eclipse Factor for Elliptical Satellite Orbits," *ARS Journal*, 32(9), September 1962, pp. 1399-1400.
193. Lesh, H.F., *Determination of Interplanetary Trajectories*, NASA CR-100490 (N69-21292), November 1968.
194. Rauschenbach, H.S., *Solar Cell Array Design Handbook, Volumes 1 and 2*, NASA CR-149364 (N77-14193), October 1976.

195. Pro, S., "Power Conditioning for Satellite Systems," Aerospace Corporation, Report TR-1001(2307)-6 (N68-12046), March 1967.
196. "Study and Analysis of Satellite Power System Configurations for Maximum Utilization of Power," NASA CR-898, October 1967.
197. Johnson Space Center, "Manned Mission Photovoltaic Power System Study Final Report Volume II, Technical Discussion," NASA Contract NAS9-5266, Houston, Texas, June 1967.
198. Reppucci, G.M., "Design of the High Energy Astronomy Observatory (HEAO) Power Subsystem," *Proc. Eleventh Intersociety Energy Conversion Engineering Conference, State Line, Nevada*, (A77-12662), 1976.
199. Nekrasov, P., "Partial Shunt Regulation," *Proc. 14th Annual Meeting of the American Astronautical Society, Dedham, Massachusetts*, May 13-15, 1968.
200. Moore, E.T., and T.G. Wilson, "Basic Considerations for DC to DC Conversion Networks," *IEEE Trans. on Magnetics*, MAG-2(3), September 1966, pp. 620-624.
201. Schwarz, F.C., *Power Processing*, NASA SP-244 (N72-15229), 1971.
202. LaVigna, T.A., "A Low Noise Switching Converter-Regulator for Main Power Control in a Space Power System." NASA TM X-55758, November 1966.
203. Farber, B.F., *Analysis of Aerospace Power Conditioning Component Limitations, Final Report*, NASA CR-97000 (N69-23417). April 1969.
204. Schoenfeld, A.D., and Y. Yu, *ASDTIC Control and Standardized Interface Circuits Applied to Buck, Parallel, and Buck-boost DC to DC Power Converters, Final Report*, NASA CR-121106 (N74-16806). February 1973.
205. Bedford, B.D., and R.G. Hoft, *Principles of Inverter Circuits*, John Wiley and Sons, Inc., New York, 1964.
206. *Study of Power Supply Configurations for Advanced Nimbus Missions, Final Report*, NASA CR-100529 (N69-22175). January 1969.

207. Krausz, A., and R.L. Robinson, "The Electric Power Supply of the Orbiting Geophysical Observatory," *AIAA Unmanned Spacecraft Meeting Record, Los Angeles, California*, March 1-4, 1965.
208. Ewen, W., D. Rusta, and R. Sternberg, "Power Subsystem Simulation Studies for the Timation IIIA Spacecraft," *Proc. Ninth Intersociety Energy Conversion Engineering Conference, San Francisco, California*, (A75-10476), pp. 26-35.
209. Reppucci, G.M., "Advanced Power System Development, Final Report," Report 76-8213.3-035, TRW Systems Group, Redondo Beach, California, December 1976.
210. Levy, E., Jr., and F.S. Osugi, "Design and Performance of the Intelsat IV Power Subsystem," *Proc. Seventh Intersociety Energy Conversion Engineering Conference, San Diego, California*, (A73-22751), 1972, pp. 483-492.
211. Obenschain, A., J. Bacher, and P. Callen, "The Atmospheric Explorer Power Subsystem," *Proc. Ninth Intersociety Energy Conversion Engineering Conference, San Francisco, California*, (A75-10476), 1974, pp. 43-52.
212. Wright, W.H., "Design and Orbital Performance of the Intelsat III Power System," *Proc. Seventh Intersociety Energy Conversion Engineering Conference, San Diego, California*, (A73-22751), 1972, pp. 472-482.
213. Brown, I., "The Nimbus B Solar Power Supply," EASTCON 67 Technical Convention Record, Supplement to IEEE Trans. on Aerospace and Electronic Systems, AES-3(6), November 1967.
214. Salim, A.A., "A Simplified Minimum Power Dissipation Approach to Regulate the Solar Array Output Power in a Satellite Power Subsystem," *Proc. Eleventh Intersociety Energy Conversion Engineering Conference, State Line, Nevada*, (A77-12662), 1976, pp. 1437-1442.
215. Briggs, D.C., and H.N. McKinney, "Electrical Power Subsystem for the Synchronous Meteorological Satellite (SMS)," *Proc. Seventh Intersociety Energy Conversion Engineering Conference, San Diego, California*, (A73-22751), 1972, pp. 493-500.

216. McKinney, H.N., and D.C. Briggs, "Electrical Power Subsystem for the NATO III Communications Satellite," *Proc. Eleventh Intersociety Energy Conversion Engineering Conference, State Line, Nevada*, (A77-12662), pp. 1408-1413.
217. Wick, H.M., "Design and Performance of the Telesat Power Subsystem," *Proc. Ninth Intersociety Energy Conversion Engineering Conference, San Francisco, California*, (A75-10476), 1974, pp. 53-60.
218. LaVigna, T.A., and F.L. Hornbuckle, "The ATS-6 Power System: Hardware Implementation and Orbital Performance," *Proc. Eleventh Intersociety Energy Conversion Engineering Conference, State Line, Nevada*, (A77-12662), 1976.
219. Graff, C., and R. Lanier, Jr., "Skylab Electrical Power System," *Proc. 1971 Intersociety Energy Conversion Engineering Conference, Boston, Massachusetts*, (A71-38901), 1971.
220. Purcell, J., and D.M. Witters, ed., "Low Cost Modular Spacecraft Description," NASA TM X-70912 (X75-10227), May 1975.
221. Nekrasov, P., et al., "Power System Analysis and Optimization Using Advanced Voltage Regulation Techniques," AIAA Paper 64-742, 1964.
222. Burns, W.W., III, et al., "A Digital Computer Simulation and Study of a Direct Energy Transfer Power Conditioning System," 1975 IEEE Power Electronic Specialists Conference Record, IEEE Publication 75 CHO 965-4-AES, 1975.
223. Nekrasov, P., "Systems Comparison and Analysis of Tracking and Non-Tracking Space Power Supplies," *Proc. Fourth Space Congress, Cocoa Beach, Florida*, 1967.
224. Bolton, Charles N., and Paul S. Nekrasov, "Analysis of the Advanced Nimbus Power Systems," NASA TM X-55852, July 1967.
225. Binckley, W.G., "Power System Configuration Study and Reliability Analysis, Final Report," NASA/Jet Propulsion Laboratory Contract 951574, TRW Report 07171-6001-R000, September 18, 1967.

226. Costogue, E.N., and S. Lindena, "Comparison of Candidate Solar Array Maximum Power Utilization Approaches," *Proc. Eleventh Intersociety Energy Conversion Engineering Conference, State Line, Nevada*, (A77-12662), 1976, pp. 1449-1456.
227. Cherdak, A.S., and J.L. Douglas, "Maximum Power Point Tracker," U.S. Patent 3,566,143, February 23, 1971.
228. Berard, C.A., Jr., "A Second Generation (High-Speed) Maximum Power Tracker for Space Applications," *Proc. Fifth Space Congress, Cocoa Beach, Florida*, (A68-37762), 1968.
229. Gruber, R., "High Efficiency Solar Cell Array Peak Power Tracker and Battery Charger," *1970 IEEE Power Conditioning Specialists Conference Record, Greenbelt, Maryland*, IEEE Publication C31-AES 70 (A70-41206), 1970.
230. Paulkovich, J., and G.E. Rodriguez, "Maximum Power Transfer by Conductance Comparison," *1970 IEEE Power Conditioning Specialists Conference Record, Greenbelt, Maryland*, IEEE Publication C31-AES-70 (A70-41206), 1970, pp. 114-127.
231. Thurman, J.L., "Optimization of Steady-State Thermal Design of Space Radiators," *J. Spacecraft and Rockets*, 6(10), October 1969, pp. 1114-1119.
232. *Introduction to the Derivation of Mission Requirements Profiles for System Elements*, NASA SP-6503 (N68-15683), 1967.
233. Trimmer, J.D., *Response of Physical Systems*, John Wiley and Sons, Inc., New York, 1950.
234. Grover, G.M., T.P. Cotter, and G.F. Erickson, "Structures of Very High Thermal Conductance," *J. Applied Physics*, 35(6), June 1964, pp. 1990-1991.
235. Harkness, R.E., "The GEOS-II Heat Pipe System and Its Performance in Test and Orbit," Report TG-1049, Johns Hopkins University Applied Physics Laboratory, 1969.
236. Hinderman, J.D., J. Madson, and E.D. Waters, "An ATS-E Solar Cell Space Radiator Utilizing Heat Pipes," AIAA Paper 69-630, 1969.

237. Eby, R.J., R.D. Karam, and W.H. Kelley, "Thermal Control of ATS F&G," *Proc. the SAE/ASME/AIAA Life Support and Environmental Control Conference, San Francisco, California*, ASME Publication 71-AV-28 (A71-36395), 1971.
238. Eninger, J.E., "The Transport Capacity of a Heat Pipe," *Quest. 1(1)*, TRW Systems Group, Redondo Beach, California, Winter 1976/1977.
239. Kunz, H.R., I.S. Langston, B.H. Hilton, S.S. Wyde, and G.H. Nashick, "Vapor Chamber Fin Studies—Transport Properties and Boiling Characteristics of Wicks," NASA CR-812, 1967.
240. Katzoff, S., "Heat Pipes and Vapor Chambers for Thermal Control of Spacecraft," AIAA Paper 67-310 (A68-21372), 1967.
241. Phillips, E.C., *Low-temperature Heat Pipe Research Program*, NASA CR-66792 (N75-70027), 1969.
242. Marcus, B.D., *Theory and Design of Variable Conductance Heat Pipes*, NASA CR-2018 (N72-23953), April 1974.
243. Mock, P.R., B.D. Marcus, and E.A. Edelman, "Communications Technology Satellite: A Variable Conductance Heat Pipe Application." AIAA Paper 74-749, 1974.
244. Wanous, D.J., B.D. Marcus, and J.P. Kirkpatrick, "A Variable Conductance Heat Pipe Flight Experiment: Performance in Space." AIAA Paper 75-725, 1975.
245. Maiden, C.E., A.F. Ahrens, R.R. Eliason, I.L. Kerper, E. Levy, and R.J. McGrath. "Near Earth Orbit Battery for Satellite Secondary Power." Contract AF33-615-73-C-2007, Report AFAPL-TR-74-21. Hughes Aircraft Company, June 1974.
246. Coggi, J.V., "Heat Pipe Thermal Control of Spacecraft Batteries." *Proc. Fifth Intersociety Energy Conversion Engineering Conference, Las Vegas, Nevada*, (A73-25976), 1970, pp. 7-20 – 7-260.
247. Fleischman, G.L., and D.J. Wanous, "Active Control Heat Pipe Performance for Long Life Battery Cooling," ASME Paper 72-WA/HT43 (A73-15813). November 1972.

248. Michalek, T.J., E.A. Stipandic, and M.J. Coyle, "Analytical and Experimental Studies of an All Specular Thermal Control Louver System in a Solar Vacuum Environment," AIAA Paper 72-268 (A72-25209), April 1974.
249. Dynatherm Corporation, "ATS F&G Heat Pipe Critical Design Review Presentation," To Fairchild Space and Electronics Company, Germantown, Maryland, August 25-26, 1971.
250. Neglia, M., L. Olshan, W. Ducan, and K. Hill, "OAO Louver Sun Compatibility Test," Report TLTR-67-14, Grumman Aerospace Corporation, Bethpage, Long Island, New York, September 1967.
251. Clausen, O.W., and J.P. Kirkpatrick, "Thermal Tests of an Improved Louver System for Spacecraft Thermal Control," AIAA Paper 69-627 (A69-33269), June 1969.
252. Streed, E., "Analysis and Test of a Thermal Control Louver Assembly," Report T05-71-48953-001, Martin Marietta Corporation, Denver, Colorado, June 1971.
253. Plamondou, J.A., "Analysis of Movable Louvers for Temperature Control," *J. Spacecraft and Rockets*, 1(5), September-October 1964.
254. Ollendorf, S., "Analytical Determination of the Effective Emittance of an Insulated Louver System," AIAA Paper 65-425, 1965.
255. Boscia, A.J., "A Laboratory Method for the Determination of Effective Emittance of Spacecraft Thermal Control Louvers," *Proc. Joint Meeting of the AAS and the ORS, Denver, Colorado*, June 17-20, 1969.
256. Parmer, J.F., and D.L. Buskirk, "Thermal Control Characteristics of Interior Louver Panels," ASME Paper 67-HT-64, 1967.
257. Rubenzer, J., "The 1972 GSFC Battery Workshop, Second Day," *Proc. Greenbelt, Maryland*, November 15, 1972, NASA TM X-69239 (N73-21957), 1972.
258. Rubenzer, J., "The 1973 GSFC Battery Workshop, Second Day," *Proc. Greenbelt, Maryland*, November 14, 1973, NASA TM X-72540 (N75-17808), 1973.

259. Newell, D.R., "The 1976 Goddard Space Flight Center Battery Workshop," *Proc. Greenbelt, Maryland*, NASA TM X-71284 (N77-21550), November 1976.
260. Rusta, D., "Power Source Requirements of Electric Propulsion Systems Used for North-South Stationkeeping of Communication Satellites," *Proc. Eleventh Intersociety Energy Conversion Engineering Conference, State Line, Nevada*, (A77-12662), 1976, pp. 1429-1436.
261. Eicke, W.G., Jr., "The 'Vicious Cycle' in Secondary Batteries - A Mathematical Approach," *J. Electrochemical Soc.*, 109(5), May 1962, pp. 364-368.
262. Bacher, Joel, and Douglas Rusta, "The Analysis of Voltage-Limited Battery Charging Systems," *IEE Trans. Aerospace and Electronic Systems*, AES-4(5), September 1968, pp. 792-798.
263. LaVigna, T.A., "The ATS-6 Power System - An Optimized Design for Maximum Power Source Utilization," *Proc. Tenth Intersociety Energy Conversion Engineering Conference, Newark, Delaware*, (A75-45920), 1975, pp. 1048-1055.
264. Oakes, J.B., and W.J. Billerbeck, "A New Charge Control System for Satellite Batteries," Report CM-1041, Johns Hopkins University Applied Physics Laboratory, July 1963.
265. Miller, W., W. Stewart, and J. Yagelowich, "OAO State of Charge Unit," NASA TM X-63757 (N70-14252), June 1968.
266. Breeskin, S.D., and A.D. Taylor, "Battery and Third Electrode Performance Characteristics for Varying Charge and Discharge Rates," *Proc. 1971 Intersociety Energy Conversion Engineering Conference, Boston, Massachusetts*, (A71-38901), 1971, pp. 181-187.
267. Corbett, R.E., M.C. Glass, and R.G. Matsui, "Development of a Power Module Using Third Electrode Battery Charge Control," *Proc. Ninth Intersociety Energy Conversion Engineering Conference, San Francisco, California*, (A75-10476), 1974, pp. 137-143.
268. Imamura, M.S., N.R. Sheppard, and T.D. Patterson, "Digital Techniques in Future Spacecraft Automated Power Systems," *Proc. Ninth Intersociety Energy Conversion Engineering Conference, San Francisco, California*, (A75-10476), 1974, pp. 10-19.

269. Imamura, M.S., L. Skelly, and H. Weiner, "Conceptual Definition of Automated Power Systems Management," *Proc. Twelfth Intersociety Energy Conversion Engineering Conference, Volume 2, Washington, D.C., (A77-48701)*, 1977, pp. 1343-1348.
270. Robertson, L.G., "Theory and Procedure for Using the Computerized Markov-and-Multinomial Single-Battery Reliability Models," CADM Report D.00608, TRW Defense and Space Systems Group, June 1973.
271. Kettler, J.R., and H.J. Killian, "Depth of Discharge for Long-Life Nickel-Cadmium Batteries in Synchronous Orbit," Aerospace Corporation Report TOR-0074(4901-02)-4, September 1973.
272. Layte, H.L., and D.W. Zerbel, "Battery Cell Control and Protection Circuits," *IEEE Power Processing and Electronic Specialists Conference, San Diego, California*, September 25-29, 1972.
273. Donovan, R.L., and M.S. Imamura, "Cell-Level Battery Charge/Discharge Protection System - Electronic Control Techniques," *Proc. Twelfth Intersociety Energy Conversion Engineering Conference, Washington, D.C., (A77-48701)*, 1977, pp. 302-310.
274. Thomas, E.U., and L.W. Wendling, "Guidelines for Reliable Relay Application and Selection," (A69-28045), Relay Division, Leach Corporation, 1969.
275. Ritterman, P.F., "Nickel-Cadmium Battery Charge Management Study, Final Report," Report 74-8216.6-059, TRW Systems Group, Redondo Beach, California, December 1974.
276. Imamura, M.S., R.L. Donovan, J.L. Oberg, L.A. Skelly, and D.H. Julseth, "Microprocessor-Controlled Battery Protection System," *Proc. Tenth Intersociety Energy Conversion Engineering Conference, Newark, Delaware, (A75-45920)*, 1975, pp. 1307-1317.
277. McKinney, H.N., and D.C. Briggs, "Electrical Power Subsystem for the NATO III Communications Satellite," *Proc. Eleventh Intersociety Energy Conversion Engineering Conference, State Line, Nevada, (A77-12662)*, 1976, pp. 1408-1413.
278. Reppucci, G.M., "Design of the High Energy Astronomy Observatory (HEAO) Power Subsystem," *Proc. Eleventh Intersociety Energy Conversion Engineering Conference, State Line, Nevada (A77-12662)*, 1976.

279. Krausz, A., *Space Vehicle Electrical Power Processing Distribution and Control Study: Volume 2, Technical Report*, NASA CR-123908 (N72-33054), June 1972.
280. "Study of Advanced Flight Vehicle Power Systems, Volume 1: Analytical Studies," Report ASD TR 61-368, The Marquart Corporation, Astro Research Division, January 1962.
281. Szego, G.C., and B. Paiewonsky, "Optimization of Energy Storage for Solar Space Power," *Proc. 1967 Intersociety Energy Conversion Engineering Conference, Miami Beach, Florida*, August 13-17, 1967.
282. Fono, P., "Battery and Cell Redundancy Considerations for Long Duration Space Missions," *Proc. Ninth Intersociety Energy Conversion Engineering Conference, San Francisco, California*, (A75-10476), 1974, pp. 128-136.
283. Bolton, Charles N., and Paul S. Nekrasov, "Multiple Operating Points in Photovoltaic Power Systems," NASA TM X-63251, May 1968.
284. Schwartzburg, M., "Analysis of Solar Array/Battery Lock-Up Computer Simulation of Electric Power System Performance," *Proc. 1971 Intersociety Energy Conversion Engineering Conference, Boston Massachusetts*, (A71-38901), 1971, pp. 995-1002.
285. Pessin, L., and D. Rusta, "A Comparison of Solar-Cell and Battery-Type Power Systems for Spacecraft," *IEEE Trans. Aerospace and Electronic Systems*, AES-3, November 1967, pp. 889-897.
286. Hyland, P., and R. Rasmussen, "Program Report - Energy Balance Computer Program for Advanced NIMBUS Power Systems," NASA Contract NAS5-11549, RCA, Hightstown, New Jersey, December 1968.
287. Imamura, M.S., A.A. Conn, A.J. Peszko, and R.C. Scott, "Computer Simulation Concept for a Large Solar Array/Battery Power System," *Proc. Seventh Intersociety Energy Conversion Engineering Conference, San Diego, California*, (A73-22751), 1972, pp. 607-619.
288. Bauer, Paul, "Computer Simulation of Satellite Electric Power Systems," *IEEE Trans. on Aerospace and Electronic Systems*, AES-5(6), November 1969, pp. 934-942.

289. Schwartzburg, M., "Performance Analysis of Satellite Electric Power Systems by Computer Simulation," *Proc. Fourth Intersociety Energy Conversion Engineering Conference, Washington, D.C.*, 1969.
290. Weiner, H., and S. Weinstein, "Power Subsystem Performance Prediction (PSPP) Computer Program," *Proc. Seventh Intersociety Energy Conversion Engineering Conference, San Diego, California*, (A73-22751), 1972, pp. 581-606.
291. Zimmerman, H.G., and R.G. Peterson, "An Electrochemical Cell Equivalent Circuit for Storage Battery/Power System Calculations by Digital Computer," *Proc. 1970 Intersociety Energy Conversion Engineering Conference, Las Vegas, Nevada*, (A73-25976), 1972, pp. 5-33-5-39.
292. Durando, A.R., *Modeling, Identification and Control Optimization of a Satellite Power System*, Thesis, University of California, Los Angeles, (N74-13758), 1973.
293. "Reliability Program Provision for Space System Contractors," NASA Reliability Publication NPC-250-1, July 1963.
294. *Practical Reliability: Volume IV - Prediction*, NASA CR-1129, August 1968.
295. Von Alven, William H., ed., *Reliability Engineering*, Prentice-Hall, Inc., New Jersey, 1964.
296. Au, T., et al, "Fundamentals of Systems Engineering: Probabilistic Models," Addison-Wesley Publishing Co., Reading, Massachusetts, 1972.
297. Kirsch, W.W., and L.E. Paschal, "Nickel-Cadmium Cell Composite Reliability Model," *Proc. Eleventh Intersociety Energy Conversion Engineering Conference, State Line, Nevada*, (A77-12662), 1976, pp. 521-527.
298. Eliason, J., "Nickel-Cadmium Battery Reliability for Shuttle Serviced Spacecraft," *Proc. Tenth Intersociety Energy Conversion Engineering Conference, Newark, Delaware*, (A75-45920), 1975, pp. 1297-1306.
299. "Reliability Prediction of Electronic Equipment," MIL-HDBK-217B.

300. Barnett, E.H., "Parallel Battery Simulation Computer Program," Report 74-2286.004, TRW Systems Group, Redondo Beach, California, January 1974.
301. Robertson, L.G., "Theory and Implementation of the 'Monte Carlo' Parallel Battery Model," Report 74-2286.055, TRW Systems Group, Redondo Beach, California, July 1974.
302. "Specification for the Manufacture of Aerospace Nickel-Cadmium Storage Cells," NASA/GSFC Specification 74-15000, March 1975.
303. U.S. Air Force, "Military Standard, Test Requirements for Space Vehicles," MIL-STD-1504A, May 1974.
304. Ford, F., "The 1972 GSFC Battery Workshop, Second Day," *Proc. Greenbelt, Maryland*, NASA TM X-69239 (N73-21957), 1972.
305. Stanley, C., "Spacecraft Battery Testing - 5 Year Storage Life," USAF/SAMSO Contract F04701-71-C-0131, Report 16439-93-002-602, TRW Systems Group, Redondo Beach, California, 1976.
306. Scott, W., "The 1973 GSFC Battery Workshop, First Day," *Proc., Greenbelt, Maryland*, NASA TM X-72536 (N75-15152), 1973.
307. Salkind, A.J., and G.W. Bodamer, "Changes in Physical Chemical Properties of Secondary Battery Electrodes During Cycling," *Proc. Fourth International Symposium, Brighton, England*, September 1964.
308. Aerospace Corporation, "Standardization and Program Effect Analysis Final Report. Volume IV: Equipment Compendium, Part C, Electrical Power Subsystem," Report ATR-75 (7364)-1, Los Angeles, California, November 28, 1975.
309. Bogner, R.S., *Mariner Mars 1971 Battery Design, Test, and Flight Performance*, NASA CR-132986 (N73-25095), April 15, 1973.
310. Armantrout, J.D., "Accelerated Life Tests on NATO III Batteries," *The 1976 Goddard Space Flight Center Battery Workshop, Proc., Greenbelt, Maryland*, NASA TM X-71284 (N77-21550), November 1976.
311. Ritterman, P.F., *The 1977 Goddard Space Flight Center Battery Workshop*, NASA CP-2041, 1977, pp. 271-279.

312. Kerr, R.L., and D.F. Pickett, "Space Battery Technology for the 1980's," AIAA Paper 77-482 (A77-23902), March 1977.
313. Malkin, B., "Energy Cell Selections and Related Circuits," ASME 67-DE-37, 1967.
314. Howard, P.L., "Latest Battery Improvements and Mathematical Techniques for their Selection," ASME 65-MD-44, 1965.
315. Gould, J., and P. Garmally, "Power Up With Batteries," *Design News*, March 21, 1977.

APPENDIX A DEFINITIONS

INTRODUCTION

This appendix defines cell-capacity and energy-related terms and concepts used in the main text. These definitions provide a basis for unambiguous discussion and quantitative analysis of cell performance in relation to cell design, size, and mass.

CAPACITY

The term "capacity" is usually used to refer to the coulombic discharge capacity. In general, capacity is the time integral of discharge current between specified limits; i.e.,

$$\text{Capacity} = k \int_{\text{lim}_1}^{\text{lim}_2} I_d dt \quad (\text{A1})$$

where the constant, k , depends on the units used, and I_d is the instantaneous value of discharge current.

The value of capacity measured at any point in the life of a cell is a function of many variables. These variables include the cell temperature, the magnitude of the normalized discharge current (discharge rate), whether the current is constant or increasing as it does when discharging into a constant-power load, and the value of the end (cutoff) voltage. The term "capacity" is ambiguous unless all of the foregoing variables are specified.

Standard Capacity

The standard capacity, C_S , is defined as the coulombic output on discharge under the following conditions:

- Prior charge
 - Starting with the cell discharged and shorted

- Cell-wall temperature: 20 to 25°C
- Charge rate (normalized constant current): $0.1C_R^*$ ampere
- Charge time: 18 to 24 hours

- Discharge

- Cell-wall temperature: 20 to 25°C
- Rate (normalized constant current): $0.5C_R^\dagger$ ampere
- End voltage: 1.00 volt

Coulombic output data determined under conditions other than the foregoing, such as those imposed by a specific system design, should be properly qualified with pertinent charge and discharge parameters and should be closely compared only with other data taken under similar conditions.

Rated Capacity

The rated capacity, C_R , is an arbitrary value that the cell manufacturer or the user may assign. The manufacturer's rated capacity is usually less than the average value of the standard capacity for new cells by a factor of 0.8 to 0.9, depending on the manufacturer and the design.

Specific Capacity

The term "specific capacity" is ambiguous when used alone (i.e., without being associated with the units referred to). The preferred terminology is capacity per unit mass. Specific standard capacity is therefore C_s per unit mass. The units are ampere-hours per kilogram (Ah/kg) or ampere-hours per pound (Ah/lb).

*As defined here, C_R is the rated capacity. A charge rate of $0.1C_R$ is chosen to simplify charge control because all sealed spacecraft cells should be capable of continuous overcharge at this rate and at the specified temperature without developing excessive pressure (over 65 psia). Also, a large amount of background data have been accumulated for this method of charging.

†A discharge rate of $0.5C_R$ is chosen because this rate is close to that used for many applications and because a large amount of background data have been accumulated at this rate.

ENERGY

The electrical energy delivered to, or obtained from, a cell is the time integral of the product of cell voltage and current between specified limits; i.e.,

$$W_e = k_e \int_{\text{lim}_1}^{\text{lim}_2} EI \, dt \quad (\text{A2})$$

During charge, the energy supplied is

$$(W_e)_c = k_e \int E_c I_c \, dt \quad (\text{A3})$$

where E_c and I_c are the cell voltage and current on charge, respectively. Until the incremental coulombic charge efficiency, η_c , becomes significantly less than unity, all input electrical energy is stored as chemical energy. After that, an increasing fraction of the input energy is converted to heat, and, when $\eta_c = 0$, essentially all electrical energy input is converted to heat.

During discharge, part of the stored energy content of the cell is converted to electrical energy:

$$(W_e)_d = k_e \int E_d I_d \, dt \quad (\text{A4})$$

where E_d and I_d are the cell voltage and current on discharge, respectively, and part of the stored energy is converted to heat, even though the incremental coulombic efficiency of discharge is always near 100 percent. The only deviation is a small one caused by self-discharge during the discharge interval. However, energy efficiency on discharge is considerably less than 100 percent.

According to the International System of Units (SI), the unit of energy is the joule (J), which is equal to one watt-second. For battery engineering, the unit of the watt-hour, (Wh) (= 3600 J), is more familiar and is used in the main text when a large number of joules are involved.

Because the actual value of electrical energy delivered on discharge is a function of the same variables as those of capacity as listed above, careful definition of energy terms is required. The following definitions are extensions of this definition of energy.

Standard Energy Output

The standard energy output is the electrical energy delivered by a cell during a discharge to measure standard capacity, as defined in the foregoing section on "Standard Capacity."

Specific Energy (Energy Density)

The terms "specific energy" and "energy density" are used interchangeably to refer to energy output per unit mass. The authors prefer the term "specific energy." When the meaning of "energy per unit volume" is intended, it will be spelled out.

The units of specific energy by the SI system are joules per kilogram (J/kg). For engineering purposes and in the main text, watt-hours per pound (Wh/lb) are used.

Specific Mass or Specific Weight

The term "specific mass (or weight)" is often used to refer to the ratio of mass-to-energy output (i.e., to the reciprocal of specific energy). Although this ratio is a useful parameter, the shorthand terminology is ambiguous in that the other factor besides mass in the ratio is not specified by the terms *per se*. For this reason, these terms are not recommended. Instead, the component parts of the ratio intended (e.g., mass per unit energy (kg/Wh)) should be spelled out.

STATE OF CHARGE AND DEPTH OF DISCHARGE

The term "state of charge" is used in several ways in the literature (i.e., to refer to the amount of charge put through the cell and to refer to the level of usable charge existing in the cell at any point). Because the incremental coulombic charge efficiency at high states of charge becomes low and because cell behavior correlates well with true state of charge and not necessarily to charge throughout without taking charge efficiency into account, the term "state of charge" refers only to the true state of charge retained by the cell.

As normally used, state of charge does not refer to capacity *per se*, but to the ratio of the actual (measurable) capacity, C_a , at a given point to some reference capacity, C_{ref} ; i.e.,

$$\text{State of charge} = \frac{C_a}{C_{ref}} \quad (A5)$$

C_{ref} may be chosen as equal to rated capacity or to the maximum capacity achievable under the conditions of interest.

True state of charge in a sealed nickel-cadmium cell cannot be measured reliably by any direct method in spite of considerable work to develop such a method. The only widely accepted method for determining the state of charge is to discharge the cell, measure the output, and divide by the reference capacity. Because this definition makes state of charge a function of the parameters that control discharge output (i.e., cell temperature, discharge rate, and end voltage), these parameters should be specified with the data.

APPENDIX B
AUTHOR INDEX

- Ahrens, A. F., 320
Appleby, A. J., 196, 202
Armantrout, J. D., 53, 169, 273, 455
Au, T., 400
- Bacher, J., 291, 337
Baer, D. A., 112, 126, 349
Baker, H., 22, 169, 194
Barnett, E. H., 136, 147, 155, 157, 400, 401, 406
Barney, D. L., 204
Bauer, J. L., 26
Bauer, P., 3, 4, 10, 67, 68, 70, 97, 100, 102, 103, 104, 116, 265, 327, 392
Baumstark, G. A., 118, 199
Bean, E. E., 156, 157
Bedford, B. D., 289
Berard, C. A., Jr., 302
Betz, F. E., 86, 87, 273
Billerbeck, W. J., 347
Binckley, W. G., 301, 388, 389
Bloomquist, C. E., 156, 157
Bodamer, G. W., 439
Bogner, R. S., 64, 446
Bolton, C. N., 301, 389, 390
Boscia, A. J., 322
Breeskin, S. D., 349
Briggs, D. C., 62, 169, 291, 301, 377
Broberg, H., 136, 157, 402
Brooman, E. W., 73, 74, 75, 76, 78, 104, 217, 268, 270, 309, 311
Brown, I., 291
Bulla, W., 194
Burns, W. W., III, 301
Buskirk, D. L., 323
- Cahoon, N. C., 46
Callen, P., 291
Cardwell, G. I., 29, 73, 93, 169, 196, 273, 312, 348
- Carson, W. N., Jr., 41, 43, 45, 56, 100, 152
Casey, E. J., 32
Catotti, A. J., 192, 194, 204
- Cherdak, A. S., 302
Chua, D., 205
Clausen, O. W., 321
Coggi, J. V., 320
Conn, A. A., 391
Consiglio, J. A., 100
Conway, B. E., 9, 10
Corbett, R. E., 349
Costogue, E. N., 301, 389
Cotter, T. P., 316
Cover, P. W., 179, 192, 194, 201
Coyle, M. J., 320, 322, 323
Crawford, R. L., 77, 78
Cunningham, F. G., 276
Cuthrell, W. F., 22, 169
- Donovan, R. L., 360, 369
Doran, R., 18
Douglas, J. L., 302
Dubois, A. R., 32
Ducan, W., 321
Duncan, E. C., 29, 73, 93, 169, 196, 273, 312, 348
Dunlop, J. D., 19, 111, 156, 165, 169, 173, 176, 196, 202, 205, 265, 439
Durando, A. R., 392
- Earl, M., 111, 196, 205, 265
Eby, R. J., 316
Edelman, E. A., 320
Eicke, W. G., Jr., 334
Ekpanyaskun, S., 13
Elder, J. P., 95, 107, 108, 127
Eliason, J. T., 136, 153, 154
Eliason, R. R., 320, 402
Eninger, J. E., 318

- Epstein, S. D., 136
 Erickson, G. F., 316
 Ewen, W., 291, 296, 297, 391
- Falk, S. U., 9, 13, 32, 115, 123
 Farber, B. F., 289
 Faust, C. L., 179, 181, 183, 192, 198, 201
 Finkelstein, J., 156, 157
 Fitchman, A., 118, 199
 Fleischman, G. L., 320
 Fono, P., 388
 Font, S., 67, 68, 70, 71, 84, 88, 91, 92, 93, 94, 95, 97, 98, 101, 104, 109, 128, 205
 Ford, F. E., 43, 45, 86, 111, 140, 149, 150, 151, 152, 168, 174, 188, 260, 265, 291, 337, 339, 348, 351, 370, 376, 438, 439
 Fougere, P., 169, 170, 171
 Francis, H. T., 3
- Garcia, A., 26
 Garmally, P., 458
 Garrett, P., 135, 136, 142
 Gaston, S. J., 53, 148, 149, 258, 260, 265, 391
 Gibson, L., 136
 Gileadi, E., 9, 10
 Glass, M. C., 349
 Glocking, R. J., 108, 128, 203, 204, 205, 207
 Gondusky, J. M., 77, 78
 Goodman, L. A., 196, 216, 217, 219
 Gordon, L., 156, 158, 159, 160, 400, 401, 402
 Gordy, D. J., 128, 202
 Gottlieb, M. H., 111
 Gould, J., 458
 Graff, C., 291, 301, 352
 Gross, S., 39, 41, 108, 109, 128, 201, 202, 203, 204, 205, 207, 273
 Grover, G. M., 316
 Gruber, R., 302, 352
- Haas, R. J., 62
- Halpert, G., 4, 10, 13, 16, 53, 136, 192, 193, 194, 196, 198, 202, 216
 Harivell, J. P., 108
 Harkness, J. D., 142, 150, 165, 169, 170, 174, 196
 Harkness, R. E., 316
 Haugen, H., 73, 119, 273
 Häusler, E., 53
 Hennigan, T. J., 217, 219, 271
 Henningson, A., 136, 157, 402
 Hess, H. J., 205
 Hill, K., 321
 Hilton, B. H., 318
 Hinderman, J. D., 316
 Hoft, R. G., 289
 Holleck, G., 15, 16, 47, 114, 124, 198
 Hornbuckle, F. L., 291, 301, 341
 Howard, P. L., 458
 Howden, W. E., 32
 Hyland, P. J., 391
- Imamura, M. S., 352, 360, 369, 391, 457
- Jakobi, W. W., 24, 77, 123
 Johnson, C. R., 136, 139, 140, 148, 265, 271
 Jones, C. C., 192, 193, 194
 Jost, E. M., 95, 107, 108, 127
 Julseth, D. H., 369
- Kantner, E., 47, 49
 Karam, R. D., 316
 Katzoff, S., 318
 Kelley, J. J., 194
 Kelley, W. H., 316
 Kent, J., 136, 185, 186, 187, 192, 194, 216
 Kerper, I. L., 320
 Kerr, R. L., 457
 Kettler, J. R., 356
 Killian, H. J., 356
 Kirkpatrick, J. P., 320, 321
 Kirsch, W. W., 43, 45, 136, 139, 140, 150, 152, 167, 168, 348, 352, 358, 400, 402

ORIGINAL PAGE IS
 OF POOR QUALITY

- Krause, S., 169, 173, 176
Krausz, A., 291, 382
Kröger, H. H., 16, 18, 19, 32, 50, 53,
124, 125, 127, 192, 194, 198, 207
Kunz, H. R., 318
- Lackner, J., 92, 176
Lake, P. E., 32
Langston, I. S., 318
Lanier, R., 168, 291, 301, 352
LaVigna, T. A., 289, 291, 301, 341,
391
Layte, H. L., 357
Leary, J., 136, 154, 155, 402
Lerner, S., 18, 43, 45, 95, 126, 152
Lesh, H. F., 276
Levy, E., Jr., 29, 73, 93, 169, 196,
273, 291, 312, 320, 348, 357
Lim, H. S., 24, 165, 166, 205, 206,
440
Lindena, S., 301, 389
Loewner, A., 136, 157, 402
Luksha, E., 128, 202
- MacArthur, D. M., 10
Madson, J., 316
Maiden, C. E., 29, 73, 93, 169, 196,
273, 312, 320, 348
Malkin, B., 458
Marcus, B. D., 320
Matsui, R. G., 349
Mauchly, J. W., 136
Maurer, D., 108, 109, 111, 129, 194,
204
Mayer, S. W., 204
McCallum, J., 73, 74, 75, 76, 78,
104, 179, 180, 181, 183, 192, 194,
198, 201, 217, 218, 268, 270, 271,
309, 311
McDermott, P. P., 13, 196, 202, 203,
216, 217, 219, 271
McGrath, R. J., 320
McHenry, E. J., 32
McKinney, H. N., 291, 301, 377
Menard, C. J., 16, 124
Michalek, T. J., 320, 322, 323
- Michel, W., 29, 73, 93, 169, 196,
273, 312, 348
Migeon, J., 108
Miller, G. H., 104, 179, 180, 181,
183, 192, 198, 201, 217, 218, 268,
270, 271
Miller, L., 51, 52, 114, 125, 126, 130
Miller, W., 348
Milner, P. C., 124
Mock, P. R., 320
Moore, E. T., 288
Morignat, B., 108
Moroz, W. J., 32
- Napoli, J., 176
Nashick, G. H., 318
Nche, P., 13
Neglia, M., 321
Nekrasov, P., 287, 301, 398, 390
Newell, D. R., 129, 166, 327, 446
- Oakes, J. B., 347
Obenschain, A., 291
Ober, J. L., 369
Ogunyankin, O., 192, 193, 194
Okinara, Y., 32
Oliver, R. L., 47, 53, 124
Ollendorf, S., 322
Olshan, L., 321
Orenstein, S., 194
O'Rourke, J. A., 53, 148, 149, 258,
260, 265, 391
Osugi, F. S., 291, 357
Otzinger, B., 101, 102
- Paiewonsky, B., 388
Parmer, J. F., 323
Parry, J. M., 192, 194
Paschal, L. E., 265, 400, 402
Patterson, T. D., 352
Paulkovich, J., 320
Pensabene, S. F., 204
Pessin, L., 391
Peszko, A. J., 391
Peterson, R. G., 392
Phillips, E. C., 318
Pickett, D. F., 47, 53, 124, 176, 457

- Plamondou, J. A., 322
Pomroy, S., 135, 136, 142
Popat, P. V., 77, 78, 129
Preusse, K. E., 273
Pro, S., 281, 283, 286
Puglisi, V. J., 46, 47, 53, 123, 124,
125, 128
Purcell, J., 296
- Ralph, E. L., 46, 123, 124, 125, 128
Rampel, G. G., 19, 20, 36, 41, 43,
45, 56, 114, 115, 152, 203
Rasmussen, R., 391
Rauschenbach, H. S., 279
Reed, A. H., 179, 192, 194, 201,
218, 270
Reppucci, G. M., 284, 290, 291, 292,
330, 331, 377
Ritterman, P. F., 11, 18, 47, 118,
124, 362, 455
Robertson, L. G., 136, 147, 155,
156, 157, 158, 159, 160, 353, 400,
401, 402, 406
Robinson, R. L., 291
Rodriguez, G. E., 302
Roeger, E. A., Jr., 104, 201, 217,
218, 268, 270, 271
Rubenzer, J. F., 327
Rubin, E. J., 18, 77, 78, 108, 124,
198
Rusta, D. W., 291, 296, 297, 327,
337, 391
- Salim, A. A., 291
Salkind, A. J., 9, 13, 32, 115, 123,
439
Sanders, J. A., 265
Schoenfeld, A. D., 289
Schulman, I. M., 64, 176
Schwartzburg, M., 390, 392
Schwarz, F. C., 288
Scott, R. C., 391
- Scott, W. R., 16, 17, 18, 29, 41, 43,
44, 45, 73, 101, 102, 112, 118,
119, 124, 129, 130, 156, 168,
169, 170, 171, 173, 174, 176, 177,
188, 196, 198, 207, 253, 254, 255,
257, 265, 266, 267, 268, 273, 303,
343, 346, 349, 406, 433, 439
Seiger, H. N., 9, 10, 18, 43, 47, 49,
53, 95, 114, 122, 124, 126, 129,
202
Shair, R. C., 273
Sheppard, N. R., 352
Shikoh, A. E., 43, 45, 136, 139, 140,
150, 152, 167, 168, 348, 352, 358
Skelly, L. A., 352, 369, 457
Sommerfeldt, E. E., 196, 216, 217,
219, 271
Sparks, R. H., 265, 268, 343
Stager, D. N., 73, 119, 273
Stanley, C. L., 258, 439, 442
Sternberg, R., 291, 296, 297, 391
Stewart, W., 348
Stipandic, E. A., 320, 322, 323
Stofel, E., 192
Streed, E., 321
Sylvia, J., 273
Szego, G. C., 388
- Taylor, A. D., 349
Thierfelder, H., 136, 139, 148
Thomas, E. U., 360
Thomas, R. E., 179, 270
Thomas, U. B., 124
Thornell, S., 188, 199
Thurman, J. L., 303
Toner, S. D., 22, 169
Trimmer, J. D., 307, 310
Tuomi, D., 32
Turchan, M. J., 18
Turner, D. R., 32, 109
- Uchiyama, A. A., 64
van Ommering, G., 196, 202
Von Alven, W. H., 400, 403
Voyentzie, P. R., 41, 43, 45, 152

- Wagner, O. C., 207
Waite, J. H., 136, 179, 270
Wanous, D. J., 320
Waters, E. D., 316
Webster, W. H., Jr., 13, 192, 193,
194, 340
Weiner, H., 352, 392, 457
Weinstein, S., 392
Weinstock, I. B., 43, 45, 56, 152
Wendling, L. W., 360
Wertheim, M., 53, 148, 149, 258,
260, 265, 391
Wick, H. M., 291
Wilbore, J. F., 100
Will, F. G., 205
Williams, D. D., 207
Willis, T. H., 111
Wilson, T. G., 288
Witters, D. M., 296
Wolverton, R. W., 276
Wright, W. H., 291, 357
Wyde, S. S., 318
Yagelowich, J., 348
Yamashita, D., 32
Yu, Y., 289
Zerbel, D. W., 73, 273, 357
Zimmerman, H. G., 392

**APPENDIX C
ORGANIZATION INDEX**

Aero Propulsion Laboratory (U.S. Air Force), 1, 365	NASA Headquarters, 445
Aerospace Corporation, 445	NASA/MSFC, 268
Armed Services, 246, 271	NWSC/Crane, 2, 68, 134, 139, 142, 143, 144, 145, 147, 148, 149, 150, 151, 153, 154, 155, 156, 158, 160, 161, 162, 164, 165, 166, 167, 169, 172, 174, 192, 194, 195, 196, 205, 217, 219, 265, 268, 271, 339, 340, 365, 400, 402
Battelle Columbus Laboratories, 270, 271	
Canadian Defence Research Establishment, 24, 43	
COMSAT Laboratories, 265	Pellon Corporation, 22
Eagle Picher Industries, Inc., 14, 15, 20, 47, 51, 52, 53, 59, 60, 61, 62, 63, 75, 81, 134, 136, 162, 165, 239, 261, 273, 419, 446	Radio Corporation of America, (RCA), 358
General Electric, Battery Business Department, 14, 15, 19, 20, 34, 36, 38, 47, 53, 59, 60, 61, 63, 75, 82, 87, 88, 92, 93, 114, 115, 116, 117, 124, 126, 134, 136, 139, 142, 143, 144, 145, 148, 153, 155, 161, 162, 163, 170, 175, 190, 203, 239, 261, 267, 269, 273, 341, 364, 366, 419, 447, 448, 450, 452, 453	SAFT-America, Inc., 14, 15, 20, 34, 38, 41, 43, 47, 48, 49, 50, 53, 59, 60, 61, 63, 64, 69, 70, 71, 75, 83, 86, 89, 91, 93, 94, 95, 96, 97, 98, 105, 117, 126, 134, 136, 139, 140, 142, 143, 144, 145, 148, 149, 152, 155, 161, 162, 170, 173, 239, 261, 271, 273, 339, 340, 419, 449, 451
Gould 124, 155	SAFT-France, 14, 15, 20, 47, 53, 58, 59, 60, 84, 92
Gulton Industries, 59, 60, 89	Satellite Business Systems, 364
Jet Propulsion Laboratory, 1	Sonotone Corporation, 47, 136, 155
Marathon Battery Corporation, 47	
NASA, 1, 2, 3, 4, 51, 64, 158, 195, 219, 226, 235, 246, 247, 259, 262, 265, 271, 329, 332, 338, 391, 400, 418, 419, 425, 433, 439	TRW, 175, 247, 355, 358, 364
NASA/GSFC, 1, 3, 246, 247, 248, 251, 252, 253, 254, 256, 257, 262, 340, 370, 371, 372, 375, 418, 419, 438, 457	U.S. Air Force, 247, 248, 349, 356, 365, 425
	U.S. Navy, 334, 425
	Yardney Electric Company, 64, 419



APPENDIX D SUBJECT INDEX

The index is presented alphabetically with hierarchical notations to assist the reader in quickly locating the correct term. To find a term that is not used in the index, for which there is a synonym that is used, the reader will encounter the following reference:

Muspratt solution
Use: Ammonium hydroxide/chloride solution

There will also be a reference to indicate that the reader need not look under synonymous terms that are not used in the index:

Ammonium hydroxide/chloride solution
Use for: Muspratt solution

The following hierarchical notes are used: RT, NT, and BT. RT indicates that another term appears at the same hierarchical level that may refer the reader to other useful information. NT notifies the reader that there are more specific terms (narrower terms) that might be more useful. BT notifies the reader that there are broader terms that might be more useful; for example:

Measurement methods
NT: Accelerated-time tests, Acceptance tests, Atomic-absorption spectroscopy

Accelerated-time tests
BT: Measurement methods

The abbreviations, ff. and def., are used in the index. Ff. means that the term appears on many of the following pages. Def. means that on that page the term is defined, for example:

Capacity
120 ff., 352

Normalized current
79 (def.), 86, 88

- Absolute temperature, 303, 361
- Absorber-type separators, 21, 24
- Accelerated cycling, 258
 - tests, 174, 176, 196, 198, 217, 218, 266, 267, 269, 343
 - BT: Measurement methods
- Acceleration factor, 269 (def.), 270
- Acceptance requirements, 258, 433
 - tests, 54, 65, 68, 100, 115, 131, 230 ff., 250, 259, 264
 - BT: Measurement methods (batteries), 246, 261, 429, 430 (cells), 246-251, 262
- Accordion-fold separators, 25 (def.)
- Accountability, 238
- Active-bypass circuits, 360, 363
 - Use for: Active-element failure-protection circuits
- Active charge, 79, 182, 208
 - voltage, 107
 - BT: Cell voltage
 - charged-negative material, 41
 - BT: Charged-negative material control elements, 290
 - element failure-protection circuits
 - Use: Active-bypass circuits
 - filter
 - Use: Series dissipative regulator
- Additives, 193
- Adhydrode electrode
 - Use: Oxygen signal electrode
- Adsorbed-hydrogen electrode
 - Use: Oxygen signal electrode
- Advanced battery systems, 454
- Aerospace part-derating policies, 298
- Agglomeration, 205
- Aging, 153
- Air, 202
- Albedo, 384
- Aluminum, 315
- Ambient temperature, 79, 143
- Ammonium hydroxide/chloride solution, 194
 - Use for: Muspratt solution
- Ampere-hour capacity, 121-2
 - integration, 351
 - hours, 181, 185
- Analog signals, 296, 396
- Anomalous cell behavior, 179
- Anomalous cell-voltage behavior, 46
- Antipolar material, 19
- Apparent reactance, 70
- Apparent resistance, 70
- Applications Technology Satellite 6 (ATS-6), 451
- Area loading, 106, 123 (def.), 124
 - RT: Plate loading
- Array
 - Use: Solar-cell array
- Assembly drawing, 8
- Asymptotic value of taper current, 336 (def.)
- Atmospheric Explorer C (AE-C), 448
- Automatic power systems, 327
- Atomic-absorption spectroscopy (AA), 194
 - BT: Measurement methods
- Autonomous power systems, 327
- Auxiliary devices, 8, 414-15, 420
- Auxiliary electrodes, 43, 138, 152, 348
 - NT: Oxygen signal electrode, Recombination electrode, Reference electrode
- Average charge efficiency, 92
 - BT: Charge efficiency
- Bag separators, 25
- Battery, 8 (def.)
 - assembly qualification, 435
 - cell dissipation, 389
 - cell failures, 299
 - cell thermal analysis, 311-12
 - characteristic curve, 295
 - charge bus, 296
 - charge controls, 259, 281-297, 300, 343, 364, 457

- charge current control, 296-7
- computer programs, 388
- configuration, 409, 410
- current, 132
- design, 239, 395, 411-413
- design review, 268
- development, 380, 411-413, 446
- discharge control, 281, 292, 298, 377
- engineer, 222 ff., 256, 395, 409, 416, 429, 443
- equipment specification, 414, 424 (def.)
- failure, 180 (def.), 416
- failure criteria, 180 (def.)
- harness, 260
- heater, 347
- installation, 437
- isolation diodes, 297, 377
- limited power system, 65
- logistics plan, 437, 443
- maintenance, 437
- manufacturing, 245, 426
- mass, 422
- measurements, 436
- model, 416
- performance analysis, 97
- procurement, 221, 239-40
- qualification, 262-3, 425, 434
- reliability, 157-8, 164, 402
- responses, 67
- sizing, 120, 276, 385, 392, 393
- specification, 222, 224, 240, 409
- standby operations, 440
- structure, 131
- system, 8 (def.), 96, 409
- system configuration, 227, 385-7
- system design, 275, 280
- system interfaces, 384
- system mass, 328
- system reliability, 280, 355, 387
- temperature, 186, 334, 337, 343, 347, 371-5
- testing, 243-5
- thermal-control system, 8 (def.), 276
- thermal environment, 394
- voltage limit (BVL), 337, 344, 372, 374
- voltage limit families, 339
- voltage sensing points
 - Use: Taps
- Beginning-of-charge voltage, 109, 187
- Beginning-of-discharge voltage, 116, 187
- Blisters, 195
- Boost-discharge regulator, 298-300
- Breakage, 200
- Brushing, 51
- Buck/boost charger, 295
- Buck discharge regulator, 298-300
- Bus ripple, 288
 - voltage, 294, 297, 346, 407
 - voltage regulation, 279, 296, 300, 370
- Butt-type geometry
 - Use: Interface geometry
- Bypass circuits, 405
- Cable mass, 382
- Cables, 382, 420
- Cadmium active material, 18, 38-9, 56, 108, 195
 - Use for: Negative active material
- Cadmium additives, 18
 - cadmium cell, 199
 - hydroxide, 195, 204
 - migration, 191, 203-5, 216-17
- Cady gage, 36
- Calendaring, 25 (def.)
- Can
 - Use: Cell case
- Capacitive reactance, 72
- Capacity, 11, 14, 33, 54, 66, 76-7, 94-99, 107-9, 120-26, 123-7, 128-30, 135, 141, 150-51, 160-68, 174, 187 (def.), 218, 250,

- 257, 263, 371, 395
BT: Performance characteristics
NT: Discharge capacity, Negative capacity, Rated capacity, Relative capacity, Specific capacity, Theoretical capacity, Thermal capacity.
 degradation, 41, 174-5, 353-5, 361
 loss, 188, 196, 198, 217
 matching, 259-61
 measurement, 131, 188, 193, 258-9
 ratios, 33, 38, 54, 107, 108, 111, 114, 128, 166, 216
 Use for: Negative-to-positive ratios requirements, 56
 retention, 102, 339
 verification test, 432
BT: Measurement methods
- Caps,** 28
- Carbonate,** 33, 56, 163, 193, 196, 204, 217
- Case wall**
 Use: Cell case
- Catalog-item sealed aerospace cells,** 34
- Caustic treatment,** 49-56
- Cd(OH)₂,** 10
- Cell,** 8
 acceptance, 239, 419
 acceptance failure, 247-8
 area, 57
 assembly, 55, 202
 bypass circuitry, 299
 capacity, 41, 53, 74, 129, 134, 138, 219, 300
 case, 25 (def.), 26-7, 44-6, 362
 case dimensions, 112
 case height, 58, 61
 case materials properties, 27
 case temperature, 66, 79, 80, 133, 303
 case thickness, 26, 27, 58, 61, 76
 case volume, 37, 58
 configuration, 42, 356
NT: Cylindrical cells
- Prismatic cells**
 construction, 361
 cover, 25 (def.), 26-31
 current, 121, 138, 181-5
 current voltage, 386
 -definition studies, 385
 degradation, 140, 176, 180 (def.), 239, 264, 271, 362, 379, 406
NT: Degradation/failure determinants, Degradation/failure mechanisms: Degradation/failure modes; Degradation models, Degradation rate
RT: Cell failure
 degradation analysis, 179
 degradation/failure mode, 182
 design, 12, 38, 46, 100-111, 122-3, 159, 176, 180, 209, 229, 235, 262, 361
 design audit, 224
 development testing, 417
 dimensions, 66, 76
 failure, 180 (def.), 181, 264, 379, 383, 405-6, 416
RT: Cell degradation
 failure analysis, 179, 198
 failure criteria, 180 (def.)
 failure mechanisms, 179
 failure rate, 152-155, 164, 175
 geometry, 33
 internal pressure, 66
 leakage, 42, 215, 362
 -level design verification, 434
 level protection 376 ff.
 lot acceptance, 256
 manufacturer's tests, 100
 manufacturing, 47, 54, 65, 80, 107, 113, 123-130, 150, 176, 180, 216, 245
 Use for: Manufacturing mass, 33, 58 ff., 126, 128
BT: Static properties
 matching, 258-62, 378
 model, 311, 392, 416

- parameter sensing, 363-9
- pressure, 42, 103, 108, 132, 135, 170, 181-187, 246, 250, 333, 346, 353, 362, 421
- procurement, 221-4, 418
- protection circuitry, 410
- rejection rates, 256
- qualification, 262-3, 419
- reliability, 153-160, 256, 264, 399, 402
- reversal, 356, 362, 368
- selection, 258, 416
- size, 33, 38, 392, 414
- specification, 224-5
- teardown analysis, 179
- temperature, 66-7, 86-95, 120, 132-9, 181-5, 279, 333, 374
- terminal voltage, 66, 103
- testing, 243, 245, 260
- venting, 39, 40, 56, 57
 - Use for: Flooded cells
- voltage, 79 ff., 240, 250, 262, 279, 299, 352, 357, 365, 393
 - BT: Voltage
 - NT: Active charge voltage, Over-charge voltage, Peak voltage
- voltage change, 67, 368
- voltage scanning, 369
- volume, 38, 63
- wall
 - Use: Cell case
- weight, 37, 73, 227
- Ceramic, 30
- Ceramic-to-metal braze bonds, 29
- Certificate of conformance, 230-33
- Charge, 168
 - NT: Pulse charge, Taper charge, Trickle charge
- acceptance, 88-93, 106, 126-7, 332
- behavior, 112, 261
- characteristics, 79, 106
- coefficient, 127 (def.)
- control, 80, 116, 131, 152, 295, 302, 329-336, 355-6, 370, 375, 386, 414, 418
 - NT: Constant current charging
 - Recharge-ratio control
 - Temperature-limited charging
 - Voltage-limited charging
- controller, 8, 300, 396
- current, 79-83, 90, 100, 235, 293, 332-3, 372, 391, 416
- cutoff, 351 (def.)
- efficiency, 32, 79, 91-97, 122, 167, 259-61, 371
 - NT: Average charge efficiency, Coulombic charge efficiency, Energy charge efficiency, Incremental charge efficiency
- level, 108 (def.)
- rate, 80 ff., 266, 272, 292, 333, 383, 384, 399
- regulator, 292, 402
- retention, 100-101, 255-263, 432
- temperature, 103
- throughput, 79, 96-98, 108, 170
- voltage, 46, 80-108, 134, 139, 170, 190-199, 231, 250, 366, 416
- Charge-voltage characteristic matching, 259, 364
- Charged-negative material, 40-41
 - NT: Active charged-negative material, Total charged-negative material
- Chemical analysis, 110
 - BT: Measurement methods
- degradation, 21
- impregnation
 - Use: Impregnation
- Circuit application procedures, 360
 - power consumption, 360
 - techniques, 369, 396
- Circular orbits, 277
- Cleanliness, 436
- Cobalt additives, 18-19, 107, 126-7,

- 161, 194
- Coining, 16-18, 48-52, 125
- Collars, 28
- Collector resistor, 288
- Collector-to-emitter short circuit, 288
- Combs, 28-31
- Communications satellites, 171
- Comparator, 281-2
- Component-mass properties, 387
- Compressed-polymer bonds, 29
- Compression geometry
 - Use: Interface geometry
- Computer programs, 46
- Conceptual design, 410-15
- Conduction path, 322
- Conductive element, 305
- Conductor, 382
- Configured-item identification number, 8
- Connector bonding resistance test, 431
 - BT: Measurement methods
- Constant-current charging, 88, 135-7, 170, 188, 332-6, 341
 - Use for: Current-limited charging
 - Constant-current charge control
 - BT: Charge control
 - discharge, 121, 259
 - electrical input, 281
 - loads, 278
- Constant discharge tests, 174
 - BT: Measurement methods
- Constant power, 259, 390
 - discharge, 142, 182
 - electrical input, 282
 - power loads, 278, 393
- Constant resistance, 259
 - loads, 278, 393
- Constraints analysis, 414
- Construction materials and requirements, 227
- Contact joints, 305
- Contact life, 360
- Continuous cycling, 131 (def.), 134, 153, 186
- Contract Data Requirements List, 232
- Contraction, 184
- Control-circuit losses, 283
- Control electrode
 - Use: Oxygen signal electrode
 - transistor, 286-8
- Conversion factor, 10
- Converter circuits, 289
- Converter/regulator, 280, 378-9, 389
- Cooling, 309
- Copper-silver alloy, 29
- Corrosion, 26, 184, 202
- Cost, 409, 414
- Coulombic charge efficiency, 12, 91-2
 - BT: Charge efficiency
- Cover assembly
 - Use: Cell Cover
 - plate flexing, 28
- Critical assemblies, 221
- Crystal growth, 205
- Crystal structure, 193
- Cumulative distribution function, 398
- Cup, 29-30
- Current, 284, 393
 - density, 108, 123, 208
 - imbalances, 379
 - limit, 351
 - limited charging
 - Use: Constant-current charging
 - limiting device, 288
 - reduction, 170
 - sensing, 396
 - sensing resistor, 297
 - sharing, 368-379
 - taper, 139, 170
- Cutoff voltage, 114-15
- Cycle life, 12, 15, 36-8, 127, 139-40, 152-63, 218, 355
 - period, 399
- Cycles to failure, 270
- Cycling, 16-20, 32-6, 50, 57, 64, 87,

- 109, 114-29, 135, 139-52,
165-206, 258
Cylindrical cells, 42-3, 73-7, 136, 153
BT: Cell configuration
- Data weighting factors, 261
Decarbonation, 33, 107, 115
Decomposition, 125
Defense Contract Administration Service, 224
 Meteorological Satellite Program (DMSP), 452
 Satellite Communications System, 266
Definition studies, 380
 NT: Battery-system thermal and mechanical interfaces; Load bus voltage level and regulation studies; Load power-profile analysis; Power-source regulation definition
Degradation/failure determinants, 111, 183 ff.
 BT: Cell degradation mechanisms, 184 (def.), 185-209, 216, 219
 Use for: Failure mechanisms
 BT: Cell degradation modes, 186-91, 353
 BT: Cell degradation
Degradation models, 209-15
 BT: Cell degradation rate, 191
 BT: Cell degradation
Deliverables list, 225
Delivery schedules, 232
Density, 76, 304
 function, 401
Deposits, 195
Depth of discharge, 43, 69, 77, 86-7, 116-17, 131 ff., 198, 216-19, 250 ff., 299-302, 326 ff.
Derating, 377
Design lifetime, 291
 methodology, 276
 package, 233
 requirements, 227
 reviews, 425, 427
 variation, 66, 76
Destructive testing, 258
Detail specification 226 (def.)
Device selection, 396
Dewetting, 203
Diffusion, 184
Digital shunt regulator, 288
Dimensional stability, 21
Diode junctions, 359
Direct discharge method, 370
 Energy Transfer (DET) Systems
 Use: Shunt-regulated electric power system
 -reading milliohmmeters, 255
Discharge, 68-70, 80, 100, 113-17, 182, 206-8
 bypass diode, 359
 capacity, 96-7, 108, 119, 127, 129
 BT: Capacity /charge cycle profile, 326
 conditions, 92
 control, 370
 current, 11, 79, 116-19, 218, 235, 370-6, 391-4, 416
 diode dissipation, 359
 energy, 121
 output, 79
 paths, 375-6
 rate, 116, 117, 119, 120, 123, 127, 128, 142, 196, 218, 219, 270, 271, 272, 399
 ratio, 97
 regulator, 8, 382, 402
 time, 218-19
 voltage, 46, 115-16, 121-9, 141-9, 160 ff., 202, 231, 250, 366, 376-7, 394, 416
 voltage characteristic matching, 259-60

- Dischargeable energy content, 66
- Discrete devices, 276
- Dissipative series regulator, 278
- Dormancy, 153
- Double-insulated cell, 42, 46
- Drawing tree, 253 (def.)
- Duty cycle, 402, 420

- Earth orbiters
 - Use: Orbiting spacecraft
- Earth synchronous applications, 78
- Eccentric orbit applications, 153
- Eclipse period, 141, 276-8, 294-8, 326, 416
- Eclipse seasons, 131, 169-77, 265-8, 365-7
- Effective inductance, 72
- Efficiency, 282
- Electric power system, 67, 78, 239, 414
 - classification, 289
 - modeling, 388, 391
 - regulation, 280
- Electrical continuity test, 431
 - BT: Measurement methods degradation/failure mode, 187
 - design requirements, 409, 415
 - insulation resistance test, 431
 - BT: Measurement methods interface characteristics, 279
 - performance analyses, 415
 - schematic diagram, 414, 420
 - testing, 179, 420
- Electroactive surface area, 208
- Electrochemical cleaning, 50 (def.), 130
 - efficiency, 122
 - impregnation, 49-53, 64, 127-9, 176, 216
 - BT: Impregnation shorting path, 199 (def.)
 - testing, 53-4, 114, 130
 - Use for: Flooded formation cycling, Measurement methods
- Electrochemically measured negative-to-positive ratio
 - Use: Measured capacity ratio
- Electrode area, 43-5
 - potential, 11, 88-9, 106-8, 183, 209
 - reactions, 9 ff.
- Electrodes, 201, 302
- Electrolyte, 27 ff., 56 ff., 107 ff., 126-9, 161-6, 184, 192-209, 227, 233
 - distribution, 78, 90-91, 109-12, 152, 194-203, 216, 250, 349
 - leak test, 257, 263
 - retention, 24, 165
 - viscosity, 203
- Electronic auxiliaries, 395
 - design, 410
 - shorting, 199-204
 - Use for: Metal-to-metal shorting, Plate-to-plate shorting
- Elemental cadmium, 110
- EMF, 103
- Emittance, 322
- End-of-charge current, 90, 139, 170, 190
 - impedance, 171
 - pressure, 37, 107, 115
 - voltage, 107-15, 134-7, 167-71, 182-91, 272, 417
- End-of-discharge current, 342, 371
 - pressure, 342
 - voltage, 110-120, 141-9, 163 ff., 217-18, 270-71, 341, 368
- End-of-life solstice, 293
- End voltage, 115, 150
- Energy, 12, 66, 76, 123
 - BT: Performance characteristics balance, 332, 370, 380, 390-92
 - charge efficiency, 91-2
 - BT: Charge efficiency content, 121
 - conversion, 65
 - BT: Performance characteristics density
 - Use: Specific energy

- output, 126, 259
 - storage system, 8
- Enthalpy, 104
- Entropy, 103
- Environmental acceptance test, 433
 - BT: Measurement methods
- Environmental conditions, 199, 230, 326-8, 391
- Equinox season, 294-5, 380
- Excess cadmium
 - Use: Excess negative
 - negative, 39, 41, 56-7, 108-15, 128-29, 139, 150, 166-70, 208, 250
 - Use for: Excess cadmium
 - polarization
 - Use: Fading
- Expansion, 184
- Exponential distribution, 400-404
- External finish, 227
- External heat input, 276, 347

- Fabricated case
 - Use: Welded cell case
- Fading, 19, 128, 129, 139, 198, 208, 258
 - Use for: Excess polarization
- Failure analysis. 186, 192 (def.), 201, 207, 271
 - frequency. 186
 - mechanisms. 1
 - Use: Degradation/failure mechanism
 - mode. 181 (def.)
 - Modes and Effects Analysis (FMEA). 397
 - pathology. 361
 - rate. 154-60, 399, 406
- Faraday constant, 103
- Fault isolation 285, 383
- FED-STD-209B. 436
- FED STD PPP-B-566. 443
- FED STD PPP-B-636. 443
- Fiber density. 25
- Filament bonding. 25

- Fill tube, 26-7
- Final design, 414
- Final discharge voltage, 146
- Fixed resistor, 286
- Flanges, 28, 31
- Fleet Satellite Communications (FLTSATCOM) system, 334, 343-4, 452
- Flight altitude, 276
- Flight data, 267
- Flooded capacity, 54, 126, 130
 - cells
 - Use: Cell venting, Vented cells formation cycling
 - Use: Electrochemical testing
- Fluid-loop cold-plate design, 303
- Forcing functions, 307, 345
- Formation process, 33, 48-54, 114, 130, 150, 202
- Fourier equation, 304
- Frequency, 69-71
- Full-cell electrode
 - Use: recombination electrode

- Full charge current, 339
- Full linear dissipative shunt regulator, 283-7, 296-7

- Gas analysis. 192
 - evolution. 117, 137, 362
 - NT: Hydrogen gas, Oxygen gas sampling. 192
- General specifications, 226 (def.), 236
- Geosynchronous orbit applications, 153, 176, 188, 256, 258-9, 261, 264-6, 268, 271, 292, 301, 326, 331-3, 341, 346, 351, 356-7, 369-70, 376, 380, 384, 392, 418
- Germanium devices, 360
- Glass. 31
- Gompertz model, 402
- Graphical analyses, 388-9
- Grid. 13

- expansion, 216
 - preparation, 47-8
 - Use for: Substrate preparation
 - Ground mode, 434

 - Harness-resistance ratio, 375
 - Harnesses, 382, 420
 - Hazard function, 152, 398-402
 - Hazard rate, 153, 175
 - Heat, 12, 24, 32, 36, 41-2, 343
 - conduction equation, 303
 - conduction paths, 305
 - flow
 - Use: Thermal conductivity
 - flux densities, 319
 - generation, 66, 72, 95-6, 102-6, 118-19, 303, 311, 380-86, 391, 396, 414-18
 - RT: Performance characteristics, Thermophysical properties
 - generation measurement, 273
 - pipe, 316-19
 - rate, 79, 104, 119
 - rejection surfaces, 416, 423
 - sink, 12, 131, 133, 231, 303, 305, 309, 312, 319
 - source, 305, 319
 - sterilization, 165
 - transfer, 303, 312, 320, 410, 421
 - Heater-circuit operation test, 432
 - BT: Measurement methods
 - Hemispherical emittance, 312
 - High altitude applications, 78-80, 134, 153, 169, 176, 266, 396
 - Use for: Long cycle applications
 - charge voltage, 200, 215
 - Energy Astronomical Observatory, 337
 - frequencies, 70
 - power applications, 288, 301
 - rate dc discharge current, 255
 - rate operation, 15, 34, 128
 - reliability designs, 116
 - resistance connector contacts, 186
 - voltage batteries, 381-2
 - voltage load, 381
 - voltage on charge, 190
- Hot spots, 14
- Hydrogen burst phenomena, 440
- gas, 11, 39, 41, 45, 88-90, 108-11, 118-19, 152, 333, 348, 361-2, 383-4
 - BT: Gas evolution
 - pressure, 39, 111
 - recombination, 117-18, 362
- Hydrolysis, 184
- Hydrophilic side-chains, 25
- Hysteresis effects, 337, 348, 396
-
- I-V characteristics, 335, 371, 388-9
- Illumination, 279, 290, 301, 389, 391
- Impedance, 66-72, 77-8, 89, 140, 170, 180, 190, 198, 218, 255, 376
 - BT: Static properties
- Impregnation, 16-19, 33, 48-54, 114, 123-4, 126, 129-30, 176, 201, 216
 - RT: Electrochemical impregnation
- Improved TIROS Operation System (ITOS-D), 447
- Impurities, 29, 50, 54, 92
- In-cycle capacity, 187-8
- Incremental charge efficiency, 90, 92, 96-99, 103, 120-21
 - BT: Charge efficiency
 - Use for: Instantaneous charge efficiency
- Incremental coulombic efficiency, 96
 - Use for: Instantaneous coulombic efficiency
- Indium, 128
- Inert gasses, 203
- Initial discharge characteristics, 115, 122, 128
- Input filter, 282
- Input voltage, 282, 299

- Insertion loss, 297, 393, 396
 Instantaneous charge efficiency
 Use: Incremental charge efficiency
 Instantaneous coulombic efficiency
 Use: Incremental coulombic efficiency
 Instantaneous failure rate
 Use: Hazard rate
 Instrument calibration, 436
 Insulated terminals, 41
 Insulation resistance, 41
 Insulator seals, 28-9, 41
 Integrated circuits, 276
 Integrity, 12
 Intelsat, 378, 439
 Interelectrode ohmic resistance, 183
 Interface compatibility, 262, 414
 Interface geometry, 29, 32
 Use for: Butt-type geometry,
 Compression geometry
 Intermediate altitude applications, 153
 Internal shorting, 101, 204, 255, 258
 Interplanetary probes and orbiters, 78,
 176, 301, 327, 351
 Interplanetary trajectory, 276, 326,
 414
 Use for: Trajectory
 Inverter circuits, 289
 Ionic solids, 184
 IR drop, 184, 197, 201, 209
 Iron, 194
 Isolation diode, 376, 402
- Kapton, 315
 Kirchhoff's current and voltage laws,
 307
 KOH
 Use: Potassium hydroxide
 Kovar, 28
- Laplace equation, 304
 transform methods, 307
 Last-cycle capacity, 165
- Launch/ascent timeline, 381
 mode, 434
 trajectory, 414
 vibrations, 12
 Life-cycle tests, 203, 343
 Life expectancy, 135, 152 (def.)
 requirements, 36, 231, 258
 testing, 64, 176, 229, 262-8
 BT: Measurement methods
 Lightweight batteries, 455-6
 cells, 62-4, 455
 Limited-voltage (LV) dc-bus system,
 289, 295
 Use for: LV dc-bus system
 Limiting function, 335
 Linear control element, 281
 voltage regulator, 286
 Lithium hydroxide, 32
 LiOH
 Use: Lithium hydroxide
 Load bus, 296
 -bus voltage, 292-7, 381, 394
 -bus voltage level and regulation
 studies, 381
 BT: Definition studies
 growth, 300
 power-profile analysis, 380
 BT: Definition studies
 power-time profiles, 380
 -sharing, 372-74, 406
 transients, 298
 Loading, 19 (def.), 108, 123-5, 393
 RT: Plate loading
 level, 19, 109, 126, 130, 202
 Manufacturers' Specifications, 20
 Long-cycle testing, 174
 mission life applications, 45, 111,
 202, 235, 257, 260, 376
 -term characteristics, 65-6, 159
 -term effects, 111, 198
 -term performance, 126, 134, 167,
 229, 302
 Low Earth-orbit applications, 78,

- 134-7, 147-59, 168, 175, 190, 218, 259, 301, 330, 337-9, 341, 349, 351, 355, 363, 370, 396, 416, 418
- Earth-orbit life test, 139-52, 166-9, 196, 205, 265
- frequencies, 67, 70
- impedance output bus, 281
- impedance source, 298
- pressure operation, 110
- rate charge acceptance, 261
- rate discharge, 207
- temperatures, 88, 104, 108-11, 117, 128, 141-2, 150, 171, 260, 357, 417
- voltage batteries, 381-2
- voltage on charge, 188-9
- Lower resistive element, 286
- Lunar Orbiters
 - Use: Orbiting spacecraft
- LV dc-bus System
 - Use: Limited-voltage (LV) dc-bus system
- Magnetic amplifier, 396
 - cleanliness, 326
- Main power terminal conductors, 28-9
- Make-or-buy decision, 241
- Manual power systems, 327
- Manufacturer's quality control program, 236
 - rating, 79, 116
- Manufacturing
 - Use: Cell manufacturing
 - Control Document
 - Use: MCD
 - methods, 422
 - process data, 258
- Markov reliability model, 406
 - transition rate, 354
- Mars orbiters
 - Use: Orbiting spacecraft
- Mass transfer, 65
 - BT: Performance characteristics
- Master production schedule, 233
- Material ratio
 - Use: Theoretical capacity ratio
- Materials selection, 421
- Maximum power point, 298
 - power point-tracking (MPT) system, 289, 301
 - Use for: MPT system, Point-tracking system
- MCD, 225, 232-7, 243-6, 414-19
 - Use for: Manufacturing Control Document
- Mean failure rate, 399
 - time to failure, 216, 399
- Measured capacity ratio, 38-9, 187
 - Use for: Electrochemically measured negative-to-positive ratio
- Measurement methods, 67, 74
 - NT: Accelerated-time tests, Acceptance tests, Atomic-absorption spectroscopy, Capacity verification test, Charge retention, Chemical analysis, Connector bonding resistance test, Constant discharge tests, Electrical continuity test, Electrical insulation resistance test, Electrochemical testing, Environmental acceptance tests, Heater-circuit operation test, Life-testing, Mercury intrusion, Nonoperating bench tests, Peak loads, Qualification tests, Real-time tests, Reference electrodes, Seal leakage test, Temperature sensor operation test, Thermostatic switch operation test, Variable discharge tests, Voltage recovery test
- Mechanical design, 421
 - design requirements, 409
 - performance, 387
 - strength, 28, 193
- Mercury intrusion, 16, 124-5

- Use for: Measurement methods
- mercuric oxide electrode, 46
- Metal substrate
 - Use: Plaque
 - to-metal shorting
 - Use: Electronic shorting
- Metallic cadmium, 204
- Mid-charge voltage, 187, 189
- Mid-discharge characteristics, 142-6, 165, 187
- Migration, 195-6, 216
- MIL-C-45662A, 436
- Mild steel, 47
- Minimum temperature conditions, 286
- Mirrors, 315
- Mission length, 352
 - requirements, 326, 394-5
- Modeling, 74, 75, 395-402
- Modulator, 282
- Monte Carlo simulation, 406
- Motors, 276
- Mounting, 414, 421
- MPT system
 - Use: Maximum-power point-tracking system
- Multimission Modular Spacecraft, 374
- Multiple-battery configurations, 297
- Muspratt solution
 - Use: Ammonium hydroxide/chloride solution
- NASA/GSFC Specification 74-15000, 248, 256, 418-19
- NASA/GSFC Specification S-711-16, 262
- NATO-III battery, 456
- Negative active material
 - Use: Cadmium active material capacity, 110, 218, 258
 - BT: Capacity electrode, 39-40, 54-6, 90, 128, 139, 183, 197-213, 250
 - limited cell, 118
 - overtoltage, 108
 - plates, 108, 128, 142, 163, 194
 - terminal, 44
 - to-positive ratios
 - Use: Capacity ratios
- Net-energy conversion, 65
- Network equations, 389, 391
- Nickel, 73
 - active material, 9, 18-19, 38-9, 79, 126, 193, 202
 - braze material, 29
 - cell cases, 26-7
 - hydroxide, 10, 128
 - powder, 48, 51-2, 123, 125, 130
 - substrate, 47, 51-2
- NiOOH, 9 ff.
- Nitrate, 192-3, 217
- Nitrogen gas, 57, 202
- Noncondensable gas, 319-20
- Noncyclic conditions, 186
- Nonhardware items, 232
- Nonnormal environmental conditions, 228
- Nonoperating bench tests, 261
 - BT: Measurement methods
- Nonwoven separators, 67, 165
- Normal environment requirements, 228
- Normalized current, 79 (def.), 86, 88
- Nylon, 73, 107, 112
 - hydrolysis, 205-6, 216
 - separators, 67, 76-7, 112, 129, 155, 163-5, 198, 203, 206
 - NT: Pellon separators
- Off-pointing requirements, 338
- Off-time/on-time ratio, 282
- Ohmic conduction, 354
- Ohmic resistance, 43, 67
- One-at-a-time cycles, 78 (def.), 80
- One-dimensional cell model, 311
- Open circuit, 100-101, 180, 191 (def.), 200-201, 299, 353-7, 405
 - circuit cell voltage, 104-5, 255, 270

- circuit failure, 43, 359
- circuit potential, 10
- Operating conditions, 66, 141, 180-81
 - 187, 191, 216
 - Use for: Use conditions mode, 352
 - temperature, 111, 126-7, 131, 135, 141-2, 149, 150, 174, 216-17, 259-60, 326, 332, 358, 402
 - time, 186
- Operational requirements, 327
- Optimization techniques, 276
- Orbit-average solar input, 312
 - characteristics, 276, 291, 326, 414
 - period, 278
- Orbital mode, 434
- Orbiting Astronomical Observatory, 348, 376
 - Astronomical Satellite, 260
 - Solar Observatory I (OSO-I), 450
 - spacecraft, 12
 - Use for: Earth orbiters, Lunar orbiters, Mars orbiters
- Out-of-cycle behavior, 186
- Out-of-cycle capacity, 188
- Outline drawings, 420
- Output energy, 122
- Output filter, 282
- Overcharge, 10-12, 36-41, 68, 79-80, 86, 91-5, 102, 110, 127-34, 168, 182, 201-8, 257, 302, 332-6, 343, 347, 359-60, 374-5, 396, 405
 - current, 90, 349
 - pressure, 21, 37, 41, 57, 90-91, 108-14, 164, 349, 417
 - protection, 41, 90, 152, 166, 205-8, 216, 250, 329, 363, 439
 - rate, 89
 - voltage, 88-9, 106, 111, 114, 250, 261, 417, 439
 - BT: Cell voltage
- Overdischarge, 11, 37, 39, 118-19, 199, 299, 352, 357, 360-62, 368, 405
 - current, 361
 - voltage, 117
- Overtemperature protection, 347
- Overvoltage, 352, 357, 364
- Oxidation, 184, 206
- Oxygen gas, 45, 57, 90, 100, 108, 118-19, 202, 206, 208, 333, 345, 348, 362, 365
 - BT: Gas evolution
 - overvoltage, 365
 - permeability, 36
 - pressure, 11, 39, 43, 90-91, 109, 152, 332
 - recombination, 11 (def.), 117, 333
 - recombination rate, 21, 208
 - signal electrode, 43-5, 112, 131-2, 152
 - BT: Auxiliary electrodes
 - Use for: Control electrode, Adsorbed hydrogen electrode, Adhydrode electrode
 - transfer reaction, 105
 - venting, 129
- Packaging, 42, 409-10, 414, 420, 443
- Paint, 315
- Paralleled multiple battery systems, 260
- Parallel battery operation, 371-6
- Parametric testing, 272
- Partial linear dissipative shunt regulator, 283, 286-8, 297
- Passive bilateral element, 290
- Passive thermal properties, 72
- Payload duty cycles, 380
- Payload power profile, 381
- Peak loads, 326, 433
 - BT: Measurement methods
- Pellon separators, 22, 24, 35, 76
 - BT: Nylon separators
- Performance analysis, 65-7, 78
 - characteristics, 65, 78, 414

- NT: Capacity, Energy, Energy conversion, Heat generation.
 Mass transfer, State of charge
 degradation, 168
 goals, 229
 requirements, 227-31
 tests, 248, 259
 Phase angle, 70-72
 Pinch tube, 27
 Plaque, 14-17, 33, 49, 51, 107, 123-5, 128, 130
 RT: Void fraction
 Plate area, 17, 19, 33-4, 38, 67, 77-80, 102, 109, 125, 193, 205, 216, 439
 buckling, 14
 capacity, 16, 53, 128
 design, 209, 235
 deterioration, 191
 edges, 17, 49
 loading, 80, 106-7, 125, 127, 161, 163-4, 216
 RT: Area loading, Volumetric loading
 manufacturing, 47
 materials, 114
 separation distance, 35, 37, 107, 111-12, 227
 Use for: Separation distance
 storage, 51
 -surface resistance, 208
 tabs, 14, 42, 56
 temperature, 312
 thickness, 130, 146, 193, 196, 227
 -to-plate shorting
 Use: Electronic shorting
 treatments, 20 (def.)
 volume, 37, 124
 weight, 14, 125, 193
 Plates, 12-15, 51, 56, 76, 78, 90, 112, 130, 193, 229
 RT: Void Fraction
 NT: Negative Plates, Positive plates
 Platinum, 45
 Point-tracking system
 Use: Maximum-power point-tracking system
 Poisson equation, 304
 Polar orbit applications, 266
 Polar side chains, 165
 Polarization, 51, 53, 183 (def.), 197-8, 201, 207-8
 Polarization loss, 34
 Polymer decomposition, 24
 Polymeric sealant, 29
 Polypropylene, 77-8, 107, 112, 129, 161
 Polypropylene separators, 163, 165-6, 198, 203, 216
 Pore blockage, 15, 204-5, 216
 fill fraction, 125 (def.), 126
 flooding, 196
 size, 16, 80, 123-5, 128
 volume, 33, 35, 108
 Porosity
 Use: Void fraction
 Positive active material
 Use: Nickel-active material
 capacity, 110-11, 129
 BT: Capacity
 electrode, 39, 54, 56, 90, 100, 124-6, 183, 197, 201, 205-10, 218
 -electrode voltage fading, 19
 -limited cell, 11 (def.), 86, 118-19, 128
 plate expansion, 201, 203
 plate swelling, 250
 plates, 14, 50, 64, 79, 108, 123-4, 126, 142, 150
 BT: Plates
 Post
 Use: Terminal conductors
 source conversion equipment, 383
 Potassium hydroxide, 32-3, 46, 73, 192, 205
 Use for: KOH
 Potential, 46, 306

- Power-bus voltage, 295, 371, 383
 - conversion equipment, 290
 - converter, 288
 - dissipation, 45, 321
 - distribution cabling, 371
 - inversion equipment, 288, 290
 - loss, 288, 382
 - regulator unit system, 296
 - source mass, 382
 - source regulation definition, 383
 - BT: Definition studies
 - switches, 402
 - system, 150, 291, 328, 380, 409, 415
 - systems engineer, 222, 224, 385
 - to-mass ratio, 321
 - transfer, 298
 - transistor, 298
 - voltage characteristic curves, 293
 - Preacceptance manufacturing tests, 246
 - Precharge, 33, 39-41 (def.), 56-7, 107-11, 128-9, 162, 166-7, 227, 258
 - Precipitation, 184
 - Prelaunch storage lifetimes, 258
 - testing, 111
 - Preliminary design, 414
 - power-system configurations, 380
 - Preload conversion equipment, 383
 - Preregulation requirements, 298
 - Pressure, 12, 27, 57, 103, 112, 117-18, 131-4, 137, 166, 191, 195, 216, 332, 352, 361, 409
 - limited charging, 348
 - transducer, 152, 177, 348
 - Primary power bus, 298, 300, 346, 370, 380
 - Prismatic cells, 42, 62, 67, 73-4, 136, 153, 161, 348
 - BT: Cell configuration
 - Probability density function, 398
 - Process Identification Document, 234
 - Procurement personnel, 225
 - sequence, 222
 - specification, 246
 - Production, 233, 237-8
 - Project engineering, 224-5
 - Proposal evaluation, 231
 - Pulse charge, 207
 - BT: Charge
 - Purchase orders, 222
 - Purchasing agent, 230
 - Pyrotechnic devices, 381
 - Qualification tests, 228-30, 239, 245, 261-2
 - BT: Measurement methods
 - "Quality" (Qv), 270 (def.)
 - assurance, 225, 229, 429
 - control, 29, 228-9, 236-7, 256
 - Recharge-ratio control, 351, 371
 - BT: Charge control
 - Recharging, 93
 - Recombination, 109
 - electrode, 43-5
 - BT: Auxiliary electrodes
 - Use for: Full-cell electrode rate, 108
 - Reconditioning, 65, 78, 134, 168-9, 176 (def.), 180, 181, 207, 268, 271, 356-8, 367, 386, 402
 - Reduction, 184
 - Redundancy, 355, 357, 370-71, 376, 387, 404-6, 414
 - Reference capacity
 - Use: Rated capacity
 - circuits, 363
 - design cells, 58-80, 115, 122, 126, 134, 141-2, 166, 169
 - design data, 58 (def.), 74-5
 - electrodes, 43, 46, 198
 - BT: Measurement methods
- Regenerative action, 209
- Regulated bus voltage, 298

- Regulated-voltage (RV) dc-bus system.
 289, 297-8
 Use for: RV dc-bus system
 Regulator efficiency, 299
 Relative capacity, 120
 BT: Capacity
 Relay closure, 294
 contact ratings, 360
 protection, 360
 Reliability block diagrams, 403
 function, 398-401
 goals
 Use: System reliability
 Request for Proposal, 222-31
 Requirements analysis, 414
 section, 228
 Resistance, 14, 35-6, 45, 67, 198-204,
 214-16, 255, 263, 281, 286,
 306, 376
 Resistivity, 15, 27, 32
 Rest, 167
 Reversal, 19, 117-18
 Reversal voltage, 361
 Reverse leakage currents, 360
 Runaway condition, 334
 RV dc-bus system
 Use: Regulated-voltage (RV)
 dc-bus system

 Safety margins, 434
 Sampling instructions, 230
 Saturated voltage drop, 281
 Scaling, 79
 Seal failure, 28, 155
 leakage test, 432
 BT: Measurement methods
 Sealed cells, 115, 123-30, 198
 Use for: Starved cells
 Self-discharge, 95, 101
 Semiautomatic power systems, 327
 Semiconductor switch, 282
 Separation distance
 Use: Plate separation distance
 Separator compression, 36, 44, 56
 degradation, 110, 191, 195-6,
 205, 217, 439
 design, 21, 78, 129
 drying, 36, 191, 202
 forms, 25
 materials characteristics, 21-4,
 36-7, 45, 77, 229
 oxidation, 205
 redistribution, 36
 structure, 25
 Separators, 26, 35, 56, 64, 69, 76, 78,
 183, 194, 197, 199-201, 209, 213
 Sequentially controlled full linear
 dissipative shunt regulator, 283,
 285, 297
 Sequentially controlled partial linear
 dissipative shunt regulator, 283,
 297
 Series cells, 300
 Series dissipative regulator, 281
 Use for: Active filter
 Series switching regulator, 282, 288,
 296, 298, 301
 Service history, 279, 352, 361
 life, 256, 258, 262, 265, 268,
 398, 409
 Shelf life, 429
 Shipping conditions, 239
 Shock environments, 12, 21, 262, 419
 Short-circuits, 299, 335, 353-4, 368
 Short-cycle applications, 78, 90, 134,
 141, 152, 155, 167-8, 188
 -cycle testing, 136, 141, 198
 Short orbit operation, 80, 152, 176,
 374
 Shorted failure mode, 199
 Shorting paths, 199
 Shorts, 14, 21, 35, 42, 44, 56, 93,
 101, 109, 118, 140, 155, 166,
 175, 180, 190 (def.), 201, 205,
 214, 218
 Shottky-barrier power rectifiers, 360

- Shunt-regulated electric power system, 300
 - Use for: Direct Energy Transfer (DET) Systems
- Shunt regulator/limiters, 283, 301, 346, 381
- Shunt transistor, 361, 363
- Shunting resistance, 70
- Signal behavior, 152
 - electrode
 - Use: Oxygen-signal electrode performance, 45
 - sensitivity, 152
 - voltage, 112
- Silver, 194, 199
 - cadmium cells, 129
 - treatment, 20, 162-5
- Simplified equivalent circuit, 70, 72
- Sine-wave ac current, 255
- Single-insulated cell, 41-2
- Single-orbit profile, 380
- Single-pole double-throw (SPDT) relay, 360
- Single-pole double-throw normally open relay, 360
- Sinter, 14-19, 48 (def.), 50-52, 108, 114, 125, 130, 194, 196, 202
- Sintered-nickel substrate, 32, 50
- Sintered plate, 13, 209
- Sintering process, 125
- Sizing, 125 (def.), 355, 414, 421
- Skylab Airlock Module, 352
- Slurry viscosity, 48, 125
- Small Astronomy Satellite C (SAS-C), 449
- Solar absorptance, 312
- Solar-array/battery load sharing, 332
 - cell array area, 302, 380
 - cell array power, 292, 294
 - cell array regulation, 280
 - cell array tap point, 286
 - cell array temperature, 295
 - cell array voltage, 294
 - constant, 321
 - pressure torques, 302
- Solder joints, 186
- Solder lug, 26-31
- Solid-state thermal switches, 396
- Solstice season, 380
- Source impedance, 286
 - inspection, 224-5, 237-8
 - load matching, 280, 302
- Space radiator thermal modeling, 312
- Spacecraft characteristics, 291, 414
 - electrical loads, 259, 276, 278
 - integration, 438-9
 - interface qualification, 435
 - load characteristics, 295, 415
 - logistics plan, 443
 - power systems, 121, 414
 - stabilization, 291, 414
 - thermal balance, 293
 - thermal system design analyses, 415
- Special tests, 245, 246, 258, 263
- Specific capacity, 121-2, 128, 130
 - BT: Capacity
 - energy, 16, 17, 34, 46, 62, 64, 76, 111, 121-3, 127, 130
 - Use for: Energy density
 - gravity, 73
 - heat, 73, 78, 304
 - mechanism, 184 (def.)
- Specification performance requirements, 250
 - sheets, 226 (def.)
- Specifications, 396
- Specimen contract, 225
- Split bus electric power systems, 378
- Sponge type plates, 129
- SSTS
 - Use: Solid-state thermal switches
- Stabilization cycling, 250
- Stainless steel, 73, 315
- Stainless steel cell cases, 26-7
- Stainless steel combs, 28
- Stand periods, 101
- Standard capacity
 - Use: Rated capacity
- Standard specifications, 226 (def.)
- Starved cells

- Use: Sealed cells
- State of charge, 39, 57, 66-7, 74, 79-80, 93, 96-104, 120, 134-5, 139, 168, 197, 260, 279, 335-6, 351, 371-2, 378, 383, 388-9, 391, 416
- BT: Performance characteristics
- Statement of work, 225
- Static properties, 65
 - NT: Cell dimensions, Cell mass, Cell temperature, Impedance, Thermal capacity, Thermal conductivity
- Steady-state charge rate, 112
 - current, 90
 - operating temperatures, 279
 - overcharge voltage, 86
 - temperature conditions, 286
- Stephan-Boltzmann constant, 312, 321
- Sterilizable battery, 446
- Storage, 203, 206, 326, 420, 437, 439
- Strain gage, 348
- Stress, 141, 266, 270
- Stress-relief member, 30
- Structural analyses, 422
- Stud
 - Use: Terminal conductor
- Subcontract arrangements, 222
- Substrate, 216
- Substrate preparation
 - Use: Grid preparation
- Sunlit periods, 276-7, 298, 326, 416
- Supplier, 230
- Surface buildup, 15
- Surface emittance, 322
- Surfactants, 25
- Swelling, 14, 16-17, 32, 50
- Switching shunt regulator, 283
- Synchronous Meteorological Satellite (SMS), 446
 - orbit applications, 77, 111, 131, 169-76, 205
 - orbit tests, 198, 266
- System design constraints, 328
 - reliability, 262, 297, 326, 370, 394-407, 414-16
 - Use for: Reliability goals
 - reliability measures, 398
 - requirements, 327
 - stability, 390
- Synthesis procedures, 276
- Tabs
 - Use: Plate tabs
- Taper charge, 80, 336
 - current, 372
- Taps, 368, 383
 - Use for: Battery-voltage sensing points
- Teardown analysis, 192 (def.), 195-6, 216, 231, 258
- Teflon, 43
 - fibers, 24
- Teflonation, 20, 37, 56, 107, 108, 112, 128, 161-4, 176, 203, 216
- Temperature, 38, 80-81, 85, 88, 91, 93-4, 96-7, 100, 103-5, 108, 110, 112, 116, 127, 133, 136-7, 140, 146, 148, 151, 153-4, 164, 167, 170, 172, 174, 191, 196, 198, 203, 205-6, 217, 260-61, 265-6, 268, 270, 272, 279-80, 290, 301, 335-6, 338-9, 349, 351-2, 356, 360-61, 370-72, 383, 388-9, 391-2, 399, 414, 416
 - compensated battery voltage limits (BVL), 293, 297, 334, 341, 343, 359, 363, 396
 - control, 280, 302, 332
 - distribution, 304
 - gradients, 75, 305
 - limited charging, 343-6
 - BT: Charge control
 - response equation, 309
 - sensitive controls, 329
 - sensor, 345

- sensor operation test, 432
 - BT: Measurement methods
- transient, 343, 345
- Terminal conductors, 28-31, 76, 155
 - Use for: Post, Stud
- seal, 26-9, 30, 32, 229, 337, 362
- voltage, 240, 299, 359, 368
- Terminals, 200
- Terrestrial applications, 457
- Testing, 55, 67, 230, 236, 250, 259, 266, 272, 435, 437
- Theoretical capacity, 108
 - BT: Capacity
- capacity ratio, 38-9
 - Use for: Material ratio
- Thermal analyses, 422
 - capacitance, 305
 - capacity, 66, 72-3, 78
 - BT: Static properties, Thermophysical properties
 - conductivity, 27, 66, 72-8, 303, 305
 - BT: Static properties, Thermophysical properties
 - Use for: Heat flow
- control, 95, 100, 231, 283, 296, 333, 335, 337, 363, 371, 386, 409, 414, 424
- control heaters, 293
- control materials, 314, 315, 424
- cycling, 409
- decomposition, 100
- design, 131, 392, 409, 423
- diffusivity, 303
- dissipation, 280, 288, 298, 302, 329, 332, 335, 337, 345, 359
- electrical models, 310
- gradients, 302-3, 421, 423
- interface, 279-80
- louvre system, 320, 322
- modeling, 303
- radiation time constant, 316
- resistance, 66, 78
 - BT: Thermophysical properties
- schematic diagram, 305
- systems engineer, 385
- time constant, 345
- transformer, 319-20
- transience, 301
- Thermally isotropic body models
 - Use: Battery-cell thermal analysis
- Thermodynamic constants, 10
- Thermophysical properties, 73, 75-7
 - NT: Heat generation, Specific heat, Thermal capacity, Thermal changes, Thermal conductivity, Thermal resistance
- Thermostatic switch operation test, 432
 - BT: Measurement methods
- Thickness reduction, 16
- Three-dimensional cell model, 311
- Throughput, 81-4, 93-5
- Time, 106, 121, 139, 142, 185, 206, 304-6
- Time-accelerated tests, 170
 - BT: Measurement methods
- Time constant, 306
- Tolerance requirements, 386
- Total charged-negative material, 41
 - BT: Charged-negative material
- Tradeoff studies, 387
- Trajectory
 - Use: Interplanetary trajectory
- Transducers, 402
- Transient charge, 80
 - period, 309, 384
 - response, 288
 - temperature response, 314
- Transistor dissipation, 284, 286
 - drive circuits, 363
- Transmission voltage level, 382
- Transmitted power, 382
- Transponder, 293, 378
- Travel cards, 236
- Trickle charge, 79, 86, 100, 170, 293, 334, 343, 348, 420, 439, 441

- U-fold separators, 25
- Unbalanced discharge currents, 371
- Unchargeable discharged material, 207
- Undertemperature protection, 347
- Undervoltage, 364, 371, 383, 393
- Undischargeable charged material, 207
- Unit capacity, 34
- Unit-load power data, 381
- Unregulated-voltage (UV) dc-bus system, 289-90
 - Use for: UV system
- Upper resistive element, 286
- Use conditions
 - Use: Operating conditions
- Utilization, 16 (def.), 33, 38-9, 43, 111, 122 (def.), 123-7, 130, 208
- UV system
 - Use: Unregulated-voltage (UV) dc-bus system
- Vacuum tubes, 276
- Variable discharge tests, 174
 - BT: Measurement methods
- Vented cells, 123
- Verification, 228
- Vibration tolerance, 420
- Void fraction, 14-16, 19, 33, 36-7, 49, 51, 108-9, 111, 115, 123-5, 130, 193, 196
- Void volume, 19, 37-8, 57, 90, 107, 112, 115, 129, 202
- Voltage, 80, 88, 112, 282
 - NT: Cell voltage
 - balance, 433
 - behavior, 187
 - conversion element, 279
 - degradation, 78, 134, 147, 168, 189, 365, 367-8
 - divider network, 286
 - drop, 298, 359, 378, 382, 393, 396
 - limit, 86, 90, 131, 133, 137-40, 146, 151, 170-71, 182, 190, 292, 336, 338-9, 342, 351, 399
 - limited charging, 334-6, 340-41, 417
 - BT: Charge control
 - recovery test, 255, 257, 263
 - BT: Measurement methods
 - reference, 281-2
 - regulation, 12, 278, 390, 416
 - variations, 296, 281
 - Volume, 19, 409, 414
 - Volumetric loading, 106, 123, 125
 - BT: Plate loading
 - Watt-hours, 181, 185
 - Watt-hour capacity, 168
 - Weibull distribution, 400-401, 404-5
 - Weight, 12, 34, 53, 205-6, 296, 382, 409, 414, 417, 421
 - Weldability, 28
 - Welded cell case, 27 (def.)
 - Use for: Fabricated case
 - Wettability, 20, 24-5, 77, 165, 203
 - Wick, 44-5
 - Wicking, 112
 - Wire-loop flux detector, 396
 - Work flow plan, 410
 - Working fluid, 316-17
 - Year, 174 (def.)

